Pure

Bangor University

DOCTOR OF PHILOSOPHY

Holocene evolution of a coastal barrier complex, Pendine Sands.

Walley, Stuart Shelby

Award date:
1996

Awarding institution:
Bangor University

Link to publication

General rights
Copyright and moral rights for the publications made accessible in the public portal are retained by the authors and/or other copyright owners and it is a condition of accessing publications that users recognise and abide by the legal requirements associated with these rights.

- Users may download and print one copy of any publication from the public portal for the purpose of private study or research.
- You may not further distribute the material or use it for any profit-making activity or commercial gain
- You may freely distribute the URL identifying the publication in the public portal ?

Take down policy
If you believe that this document breaches copyright please contact us providing details, and we will remove access to the work immediately and investigate your claim.

Download date: 22. Nov. 2024

HOLOCENE EVOLUTION OF A COASTAL BARRIER COMPLEX, PENDINE SANDS.

STUART SHELBY WALLEY

Thesis submitted in accordance
with the requirements of the
University of Wales
for the degree of
Doctor in Philosophy

I'W DDEFNYDDIO YN Y
LLYFRGELL YN UNIG

TO BE CONSULTED IN THE
LIBRARY ONLY

School of Ocean Sciences
University of Wales, Bangor
Menai Bridge
Anglesey
North Wales

July 1996

BEST COPY

AVAILABLE

Variable print quality

CONTAINS

PULLOUTS

Abstract

This study uses a multidisciplinary approach to elucidate the formation and evolution of a large coastal sand barrier complex in South Wales during the Holocene. Foraminifera, pollen, and geophysical evidence is used to interpret the geometry, lithology and stratigraphical relationships between deposits within the back-barrier area. Heavy mineral analysis and XRDA provide information on potential sediment sources.

Geophysical surveys show that the western portion of the barrier at Pendine Sands rests on a ridge of Pleistocene glacigenic sediment. This study shows that the barrier formed during the early Holocene (*ca.* 8,000 to 7,000 years BP) in response to the drowning of the antecedent topography by rapidly rising relative sea-levels; lithostratigraphic and biostratigraphic evidence from cores recovered within the back-barrier area show that the high energy surf zone did not overstep the gravel ridge and rework the fossil cliffline behind the western portion of the barrier. Sediment reworked from glaci-fluvio deposits in Carmarthen Bay was supplied to the prograding dune system by strong westerly and southwesterly winds and longshore drift. Between *ca.* 6,200 and 5,700 years BP and between *ca.* 4,500 and 3,500 years BP the barrier underwent two phases of long-term stability. These periods of barrier progradation and stabilisation were punctuated by relatively short phases of erosion, instability and barrier breakdown. Periods of barrier stability were probably triggered by regressive phases in relative sea-level change, which promoted spit development, whereas the intervening instability and breakdown was probably caused by an increase in storm frequency.

The response of this system to increased storm activity was primarily controlled by local topographic and sedimentological factors. The ridge beneath the western portion of the barrier prevented the total breakdown and or landward migration of the barrier dunes. Consequently, the back-barrier sediments deposited behind the barrier were preserved whereas the tidal inlet sequences east of the gravel ridge were reworked by wave action and tidal scour. Reclamation of the back-barrier area during the 17th and 19th centuries has had a significant effect on the configuration of the coastline at Pendine Sands. The construction of seawall defences stabilised the barrier dunes and promoted rapid accretion along the seaward side of the barrier dunes and at the distal end of the spit. The large expanse of sandflats which are exposed in Carmarthen Bay at low tide, and the frequency of strong westerly and southwesterly winds, were critical factors in the formation and development of the barrier dunes at Pendine Sands.

The significance of antecedent topography indicates that the formation and evolution of this particular barrier should not be considered as typical of regional barrier development.

Acknowledgements

I would like to thank:

Dr. James Scourse and Dr. Colin Jago for help and supervision during this project and for reading and commenting on the thesis.

The University of Wales for providing a postgraduate research studentship and NERC for funding radiocarbon dating.

Dr. Pete Brabham and Dr. Adrian Cramp (University of Wales, Cardiff) for the loan of essential field work equipment.

Dr. Jim Bennell and Dr. Dei Huws (University of Wales, Bangor) for support and advice during geophysical fieldwork and for helpful discussion.

Prof. Frank Oldfield (University of Liverpool) for the use of geomagnetic instrumentation.

Dr. David Jenkins (University of Wales, Bangor) for the provision of XRD and heavy mineral separation facilities.

The M.O.D. establishment at Pendine for allowing access to sites and for providing necessary maps.

Dr. Ron Haynes (University of Wales, Bangor) for advice and help with seismic data processing.

I am very grateful to the people of Laugharne for the warm welcome I received on every visit; long may this unique township's drinking traditions continue.

I am deeply indebted to the following friends for all their help with fieldwork and the sessions which followed; Dom Wren, Rob Dowsett, Rob Wells.

In particular I would like to thank Christopher Langrill who endured sub-zero conditions whilst we were coring at Laugharne. His encouragement and support was invaluable.

Finally, and most importantly I would like to thank my family without whose support, encouragement and generosity none of this would have been possible.

To John Shelby James

The wisest man I know.

Contents

Abstract
Acknowledgements
Contents
List of Figures
List of Tables
List of Appendices

Chapter 1 Introduction 1

1.1 Aims and objectives 1
1.2 Site description and recent history 2
1.2.1 The barrier complex 2
1.2.2 The Taf Estuary 4

1.3 Relative sea-level rise and contemporary dynamics 5
1.3.1 The Bristol Channel 6
1.3.2 Pendine Sands 7
1.3.3 The Taf Estuary 7

Chapter 2 Sea-level change and barrier formation/development 9
2.1 Sea-level change 9
2.1.1 Historical development of sea-level studies 9
The sea-level debate and approaches to sea-level studies 10
2.1.2 Sea-level methodology and inaccuracy 14
2.1.3 Sea-level change and crustal movements during the Holocene in Southwest England and Wales 21
2.1.4 Future direction of sea-level research 29

2.2 Barrier formation and evolution 32
2.2.1 Historical development of theories regarding barrier island genesis 32
2.2.2 Barrier complex response to relative sea-level rise 38
2.2.3 Summary 46

Chapter 3 Methods 49

3.1 Fieldwork/Site investigation 49
3.1.1 Coring methods 49
3.1.2 Sediment description 50
3.1.3 Sampling 51
3.1.4 Levelling 51
3.1.5 Seismic methods 51
Fundamental theory 51
Seismic refraction surveying 54
Seismic reflection surveying 57
Marine reflection profiling 61
3.1.6 Electrical resistivity surveying 63

3.2 Laboratory procedures 66
3.2.1 Heavy mineral analysis 67
Introduction 67

		Hydraulic relationships between light and heavy minerals	67
		Sample strategy and pretreatment	70
		Heavy mineral separation	71
		Heavy mineral identification	71
		Data analysis	72
	3.2.2	X-Ray Diffraction procedures	73
		Introduction	73
		Sample preparation and strategy	73
		Data analysis	74
	3.2.3	Geomagnetic measurements	74
		Introduction	74
		Magnetic minerals in sedimentary environments	75
		Sampling	76
		Magnetic measurement	77
		Processing and analysis	77
	3.2.5	Foraminiferal analysis	78
		Introduction	78
		Taphonomic considerations	80
		Sampling preparation	83
		Assemblage counts	83
		Identification and classification	83
		Diagram construction	84
		Analysis	84
	3.2.5	Pollen analysis	84
		Introduction	84
		Pollen taphonomy	86
		Sampling	89
		Sample preparation	89
		Gravity separation	89
		Preparation of organic sediments	90
		Pollen counting and sum	90
		Identification	90
		Pollen concentration	91
		Diagram construction	91
		Zonation	92
	3.2.6	Grain size analysis	92
		Sieving and Sedigraph analysis	92
		Particle size analysis using laser-based optical analysis	93
3.3		Radiocarbon dating	95
	3.3.1	Introduction	95
	3.3.2	Sources of error	95
	3.3.3	Sampling	96
	3.3.4	Radiocarbon measurement	97
	3.3.5	Interpretation	97
Chapter 4		**Lithostratigraphy, mineralogy and magnetics**	**98**
4.1		Core descriptions	98
	4.1.1	Introduction	98
	4.1.2	West Marsh	98
		Pendine Woodend Section	98
		Westmead Section	100
		Brook Section	101
	4.1.3	East Marsh	103
		Coygan Quarry Section	103

		Causeway Section	104
		Salt House Section	106
		East House Section	106
	4.1.4	Pendine Burrows	107
	4.1.5	Taf Estuary	107
		Delacorse Marsh	108
		Blackscar Marsh	109
		Lithology of physiographic sub-environments within the Taf Estuary	109
	4.1.6	Summary	109
4.2		Provenance studies	111
	4.2.1	Heavy mineral analysis	111
		The heavy mineralogy of saltmarsh and back-barrier sediments	111
		The origin of sediments within the Taf Estuary and barrier complex	113
	4.2.2	X-Ray Diffraction Analysis	118
		Clay mineralogy and indications of sediment source	118
4.3		Environmental magnetism	121
	4.3.1	Magnetic measurements	121
		West Marsh	121
		East Marsh	123
	4.3.2	Summary	125
Chapter 5		**Geophysical methods**	**127**
5.1		Seismic methods	127
	5.1.1	Seismic refraction surveying	127
		Description of refraction data	127
		Comparison of refraction data to borehole information	129
		Surface models derived from refraction data	130
		Implications for barrier formation and development	132
	5.1.2	Seismic reflection surveying	133
		Description of land based shallow reflection data	133
		Discussion of high-resolution seismic reflection data	135
	5.1.3	Marine reflection profiling	136
		Description of shallow marine reflection data	136
		Discussion of shallow marine reflection data	137
5.2		Electrical resistivity surveying	138
	5.2.1	Description of resistivity data	138
5.3		Summary	139
Chapter 6		**Palaeoenvironments and Radiocarbon Dating**	**141**
6.1		Foraminifera	
	6.1.1	Description of foraminiferal data	141
		Site 12	141
		Site 4	142
		Site 11	144
		Site 17	146
		Site 20	147
		Site 22	148
	6.1.2	Modern foraminiferal associations in the Taf Estuary	149
	6.1.3	Comparison of modern and fossil assemblages	151

6.1.4 Interpretation of fossil data 153
Site 12 153
Site 4 154
Site 11 155
Site 17 156
Site 20 156
Site 22 157
6.1.5 Summary 157

6.2 Pollen analysis 160
6.2.1 Description of pollen analytical data 160
Site 7 160
Site 12 162
Site 4 164
6.2.2 Pollen sources in West Marsh and regional vegetation succession during the Holocene 166
6.2.3 Vegetational development within West Marsh 169
Site 7 169
Site 12 172
Site 4 174
6.2.4 Summary 175

6.3 Radiocarbon dating 178
6.3.1 Radiocarbon results 178
Site 7 178
Site 12 178
Site 4 178
6.3.2 Discussion of ^{14}C dates 179

Chapter 7 Discussion 181

7.1 Introduction 181
7.2 Sedimentary facies development 182
7.2.1 West Marsh 182
Pendine Woodend Section 182
Westmead Section 184
Brook Section 185
7.2.2 East Marsh 187
Causeway Section 187
Salt House/East House Section 188

7.3 Coastal evolution 189
7.3.1 Deglaciation and the onset of the Holocene transgression: 18,000-10,000 years BP 189
7.3.2 Formation and evolution of the Pendine and Laugharne Burrows 190
Onset of the Holocene transgression: 10,000-8,000 years BP 191
Barrier formation, progradation and stability: 8,000-5,500 years BP 191
Barrier instability, breakdown and reworking: 5,500-5,000 years BP 193
Barrier progradation and stability: 5,000-3,500 years BP 194
Barrier instability and the formation of the Pendine and Laugharne Burrows: 3,500-2,000 BP 195
Progradation of the Pendine and Laugharne Burrows: 2,000-500 years BP 196

Reclamation of West and East Marshes: Late 17th century to present day 197

7.4 Mechanisms controlling barrier formation and evolution in South west Wales 197

Chapter 8 Conclusions **206**

8.1 Conclusions 206
8.2 Further research 209

References **210**

Appendices

List of Figures

Figure 1.1 Location of Carmarthen Bay, South Wales.

Figure 1.2 The Pendine/Laugharne barrier complex.

Figure 1.3a Fossil cliffline from Pendine to Coygan.

Figure 1.3b Steep eroded fossil cliffline between Coygan and Laugharne.

Figure 1.4a Low irregular dune at the back of the Laugharne Burrows.

Figure 1.4b Shore-parallel beach/dune ridges along the front of the burrows.

Figure 1.5a Ordnance survey map showing Ginst Point in 1908.

Figure 1.5b Aerial photograph showing contemporary marshes extending from the 'Freathing' sea wall between sir John's Hill and Ginst (April, 1993).

Figure 2.1 Different interpretations of sea-level history during the Holocene (Kidson, 1986).

Figure 2.2 Sea-level methodology with reference to errors (Shennan, 1983)

Figure 2.3 Sea-level curves for the English Channel, Bristol Channel, and Cardigan Bay (Heyworth & Kidson, 1982).

Figure 2.4 A time-altitude graph for 311 ^{14}C-dated sea-level index points; each date is represented by four proportional ellipses to visually represent age and altitude error estimates (Heyworth and Kidson, 1982).

Figure 2.5 Sea-level curves drawn for: 1, Bristol Channel; 2, English Channel; 3, Cardigan Bay; 4, Somerset Levels Trackways; 5, North Wales. MHWST is used as the common datum (Heyworth and Kidson, 1982).

Figure 2.6 Map of estimating current rates (mm/yr) of crustal movement in Great Britain. Isolines cannot be drawn for much of southern England and point estimates are only shown for guidance (Shennan, 1989b).

Figure 2.7 A sea-level curve for the Bristol Channel (Allen, 1990).

Figure 2.8 Cross section of narrow Holocene barrier and salt marsh along front of Sapelo Island, Georgia. SL= sea-level (Hoyt, 1967).

Figure 2.9 Idealized diagram showing barrier island formation from spit. 1 and 2, Spit develops in direction of longshore sediment transport. 3, Spit breached to form barrier island (Hoyt, 1967).

Figure 2.10 Formation of barrier islands by submergence. 1, Beach or dune ridge forms adjacent to shoreline. 2, Submergence floods area landward of ridge to form barrier island and lagoon (Hoyt, 1967).

Figure 2.11 A barrier island may 1, prograde; 2, erode; or 3, remain in place, depending on sediment supply, rate of submergence, and hydrodynamic factors (Hoyt, 1967).

Figure 2.12 The unit volume of coastal water column and its substrate. Arrows indicate components of sediment and water transport. Coast-parallel water movements are more intense than coast-normal movements, hence the resultant transport vectors tend to make low angle with coast (Swift, 1975).

Figure 2.13a Evolution of the shoreface as a rugged coast passes from stillstand to transgression. A mature configuration is replaced by a transient state of mainland beach detachment, then by a quasi steady-state regime of cyclic spit building (Swift, 1975).

Figure 2.13b Evolution of the shoreface as a low coast passes from stillstand to transgression. A mature coastal configuration passes via mainland beach detachment into a steady state of barrier retreat (Swift, 1975).

Figure 2.14 New South Wales showing coastal Quaternary deposits and locations (Roy *et al.*, 1980).

Figure 2.15 Three primary types of Holocene embayment fill, illustrated diagrammatically (Roy *et al.*, 1980)

Figure 2.16 Schematic sections showing progressive stages of evolution, according to the model, of three embayment types (Roy *et al.*, 1980).

Figure 2.17 Local sea-level curves for Delaware constructed from ^{14}C dated basal peats (Belknap and Kraft, 1981).

Figure 2.18 Flow chart of concepts leading to a model of fractional preservation related to rate of sea-level rise as well as variables of incident wave energy, net sedimentation input or export, change of tidal range, antecedent topography, and other minor factors (Belknap and Kraft,1981).

Figure 2.19a Coastal sedimentation in Nova Scotia can be considered as a 6-stage transgressive sequence of barrier genesis, destruction and re-establishment dominated by localised glacial sediment sources, rising RSL and tidal inlet processes. Initial barrier genesis (Stages 1 and 2) was related to advance and ablation of continental ice sheets. Subsequent evolution consists of a cyclic repetition of Stages 3-6 (Boyd and Penland, 1984).

Figure 2.19b A conceptual model of barrier formation on the N.S.W. coast. Two alternative mechanisms are identified to produce stages of shoreline progradation by landward sediment transfer from the shoreface (Boyd and Penland, 1984).

Figure 2.19c Sediment input to coastal barrier systems of the Mississippi Delta is controlled by the processes of subsidence and erosional shoreface retreat. The original sand source lies in distributary and pre-existing barrier deposits. During transgression of this source is reworked to form new barrier deposits by erosional shoreface retreat until on-going compactional subsidence removes the sand source below the base of the shoreface resulting in eventual barrier submergence (Boyd and Penland, 1984).

Figure 2.20 The control hierarchy associated with sea-level control of coarse clastic barrier and lagoon evolution (Carter *et al.*, 1989)

Figure 3.1 a) The drilling assembly; b) the extraction system; c) the closed sampler.

Figure 3.2 Location of Ordinance Survey Bench Marks

Figure 3.3 Refraction at an interface between two layers; I= angle of incidence; t= angle of transmission.

Figure 3.4 Critical refraction at an interface between two layers; c= critical angle of incidence.

Figure 3.5 Schematic representation of the critically refracted raypaths from A to B and B to A.

Figure 3.6 Raypaths between a single source and a series of receivers.

Figure 3.7 Raypaths between source and receivers for a CMP with 6-fold coverage.

Figure 3.8a The processing routine used to read SEG-Y data from disk into SierraSEIS.

Figure 3.8b The pre-stacking processing routine.

Figure 3.8c The processing routine used to define the velocity structure, correct for normal moveout and stack CDP gathers.

Figure 3.9 Plan view of the IKB-SEISTEC.

Figure 3.10 The 'Line and Cone' receiver.

Figure 3.11 Schematic diagram showing the expanding Schlumberger electrode array.

Figure 3.12 Heavy mineral separation, adapted from Jenkins (1964).

Figure 3.13 Electron transitions in an atom bombarded by an SEM electron beam (Welton, 1984).

Figure 3.14 Various sources of pollen in a small lake or mire within a wooded landscape (Tauber, 1965).

Figure 3.15 Relationship between the size of a site and the various sources of pollen entering it (Jacobson & Bradshaw, 1981).

Figure 3.16 The pollen preparation method (Watkins, 1991).

Figure 4.1 The Pendine/Laugharne barrier system.

Figure 4.2 Location of borehole sites within West Marsh and East Marsh.

Figure 4.3 Lithology at sites 7 and 8.

Figure 4.4a A detailed description of the lithology at site 7.

Figure 4.4b. A detailed sedimentary log describing the organics recovered from site 7.

Figure 4.5 Lithology at sites 6, 5, 12 and 9.

Figure 4.6a A detailed description of the lithology at site 12.

Figure 4.6b A detailed sedimentary log describing the organics recovered from site 12.

Figure 4.7 Lithology at sites 3, 4 and 11.

Figure 4.8a A detailed description of the lithology at site 4.

Figure 4.8b A detailed sedimentary log describing the organics recovered from site 4.

Figure 4.9 A detailed description of the lithology at site 11.

Figure 4.10 Lithological log drawn from borehole data obtained from F.H. Gilman & Co.

Figure 4.11 Lithology at sites 15, 16, 17, 18 and 19.

Figure 4.12 A detailed description of the lithology at site 17.

Figure 4.13 Lithology at sites 24 and 20.

Figure 4.14 A detailed description of the lithology at site 20.

Figure 4.15 Lithology at sites 23, 21 and 22.

Figure 4.16 A detailed description of the lithology at site 22.

Figure 4.17 Location of the MOD test track section.

Figure 4.18 Lithological sequence through Laugharne Burrows drawn from boreholes obtained from BGS.

Figure 4.19 Location of cores recovered from Delacorse Marsh.

Figure 4.20 The lithology in Delacorse Marsh.

Figure 4.21 PCA applied to the untransformed non-opaque heavy mineral assemblages; estuarine samples (◆), back-barrier deposits (◊), Carmarthen Bay sands (■), loess (X), Irish Sea Drift (∗), Breconshire Drift (⊗), moraine within the Taf Estuary (⊙), and the soil sample (+).

Figure 4.22 XRDA diffraction patterns for (a) the Delacorse Marsh sediments and (b) the Black Scar Marsh sediments.

Figure 4.23 XRDA diffraction patterns for (a) the back-barrier material and (b) the Carmarthen Bay sample.

Figure 4.24 The major sources of clay minerals within the Severn Estuary and the lower Bristol Channel (Allen, 1991).

Figure 4.25 Whole core susceptibility (*k*) measurements for (a) site 7; (b) site 12; © site 9; (d) site 4; (e) site 11.

Figure 4.26 Magnetic parameters, quotients and ratios for site 17.

Figure 4.27 Magnetic parameters, quotients and ratios for site 24.

Figure 4.28 Magnetic parameters, quotients and ratios for site 20.

Figure 4.29 Magnetic parameters, quotients and ratios for site 23.

Figure 4.30 Magnetic parameters, quotients and ratios for site 21.

Figure 4.31 Magnetic parameters, quotients and ratios for site 22.

Figure 5.1 Distribution of refraction data within West Marsh (WM), East Marsh (EM) and the Pendine Burrows; black points indicate shot positions.

Figure 5.2 Model of bedrock basement (L4).

Figure 5.3 Model of pre-Holocene surface (L3/L4).

Figure 5.4 Position of reflection profiles on Pendine Sands.

Figure 5.5 Final processed section for Transect 1; the geological interpretation is based on an average velocity of 1650 m/sec.

Figure 5.6 Final processed section for Transect 2; the geological interpretation is based on an average velocity of 1650 m/sec.

Figure 5.7 Final processed section for Transect 3; the geological interpretation is based on an average velocity of 1650 m/sec.

Figure 5.8 Marine reflection survey track within the Taf Estuary.

Figure 5.9 A section of marine reflection data recorded using the SEISTEC along line 6; the geological interpretation is based on an average velocity of 1650 m/sec.

Figure 5.10 A section of marine reflection data recorded using the SEISTEC along line 9; the geological interpretation is based on an average velocity of 1650 m/sec.

Figure 5.11 Model of bedrock basement.

Figure 5.12 Model of pre-Holocene surface.

Figure 5.13 Bedrock basement beneath study area.

Figure 5.14 Pre-Holocene beneath the study area.

Figure 5.15 Thickness of Pleistocene beneath study area.

Figure 6.1 Location of sites 12, 4, 11, 17, 20 and 22.

Figure 6.2 Foraminiferal diagram for site 12.

Figure 6.3 Foraminiferal diagram for site 4.

Figure 6.4 Foraminiferal diagram for site 11.

Figure 6.5 Foraminiferal diagram for site 17.

Figure 6.6 Foraminiferal diagram for site 20.

Figure 6.7 Foraminiferal diagram for site 22.

Figure 6.8 Location of Delacorse Marsh.

Figure 6.9 PCA applied to both modern (▲) and fossil (O) data.

Figure 6.10 Location of sites 7, 12 and 4.

Figure 6.11 Pollen diagram for site 7.

Figure 6.12 Pollen concentration diagram for site 7.

Figure 6.13 Pollen diagram for site 12.

Figure 6.14 Pollen concentration diagram for site 12.

Figure 6.15 Pollen diagram for site 4.

Figure 6.16 Pollen concentration diagram for site 4.

Figure 6.17a Schematic cross-section showing the various pollen sources within West Marsh during the accumulation of saltmarsh sediment.

Figure 6.17b Schematic cross-section showing the various pollen sources within West Marsh during phases of organic accumulation.

Figure 6.18 Radiocarbon dated Holocene pollen zones in Tregaron Bog, Wales (from Hibbert and Switsur, 1976).

Figure 7.1 The Pendine/Laugharne barrier system.

Figure 7.2 Position of stratigraphic sections in West Marsh and East Marsh.

Figure 7.3 Stratigraphic section (T1) based on lithological data from sites 7 and 8.

Figure 7.4 Stratigraphic section (T2) based on lithological data from sites 6, 5, 12 and 9.

Figure 7.5 Stratigraphic section (T3) based on lithological data from sites 3, 4 and 5.

Figure 7.6 Stratigraphic section (T4) based on lithological data from sites 15, 16, 17, 18 and 19.

Figure 7.7 Stratigraphic section (T5) based on lithological data from sites 24, 20, 21 and 24.

Figure 7.8 Coastal configuration at the onset of the Holocene transgression.

Figure 7.9 Coastal configuration at 9,000 years BP.

Figure 7.10 Barrier formation through mainland detachment of antecedent topography.

Figure 7.11 Barrier progradation in response to high sediment supply.

Figure 7.12 Barrier stability, marsh development and organic accumulation.

Figure 7.13 Barrier breaching and breakdown.

Figure 7.14 Barrier progradation, marsh development and organic accumulation.

Figure 7.15 Barrier thinning and spit elongation.

Figure 7.16 Barrier breaching and breakdown.

Figure 7.17 Formation of the Pendine and Laugharne Burrows.

Figure 7.18 Dynamic equilibrium and sediment by-passing.

Figure 7.19 Reclamation of West Marsh and East Marsh.

Figure 7.20 Reclamation of Lower Marsh.

Figure 7.21 Contemporary barrier system.

List of Tables

Table 4.1 The description and position of samples examined using heavy mineral analysis.

Table 4.2 Composition of heavy mineral assemblages from Delacorse Marsh and East Marsh.

Table 4.3 Composition of heavy mineral assemblages from potential source materials.

Table 5.1 Seismic velocities and refractor depths obtained from refraction lines within the dunes and the back-barrier area.

Table 6.1 Authorities and ecological requirements for the foraminifera identified in the back-barrier complex sediments.

Table 6.2 Radiocarbon dates obtained from organic levels in West Marsh.

Table 7.1 Facies development at site 7 during the Holocene.

Table 7.2 Facies development at site 12 during the Holocene.

Table 7.3 Facies development at site 4 during the Holocene.

Table 7.4 Facies development at site 11 during the Holocene.

Table 7.5 Facies development at site 17 during the Holocene.

Table 7.6 Facies development at site 20 during the Holocene.

Table 7.7 Facies development at site 22 during the Holocene.

List of Appendices

Appendix 3.1 Multiple layer refraction shooting.

Appendix 6.1 Modern foraminiferal associations from the Taf Estuary.

Appendix 6.2 Ecological and environmental requirements of certain tree, shrub, herb and lower plant taxa

Chapter 1

Introduction

Diverse and complex natural processes continually modify the world's coastlines which are consequently in a permanent state of flux. The scale of coastal change may range from microscopic biological, chemical or physical processes affecting individual grains of sand to global changes in relative sea-level. During the Late Devensian the mass wastage of the terrestrial ice sheets caused the world's oceans to transgress the continental shelves, inundating former glacial and river valleys. The rate of relative sea-level rise and the response of certain areas of coastline to the removal of terrestrial ice sheets depended upon their proximity to the former ice masses and the availability of sediment to supply and maintain coastal systems. Human activity during the last few hundred years has added a further dimension to coastal change by modifying and disturbing coastal environments and the natural processes of change.

Studies into the long-term behaviour and response of coastal systems to these natural processes are the key to predicting future coastal changes and providing the understanding necessary to resolve the coastal crisis. Models describing long- (10^3 years) and short-term (10^0 years) coastal evolution should be used to devise and construct management policies which aim to the control the increasing demands exerted on the coastal resource; the latter requires an understanding of contemporary processes and analysis of the Holocene stratigraphic record.

1.1 Aims and objectives

The Pendine and Laugharne Burrows, situated on the north coast of Carmarthen Bay in SW Wales (Figure 1.1), form an extensive barrier complex which covers an area of approximately 20 km^2. The aim of this multidisciplinary study is to investigate the formation and evolution of this large coastal sand barrier complex in response to relative sea-level rise and differential sediment supply during the Holocene. This feature is one of the largest barrier complexes in western Britain, and unlike the majority of the barriers in the Gulf of Mexico and on the eastern seaboard

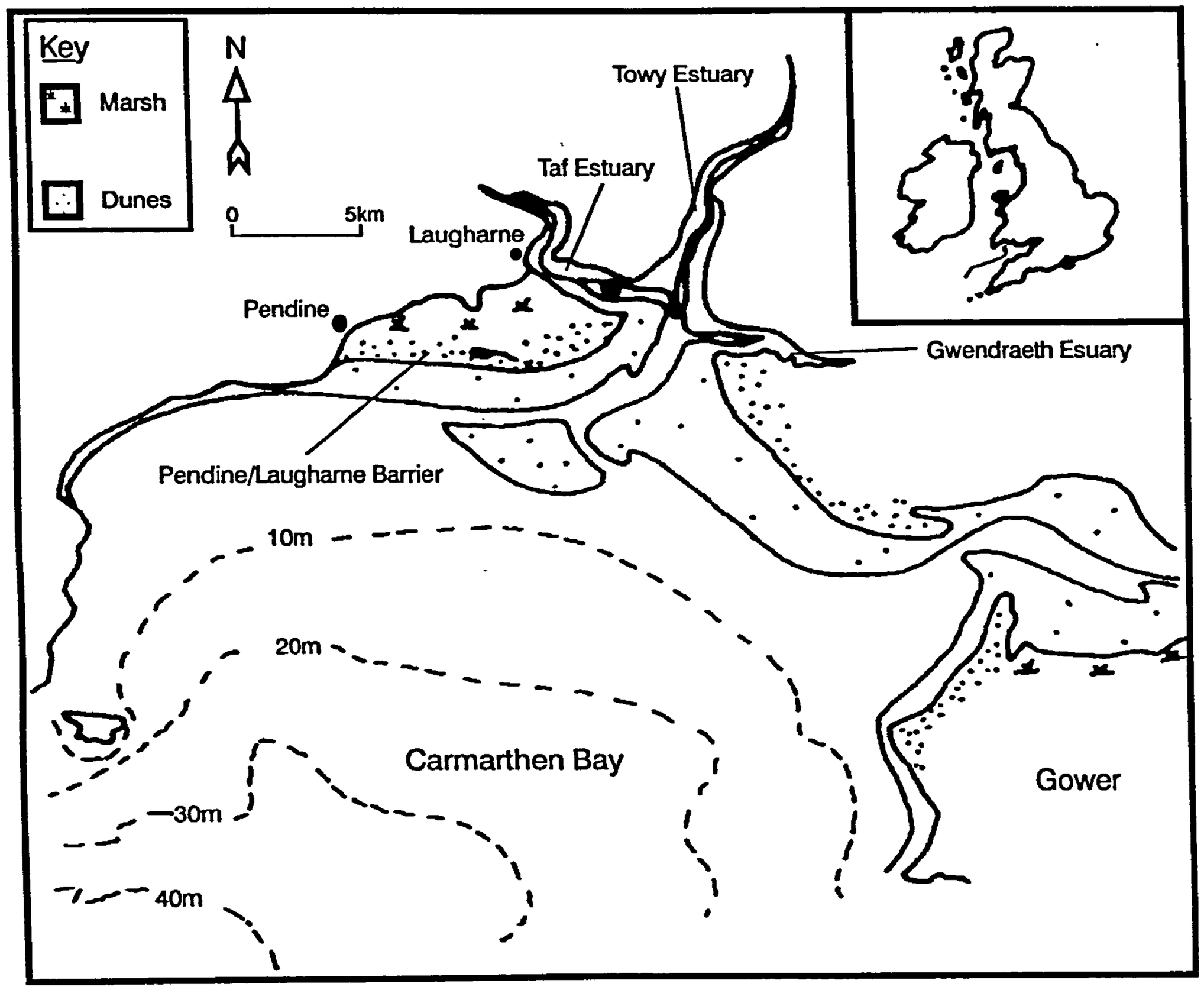

Figure 1.1 Location of Carmarthen Bay, South Wales.

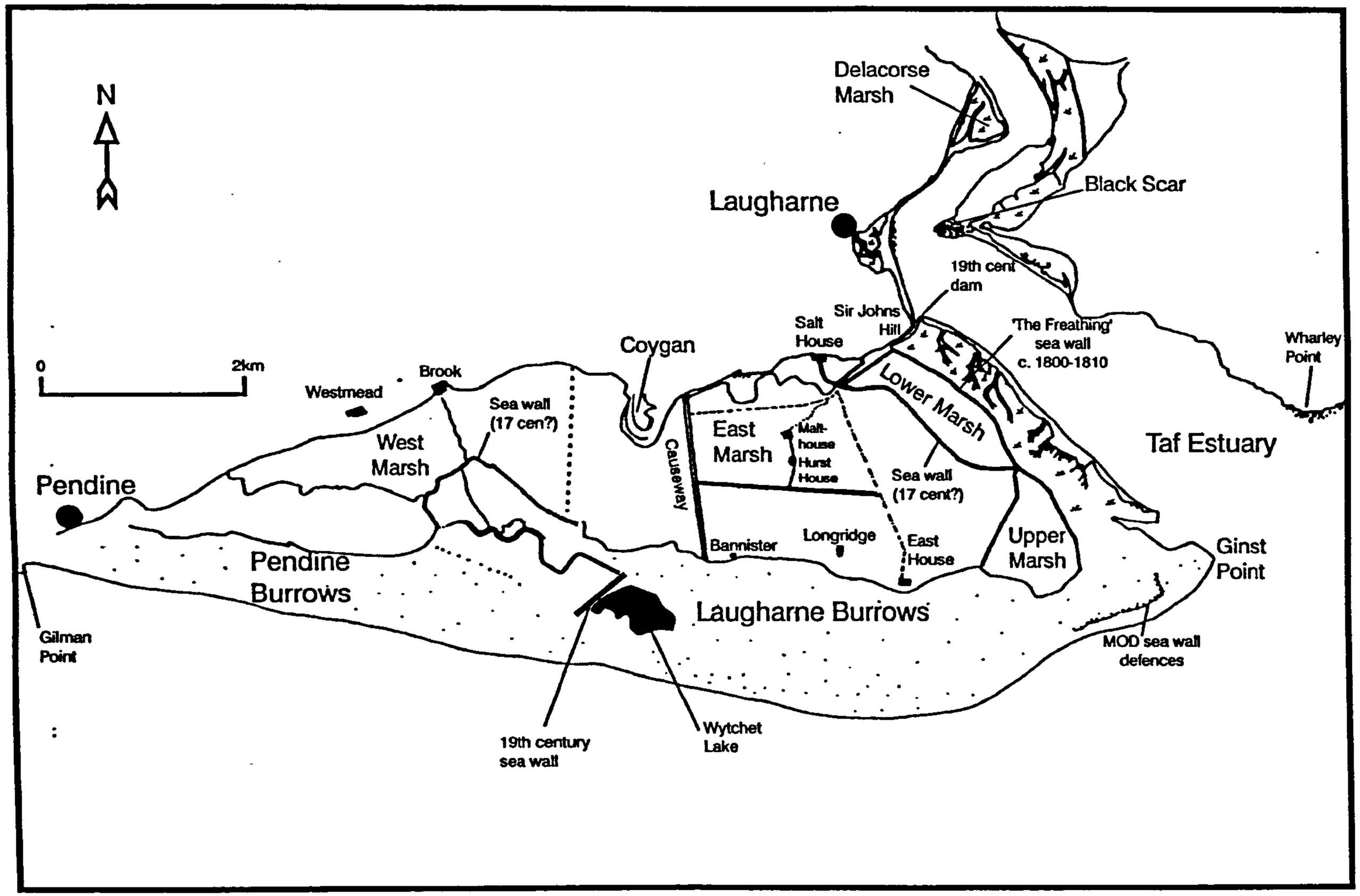

Figure 1.2 The Pendine/Laugharne barrier complex.

of the USA, it formed and developed in a macro- rather than micro-tidal environment. Previously established hypotheses of barrier genesis, evolution and development will be tested against the hypotheses produced in this study; the latter will be used to establish whether or not this feature formed and developed in response to regional processes or was controlled primarily by local phenomena. To achieve these aims biostratigraphic and lithostratigraphic evidence, obtained from boreholes drilled into the back-barrier area, will be used to establish facies changes within the system which will be constrained by radiocarbon dating of organic levels and correlated by using laboratory induced magnetic measurements. Heavy and clay mineral analysis will be used to determine sediment provenance, and geophysical data will be used to establish the antecedent topography upon which this feature rests. Knowledge of pre-transgressive surfaces are necessary as coastal barrier evolution is often intimately tied to the surfaces upon which these systems form and subsequently migrate.

1.2 Site description and recent history

Carmarthen Bay is a shallow embayment bound by rocky clifflines which is believed to have formed by the erosion of relatively soft shales within the Millstone Grit and Coal Measure series (Strahan, 1909). The area contains considerable quantities of glacigenic material which has been reworked to form abundant sandwaves offshore and numerous near-shore bars and intertidal sandbanks (Jago, 1974, 1980).

1.2.1 The barrier complex

The barrier complex extends a distance of 10 km from Gilman Point near Pendine to the confluence of the rivers Taf, Towy and Gwendraeth (Figure 1.2). This feature extends across the lower reaches of the Taf Estuary and the barrier dunes form the landward portion of extensive sandflat deposits which are exposed within Carmarthen Bay at low tide. The barrier is attached to a steep cliffline at Gilman Point which runs behind the barrier system from Pendine to Sir John's Hill (Figure 1.3a). This fossil cliffline, cut into Devonian Old Red Sandstone and the Carboniferous Limestone promontory at Coygan, is though to represent the coastline prior to the formation of the barrier. Savigear (1953) indicate that, as the slope of the cliffs increases

Figure 1.3a Fossil cliffline from Pendine to Coygan.

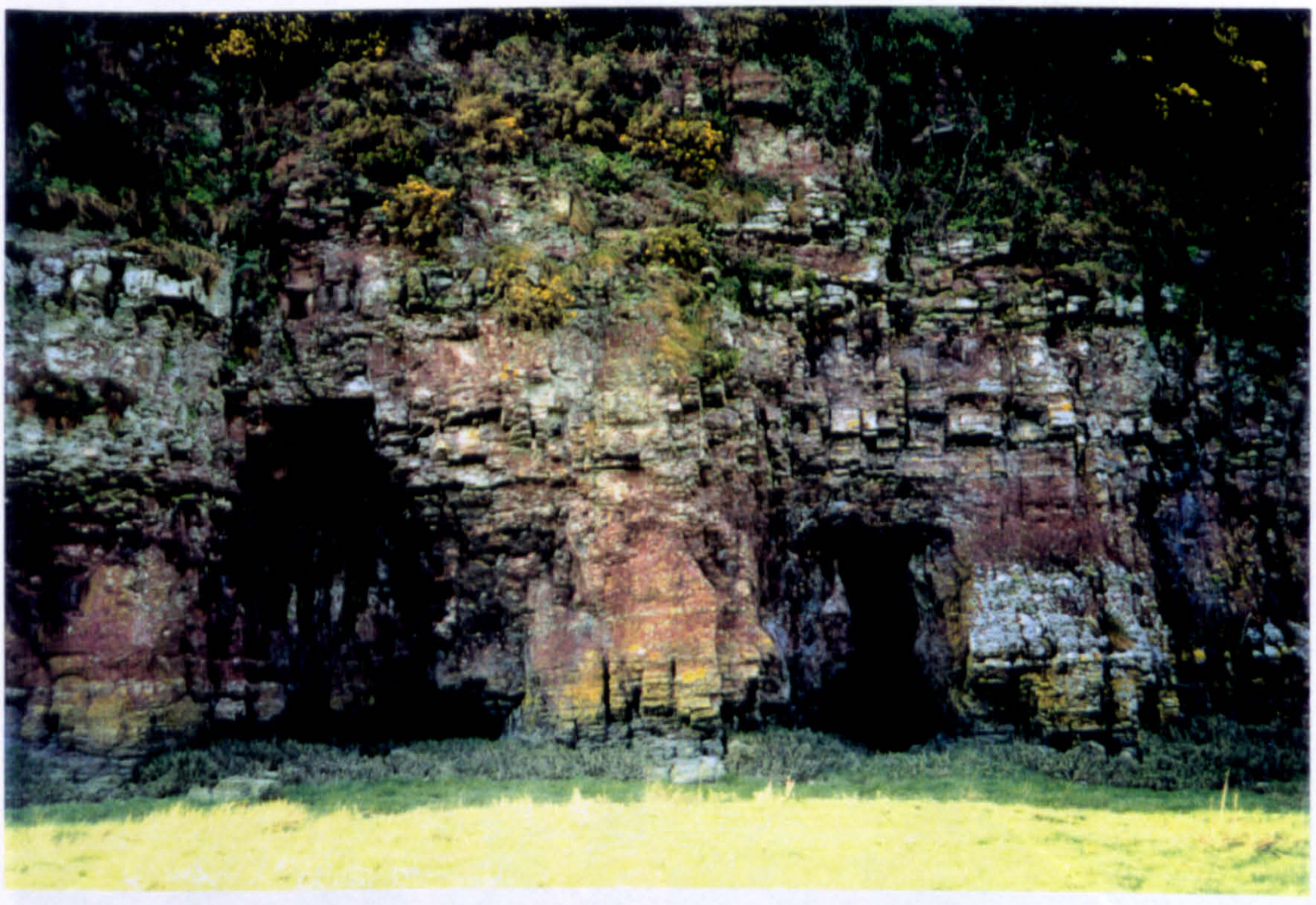

Figure 1.3b Steep eroded fossil cliffline between Coygan and Laugharne.

Figure 1.4a Low irregular dune at the back of the Laugharne Burrows.

Figure 1.4b Shore-parallel beach/dune ridges along the front of the burrows.

progressively from Pendine to Laugharne, the barrier probably formed through the longshore development of the dunes and foreshore.

Pathways and roads cut into the fossil cliffline west of Coygan show that brick red Pleistocene till has been pushed up and smeared against this portion of the fossil cliffline; these deposits are similar to the ridge of moraine within the Taf Estuary known as Blackscar (Figure 1.2). The latter is believed to represent a slight readvance during the retreat of Central Welsh ice during the Late Devensian (Griffiths, 1939). In contrast the cliffs to the east of Coygan are far steeper and contain numerous caves infilled with coarse gravel and sand (Figure 1.3b). The absence of similar features west of Coygan suggests that this portion of the fossil cliffline was not subject to significant erosion prior to the formation of the coastal barrier.

The Wytchet brook dissects the barrier forming the boundary between West and East Marshes and the Pendine and Laugharne Burrows (Figure 1.2). The dunes at the back of the burrows are relatively low and exhibit no clear orientation, suggesting that this portion of the barrier was periodically breached and therefore experienced washover and blowout events (Figure 1.4a). In contrast the fore- dunes are composed of a series of low shore-parallel beach ridges which prograde seawards (Figure 1.4b). During barrier development the back-barrier area would have been dominated by an expansive saltmarsh-tidal creek complex. Tidal inlets similar to Wytchet inlet generally exhibit little or no down drift migration, in response to sediment accretion and sediment by-passing, and are more stable than inlets in wave dominated environments.

Documentary references indicates that West Marsh was under pasture prior to the construction of any sea walls and that the evolution of the marsh for agricultural purposes was an eastward moving phenomenon (James, 1991). The back-barrier marshes now form a relatively flat area which was first reclaimed during the 17th century by the construction of embankments across the Wytchet inlet and from the fossil cliffline at the foot of Sir John's Hill to the Laugharne Burrows (Curtis, 1880; James, 1991). A second embankment referred to as 'The Freathing' sea-wall, was constructed between 1800 and 1810 to reclaim Upper and Lower Marsh (Figure 1.2). Prior to the construction of the dam across Wytchet in the late 19th century this inlet was still open to the sea and West Marsh and East Marsh were periodically inundated by the tide (James, 1991).

The marine chart for 1800 AD shows no dunes east of Wytchet but name the Laugharne Burrows. Cantrill (1909) records the findings of early Iron Age or late Stone Age shell mounds in the Laugharne Burrows. The preservation of these findings suggest that the dunes have not been completely broken down and reworked since that period and that the barrier was sufficiently developed and stable over 2,000 years ago to protect the inhabitants from strong westerly-southwesterly storms. Although, marine charts may be better tools for reconstructing the position of former coastlines, schematic representations of coastal features are often misleading. Care should be taken when using different types of cartographic evidence to reconstruct the configuration of former coastlines. Cartographic evidence shows that the reclamation of the back-barrier area stabilised the barrier system and has promoted the futher development of this feature (James, 1991).

The Pendine and Laugharne Burrows were taken over by the Ministry of Defence during the Second World War and have since been used as an experimental and test establishment. During the early 1970s the MOD stabilised the dunes at Ginst Point in order to prevent the rapid erosion and possible breaching of the barrier. This has subsequently promoted the longshore development of the distal end of the spit which now extends further across the mouth the Taf Estuary towards Wharley Point. Ordnance survey maps for 1907 (Figure 1.5a) indicate that the saltmarsh adjacent to the sea wall which encloses Upper and Lower Marsh developed within the last eighty or so years (Figure 1.5b)

1.2.2 The Taf Estuary

The River Taf drains into a macro-tidal estuary which is currently being infilled with well sorted sand transported up-estuary as a result of tidal asymmetry (Jago, 1980). Although the inner estuary and barrier complex form part of the same sedimentary dispersal system they may be divided on the basis of their physiography and hydrodynamics. The estuary is 8 km in length and less than 1.5 km wide at its mouth; although the cross-sectional area increases towards the mouth Jago (1980) suggests that an equilibrium between erosion and accretion has not yet been attained.

The estuary contains a number of physiographic sub-environments which may be differentiated by sediment type, vegetation cover, surface and sub-surface fauna and currents (Jago, 1980). At

low tide the estuary appears like an intertidal flat with saltmarshes and mudflats fringing low lying sandbanks which are dissected by a complex pattern of shallow drainage channels. Although the position of the main channels remain relatively stable the orientation and position of the smaller channels depends upon the magnitude of river discharge. These channels migrate across the sandflats often causing the erosion of mudflats and saltmarshes which extend into the main channel.

Spartina townsendii, allegedly introduced into the area by an East Marsh farmer during the 1920s (Jago, 1974), dominates the more recent low lying saltmarshes and upper mudflats within the estuary. The more established high marshes are inhabited by well developed floras which may include *Glyceria maritima, Armeria marctima, Festuca rubra, Aster tripolium, Atriplex* and *Halomione portulacoides.* The saltmarshes are dissected by a hierarchy of self perpetuating creeks which drain sinuously onto the sandflats in the centre of the estuary. Changes in marsh elevation and vegetational composition indicate progressive stages of saltmarsh accretion and development which may relate to the position of the main channel.

The morphology and development of the contemporary saltmarshes within the Taf Estuary highlight the complex patterns of sedimentation within this system. It is likely that the position and size of the tidal inlets, the back-barrier drainage channels and marsh creeks significantly influenced back-barrier sedimentary facies development. Knowing the distribution and inter-relationships between physiographic sub-environments within the contemporary estuary will prove critical when developing models which aim to describe back-barrier facies development.

1.3 Relative sea-level rise and contemporary dynamics

The British Isles have experienced a complex pattern of relative sea-level rise during the Holocene. Variations in glacial-isostasy, glacial-eustasy and tectono-eustasy have resulted in different areas experiencing differing rates and patterns of relative sea-level rise. South Wales is an area located within close proximity to the maximum limit of ice advance during the Late Devensian. Sea-level studies indicate that reconstructions of relative sea-level rise within the Bristol Channel during the Holocene are further complicated by the wide continental shelf, the crenulate coastline, by convoluted changes in the position and strength of amphidromes and by

PAGE

MISSING

IN

ORIGINAL

models are not exclusive and that the mutually evasive sediment transport mechanism may operate mainly in sand choked estuaries.

1.3.2 Pendine Sands

Carmarthen Bay is open to southwesterly storms and oceanic swell which may have travelled over 5,000 miles across the Atlantic. Jago and Hardisty (1984) suggest that the energy loss as waves sweep across the shallow bay prevents the majority of large waves from reaching the shoreline. They predicted that for the waves that approach from 203°, 4s waves will be reduced by 50% and 10s waves will be reduced by 70% as they shoal from the 40m to 5m isobaths off the eastern end of the barrier. During extreme spring tides the tidal range on the Pendine sands approaches 10.0 metres and surface currents reach 1.0 m/s in the middle of the bay. Jago and Hardisty (1984) suggest that the beach profile is self-stabilising in the short term, and periodic levelling shows that the beach is in long-term equilibrium with the prevailing conditions. The barrier shoreface does however exhibit significant dynamic response to changing tides and waves. As the tide ebbs, wave generated stresses on the shoreface decrease. Consequently there is an overall seaward-fining of the intertidal sand texture. Jago and Hardisty (1984) conclude that tide- and storm-induced modification of the near-shore flow regimes produces a distinctive array of shore-normal sedimentary facies, which are more laterally extensive than comparable micro-tidal sequences.

1.3.3 The Taf Estuary

The Taf Estuary is characterised by a well established tidal asymmetry so that maximum currents during spring tides are 3-4 times greater in the estuary than in Carmarthen Bay (Jago, 1980). The accumulation of sand within the estuary has generated an elevated profile which delays the tide from entering the estuary. By the time the sea enters the estuary the tide is well advanced in the bay causing maximum currents to occur as the sea enters the estuary and just prior to its withdrawal (Jago, 1974, 1980). The tidal asymmetry within the Taf is exaggerated because the tide is forced to rise two metres when entering the estuary.

The Taf is presently being infilled and levelled transects within the estuary indicate that between 1968 and 1978 there was a net rise in the volume of sand within the estuary (Jago, 1980). The texture mineralogy and composition of these sands is almost identical to those in Carmarthen Bay. Jago suggests that southwesterly storms push material from the bay to the mouth of the estuary reinforcing the tidal asymmetry which in turn pumps sediment into the estuary.

The predominant sedimentological trend is depositional in the north western portion of Carmarthen Bay with the progressive movement of sediment into the estuaries (Jago, 1980; Jago and Hardisty, 1984). Comparison of foreshore and estuarine sands indicates that sands stripped from the foreshore are not simply deposited within the Taf Estuary; the selection of sand for deposition within the estuary occurs offshore in Carmarthen Bay and is probably controlled by both tidal and wave action.

Chapter 2

Sea-level change and barrier formation/development

2.1 Sea-level change

2.1.1 Historical development of sea-level studies

Early observations of land/sea-level change were not exclusively confined to Europe in the late 17th century. For instance, the phenomenon of raised shorelines and changing sea-levels have been investigated by the Chinese for some 2200 years and non-literate societies have noted changing land levels and associated shorelines. As these societies were dependent upon harmony with nature for their survival, they must have been aware of the affect of shoreline changes upon the location of food resources (Devoy, 1987). The implications of continued sea-level rise are no less important today. The anthropogenic input of greenhouse gases such as carbon dioxide, methane, nitrous oxide and chloroflurocarbons, are expected to cause a substantial global warming, which may result in the global mean sea-level rising due to the thermal expansion of the oceans and the melting of terrestrial ice. Accurate prediction of future sea-level change is paramount in developing coastal management strategies to predict changes in low lying regions which may be inundated by a small rise in eustatic sea-level.

However, to predict future sea-level variations one must first be able to understand past sea-level changes and estimate future variations in climate, which would ultimately control future sea-level changes. Furthermore, the nature of the rise in sea-level during the Holocene is of significant importance since this controls sedimentation and therefore influences the manner in which coastal environments such as estuaries and barrier complexes evolve.

During the last thirty years or so there has been an increase in the number of detailed studies investigating sea-level change during the Holocene, and with these a number of different schools of thought have emerged, resulting in often fierce debates.

2.1.2 The sea-level debate and approaches to sea-level studies

In western scientific literature the fundamental concepts of sea-level studies covering glacio-eustasy and glacio-isostasy were developed in the nineteenth century. McLaren is regarded widely as a founder of ideas regarding the exchange of water masses between the land and ocean, through the build up and decay of ice sheets, indicating that this is the controlling factor in sea-level fall and rise. In 1842, McLaren, noting the publication Agassiz's new and controversial book on the glacial theory two years earlier, wrote "if we suppose the region from the 35 parallel to the North Pole to be invested with a coat of ice thick enough to reach the summit of Jura... it is evident that the abstraction of such a quantity of water from the ocean would immediately affect its depth".

In 1888 Suess introduced the term eustasy; however, he interpreted the origin of eustatic changes in the formation of ocean basins and in the infill of sediments and referred to them as tectono-eustasy and sediment-eustasy respectively, rather than glacio-eustasy (Mörner, 1987). By the end of the 19th century the main models for explaining absolute sea-level changes included glacial-eustasy, tectono-eustasy and the mass attraction of water masses. Not until the work carried out by Daly in 1910 and 1925, on the glacial control on coral reef development, did the glacio-eustatic concept gain wider acknowledgement (Mörner, 1987).

In 1934 Daly published a book entitled *'The Changing World of the Ice Ages'*, in which he stated that surficial redistribution of both ice and water loads involved immediate crustal elastic responses, as well as deep seated plastic deformation and mass transfer. His work formalised many of the concepts of earth rheology, ice marginal crustal forebulge, geoidal changes and ice-water surface gravitational attraction, that have become influential in sea-level/shoreline thinking since 1970 (Devoy, 1987).

The advent of the radiocarbon method, of age determination, by Libby in the early 1950s facilitated greater detail in the study of Late Quaternary sea-levels (post 20,000 BP). The application of such techniques led to an intensified search for the Holy Grail, the identification of a single universally valid sea-level curve, a eustatic curve (Devoy, 1987). Attention focused on establishing the form and pattern of Holocene eustatic sea-level recovery. During the late 1950s and early 1960s a number of significant papers were published, highlighting both the

worldwide interest in the phenomenon of sea-level change and the assumption that since the oceans are interconnected, the change in ocean-level would follow a universal pattern (Kidson, 1986).

Three contrasting schools of thought emerged during the search for a single global eustatic sea-level curve for the Holocene period. The first group supported an oscillatory pattern of global sea-level recovery, showing sea-level rising rapidly to a high point above present levels during the expected thermal maximum, the Hypsithermal, reaching some +3 meters above the present-sea-level (PSL) by 5000 BP (Fairbridge, 1961). Fairbridge argued that the post-glacial rise of the sea was spasmodic and included regressive as well as transgressive phases. He further suggested that since approximately 5000 years BP sea-level has experienced a number of stands at heights up to 3.7 meters above PSL, and that sea-level has therefore oscillated in the later Holocene with an amplitude of 6 meters around its present position (Kidson, 1986; Devoy, 1987). This concept of higher than present sea-level grew from Daly`s work in the 1920's and 1930`s, where coral terraces in the Indian and Pacific, interpreted as Mid-Holocene in age, are apparently elevated some six meters above PSL. Daly postulated that these terraces formed during the Hypsithermal, where through increased ice melt and thermal expansion of the ocean water, global sea-levels were higher, and the subsequent fall in sea-level occurred as a result of cooling (Devoy, 1987).

The second group favoured the concept of a standing sea-level after 3600 BP, with the global sea-level shown as rising to its present position between 5000 and 3600 years BP (McFarlan, 1961; Coleman and Smith, 1964). Data in support of this view came predominately from the Gulf coast of the USA which has been subject to long-term subsidence during the Holocene.

The third group found no evidence of past sea-levels rising above present levels. Shepard (1963) indicated that there was general agreement on the nature of sea-level change in the late glacial, but that in the later post-glacial this agreement broke down. Shepard argued that in this later period the rise in sea-level was a continuous one, at a rate diminishing in time but going onto the present day. However, he did not entirely rule out the possibility of a slightly higher than present late Holocene level, but considered it to be unproven and drew attention to the fact that all Fairbridge`s evidence for such higher levels came from Australia, in his own words *an enigma* (Kidson, 1986). Initial data supporting a smooth exponential decay curve came predominately from low lying, long term depositional coastlines, based largely on biostratigraphic data.

There followed a sequence of papers from around the world which showed a broad division into either the Fairbridge or Shepard schools of thought, and the resulting curves are summarised by Kidson (1986), and can be seen in figure 2.1. The large number of time depth diagrams or sea-level curves were constructed during the 1970s reflect the wide differences in approach to sea-level studies.

This period of growth and debate in studying sea-level surface movements culminated in the International Geological Correlation Programme (IGCP) Project 61, Sea-level movements during the Last Deglacial Hemicycle (15,000 years), which ran from 1974 to 1982. Project 61 initially set about producing an Atlas of Sea-level Curves (Bloom, 1977); attempts to compare curves from different parts of the world emphasised their differences, rather than their similarities which might have been expected from a world wide eustatic event (Kidson, 1986). This served to underline the growing awareness of many researchers during the project that sea-level variations are modified by many local, regional and global factors (Mörner, 1987). Furthermore, spatially uniform changes in sea-level, as characterised by a single global eustatic curve, represent an unrealistic response of the earths crust to water-mass transfers, and no point on the earth surface can be regarded as having provided a stable datum for recording eustatic sea-level (Devoy, 1987).

Bloom (1977) gave a critical assessment of five published eastern US submergence curves and, in proposing the use of sea-level records to test the theory of isostasy, emphasized the significance of mass transfer between oceans and glaciated regions during the glacial-interglacial cycles. Bloom (1977) found that "the postglacial submergence histories of five eastern United States coastal sites support the hypothesis that the load of water added to the continental margins by post-glacial rise of sea-level has been sufficient to isostatically deform coastal areas in proportion to the average depth of water in the vicinity. It is therefore reasonable to hypothesize that the entire ocean floor could deform in response to changes of sea-level of the magnitude of the glacial-interglacial cycle".

Clark *et al.* (1978) proposed a number of numerical models based on a spherical viscoelastic earth with varying layered structures, and on different assumptions regarding the rate of northern hemisphere ice melt. These models indicated that the relationship between eustatic change and isostatic adjustment is far more complex than generally assumed. They also confirmed the

PAGE/PAGES
EXCLUDED
UNDER
INSTRUCTION
FROM
UNIVERSITY

demise of the concept of a world wide eustatic response, and underlined the belief that no part of the earth's crust can be considered as being stable.

Tooley (1987) suggests that the lack of concurrence in data results partly from the failure to employ a unified methodology and an homogenous data base, making correlation of events at best elusive, and at worst erroneous and misleading. This lack of agreement is not solely due to methodology, and fundamental problems remain with understanding the nature of the sea-level itself (Devoy, 1987).

Opinions regarding the nature of sea-level change during the Holocene deglacial have proliferated with studies generating greater volumes of reliable data which can be used to support each of the schools of thought. The debate between the smooth or oscillatory patterns of sea-level recovery is today less pronounced due the recognition of various local factors that are only really of local significance.

The aims of IGCP Project 200, which marked the end of Project 61, were to identify and quantify the process of sea level change by producing detailed local histories that can be analysed and correlated for tectonic, climatic, tidal and oceanographic fluctuations. The ultimate purpose was to provide a basis for predicting near future changes in sea-level, for applications to a variety of coastal problems, with particular reference to densely populated low lying coastal areas (Shennan, 1989a). To achieve these aims three main lines of approach were adopted. First, the collection, analysis and correlation of new and existing sea-level data, both from areas deficient in data and from key areas, to provide diagnostic evidence, for the evaluation of assumptions underlying any models developed. Second, to acquire data from coastal and shelf deposits to provide valuable information on resource exploitation, coastal land use planning, subsidence, reclamation, aquaculture and ecological studies. Third, to analyse tide-gauge records and model other short term sea-level fluctuations, such as changes in tidal range, storm surges and tsunami, using computer simulation techniques controlled by reliable and accurate sea-level data (Shennan, 1989a).

Over the last thirty or so years the attitudes towards sea-level change, methodology and approaches employed in such studies have changed, reflecting intensive strategic research. The progression of IGCP Project 61 saw the abolition of the global sea-level curve, recognising that

PAGE/PAGES
EXCLUDED
UNDER
INSTRUCTION
FROM
UNIVERSITY

local factors play an important role in altering the recorded nature of sea-level change, producing relative sea-level as opposed to absolute responses. Regional variations in response to deglaciation due to variable factors such as glacio-isostasy, hydro-isostasy, glacio-eustasy, geoidal-eustasy result in recent sea-level studies concentrating on the generation of detailed local histories which can be correlated with other local studies to asses and infer regional sea-level changes.

2.1.2 Sea-level methodology and inaccuracy

In the correlation of sea-level data from numerous detailed sea-level studies it would be desirable to have a generally accepted methodology of applied sea-level work in order to generate a rigorously tested and refined sea-level data base, upon which subsequent analysis can be based (Tooley, 1992). Tooley suggests that three criteria should be used to select sea-level index points used in the construction of age-altitude graphs.

First, index points should come from a small homogenous area, so that the effects of tidal inequalities, earth movements and variations in the geoid configuration are minimised. Second, sea-level index points should come from similar palaeoenvironments and have the same indicative meaning i.e. each index point should be obtained from material, deposited *in situ* over a very narrow vertical range, which can be related to palaeo-water depth. For instance, in temperate coastal lowlands samples of monocotyledonous turfa or limus with pollen or seeds of salt marsh taxa and epiphytic diatoms of marine or brackish water preference provide ideal material for sea-level index points (Tooley, 1992). Second, sea-level variates should be assigned an altitudinal error band which includes, for instance, levelling errors and errors due to consolidation. Third, radiocarbon dates should be capable of independent corroboration, achieved where standard regional pollen diagrams are available. All samples should be dated at the same laboratory, several dates should be obtained from the same core, and all radiocarbon dates should be displayed with two standard deviations.

In figure 2.2 taken from Shennan (1983), one can see three possible routes to take in the analysis of past sea-levels. Route 1, *local sea-level analysis* is the simplest option, which is no more than the development of a local sea-level curve or chronology and an estimate of data collection and

interpretation errors. This route may represent how existing sea-level studies may be developed if relevant information is available for each sea-level index point. Shennan *et al.*(1983) have shown that when the tendency of each sea-level index point can be evaluated, a chronology of periods of positive and negative tendencies in sea-level can be developed for each area. Route 2 proposed by Shennan (1983) allows the analysis of regional sea-level tendency, identifying data which may disagree with proposed models of regional sea-level change. Route 3, *analysis of crustal movements* is designed to estimate isostactic rates for the whole region and isolate the eustatic component within relative sea-level rise.

Shennan *et al.* (1983) suggest that the use of the terms transgression and regression have been a major cause of misinterpretation in the correlation of sea-level index points used to produce a global eustatic sea-level curve, as attempted by IGCP Project 61. Shennan (1983) explains that the terms *transgressive overlap* and *regressive overlap* should be used as lithostratigraphic descriptive terms in which no process, such as sea-level rise or fall, is implied. These terms would only describe a change in sediment type and should not be used in interpreting the cause of such changes (Van der Plassche, 1986). The processes involved in the development of coastal stratigraphic sequences are dependent on the position and rate of sea-level change, and these sequences contain evidence of tendencies in sea-level. Shennan defines a positive and negative tendency in sea-level movement as an apparent increase or decrease of marine influence.

Shennan *et al.* (1983) concluded that tendencies in sea-level and their application permit meaningful correlations between rising and subsiding areas, and introduce objectivity in correlation schemes showing transgressive sequences. Positive and negative tendencies of sea-level movement can be established, and although the sea-level index points are site specific, indicators from many sites within an area show a general tendency of sea-level movement, and this is the basis for wider geographical correlations (Tooley, 1992). Whether a positive or negative tendency in sea-level movement can be shown to actually indicate a rise or fall in sea level is a further step in the analytical process (Van der Plassche, 1986).

As previously indicated it is quite clear from the literature that smooth and spasmodic schools of thought (Fairbridge, 1961; Shepard, 1963) still remain; however, researchers now agree that the limitations of present techniques and the possibility of in-built errors mean that the construction of sea-level curves, whether smooth or irregular, has been attempted in the past with too much

confidence (Kidson, 1986). The standard methodologies has facilitated the generation of a sea-level data base which contain some 915 dated sea-level index points from sites around the UK (Shennan, 1987, 1989b). This data base has enabled researchers to construct regional sea-level curves and evaluate Holocene crustal movements within the UK (Shennan, 1989b).

However, sea-level researches have realised that lines joining sea-level index points gives a false sense of accuracy (Kidson, 1982; Heyworth and Kidson, 1982; Kidson, 1986). Error terms built into many sea-level curves have been inadequate, and many sea-level indicators used in the construction of such curves have only a crude, tenuous relationship to sea-level. Heyworth and Kidson (1982) have argued that the wide range of potential sources of error and the possible cumulative significance of these would reduce the value of a good deal of published data. Kidson (1986) suggested that even before attempts are made to derive eustatic changes from a relative sea-level curve, by correcting for isostatic and tectonic deformation, a wide range of other potential errors must be accounted for. Such errors may arise from the choice of datum, altitude of sample correction points, age determinations and so on, all of which vary and may be critically important.

Careful levelling of a sample point at or near to the surface, from a bench mark on solid rock, should introduce an error of no more than ± 1 cm (Heyworth and Kidson, 1982). However, many coastal sites are a considerable distance from such bench marks, and bench marks resting on substantial thicknesses of estuarine clays are not always at their original height, due to the varying affects of compaction and consolidation. Greater errors are generated in deep bore-holes, where errors introduced by drilling, sampling and measuring procedures make it difficult to ascertain the exact depth from which a sample has come. In general offshore boreholes have the greatest source of levelling error and, since many of the oldest sea-level dates come from such sites, this may explain the large discrepancies in altitudes of some of these samples (Heyworth and Kidson, 1982).

As Holocene sea-level studies require an accuracy of a few decimeters it is essential to begin with precision in the Datum to which sea-level data is related. Although this is particularly important when, for instance, sea-level data within a region is to be compared, many authors ignore the problem simply referring to present sea-level (Kidson, 1986). Kidson further highlights the fact

that most researchers do not determine the local sea-level, however defined, but refer their height to the national Geodetic Datum.

The Geodetic Datum must not be confused with local mean sea-level, since the first is obtained by holding sea-level fixed, as observed at a number of tide stations, whereas the second is made at the local tide station. Often before a sea-level study begins an error of unknown dimensions may be introduced by the choice of datum used to define the present sea-level (Kidson, 1986). Fairbridge (1961) used Mean-Low-Water-Spring-Tides (MLWST) as his datum; however, other authors have adopted different sea-levels, such as Mean-Sea-Level. Prior to the comparison of sea-level data from different sites/areas one must first reconcile discrepancies between the datums used (Kidson, 1986).

Where tidal ranges are significant, the vertical spread over which marine processes operate becomes very wide and the potential errors may multiply, where in extreme situations the vertical spread may be several orders of magnitude greater than postulated sea-level changes over time spans of millennia. For instance, the Bristol Channel has a predicted spring tidal range of some 14 meters, and when wave heights of 7 metres are superimposed on such a variation, together with heights of high water being regularly exceeded by some 2 metres, then dependent on its definition sea-level could fall anywhere within a 23 metre band.

Many studies of sea-level change are conducted in estuaries and embayments where frictional forces generated by shallowing and narrowing arms of the sea result in the enhancement of tidal prism causing the height of high water above geodetic mean to increase. Kidson (1986) suggests that the height of HWST (High-Water-Spring-Tides) above ordnance datum in the Bristol Channel increases by some 3 metres from the mouth of the Channel to the head of the estuary (Kidson, 1986).

When comparing the altitude of samples from different sites correction has to be made for differences in tidal range, usually done using published figures in tide tables. For sites some distance from a Tide Table port, considerable errors can be introduced using figures of HWST for that port, and in estuaries with large tidal gradients the problem is particularly serious. Heyworth and Kidson (1982) suggested that this source of error can be largely eliminated by levelling the height of MHWST (Mean-High-Water-Spring-Tides) at the site when weather and

wave conditions are such that predicted MHWST is reached at the Tide Table port. The occurrence of tidal bores in estuaries, which in the past may have been responsible for wide spread flooding at levels greater than expected, may further complicate the construction of sea-level curves.

As previously suggested, the tidal range in a particular area may have experienced significant changes during the last deglaciation (Austin, 1991), and although these variations have reduced in scale they probably continued throughout the Holocene. Whilst tidal range may have changed at some sites, while remaining unaltered at others, considerable changes may have occurred in the pattern of variation at any one locality. In such circumstances the possible sources of error are large, and the comparison of two or more sea-level curves by simply allowing for present differences in MHWST levels is inadequate to account for such sources of error (Heyworth and Kidson, 1982).

Rare events, where tides inundate areas normally free of salt water introducing further uncertainties in the reconstruction of past sea-levels. The effects of high tidal or storm levels tend to remain in the sedimentary record until eliminated by even higher ones. Although it is unlikely that permanent changes would be produced, there is little doubt that the impression left could be of an apparent sea-level which would be higher than the actual sea-level at that time. This source of error would only operate in one direction, the true sea-level would always be lower than indicated by index points (Heyworth and Kidson, 1982). The difficulty of separating the effects of rare events from normal sea-levels introduces a source of error, which is ill-defined but may be considerable.

Tidal problems are therefore so complex that not to take them into account can only lead to inaccuracies in palaeoenvironmental reconstruction, but since many cannot be assessed it suggests that real precision is probably unattainable in such reconstructions. One facet of the problem which has not so far received significant attention is the change in tidal regimes/climates through time. As palaeo-tidal models generally omit subtle changes in bathymetry and coastal configuration their application in sea-level studies is to some extent limited.

In a review of the diagnostic criteria reflecting the waxing and waning bidirectional tidal flow, in tidal deposits and sub inter- and supra-tidal sub-environments, Terwindt (1988) suggested that

shifts in the position of major tidal channels and intertidal drainage channels produce local micro-transgressive and regressive sequences, superimposed on the general trends. Terwindt (1988) concluded that although it is possible to infer a tidal origin for a particular sediment complex, establishing convincing distinctions between sub- and inter-tidal environments remains difficult. Furthermore, it is even more difficult to determine the position of the low-water zone in the section, therefore making the assessment of the palaeo-tidal range extremely difficult. From his review of the literature, Terwindt indicated that the number of spatial reconstructions of palaeo-tidal basins are limited, and that careful investigations of the lower inter-tidal and upper sub-tidal environments are a clue to better palaeo-tidal reconstructions.

The use of ambiguous indicators of former sea-levels can lead to artificial multiplication of oscillations on already published sea-level curves (Kidson, 1986). Erosional features such as shore platforms can rarely be used by themselves as precise indicators of past sea-levels. Even marine deposits covering a wide range, from the seaward margin of the near shore sand wedge to the crests of storm beaches, must be interpreted with care. Kidson (1986) suggested that the only wholly reliable indicators of former sea-levels are organic remains in growth positions, where their relationship to sea-level or the water table can be determined within acceptable limits.

Heyworth and Kidson (1982) have suggested that the interface between saline and fresh water representing the lower limit of freshwater conditions, occurs at present between MHWST and HAT (Highest-Altitudinal-Tide), and horizons (peats) representing this interface give the best starting point for determining past sea-levels. They conclude that this could be done to an accuracy varying from ±15 to ±35 cm depending on tidal range i.e small and large tidal ranges respectively. However, their estimates apply to present day sites and no allowance has been made for the possibility of local change, such as the formation or destruction of coastal barriers, which would increase uncertainties and errors associated with particular sea-level indicators.

It is now widely recognised that even where biogenic material giving precise relationships to sea-levels is not available, then more ambiguous evidence such as erosional contacts/features must be used but only with full recognition of its limitations. The present trend is therefore to use only those indicators expressly related to sea-level, and where not possible more equivocal evidence is treated with much more caution than has sometimes been assigned in the past (Kidson, 1986). Much attention has been given in the literature to errors associated with Radiocarbon Dating;

many authors still appear to believe that the age of a sample probably lies within one standard deviation given by the laboratory. Although the limitations associated with this method are covered elsewhere, it must be stated that the precision attributed to radiocarbon ages in some particularly earlier sea-level studies, is not justified, and relatively recent sea-level studies have adopted two standard deviations as the error term used to plot sea-level radiocarbon dates on age/altitude graphs (Kidson, 1982; Heyworth and Kidson, 1982; Kidson, 1986). Most radiocarbon samples used in sea-level studies are from buried peats, which have been waterlogged in an anaerobic environment since they were formed. Contamination by recent carbon is less likely than for other materials, but penetration by younger roots and other stratigraphical disturbances are well known sources of error. Many other sources of error may falsify the resulting age determination, but in most cases there is no way to detect their individual influence (Heyworth and Kidson, 1982).

When radiocarbon dates are being used to construct a sea-level curve, it matters little whether the wide spread of results for a single sample are due to differences in the original radiocarbon content or to difficulties in measurement. The main consequence of this, as previously stated (Kidson, 1982; Heyworth and Kidson, 1982; Kidson, 1986), is that one standard deviation is not great enough an allowance to account for the majority of errors associated with the age determination of a particular sea-level index point using the radiocarbon technique.

Consolidation of clays is much less than that of peats, but in a normal estuarine stratigraphy where thin peats occur within thick clay layers, consolidation is roughly equal between the two (Heyworth and Kidson, 1982). Mixed successions of strata with a wide range of physical attributes are more frequent in coastal marine areas, and their variability ensure that a high degree of accuracy in assessing the effects of compaction and consolidation is unlikely to be obtained (Greensmith and Tucker, 1986). The greatest effect of compaction/consolidation on the altitude of a peat layer occurs where the underlying and overlying clays are approximately equal, and in the view of uncertainties in correction calculations it is often more desirable to sample from areas not significantly affected by consolidation. If no other samples are available then the correction for compaction and consolidation must be made and since it is often clear that samples must have originally been higher, then only the magnitude of the correction is in doubt. Due to their unpredictability, compaction and consolidation have largely been ignored by the Holocene sea-level worker; however researchers must try to assess and quantify compaction and consolidation

using all the available evidence from geological, geotechnical, geomorphological, biological and archaeological fields (Greensmith and Tucker, 1986). Problems attendant on compaction and consolidation cannot be divorced from tectonic effects. For instance, the subsidence due to tectonic down warping is an additive to that caused by the compaction and consolidation of sedimentary sequences.

2.1.3 Sea-level change and crustal movements during the Holocene in Southwest England and Wales

Most of the problems associated with recent palaeoenvironmental reconstructions are encountered, some in extreme form, along the southwestern coasts of Britain. Heyworth and Kidson (1982) in a compilation of available sea-level radiocarbon dates for Wales, SW England and the Channel Islands suggest that the reconstruction of eustatic changes along this coast is complicated by its location. The region is located on one of the widest continental shelves in the world, has a complex pattern of amphidromes and is in one of the world's great westerly storm belts.

Sea-level may be thought of as the interface between saline and fresh water, as indicated by living organisms, rather than some abstract term such as mean-sea-level, and such an interface is considerably higher and more variable from place to place than mean-sea-level (Kidson and Heyworth, 1979). The crenulate nature of the southwest coast of Britain results in significant differences in exposure and fetch, so that different portions of the coast experience different wave energies/climates. The tidal variations are often more variable than the wave energy, since the forecast height of MHWST (astronomical component without meterological forcing) ranges from some 1.17 to 6.70 meters above Ordnance Datum, with mean spring tidal variations range between 1.9 and 12.3 meters at Portland and Bristol respectively (Heyworth and Kidson, 1982). Therefore as already discussed, prior to the interpretation of former sea-levels, large variations in wave climate and tidal range need to be assessed, otherwise additional errors are introduced. Heyworth and Kidson (1982) indicated that sea-level studies have not allowed for changes in tidal regimes as coastal configuration and ocean water depth have changed in response to the Holocene transgression. The exclusion of palaeo-tidal variations, in the reconstructing of former sea-levels, was due to the lack of an adequate technique to assess such changes (Heyworth and Kidson,

1982; Greensmith and Tucker, 1988). Although Heyworth and Kidson (1982) suggested that for much of the coast the consequence of such changes are relatively minor, they indicate that for the coast for the English Channel and the Bristol Channel, there must have been significant differences in the tidal regimes at the start and end of the Holocene transgression.

Austin (1991) argued that tides on the N.W. European continental shelf must have undergone considerable changes during the Holocene, in response to rising sea-levels and associated coastline movement. Sea-level researchers commonly use indicators related to past tidal levels (Greensmith and Tucker, 1988; Austin, 1991), and accurate estimates of palaeo-tidal variations are needed if the tectonic component of change is to be isolated. Austin (1991) used a numerical model of the M2 tide on the NW European continental shelf to estimate the effect of uniform depth changes (of the order of the Holocene eustatic variation), on tidal elevation amplitudes (amphidromes), sand transport paths and the position of tide generated fronts. Austin concluded that shifts in the position and strength of amphidromes are shown to cause strong spatial gradients in the rate of change of tidal amplitudes in the Irish Sea and English Channel. However, Austin calculated that the tidal contribution to absolute changes in mean high water levels, is everywhere less than 5% of the eustatic contribution, and also states that a more realistic description of bathymetric variation is required to further develop this modelling approach, thus limiting its present application to palaeo-tidal modelling.

In investigating the low sea-level origin of Celtic Sea sand ridges, Belderson *et al.* (1986) using a numerical model of M2 tidal steams, found that the tidal currents at the time of the lowered sea level were approximately twice the strength of present day levels. The major axes of the great majority of the tidal ellipses were rotated in a clock-wise sense with respect to those of the present day. The actual age of the sand banks is likely to be Late Devensian/early Holocene (Bouysse *et al.*, 1976; Pantin and Evans, 1984), corresponding to the early stages of sea-level rise where sea-level was estimated as -110 to -120 meters (Bouysse *et al.*, 1976) and -135 metres (Pantin and Evans, 1984) below present.

Holocene and late Devensian sea-level and crustal movements in England and Wales have been studied generally by small groups or individual workers specialising in relatively short sections of coastline (Shennan, 1983). Numerous researchers have shown that no part of the earth's surface can be regarded as geologically stable over time scales of a few thousand years or more

(Clarke *et al.*, 1978; Walcott, 1980; Flemming, 1982). Platetectonics has provided an explanatory mechanism for long-term tectonic and isostatic movements of continental margins, while the glacio-isostatic and hydro-isostatic theories have been combined to show that all coastal parts of the earth are subject to a greater or lesser degree of isostatic reaction to the glacial-deglacial cycle (Flemming, 1982).

The British Isles are in a zone of glacial isostatic readjustment caused by the removal of the Scottish and Scandinavian ice sheets. In assessing the geological factors causing vertical movements, one could in principle derive a correction so as to arrive at the most probable absolute sea-level curve for the area. Flemming suggests that such an analysis would produce a different curve for each area due to both inevitable approximations made locally, and unquantified regional responses to hydro-isostasy, glacio-isostasy and so on. Flemming (1982) used a partial data set of the total data available in 1978, consisting of some 143 data points, in a numerical analysis of crustal movements. Although the results provide a model for deformation of the British Isles, Flemming (1982) stresses that the results must be regarded as provisional and that they are intended to demonstrate the potential of a method, rather than to prove a particular result.

The method is based on the assumption that the observed present distribution of sea-level indicators of various ages is the summed effect of a eustatic sea-level change which is coherent through time, but independent of geographical location and local geological vertical displacement which has taken place at a constant rate at each locality, with that constant varying from place to place (Flemming, 1982):

$$Z = f(T) + g(x,y) \times T \qquad 2.1$$

Z is the relative vertical displacement, T is the age in 10^3 years, x and y are geographical co-ordinates, f and g are unknown polynomial functions.

Walcott (1980) notes that the rheology of the lithosphere and the mantle of the earth is such that the stresses involved in post-glacial rebound are near the boundary between linear and non-linear behaviour. At low values of stress rates of strain should be linear, whereas at high values rates of strain are proportional to the cube of the stress. For the purpose of his model, Flemming

(1982) assumes that the vertical displacement during the period 9000 years BP to present was small in relation to the total displacement between the maximum glacial depression and the final deglacial isostatic equilibrium. On the basis of this assumption, Flemming proposes that it is reasonable to assume that the stress is constant, and that the stress strain relationship is linear. It is difficult to model the period of ice melting, and Flemming overcame this by assuming an equilibrium state of isostasy at the maximum glaciation, followed by a disequilibrium as the ice thinned. If ice melted at such a rate that isostatic forces increase, then the imbalance of isostatic forces would simultaneously increase causing the crust to accelerate vertically. Flemming made no attempt to model this first stage of isostatic rebound since his data referred to the past 9000 years, and all ice is presumed to have melted in Scotland by 10,000 BP.

Even so, rapid wasting of terrestrial ice sheets during the Late Devensian (Hughes, 1987) may have caused accelerations in isostatic response to deglaciation, and surely these would still influence crustal movements during the period Flemming describes. Flemming (1982) therefore introduced a simple polynomial or exponential expression based on the assumption that the direction of isostatic recovery has been constant at each location, but has varied between sites. He explicitly did not refine the analysis to account for regional or oceanographic factors which may have influenced the analysis, but his summary of crustal movement is well known, showing a range from + 2.5 mm/yr over the highlands of west Scotland to - 0.5 mm/yr over the extreme south west of England.

During the IGCP Project 61 the international data bank of radiocarbon dated sea-level index points was established and the UK working group started to collect the relevant information. Whilst undertaking a compilation of the radiocarbon data bank for the UK, Shennan (1987, 1989b) experimented with an alternative approach to differential crustal movements, using published sea-level curves. Although such an approach may have a number of advantages over using individual sea-level points, curves include limitations such as interpretational differences made by the original authors.

By the end of Project 200, some 915 radiocarbon dates were held; however, due to the problems of acquiring all the relevant information Shennan (1989b) restricted his analysis to dates on peats. Various conditional filters, such as contamination, eroded contact, stratigraphic context, and age context were applied to the remaining peat dates, leaving 429, which Shennan believed to be

related to past sea-levels. In noticing that the relevant tidal information was being submitted in different ways Shennan, in order to standardise the procedure, produced a separate data base containing 14 tidal variables for some 400 coastal locations obtained from Admiralty Tide Tables.

The approach Shennan (1989b) adopted to calculate Holocene crustal movements in Great Britain required a eustatic correction to be applied to each radiocarbon date used. Flemming (1982) calculated the eustatic factor, which was in fact a geographically independent factor combining a eustatic sea-level factor and a linear factor assumed to be of tectonic origin. Shennan (1989b) used the regional eustatic curve proposed by Mörner (1984), and subtracted this from a relative sea-level value to give an estimate of uplift/subsidence. This value includes glacio-isostatic, hydro-isostatic and tectonic components, as well as local-scale factors, such as sediment compaction and oceanographic/hydrological effects, including palaeo-tidal changes (Shennan, 1989b). For each area with an adequate number of reliable sea-level index points Shennan attempted to identify and quantify, where possible, the general form of crustal movements and the magnitude and pattern of residuals.

Heyworth and Kidson (1982) compared three sea-level curves from detailed studies in Cardigan Bay, Bridgwater Bay and the Bay of Mont Saint-Michel (Figure 2.3). They found that the curves from the first two sites are almost identical, suggesting that over the last 8000 years the rate and timing of sea-level rise is comparable between Mid-Wales and SW England.

In reconstructing eustatic changes in sea-level, Heyworth and Kidson used three main sites, Cardigan Bay (Borth, Ynylas and Clarach), Bridgwater Bay (Salford) and the Somerset Levels since detailed studies had been carried out, and large numbers of radiocarbon dates had been obtained at these sites. They also produced sea-level curves for North Wales and the English Channel but these were not based on large numbers of radiocarbon dates. Dated sea-level index points from Cardigan Bay and Bridgwater Bay were taken from submerged forests, peats and so on; in contrast the radiocarbon dates from the Somerset Levels were obtained from the prehistoric trackways. Although these index points were not directly controlled by changing sea-levels, Heyworth and Kidson (1982) believe that the trackways were built in response to higher water levels (reflected in the surrounding peats), and that since they were constructed of small timber, used almost immediately, the measured radiocarbon dates should represent dates of construction. It may be that the trackway sites in such a position cushioned from the *extreme events* which may

PAGE/PAGES
EXCLUDED
UNDER
INSTRUCTION
FROM
UNIVERSITY

influence coastal sediments, yet controlled by water-table movements, provide the most reliable indication of long-term sea-level change (Heyworth and Kidson, 1982).

Instead of using bars or rectangles, Heyworth and Kidson (1982) represent age and altitude error estimates as either ellipses or circles. Estimates of uncertainty in the sea-level figures are used to construct these error ellipses, an error range of ± two standard deviations being assumed for both axes; the standard deviations used by Heyworth and Kidson for the altitudinal measurements have no statistical basis. For each sea-level index point values of age and altitude were plotted in a way which attempts to show the probability distribution of a particular radiocarbon date representing a particular sea-level (Figure 2.4). The four concentric ellipses given to each date represent the probability distribution of the true point lying within each of the four zones, and therefore a date with small associated uncertainties will appear as a dense circle or ellipse, whereas one with large uncertainties will appear large and faint.

Heyworth and Kidson (1982) used such a method to overcome the problem of imprecise results appearing more important than precise ones, giving a more accurate graphical representation which displays overlapping results. In not displaying uncertainties in the relative altitudes of samples from different sites the sea-level curves from those sites may appear significantly different, when in fact their differences may be only slight. In figure 2.5 Heyworth and Kidson (1982) give a general indication of curves which can be drawn for various parts of the coastline. Radiocarbon dates are plotted relative to the MHWST level, with no correction being made for the uncertainty in the height of the present MHWST level.

Heyworth and Kidson (1982) argued that this diagram does not imply that these curves are significantly different. If MHWOT had been used to bring points to a common datum rather than MHWST, then curves 1 (Bristol Channel) and 3 (Cardigan Bay) would be almost identical. Only curve 5 for North Wales displays a difference which seems to be outside the expected range of error for a single curve, and this curve is plotted for only two dates, so that too much should not be deduced from the divergence (Heyworth and Kidson, 1982). These curves suggest that no sea-level stand higher than present occurred in SW England or Wales during the Holocene, and that any oscillations are smaller than the sum of uncertainties (Heyworth and Kidson, 1982).

PAGE/PAGES
EXCLUDED
UNDER
INSTRUCTION
FROM
UNIVERSITY

In investigating sea-level changes on the coasts of Ireland, Mitchell and Stephens (1979) reported a eustatic transgression up to 3.5 metres above present sea-level some 5000 years BP in Dublin Bay, at the same latitude but on the opposite side of the Irish Sea to Cardigan Bay. These opposing views which can be explained in the context of regional eustasy and changes in the geoid, may also arise from different interpretations of the eustatic component of relative sea-level data or from different compensation of errors (Kidson, 1986).

Inevitably, due to the incompatibility of definitions the simple comparison of sea-level curves cannot be used to accurately reconstruct regional changes in sea-level or crustal movement but they may serve as a working hypothesis (Shennan, 1983). That complex discrepancies in sea-level studies around the Bristol Channel are largely due to the presence of a wide continental shelf and an amphidromically complex situation with the largest tidal range in the UK Furthermore, this coastline consists of numerous narrow valleys, the entrances to which are restricted by shingle spits or barriers. These factors would combine with the problems associated with the drainage of important and variable amounts of freshwater and sediments from drainage basins, to confound the interpretation of Holocene sea-level data, making it extremely difficult to observe any regional effect due to local noise.

Shennan (1983) suggests that whereas there appears a clear subsidence of the Bristol Channel relative to North Wales, movement relative to Cardigan Bay is unclear. All the data for Cardigan Bay indicates a slight subsidence, and a rate of -0.11 ± 0.08 mm/yr may be the best summary of that subsidence, but due to the almost invariant nature of the altitudinal data (errors from an offshore vibro-core) this rate is poorly established (Shennan, 1989b).

The data used by Shennan (1989b) for the Bristol Channel was poorly resolved, coming from a wide range of sites, with different palaeo- environmental conditions, and perhaps most significantly comes from the estuary with the largest tidal range in Great Britain, the Severn Estuary. As already discussed the tidal regime is unlikely to have remained constant during the Holocene transgression (Belderson *et al.*, 1986; Austin, 1991; Scourse and Austin, 1995), contributing to scatter and poor numerical solutions. Shennan (1989b) concluded that the only clear signal is that subsidence is apparent, in the order of -0.24 ± 0.19 mm/yr. Furthermore, it is not possible to specify the cause of subsidence, making it almost impossible to determine to what

PAGE/PAGES
EXCLUDED
UNDER
INSTRUCTION
FROM
UNIVERSITY

extent crustal movements are a manifestation of forebulge collapse, reactivation of tectonic structures or sediment loading and/or hydro-isostasy (Shennan, 1989b).

Shennan (1989b) summarised rates of relative subsidence in Great Britain as a series of isolines, estimating *current rates* of crustal movement (Figure 2.6). For England and Wales Shennan interpolated between a few fixed points, and therefore concludes that these isolines should not be interpreted as precise lines, but used as point estimates which provide a regional pattern of crustal movements.

Whatever the thought about the idea that the position of relative sea-level may have oscillated with height on the scale of hundreds of years, it is clear that in general there is an upward trend in sea-level during the Holocene in Southwest England and Wales (Heyworth and Kidson, 1982; Shennan, 1983; Allen and Rae, 1988; Allen, 1990). Referring elevations to MHWST, Shennan (1983) indicated that the relative sea-level some 2500 years ago was roughly 2.5 metres lower than today. There is no evidence of sea-levels higher than present which supports the hypothesis that sea-level has risen in England and Wales continuously at a decreasing rate up to the present time.

Within the Severn Estuary, Allen and Rae (1988) used levellings across dated sea-banks and the dated history of the salt marsh chemical pollution to construct a generalised sea-level curve for approximately the last 2000 years. The origin of their curve is some 0.5 to 0.6 metres above the local level of MHWST, but is reduced to this level to achieve maximum compatibility with the curve drawn by Shennan (1983) using Heyworth and Kidson's (1982) data from the Bristol Channel (Figure 2.7). Allen and Rae concluded that depending on the extent to which the Severn Estuary is regarded in retreat, that since the first reclamations made during the Roman Period (AD 43-410 in Britain) the spatially averaged rise in relative sea-level has been no less than 1.22 metres and no more than 1.6-1.7 metres.

Allen (1990) concluded that a discrepancy of 0.8-0.9 metres between the start of Allen and Rae's curve and the end of that drawn by Shennan (1983), as displayed in figure 2.7, may be due to different methodologies applied to areas which merely adjoin. However, the two curves serve to define an early phase of rapid rise in relative sea-level, which gave place some 6000 radiocarbon years ago to a more gradual upward trend followed by a further acceleration over the

last few centuries (Allen, 1990). The current rate of rise averaged over the Severn Estuary is a few mm/yr (Allen and Rae, 1988), which is much greater than the rate of eustatic movement in recent decades.

2.1.4 Future direction of sea-level research

The quest to obtain a record of a global eustatic response to the transfer of mass between terrestrial ice-sheets and the oceans has been judged to be too simplistic since such studies omit the effects of regional variations introduced by glacio- and hydro-isostasy. In fact the most recent sea-level studies have concentrated on the construction of local sea-level curves in an attempt to infer a regional response to sea-level change.

Due to the dynamic nature of the earth's crust it seems useless to construct a global eustatic sea-level curve, as different localities have distinct Late Quaternary tectonic histories. Glacio-isostasy, ice loading or unloading results in regional terrestrial depression or rebound which may amount to tens of metres. Hydro-isostasy, or crustal response to the shifting of water loads on continental margins takes place at similar rates to glacio-isostasy, but typically of magnitudes of only a few metres. Finally, long term continental margin subsidence, due to the thermal contraction of adjacent oceanic lithosphere, may also significantly contribute to rising sea-levels. To understand Late Quaternary changes in climate, driven by the dissipation of internal energy and by changes in solar radiation received by the earth, one must first understand changes on a much longer time scale (Boulton, 1992). This concept can also be applied to regional tectonic responses in that although an area may be rebounding in response to the removal of terrestrial ice sheets during the present interglacial that same area may also be subject to a sustained long term subsidence. For instance, the southern coast of England is presently subsiding in response to the removal of ice from the Scottish Highlands (Shennan, 1989b); however, Preece *et al.* (1990), in studying the Pleistocene sea-level and neotectonic history of eastern Solent, southern England, inferred that regional tectonic uplift has been active in the eastern Hampshire Basin at some stage during and or since the middle Pleistocene. Crustal movements, in response to the growth and decay of terrestrial ice masses, may simply be superimposed upon long-term regional tectonic patterns suggesting that in the construction of accurate sea-level curves one should try to assess

the long term tectonic patterns which ultimately effect the altitude of particular sea-level index points.

IGCP Project 274 has been formulated to establish models of coastal processes and Quaternary evolution of the coastline and shelf areas; to examine coastal evolution in critical earth environment zones; to assess the impacts of past and future sea-level change on coastal environments; and to promote education of matters concerning coastal evolution and impacts of sea-level change (Shennan *et al.*, 1992). The United Kingdom Working Group hope to combine present shoreline evolution and sea-level data in the British Isles producing a framework for exploring and predicting coastal changes to examine the sensitivity of coastal response to sea-level change, sediment supply, wave power, basement geometry and basement material, in environments such as gravel beaches, sand beaches, saltmarshes and so on (Shennan *et al*, 1992). It appears therefore that a number of recent research papers presented in response to IGCP Project 274 are concerned with the evolutionary sensitivity of coastal environments to Holocene sea-level rise. Shennan *et al.* (1992) suggests that although Holocene sea-level change is well documented for most parts of the British Isles, the causes for the spatial response of coastal environments to changing sea-levels is poorly understood. They further indicate that sea-level variation may not be the principal agent of coastal differentiation but they suggest that sediment availability is more likely to prescribe patterns of coastal deposition.

Hinton (1992) described a new approach to the study of Holocene sea-level change suggesting that palaeotidal changes are one of the least known factors recorded in local sea-level changes. By integrating numerical tidal models with stratigraphic data recording former tidal heights one can extend the knowledge of tidal alterations with sea-level change, and such knowledge will permit a higher degree of accuracy in the construction of regional and local sea-level variations during the Holocene (Hinton, 1992). Modelling approaches of this kind, such as the study by Austin on the NW European continental shelf, are used to fine tune palaeoenvironmental data (Scourse, 1992); however, due to the resolution permitted by many of the tidal models employed such assessments have not provided detailed information on a local scale. The refined tidal model of the Wash developed by Hinton (1992) may simulate greater research into detailed assessments of tidal variations at any one locality which may subsequently be used to construct more accurate sea-level curves.

The general public are becoming increasingly aware of the effect of global warming on sea-levels and how such a phenomenon may affect their everyday lives. However, predictions of postulated sea-level rises vary considerably confusing the public making them more suspicious such predictions. Informed predictions of future coastal changes, on which strategies for management and engineering may be based (Scourse, 1992), require detailed studies on shoreline response to rising sea-levels. Recent studies (IGCP Project 274) hope to provide such information and seem to concentrate on obtaining more accurate sea-level curves, from which more informative predictions of future coastal response to sea-level changes can be made.

2.2 Barrier formation and evolution

2.2.1 Historical development of theories regarding barrier island genesis

The coastal plain and continental shelf of the west coast of mainland Mexico were investigated as a part of the Scripps Institution of Oceanography's project on the geology and oceanography of the Gulf of California. One of the areas of greatest interest was the area south of Mazatlan, Sinaloa, and the north of San Blas, Nayarit on the mainland side of the Gulf of California (Curray and Moore, 1963).

The coastal plain here consists of a low-lying marsh roughly at sea-level which exists, mainly in depressions, between scores of parallel abandoned beach-dune ridges. This strand plain of abandoned beach ridges averages some 5 km in width, for the 225 km distance from Mazatlan to San Blas, and is uniformly furrowed by the parallel ridges which are typically 30-200 metres apart. The sand body is continuous between the ridges and across the strand plain, being found beneath elongate surface lenses of modern alluvium deposited between the ridges (Curray and Moore, 1963). This continuous sand sheet rests upon the pre-transgressive or Pleistocene flood plain deposits of the coalescing river system. Curray and Moore (1963) suggest that each ridge was formed individually as a shoreline deposit, with the oldest lying furthest from the present shoreline, and that the present shoreline is analogous to each of the ridges at the time of their formation. They postulate that each ridge initially formed as a longshore bar in front of the existing beach and that given a sufficiently high rate of sediment supply and conditions of low wave action the bar can accrete up to the water surface. If this were to occur during a high tide, with the persistence of low wave conditions through several successive tidal cycles, the long-shore bar would in effect become the new shoreface isolating the former beach (Curray and Moore, 1963).

Curray and Moore suggest that this process has apparently repeated itself cyclically since the time sea-level approached its present position. Furthermore, throughout the formation of the strand plain sediment supply and hydrodynamical conditions have remained approximately uniform. After the formation of each successive new beach ridge the process is repeated after a sufficient supply of sediment was introduced into the area either by long-shore transport or by the

PAGE/PAGES
EXCLUDED
UNDER
INSTRUCTION
FROM
UNIVERSITY

reworking of relict sediments offshore. Curray and Moore proposed that barrier islands originate from bars, built to sea-level by the rapid supply of sediment during periods of low wave intensity isolating the former beach surface, creating a lagoon which is subsequently infilled by both sand and alluvium. However, at the time of their study there was only one available ^{14}C date, and in recognising this, Curray and Moore indicated that both the rate at which the strand plain formed and the position of the late Holocene sea-level could not be accurately assessed.

Price (1963) suggested that small barriers form a short distance from the shore during periods of high water associated with storm setup. A bar develops in front of the beach and builds vertically almost to the height of the temporarily raised sea-level and with a subsequent fall in sea-level remains as a low barrier.

Hoyt (1967) suggested that several difficulties arise in applying the theory of barrier formation from the building of offshore bars. First, although offshore bars may develop under certain wave conditions, their vertical progression is arrested as the water level is approached due to the washing of waves over the top of the bar. Second, if barriers develop directly from bars then evidence of this process should be observable somewhere. Hoyt (1967) indicated that the lack of examples at various stages of barrier development suggests that barriers do not in fact form from the build up of offshore bars. Furthermore, he highlighted the absence of beach and shallow neritic deposits landward of barriers arguing that if barriers did form from offshore bars then open-ocean conditions should have prevailed landward of that bar during the early stages of barrier formation.

Hoyt (1967) examined the contact between Holocene salt-marsh deposits and Pleistocene sediments at many locations along the Georgia coast and found no beach deposits landward of the saltmarsh (Figure 2.8). He supported this evidence by reappraising numerous other studies, all of which indicated the absence of beach and shallow neritic deposits landward of barrier islands, but was careful to point out that although there may be minor exceptions most major barrier features formed by some other mechanism.

Gilbert (1885) suggested that barriers form by the accretion of sediments transported along the shore by littoral and longshore currents. Although this theory was dismissed at the time there can be little doubt that barrier islands form by the breaching of spits during storms (Figure 2.9).

PAGE/PAGES
EXCLUDED
UNDER
INSTRUCTION
FROM
UNIVERSITY

However, Hoyt (1967) suggests that this mechanism does not adequately account for major barrier systems and is probably limited to small sections of the coast.

Swift (1975) suggests that barriers developed at a low sea-level stand, and have transgressed the continental shelf during the Holocene transgression, but this does not solve the problem of formation. Hoyt (1967) presented a hypothesis which considered the rapid submergence which began some 18,000 years BP, the absence of a world-wide sea-levels higher than present during the Holocene, the slow submergence during the past 3,000-4,000 years (Shepard, 1963), the absence of marine deposits and faunas landward of barriers, and the ability of barriers to reform after being destroyed by an emergence.

Along some shorelines aeolian deposits build dunes over 100 feet high and waves can form beach ridges some 20 feet above high water level. Hoyt (1967) suggested that the combination of both wind and wave action may produce a topographic ridge along the upper edge of the shoreline. Suppose that during their formation there was a relative rise in sea-level, then the area landward of the ridge would flood to form a lagoon and the topographic ridge would become a barrier to marine influence (Figure 2.10). The actual width of the barrier would depend upon the amount of progradation prior to submergence which is dependent on the rate of sediment supply and hydrodynamics (Hoyt, 1967). Once formed, barriers can be maintained as long as there is a balance between the sediment supply, the rate of submergence, and the local hydrodynamic factors (Figure 2.11). Although submergence may result in the landward retreat of the shoreline, too fast or too slow a submergence rate may be detrimental to continued barrier development (Hoyt, 1967). Submergence is the pillar stone in the theory proposed by Hoyt and such a rise in relative sea-level has occurred during the Holocene epoch by the transfer of water from continental glaciers to the oceans.

Pierce (1969) examined the physiographic changes, along the North Carolina coast, where he found that the barrier system has accreted sediment at an annual rate of some 796,000 m^3. He postulated that the continental shelf acts as a reservoir of sediment which is at present contributing to the accretion of the nearshore zone. This would suggest that if sufficient sediment is not supplied by longshore/littoral processes, a barrier system may be maintained by relict sediments.

Otvos (1970a) stated that barrier formation by beach-ridge engulfment would probably occur when a stable shoreline with well developed ridges is engulfed by a relatively sudden marine transgression which ultimately does not erode or displace the ridges landward. This would be followed by a slower sea-level rise during which the islands maintain their upward growth. Otvos (1970a) argued that although such a transgression may have existed at the onset of the Holocene, in the Gulf of Mexico, most of the barriers started to form some 5,000 to 3,500 years BP when the transgression had slowed or stopped altogether.

The failure to recognise beach and shallow marine sediments landward of the barrier islands, as highlighted by Hoyt (1967), can be attributed to several factors other than barrier formation through the engulfment of beach ridges. Otvos (1970a) argued that the presence or absence of beach sediments is not sufficient proof to eliminate barrier formation from spits or bars. For instance, when a transgression reaches a lagoon the first sediments to be reworked into the sedimentary column would be beach and shallow neritic deposits, and Otvos argues that this would make them indistinguishable from earlier Pleistocene sediments. However, if shallow marine sediments existing landward of barriers were reworked into the sedimentary column then they would form a distinctive sedimentary unit distinguishable from earlier Pleistocene sediments. Otvos (1970a) suggested that the rapid development of bay-mouth bars or spits do not allow the accumulation of noticeable volumes of open marine sediments before sedimentation becomes lagoonal. He stated that it must also be proven that the total section, between the pre-transgressive and island surfaces, was formed in the supra-tidal environment before one can conclude that barriers did in fact form through beach and dune ridge engulfment.

Hoyt (1967) maintained that only a few small short lived barrier islands located close to the shoreline formed from off-shore bars. Otvos (1970a) indicated that records from the Louisiana and Mississippi coastal areas do not support this hypothesis because several major and minor examples of barrier development from underwater shoals took place in the Chandeleur, Mississippi Sound, and Timbalier Island groups. For instance, in the southern Chandeleur Island group the 7.5 km long Grand Grosier Island has developed since 1869 through numerous stages of the development and merger of small islands from the shallow sea-floor. Otvos (1970a) concluded that beach ridge progradation of coastal plain, barrier spit, and barrier island shores is essentially an identical process. Furthermore, new ridges added to the land form not only by seaward beach expansion but also by beach formation and by the development of near-shore bars.

Hoyt responded in 1970 in an attempt to answer many of the points raised by Otvos. Hoyt (1970) pointed out that Otvos principally argued that barrier islands form from offshore bars or shoal areas. In order to substantiate his theory Otvos (1970a) gave a number of examples. Careful reading reveals that only one of the examples used by Otvos, which comes from the southern Chandeleur Island group, developed from the shallow sea-floor and Hoyt argues that even this example is not valid since the development of Grand Grosier from a number of small islands does not establish its origin.

Hoyt (1970) suggested that the question of barrier island formation was left unanswered by Otvos in his discussion. Furthermore, there is no evidence given by Otvos to show that the Chandeleur Islands, or any other, formed through the vertical accretion of offshore bars and the absence of open marine deposits landward of the barriers seems to contradict their postulated mode of formation. Hoyt (1970) preferred an alternative hypothesis indicating that such barrier islands appear to be outstanding examples of beach/dune ridge engulfment.

In summary, Hoyt (1970) concluded that much of the evidence mentioned by Otvos (1970a) has no bearing on the original formation of barrier islands but simply reiterates information regarding their erosion, progradation, and migration. Otvos ignores criteria (Hoyt, 1967) which would be useful in rejecting some of the possible ways in which barriers have been considered to form, and his lack of examples has some significant implications (Hoyt, 1970).

Otvos (1970b) indicated that one of the main aims of his previously published paper was the illustration of processes which may obscure or destroy sedimentary proofs of barrier island genesis. Otvos argued that clear-cut examples should have been stated in defence of the barrier through engulfment theory. Although, Otvos (1970b) did not totally reject the hypothesis proposed by Hoyt, he reiterated that the absence of marine deposits landward of barrier islands can be accepted only as supplementary evidence in support of that theory. No marine deposits can be expected landward of barrier islands which have formed adjoining or within lower salinity basin areas such as estuaries, bays, or sounds. Assuming that fully saline conditions prevailed landward of future barriers, following the transgression, low sedimentation rates might have produced only a thin veneer of open marine sediments which may, as already indicated, be reworked into the sedimentary column making them indistinguishable from succeeding brackish deposits (Otvos, 1970b).

Swift (1975) stated that a barrier island is a littoral sand body consisting of a shoreface maintained by the prevailing hydraulic regime and attached wash-over fans whose surfaces are modified by aeolian and biological (including human) activity (Figure 2.12). The beach and shoreface response surfaces are clearly the critical zones suggesting that the existence and behaviour of other parts of the barrier are dependent on the behaviour of the shoreface. Swift (1975) postulated that if barriers have transgressed the continental shelf in response to a post-Pleistocene sea-level rise, the problem of barrier genesis is transferred "out there" to some late Holocene still stand position on the continental shelf.

Otvos (1970a,b) made it clear that migrating barriers are in a constant state of morphologic flux with individual barriers continually undergoing expansion, contraction, fragmentation and integration. The long-term behaviour of the shore-face during a marine transgression, whether retrogradation or progradation, depends on the balance between fair weather accumulation and storm erosion over the observational interval.

Swift (1975) detailed two time mechanisms for barrier formation by considering such shore-face dynamics, coastwise spit progradation and mainland beach detachment. He considered a third mode of formation, as proposed by Otvos (1970a,b), but suggested that there are two basic problems associated with this hypothesis. First, it is necessary that the previous withdrawal of the sea is such that at time zero a metastable condition prevails where the sea-floor slope is gentler than that required by the equilibrium profile; the equilibrium profile is a surface that when stressed will respond in such a way as to relieve that stress. However, the response time of the shoreface is instantaneous with respect to glacio-eustatic sea-level fluctuations. Second, associated with the up-building bar hypothesis is the inadequacy of known mechanisms of swash bar formation for building barriers of appropriate scale and distance from the shore. Swift further argued that break-point bars are small scale features which tend to migrate on-shore as swash bars, welding themselves to the shoreface. On prograding coasts break-point bars become stabilized by accretion on their seaward faces and they may accrete high enough to become shoreline initiated dunes, not barrier islands (Swift, 1975). Although Otvos (1970a) advocated the emergence of off-shore bars as a mechanism for barrier formation, Swift claims that his subsurface evidence is ambiguous and does not show the bore-hole spacing or the criteria used to distinguish barrier sub-environments, a notion echoed earlier by Hoyt (1970). Swift suggests

PAGE/PAGES
EXCLUDED
UNDER
INSTRUCTION
FROM
UNIVERSITY

that the earlier conclusion of Hoyt (1967) that minor barriers may form from bars is valid, but that these features are short lived.

Spits are characteristic of coasts of high relief undergoing a rapid transgression, because barrier formation through mainland beach detachment is severely inhibited by this type of coastal configuration (Swift, 1975). The submarine valley floor adjacent to retreating headlands would be in increasingly deeper water after the onset of the transgression, and as the submarine surface area of the barrier requiring nourishment increases the capacity of littoral drift to nourish the shore-face may eventually be exceeded (Figure 2.13a). As this point is reached storm wash-over will cause the barrier to retreat until equilibrium is restored (Swift, 1975) at a point possibly inland from the tips of the headland.

Conversely, Swift (1975) theorised that the submergence of a coast of very subdued relief, as in the case of most coastal plains, would tend to promote mainland beach detachment at the expense of spit progradation (Figure 2.13b). Therefore on an initially low straight coast, barrier spits and islands would form preferentially by mainland beach detachment rather than by coastwise spit progradation. Swift concluded that the lagoonal carpet of the Central Atlantic Shelf indicates that modern barriers have retreated to their present positions from the shelf edge during the Holocene transgression. Barrier genesis in the classical sense of mainland beach detachment (Hoyt, 1967) or coastwise spit progradation can only occur when a regression passes through stillstand into transgression (Swift, 1975).

Ultimately, the roles of these two mechanisms of barrier formation depend upon the configuration of the substrate, with spit building favoured by greater relief, and mainland beach detachment favoured by low flat coasts.

2.2.2 Barrier complex response to relative sea-level rise

The southeastern coast of Australia is an embayed bedrock margin with drowned river valleys infilled to varying degrees with Quaternary sediments. Studies of a number of Holocene barriers and estuaries in New South Wales have documented three primary types of embayment fill, characterised by different morphologies, lithofacies associations, and hydrodynamic regimes

(Roy *et al.*, 1980; Figure 2.14). These primary types show varying degrees of modification which suggests a general evolutionary model for sedimentation on an embayed high energy coast at the culmination of a marine transgression.

Radiocarbon dates used to construct an envelope of sea-level change in the Holocene indicates that along this apparently stable coastline, sea-level rose rapidly until some 6000 years BP after which it is unlikely that sea-level has oscillated more than ± 1m (Thom and Chappell, 1975). This would suggest that for the last 6000 years this area has been subject to a stillstand in sea-level which contrasts with other workers such as Fairbridge (1961) who show sea-level rising some 2-5 m above its present level in the mid-Holocene (section 2.1). Roy *et al.* (1980) summarised the lithofacies of Holocene age identified along this coast (Table 2.1.). Environments of deposition within embayments include: dune, barrier beach and near-shore; flood tide delta, and back barrier; estuarine mud basin, channel and tidal flats; and river delta including channel, flood plain and fresh water swamp (Roy *et al.* 1980).

The first type are open ocean embayments dominated by ocean swell and wind waves, where estuarine and fluvial processes have negligible influence (Figure 2.15). Roy *et al.* indicate that these embayments are characterised by marine depositional environments containing bay barriers which consist of both shelly beach/near shore sands extending to depths of -30 m at the shoreline, and transgressive dunes which may reach elevations of +35 m. Prograded barriers reach widths of 2 km and disconformably onlap onto either bedrock or Pleistocene substrate, behind which limited swamp or estuarine deposits may occur (Roy *et al.*, 1980).

The second type, barrier estuaries, are embayments in which lagoons or estuaries occupy drowned valleys impounded by coastal sand barriers. They may follow the irregular outline of the drowned bedrock valley they occupy, or be coast-parallel and more oval, similar to barrier lagoons on the Texas coast (Roy *et al.*,1980). Barrier estuaries are characterised by estuarine and fluvial depositional environments where muds form extensive subaqueous mud basin deposits, and where tidal flats with the occasional occurrence of biohermal shell reefs are found in estuaries which are permanently open to the sea. Roy *et al.* states that barriers of all types are associated with these embayments (dependent on the regressive-stillstand-transgressive sequence), where process regimes, and the associated near-surface geometries of lithofacies are complex and

PAGE/PAGES
EXCLUDED
UNDER
INSTRUCTION
FROM
UNIVERSITY

dependent upon the degree of infill which is in turn dependent upon the estuary size and the rate of sediment input.

The final type of embayment Roy *et al.* (1980) describes are classical ria estuaries or drowned river valleys with wide exposed deep water entrances. They postulate that in such estuaries ocean waves influence the morphology and sediment distribution, both around the entrance and, for distances of up to 5 km in land, with tidal and fluvial processes being dominant upstream.

Roy *et al.* proposes an evolutionary model for the development of these three embayment types, based on different estuaries which show varying degrees of evolution (Figure 2.16), suggesting that variations between embayments identified on the New South Wales coast depend on the configuration of the pre-Holocene coastal margin, and the nature of the marine sand bodies that accreted on it at the end of the Holocene marine transgression. The model describes two modes of shoreline displacement as sea-level reached its present level some 6,000 years BP. First, there is abundant ^{14}C evidence to support the view that most bay barriers, particularly the prograded type, accumulated at a declining rate between 6,000-3,000 years BP. The second mode of displacement is erosional and appears to have predominated along the New South Wales coastline over the last 3,000-4,000 years.

Roy *et al.* (1980) conclude that the severity and duration of these modes varies from locality to locality, and that it is not known whether erosion is episodic, involving changing energy conditions, or is basically a long term trend reflecting the progressively declining sediment supply within embayments.

Development of barriers and other sediment bodies in embayments along the New South Wales coast represents a depositional response to environmental conditions which differs somewhat from the well studies barrier complexes of the USA (Hoyt, 1967; Otvos, 1970a,b; Swift, 1975). In contrast with the US Gulf coast, in NSW it can be shown that because of the compartmented nature of the embayments the bulk of the sand forming the barriers was derived from offshore sources by onshore rather than by along shore processes (Roy *et al.*, 1980).

As has been suggested a complex set of parameters control shoreface translation and the generation of coastal facies during sea-level regressions and transgressions. In understanding

PAGE/PAGES
EXCLUDED
UNDER
INSTRUCTION
FROM
UNIVERSITY

coastal sedimentation it is necessary to identify the dominant factors which control the vertical and horizontal translation of the depositional shoreface (Boyd and Penland, 1984). Once identified, relationships between these parameters may be established which are possibly capable of predicting quantitatively the geometry and distribution of coastal stratigraphic sequences in modern and ancient environments.

Initial contributions by Sloss (1962) and Allen (1964) identified the concepts of facies generation during sea-level regressions and transgressions. Swift *et al.* (1972) grouped the variables used by Sloss in a quantitative manner to produce an empirical relationship. For the coastline position to remain constant the ratio of sediment input to the energy available for its dispersal must be balanced by an equivalent change in relative sea-level:

$$\left(\frac{Q}{E}\right)_{G} - R = K \qquad 2.2$$

where Q is the material supplied to the depositional site, E is the energy input, K is a constant coastline position, g is a variable, and R is the rate of subsidence at the site. Swift (1975) restated the problem in the form of the sediment continuity equation:

$$\frac{\delta C}{\delta t} + VC = \frac{\rho}{d} \cdot \frac{\delta h}{\delta t} \qquad 2.3$$

where C is the sediment concentration, V is a velocity vector, ρ is the sediment density and d is the water depth. Swift indicates that the rate of change of the coastal sediment-water-interface, $\delta h/\delta t$ is proportional to the time rate of change of sediment advected into and out of the unit volume.

Belknap and Kraft (1981) indicate that the migration of coastal lithosomes (barrier systems) across the US Atlantic Shelf is a response to rising sea-levels during the Holocene. A relative sea-level curve for Delaware (Figure 2.17) constructed from ^{14}C dates on basal peats, rises smoothly from 25 m below present sea-level some 10.000 years BP. The rate of relative sea-level rise decreases with time and caused in rates of coastal retreat of up to 20 m/yr at 10,000 years BP, which subsequently slowed to some 5 m/yr around 5,000 BP (Belknap and Kraft, 1981). In examining the preservation potential of transgressive coastal lithosomes and extending the controlling factors to include pre-existing topography, erosion resistance and tidal range, Belknap

PAGE/PAGES
EXCLUDED
UNDER
INSTRUCTION
FROM
UNIVERSITY

and Kraft (1981) concluded that the depth of shore-face erosion was related to the rate of sea-level rise with faster rates of sea-level rise being capable of greater preservation (Figure 2.18).

Boyd and Penland (1984) presented three regional examples from the central coast of New South Wales, Louisiana and Nova Scotia to provide a spectrum of contrasting case studies, where for each example variables controlling sedimentation were identified. For instance, in New South Wales rising sea-levels are followed by stillstand under a moderate to high energy wave climate; in Louisiana very rapid rates of relative sea-level rise and low wave energy are punctuated by storm events on a low gradient coast; whereas in Nova Scotia drumlin point sources supply sediment to topographically controlled estuaries by under relative sea-level rise and moderate levels of wave energy. Boyd and Penland presented the stratigraphic records for each example in order to illustrate the contrasting process interactions can produce an array of barrier sedimentary sequences. They infer that coastal sedimentation during transgressive and regressive cycles is determined by the parameters which control the shape of the shoreline profile and factors which result from profile translation.

In Nova Scotia a continuing rise in relative sea-level causes initial barrier progradation which is followed by destruction and breakdown. During the erosive phase, Boyd and Penland postulate that estuarine headlands act as effective barriers to longshore transport where sediment is moved landward by aeolian, wash-over, and tidal inlet processes. Sediment remaining on the shoreface is transported onshore by wave action leaving a thin veneer on the shelf (Figure 2.19a). They conclude that transgressive sedimentation on the eastern shore of Nova Scotia supports the shoreface retreat concept devised by Swift (1975).

As previously illustrated (Roy *et al.*, 1980), on the central coast of NSW a rapid relative sea-level rise occurred prior to the stillstand reached some 6,000 years BP (Thom and Chappel, 1975), after which sediment supplied from the adjacent disequilibrium shelf formed regressive barrier deposits (Figure 2.19b). Boyd and Penland suggest that barrier progradation slowed or ceased as sediment supply diminished (Roy *et al.*, 1980) and that the resulting barrier sequence consists of a thin basal transgressive sand sheet overlain by regressive beach ridge and dune complexes. Although the barriers retreat in response to relative sea-level rise, barrier sediments are retained on the inner shelf as postulated by Belknap and Kraft (1981); during the stillstand sediment is

PAGE/PAGES
EXCLUDED
UNDER
INSTRUCTION
FROM
UNIVERSITY

moved landward to produce a form of punctuated stepwise shoreface retreat (Boyd and Penland, 1984).

Finally in Louisiana rapid rates of relative sea-level rise generate barriers during the reworking of the underlying deltaic sand sources. As the transgression continues over a low regional gradient the sandy barrier systems are transformed into subaqueous shoals. Boyd and Penland suggest that the resulting stratigraphy is a dispersed sand lens overlying lagoonal muds, and that coastal processes therefore incorporate reworked barrier sand bodies into the stratigraphic record (Figure 2.19c). Boyd and Penland (1984) indicate that sufficient variability exists within the three studies to suggest that existing coastal models and concepts of barrier genesis and evolution cannot fully describe the formation and subsequent response of barrier island systems (lithosomes) to relative sea-level changes.

In investigating coastal dune building episodes and their relationship to Quaternary sea-level changes, Pye (1984) inferred that during the Holocene marine transgression, rising sea-level caused the reworking of regressive marine deposits laid down during the preceding glacial period. A rising sea-level would have also led to sustained shoreline erosion as the near shore profile sought to achieve a new profile of equilibrium. Strong winds would have transferred a substantial proportion of the shoreface sands landwards feeding the transgressive sand sheets and dunes.

Pye proposes that transgressive dune activity may have been self-maintaining, in that winds supplying transgressing dunes with sediment would effectively promote the erosion of the shoreface, and that only after sea-level had ceased to rise would a new profile of equilibrium be attained, terminating shoreline retreat. Pye (1984) suggests that as dunes were locally and intermittently active within the last 6000 years in Australia, when sea-level is thought not to have fluctuated more than ± 1 m (Thom and Chappell, 1975), transgressions are not the only factor capable of initiating dune instability phases.

Shoreline erosion and degradation of vegetation may be caused by variations in wind wave climate or by changes in the pattern of near shore sediment supply and the profile of equilibrium (Pye, 1984). He noted that the marine transgression model of coastal dune instability is unlikely to have worldwide applicability due to variations in the balance between sand supply, wind energy and sand binding vegetation under differing environmental conditions, and because areas

have experienced contrasting sea-level histories during the Holocene. Nevertheless, this model highlights the complexity of dune and barrier system retreat in response to rising sea-levels.

Carter *et al.* (1989) attempted to explore barrier and lagoon coast evolution under differing relative sea-level regimes using examples from Ireland and Nova Scotia. They propose that it is the rate rather than the magnitude of relative sea-level change which determines the evolution of coarse barrier and lagoon coasts.

Heron *et al.* (1984) suggested that while the hydrographic regime is an important control on sedimentation pattern other natural controls are equally important. They suggest that perhaps the most important process has been the Holocene rise in sea-level, a process resulting in a shoreline transgression.

Rampino and Saunders (1981) used evidence from the transgressive sediments beneath and behind modern barriers, the remnant depositional record on the shelf, and the nature of the surface being transgressed by the sea to reconstruct the long term history of the barrier Islands of Southern Long Island during the past 9,000 years.

At approximately 9,000 years BP sea-level stood 24 m below the present mean sea-level, and a chain of barrier islands existed on the present shelf roughly 7 km offshore. These barriers are thought to have continued their build up until some 7,000 years before present at which time the sea stood 15 m below its present level. Rampino and Saunders (1981) went on to suggest that these barriers were then overstepped by the rapidly rising sea and that the surf-zone shifted rapidly landwards to a position some 2 km offshore. Due to the rapid rate of relative sea-level rise back-barrier deposits were extensively preserved on the continental shelf. They conclude that a rapid relative sea-level rise and low sediment supply has the potential to overstep and preserve barrier deposits, whereas slow rates of submergence and a greater supply of sediment favours continuous shoreface retreat.

Although the coasts of southern Ireland and eastern Nova Scotia possess many basic similarities, especially in terms of geology, glacial history, sediment character, resistance to erosion and hydrodynamic regimes, there is a fundamental difference in their Holocene sea-level histories (Carter *et al.*, 1989). During the last 4,000 years Ireland has experienced a slow sea-level rise of

less than 1 mm/yr, whereas the Atlantic coast of Nova Scotia has been experiencing sea-level rises up to three times greater over the same period. On the basis of their studies Carter *et al.* (1989) proposed a hierarchy of intrinsic controls resulting in the evolution of coarse clastic barrier lagoon coasts (Figure 2.20).

Facies associated with slow sea-level rise in Ireland tend to show a gradual encroachment of marine conditions from terrestrial through fresh and then saltwater wetlands, to intertidal flats and eventually, into open sea-conditions. Carter *et al.* (1989) inferred that over a short time period, the coastal sedimentary facies associated with slow relative sea-level rise are largely reworked *in situ* while, the lagoonal areas show a slow transition from fresh to saltwater conditions. The general scarcity of sediment, typical of many Irish sites, would lead to the preservation of very thin representative units as the shoreface migrates (Carter *et al.*, 1989).

As relative sea-level rises against an intricate coast, like that of eastern Nova Scotia, there is a need to redistribute sediment across and along the leading edge of a barrier. Carter *et al.* indicated that when and where sediment is scarce barriers must respond through morphological change in order to survive the impact of rising sea-level. This may involve changes in barrier geometry and the cannibalization or reworking of existing forms to supplement some of the deficits in the sediment budget. These processes, driven by rising sea-level, may cause barrier stretching, segmentation into sub-cells, breaching and sediment dispersal away from the shoreline.

Carter *et al.* (1989) argued that the stress imposed on barriers by a rapid relative sea-level rise may either lead to the destruction, the overstepping, or drowning of that barrier and examples of drowned barriers are evident in the literature (Oldale, 1985). Although the rate of sea-level rise is a primary control, basement expression (i.e. the pre-existing morphology of the transgression surface) plays an important role in shoreface evolution. For instance, in Ireland barrier-lagoon form is controlled by local basement expression, particularly through the emergence of headlands, creating largely closed sediment systems. The Nova Scotian examples are associated with rapidly moving erosional fronts where local basement control is regulated to a subordinate role at the expense of rapid changes in sediment supply (Carter *et al.*, 1989).

PAGE/PAGES
EXCLUDED
UNDER
INSTRUCTION
FROM
UNIVERSITY

2.2.4 Summary

The actual origin of coastal barriers is still a matter of debate (section 2.2). Although, intense discussion during the 1960s and 1970s did not resolve the problem of barrier genesis *per se*, four theories have been persistently used in the literature to explain the origin of these features. First, barriers may form through the build up of offshore point-break bars i.e. via coastal emergence (DeBeaumont, 1845; Price, 1963; Otvos, 1970a,b). Second, barriers and barrier islands may form in response to longshore transport, spit elongation and inlet breaching (Hoyt, 1967). Third, barriers may be initiated through in-place drowning of coast parallel antecedent topography i.e mainland detachment in response to relative sea-level rise (Hoyt, 1967). The final theory suggests that barriers located offshore on the continental shelf may have migrated landward and become detached from their point of origin (Swift, 1975).

As modern barrier systems have been used to support each of these theories it is likely that the mechanisms responsible for the formation of these features are site specific. However, the utilitarian approach to barrier genesis suggests that more than one of these mechanisms may have operated during the formation and subsequent evolution of the barrier system; this view of 'multiple causality' has prevailed following the debate in the mid-1970s (Carter, 1988).

Although the mechanisms described above are controlled primarily by changes in relative sea-level, sediment supply and local hydrodynamics, barriers evolution is intimately tied to the antecedent topography and the geologic systems upon which they form and migrate (Belknap and Kraft, 1985). The pre-existing topography has been shown to be of critical importance in determining the evolution and preservation of barrier systems in Delaware, Florida and Carolina (Belknap and Kraft, 1985; Davis and Kuhn, 1985; Riggs *et al.*, 1995).

It is known that barriers did exist on what is now the continental shelf (Swift, 1975; Roy *et al.*, 1980; Belknap and Kraft, 1981; Rampino and Saunders, 1981; Oldale, 1985) indicating that modern barriers may have been derived from landward retreating barriers which originated on what is now the submerged continental shelf. A complex set of parameters control shoreface translation and the generation of coastal facies during sea-level regressions and transgressions.

It has been widely suggested that the rate of sea-level rise and the nature of sediment supply are controlling factors in determining the nature of barrier migration under rising sea-levels. Rapid rates of relative sea-level rise and low sediment supply seem to favour the overstepping of barriers, preserving them on the continental shelf, whereas slow rates of submergence and a greater supply of sediment seem to favour continuous shore-face retreat (Roy *et al.*, 1980; Belknap and Kraft, 1981; Rampino and Saunders, 1981; Heron *et al.*, 1984; Boyd and Penland, 1984; Carter *et al.*, 1989). It is therefore the rate rather than the magnitude of sea-level rise which ultimately controls the evolution of barrier systems retreating under rising relative sea-levels (Carter *et al.*, 1989).

Although rapidly rising sea-levels at the onset of the Holocene may have preserved barriers on the continental shelf of New South Wales, reworking by waves and the subsequent onshore transport of those sediments to maintain contemporary barriers has effectively erased evidence of barriers existing on submerged portions of the continental shelf (Roy *et al.*, 1980; Boyd and Penland, 1984). This would indicate that although the rate of sea-level rise initially plays an important role in the preservation of barriers, their subsequent maintenance is dependent upon the contemporary hydraulic regime which acts to redistribute those sediments.

Hoyt (1967) maintained that the key to discovering the mechanism of barrier genesis was study of the sediments beneath modern barrier island sands and associated back barrier lagoonal sediments. One of the fundamental concepts of sedimentary geology is that major breaks in the stratigraphic record result from important marine regressions due to eustatic and/or tectonic phenomena. By studying the stratigraphic record and using certain sea-level indicators, one can infer the relative sea-level rise for a particular location from which theories regarding the evolution of coastal sedimentary facies can be formulated.

Sea-level change is no doubt fundamental to the generation of coastal sedimentary sequences; however, the evolution of barrier systems is dependent upon complex interrelationships between numerous factors which may operate locally if not regionally. If as in the case of Story Head, Nova Scotia, an inherently poor sediment supply was to cease then the hydrodynamic regime would lead to both the cannibalization and destruction of the barrier (Carter *et al.*, 1990). Therefore, although the rate of sea-level rise may determine the nature of barrier retreat (Carter

et al., 1989), numerous other factors as well as sea-level dictate the evolution of coastal sedimentary environments.

Chapter 3
Methods

3.1 Fieldwork / Site investigation

The seismic refraction surveys were conducted in order to identify and model sub-surface refractors beneath West Marsh, East Marsh and the Pendine Burrows. The velocity data obtained from refraction lines within the survey area would provide a basis for establishing the range of velocities exhibited by each of the seismic facies. The aim of conducting high-resolution reflection profiles was two fold. First, to locate and identify the pre-Holocene and bedrock surface beneath the Pendine Sands and the back-barrier deposits. Second, to determine whether back-barrier deposits lie beneath the contemporary foreshore. Marine reflection data were acquired within the Taf Estuary in order to determine the depth to bedrock basement and model the shape of the pre-Holocene surface within this area.

The aim of conducting Schlumberger depth probes was two-fold. First, to provide information regarding the depth to bedrock and the composition of the overlying sediments. Second, to use this information to corroborate the data obtained from the seismic surveys.

3.1.1 Coring methods

Two coring methods were applied in this study. Initially short cores were obtained from the saltmarshes within the Taf Estuary, using a hand held Dutch auger (Eijkelkamp steel gouge auger, model 04.03). The method was well suited to coring through fine cohesive sediment, but became ineffective when sandy sediments were encountered.

Relatively longer cores (3-13 metres) were recovered from the back-barrier deposits using an Eijkelkamp percussion drilling set (Model 04.18). The sampler body consists of a reinforced gouge auger (diameters 50 and 100) with a hardened steel cutting head. The auger is driven into the ground by a two stroke wrecking hammer without the use of drilling fluid (Figure 3.1a). The sampler is recovered using an extraction system consisting of a mechanical rod puller and a ball

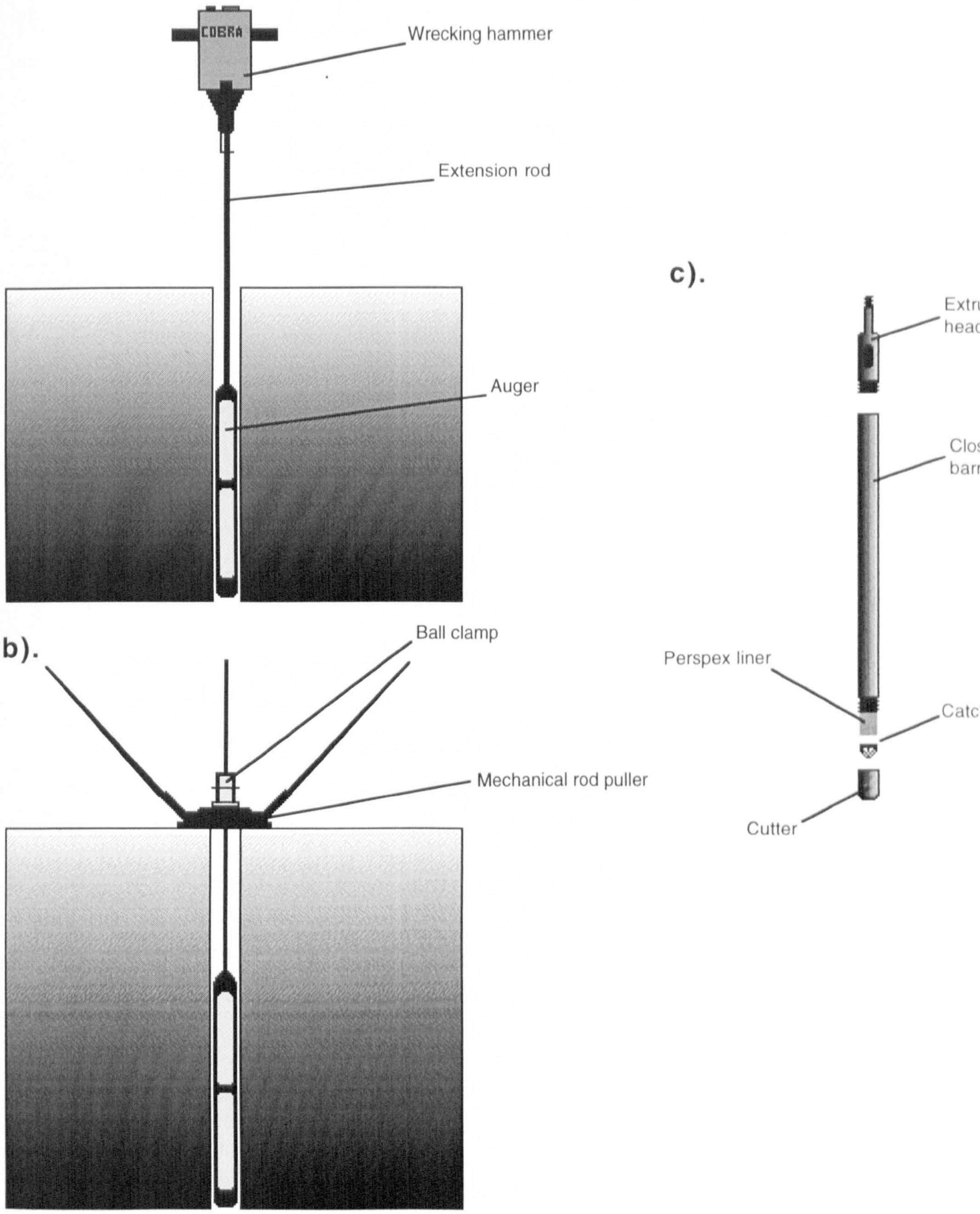

Figure 3.1 a) The drilling assembly; b) The extraction system; c) The closed sampler

clamp with hand grips which when placed over the extension rods can pull the assembly out of the sediment (Figure 3.1b). Sub-samples were taken from the auger and the sediment was described in the field (Section 3.1.2). The borehole depth was extended by adding metre long extension rods to the sampler; the time taken to drill and extend the assembly increased significantly for depth greater than eight metres. A closed sampler, containing a perspex liner, was used to recover whole cores for subsequent analysis in the laboratory (Figure 3.1c). As for the auger, the closed sampler was driven into the ground using the wrecking hammer and recovered using the extraction system.

The percussion drilling set proved extremely effective when coring through fine cohesive sediment, but became less useful when clean sands were encountered. The technique caused relatively little compression of the sediment (5-15%) and preserved the majority of depositional features.

3.1.2 Sediment description

The Troels-Smith (1955) descriptive method was used to describe and log sediments within the field and subsequently in the laboratory. This system describes the basic components of the sediments and is used to make a qualitative estimate of the relative abundance of gravel, sand, silt, clay, turfa, humus, organic detritus and calcareous material. Each of these components has an abbreviation and the Troel-Smith system estimates the quantity of each material using a five point scale. For instance, if a particular deposit contained no clay and was composed entirely of sand then the values for these two components would be 0 and 4 respectively.Sediments described in the laboratory were also characterised using the Munsell Colour Chart (1975) and photographs were taken to provide a visual record. The descriptive scheme utilises lithology, texture, colour and structures within the sediment, as well as variation within units and the contacts between units as criteria for characterising the sediment.

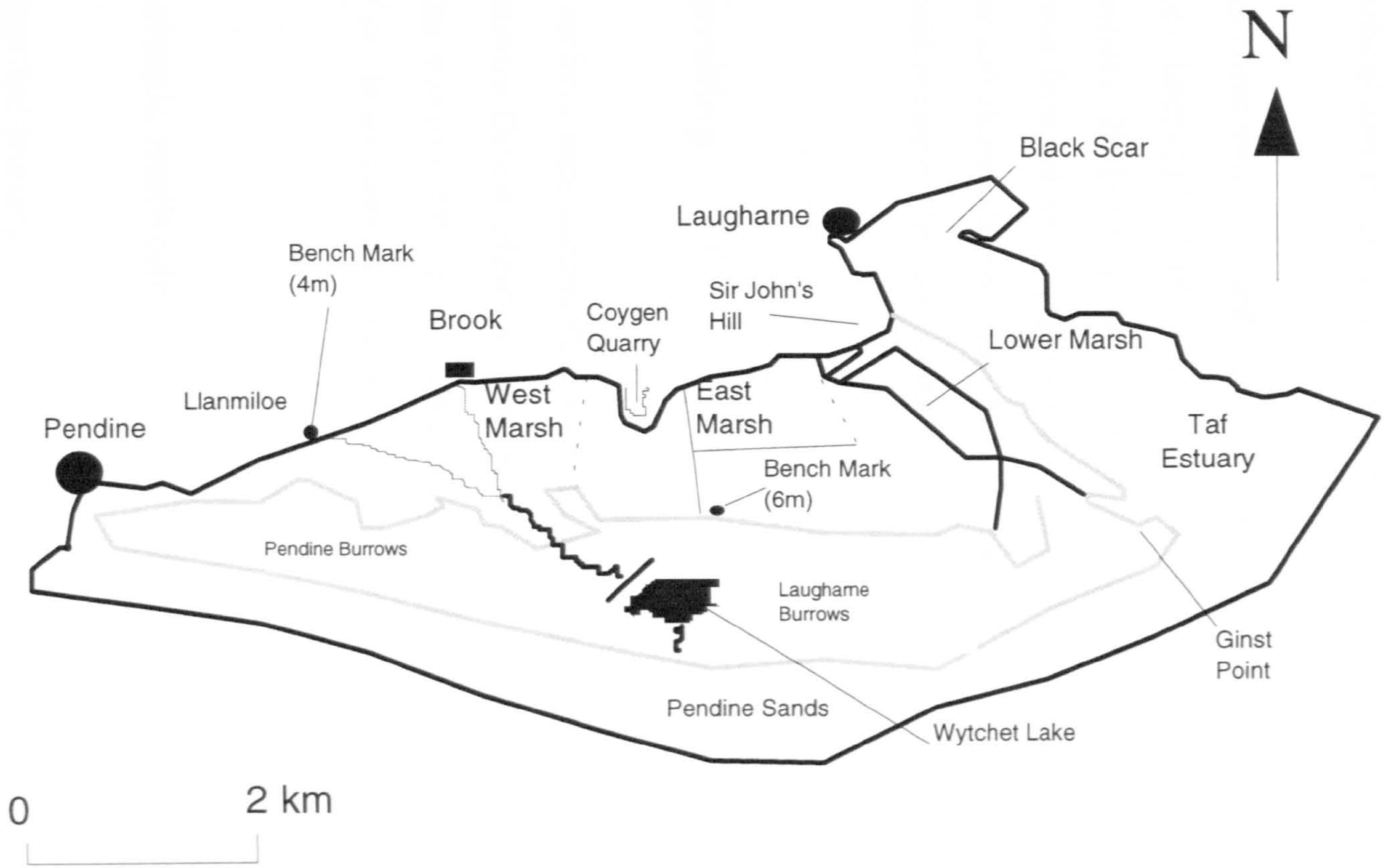

Figure 3.2 Location of bench marks in West and East Marshes

3.1.3 Sampling

Samples obtained in the field for later analysis were stored in sealed plastic bag. When taken from the augers care was taken to ensure that there was no risk of contamination by cleaning the sample surfaces and avoiding any clearly remoulded material.

Continuous cores were obtained from appropriate sites using the method previously described. The perspex liners (1 by 0.05 metres) were sealed and stored in a refrigerator at the School of Ocean Sciences. Rather than extrude the sediment a Miller saw was used to split the liner, the material was then halved using a cheese wire and the cores were described then resealed in plastic film and aluminium foil. One half was used for analysis and the other was archived, with the materials preserved for radiocarbon dating.

3.1.4 Levelling

Borehole surfaces were accurately levelled using a Nikon Automatic Leveller to provide heights above Ordnance Datum (Newlyn). Temporary bench marks were levelled into the estuary and back-barrier area from OS bench marks, located in Laugharne, Llanmiloe and at Bannister Farm (Figure 3.2). In all cases the transects were closed to assess the borehole levelling accuracy.

3.1.5 Seismic methods

Fundamental theory

In applied seismology the interpretation of the majority of seismic information is based upon recordings of the sub-surface response to a compressional disturbance generated by a seismic source at or below the ground surface. Energy travels outwards from the point of firing, as a spherical pulse, by vibrating particles within the propagating medium; the radius of the seismic pulse increases until the wavefronts approximate plane surfaces. In seismic techniques the transmitting medium is assumed to behave in an 'elastic' manner as the passage of seismic energy

through the propagating media leaves the material undeformed. The type of seismic source used and media of propagation determine the basic shape of the seismic record, which contains wavelets of differing amplitude, frequency and velocity.

Two types of wave are propagated within an homogenous medium. The first referred to as compressional or P-waves, propagated by alternatively compressing and dilating the elastic media. The second type are known as shear or S-waves, propagated by displacing the media in a direction perpendicular to the propagation axis. Equations 3.1 and 3.2 describe compressional (Vp) and shear wave (Vs) velocities in terms of the elastic moduli and bulk density of the transmitting medium:

$$V_p = \sqrt{\frac{k + \frac{3}{4}\mu}{\rho}} \qquad (3.1)$$

where k is the bulk modulus, μ is the rigidity modulus and ρ is the bulk density of the propagating media:

$$V_s = \sqrt{\frac{\mu}{\rho}} \qquad (3.2)$$

where μ is the rigidity modulus and ρ is the density of the propagating media. Because rigidity is zero in fluids, S-waves cannot propagate through liquids.

The path along which a seismic pulse travels is known as the raypath (drawn perpendicular to the wave front), and for any source-receiver pair on or below the ground surface there are a multitude of time travel paths, each related to a specific seismic event. For instance, air waves, surface waves, multiples, refracted waves, reflected waves, side swipes, diffracted waves and converted waves (Telford *et al.*, 1990). Although the earth often consists of a complex series of stratified materials, seismologists use simplified models to approximate reality. The simplest model consists of two horizontal homogenous layers with different seismic velocities. Consider one horizontal interface at a depth h separating two media which exhibit an increase in compressional velocity with depth (Figure 3.3). The first raypath is that between the source and the receiver (g) which travels along the same axis as the surface or Rayleigh wave, but at a much

greater velocity (V_1). The second raypath travels from the source and strikes the interface at depth *h* (Figure 3.3). Any wave meeting this interface is partly reflected, partly transmitted and partly refracted; the change in raypath direction is described by *Snell's Law*:

$$\frac{\sin \theta_i}{V_1} = \frac{\sin \theta_t}{V_2} \qquad (3.3)$$

where θ_i and θ_t are the angles of incidence and transmission respectively, and V_1 and V_2 are the seismic velocities of the two media. The *refractive index* (Equation 3.4) at that interface determines the change in the transmitted wave raypath direction; for $V_2 > V_1$ the refraction is away from the normal (Figure 3.3):

$$\frac{\sin \theta_i}{\sin \theta_t} = \frac{V_1}{V_2} \qquad (3.4)$$

Although the amplitudes of the reflected and transmitted waves vary with the angle of incidence the actual proportion of energy reflected depends upon the properties of the media, namely the *acoustic impedance* contrast across the interface; the acoustic impedance is the product of seismic velocity and density of the layer medium. For instance, an interface between layers with a large velocity contrast and similar density will produce a strong reflection; if the velocity of the lower layer is less than that of the upper then the reflection coefficient will be negative and the refraction will be towards the normal.

Accurate determinations of velocity values are essential to calculate the depth, dip, and horizontal location of sub-surface reflectors and refractors and to ascertain the nature of the rocks, sediments and interstitial fluids from velocity measurements (Sheriff and Geldart, 1995). As shown by equation 3.1 P-wave velocity in an homogenous elastic solid is a function of the elastic constants and density. Although lithology is the most obvious factor, porosity is the single most important component determining velocity; density, age, depth of burial, cementation and the composition of the interstitial fluid also influence velocity (Sheriff and Geldart, 1995). The large velocity ranges exhibited by most rocks and sediments consequently

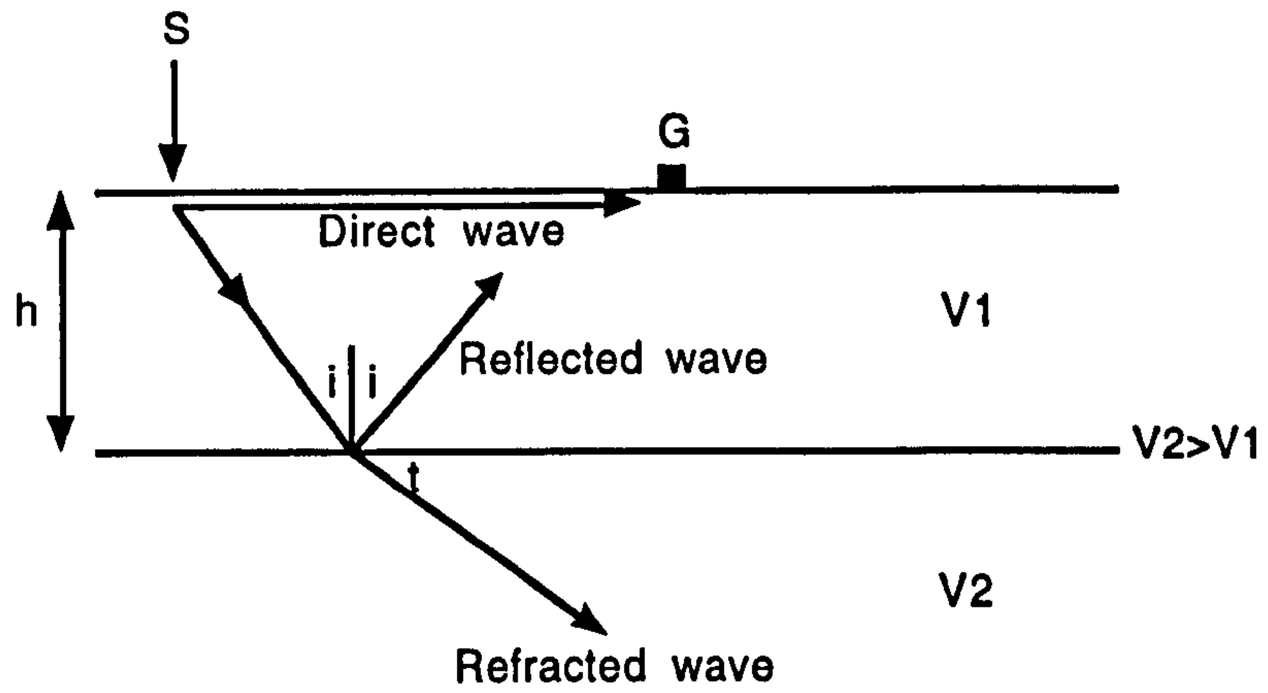

Figure 3.3 Refraction at an interface between two layers; i= angle of incidence; t= angle of transmission.

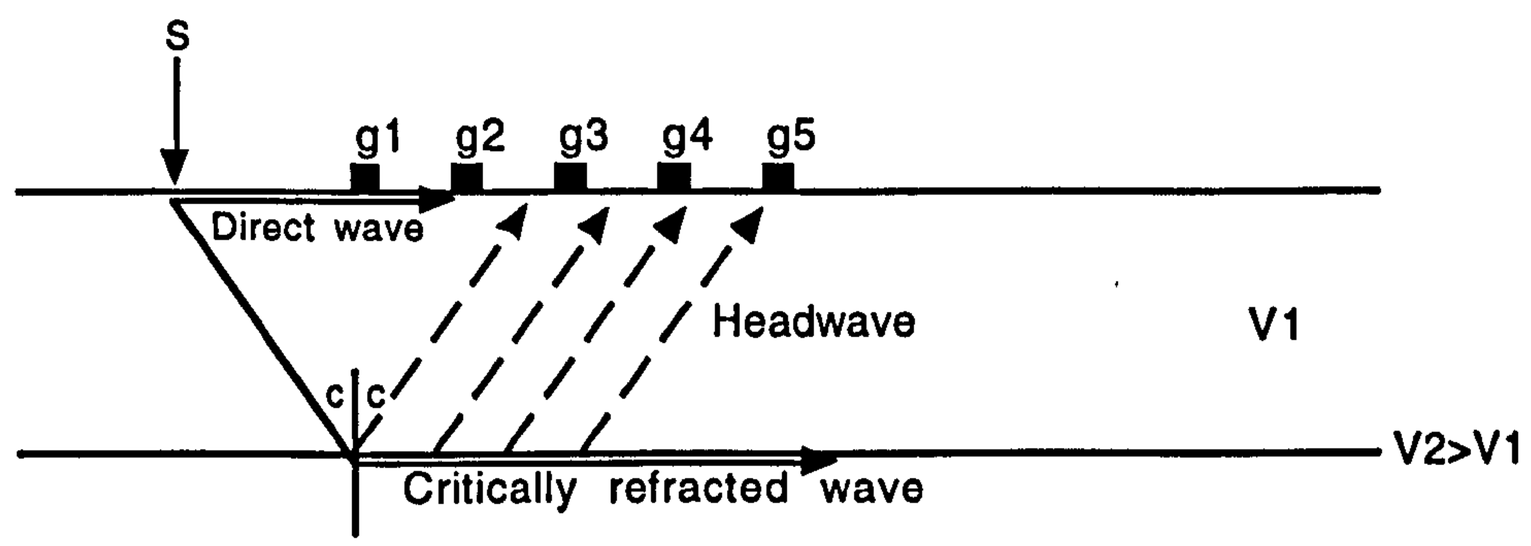

Figure 3.4 Critical refraction at an interface between two layers; c= critical angle of incidence

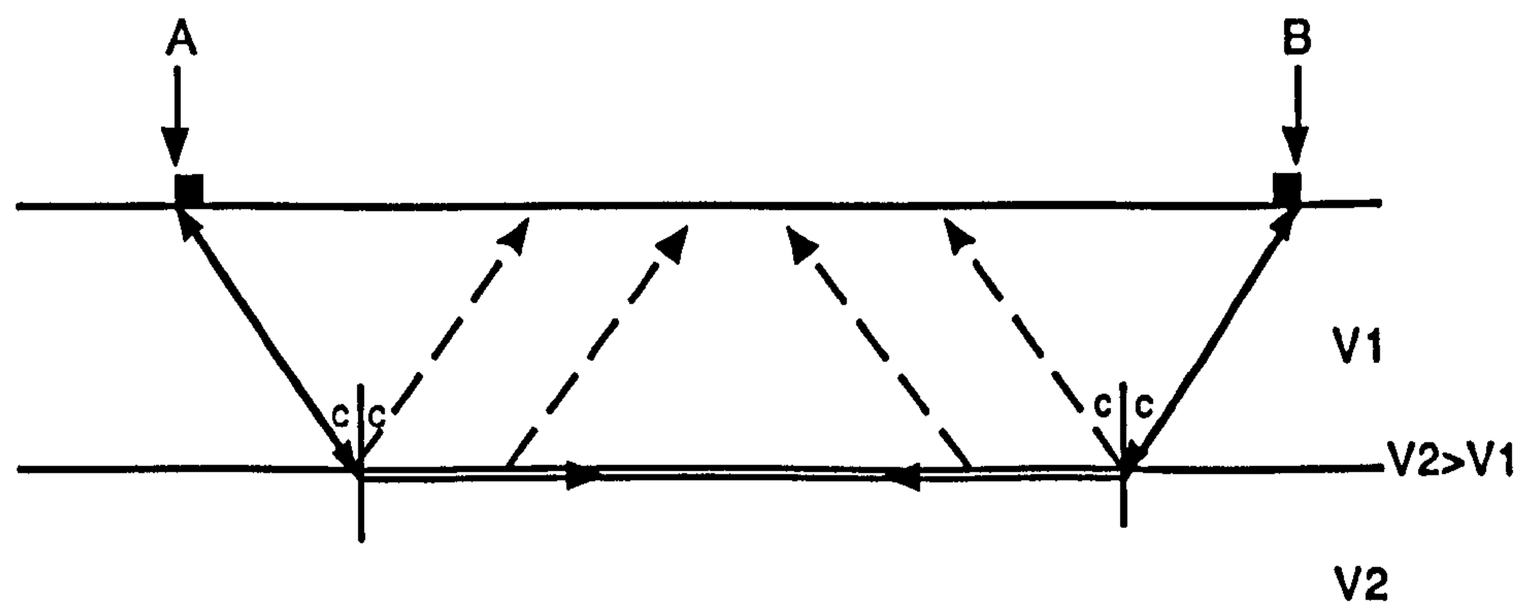

Figure 3.5 Schematic representation of the critically refracted raypaths from A to B and B to A

mean that seismic velocity alone does not provide an adequate basis for distinguishing lithology.

However, in the case of sedimentary rocks a general rule can be applied; high velocities generally indicate carbonates, low-velocities are characteristic of sandstones and shales whereas intermediate velocities can indicate either (Sheriff and Geldart, 1995). As unconsolidated materials generally exhibit distinctly lower seismic velocities than lithified rocks. Although, some sediments and rocks have similar seismic velocities, this property can still be used to distinguish between lithified and non-lithified materials (Telford *et al.*, 1990). For instance, till and shale have similar compressional wave velocities but exhibit very different shear wave velocities (Davis and Bennell, 1988). Where compressional wave velocities do not distinguish between rocks and sediments, shear waves can be used to resolve the problem and establish the near surface velocity structure.

Seismic Refraction surveying

Background

Refraction surveying utilises waves which have been refracted at the *critical angle* (θ_c) of incidence (Figure 3.4). When a P-wave strikes an interface between two layers at θ_c it is critically refracted along the boundary and travels parallel to the refractor in the lower medium. In doing so the refracted wave generates oscillatory motion immediately below the refracting horizon which causes the upper media of velocity V_1 to move in phase with the lower media of velocity V_2; this disturbance travels along the interface at the velocity of the lower media (Figure 3.4). *Huygens* principle suggests that oscillatory motion along the interface generates a *headwave* (plane wave) within the upper media which propagates back to the surface at θ_c (relative to the normal) and is transmitted at the upper layer velocity (V_1).

Critical refraction at an interface only occurs where there is a layer increase in velocity with depth and is governed by *Snell's Law*:

$$\sin \theta_c = \frac{V_1}{V_2} \qquad (3.5)$$

where θ_c is the *critical angle of incidence,* V_1 is the seismic velocity within the upper media and V_2 is the seismic velocity within the lower media.

At and beyond a *critical distance* away from the source it is quicker for the seismic energy to travel down to the first acoustic impedance interface, along the refracted raypath and back to the surface via the headwave, than it is to travel directly through the upper media at lower V_1 velocity (Figure 3.4). Refractors are thus observed only at offsets greater than twice the depth to the refractor (Telford *et al.*, 1990).

The interpretation of seismic refraction data is based upon 'first arrivals' picked from a seismograph - the latter permitting an accurate evaluation of travel-times. These data are plotted on a *time-distance graph* which can be used to determine the number of layers, their apparent velocities, shot terms and geophone terms. To establish the sub-surface geometry refraction lines are generally reversed and the *principle of reciprocity* is utilised *i.e.* the travel time from a source at point A to a receiver at point B (tr) is the same as that from a source at point B to a receiver at point A (Figure 3.5). If the reciprocal times do not match then the seismic pulses, generated in the normal and reversed directions, must have travelled along different raypaths.

Because of the distinct contrast in velocity between unconsolidated sediment and lithified rock mentioned above, seismic refraction techniques are particularly suited to evaluating the depth of overburden above bedrock. However, one chief control on the quality of the interpretation of refraction data in general is the definition of the near surface velocity (V_1). Errors in establishing an accurate value for V_1 directly transfer to errors in depth estimates. In unconsolidated sediments the near surface layer maybe unsaturated and can consequently exhibit seismic velocities lower than the velocity through water (1500 m/sec) since the bulk modulus may reduce drastically under such circumstances (refer to equation 3.1). This aerated low velocity layer (LVL) can absorb a large proportion of the seismic energy and has a disproportionally large affect on travel-times. Over-estimating the LVL velocity can introduce errors in the subsequent determination of refractor depths. It is therefore important to use a geophone spacing which can accurately define the near surface velocity and any subsequent increase in velocity with depth through the saturated overburden. Because this technique depends upon critical refraction it should only be used at sites which exhibit an increase in seismic velocity with depth. Layers which exhibit decreases in velocity with depth are not accommodated in the critical refraction

models and their existence cannot be established from analysis of the first arrival data. As such, any LVL in the vertical sequence may give rise to substantial errors in depth to bedrock calculations. A further complication arises where refracted energy from 'thin' layers which exhibit a small velocity contrast to the underlying strata within a vertical sequence may become 'hidden' amongst refractors from lower layers. Although, hidden layers can introduce additional errors in the analysis of refraction data, they can often be identified in seismic reflection surveys.

Seismic refraction techniques were applied in this study to investigate the sub-surface velocity structure and to map the distribution of horizons beneath West Marsh, East Marsh and the Pendine Burrows.

Refraction surveying data acquisition and position fixing

12 & 24 multi-channel Atlas Copco ABEM Teraloc Seismic System (Mark 3) were used in this study to record and view seismic refraction data. A 13 take-out (120 metre long) geophone cable and an external trigger were connected to the seismograph. The trigger geophone was placed at the shot point and the first geophone was connected to the second take-out, whose offset depended on the total spread length. A 14 lb sledge hammer and a metal plate were used as the seismic source, and the data were recorded into 12 channels. The line was reversed by placing the source and trigger at the opposite end of the spread, disconnecting the geophone from that end and then reconnecting it to the first take-out, which was positioned at the previous shot point. Although the strategy did vary, generally at any one site data were collected from a 120 metre spread, and then from a 24 metre line. This was done to calculate the thickness and velocity of any near surface *low velocity layer*, which is accounted for when interpreting the longer spread.

Due to constraints imposed by the availability of suitable seismic sources and the near surface velocity structure the maximum refraction spread length was limited to 120 metres, because when greater offsets were attempted seismic signals could not be resolved from the ambient 'noise' due to severe energy attenuation. Therefore, depending upon the sub-surface geometry and velocity structure, the maximum penetration was approximately 50 metres.

The line positions were obtained by taking bearings from prominent landmarks and by measuring from the shot points to field boundaries. The refraction lines could then be accurately marked onto a base map with an error of less than two metres.

Geophysical and geological interpretation

Multiple dipping layers were encountered at the majority of sites, with 3 or 4 layers of differing velocity. This, coupled with insufficient overlap of corresponding refractors, on the reversed time-distance graphs, limited the type of analysis which could be applied to the data *i.e.* the data could not be processed using the *Generalised Reciprocal Method* (Palmer, 1980). The depths to the refractors, beneath the shot points, and their relevant velocities were calculated assuming a plane layer forward model (Appendix 3.1).

Seismic reflection surveying

Background

The seismic reflection method utilizes arrivals of energy that vary systematically from trace to trace, believed to represent energy reflected from sub-surface acoustic impedance interfaces (Sheriff and Geldart, 1995). The arrival travel times for reflection events are measured for various geophone groups, from which the location and geometry of the sub-surface interfaces can be calculated. Seismic reflection sections are often referred to as *normal incidence sections* and an important aspect of their geometry is the displacement of a reflection point (which corresponds to a data point) along the traverse. This dynamic shift or *normal moveout* (NMO) is defined as the difference between a recorded reflection time, for a source-receiver pair, and the corresponding normal incidence reflection time at the midpoint between the source and receiver.

For the simplest case when a plane horizontal reflector is overlain by a homogenous medium of constant velocity (Figure 3.5), the travel-time between a source and receiver is described by:

$$t = \frac{2\sqrt{h^2 + (x / 2)^2}}{v} \qquad 3.6$$

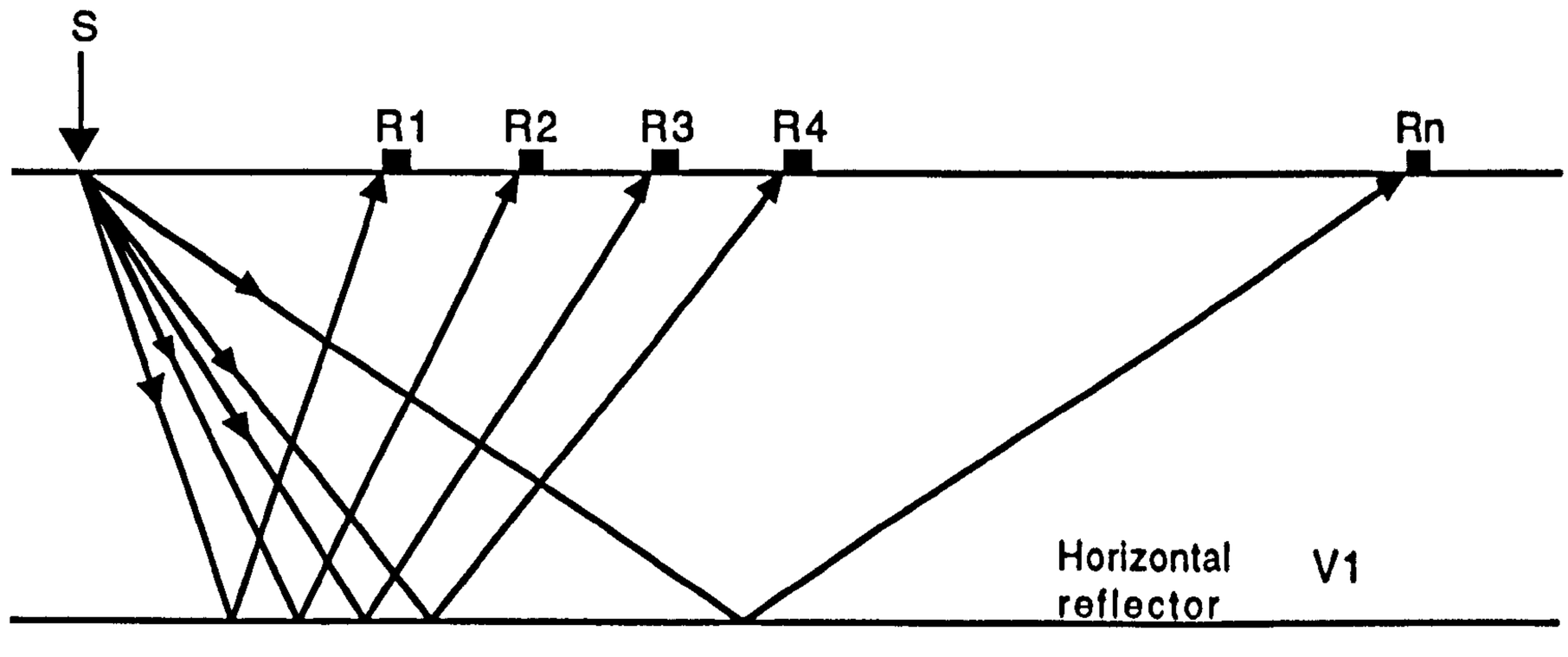

Figure 3.6 Raypaths between a single source and a series of receivers

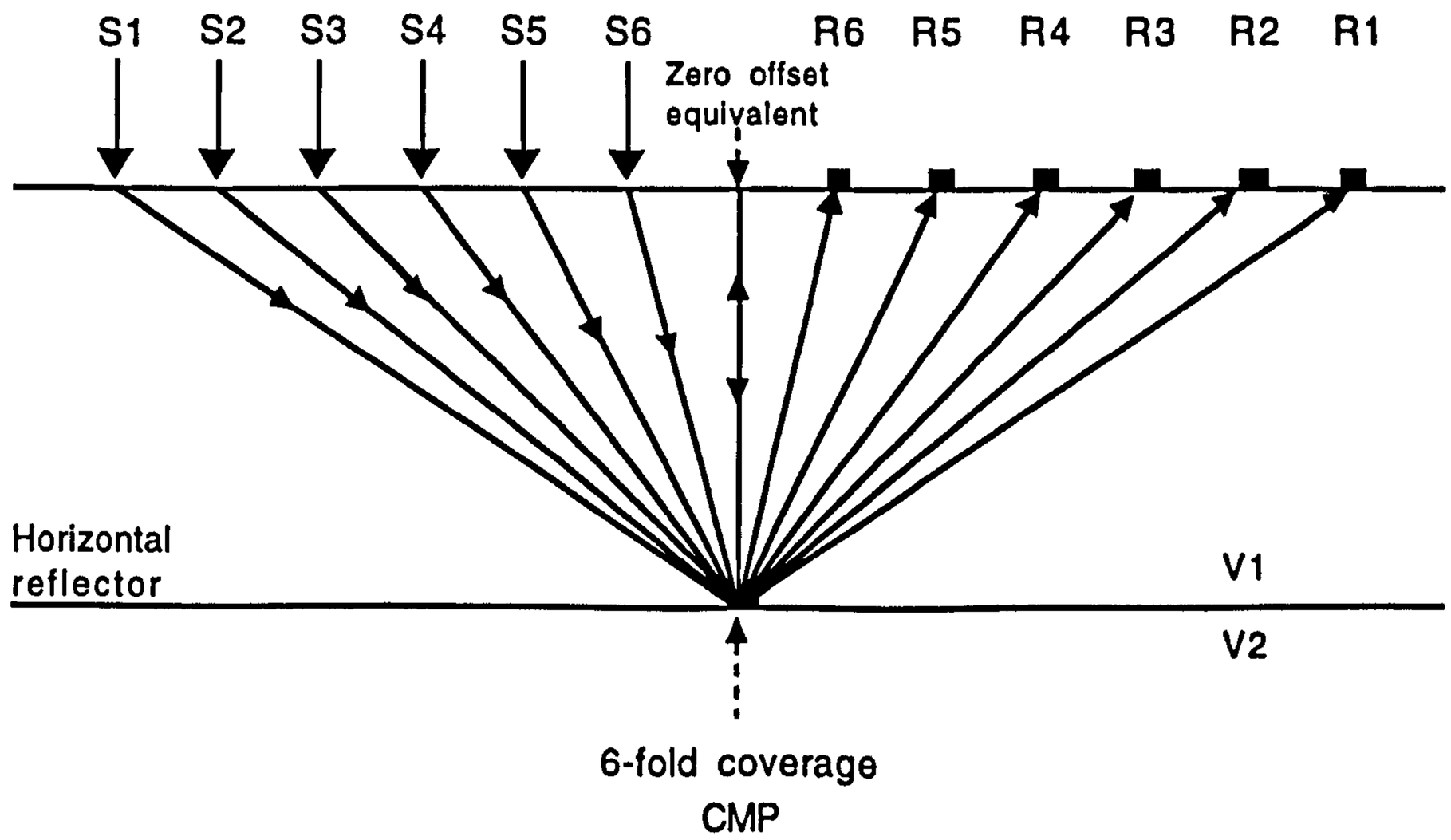

Figure 3.7 Raypaths between source and reiceivers for a CMP with 6-fold coverage

where x is the source-receiver offset, t is the travel time, v is the seismic velocity and h is the depth to the reflector. At normal incidence the travel time (t_0) would be $t_0 = 2h/v$, and is often termed two way travel time. The increase in travel-time from t_0 with offset effectively defines the NMO, and can be simplified as:

$$t^2 = t_0^2 + \frac{x^2}{v^2} \qquad 3.7$$

The affect of NMO causes travel times, for a shot and geophone array, produce a hyperbolic curve when plotted on a time distance graph (Figure 3.6).

Extending this model to n horizontal layers, of differing thickness and velocity, the equation becomes:

$$t^2 = t_0^2 + \frac{x^2}{v^2_{rms}} + c_1x^4 + c_2x^6 + \ldots . \qquad 3.8$$

where v^2_{rms} is the root-mean-square velocity and c_i is a function of the thickness and velocity of the n layers. In the case of a dipping reflector the affect of NMO is the same, but the apparent velocity is altered by:

$$t^2 = t_0^2 + x^2\cos^2\alpha \,/\, v^2 \qquad 3.10$$

where α is the component of dip.

Multi-channel reflection seismics

In multi-channel data acquisition, a series of source and receiver offsets are combined to increase the signal to noise ratio by stacking individual traces with the same subsurface *common mid-point* (Figure 3.7). When processing the data, traces contained within reflection shot records are sorted into common mid-points (CMP), using the source and receiver positions, and prior to stacking, the individual traces within a CMP-gather are corrected for normal moveout. This results in a series of zero-offset traces which can be stacked to produce a final time section. As well as improving the signal-to-noise ratio, stacking partly attenuates multiple energy produced by interlayer reverberations. The NMO corrections, made when stacking CMP gathers, provides

information on the velocity structure which can be used to convert two-way travel time into depth. The final stacked output represents a zero-offset section, which may be taken to approximate the geological structure.

Seismic methods have been applied mainly in the exploration of oil and gas, but with the development of new improved seismic sources giving improved penetration and/or resolution (Doornebal and Helbig, 1983) multi-channel data acquisition techniques have been adapted to suit a wide range of land based investigations (Bredewout and Goulty, 1986; Knapp and Steeples, 1988; Jongerius and Helbig, 1988; Brabham and McDonald, 1992; Miller *et al.*, 1992; Miller *et al.*, 1995; Jeng, 1995). To conduct a successful survey, detailed consideration must be given to the acquisition system which consists of a seismic source, geophones, geophone cables, amplifiers/filters (which condition the signal), analogue to digital converters and the data storage device (seismograph). For instance, high frequency geophones are also usually used for high resolution shallow reflection work. Furthermore, Miller *et al.* (1995) conclude that in situations where the surface materials are composed of fine grained saturated sediment, down hole sources work extremely well whereas if the surface is hard, weight drop sources should be used. The selection of a suitable source depends upon the near surface conditions (Miller *et al.*, 1995) and the use of an unsuitable source can result in poor data quality.

Shallow seismic investigations are particularly suited to in intertidal environments for a number of reasons. Firstly, as the near surface sediments are generally saturated the majority of the seismic energy is allowed to penetrate into the subsurface rather than being absorbed or internally reflected within a near surface low velocity layer. Secondly, the seismometers (geophones) can be placed beneath the surface to improve ground coupling and reduce ambient environmental noise. Furthermore, as beaches are often easily accessed, the logistical problems encountered when surveying on land are generally avoided.

Although shallow seismic investigations are commonly applied to coastal engineering problems their application in the analysis of Quaternary environments is relatively limited until recently, but is rapidly increasing. High-resolution seismic profiling is applied in this study to investigate the sub-surface geometry of reflectors beneath the Pendine Sands to improve models of the subsurface lithology produced by refraction analysis within the burrows and the back-barrier area.

Seismic reflection data acquisition and position fixing

Data were acquired using 12 & 24 channel ABEM Teraloc Seismic System, 24 geophones, two 12 channel geophone cables, a Geostuff (Model RS-48/24) Rollalong Switch, together with a 14 lb sledge hammer and steel plate. A refraction traverse was used to establish the optimal reflection geometry *i.e.* a suitable geophone spacing and shot offset. Once the two cables were laid out, and the geophones connected, the cables were attached to the rollalong switch. The switch was then connected to the Teraloc and the trigger geophone was placed at the shot point. Once five shots were recorded the shot point and switch were advanced and the process was repeated. When the shot point had advanced twelve times the first cable was disconnected and reconnected to the end of the second cable. In doing so the reflection traverse advanced across the beach surface. Using this *common mid-point shooting* technique 6-fold coverage was achieved *i.e.* a maximum of six traces shared the same CMP. The raw data were recorded using zero-delay over record lengths of 100 & 200 milliseconds, gain was applied and where appropriate the signal was passed through bandpass filters (10-600 dB).

On the Pendine Sands the position fixing was done by surveying near prominent landmarks and by taking a number bearings. Using these two methods the positions of the reflection lines could be obtained with an accuracy greater than that provided by non-differential GPS.

Data processing

The data were processed using two packages, QSEIS and the UNIX based SierraSEIS system (Halliburton Company, Precision Software Solutions). QSEIS was used initially to process the data because at that time there was no available software to convert the Teraloc files to a SEGY format suitable for SierraSEIS. A Basic program was developed to convert the Teraloc files to OYO format so the data could be processed using QSEIS. Due to the lack of sophistication of the software data processing was very cumbersome and the types of velocity analysis, available to establish the velocity structure prior to stacking were very limited. It was for this reason that when the Teraloc files could be converted to SEGY format the majority of the reflection data from Pendine Sands was reprocessed using Sierra SEIS.

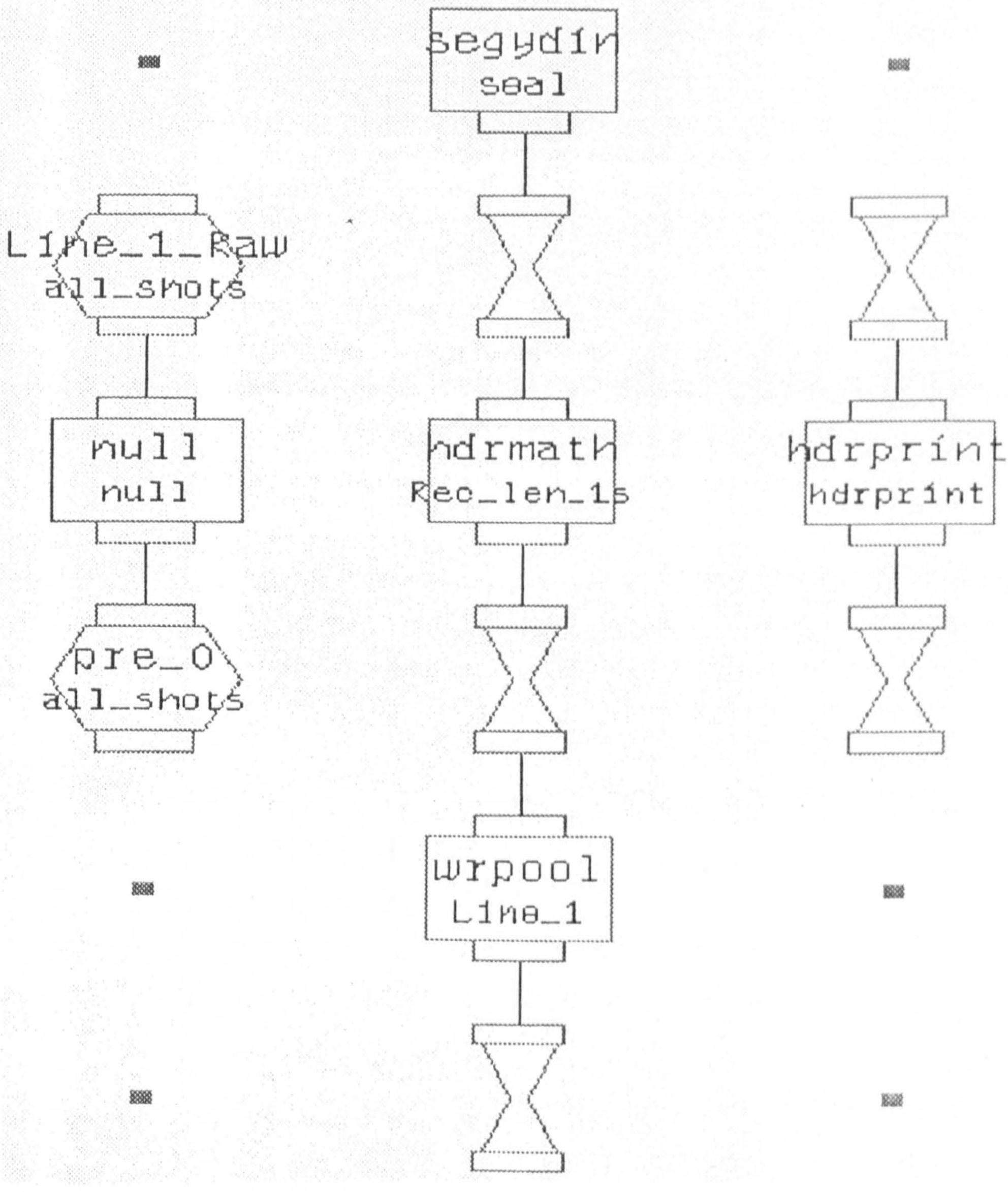

Figure 3.8a The processing routine used to read SEG-Y data from disk into SierraSEIS.

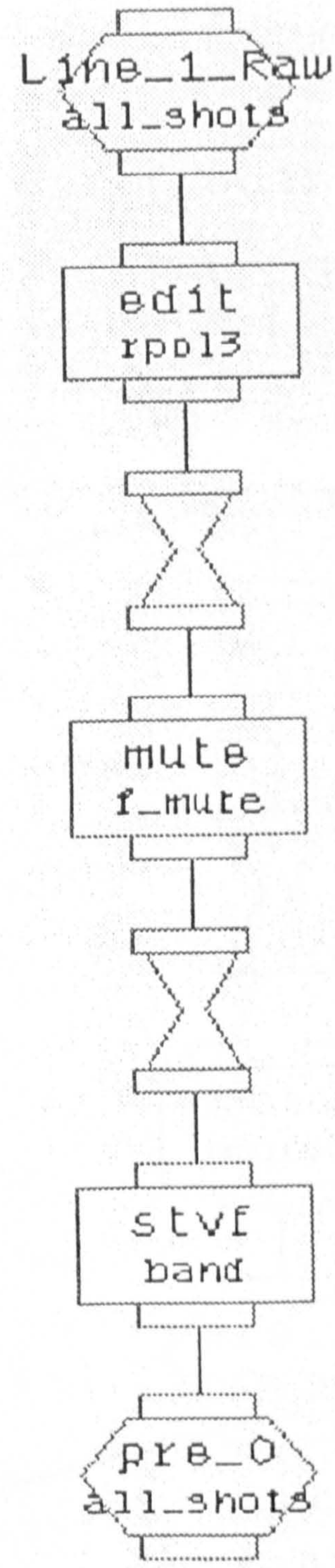

Figure 3.8b The pre-stacking processing routine.

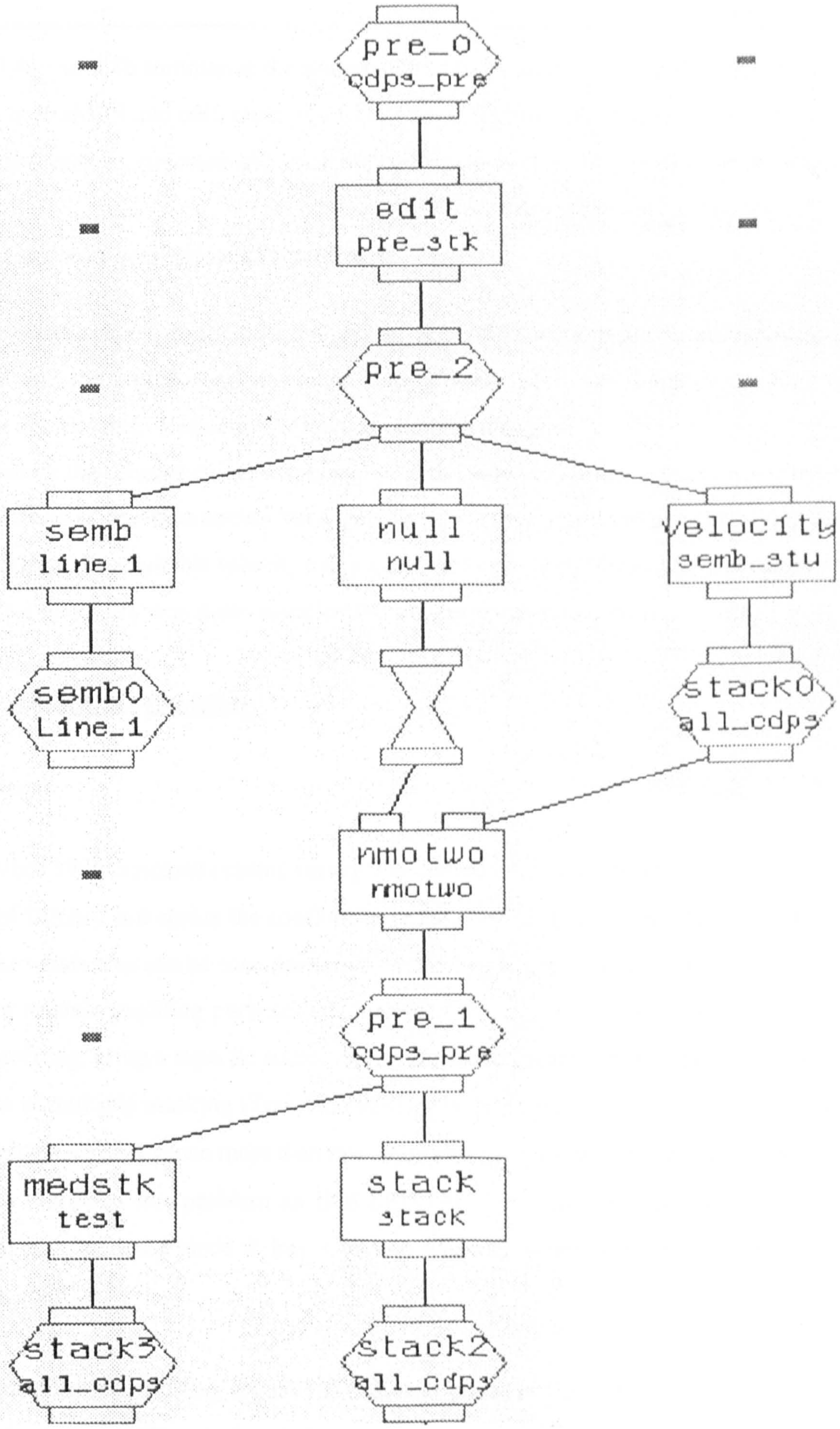

Figure 3.8c The processing routine used to define the velocity structure, correct for normal moveout and stack CDP gathers.

Figures 3.8a and 3.8b summarise the processing routines used to read in the SEG-Y data from disk into SierraSEIS and edit, mute and filter traces. Figure 3.8c displays the routine used to establish the velocity structure and stack the CMP gathers to produce a final stacked section.

Geophysical and geological interpretation

Using the final stacked sections, which represent zero-offset sections, the seismic reflectors were identified and their geological character was inferred using the semblance velocities and reflection coefficients. Refraction velocities obtained along the reflection traverses were used to corroborate the semblance velocities and tune the velocity structure used in the final stack. The conversion of the 'time section' to a 'geological section' was done by multiplying the two-way travel times by a suitable velocity using a layer cake method (McQuillin *et al.*, 1984); where the reflector geometry was more complex this conversion became more intricate.

Marine reflection profiling

Background

In September 1993, a marine seismic survey was carried out within the upper and lower reaches of the Taf Estuary and across the confluence of the rivers Taf, Towy and Gwendraeth (Figure 5.13). The whole area can be considered to be a 'shallow water environment' (5-15 metres water depth) for seismic profiling purposes. Under such circumstances the traditional approach to seismic profiling, using a separate source and hydrophone streamer, would probably suffer from the effects of multiple masking (Trabant, 1984), where the real reflector signal is obscured by events which have undergone more than one reverberation cycle within the water column. In an attempt to minimise this problem an IKB-SEISTEC™ profiling system, developed by IKB Technologies, was used since it has a quoted working water depth of less than 2 metres (Simpkin, 1993).

In seismic reflection profiling acoustic signals transmitted by a surface towed seismic source, reflected from the sea-floor and underlying strata, are detected at the surface by a hydrophone or a series of hydrophones making-up a streamer. Hydrophones consist of piezo-electric acoustic

crystals which generate a small electric current in response to the pressure of the returned acoustic signals and ambient noise. Hydrophone cables contain a number of these crystals and when profiling the streamer needs to be set below the sea-surface to reduce noise from surface waves and cavitation. The buoyancy of the hydrophone cable has to be balanced to maintain the cable at a specific depth beneath the sea surface.

The SEISTEC profiler combines a *Boomer* source and a *In-line cone* receiver (Simpkin, 1993), both of which are mounted onto a single catamaran which is floated and towed behind the vessel (Figure 3.9). The profiler minimises multiple masking by fixing the geometry of the source and receiver, in respect to one another and the sea surface, and by using an In-line cone system which focuses the return signal thus cutting out much of the multiple energy (Figure 3.10). It is by design that the SEISTEC system is able to successfully record reflection data in shallow water environments

Data acquisition, processing and position fixing

The survey was conducted using the SEISTEC's standard components, power for the boomer source was provided by a 240 Volt generator through a Geopulse Power Supply (Model 5420A). The signal was processed using the IKB Dual Scope Signal Processor (Model SPA1) and the data were recorded on a Waverley Thermal Linescan Recorder (Model 3700).

Voltage and frequency selection was accomplished by changing two plug-in configuration boards within the power supply. As the unit uses filters to suppress high current surges a smaller generator than usual is required to power the boomer; a second generator was used to run the SPA1 and Thermal Line Scan Recorder. An energy level of 175 Joules was used with the internal trigger mode and the data were recorded with a sweep time of 30 milliseconds. The SPA1 is a single channel analogue signal processor. When recording data from the Taf Estuary, a fixed gain of 20dB, a 6.3 kHz low pass filter and a 1 kHz high pass filter were applied to the signal.

Within the Taf estuary, the data were recorded between the fixed geographical points used to level the main channel. The survey vessel position was logged every four seconds using non-

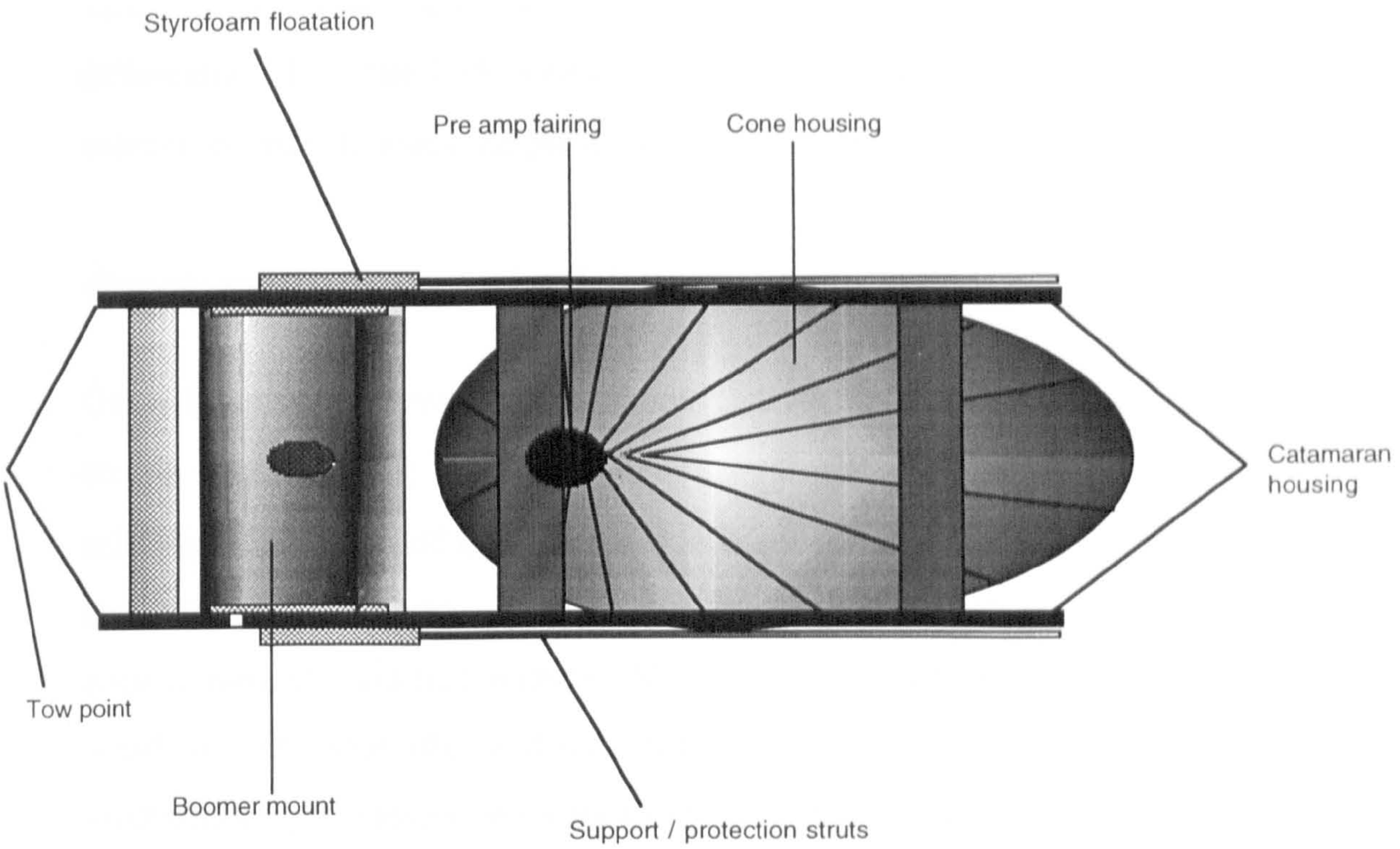

Figure 3.9 Plan view of the IKB-SEISTEC

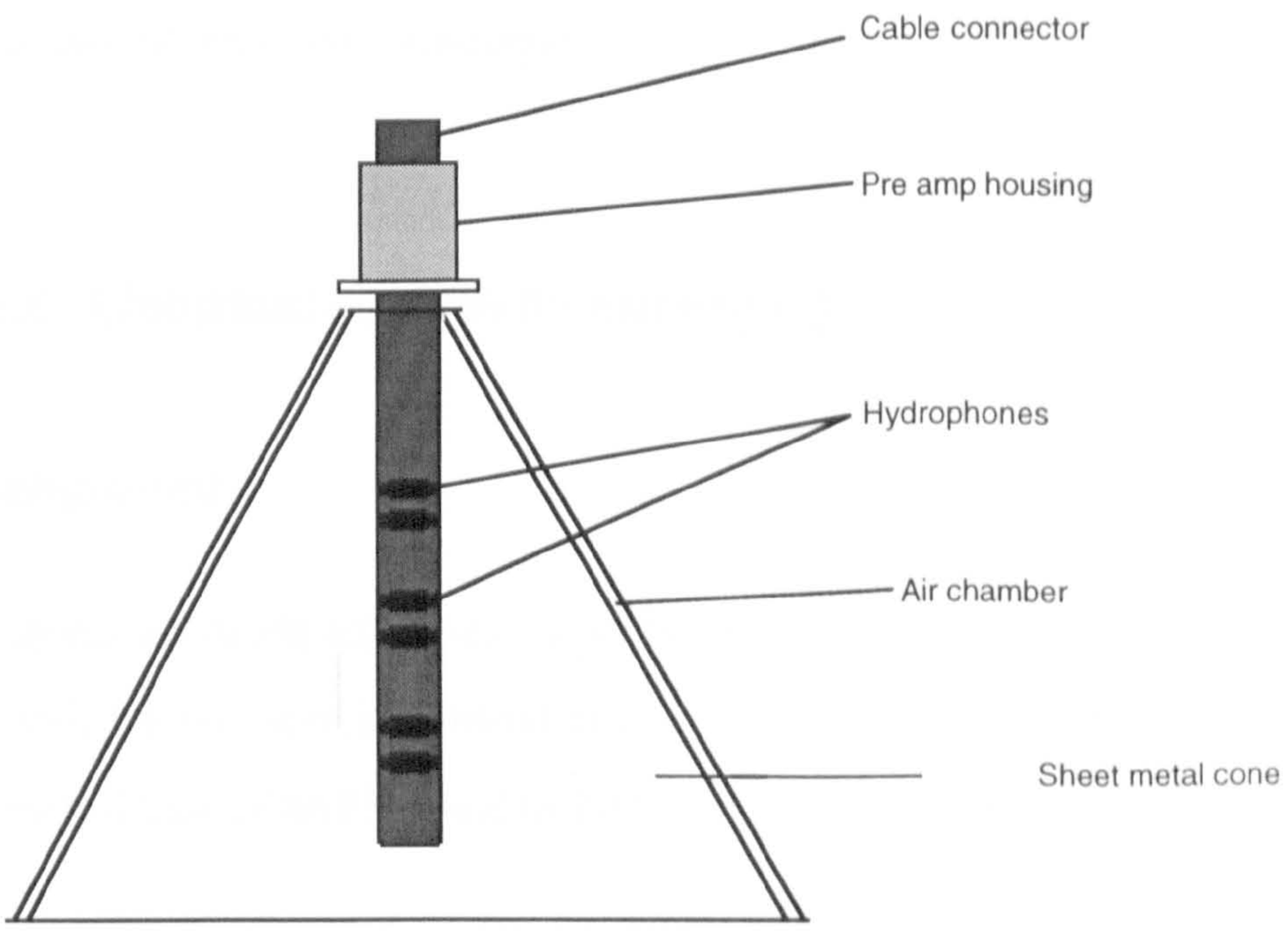

Figure 3.10 The 'Line and Cone' reciever.

differential GPS. The GPS positions were compared to the fixed geographical points within the estuary in order to asses the position fixing accuracy.

Geophysical and geological interpretation

Other than the primary signal processing described above no subsequent processing was carried out on the data. The seismic reflectors were identified on the records and then compared to refraction data acquired from the sand flats within the Taf Estuary. Further information used to aid the interpretation was obtained from exposures within the estuary, associated with reflectors approaching the sea-bed surface. Velocities, required to convert the two-way time data to a depth section, were obtained from the refraction data and the times through each layer were multiplied by a relevant velocity to yield depth. In doing so the depth to each reflector was determined in turn using a 'layer cake' method (McQuillin *et al.*, 1984). By combining seismic velocities and lithological 'ground truth' information, obtained from outcrop data, it became possible to make estimates as to the geological character of the reflectors and the relative thickness of Holocene sediments.

6.1.6 Electrical resistivity surveying

Background

Electrical methods are based upon the application of an artificially produced current into the ground, whose flow is controlled predominantly by pore waters. *Ohm's Law* states that the current (I) transmitted is equal to the voltage (V) across the ground, divided by the resistance (R):

$$I = \frac{V}{R} \qquad 3.11$$

The resistivity (ρ) is the resistance of a unit cube to a current passing between opposite faces and is measured in ohm-metres. Resistance is therefore given by:

$$R = \frac{\rho x}{A} \qquad 3.12$$

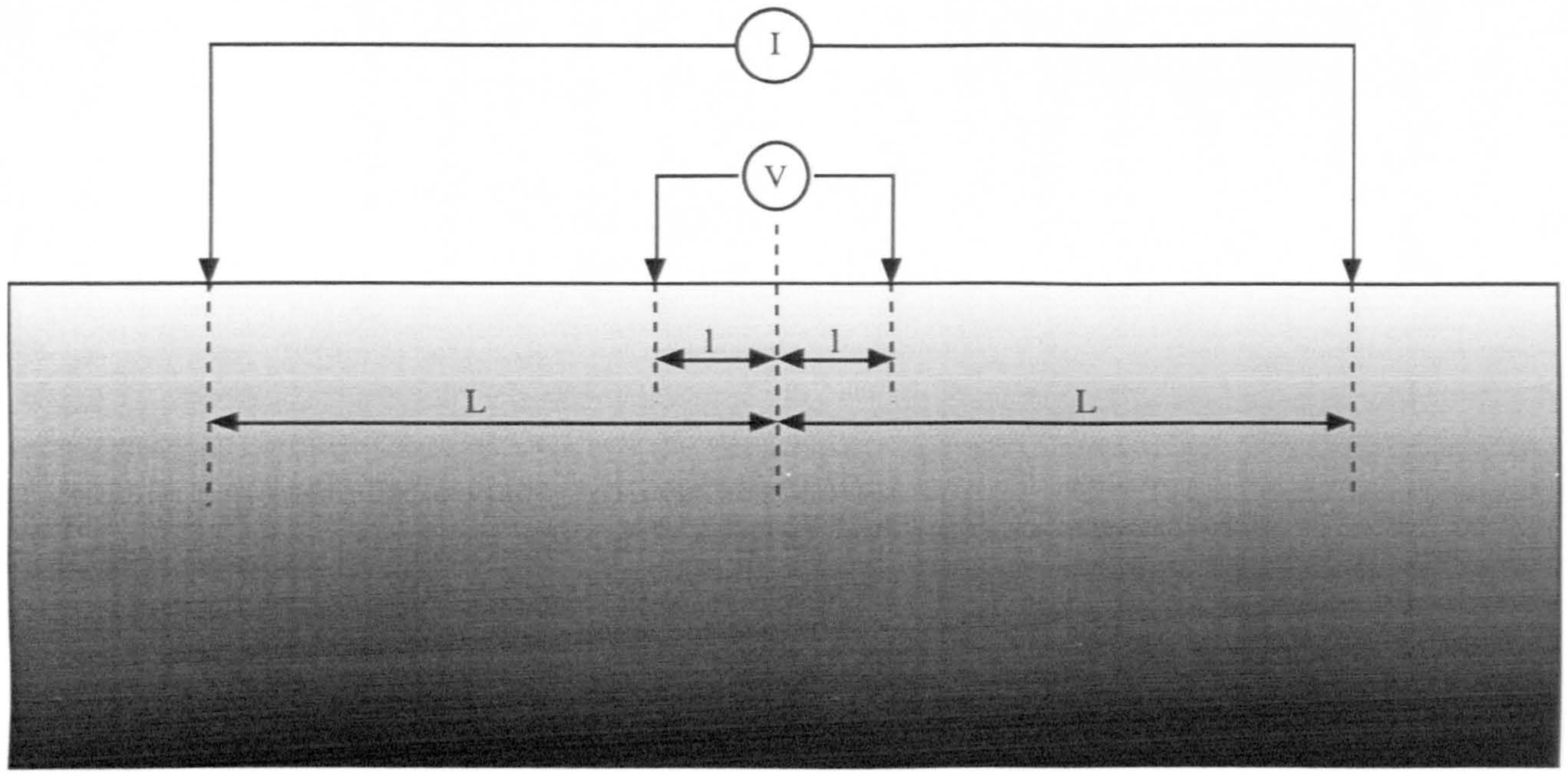

Figure 3.11 Schematic diagram showing the expanding Schlumberger electrode array

where x is the distance the current must travel and A is the cross-sectional area. Numerous arrays are used to make resistivity measurements and any specific value of resistivity, obtained using a particular electrode configuration on the surface, can be considered to be some form of 'average' of the underlying medium. These values are referred to as *apparent resistivities* (ρ_a).

The Wenner and Schlumberger arrays are two commonly used electrode configurations which are favoured for 'depth sounding' (Telford et al., 1990). The Schlumberger array is an 'expanding' electrode system which consists of two current and two potential electrodes (Figure 3.11). When using this system both current electrodes are expanded outwards from an inner potential pair until the potential difference becomes too small to measure. The potential pair spacing is then increased and the current electrodes are further expanded. Each time the current electrodes are moved the resistance is measured. The apparent resistivities, calculated from the measured resistance and a geometric factor, are then plotted against the electrode separation on logarithmic paper. Although the depth to which a fraction of the current penetrates is in general increased by increasing the current electrode spacing, the lithology can have a profound affect upon current penetration into the ground (Telford *et al.*, 1990).

In a simple two layer case, the 'shape' of the resistivity electrode separation curve depends upon the resistivity contrast between the two layers and thickness of the upper layer. Resistivity curves are interpreted using a series of 'master curves', the selection of which depends upon a qualitative estimate of the number of layers present. As the direct interpretation of resistivity cures is a complex and sometimes subjective procedure, computer packages designed to process and model resistivity data are commonly used.

Data acquisition

Geopulse and ABEM terrameters were used, together with four electrodes and four cables, to conduct a series of Schlumberger depth-soundings behind the barrier. The maximum current base separation used in this study was restricted to 300 metres by the length of the cables connected to the current electrodes (150 metres). Further restrictions were imposed by field boundaries. At some sites a greater separation would have been desired.

Data processing and interpretation

The data were processed using the PC-based package RESIXS-Plus. The apparent resistivities and corresponding electrode spacings were input into the together with an initial estimation of the number of layers, their relative thickness and resistivity. The computer makes a forward calculation to compute a synthetic sounding curve from the initiation ground model which can be compared to the original measured curve. The model can then be fine tuned to provide a better fit of the measured data by trial and error. Alternatively an iterative procedure can be used to provide a best fit model using a least squares method.

Estimates of the geological character of the layers are inferred by comparing the modelled resistivities to published values of resistivity for common materials (Griffiths & King, 1981).

3.2 Laboratory procedures

Heavy mineral analyses were used to investigate the sources of materials presently accumulating within the Taf Estuary. Samples, taken from cores recovered within the estuary and back-barrier area, are compared to sands from Carmarthen Bay and other potential sources in an attempt to elucidate spatial and temporal changes in the sedimentary dispersal patterns during the late Holocene. X-Ray Diffraction Analyses were used to determine whether there are any significant temporal or spatial changes in clay mineralogy, and to correlate these to similar changes in the composition of the heavy mineral assemblages.

Environmental magnetic measurements were used to correlate cores recovered from the West Marsh and more detailed measurements undertaken on cores recovered from East Marsh were used to analyse variations in the magnetic mineral compositions of sedimentary units within the back-barrier complex. No attempt was made to trace sediment source using magnetic measurements; this analysis was conducted as it is a relatively rapid, nondestructive and inexpensive means of comparing a large number of samples.

Foraminiferal analyses were used to identify back-barrier facies changes and to infer local relative sea-level tendencies within West and East Marshes. This information can be used to generate hypotheses which aim to describe the evolutionary history of the barrier complex and the mechanisms which cause those changes. The aim of conducting pollen analyses were two fold. First, to elucidate regional changes in vegetation for comparison with well dated regional pollen records. Second, to provide evidence for local ecological changes within West Marsh.

The purpose of radiocarbon dating was to establish a chronostratigraphic framework for the studied sequences and provide a timescale over which the barrier complex developed; the sampling strategy was therefore designed to date the main phases of organic accumulation in West Marsh. Grain size analyses were used to determine the composition of the back-barrier and estuarine sediments, and provide supplementary evidence for the interpretation of heavy mineral assemblage data.

3.2.1 Heavy mineral analysis

Introduction

Assemblages of heavy minerals, which rarely constitute more than 1% of a sediment, have been used for many years to analyse sedimentary sources and transport paths (Griffiths, 1967). The technique is based upon the assumption that every potential sedimentary source possesses its own unique assemblage of heavy minerals. The first step in the analysis is to search for a unique heavy mineral which ties the sediment to a unique source. Where this proves unsuccessful the emphasis is switched from unique minerals to unique assemblages reflected in the bulk mineralogy of the heavy fraction. However, to trace sedimentary dispersal patterns prior knowledge of both the potential sources and their heavy mineral compositions is required.

Hydraulic relationships between light and heavy minerals

An understanding of the processes which result in the transport and deposition of sand grains is necessary before useful interpretations can be made using heavy mineral data. The concept of hydraulic equivalence and the relationships between light and heavy minerals was first considered by Rubey (1933). He stated that 'whatever the conditions may have been which permitted the deposition of quartz grains of a certain size would also permit the deposition of magnetite grains (of a size) that had the same settling velocity'. Rubey used known settling velocity laws to calculate the grain diameter ratios of hydraulically equivalent minerals within a deposit; these ratios are inversely proportional to a power of the ratios of their densities. The theory therefore states that when two detrital minerals accompany each other, in a sediment or sedimentary rock, they must be hydraulically equivalent.

Subsequent studies reveal that in most natural sands and sandstones light and heavy minerals are rarely hydraulically equivalent (Rittenhouse, 1943; Briggs, 1965; Lowright *et al.*, 1972; Slingerland, 1977). Hydraulic inequivalence either results from differentially inherited mineral size restrictions within the source materials, or is caused by the differential transport of particular minerals within the sand fraction.

Rittenhouse (1943) and Briggs (1965) have both published data which supports the first hypothesis; however, Lowright *et al.* (1972) have shown that it is differential transport, not source restrictions, which result in the observed deviations from hydraulic equivalence in most natural sands. They examined the distribution and settling velocities of both light and heavy minerals in river, beach, dune, offshore sands and Pleistocene till near Presque Isle, Lake Erie. The results indicate that due to an 'equivalent range of heavy mineral sizes' within the tills no source availability problem existed for the larger heavies. Even so the largest and smallest heavy minerals, present within the source material, were absent from the Presque Isle beach or dune sands, subject to over 20 miles of river and longshore transport (Lowright *et al.*, 1972).

Lowright *et al.* (1972) conclude that 'source influence' extends to the river mouth and that only five miles of longshore transport is required to selectively remove the smallest and largest heavy minerals. In this instance differential entrainment by longshore processes selectively sort the heavy minerals and result in hydraulically inequivalent sands.

The differential entrainment theory was further extended by Slingerland (1977). He developed critical entrainment and critical suspension velocity equations to explain the effects of entrainment, with respect to settling velocities, on grains of differing density contained within the sand fraction. Using the critical equations, supported by experimental data, Slingerland (1977) constructed a four-fold classification of constant terminal settling velocity (CTSV) and in doing so placed boundaries on the hydraulic equivalent sizes of light and heavy minerals. He used a range of boundary Reynold's numbers (R*) and the ratio heavy mineral grain size to the bottom roughness grain size (d_h/ BKS). If R* is less than five and d_h/BKS is roughly one then this combination will result in a heavy enriched well sorted medium sand deposit. Slingerland (1977) states that deviations from standard hydraulic equivalence (SHE) not only result from transport distance but are primarily controlled by hydraulic and boundary roughness conditions.

Slingerland (1984) considered the role of hydraulic sorting in the origin of fluvial placers. He subdivided sorting into entrainment sorting and differential transport; the latter is influenced by entrainment as well as the motion and mean velocity of a grain already moving in the flow. Differential transport therefore includes both entrainment and suspension sorting. Slingerland concludes that heavy mineral enrichment, on any scale within streams, occurs in response to selective sorting by size and density due to differential entrainment, differential suspension,

differential bedload transport, and shear sorting or kinetic sieving. For instance heavy minerals are concentrated on the backs of mega ripples as larger and typically lighter grains are more readily entrained and transported than the smaller denser grains.

Li and Komar (1992a) examined longshore grain sorting and beach placer formation, on beaches adjacent to the Columbia River. The results reveal a complex pattern of sorting which they interpreted at representing three superimposed levels of sorting. The first level of sorting involves the selection of which grains remain on the beaches as opposed to those which move offshore. Li and Komar argued that this process is controlled by particle settling velocities; particles with low settling rates, compared to turbulence velocities within the surf zone, are preferentially moved offshore. They also analysed the settling velocity distributions for the principle heavy minerals within beach sands and found an inverse relationship between the densities of individual minerals and their median diameters.

Beyond 10km distance, from the mouth of the Columbia River, the median grain sizes and settling velocities decreased. Li and Komar suggest that after being delivered to the beach, from the Columbia River by settling velocities, the sediments undergo a second level of sorting during longshore transport and that settling velocities continue to be important to that sorting. The dependence on settling velocities suggests that longshore transport occurs as suspended load, possibly within the high energy beaker/surf zone. Li and Komar (1992a) also argued that as grain-settling velocities increase, in the longshore direction, differential grain settling plays a minimal role in concentrating heavy minerals close to the river mouth. They concluded that the sorting of individual minerals within placer deposits depends upon their densities and median diameters; the higher the density and smaller the diameter the more concentrated the mineral is within the placer. The mineral is then less likely to move longshore away from the river mouth (Li and Komar, 1992a). Superimposed on this is selective sorting due to selective entrainment and transport, during periods of beach erosion, which effectively modifies sorting due to differential settling velocities. Li and Komar (1992a) concluded that sorting by contrasting entrainment stresses and differential transport rates are the main cause of heavy mineral concentration close to the mouth of the Columbia River.

Spatial variations in heavy minerals and patterns of sediment sorting along the Nile Delta exhibit a similar relationship (Frihy *et al.*, 1995). Lower density and coarser sized minerals are

selectively entrained by waves and currents in areas of beach erosion are subsequently transported and deposited in zones of beach accretion. Conversely, higher density smaller sized minerals are concentrated in areas of beach erosion. Frihy *et al.* (1995) also discovered a distinctive pattern of cross-shore sorting in which heavy mineral concentrations are highest along the shoreline and progressively decrease offshore. They conclude that enhanced levels of high density minerals such as the opaques, rutile, zircon and monozite occur in coastal areas subject to erosion.

Field measurements like those described are supported by both theoretical analyses and laboratory experiments. Li and Komar (1992b) developed a model for selective entrainment based upon flume experiments. The study examined selective transport using an artificial mixture of light and heavy minerals which have equivalent settling velocities, eliminating differential settling as a sorting mechanism. Their results reveal that pronounced sorting occurs as light minerals are preferentially entrained and transported, leaving behind a concentration of heavy minerals. Furthermore, experiments using a range of stresses indicate that as the magnitude of the flow increases the efficiency of mineral sorting and separation decreases. Li and Komar (1992b) concluded that relative grain size as well as mineral density are important factors which influence hydraulic sorting. For instance, as the heavy minerals typically have smaller grains sizes they have larger pivoting angles within the bed fabric and lower protrusion distances into the flow. The results clearly indicate that greater stresses are required to entrain these smaller dense grains into the flow (Li and Komar, 1992b).

Selective sorting of grains by differential entrainment, differential transport and differential settling can significantly alter the heavy mineral composition of fluvial, estuarine, beach and dune sands. Care must therefore be taken when interpreting differences between samples, taken from within the same sedimentary dispersal system, as hydrodynamic sorting processes can mask all but the major changes in mineral composition.

Sample strategy and pretreatment

Material was sub-sampled from a series of short cores (1-4 metres), recovered from the saltmarshes within the Taf Estuary. Fifty grams of sediment were dispersed in sodium hexametaphosphate using a mechanical food mixer. The dispersant was then sieved through a

63μm sieve, and the material which passed through was subsequently used in the investigation of clay mineralogy (section 3.2.2). Samples were taken from sedimentary units which exhibited contrasting textural characteristics, as changes in grain size may reflect changing provenance.

Heavy mineral separation

Light and heavy minerals were fractionated using the method described by Jenkins (1964). Approximately 5 grams of the sand size fraction was placed in a tapered centrifuge tube (M.S.E. 69386) and then dispersed in tetrabromoethane, whose density is 2.95 g/cm. The sample was then centrifuged for ten minutes at approximately 1300 rpm; faster rates shatter the centrifuge tubes. The two fractions were then redispersed (using a glass rod) and recentrifuged so as to increase the separation efficiency. Jenkins (1964) indicates that three successive periods of centrifugation recovers up to 97% of the heavy mineral fraction.

Once the centrifugation was complete the two density fractions were separated by the introduction of a polythene plunger designed to isolate the heavy minerals at the bottom of the tapered tube(Figure 3. 12). The light fraction was then redispersed and filtered under suction through hardened filter paper (Whatman 541). The remaining light minerals and tetrabromoethane were flushed out of the tube and onto the filter paper. The light fraction was then thoroughly washed under suction, using acetone, to remove any remaining tetrabromoethane.

The heavy fraction was dispersed in acetone and the diluted tetrabromoethane was decanted. The minerals were then pipetted onto a watch glass, washed in acetone and placed in a drying cabinet. The dry heavy minerals were weighed, to quantify their total percentage, and split by coning and quartering. In most cases a fraction of the heavy mineral fraction was mounted onto a glass slide using Epoxy Resin (Logitech 2), which has the same refractive index as Canada Balsam (1.54)

Heavy mineral identification

The analysis was accomplished in transmitted light using a Swift Polarising Microscope. Minerals were counted using the Ribbon method whereby all the minerals, along equally spaced

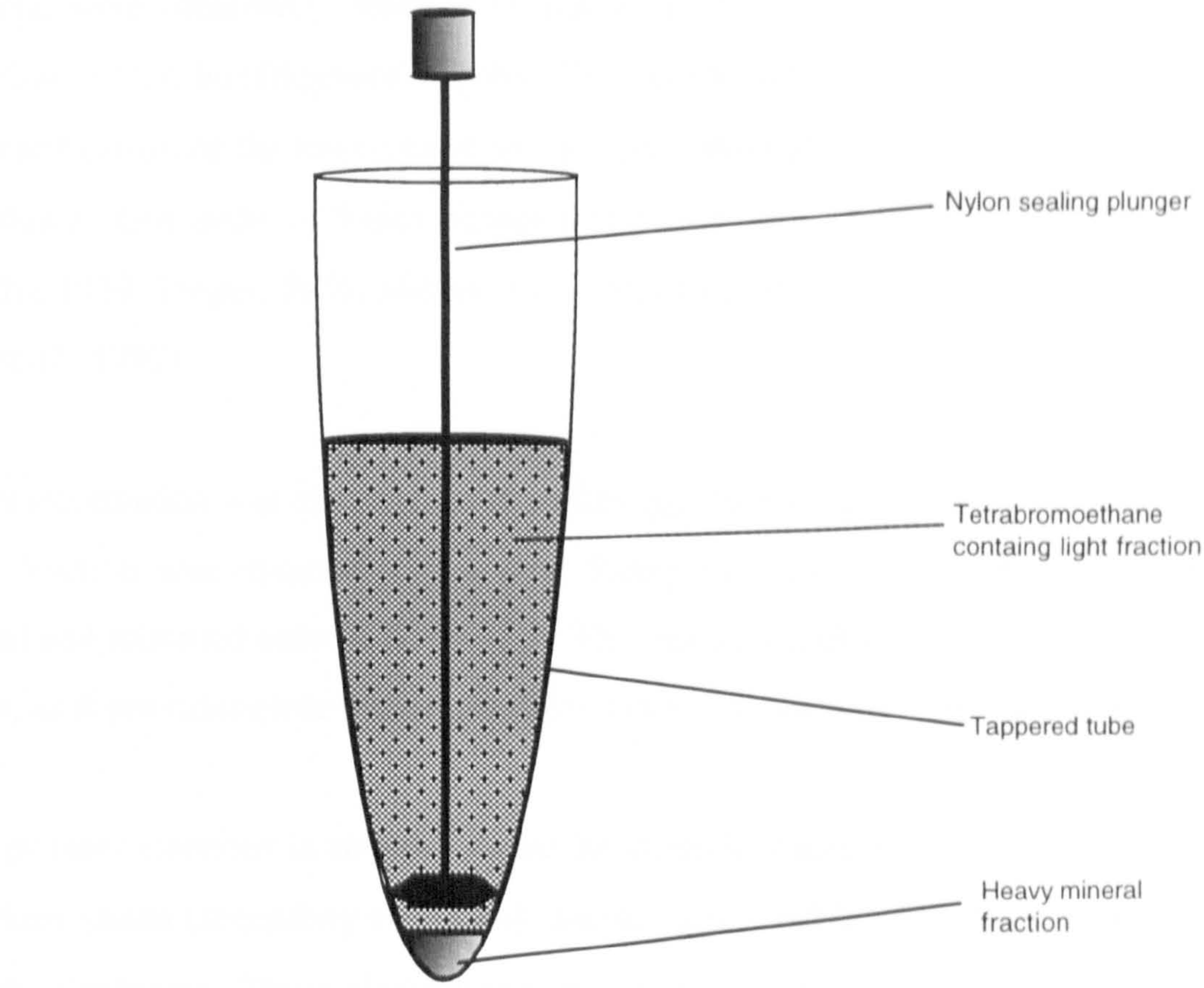

Figure 3. 12 Heavy mineral separation, adapted from Jenkins (1964).

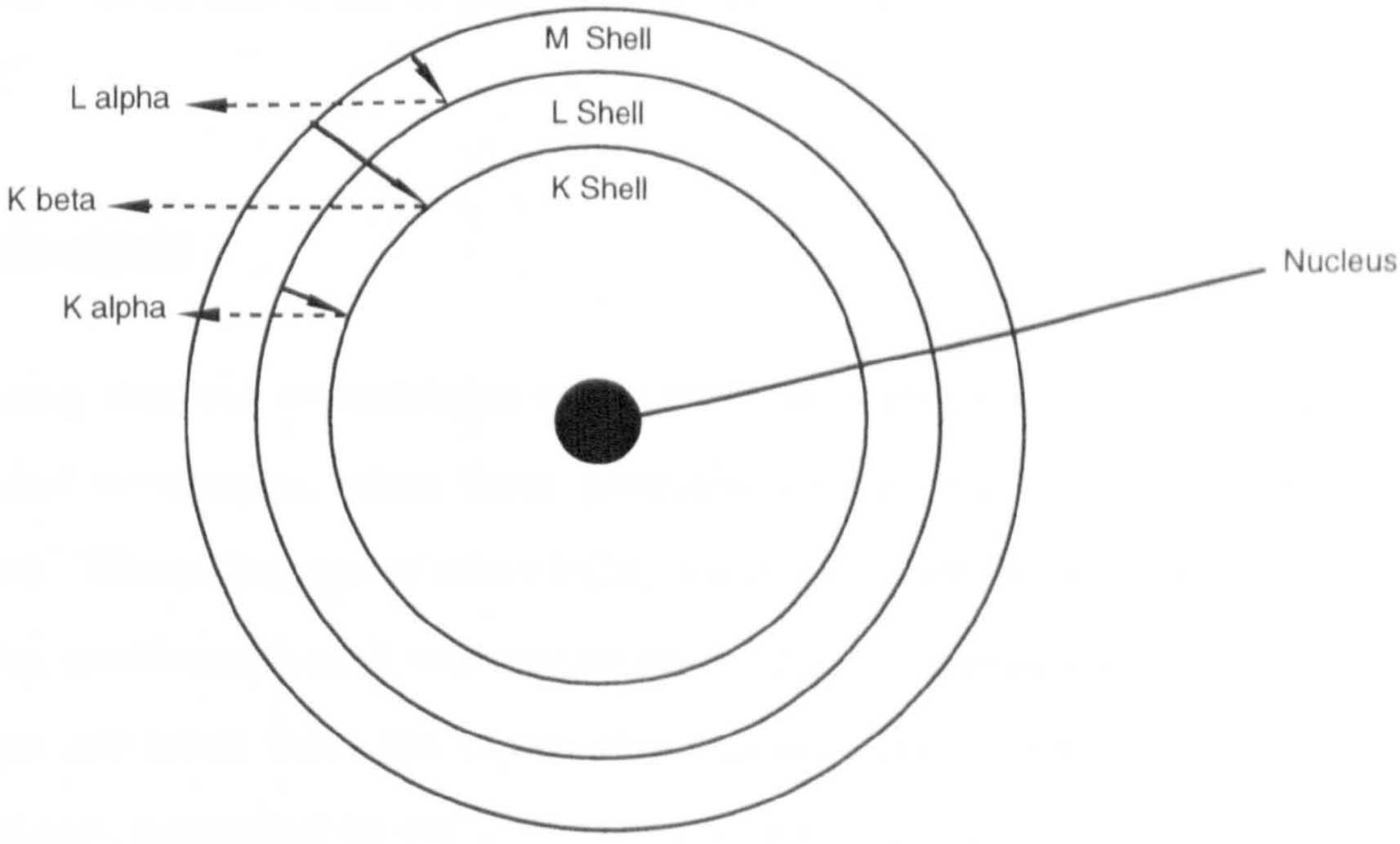

Figure 3.13 Electron transitions in an atom bombarded by an SEM electron beam (Welton, 1984).

transects, were identified. Optical properties such as refractive index, optical orientation, extinction angles, birefringence colours, 2V, pleochroism and the mineral colour were used in the identification of the heavy mineral fraction. Minerals were also compared to a reference collection in University of Wales Bangor and to examples given in the literature (Stuart, 1924; Griffiths, 1939; Troger, 1956; Milner, 1962; Jenkins, 1964; Barrie, 1978, 1980; Gribble, 1988; Deer *et al.*, 1992).

Further information was obtained using an Energy Dispersive X-Ray Spectrometer (EDX). The heavy fraction was immersed in Methyl Salicylate (R.I.=1.54) and specific minerals were pipetted and mounted onto an SEM stub. The minerals and stub were coated in a thin layer of carbon, as it provides clear images but does not hinder mineral identification.

When primary electrons in an SEM ionize the atoms in a mineral, the atoms eject electrons from their inner shells (secondary electrons), and to regain stability electrons from the outer shells enter the vacancies. These electron transitions release specific amounts of energy in the form of X-rays (Figure 3.13), whose energy levels depend upon the difference between the electron shells, differences in electron spin and the number of protons in the nucleus (Welton, 1984). When using the EDX, X-rays emitted from an isolated area of a particular mineral are separated in a multichannel pulse analyser. The major elements (>1%) are represented by peaks, whose energy levels (KeV) are diagnostic of that element. A semiquantitative estimation of each elements concentration can be obtained by calculating the integral of the KeV window (energy range).

Data Analysis

The heavy mineral assemblages obtained from saltmarsh and back-barrier sediments were compared to samples taken from probable source materials using Principle Components Analysis. The advantage of using PCA, which is a preliminary form of factor analysis, is that complex multivariate data sets can be reduced and summarised by the major components of variance extracted from the correlation matrix (Kline, 1994). In plotting the correlation coefficients, generated by the two major principle components of variance, the samples are displayed on scatter graph from which the similarity of samples can be assessed. PCA analysis

does not directly correlate samples but compares them to a particular 'factor' within the data set (Kline, 1994).

3.2.2 X-Ray Diffraction Procedures

Introduction

The minerals contained within the clay fraction of samples taken from core 006, 103 and the back-barrier deposits (P1) were analysed using X-ray Diffraction Analysis (XRDA). These samples are compared to surface sediments taken from the river bank at St Clears, Ginst Marsh and Carmarthen Bay. The analysis is qualitative at best and has been used to indicate the composition and relative proportion of clay minerals within a small number of samples. No attempt is made to either calculate the concentration of particular minerals or to correlate the assemblages contained within different samples.

Sample preparation and strategy

Fifty grams of material was dispersed in sodium hexametaphosphate and distilled water, using a mechanical food mixer. The material was washed into 1 litre measuring cylinder, shaken, and left for 16 hours. The clay fraction, contained within the top 20 cm (*Stokes Law*), was then syphoned off for subsequent analysis.

The clay fraction was divided in two and saturated in either a 0.5 molar solution of magnesium acetate (MgAc), or a 1.0 molar solution of potassium chloride (KCl). The saturated clays were then centrifuged and washed in distilled water, to remove excess Cl and Ac cations. The clay sludge was resuspended in a small volume of distilled water and pipetted onto a glass slide producing an orientated mount. Orientated mounts greatly enhance the intensities of basal reflections as the clay minerals are orientated parallel to the slide surface.

Expandable clays, such as smectite and vermiculite, as well as interstratified minerals, contain numerous cations whose properties vary. In saturating the samples in MgAc and KCl, the cations are replaced by either Ac or Cl making those minerals more easily identifiable.

Additional information is obtained by saturating MgAc mounts in ethylene glycol and by heating KCl mounts to 300°C and 550°C. For instance, smectites swell when saturated in ethylene glycol and kaolinite and vermiculite collapse when heated to 300°C.

Two samples taken from cores recovered within the Taf Estuary were compared to sediments from the barrier complex, a sample taken from Carmarthen Bay and surface samples taken from the contemporary marshes and river bank.

Data Analysis

Clay mineral analysis is generally a qualitative technique whereby the relative concentration of a specific mineral, within an assemblage, may be estimated by approximating the height of the diffraction maxima. Estimates of sediment provenance were inferred by comparing the back-barrier and saltmarsh mineralogy to probable sources and catchment geology.

3.2.3 Geomagnetic measurements

Introduction

The magnetic properties of numerous materials are presently used by scientists world wide to investigate a whole series of environmental problems. Environmental magnetic measurements *per se* are made using the techniques developed by palaeomagnetists to analyse the properties of remanence carrying magnetic minerals in rocks and sediments. Unlike palaeomagnetic studies, which measure the natural magnetic properties of materials, geomagnetic studies measure a series of laboratory induced magnetic properties which relate to the composition of the magnetic mineral assemblage within the sediment *i.e* the size and mineralogy of the magnetic component. Environmental magnetic studies are generally applied to those systems in which magnetic grains have undergone transport, deposition or transformation in response to processes within the atmosphere, lithosphere and hydrosphere. A comprehensive guide to environmental geomagnetics is provided by Thompson and Oldfield (1986) and recent publications which review the potential applications of this field include Oldfield (1991) and Verosub and Roberts (1995).

Magnetic minerals in sedimentary environments

Large multidomain grains of magnetite are generally formed in the earth's interior by slow cooling, whereas smaller single-domain, pseudo-single-domain and superparamagnetic grains are often produced by rapid cooling at the earth's surface or by surface processes such as erosion, weathering, chemical alteration, biogenesis or pedogenesis (Verosub and Roberts, 1995). Magnetic minerals, contained within a source material, may undergo chemical transformations in response to chemical weathering and soil formation. These processes can either be constructive (convert paramagnetic iron to ferri- or antiferrimagnetic forms), transformative or destructive (ferri- or antiferrimagnetic to paramagnetic compounds), leading to significant changes in the magnetic remanent properties of these materials. For instance, Maher and Taylor (1988) describe the inorganic formation of ultra fine-grained magnetite in some UK soils; they suggest that soil derived magnetite may contribute to the remanent magnetism of sediments and can be used to indicate specific erosional events.

Physical weathering, erosion and transport by water, wind or ice can cause changes in the size and shape of the magnetic minerals. This may lead to the formation of pseudo-single-domain or small single-domain grains from larger multidomain minerals (Thompson and Oldfield, 1986). As superparamagnetic (0.001-0.01 μm), small single-domain (0.02- 0.05 μm), pseudo-single-domain (0.08-0.5 μm) and multidomain (> 1 μm) grains respond very differently to the extrinsic magnetic properties, changes in the shape and size of magnetic minerals during physical weathering and transport can lead to the magnetic properties of a sediment being different to the source from which they were derived.

During sedimentation, sorting processes alter the composition of the magnetic and non-magnetic components within a sediment. The deposition of magnetic grains with an equivalent spherical diameter >10μm is primarily controlled by mechanical and gravitational forces rather than by magnetic forces (Ellwood, 1979). As these grains are included in the opaque component of the heavy mineral fraction, the distribution of larger multidomain grains may be influenced by differential entrainment, differential transport and differential settling within the depositional basin. Consequently, the distribution of larger magnetic grains in coastal sands and silts may be significantly affected by selective sorting processes. Deposition in coastal environments is extremely complex and there is a need to differentiate between magnetic variations caused by

changing sedimentary dispersal patterns and those resulting from secondary physical processes within the depositional environment.

Postdepositional diagenetic processes can result in the formation of authigenic magnetic minerals (Thompson and Oldfield, 1986; Oldfield, 1991; Verosub and Roberts, 1995). Fine grained sediments, buried under anoxic/sulphate reducing conditions, often contain trace amounts of iron sulphates. Intermediate ferrimagnetic iron sulphide minerals, such as pyrrhotite (FeS) and greigite (Fe_3S_4) which lead to the formation of paramagnetic pyrite, through sulphurisation reactions, are extremely magnetic and the preservation of these phases within a sediment can significantly affect the magnetic properties of that deposit.

Recent studies have revealed that magnetotactic bacteria are an additional source of authigenic magnetic phases in sedimentary environments (Farina *et al.*, 1990; Mann *et al.*, 1990; Bazylinski *et al.*, 1993). Magnetotactic bacteria, such as *Coccus* and prokaryotes, contain magnetosome chains of either magnetite or greigite, which they use to orientate and navigate along geomagnetic field lines (Mann *et al.*, 1990). These bacteria are able to control the mineralisation of iron sulphide and magnetite, in contrast to the biologically mediated processes which result in sulphate reducing bacteria generating high concentrations of H_2S which subsequently combines with iron to form greigite, pyrrhotite and pyrite (Mann *et al.*, 1990). Claims that fossil magnetosomes can significantly influence the remanent characteristics of sediments has sparked a debate between the 'detrital' and 'biomagnetic' schools of thought (Verosub and Roberts, 1995). Biomagnetic contributions to magnetic remanence in sediments cannot be ignored and recent studies have suggested criteria which can be used to distinguish between biogenic magnetite and other fine grained ferrimagnets in sediments (Oldfield, 1994).

Sampling

Material was sub-sampled at suitable levels from the cores recovered at sites 18, 20, 21,22, 23 and 24. Ten grams of wet sediment was dried at 40°C over night, disaggregated, and then tightly packed into 10 ml styrene sample holders using plastic film.

Magnetic measurements

All the measurements made in this study were done using the equipment in the Department of Geography at Liverpool University. Whole core susceptibility (χ) measurements were obtained for the cores recovered at sites 4, 7, 9, 11 and 12. Susceptibility was measured at 2cm intervals using a Bartington Susceptibility meter connected to a PC. These measurements were designed to provide preliminary data for the correlation of sedimentary units.

Five magnetic properties were measured using the samples taken from sites 18, 20, 21, 22, 23 and 24:

- Low frequency susceptibility ($\chi_{LF} \approx \chi$);
- High frequency susceptibility (χ_{HF});
- Anhysteretic Remanent Magnetisation (ARM);
- Isothermal Remanent Magnetisation (IRM) at 1000 mT (SIRM);
- Isothermal Remanent Magnetisation using successively increasing reverse fields of -20 mT, -30 mT, -40 mT, -50 mT, -100 mT and -300 mT.

The remanence measurements were made using a portable Minispin slow speed spinner Fluxgate Magnetometer. ARM remanence were grown in a modified Molspin AF demagnetiser (*cf.* Oldfield & Yu, 1994) and IRM remanence were grown using a Molspin Pulse Magnetizer.

Processing and analysis

From the magnetic measurements a series of mass-specific magnetic properties were calculated:

- susceptibility ($\chi LF=\chi$) (m^3kg^{-1});
- frequency dependent susceptibility ($\chi_{fd\%}$)(m^3kg^{-1})1;
- ARM (Am^2kg^{-1});
- susceptibility of ARM (χ_{ARM}) (m^3kg^{-1});
- SIRM (Am^2kg^{-1});
- 'Soft' IRM and 'Hard' IRM as well as other ratios and percentages (*cf.* Oldfield & Yu, 1994).

These mass-specific magnetic properties were compared to information summarized in Thompson and Oldfield (1986), Thompson (1986), Maher (1988), Maher and Taylor (1989), Oldfield (1991), Oldfield (1994) and Oldfield and Yu (1994). This comparison formed the basis of the interpretation from which inferences regarding magnetic provenance and the correlation of sedimentary were made.

3.2.4 Foraminiferal analysis

Introduction

Foraminifera are unicellular protists which construct a hard test to enclose and protect soft cytoplasm from predators and unfavourable environmental conditions (Murray, 1979, 1991). The test may also serve as a receptacle for excreted matter, aid in reproduction or provide buoyancy. The test is built incrementally, each addition consisting of a new chamber covering the preceding aperture, to allow cytoplasmic continuity through the test. Since there are limited ways in which this can be achieved many unrelated genera have repeated these arrangements through geological time. Chamber arrangements can be described as *uniserial*, *biserial* or *triserial* and the tests can also posses *planispiral, trochospiral,* or *streptospiral* coiling, as well as discrete or enveloping chambers (Loeblich & Tappan, 1988).

The composition of modern foraminiferal tests are sub-divided into two main groups, agglutinated and calcareous. Agglutinated tests are composed of detrital grains, usually quartz, glued together with an organic cement which often contains iron (Murray, 1979). When constructing a new chamber an agglutinating foraminifera creates a pile of grains at the entrance to its test from which it selects suitable sized particles for building using its pseudopodia. Calcareous tests are composed of calcite, secreted by the foraminifera, which is either arranged in a random fashion or in an ordered radial pattern; these two wall structures are described as porcelaneous and hyaline, respectively (Murray, 1979).

The classification of foraminifera is constantly being revised, as new genera are discovered. Taxonomy is based upon characteristics such as test composition, mineralogy, ultrastructure, and

the method of test construction. It is these features of test morphology which delimit the 12 suborders, 74 superfamilies, 296 families, and 302 subfamilies in which foraminifera are classified (Loeblich & Tappan, 1988). For instance, agglutinated tests are classified in the suborder Textulariina whereas porcelaneous and hyaline foraminifera are classified into the suborders Miliiolina and Rotaliina respectively.

To survive in a variety of dominantly marine environments, benthic foraminifera have developed contrasting feeding strategies. Individuals may be herbivores, actively or passively feeding on algae; carnivores, capturing small arthropods by spreading their pseudopodia nets; passive suspension feeders, detritivores living on fine grained sediments, or omnivores (Murray, 1991).

In addition to the variety of substrates (rocks, shells, seaweeds or soft unconsolidated sediment) inhabited by foraminifera, individual species may have specific ecological requirements which are reflected in their mode of life (Murray, 1991). Foraminifera may be described as epifaunal, living on or above the sediment surface; semi-infaunal, living partly below and above the sediment surface; or infaunal, living below the sediment surface. These three ecological levels are further subdivided into *sessile, clinging* and *free* living to describe whether individual forams are permanently attached to the substrate, semi-permanently attached or free to move around.

Test architecture is affected by the ecological requirements of specific foraminifera and environmental controls exerted upon the individual. For example, *Cibicides* is an epifaunal/sessile foram which constructs a test with low broad trochospiral architecture whereas *Bulimina* is infaunal/free living and constructs a test with high upright trochospiral architecture (Murray, 1991). The low streamline form developed by *Cibicides* is designed to reduce frictional drag in the high energy environments they inhabit.

Many temperate tidal marshes, which develop in the upper half of the intertidal zone, display strong vertical ecological zonation that reflects the different tolerances of organisms to strong environmental gradients across the marsh surfaces. These gradients are controlled primarily by elevation relative to mean sea-level, salinity and proximity to tidal creeks (Scott and Leckie, 1990; Patterson, 1990; Jennings and Nelson, 1992; Jonasson and Patterson, 1992; Williams, 1994; Gehrels, 1994 and Jennings *et al.*, 1995).

Because foraminifera are vertically zoned within temperate marshes, and are sensitive to small changes in relative sea-level, analysis of fossil assemblages can be used to reconstruct former Holocene sea-levels (Scott and Medioli, 1978, 1986).

Analysis of fossil assemblages contained within former intertidal sediments can also be used to identify the depositional environments. For instance, Jonasson and Patterson (1992) examined foraminiferal biofacies in down-core samples from the Fraser Delta. Although fewer biofacies could be resolved in the palaeomarsh sediments than on the contemporary marsh surface, in response to differential preservation of tests, foraminiferal biofacies were used to reconstruct palaeoenvironments in this area.

Taphonomic considerations

Modern benthic foraminifera populations are described in terms of the living, dead or total assemblages. As differences exist in the composition of the living and dead populations (cf. Murray, 1991), the total assemblage is often examined as it is believed that a combination of the two fractions is more accurate when using modern analogues to interpret the fossil record (Scott & Medioli, 1980). However, the relative contribution from the living and dead assemblage must be considered before meaningful conclusions can be made from examining the total assemblage. For instance, in areas of rapid sedimentation the living and dead assemblage may be similar and as a result they will both be represented in the total assemblage. However, in areas of slow sedimentation the living and dead assemblages are likely to be dissimilar; their similarity to the total assemblage will depend upon the relative contribution from each population (Murray, 1991).

Through time total population ultimately converts to the fossil assemblage which is modified by a series of taphonomic processes. The total assemblage is in a state permanent dynamic flux and represents a composite of the processes active at the time of its formation; as tests grow and form, others are moved into or out of the environment, or are destroyed by dissolution. The faunal composition of the fossil assemblages may be further altered during diagenesis which effectively reduces species diversity and specimen numbers. The composition of the fossil assemblage may be further modified by the introduction of tests from living infaunal species.

Smith (1987) uses three examples to describe distinctly different fossilization potentials in the transition from living to fossil assemblages. He concludes that taphonomic changes are related to test composition and structure. Loosely cemented agglutinated tests have little or no fossilization potential whereas well cemented tests are much more likely to be preserved in the fossil assemblage. In calcareous specimens the fossilization potential varies between perforate and imperforate forms, and between tests with or without organic linings. For example, individuals with thinner walls and larger pores are more susceptible to dissolution due to their greater surface area (Smith, 1987).

Boltovskoy and Totah (1992) conducted a study to investigate the reaction of foraminiferal species to dissolution and developed an 'index of preservation' which describes the preservation potential of a number of species. Although the preservation potential of benthic tests is generally greater than planktonic tests it varies considerably. For instance, after being immersed in a container filled with distilled buffered water (pH 6.7) for 50 days only 25% of an *Elphidium excavatum* test was still intact. In contrast it took 130 days for an *Ammonia beccarii* specimen to degrade into a similar condition (Boltovskoy and Totah, 1992).

The loss of specific taxa upon death and differences in species diversity between live, dead and total populations may significantly affect the composition of the fossil assemblage; species diversity and specimen numbers are generally considered to decrease in the fossil assemblage (Smith, 1987).

Postmortem transport can also significantly affect the fossilization potential of the living population. Although the dead assemblage at a particular locale may have a low fossilization potential in its living site it may be a significant component of the total or fossil assemblage at an adjacent site. For instance, living and dead benthic and planktonic specimens may be swept from the continental shelf during high energy storms and deposited in adjacent environments.

Allochthonous depletion or enrichment may play a significant role in the ultimate generation of the fossil assemblage at particular site. For example, in the Bristol Channel powerful tidal currents and storms can transport foraminiferal tests from the outer shelf to low energy marginal marine environments. Estuaries in southwestern Britain receive tests ranging in size from 100-

150 μm, transported in suspension from the shelf, and the proportion of exotic tests in modern estuarine sediments can vary between 30 to 70% (Murray & Hawkins, 1976).

The depth to which infaunal foraminifera penetrate is controlled primarily by the sediment grain size, the extent of oxic sediments beneath the substrate surface and the availability of food (Murray, 1991). Foraminiferal production in the near surface sediments may vary and differences between the surface and infaunal populations depends upon whether or not the foraminifera exhibit distinct vertical microhabitat zonation. The most active taphonomic zone is located within the upper few centimetres of the sediment column (Loubere *et al.*, 1993). Sediment mixing controls both the sediment interval over which species production will be blended and the movement of infaunal tests through the vertically segregated taphonomic zones. If the level of bioturbation at a particular site is relatively low then deeper production from infaunal species may never pass through the most active taphonomic zone. Consequently, the preservation potential for deeper infaunal tests is probably greater than for epifaunal production at this site. Loubere *et al.* (1993) concluded that bioturbation controls both the mixing of vertically stratified test production and whether deeper infaunal populations pass through the taphonomic filter. These taphonomic processes may vary in response to the depositional environment (Loubere et al., 1993).

Goldstein and Harben (1993) indicated that infaunal production in a Georgia salt marsh may modify the death assemblages which accumulate in the subsurface sediments. Infaunal forams may become 'enriched' in relation to epifaunal species in response to selective preservation beneath the active taphonomic zone. The fossil assemblages preserved within the subsurface sediments may therefore differ from the living population on the marsh surface and the fossil assemblage is unlikely to adequately characterize the foraminiferal species accumulating at this site (Goldstein and Harben, 1993).

Foraminiferal taphonomy is extremely complex and can significantly influence the composition of fossil assemblages. The *uniformitarian* approach uses modern analogues to assist in the reconstruction of former palaeoenvironments and is useful when the processes which result in the formation of the total assemblage are considered in context with the depositional environment.

Sampling and preparation

In the fossil assemblage study, 40 g of sediment was taken from suitable levels within the cores recovered at sites 4, 11, 12, 18, 20 and 22. The samples were decanted into clean 63µm sieves and washed in water to remove any fine grained sediment. The residue was then washed into an evaporating basin and dried at 60-100°c.

In the modern foraminiferal study, 40g of material was scraped from a known area on the saltmarsh, mudflat, or sandflat surface using a clean trowel. The sediment was washed through a 63µm sieve and then stained in Rose Bengal. Once washed the residue was dried in an oven at 60-100°c.

Assemblage counts

A known proportion of the 500-125µm fraction was transferred onto a gridded picking tray. Foraminifera were picked from evenly spaced transects, using a fine brush, and the individuals were placed onto a gridded adhesive slide for subsequent identification.

When 250 or more individuals are counted the relative proportions of each component species becomes reasonably constant (Murray, 1991). In this study counts of between 300-400 individuals were made, where possible, using an Olympus (Model C011) low power stereoscopic microscope with x40 magnification. However, in some levels where foraminiferal preservation was poor or concentrations were low, this number was greatly reduced and counts of less than 50 individuals were obtained for the total sample.

Identification and classification

Individuals were identified to the lowest taxonomic level using a reference collection in the University of Wales, Bangor, the keys of Haynes (1973), Murray (1979) and Loeblich and Tappan (1988), and using the micrographs in Austin (1991). The classification was based on Loeblich and Tappan (1988).

Diagram construction

The diagrams were constructed using version 2.26 of Psimpoll, a program written in 'C' by K. D. Bennet (Cambridge University). The advantage of using Psimpoll, over other packages, is that the sediment description can be displayed adjacent to the percentage diagrams. Species percentages were calculated from the total number of individuals counted in that level. All the horizontal scales are comparable and are plotted with a x10 exaggeration to emphasize species of lower abundance. The diagrams were zoned at levels where there was a clearly defined change in the composition of the fossil foraminiferal assemblages.

Analysis

Principle Components Analysis (Kline, 1994) was used to compare fossil assemblages with modern ecological data, in order to characterise palaeoenvironments within the back-barrier complex. The number of taxa within the data set was reduced to approximately 20 and the analysis was then applied to both modern and fossil data. The correlation scores, for the two major principle components, were plotted on a scatter diagram facilitating the direct comparison of all assemblages. As the principle component axis represent the two major sources of variance within the data set further information regarding the cause of this variance was inferred from these plots.

3.2.5 Pollen analysis

Introduction

Pollen analysis is a technique used to reconstruct former vegetation by studying the pollen grains and spores produced by plants, preserved in deposits. The pollen grains are extracted using various physical and chemical techniques and are identified to the lowest taxonomic level using critical morphological features. This technique has become the most widely used method for the reconstructing past flora, vegetation and environments; pollen grains are extremely resistant to diagenesis, they are produced in enormous quantities, they are widely and evenly distributed and can be retrieved in great quantities (Fægri & Iversen, 1989).

Pollen grains result from meiosis and their function is to transfer the male gamctophyte generation of the angiosperm or gymnosperm to the female gamete (Moore *et al.*, 1991). The pollen grain needs to be transported to the stigma of a plant of the same species before it is considered to have successfully completed its purpose. Pollination therefore requires the dispersal of pollen grains and the modes of transport are fundamental in the evaluation of pollen-analytical data (Fægri & Iversen, 1989). Pollen grains are produced in tetrads and the gymnosperm grains tend to be spherical, may be invested with air sacs for wind dispersal and have poorly developed wall structures. Angiosperm pollen, due to their initial formation, posses apertures which follow critical patterns related to their position within the tetrad. These apertures may be described as pores, if both diameters are the same, or furrows if one diameter exceeds the other (Birks & Birks, 1980). Pollen grains may possess pores, furrows, or a combination of both and the apertures tend to be three or multiples of three. The angiosperm pollen grain is composed of three main concentric layers which contain the living cell (Fægri and Iversen, 1989). The middle layer, termed the *intine*, envelops the whole grain forming a uniform cellulose sheath. No part of this layer is known to be fossilized (Fægri & Iversen, 1989).

If a pollen grain fails to reach the stigma it soon perishes, and both the cytoplasmatic interior and the intine are rapidly destroyed. What is left, the *exine*, may survive for a longer period as it is comprised of extremely resistant materials called sporopollenins (Fægri & Iversen, 1989). The exine is stratified into two main layers. The inner layer, the *endexine*, forms a microscopically homogenous membrane and other than where it is connected to apertures it has few morphological developments. The *ektexine* may be distinguished optically from the endexine as they react differently to staining. The ektexine is comprised of small radial, rod-like, elements whose development and distribution reflect the extreme variability of the exine (Fægri & Iversen, 1989). This layer may be further subdivided into three layers in which *columellae* separate an outer and inner stratum, referred to as the *tectum* and *foot layer.* The structure and development of the layers within the ektexine, together with the apertures arrangement, are some of the morphological features used to identify pollen taxa.

Pollen grains are usually preserved in peat and sediments even when most other organic constituents are reduced to a structureless mass (Fægri & Iversen, 1989). If a sediment or peat is weathered then pollen grains may be destroyed, and due to their varying resistance to corrosive agents there is a risk of differential destruction of pollen grains.

Pollen taphonomy

The assumption made in pollen analysis is that changes in pollen frequencies represent a corresponding change in the contemporary pollen producing flora (Davis *et al.*, 1973) which result from changing environmental conditions (Moore *et al.*, 1991). Due to variations in pollen production and dispersal, pollen percentages and concentrations invariably do not correspond to vegetation cover as they are biased to certain taxa. For instance, wind pollinated trees such as *Pinus* are over-represented in comparison to insect pollinated plants such as *Tilia* (Traverse, 1988). Pollen taphonomy considers the production and dispersal of grains, from modern plant communities, along with the processes which result in grains reaching the site of preservation.

Plants use one of three mechanisms for pollen dispersal, driven by either water, animals or the wind; the mechanism used influences the total pollen production and therefore the representation of a particular species within an assemblage. Pollen from the few aquatic plants which use water dispersal are invariably not represented in the fossil assemblage as these plants produce few pollen grains possessing thin exines which are rarely preserved (Fægri & Iversen, 1989). Zoophilous plants use animals, such as insects, birds and bats, to disperse their pollen. As the means of pollination becomes more specialised, fewer numbers of pollen are produced by the zoophilous blossom. Wind pollinated anemophilous plants produce the largest quantities of pollen; these species tend to be over-represented at the expense of other plants.

Pollen frequencies, recorded in a fossil assemblage, are therefore greatly influenced by differential pollen production and the bias results from, for instance, different tree species producing differing amounts of pollen. Pollen production is also influenced by external environmental factors, which result in annual variations in pollen production within species.

Complications in taphonomy are introduced by certain pollen taxa being more effectively dispersed than others. Effective dispersal is linked to the size of a 'basin' and is influenced by the density of vegetation at a particular site (Watkins, 1991). As anemophilous pollen are effectively dispersed by the wind it becomes difficult to distinguish the source as being a few local stands, or having originated from a dense stand of vegetation some distance from the site of preservation. For instance, relatively high percentages of *Pinus* (25%) have to be recorded before a local presence can be interpreted (Huntley and Birks, 1983); as *Tilia* produces a

relatively heavy grain, which is ineffectively dispersed by animals, low frequencies of this taxa can be used to deduce a local origin.

It is also necessary to consider how the pollen reached the site of preservation and how it bchaves upon arrival (Moore *et al.*, 1991). When attempting to reconstruct former palaeoenvironments at a particular site the interpretation must include all the factors which influence pollen deposition and preservation in that environment.

Tauber (1965) developed a model to describe the various mechanisms which control the dispersal and deposition of pollen within a site surrounded by forest (Figure 6.14). Tauber regards the pollen input at a particular site as consisting of three components derived from the trunk space (Ct), the canopy (Cc) and from rain (Cr). The Ct component falls from the tree canopy, or is produced by shrubs of herbs beneath the canopy, and is dispersed by sub-canopy air movements. Some of this pollen may be transferred above the canopy by strong gusts of wind, but most is deposited on the forest floor. The Cc component consists of pollen carried by winds above the canopy itself. A certain amount of the Cc component may be transferred to high altitudes by thermals, where it can travel considerable distances; a similar proportion may sink in eddies down to the trunk space, where it is deposited along with the Ct component. The Cr component consists of pollen within the atmosphere which act as nuclei for water condensation. During precipitation rain drops, falling through the atmosphere, collect more dust and pollen returning the grains to the ground surface. The model produced by Tauber suggests that a small 'pond' may be dominated by the Ct component, whereas a large lake may have a considerable input supplied by the Cc and Cr components.

Moore *et al.* (1991) suggested that the local or gravity (Cl) and 'secondary or inwash' (Cw) components should be included in Tauber's model to account for all pollen input mechanisms. The Cl component is derived from plants growing in immediate vicinity of the site of deposition. For instance, from aquatic plants growing in a lake, from *helophytic* species growing on the surface of a mire, or from trees which may over-hang the site (Moore *et al.*, 1991). Problems may arise at sites which receive water from a surrounding catchment area. The drainage water may contain pollen grains which have been eroded and remobilised from sediments upstream. If the Cw component consists of recently deposited, well-preserved pollen, it is difficult to distinguish between local and non-local components (Moore *et al.*, 1991). In contrast, if this

PAGE/PAGES
EXCLUDED
UNDER
INSTRUCTION
FROM
UNIVERSITY

component is eroded and transported from older sediments then the reworked pollen introduces problems in interpretation of the observed mixed-age assemblages.

The model developed by Tauber (1965) may be used as a basis for interpreting data; however the model needs to be modified for the requirements of any one particular site (Moore *et al.*, 1991). Jacobson and Bradshaw (1981) have developed a model to describe the influence of the size of a site upon the pollen source (Figure 6.15). They related basin size to the areas from which the pollen component is transported. The model serves as a guide for estimating the source of pollen for basins that receive no-inflowing streams; when streams enter the basin, additional pollen with be supplied by the Cw component (Jacobson & Bradshaw, 1981). Local pollen is defined as having originated from plants growing within 20 metres of the site, extra-local pollen is derived from communities growing twenty to several hundred metres from the basin whereas regional pollen can be described as having travelled from plants at greater distances. Jacobson and Bradshaw suggested that as generalisations, regarding pollen transport distances, do not apply to all taxa there is a need to distinguish pollen source areas for pollen accumulating at any one particular site.

Pollen assemblages can distinguish between saltmarsh and mudflat biofacies in a stratigraphic sequence (Jennings *et al.*, 1993). However, as with the sediments accumulating within an estuary, there are complex patterns of pollen provenance in which a large proportion of the pollen influx into an estuary may be strongly influenced by aquatic transport and contain reworked material. Consequently, pollen assemblages contained within any minerogenic unit, deposited in a coastal environment, will consist of an autochthonous component, derived from local vegetation, and an allochthonous component (Cw) transported to the site of preservation. As a result any deposit formed through sediment transport, as well as autochthonous sediments (peats) containing an allogenic mineral component, are likely to contain pollen which do not represent the local vegetation. Similar taphonomical constraints exist when using marine sequences to investigate long term climatic change, but when the limitations are identified useful reconstructions can be made from analysing these sediments (Mudie & Bryne, 1980; Clark *et al.*, 1986; Jennings *et al.*, 1993).

Sampling

The core surfaces were cleaned carefully prior to sampling to avoid contamination. Sub-samples of 0.5 cm^3 were taken from both the organic and inorganic units recovered from sites 4, 7, and 12, using a calibrated sampler. The sampling strategy was designed to provide skeleton pollen diagrams to identify areas of vegetational change within the sequence. The sampling interval was then improved to resolve more rapid changes in vegetational development at site 4. This facilitated comparison of the organic units present at similar levels.

Sample preparation

There are numerous techniques designed to extract pollen from sediments, most of which are modified according to sediment composition. These techniques employ chemical and physical procedures to remove minerogenic and organic material from the sample in order to concentrate the pollen without reducing its frequency or quality.

The method employed in this study closely follows the standard technique for the preparation of organic sediments used by Fægri and Iversen (1989). A modified procedure, involving sieving and heavy liquid separation, was used to extract pollen from minerogenic sediment (Figure 3.16).

Gravity separation

The 'gravity method' of pollen preparation was developed by Judy Allen (Watkins, 1991) and is based on Bjorck *et al.* (1978). The procedure eliminates the use of hydrofluoric acid as coarse and fine material is removed by sieving. The sample is then centrifuged in zinc chloride (ρ>1.8 gcm^{-3}) to remove fine sand and silt between 10 and 118 micrometres. During separation care was taken to ensure that the sample was thoroughly mixed, to prevent pollen being trapped in the denser fraction. Although gravity methods have been considered ineffective (Fægri and Iversen, 1989), Watkins (1991) found that the $ZnCl_2$ method was more effective than HF treatment, resulting in higher pollen concentrations with reduced exposure to acid.

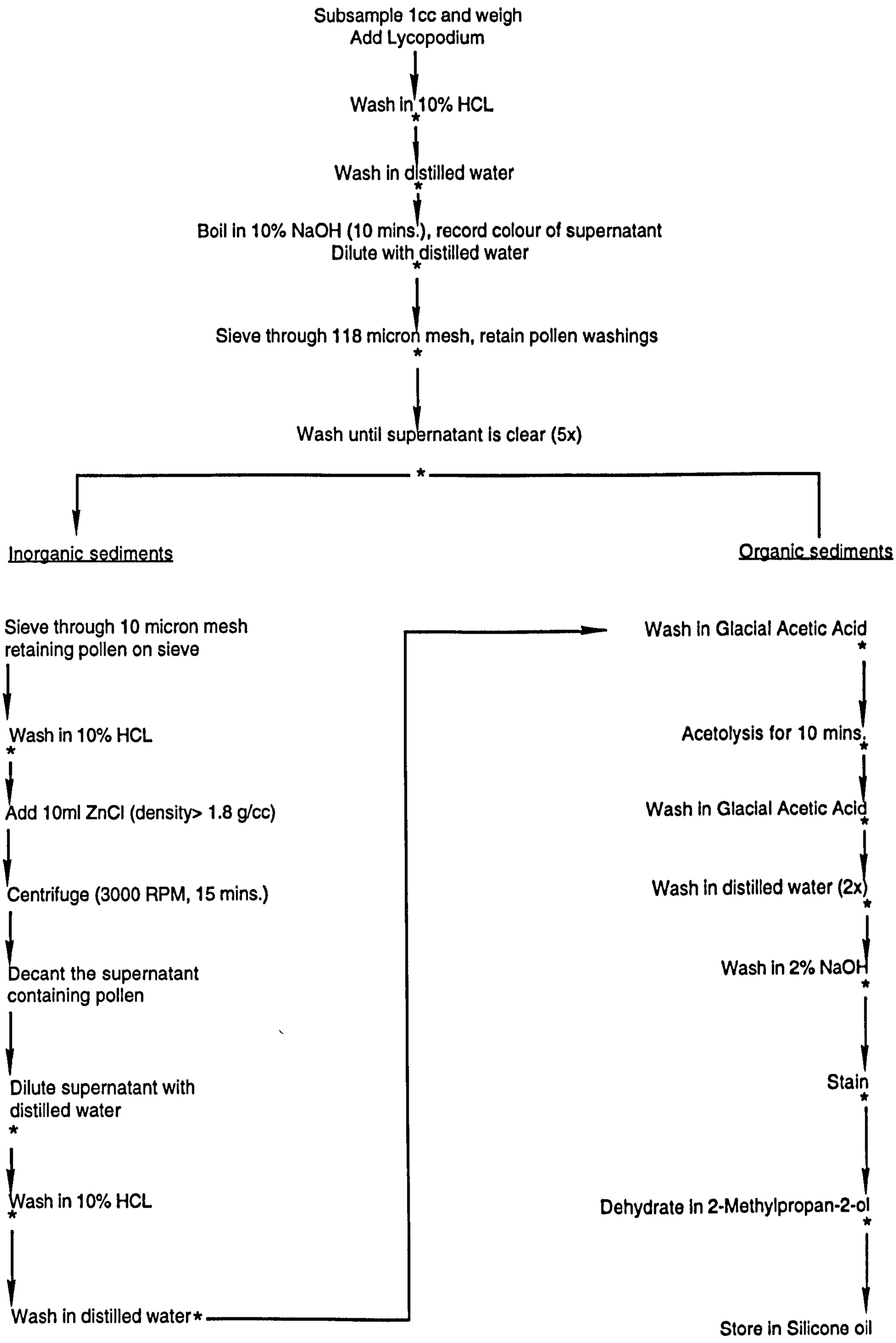

Figure 3.16 The pollen preparation method (Watkins, 1991).

Preparation of organic rich sediments

Acetolysis was used to remove cellulose from both organic and inorganic rich samples (*cf.* Erdtman, 1960). The sample was heated in nine parts anhydric acetic acid and one part conc H_2SO_4 for twenty minutes. Faegri and Iversen (1989) conclude that after acetolysis exine features become more distinct.

Pollen counting and sum

Routine counting was done using a standard HM ZEISS (16) microscope under a magnification of x400. Critical identification was done using a Leitz (Laborlux K/D) microscope with x1000 magnification, immersed in anisol. Grains were counted along regularly spaces traverses, whose spacing depended upon the pollen concentration.

In order to obtain information regarding vegetation change in as many cores as possible, a pollen sum of 300 grains was adopted. For organic samples counts of between 300-400 were obtained; for a number of the minerogenic samples analysed this figure was reduced less than 100 counts.

- Pollen Sum (P) = $\sum$(trees + shrubs + herbs)
- Sum lower plants % of $\sum$(P + lower plants)
- Aquatic (AQ) % calculated from $\sum$(P + AQ)
- Indeterminable (ID) % calculated from $\sum$(P + ID)

Identification

Pollen grains were identified to the lowest taxonomic level using the keys of Fægri and Iversen (1975, 1989), the reference collection at the University of Wales, Bangor, and the photographs / micrographs of Moore and Webb (1978) and Moore *et al.* (1991).

Supplementary information regarding the depositional environment and the method of extraction was provided by classifying indeterminable grains, following Berglund and Ralska-Jasiewiczowa (1986):

- Unknown (a grain that has not been identified but is intact);
- Corroded (exine etched, pitted and perforated);
- Degraded (exine thin, fusion of structural elements or sculpturing);
- Broken (mechanical damage to the grain);
- Crumpled (grain crushed from original shape);
- Concealed (hidden due to mineral or organic debris).

Pollen concentration

The pollen concentration (Pconc) of a sample was calculated as the number of pollen grains in a unit volume of wet sediment:

$$Pconc = \frac{Grains\ counted \times Exotic\ grains\ added}{Exotic\ grains\ counted \times Volume} = grains/cm^3 \qquad 3.13$$

Diagram construction

The diagrams were constructed using version 2.26 of Psimpoll. In the frequency diagrams the percentages of individual taxa were calculated from the *pollen sum* as described above. The percentage of indeterminable and aquatics were plotted along with the total number of grains counted at each level. All the horizontal scales are comparable and plotted with a x10 exaggeration to emphasize taxa with lower frequencies. The concentration diagrams display the concentration of each taxa per unit volume of sediment along with the total pollen concentration in each level. A vertical depth scale is displayed on the diagram, which records depths in metres below the ground surface.

Radiocarbon dates, obtained from organic units, are displayed to the left of the diagram and are given in uncalibrated years before present.

Zonation

A pollen zone represents the biostratigraphic category of an 'assemblage zone' characterized by a distinctive assemblage of individuals (Cushing, 1967). The diagrams were assessed visually and zones were placed at levels which exhibited significant changes in the composition of the flora.

3.2.6 Grain size analysis

Two different techniques were employed in this study to analyse the grain size distributions of sediments recovered from the contemporary saltmarshes and the reclaimed back-barrier deposits. The first combined sieving methods with a Sedigraph Particle Size Analyser, whereas the second used a Galai CIS-100 Particle size analyser.

Sieving and Sedigraph analysis

Samples of 40g were taken at suitable levels from the cores recovered within the estuary. The sediment was first dispersed in distilled water, using sodium hexametaphosphate and a mechanical food mixer, and was then sieved through a 63μm sieve. In samples with a high organic content, the organics were removed prior to dispersion by treating the material with dilute hydrogen peroxide.

The grain size distribution within the sand fraction was determined by sieving. The silts and clays were analysed using a Sedigraph Particle Size Analyser (5000ET), produced by Micrometrics.

The Sedigraph employs soft X-radiation to detect the relative particle concentration, within a 'sample cell', since X-ray absorption is directly proportional to particle mass. The instrument was calibrated prior to each analysis by placing the reference baseline at zero percent whilst the sample cell was flushed with distilled water and sodium hexametaphosphate. The sample was then transferred from the beaker, where it was held in suspension by a magnetic stirrer, to the sample cell. The recorder was then adjusted to read 100% absorption, the exact starting diameter

was set and the cell was removed and inspected for bubbles. Once all the checks were complete, the analysis was started by switching the run switch to on. The fall rates of particles were measured in a 25 mm sedimentation zone within the sample cell. To examine particles of the order of 0.1 to 0.2 μm the Sedigraph decreased the height of the zone of measurement during the analysis, by moving the cell in respect to the X-ray beam.

The output was plotted on log-log paper as equivalent spherical diameter against cumulative percent finer. To quantify the Sedigraph output, the sample concentration was determined by obtaining the dry weight of 5ml of suspended material pipetted into a weighed crucible. Once the analysis was complete, the cell was flushed with particle free distilled water, and the process was repeated.

The Sedigraph and sieving results were combined to produce a cumulative frequency curve for the whole sample. The sample statistics, which include graphic mean grain size, sorting (inclusive standard deviation), skewness and kurtosis, were then calculated using the cumulative frequency curve (Folk, 1966).

One drawback of this approach is that the Sedigraph determines the equivalent spherical diameter from the settling velocities using *Stoke's Law*, whereas sieving measures the physical dimensions of the grains.

Particle size analysis using laser-based optical analysis

Samples of 1cm^3 were taken from the inorganic sediments recovered at sites 4, 9 and 11. The samples were dispersed in distilled water using sodium hexametaphosphate and a magnetic stirrer.

The Galai CIS-100 is a laser-based optical analyser which can be used to conduct both particle size analysis and dynamic shape characterisation. The system uses a modular concept which combines separate units for data acquisition, processing, data presentation and image viewing.

The particle size analysis is based upon the time of transition theory. A He-Ne laser beam is scanned circularly by a rotating wedge prism and focused into a 1.2μm spot, which scans the

sample. When individual particles within a sample bisects the laser spot, interaction signals are detected by a PIN photodiode. As the beam rotates at constant speed, the duration and form of the obscuration signal provides a direct measurement of particle size. As the result represents the actual particle size, and not some secondary property from which an equivalent particle diameter can be derived, this type of analysis eliminates problems resulting from viscosity variations, Brownian motion, thermal convection and other physical phenomena. The shape analysis uses a CCD video camera microscope to provide an optimal images for processing, which are passed to a frame grabber card for analysis.

A variety of acquisition ranges, from 0.5μm to 3600μm, can be selected depending upon the general texture of the sample. Prior to analysis, a series of acquisition and output parameters including sample size, sample statistics, differential histograms, and volume distribution tables, were selected. These parameters were printed automatically once each analysis was completed.

The sample was introduced into a 1 litre tapered vessel, connected to the laser unit, and was held in suspension using a mechanical stirrer. The sample was then slowly pumped through the 'measurement zone' using a peristaltic pump. The analysis was initiated immediately after introducing the sample, and the total number of grains counted for each sample ranged from 10^4 to 10^6. Once the analysis was complete the sample cell was flushed with particle free water and the process repeated.

A cumulative frequency curve was produced for each sample using the percentiles obtained from the volume distribution tables. These curves were then used to calculated the sample statistics.

3.3 Radiocarbon dating

3.3.1 Introduction

^{14}C formed in the atmosphere, by the combination of cosmic ray neutrons and atmospheric nitrogen, maintains a constant level of ^{14}C within the atmospheric and oceanic CO_2 through a steady state of production and decay. Once produced this radioactive carbon isotope enters the global carbon cycle and subsequently becomes incorporated into living plants and animals. Whist alive plants and animals maintain a level ^{14}C identical to the atmosphere; however once carbon becomes fixed in plant or animal tissue the radioactive carbon isotope decays at a constant rate. By measuring ^{14}C in carbon containing matter it is possible to determine the age of that material.

The measurement of conventional ^{14}C ages is based on a number of assumptions and internationally agreed conventions (Mook and Van de Plassche, 1986):

- Over geological time, ^{14}C activity in carbon containing matter has remained constant during the formation of that material.
- Standard oxalic acid, distributed by the US National Bureau of Standards (NBS), is used to define ^{14}C activity.
- ^{14}C dated samples are corrected for isotopic fractionation, according to the $^{13}C/^{12}C$ ratio.
- The ^{14}C measurements are based on the Libby half-life of 5568 years.
- ^{14}C ages are quoted in years before present (BP.) i.e. before AD 1950.

3.3.2 Sources of Error

In radiocarbon dating a level of statistical uncertainty is associated with the random nature of radioactive decay. Errors incurred during the counting of the decay rate in modern reference standards and fossil samples along with background noise cause repeated measurements to spread around a true value (Chappell, 1978). This uncertainty in the radiocarbon measurement is generally quoted by laboratories as one standard deviation ($\pm 1\sigma$) of the normal distribution

curve. Errors can also result from the nature of the material analysed, the depositional environment and from the sampling procedures used.

Contamination by the introduction of foreign carbon during pre-formation, formation and post-formation of a deposit can have a significant affect upon the 14C age measurement (Mook and Van de Plassche, 1986). For instance, areas which receive water draining from calcareous bedrock, soils, coal or carbon rich rock flour the redeposition of older/inert carbon can result in an overestimate of the true ^{14}C age. Hard water errors occur when aquatic plants incorporate ^{14}C deficient carbon during photosynthesis; this consequently causes them become out of equilibrium with the atmosphere $^{14}C/^{12}C$ ratio. Inaccuracies are also caused by the in washing and deposition of allochtonous terrigenous material, the reworking and redeposition of older littoral sediments within the system, and by 'modern' carbon introduced during sampling or from rootlets. Furthermore, the leaching of humic acids can reduce the ^{14}C age estimate; the redeposition of mobile humic acids in a sediment profile can introduce more recent ^{14}C to older deposits within the sequence.

The possible sources of error within this study are considered fully in chapter six when discussing the ^{14}C results.

3.3.3 Sampling

In total ten samples were submitted to the NERC Radiocarbon Laboratory at East Kilbride for dating. Samples were taken from the lithostratigraphic boundaries between the organic and inorganic units, within cores recovered from freshly exposed profiles. The core surfaces were cleaned, to remove smeared and oxidised material, and a 1cm ($10cm^3$) slice was taken from the level to be dated. A further two slices were taken from either side of the level to provide reserve material for dating; this provided approximately 30 grams of wet sediment for measurement. The samples were subject to no pretreatment, were sealed in polythene bags and submitted with full site and sample descriptions.

3.3.4 Radiocarbon measurement

Samples were digested in 0.5 M. Acid at 80°C for 24 hours, to remove labile organic components and carbonates, were washed and then dried to a constant weight in a vacuum oven. The liquid scintillation counting method was used to detect and measure the ^{14}C activity within the samples. To provide sufficient carbon, for the measurement of ^{14}C activity, all the material submitted was required (Miller pers comm., 1995). The results are uncalibrated and based on the Libby half life of 5568 ± 30 years.

3.3.5 Interpretation

The dates received from the NERC Laboratory are interpreted in context with the lithostratigraphic and biostratigraphic evidence. No dates were rejected or omitted in this study.

The dates received from East Kilbride were quoted as x years ± 1σ before present (BP), BP defined as years before 1950 AD. The one standard deviation is an estimate of the error of measurement associated within reproducibility in the laboratory and the statistical uncertainty resulting from the random nature of radioactive decay. All the dates were expressed as uncalibrated years before present.

Chapter 4

Lithostratigraphy, mineralogy and geomagnetics

4.1 Core descriptions

4.1.1 Introduction

Lithological data acquired both within the Taf Estuary and the barrier complex, are presented and discussed in this chapter along with borehole data obtained from the British Geological Survey and F. H. Gilman & Co., the owners of Coygan Quarry. The system is sub-divided into four main areas according to their localities and stratigraphy; these include the West Marsh, East Marsh, Pendine Burrows and the Taf Estuary (Figure 4.1). Detailed lithological descriptions are provided for those sites from which samples were taken and analysed in the laboratory. The remainder are summarized and described using a series of lithological sections.

4.1.2 West Marsh

West Marsh extends from Pendine to a line which runs from the fossil cliffline between Brook and Coygan to the burrows (Figure 4.1). In total nine boreholes, ranging from 5 to 13 metres in depth, were either recovered or described in this area (Figure 4.2). The tidal inlet sequences in West Marsh are dominated by silts and clays intercalated with organic rich and biogenic deposits.

Pendine Woodend

Sites 7 and 8 are located at the western end of West Marsh (Figure 4.2). The sequence at site 7 (SN 2474 0833) is twelve metres deep and extends from 3.75 to -8.25 metres OD (Figure 4.3). At the base of the sequence a silty sand bed with clay laminae fines upwards into an overlying silty clay unit at -7.25 metres OD (Figure 4.4a). This silty clay, stratified by numerous sandy lenses, extends to -6.10 metres OD where it is replaced by sand and gravel. The sands at the top of this unit contain a high proportion of organics and are replaced at -5.50 metres OD by an

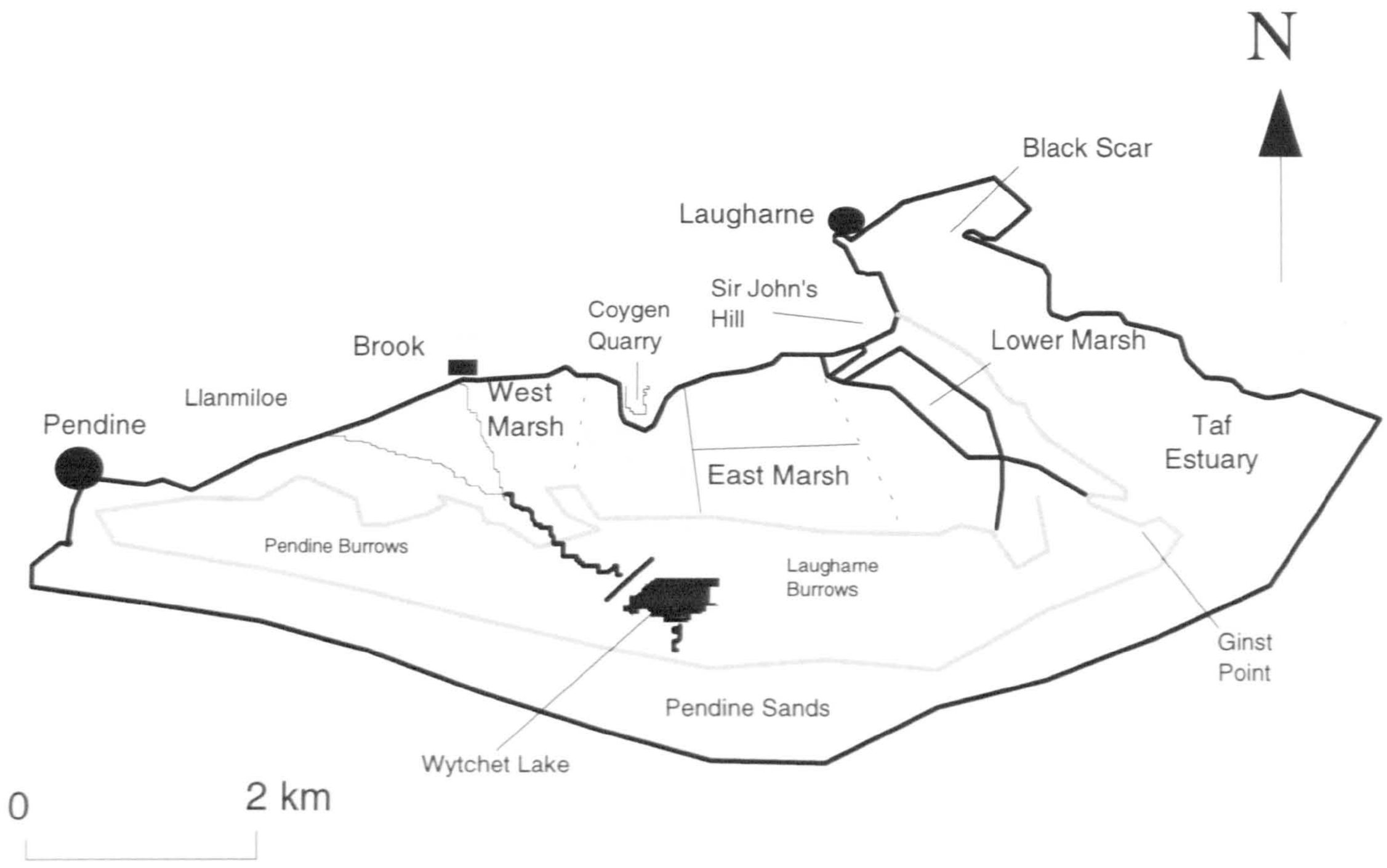

Figure 4.1 The Pendine/Laugharne barrier system

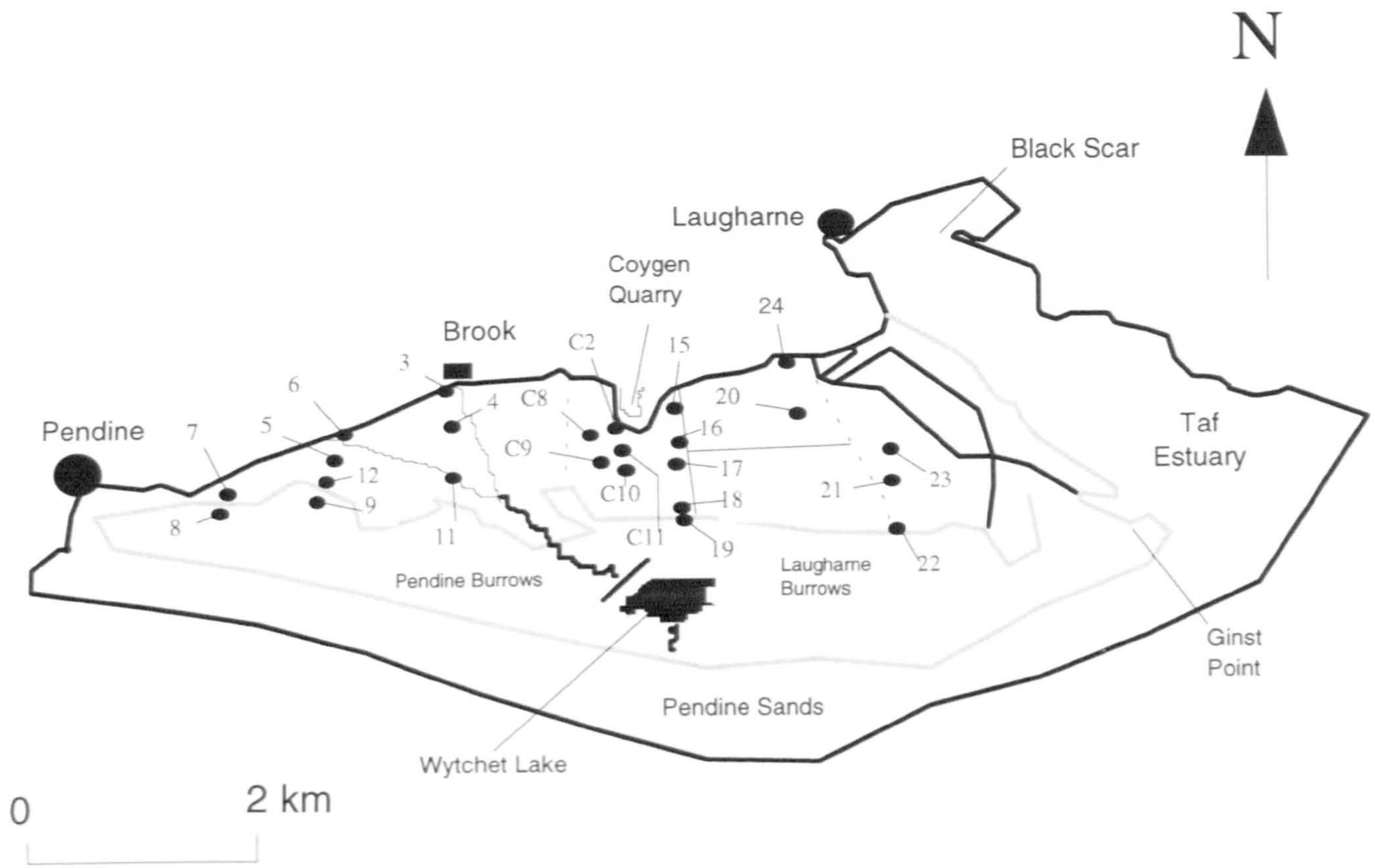

Figure 4.2 Location of borehole sites within West Marsh and East Marsh

organic rich grey silty clay unit (Figure 4.4b). The organic content increases towards the top of this unit where at -3.65 metres OD minerogenic sediment is replaced by organic detritus (Figure 4.4b). The latter extends to -3.55 metres OD where it is overlain by stratified silty clay and highly stratified silty sand (Figure 4.4a). At -0.075 metres OD the silty sand unit fines into an organic rich silty clay which grades into organic detritus at +0.06 metres OD. This upper organic bed (-0.06 to +0.70 metres OD) is composed predominately of fine grained ligneous and herbaceous fragments (Figure 4.4b). This unit is indistinctly laminated and also contains horizontally orientated wood fragments and sedge stems. The top of the organic bed is marked by a gradual boundary which grades into fine grained silty clay (Figure 4.4a). Above this the silty clay coarsens upwards into a stratified sandy silt which is replaced (at +0.80 metres OD) by a medium to fine grained sand with occasional shell fragments. The latter extends to +1.7 metres OD where it is succeeded by a stratified silty clay bed, which is oxidised and mottled near the ground surface (Figure 4.4a).

The sequence at site 8 (SN 2467 0814) is nine metres deep and extends from 5.67 to -3.33 metres OD (Figure 4.3). At the base, organic rich silty clay grades into an organic layer which is stratified by a thin layer of shelly sand. The boundaries between this sand and the organic detritus are marked by very abrupt erosional contacts. Above this the organic deposit grades into a thin layer of organic rich silty clay, which is replaced by sand (containing reworked shell fragments) stratified by organic rich silty clay (Figure 4.3). At -0.50 metres OD sand is replaced by a second organic deposit, composed of fine grained detritus. The boundaries between these organics and the sands above and below this unit are marked by very sharp erosional contacts. Sand containing reworked shell fragments extends uninterrupted to 1.6 metres OD whereupon this facies becomes stratified by silt and clay and is intercalated with layers of well sorted medium to fine sand, which contains no calcareous material (Figure 4.3).

Although the two upper organic beds at sites 7 and 8 occur at different elevations, similarities in their composition and structure suggests that they are laterally equivalent.

KEY

Silty Clay

Sandy Silt

Silty Clay containing organic detritus

Sandy Silt

Silty Sand

Organic Detritus

Sand containing shell frgaments

Sand

Red Boulder Clay containing large orientated clasts

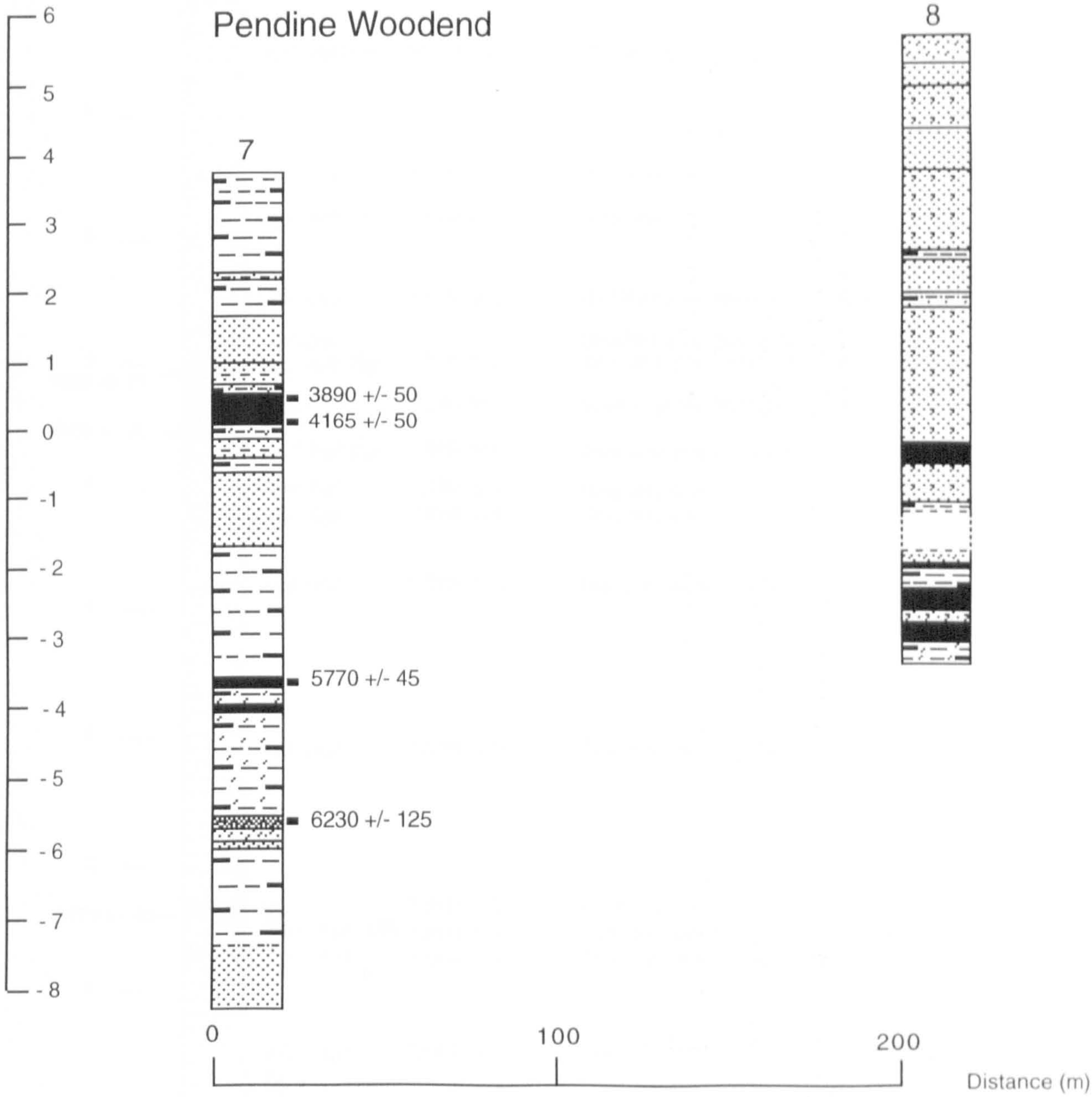

Figure 4.3 Lithology at sites 7 and 8

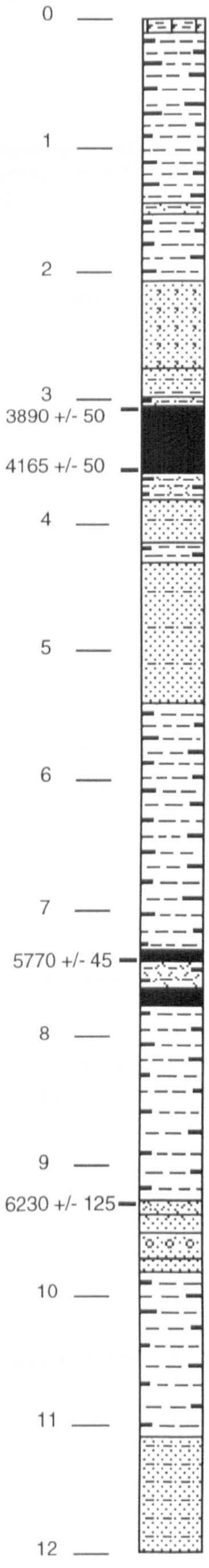

Depth (m) below surface at 3.75m OD	Troels-Smith	Munsell	Description
0	*Ag2 As1 Th1*	10YR 3/3	Dark brown sandy silt
	Ag2 Ag2 Lf+	7.5YR 4/2	Mottled brown silty clay
1			
	Ga3 Ag1	7.5YR N 5/	Grey silty sand
	Ag2 As2	7.5YR N 5/	Grey silty clay
2			
	Ga2 Gs2	7.5YR N 5/	Stratified grey sand containing shell fragments
	Ag3 Ga1		Stratified grey sandy silt
3	*Ag2 As2 Dg+*	7.5YR N 3/	Very dark grey peaty silty clay
3890 +/- 50			
	Dg4	7.5YR N 2/	Black organic detritus
4165 +/- 50			
	Ag2 As2 Dg+	7.5YR N 4/	Dark grey peaty silty clay
4	*Ga3 Ag1*	7.5YR N 5/	Grey silty sand
	As2 Ag2	7.5YR N 5/	Grey silty clay
	Ag3 Ga1	7.5YR N 5/	Highly stratified silty sand
5			
6	*As2 Ag2*	7.5YR N 5/	Stratified grey silty clay
7			
	Dg4	7.5YR N 2/	Black organic detritus
5770 +/- 45	*Ag2 As2 Dl+*	7.5YR N 4/	Dark grey silty clay containg organic detritus
	Dg3 Ag1	7.5YR N 3/	Stratified very dark grey peaty silty clay
8			
	As2 Ag2	7.5YR N 5/	Grey silty clay containing organic detritus
	Dg +		
9			
6230 +/- 125	*Ga2 Sh2*	7.5YR N 5/	Grey sandy peat
	Ga2 Gs2 Dl+		Grey sand containing organic detritus
	Gg(maj.)2 Gg(min.)1 Gs1 Ag+		Grey gravel containing rounded orientated clasts
	Ga2 Gs2		Stratified grey sand
10			
	As2 Ag2	7.5YR N 5/	Stratified grey silty clay
11			
	Ga3 Ag1	7.5YR N 5/	Stratified grey silty sand
12			

Figure 4.4a A detailed description of the lithology at site 7

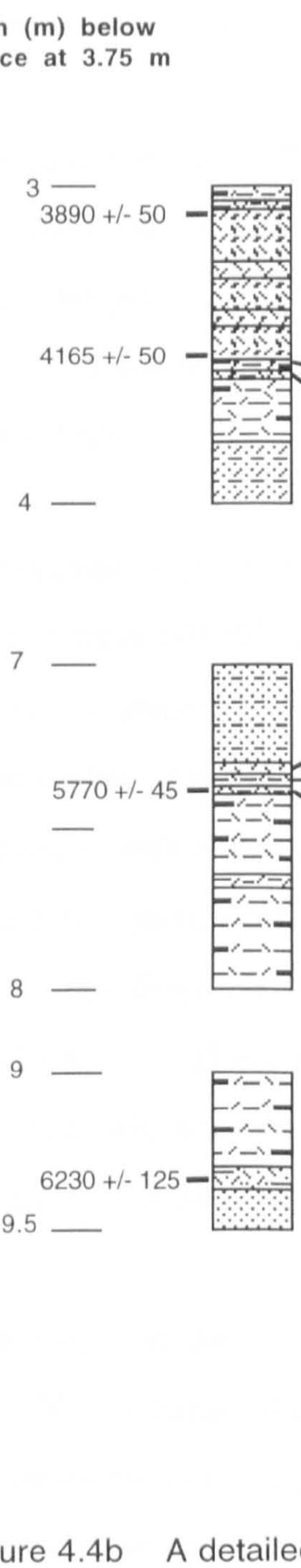

Depth (m) below surface at 3.75 m OD	Troels-Smith	Munsell	Description
3	*As2 Ag2 Dg+*	7.5YR 5 N/	Grey silty clay with organic detritus
3890 +/- 50	*Dg2 As2*	7.5YR 3 N/	Very dark grey silty peat
	Dg3 Dl1	7.5YR 2 N/	Black organic detritus with woody fragments
	Dg4	7.5YR 2 N/	Black organic detritus
	Dg3 Dl1	7.5YR 2 N/	Black organic detritus with woody fragments
	Dh2 Dg2	7.5YR 2 N/	Black organic detritus with sedge fragments
	Dg3 Dl1	7.5YR 2 N/	Black organic detritus with woody fragments
4165 +/- 50	*Ag3 As1 Dg+*	7.5YR 4 N/	Dark grey silty clay containing organic detritus
	Dg2 Dl1 Ag1	7.5YR 3 N/	Very dark grey silty organic detritus
	Ag2 As1 Dg1	7.5YR 4 N/	Dark grey silty caly with organic detritus
	Dg2 As2 Dh+	7.5YR 5 N/	Grey silty clay containing organic detritus
4			
7	*Ag3 Ga1*	7.5YR 5 N/	Grey sandy silt
	Dg4 Ag+	7.5YR 2 N/	Black fine grained organic detritus
5770 +/- 45	*Dg2 Ag2*	7.5YR 4 N/	Dark grey silty organic detritus
	Dg3 As1	7.5YR 3 N/	Very dark grey clayey organic detritus
	As2 Ag2 Dg+	7.5YR 5 N/	Grey silty clay containing organic detritus
	As2 Ag1 Dg1	7.5YR 3 N/	Very dark grey organic silty clay
	As2 Ag2 Dg+	7.5YR 5 N/	Grey silty clay containing organic detritus
8			
9	*As2 Ag2 Dg+*	7.5YR 5 N/	Grey silty clay containing organic detritus
6230 +/- 125	*Dg3 Ga1 Ag+*	7.5YR 3 N/	Very dark grey sandy organic detritus
9.5	*Ga2 Gs2*	7.5YR 4 N/	Dark grey sand

Figure 4.4b A detailed sedimentary log describing the organics recovered from site 7

Westmead Section

Sites 5, 6, 9, and 12 are located in the centre of West Marsh and lie on a line which runs perpendicular to the fossil cliff line from the fields in front of Westmead Farm to the Pendine Burrows (Figure 4.2).

The sequence at site 6 (SN 2579 0889) is six and a half metres deep and extends from 4.05 to -2.45 metres OD. At this locale a series of highly stratified silty clay and sandy silt beds overly a dense red gravel, which contains both fine grained material and large horizontally orientated clasts of sandstone. The boundary between these two facies is marked by an abrupt erosional contact (Figure 4.5).

The sequence at site 5 (SN 2570 0865) is twelve and a half metres deep and extends from 3.97 to -8.53 metres OD (Figure 4.5). The sediments at the base of the sequence fine upwards from a clayey silt, stratified by numerous sand lenses, into a silty clay bed. In between these two units is a thin layer of organic detritus, which extends from -6.4 to -6.2 metres OD. The silty clay, intercalated with relatively thinner layers of sandy silt, extends to -2.45 metres OD where it is replaced by organic detritus. This organic unit is stratified by clay lenses and grades into organic rich silty clay (Figure 4.5). This clay then extends to -0.45 metres OD where it is replaced by a second layer of red brown organic detritus. This upper organic bed grades into a thin layer of shelly sand, which is overlain by silty sand stratified by occasional clay laminae. At 2.70 metres OD silty sand grades into a dense clayey silt, mottled by Fe-nodules (Figure 4.5).

The sequence at site 12 (SN 2562 0844) is twelve metres deep and extends from 3.60 to -8.40 metres OD. A highly stratified and horizontally bedded silty sand, at the base of the sequence, fines upwards into a silty clay stratified by numerous sand lenses (Figure 4.6a). There is a distinct colour change between theses two beds; the lower unit is pinkish grey (7.5YR 6/2) whereas the upper of these two units is grey (7.5 N 5/). The latter is replaced by a grey sandy silt which grades into an organic rich silty clay at -5.25 metres OD. This silty clay bed extends to -4.65 metres OD, where it is replaced by highly stratified sandy silt unit (Figure 4.6a). The latter grades into silty clay which is intercalated with sandy silt and has an increasing organic content. At -2.235 metres OD the organic rich silty clay grades into a organic unit which is intercalated

KEY

Silty Clay

Sandy Silt

Silty Clay containing organic detritus

Sandy Silt

Silty Sand

Organic Detritus

Sand containing shell frgaments

Sand

Red Boulder Clay containing large orientated clasts

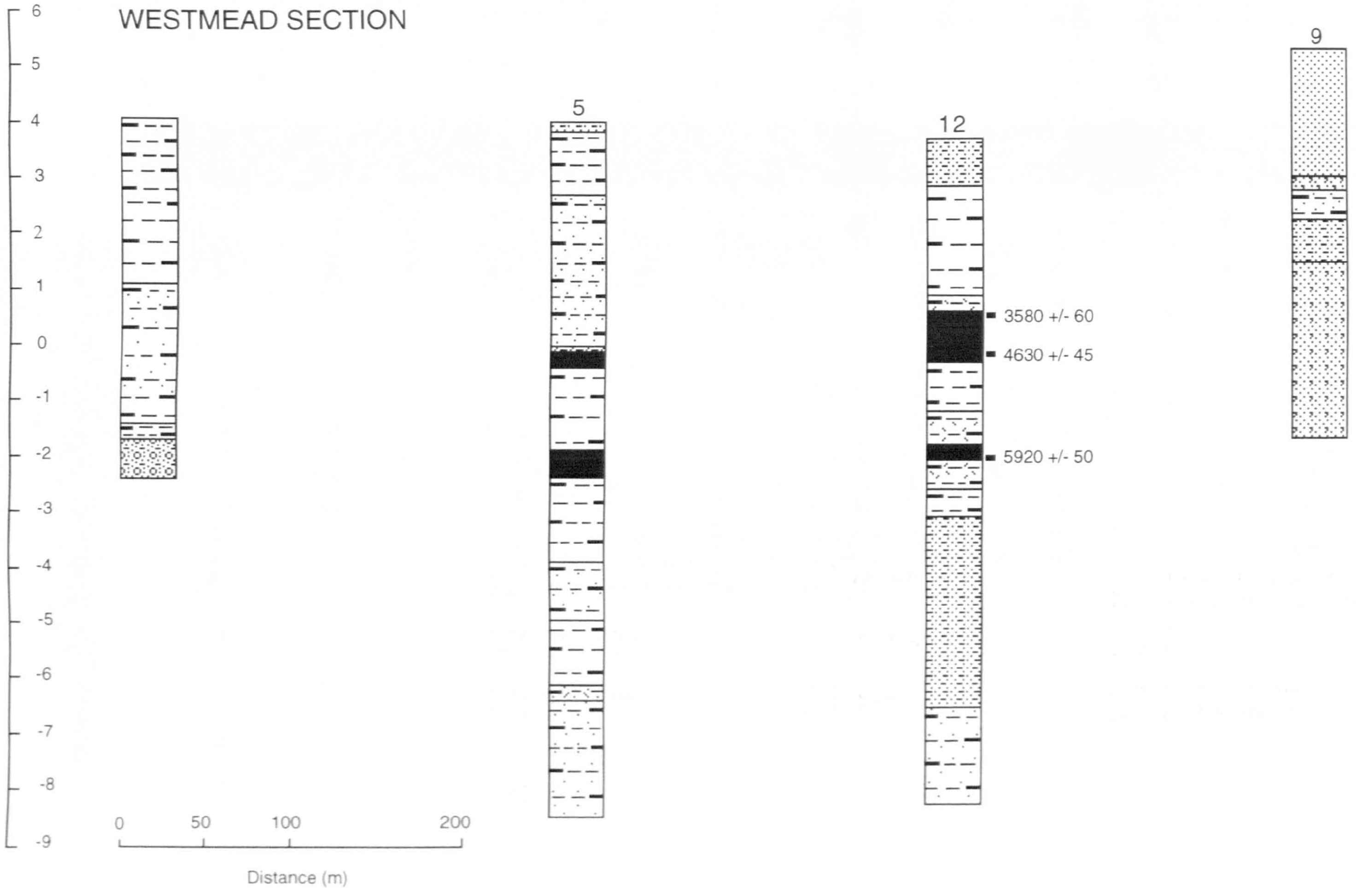

Figure 4.5 Lithology at sites 6, 5, 12 and 9

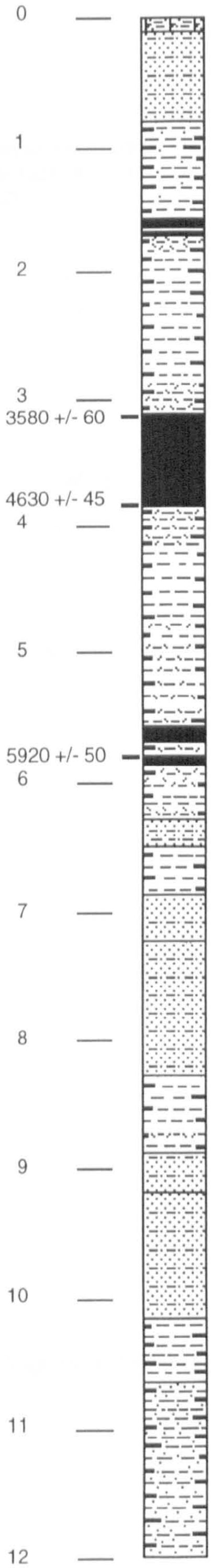

Depth (m) below surface at 3.60 m OD	Troels-Smith	Munsell	Description
0	*Ag2 Ga1 Th1*	10YR 3/3	Dark brown sandy silt
	Ag3 Ga1 Lf+	7.5YR 4/2	Mottled brown sandy silt
1	*Ag2 As2 Ga1 Lf+*	7.5YR N 5/	Mottled grey silty clay
	Dg4	7.5YR N 2/	Black organic detritus
	As2 Ag1 Dg1	7.5YR N 3/	Very dark grey silty clay containing organic detritus
2	*As2 Ag2*	7.5YR N 5/	Grey silty clay
3	*As2 Ag1 Dg1*	7.5YR N 3/	Very dark grey silty clay containing organic detritus
3580 +/- 60	*Dg4*	7.5YR N 2/	Black organic detritus
4630 +/- 45			
4	*As2 Ag1 Dg1*	7.5YR N 3/	Very dark grey silty clay containing organic detritus
	As2 Ag2	7.5YR N 5/	Grey silty clay
5	*As2 Ag1 Dg1*	7.5YR N 4/	Dark grey silty clay with increasing organic content
	Dg4	7.5YR N 2/	Black organic detritus stratified by very dark grey peaty silty clay
5920 +/- 50	*Dg4*		
6	*As2 Ag2*	7.5YR N 5/	Grey silty clay
	Ag3 Ga1	7.5YR N 5/	Grey sandy silt
	As2 Ag2 Ga+	7.5YR N 5/	Grey silty clay
7	*Ga2 Gs1 Ag1*	7.5YR N 5/	Highly stratified grey silty sand
	Ag2 Ga2 Gs+	7.5YR N 5/	Highly stratified sandy silt
8	*As2 Ag2 Dg+*	7.5YR N 5/	Grey silty clay containing organic detritus
	As2 Ag1 Dg1	7.5YR N 4/	Dark grey peaty silty clay
9	*Ga3 Ag1*	7.5YR N 5/	Grey silty sand
	Ag3 Ga1	7.5YR N 5/	Grey sandy silt
10			
	As2 Ag2	7.5YR N 5/	Stratified grey silty clay containing sand lenses
11			
	As1 Ag2 Ga1 Ga+	7.5YR 6/2	Highly stratified pinkish grey clay, silt, sand
12			

Figure 4. 6a A detailed description of the lithology at site 12

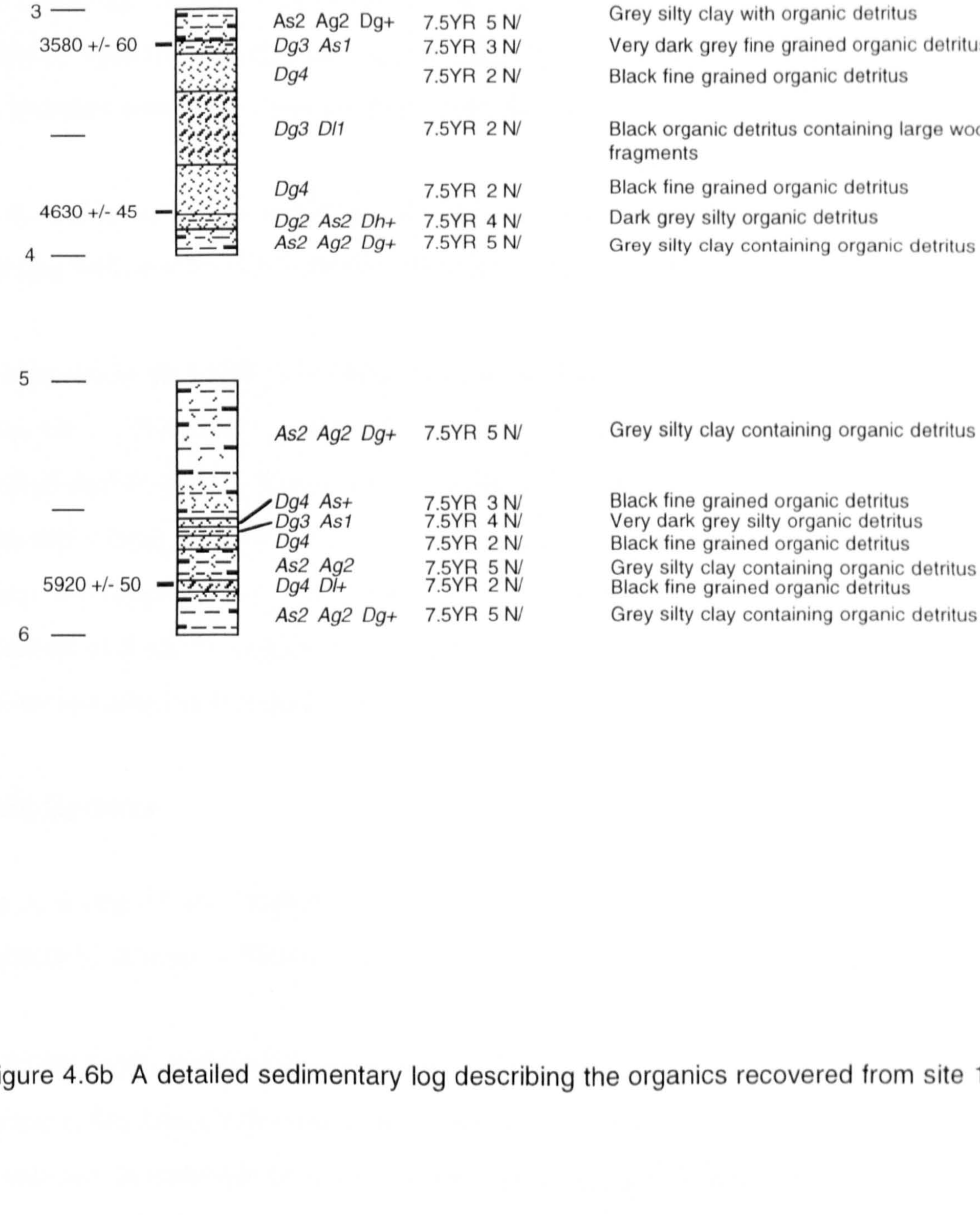

Figure 4.6b A detailed sedimentary log describing the organics recovered from site 12

with organic rich silty clay. The organics between -2.235 and -1.95 metres OD are composed of fine grained organic detritus which is horizontally laminated (Figure 4.6b).

The lower organic unit at site 12 is replaced by an organic rich silty clay bed which extends to -0.28 metres OD where it is replaced by a second organic deposit. This second organic bed ranges from -0.28 to 0.48 metres OD and is composed of both fine grained organic detritus and large fragments of wood (Figure 4.6b). The upper boundary of this second organic deposit is marked by a gradual transition into organic rich silty clay. The clay is stratified by a thin organic lens, becomes mottled towards its upper boundary and is overlain by mottled brown sandy silt.

Due to similarities in the elevation, structure and composition the organic beds at site 12, it is likely that these deposits are laterally equivalent to those described at site 7, 8 and 5 (Figure 4.5).

The sequence at site 9 (SN 2255 0825) is seven metres in length and extends from 5.35 to -1.65 metres OD. The lithology at the base of the sequence is dominated by sand which contains reworked shell fragments (Figure 4.5). This facies is replaced by silty sand which subsequently grades into a layer of clayey silt. The upper boundary of the latter unit is marked by an abrupt contact whereupon clayey silt is replaced by a thin layer of shelly sand. This shelly sand is overlain by well sorted medium to fine sand which contains no calcareous material and becomes oxidised towards the ground surface (Figure 4.5).

Brook Section

Sites 3, 4 and 11 are located at the eastern end of West Marsh and extend from the field immediately in front of Brook Farm seaward towards the Pendine Burrows (Figure 4.2).

Site 3 (SN 2670 0995) is located immediately in front of the fossil cliff line (Figure 4.2). The sequence at this locale is five and a half metres deep and extends from 4.05 to -1.45 metres OD. The sequence is underlain by a hard impenetrable material (possibly a large boulder within the gravel facies or highly compressed peat) which prevented any further penetration of the auger. The overlying lithology is dominated by grey silty clay which is stratified by silty sand and becomes oxidized towards the ground surface (Figure 4.7).

KEY

Silty Clay

Sandy Silt

Silty Clay containing organic detritus

Sandy Silt

Silty Sand

Organic Detritus

Sand containing shell frgaments

Sand

Red Boulder Clay containing large orientated clasts

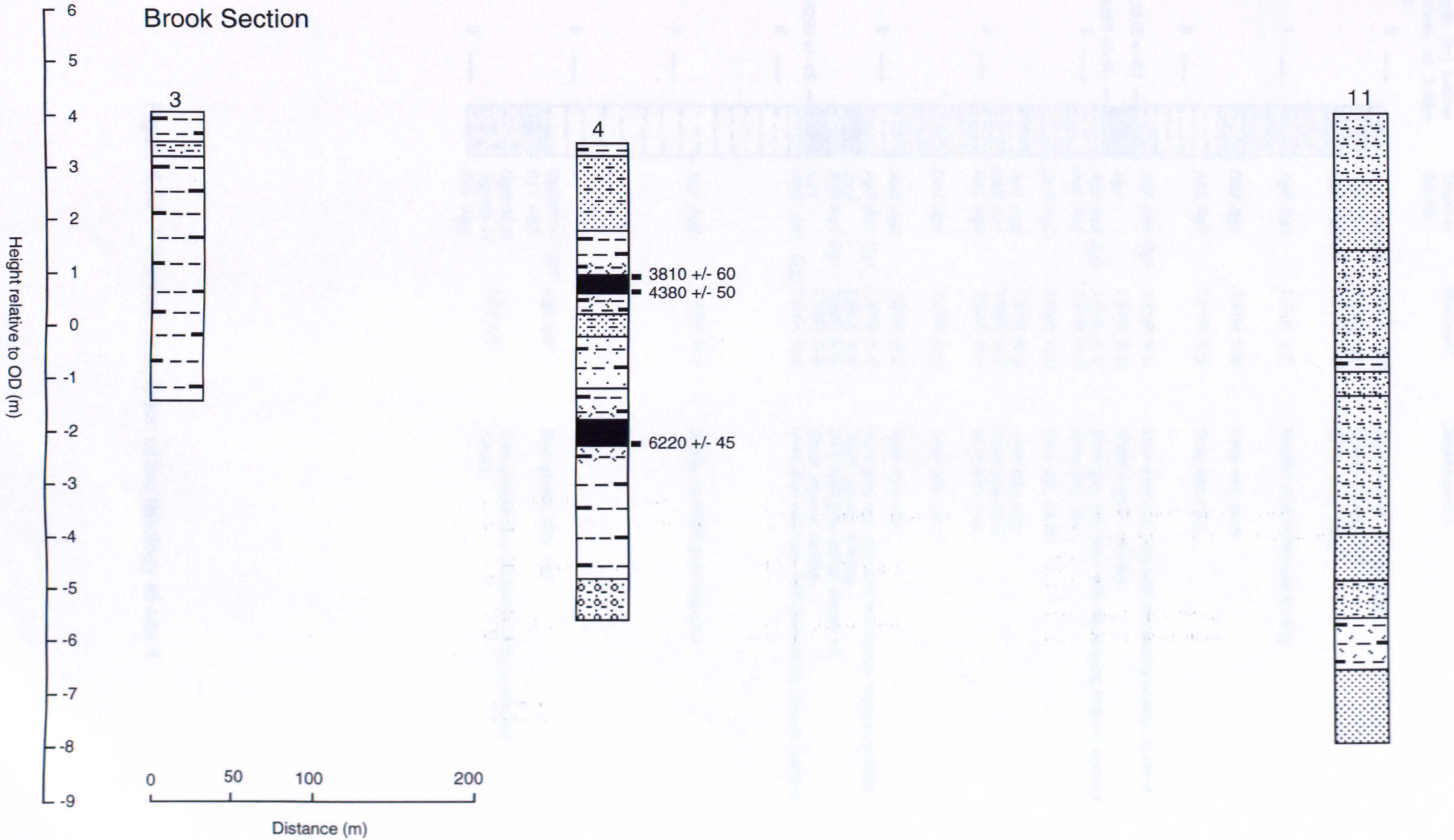

Figure 4.7 Lithology at sites 3, 4 and 11

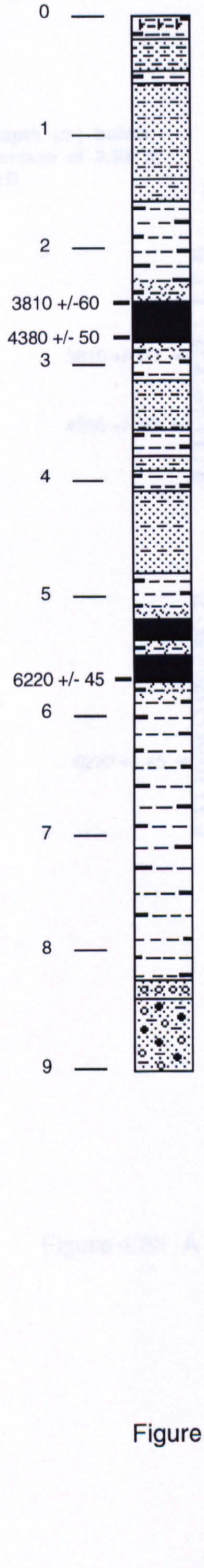

Depth (m) below surface at 3.92m OD	Troels-Smith	Munsell	Description
0	*Ag2 As1 Th1*	10YR 3/3	Dark brown clayey silt
	Ag3 Ga1	7.5YR 5/2	Brown sandy silt
	Ag2 Ag2 Lf+	7.5YR N 5/	Grey silty clay
1	*Ag3 Ga1*	7.5YR 4.2	Mottled dark brown sandy silty
	Ga3 Ag1	7.5YR N 5/	Grey silty sand
	As2 Ag2	7.5YR N 5/	Grey silty clay
2	*Ag2 As1 Dg1*	7.5YR N 4/	Dark grey silty clay with increasing organic content
3810 +/-60	*Dg4*	7.5YR N 2/	Black organic detritus
4380 +/- 50	*Ag2 As2 Dg+*	7.5YR N 4/	Dark grey silty clay with decreasing organic content
3	*Ag2 As2*	7.5YR N 5/	Grey silty clay
	Ga3 Ag2	7.5YR N 5/	Grey silty sand
	As2 Ag2	7.5YR N 5/	Grey silty clay
	Ga3 Ag1	7.5YR N 5/	Grey silty sand
4	*As2 Ag2*	7.5YR N 5/	Grey silty clay
	Ga3 Ag1	7.5YR N 5/	Grey silty sand
	As2 Ag2	7.5YR N 5/	Grey silty clay
5	*Ag2 As1 Dg1*	7.5YR N 4/	Dark grey silty clay with increasing organic content
	Dg4	7.5YR N 2/	Black organic detritus
	Ag2 As1 Dg1	7.5YR N 3/	Very dark grey peaty clayey silt
6220 +/- 45	*Dg4*	7.5YR N 2/	Black organic detritus
	Ag2 As1 Dg1	7.5YR N 4/	Dark grey silty clay with decreasing organic content
6			
7	*As2 Ag2*	7.5YR N 5/	Highly stratified grey silty clay
8	*Gg(min.)1 Gs1 Ag1 As1*	10R 4/8	Red gravel, silty, clay
9	*Gg(maj.)2 Gg(min.)1 Gs1 Ag+*	10R 4/8	Red boulder clay containing large orientated clasts

Figure 4.8a A detailed description of the lithology at site 4

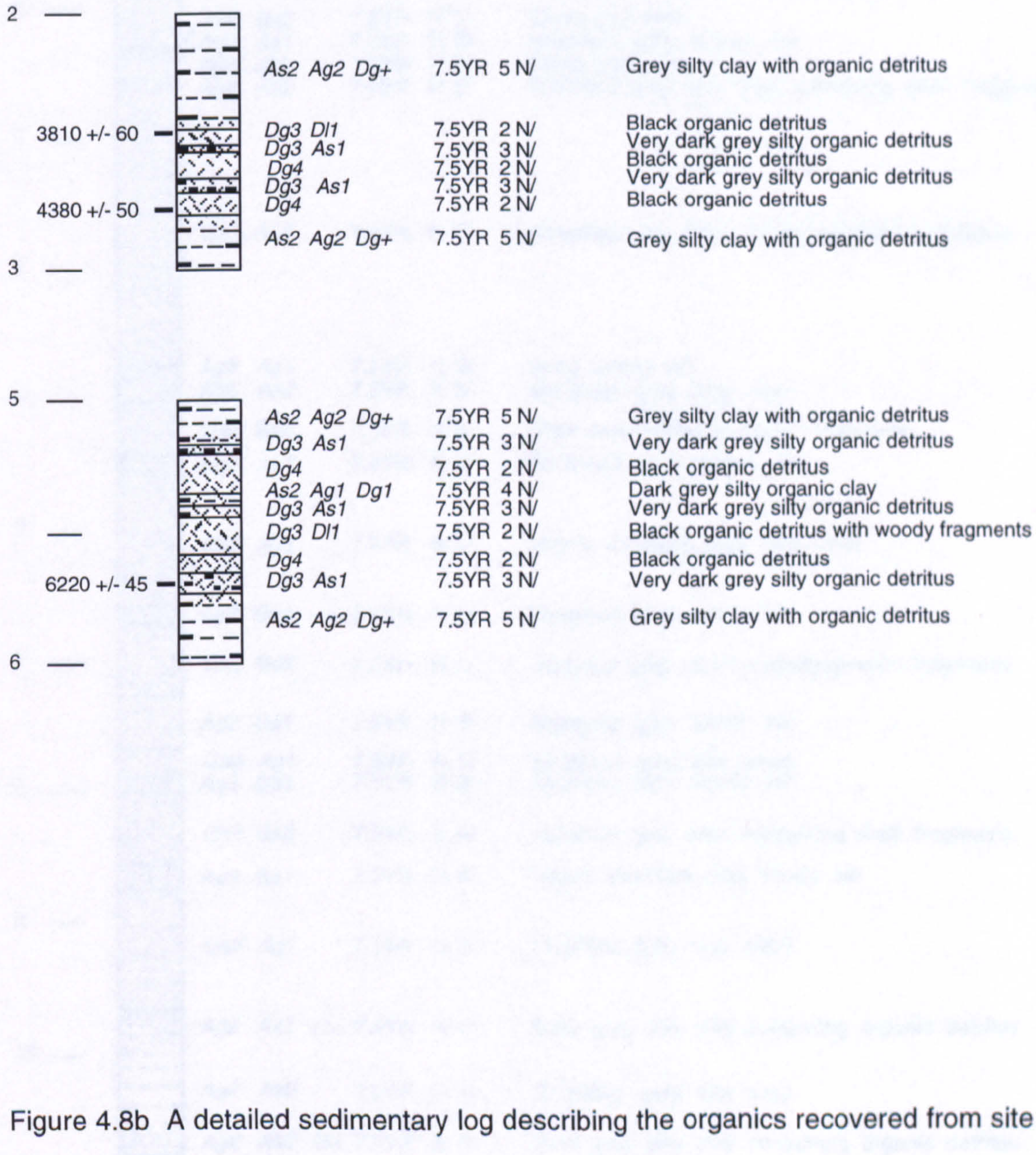

Figure 4.8b A detailed sedimentary log describing the organics recovered from site 4

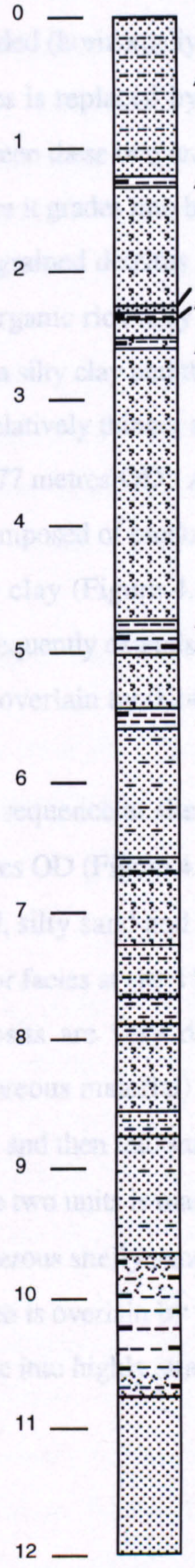

Depth (m) below surface at 4.05m OD	Troels-Smith	Munsell	Description
0			
	Ag3 Ga1	7.5YR 4/2	Highly stratified dark grey brown sandy silt
1	*Ga2 Gs2*	7.5YR N 5/	Clean grey sand
	As2 Ag2	7.5YR N 5/	Stratified grey brown silty clay
	Ga2 Gs2	7.5YR N 5/	Grey sand containing shell fragments
2	*Ga2 Gs2*	7.5YR N 5/	Clean grey sand
	Ag3 As1	7.5YR N 5/	Stratified grey clayey silt
	Ga2 Gs2	7.5YR N 5/	Clean grey sand
	Ag2 As2	7.5YR N 5/	Stratified grey silty clay containing shell fragments
3			
	Ga2 Gs2	7.5YR N 5/	Stratified grey sand containing shell fragments
4			
	Ag3 As1	7.5YR N 5/	Grey clayey silt
	Ag2 As2	7.5YR N 5/	Stratified grey silty clay
5	*Ga2 Gs2*	7.5YR N 5/	Grey sand containing shell fragments
	Ag3 As1	7.5YR N 5/	Stratified grey clayey silt
6	*Ga3 Ag1*	7.5YR N 5/	Highly stratified grey silty sand
	Ag3 Ga1	7.5YR N 5/	Stratified grey sandy silt
7	*Ga2 Gs2*	7.5YR N 5/	Stratified grey sand containing shell fragments
	Ag3 Ga1	7.5YR N 5/	Stratified grey sandy silt
	Ga3 Ag1	7.5YR N 5/	Stratified grey silty sand
8	*Ag3 Ga1*	7.5YR N 5/	Stratified grey sandy silt
	Ga2 Gs2	7.5YR N 5/	Stratified grey sand containing shell fragments
	Ag3 Ga1	7.5YR N 5/	Highly stratified grey sandy silt
9	*Ga3 Ag1*	7.5YR N 5/	Stratified grey silty sand
	Ag2 As2 Dl+	7.5YR N 4/	Dark grey silty clay containing organic detritus
10	*Ag2 As2*	7.5YR N 5/	Stratified grey silty clay
	Ag2 As2 Dl+	7.5YR N 4/	Dark grey silty clay containing organic detritus
11	*Ga2 Gs2*	7.5YR N 5/	Clean grey sand
12			

Figure 4.9 A detaited description of the lithology at site 11

The sequence at site 4 (SN 2676 0896) is nine metres deep and extends from 3.92 to -5.08 metres OD. At the base of the sequence is a poorly sorted dense red gravel bed, which contains large rounded (horizontally orientated) clasts and fine grained sediment (Figure 4.8a). The red gravel facies is replaced by a highly stratified grey silty clay at -4.305 metres OD and the boundary between these two units is marked by an abrupt contact. The latter extends to -1.815 metres OD where it grades into black organic detritus (Figure 4.8b). This organic bed is composed of both fine grained detritus and large fragments of horizontally compressed wood which are stratified by organic rich silty clay laminae (Figure 4.8b). At -1.255 metres OD the organic bed grades into a silty clay and then into silty sand at -0.86 metres OD (Figure 4.8a). The sand is stratified by relatively thinner silty clay beds and the deposit fines upwards into an organic rich silty clay at 0.77 metres OD. At 1.13 metres OD the silty clay grades into a second organic layer, which is composed of predominately fine grained organic detritus which is interstratified by organic rich silty clay (Figure 4.8b). These organics grade into a grey silty clay at 1.46 metres OD which subsequently extends to 2.345 metres OD. The latter is replaced by a mottled dark brown sandy silt, overlain by 0.24 metres of dark brown clayey silt.

The sequence at site 11 (SN 2677 0848) is twelve metres deep and extends from 3.99 to -8.01 metres OD (Figure 4.7). The lithology at this locale is dominated by well sorted medium to fine sand, silty sand and sand which contains reworked shell fragments (Figure 4.9). Although the major facies at site 11 resemble those described at site 9 the distribution and succession of these deposits are very different. At the base of the sequence well sorted sand (containing no calcareous material) is overlain by organic rich silty clay. The latter grades into stratified silty sand and then into sand containing reworked shell fragments (Figure 4.9). The boundary between these two units is marked by an abrupt contact and the latter grades into a silty sand, stratified by numerous shelly sand lenses. The sediments then grade very sharply into stratified shelly sand which is overlain by well sorted sand, containing no calcareous material. The sediments finally grade into highly stratified sandy silt which becomes oxidised towards the ground surface (Figure 4.9).

4.1.3 East Marsh

East Marsh extends eastwards from Coygan to the sea-wall which runs from Salthouse to Ginst Point (Figure 4.1). In total twelve boreholes, ranging in depth from 6.5 to 4.5 metres, are described in this area (Figure 4.2). Information for a further five boreholes, located in the fields adjacent to Coygan Quarry, were obtained from F. H. Gilman & Co.. However, as these sites were levelled by a private contractor, the absolute accuracy of the heights given is uncertain.

The lithology in East Marsh is dominated by silty clay, silt, sandy silt, silty sand, well sorted medium to fine sand and sand containing reworked shell fragments. In the western portion of this area the sequences are relatively complex with intercalated beds of shelly sand, silty sand, silty clay, sandy silt and well sorted medium to fine sand.

Coygan Quarry

Data from five boreholes, logged in the fields south west of Coygan Quarry (Figure 4.2), is summarised in figure 4.10.

Section 1

The borehole at site C8 (SN 2798 0886) is ten metres deep and extends from 4.00 to -6.00 metres OD. At the base of the sequence poorly sorted dense red gravel extends to -4.52 metres OD where it grades into a poorly sorted coarse sand. This latter unit is overlain by a stratified silty sand which fines upwards into a silty clay at -0.89 metres OD. Silty clay then extends to 2.58 metres OD where it is replaced by a coarser silt (Figure 4.10).

The sequence at site C9 (SN 2807 0861) is ten and a half metres deep and extends from 4.00 to -6.50 metres OD (Figure 4.10). The sediments are underlain by a dense red gravel facies which extends to -6.35 metres OD where it is in sharp contact with an overlying silty sand. This unit extends to -0.67 metres OD where the sediments fine upwards into an overlying silty clay bed. The latter is replaced at 2.23 metres OD by a well sorted medium to fine sand which is overlain by clayey silt.

KEY

- Silty Clay
- Sandy Silt
- Silty Clay containing organic detritus
- Sandy Silt
- Silty Sand
- Organic Detritus
- Sand containing shell frgaments
- Sand
- Red Boulder Clay containing large orientated clasts

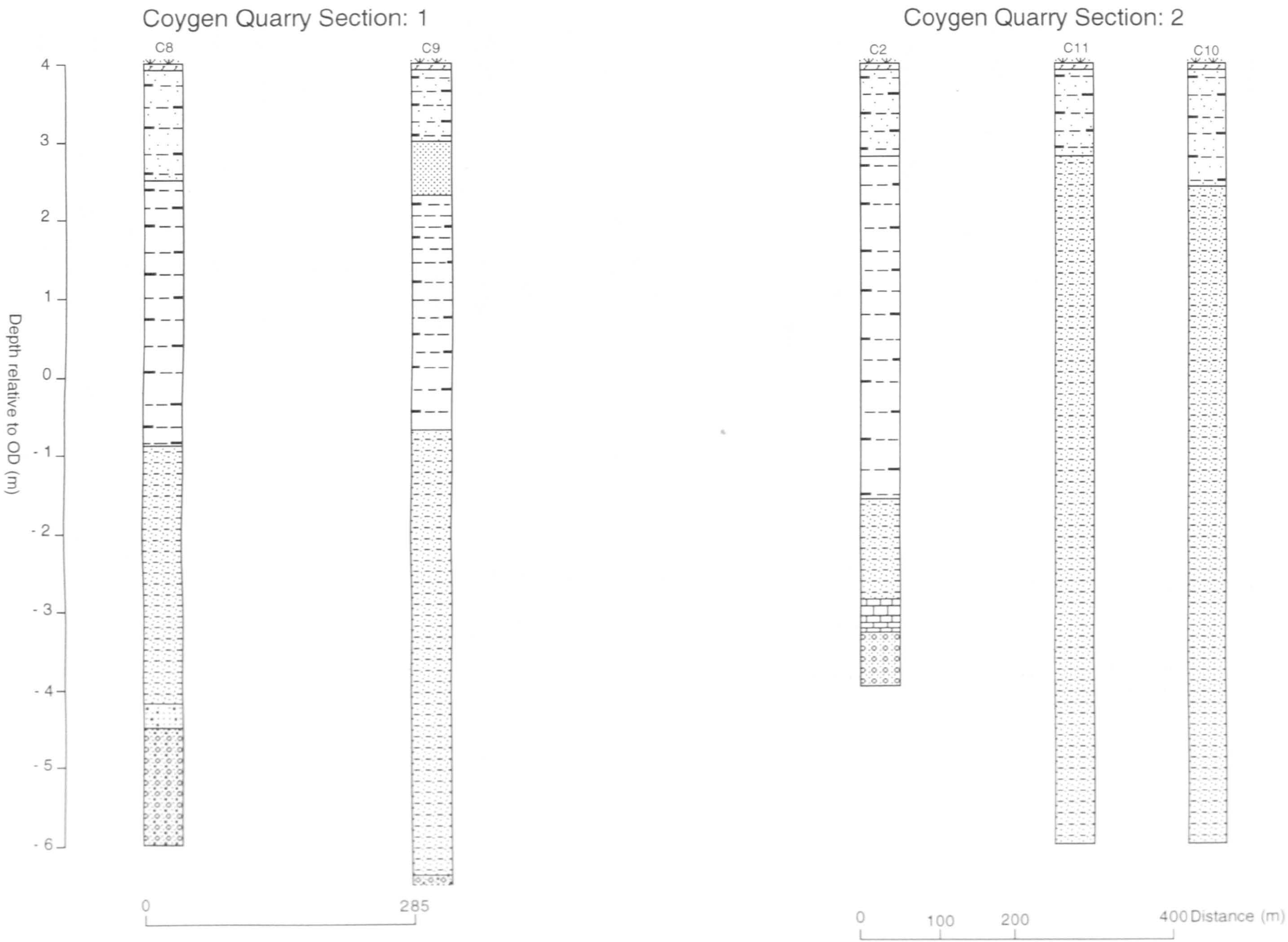

Figure 4.10 Lithological log drawn from borehole data obtained from F. H. Gilman & Co.

Section 2

An eight metre borehole was recovered and logged at site C2 (SN 2820 0893). The sequence, which extends from 4.00 to -4.00 metres OD, is underlain by poorly sorted dense red gravel and a large limestone boulder (Figure 4.10). Stratified silty sand, in contact with the limestone boulder, extends to -1.55 metres OD where it is replaced by finer silty clay. The clay deposit is overlain by coarser silt which become oxidised towards the ground surface.

The lithology at sites C11 (SN 2826 0872) and C10 (SN 2830 0853) is dominated by silty sand which extends from -6.00 to 2.81 and 2.44 metres OD respectively, where it is replaced by clayey silt (Figure 4.10).

Causeway Section

Sites 15, 16, 17, 18 and 19 are positioned on a transect which runs perpendicular to the fossil cliff line in the fields adjacent to Causeway Road (Figure 4.2).

The sequence at site 15 (SN 2875 0911) is five and a half metres deep and extends from 3.98 to -1.52 metres OD. The sediments fine upwards from a basal sand, containing reworked shell fragments, into an overlying silty clay unit (Figure 4.11). This unit grades upwards into a coarser stratified silty sand which is ultimately replaced by a second silty clay bed. The latter, which completes the sequence at this locale, contains a layer of coal fragments (3.64 to 3.74 metres OD). These coal particles may be derived from steam engines used to transport limestone from Coygan Quarry to Salthouse during the 19th century.

The sequence at site 16 (SN 2876 0879) is six and a half metres deep and extends from 3.967 to -2.53 metres OD. The sediments at the base of this sequence fine upwards from a medium to fine sand, containing reworked shell fragments into a silty sand and then into a sandy silt. The latter grades into sandy silt which is overlain by a this layer of silty sand. The upper boundary of this latter unit is marked by an abrupt erosional contact with an overlying layer of well sorted medium to fine sand. The sand is replaced by silty sand, which contains a layer of juvenile whole *Cerastoderma* bivalves in their growth positions (Figure 4.11). The sand then grades into silty clay, silty sand and sandy silt (Figure 4.11).

KEY

Silty Clay

Sandy Silt

Silty Clay containing organic detritus

Sandy Silt

Silty Sand

Organic Detritus

Sand containing shell frgaments

Sand

Red Boulder Clay containing large orientated clasts

The sediments at site 17 (SN 2874 0859) were recovered for subsequent analysis in the laboratory. The sequence is six metres deep and extends from 4.30 to -1.70 metres OD (Figure 4.11). As at sites 15 and 16 the sequence fines upwards from a sand containing reworked shell fragments into a silty clay. The clay is stratified by well sorted fine sand and sand which contains reworked shell fragments. The sediments then grade very sharply into well sorted fine sand (-0.32 metres OD) and then into sandy silt at 1.16 metres OD. The silts are overlain by finer silty clay, which is replaced by highly stratified silty sand at 1.76 metres OD. At 2.13 metres OD the sediments grade into a silty clay which is highly stratified by thin horizontal sand lenses at its base. The clay deposit grades into a sandy silt (at 3.44 metres OD) which is ultimately replaced by a well sorted medium to fine sand. The boundary between these two units is marked by an abrupt erosional contact and the upper unit becomes oxidized and mottled towards the ground surface (Figure 4.12).

The sequence at site 18 (SN 2878 0817) is five and a half metres deep and extends from 4.73 to -0.77 metres OD (Figure 4.11). The sediments fine upwards from a basal sand unit (containing reworked shell fragments) into a silty sand and then into a silty clay. The clay bed is overlain by a shelly sand and the boundary between these two units is marked by an abrupt erosional contact. The sand is overlain by a well sorted medium to fine sand which is stratified by silty sand and sandy silt lenses. The well sorted sand layer is replaced by a silty sand completing the sequence at site 18.

Site 19 (SN 2880 0805) is located immediately behind the barrier at the end of Causeway Road (Figure 4.9). The sequence is five and a half metres deep and extends from 5.13 to -0.37 metres OD. The sediments at the base of the sequence fine upwards from a shelly sand into a fine grained silty clay. This latter unit extends to 2.69 metres OD where it is replaced by a medium to fine sand (with numerous reworked shell fragments), stratified by a thin layer of organic rich sand (Figure 4.11). The boundary between the shelly sand and the underlying silty clay is marked by an abrupt erosional contact. Towards the top of the shelly sand bed the sediments grade into a well sorted medium to fine sand which is oxidised towards at the ground surface (Figure 4.11).

KEY

Silty Clay

Sandy Silt

Silty Clay containing organic detritus

Sandy Silt

Silty Sand

Organic Detritus

Sand containing shell frgaments

Sand

Red Boulder Clay containing large orientated clasts

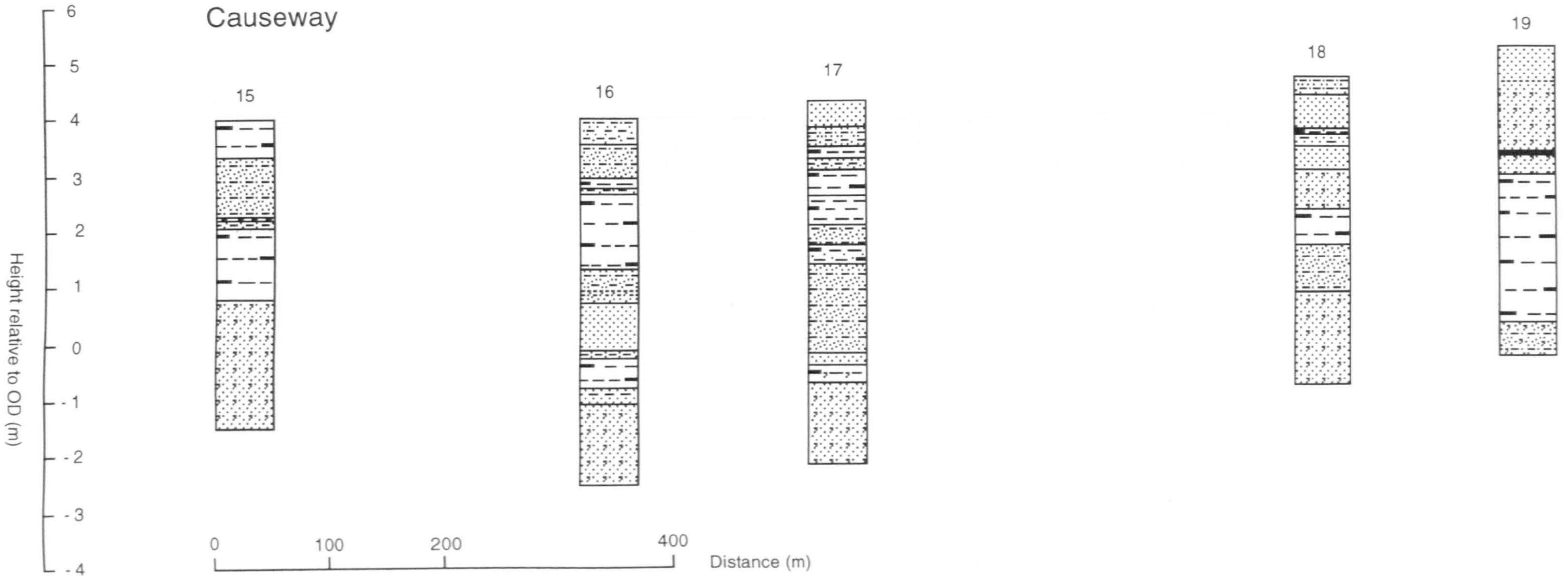

Figure 4.11 Lithology at sites 15, 16, 17, 18 and 19

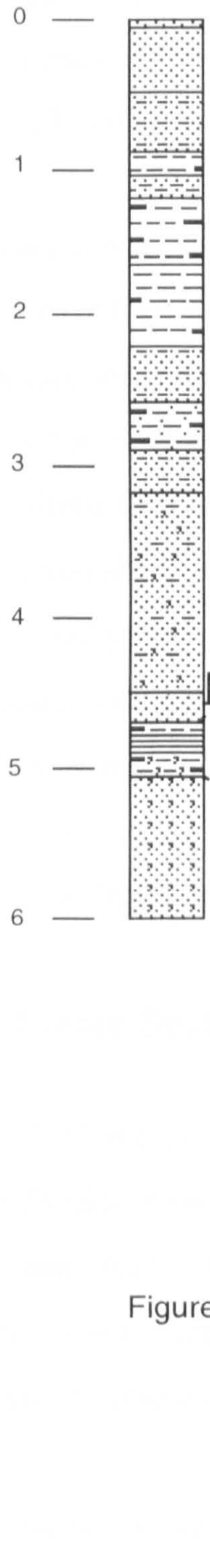

Depth (m) below surface at 4.30m OD	Troels-Smith	Munsell	Description
	Gs2 Ga2	7.5YR 5/6	Strong brown mottled sand
	Ag3 Ga1	7.5YR 5/2	Mottled brown sandy silt
	Ag3 As1	7.5YR 5/2	Mottled brown clayey silt
	Ag3 Ga1	7.5YR 5 N/	Grey sandy silt
	As2 Ag2	7.5YR 5 N/	Grey silty clay
	Ag3 As1	7.5YR 5 N/	Highly stratified grey clayey silt
	Ga3 Ag1	7.5YR 5 N/	Highly stratified grey silty sand
	As2 Ag1 Ga1	7.5YR 5 N/	Highly stratified grey sandy silty clay with shell fragments
	Ga3 Ag1 Ga+	7.5YR 5 N/	Highly stratified silty sand with clay laminations and shell fragments
	Ga2 Gs1 Ag1	7.5YR 5 N/	Grey silty sand containing shell fragments
	Ga2 Gs2	7.5YR 5 N/	Clean grey sand
	As2 Ag2	7.5YR 5 N/	Stratified grey silty clay *
	Ga2 Gs2	7.5YR 5 N/	Stratified grey shelly sand
	As2 Ag2	7.5YR 5 N/	Stratified grey silty clay *
	Ga2 Gs2	7.5YR 5 N/	Clean grey sand
	As2 Ag2	7.5YR 5 N/	Stratified grey silty clay *
	Ga2 Gs2	7.5YR 5 N/	Grey sand containing shell fragments

*Contains whole *Cerastoderma* bi-valves *in situ*

Figure 4.12 A detailed description of the lithology at site 17

Salt House Section

Sites 24 and 20 lie on a transect which extends from a field adjacent to Salt House Farm to a field next to Malthouse Farm (Figure 4.2).

The sequence at site 24 (SN 2972 0955) is 4 m 20 cm deep and extends from 4.01 to -0.19 metres OD(Figure 4.13). The sediments at the base of the sequence are composed of medium to fine sand containing numerous reworked shell fragments. These grade into well sorted medium to fine sand, with occasional shell fragments, which is overlain by silty clay (Figure 4.13).

The sequence at site 20 (SN 2982 0965) is five and a half metres deep and extends from 4.59 to -0.91 metres OD. The sediments at the base of the sequence fine upwards from a dark grey sand, containing reworked shell fragments and whole *Cerastoderma* bivalves, into highly stratified sandy silt at -0.32 metres OD (Figure 4.13). The silt is replaced at -0.096 metres OD by a series of stratified silty clay and clayey silt beds (Figure 4.14). These fine grained deposits change sharply into shelly sand, which is intercalated with a layer of dark grey silty clay. At 1.99 metres OD the shelly sand fines upwards into a silty sand and then into sandy silt; these two upper units also contain numerous reworked shell fragments. The silt is overlain by a layer of shelly sand which contains whole *Cerastoderma* bivalves (Figure 4.14). The sandy unit then grades into a layer of silty clay which is highly stratified at its base and is overlain by mottled sandy silt, containing fragments of wood.

East House Section

Sites 23, 21 and 22 at located at the eastern end of East Marsh (Figure 4.2). The borehole depth at site 23 (SN 3064 0875) is five and a half metres deep and extends from 3.64 to -1.86 metres OD (Figure 4.15). The lithology at this locale is dominated by medium to fine sand containing numerous reworked shell fragments. This unit is overlain by silty sand (containing reworked shell fragments) which grades into a finer silty clay deposit.

The sequence at site 21 (SN 3065 0842) is five and a half metres deep and extends from 3.96 to -1.54 metres OD. The deposits are very similar to those described at site 23. A basal shelly sand

KEY

Silty Clay

Sandy Silt

Silty Clay containing organic detritus

Sandy Silt

Silty Sand

Organic Detritus

Sand containing shell frgaments

Sand

Red Boulder Clay containing large orientated clasts

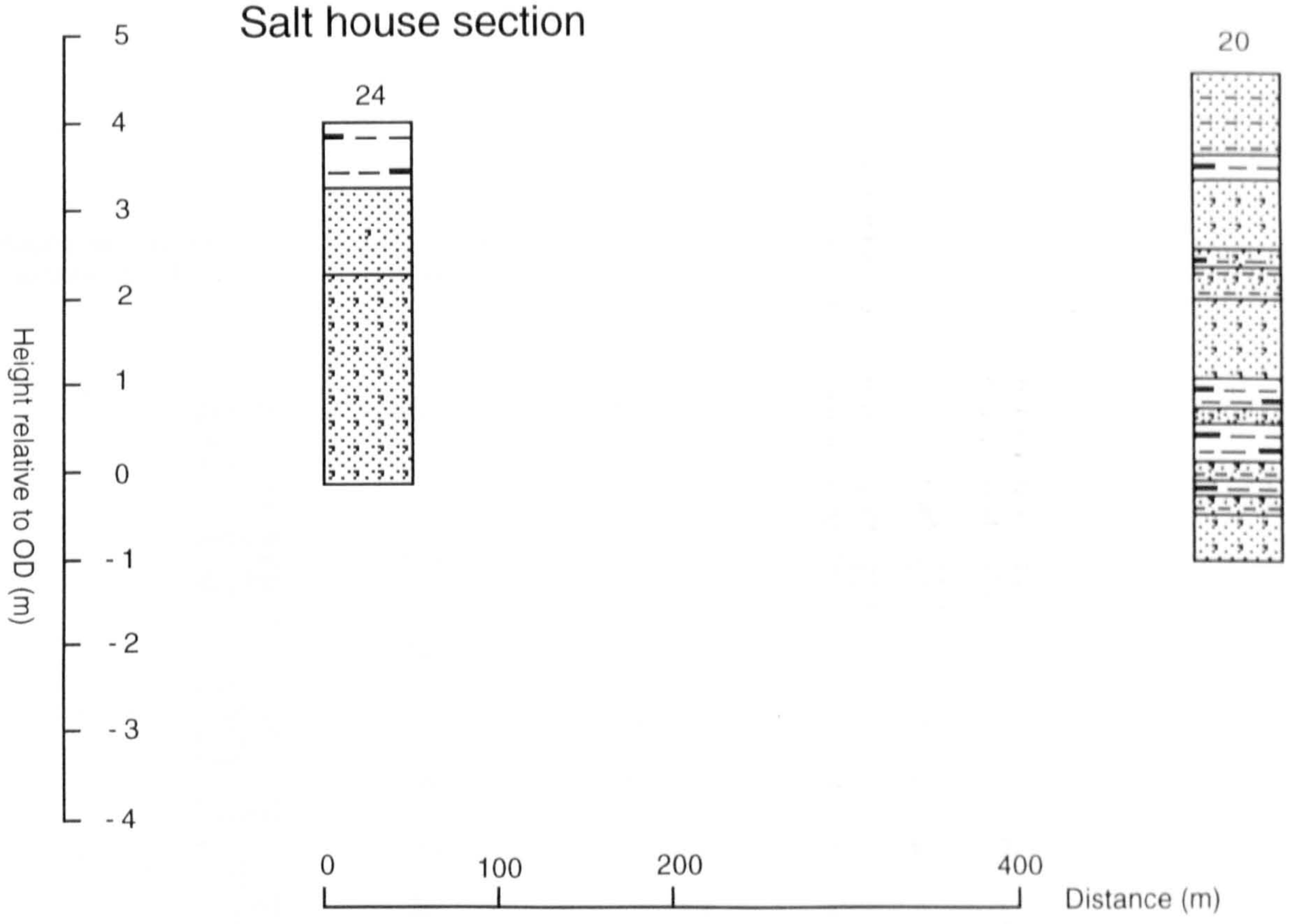

Figure 4.13 Lithology at sites 24 and 20

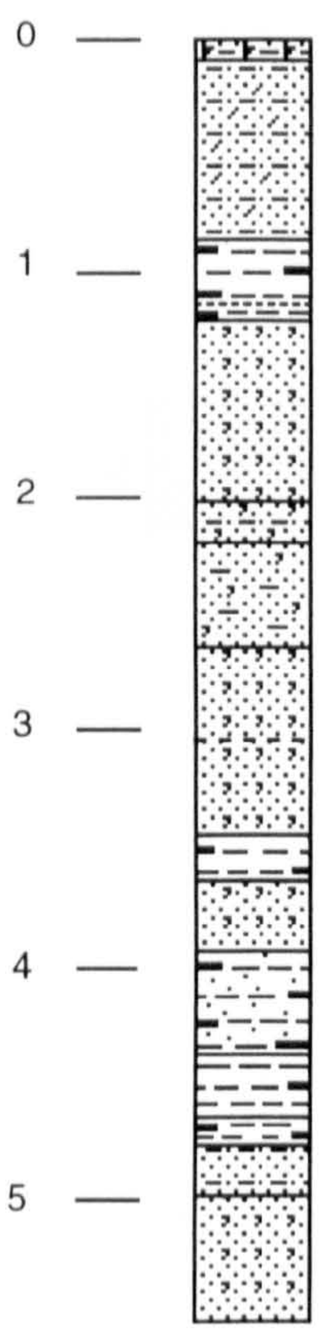

Depth (m) below surface at 4.59 m OD	Troels-Smith	Munsell	Description
0	*Ag3 Ga1*	7.5YR 5/6	Strong brown sandy silt
	Ag3 Ga1	7.5YR 5/2	Highly stratified mottled brown sandy silt with wood fragments
1	*As2 Ag2*	7.5YR N 5/	Mottled grey silty clay
	As2 Ag2	7.5YR N 5/	Highly stratified silty clay
	Ga2 Gs2	7.5YR N 5/	Grey shelly sand*
2	*Ag3 Ga1*	7.5YR N 5/	Grey sandy silt containing shell fragments
	Ga3 Ag1	7.5YR N 5/	Grey silty sand containing shell fragments
	Ga2 Gs2	7.5YR N 5/	Grey shelly sand*
3	*Ga2 Gs2*	7.5YR N 4/	Dark grey shelly sand
	As2 Ag2	7.5YR N 4/	Dark grey silty clay
	Ga2 Gs2	7.5YR N 4/	Dark grey shelly sand
4	*As2 Ag2*	7.5YR N 5/	Highly stratified grey silty clay
	Ag3 As1	7.5YR N 5/	Highly stratified clayey silt
	As2 Ag2	7.5YR N 5/	Stratified grey silty clay
	Ag3 Ga1	7.5YR N 5/	Highly statified sandy silt
5	*Ga2 Gs2*	7.5YR N 5/	Dark grey shelly sand*

*Contains whole *Cerastoderma* bi-valves *in situ*

Figure 4.14 A detailed description of the lithology at site 20

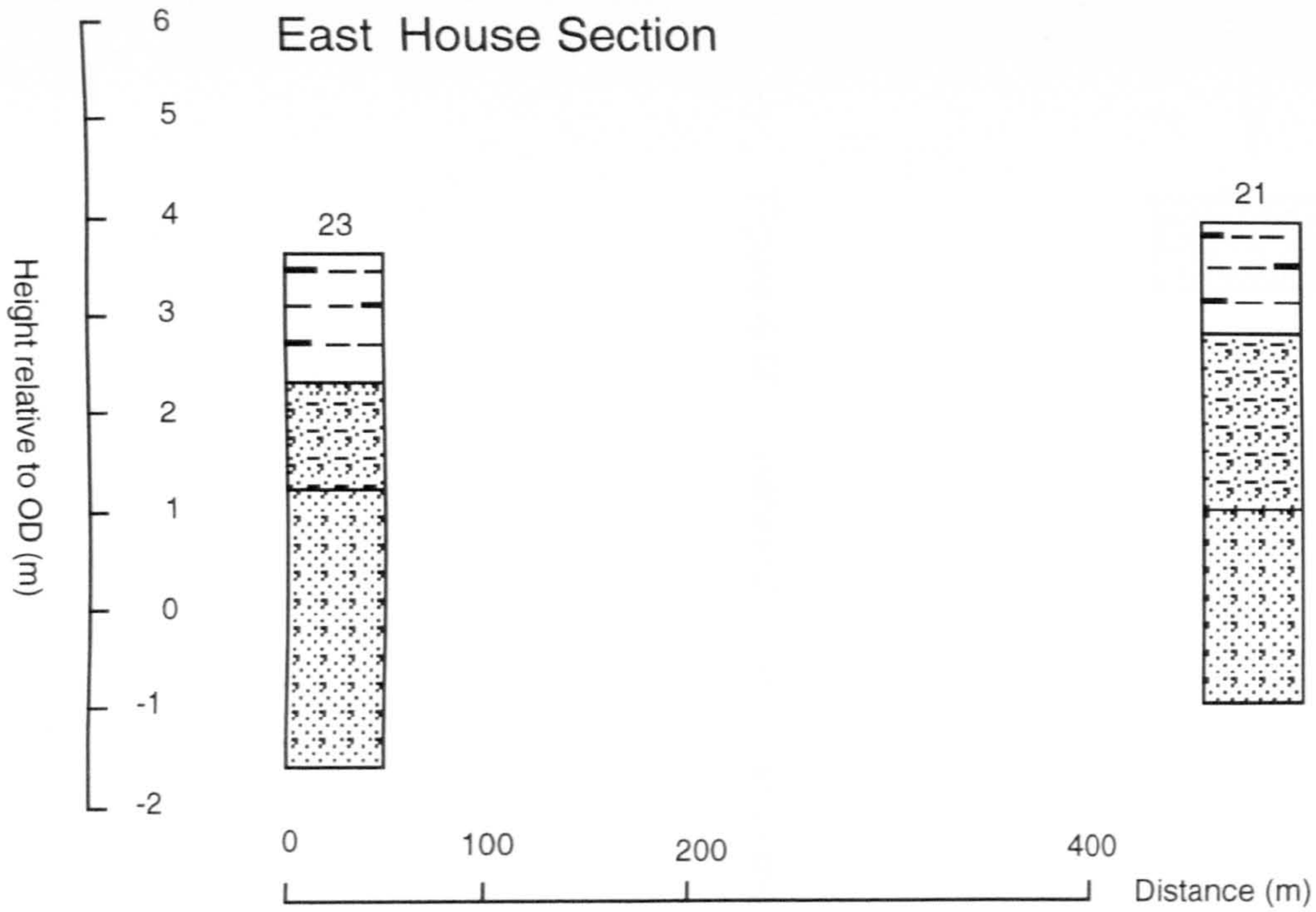

Figure 4.15 Lithology at sites 23, 21and 22

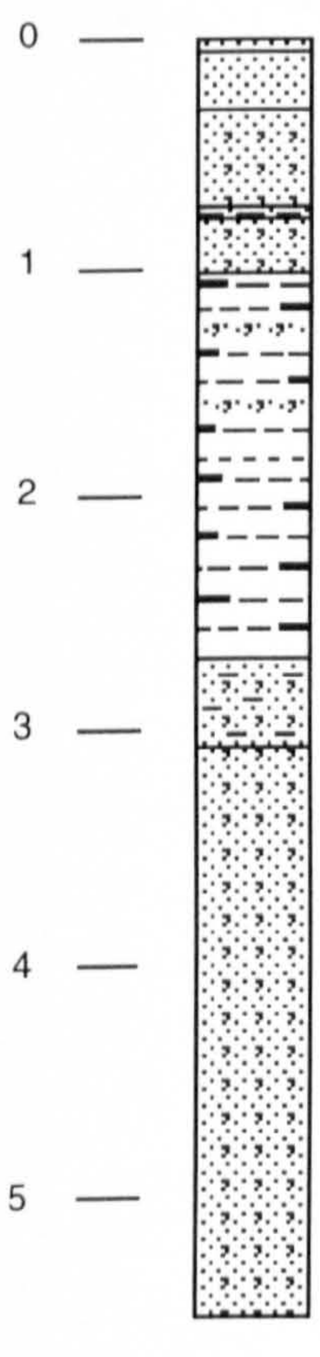

Depth (m) below surface at 4.70 m OD	Troels-Smith	Munsell	Description
	Ga2 Gs2	7.5YR 5/6	Strong brown sand
	Ga2 Gs2	7.5YR 5/2	Mottled brown sand
	Ga2 Gs2	7.5YR 5/2	Mottled brown shelly sand
	Ag3 Ga1	7.5YR N 5/	Grey sandy silt
	Ga2 Gs2	7.5YR N 5/	Grey shelly sand
	As2 Ag2	7.5YR N 5/	Highly stratified grey silty clay containing shelly sand lenses
	As2 Ag2	7.5YR N 5/	Dark grey silty clay stratified at base
	Ga3 Ag1	7.5YR N 5/	Grey silty sand containing shell fragments
	Ga2 Gs2	7.5YR N 4/	Dark grey shelly sand

Figure 4.16 A detailed description of the lithology at site 22

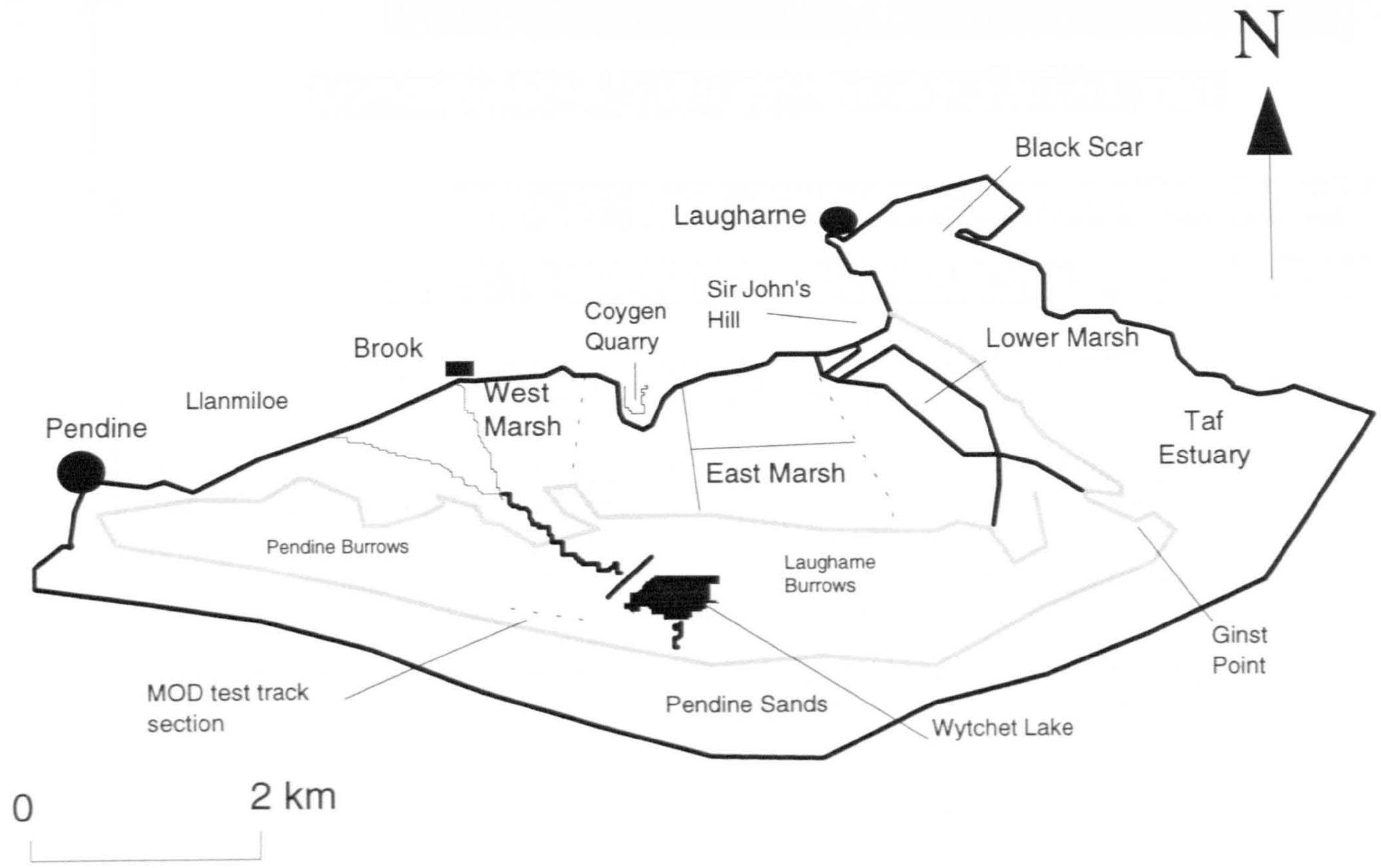

Figure 4.17 Location of MOD test track section

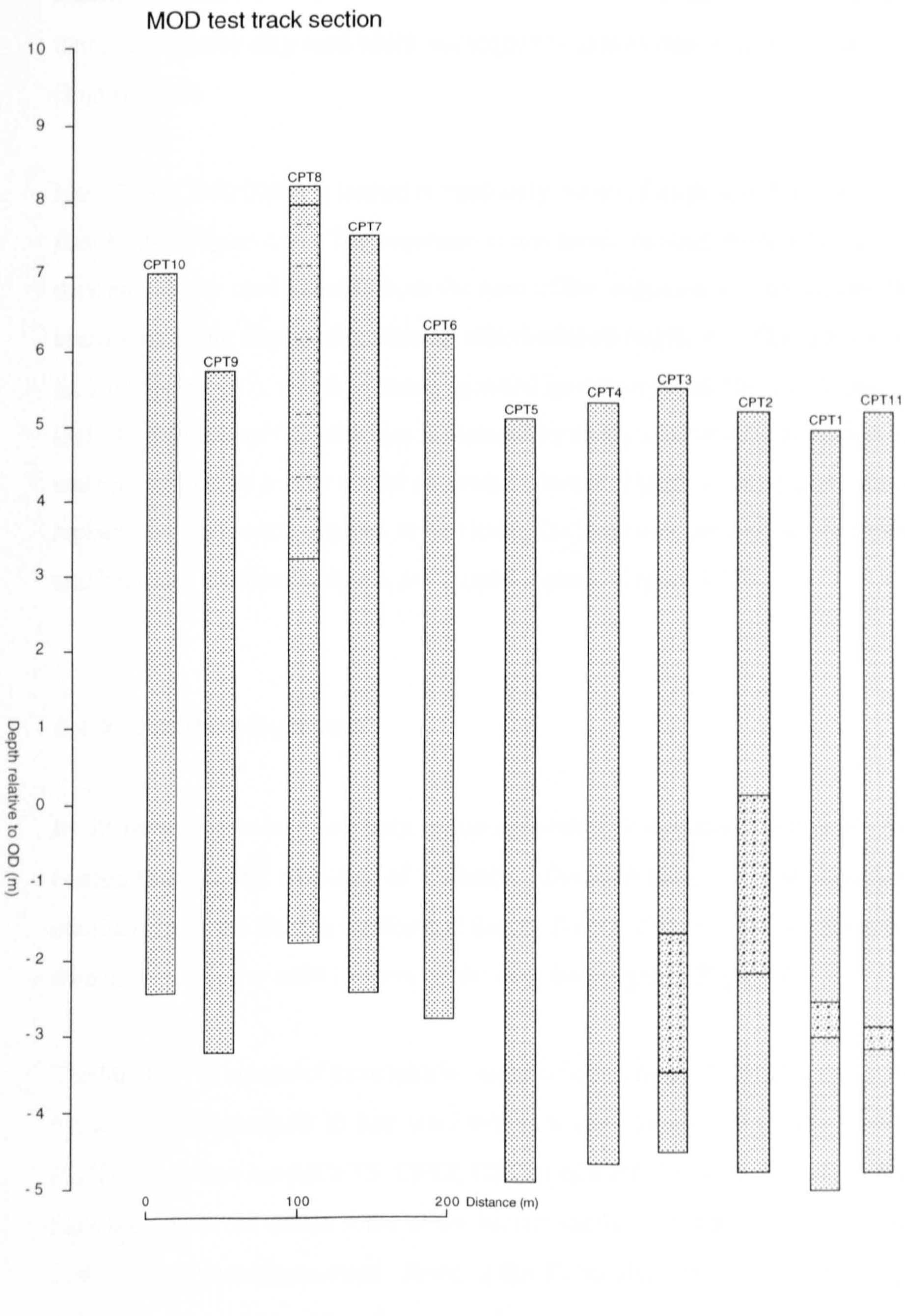

Figure 4.18 Lithological sequence through Pendine Burrows drawn from borehole logs obtained from BGS

unit is overlain by silty sand which subsequently grades into silty clay at the top of the sequence (Figure 4.15).

Site 22 (SN 3070 0796) is located immediately behind Laugharne Burrows in a field adjacent to East House (Figure 4.9). The sequence at this locale extends from 4.70 to -0.80 metres OD. A dark grey shelly sand extends from the base of the sequence to 1.62 metres OD where it grades into an overlying silty sand containing reworked shell fragments. The latter grades into silty clay (at 2.00 metres OD), which becomes stratified by numerous shelly sand lenses above 2.80 metres OD. At 3.68 metres OD silty clay is replaced by shelly sand and the boundary between these two units is marked by a very abrupt erosional contact (Figure 4.16). Above this the shelly sand is replaced by well sorted medium to fine sand; this latter unit contains no reworked shell fragments and becomes oxidised towards the ground surface (Figure 4.16).

4.1.4 Pendine Burrows

In 43 three boreholes have been either recovered or described within the burrows by private contractors for the Ministry of Defence. Detailed surveyed lithological descriptions were obtained from the British Geological Survey for all of these sites; however accurate positional data is available for only thirteen of the sites investigated (Figure 4.17).

The lithology at eleven of these sites is summarised in figure 4.18. The sediments are dominated by well sorted medium to fine sand which is occasionally intercalated with either silty sand (CPT8) or coarse sand (CPT3, CPT2, CPT1 and CPT11). Although reworked shell fragments have been observed within some of the barrier sands, no calcareous material is described at any of the eleven sites summarised. None of the 43 lithological descriptions include any reference to bedding structures within the barrier dunes.

4.1.5 Taf Estuary

A large number of relatively short cores were obtained from two of the saltmarshes within the Taf Estuary (Figure 4.19).

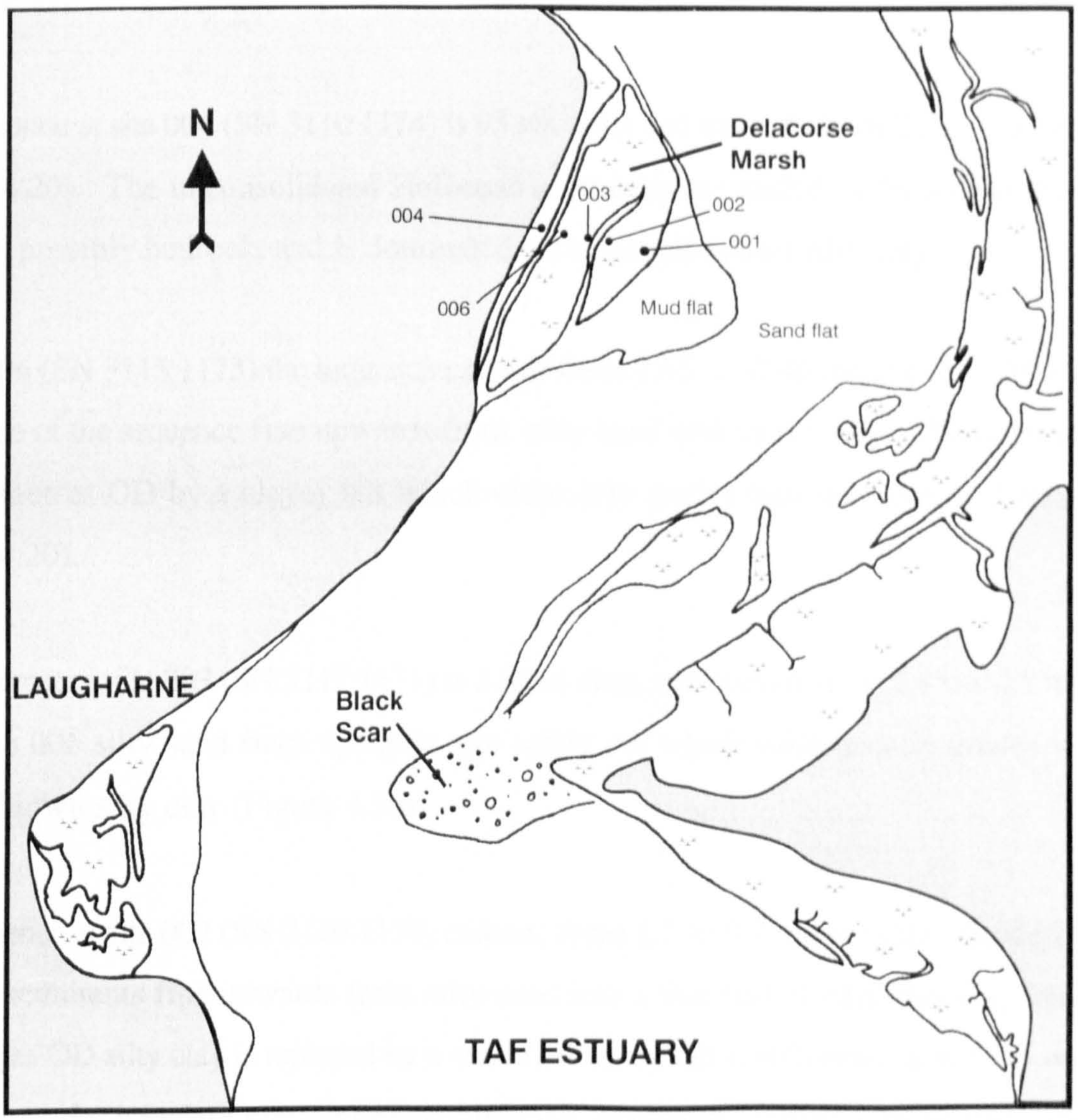

Figure 4.19 Location of cores recovered from Delacorse Marsh

Delacorse Marsh

Five cores were recovered along a transect which extends from the cliff line to the edge of Delacorse Marsh. The marsh is located inland of Laugharne on the western side of the estuary (Figure 4.19).

The sequence at site 004 (SN 3110 1174) is 93 cm deep and extends from 2.2 to 1.27 metres OD (Figure 4.20). The unconsolidated Holocene sediments are underlain by a hard impenetrable material, possibly bedrock, and is dominated dark greyish brown silty clay.

At site 006 (SN 3113 1173) the sequence extends from 2.65 to -0.40 metres OD. The sediments at the base of the sequence fine upwards from silty sand into sandy silty. The latter is replaced at 0.26 metres OD by a clayey silt which ultimately grades into silty clay at 1.80 metes OD (Figure 4.20).

The sequence at site 003 (SN 3117 1171) is 1.85 m deep and extends from 2.4 to 0.55 metres OD. As at site 006 silty sand fines upwards into sandy silt which subsequently grades into a dark greyish brown silty clay (Figure 4.20).

The sequence at site 002 (SN 3120 1170) extends from 2.2 to 0.7 metres OD. At the base of the core the sediments fine upwards from silty sand into a thin bed of silty clay (Figure 4.20). At 0.38 metres OD silty clay is replaced by a stratified sandy silt which extends to 0.95 metres OD. The latter grades into dark greyish brown silty clay, containing ferruginous nodules and organic material.

Site 001 (SN 3126 1168) is located on the edge of Delacorse Marsh. The core recovered at this locale extends from 2.80 to 1.99 metres OD. The sediments at the base of the sequence are composed of dark greyish brown sand. At 2.11 metres OD the sand is replaced by silty clay and the boundary between these two units is marked by a gradual transition.

KEY

- Silty Clay
- Sandy Silt
- Silty Clay containing organic detritus
- Sandy Silt
- Silty Sand
- Organic Detritus
- Sand containing shell frgaments
- Sand
- Red Boulder Clay containing large orientated clasts

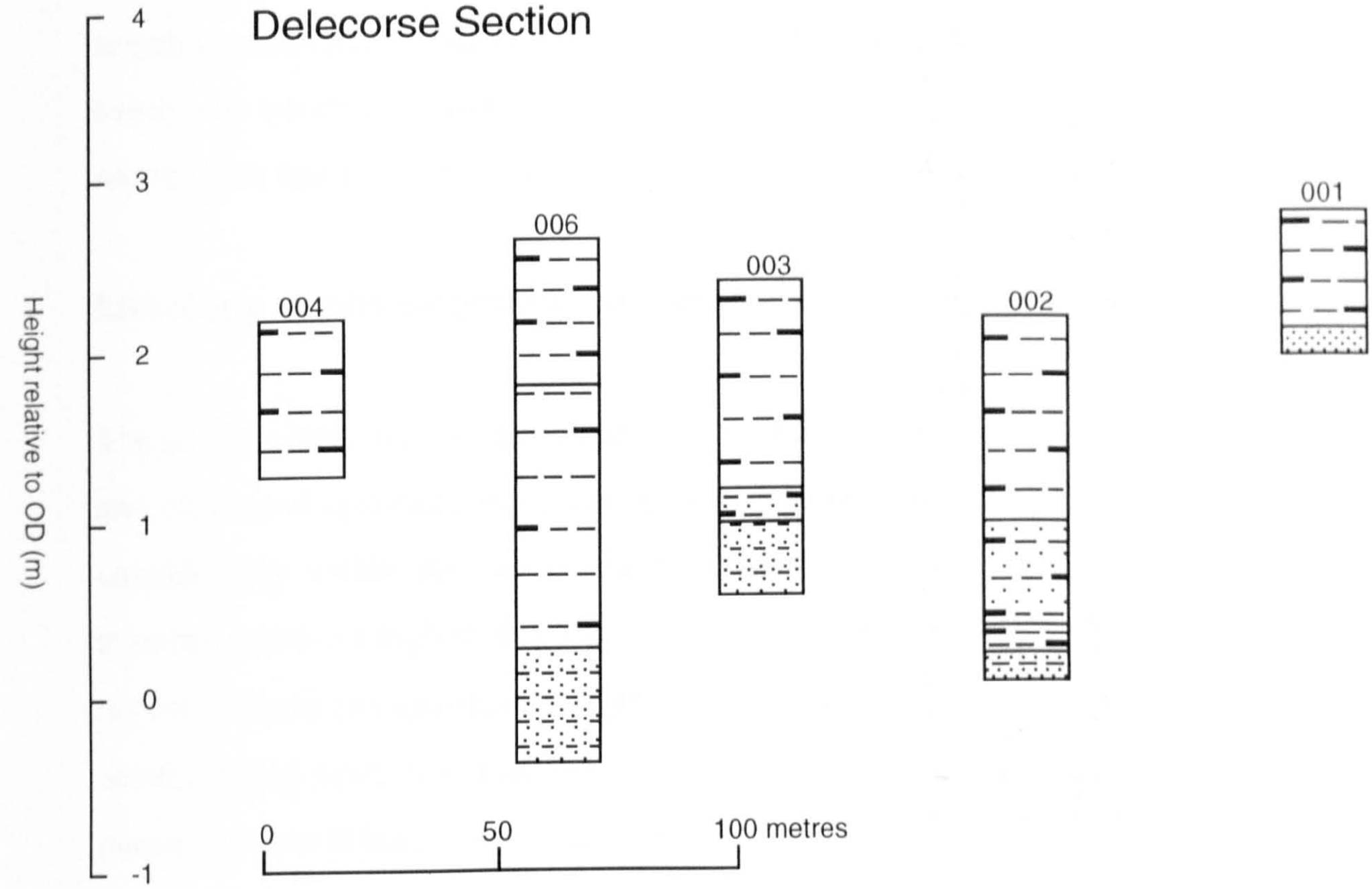

Figure 4.20 The lithology in Delacorse Marsh

Black Scar Marsh

Seventeen boreholes, one to one and a half metres deep, were recovered from Black Scar Marsh. The sediments at the base of the sequence are composed of well sorted medium to fine sand, which is underlain by boulder clay and bedrock. The sands fine upwards into highly stratified sandy silt which ultimately grades into stratified silty clay. The latter unit is on average one metre thick and extends to the contemporary marsh surface.

Lithology of physiographic sub-environments within the Taf Estuary

The contemporary saltmarshes deposits within the Taf are composed of stratified organic-rich silt and clay sized sediment; the proportion of organic matter and the level of bioturbation varies considerably within the near surface sediments. The sediments accumulating upon the low marshes contain a higher proportion of sand and are more highly stratified that the high marsh deposits. Marsh creeks contain a high proportion of silt and sand sized sediment. The sediment accumulating upon the mudflats are dominated by silt size sediment which is stratified by numerous sand lenses. In contrast sandflat deposits are composed of fine and medium grained sand.

4.1.6 Summary

The sequence in West Marsh is underlain by poorly sorted dense red gravel facies which contains large horizontally orientated clasts of sandstone. The relative depth to this facies, beneath the ground surface, varies throughout West Marsh and due to constraints imposed by the coring technique was located at only three of the nine sites investigated.

At sites 9 and 11, located immediately behind the Burrows, the lithology is dominated by well sorted medium to fine sand, silty sand and sand with occasional shell fragments. These deposits represent medium to high energy environments located within close proximity to the barrier. These coarse deposits may represent washover or blowout sediment deposited during periods of barrier instability. Sites 7, 12, 6, 5, 3 and 4 are located landward of sites 8, 9 and 11 in the back-barrier area immediately adjacent to the fossil cliff line (Figure 4.2). The lithology at these sites is dominated highly stratified fine grained silty clay and sandy silt which are characteristic of

tidally influenced low energy back-barrier environments. Two major organic beds have been described at sites 7, 8, 5, 12 and 4. Similarities in their composition, structure and stratigraphic position suggest that these units may be laterally equivalent and that they represent two major phases of organic accumulation behind the Pendine Burrows within the West Marsh area, which are stratified by fine grained organic rich silts and clays. The contacts between the these organic layers and the overlying and underlying minerogenic sediments suggest a gradual rather than abrupt change from minerogenic to organic sediment and *vice versa*.

The sediments in East Marsh are dominated by shelly sand, fine well sorted sand, silty sand, clayey silt and silty clay. These sediments may be underlain by poorly sorted red gravel though its depth and thickness is uncertain. The sediments in the centre of this area exhibit two phases of fine grained accumulation, which may have occurred during periods of barrier stability. The intervening coarser material may represent the deposition of washover or windblown sediments during periods of barrier instability. The deposits at the eastern end of this area exhibit a gradual fining upwards sequence which is overlain by washover deposits immediately behind the barrier. The thickness and extent of tidal-inlet sequences within East Marsh suggests that these deposits may have accumulated over a much shorter period than those described in West Marsh.

The MOD test track section shows that the dune material described in this study is composed of predominately well sorted fine sand. The coarse material may represent washover by storm waves, with the fine material settling out of the water column as the sea-water slowly drained off the dunes. The data presented here suggests that the dunes do not rest upon fine grained silts and clays, provided that these deposits are not preserved at greater depth. If so, the barrier may not have retreated over back barrier deposits during periods of limited sediment supply and rapid sea-level rise.

The deposits within the Taf Estuary are similar to those described along the East House section. The sediments fine upwards from a basal sand into silt clay at the top of the sequence. The large majority of the silt and clay, seaward of the 'Freathing' sea-wall (section 1.2.2), probably accumulated after the barrier had become established.

4.2 Provenance studies

4.2.1 Heavy mineral analysis

The heavy mineralogy of saltmarsh and back barrier sediments

Heavy minerals present within samples taken from Delacorse marsh and the back barrier deposits are dominated by chlorite, zircon, amphiboles(blue/green amphiboles and hornblende), augite and apatite. The sediments also contain variable quantities of garnet, epidote, andalusite, rutile and tourmaline. Chloritoid and glaucophane have been identified but they occur in extremely low frequencies. The relative contribution of each of these minerals to the total non-opaque assemblage varies in response to the samples textural composition. Details regarding sample locations and their grain size characteristics are summarised in table 4.1. The heavy minerals identified in samples taken from the Taf Estuary and the back barrier deposits are summarised in table 4.2, as percentages of the non-opaque fraction.

The heavy minerals contained within the fine sand at the base of core 006 are dominated by chlorite (22.3%), rutile (14.7%) and zircon (12.8%). These sands (006,4) also contains lesser amounts of apatite, garnet, augite, andalusite, tourmaline and epidote, as well as low numbers of zoisite, tourmaline and glaucophane (Table 4.2). Above this the sediments fine upwards into a poorly sorted silt. The heavy mineral fraction in level 006,3 is composed of chlorite (25.9%), augite (15.7%), rutile (14.7%) and zircon (12.8%); the sample also contains lesser amounts of zoisite, apatite, hornblende, tourmaline, amphibole, andalusite and epidote (Table 4.2). Towards the top of site 006 the sediments grade from fine silt into clay and associated with this is a corresponding increase in the relative proportion of chlorite from 33.8 % (006,2) to 50.1% (006,1). Both of these units contain extremely small quantities of zircon, in comparison to the underlying sand (Table 4.2). The remainder of the heavy mineral fraction in sample 006,2 is composed of augite (16.7%) apatite (13.3%) and hornblende (13.3%), with occasional grains of zoisite, tourmaline, garnet, rutile, zircon and epidote. Other common heavy minerals within the clays at the top of the sequence (006,1) include hornblende (19%), augite (15.8%) and apatite (6.3%). These fine grained sediments also contain occasional grains of garnet, zoisite, tourmaline, andalusite and epidote (Table 4.2).

Sample number	Core number	Sample depth (m OD)	Mean grain size (ϕ)	Sorting (ϕ)	Skewness (ϕ)	Kurtosis	Description
001,1	001	2.40	9.45	-3.13	0.18	0.78	Silty clay
002,4	002	0.20	5.54	-3.09	-0.86	0.87	Silty sand
002,3	002	0.35	8.79	-3.08	0.12	0.75	Silty clay
002,2	002	0.80	7.62	-3.73	-0.20	0.55	Sandy silt
002,1	002	1.80	9.88	-2.60	0.10	0.69	Silty clay
003,3	003	0.45	3.06	-1.44	-0.66	0.50	Silty sand
003,2	003	1.24	8.29	-3.07	-0.10	0.92	Sandy silt
003,1	003	1.99	9.25	-2.35	-0.01	0.66	Silty clay
006,4	006	-0.25	No data	No data	No data	No data	Silty sand
006,3	006	0.20	No data	No data	No data	No data	Sandy silt
006,2	006	1.35	No data	No data	No data	No data	Clayey silt
006,1	006	2.25	No data	No data	No data	No data	Silty clay
P2	PEN1	2.09	No data	No data	No data	No data	Clayey silt
P1	PEN1	2.30	No data	No data	No data	No data	Silty sand
CB4	Grab	Surface	2.51	0.45	-0.36	1.83	Sand
CB31	Grab	Surface	1.58	0.64	-0.41	2.19	Sand
CB55	Grab	Surface	1.89	0.51	-0.27	0.98	Silty sand
CB78	Grab	Surface	2.05	0.44	-0.27	1.33	Sand
CB101	Grab	Surface	1.91	0.36	0.06	0.91	Silty sand
CB128	Grab	Surface	1.18	0.74	-0.26	1.65	Sand

Table 4.1 The description and position of the samples examined using heavy mineral analysis

Mineral	001,1	002,1	002,2	002,3	002,4	003,1	003,2	003,3	006,1	006,2	006,3	006,4	P1,1	P1,2
Garnet	3.6	7.6	4.1	3.9	1.3	7.3	1.5	2.6	2.6	3.0	0.5	7.6	3.6	7.9
Rutile	3.6	4.3	1.6	1.7		5.0	1.9	9.4	0.7	2.7	11.9	14.7	4.0	4.6
Zircon	8.0	8.6	9.4	6.6	10.4	11.9	4.9	18.7	0.4	1.9	10.3	12.8	11.4	14.1
Apatite	9.6	6.6	4.9	5.2	4.2	6.4	2.6	8.5	6.3	13.3	6.5	8.5	10.0	8.0
Siderite														
Tourmaline	5.6	2.2	4.9	0.9	2.9	5.0	3.4	3.8	1.5	4.6	5.4	2.8	3.6	7.1
Andalusite	2.8	1.3	3.2	0.9	0.8	3.7	2.6	4.7	1.1	3.8	3.2	5.7	6.8	2.5
Brookite														
Staurolite														
Kyanite														
Amphibole	0.8	3.0	4.9	1.3		4.6	3.4	8.1		0.8	3.8		7.7	5.4
Hornblende	1.2	4.3	3.2	2.1	3.3	3.2	5.2	5.1	19	13.3	5.9	5.7	1.4	2.5
Barkevicite														1.2
Blue Green Amphiboles					7.2									
Glaucophane		0.4	0.4		0.4									
Chloritoid			0.4	0.9							1.0	1.4		
Chlorite	58.8	52.6	61.1	72.0	59.0	31.2	61.2	20.4	50.1	33.8	25.9	22.3	41.3	34
Epidote	1.2								1.1	0.7	2.2	5.2		
Clinozoizite					0.4									
Zoisite	0.8	2.6	1.6	0.9	3.8	6.9	2.2	1.7	2.0	5.4	7.6	3.8	1.4	3.7
Pyroxene	2.8	2.2	1.2	2.6	0.8	0.4								
Augite	1.2	4.3	1.6	3.1	5.9	14.2	10.0	15.7	15.8	16.7	15.7	6.6	4.1	2.5
Diopside														
Opaque %	42.2	47.9	44.0	48.7	43.4	46.4	42.9	46.1	38.7	33.2	52.4	48.5	49.3	44.2
Total	436	445	441	446	422	407	469	436	746	642	389	410	434	432
Total Non-Op	252	232	247	229	239	218	268	235	457	428	185	211	220	241

Table 4.2 Composition of heavy mineral assemblages from Delacorse Marsh and East Marsh

The poorly sorted fine sands at the base of site 003 are dominated by chlorite (20.4%), zircon (18.7%) and augite (15.7%) and contain lesser amounts of rutile, apatite, amphiboles, hornblende and andalusite, with the occasional grain of tourmaline and zoisite (Table 4.2). These sands fine upwards into very fine silt which is dominated by chlorite (61.2%). Level 003,2 also contains fewer numbers of augite, hornblende and zircon with the occasional grain of tourmaline, amphibole, apatite, zoisite, rutile and garnet (Table 4.2). At the top of the sequence the sediments fine into poorly sorted clay. The heavy minerals identified in level 003,1 contain relatively fewer numbers of chlorite (31.2%) and higher numbers of augite (14.2%), zircon (11.9%), garnet, zoisite, apatite, tourmaline and andalusite, than observed in the underlying very fine silt bed (Table 4.2).

At the base of site 002 the sediment is composed of very poorly sorted medium silt which contain a heavy mineral fraction dominated by chlorite (59%). Level 002,4 also contains zircon (10.4%), blue/green amphiboles (7.2%) and augite (5.9%) together with occasional grains of apatite, zoisite, hornblende, tourmaline and garnet (Table 4.2). Overlying the latter unit is a thin layer of poorly sorted clay dominated almost exclusively by chlorite (72%). Level 002,3 also contains zircon (6.6%) and apatite (5.2%) with the occasional garnet, augite, rutile and amphibole (Table 4.2). Above this the sediments grade into fine silt which is very poorly sorted and skewed towards the coarse fraction. The assemblage in level 002,2 is dominated by chlorite (61.1%) and contains lesser amounts of zircon (9.4%), apatite (4.9%) and tourmaline (4.9%) with the occasional garnet and andalusite (Table 4.2). This sample also contains extremely low quantities of rutile, hornblende, zoisite, augite, pyroxene, glaucophane and chloritoid. The poorly sorted clay at the top of core 002 contains relatively lower number of chlorite minerals (52.6%). The remainder of the heavy mineral fraction in level 002,1 is composed of zircon (8.6%), garnet (7.6%), apatite (6.9%) and contains small quantities of rutile, augite, zoisite, pyroxene, tourmaline, andalusite and chloritoid (Table 4.2).

The very poorly sorted clay at site 001 has a heavy mineral fraction composed of chlorite (58.8%) with lesser amounts of apatite (9.6%), zircon (8%) and tourmaline (5.6%). Level 001,1 also contains low numbers of garnet, rutile, andalusite, pyroxene, epidote and augite (Table 4.2).

The two samples taken from the back barrier area have very similar heavy mineral compositions to those described from Delacorse Marsh. Sample P2, which is a poorly sorted fine sand, has a

heavy mineral fraction dominated by chlorite (34%) and zircon (14.1%). The sample also contains apatite, garnet, tourmaline and amphiboles, with the occasional rutile, zoisite, andalusite, augite, hornblende and barevicite (Table 4.2). As the sediments fine upwards, into very fine poorly sorted silt, there is a corresponding increase in the relative proportion of chlorite (41.3%), apatite (10%), amphibole and andalusite minerals, with a decrease in the frequency of zircon (11.4%), garnet, rutile and tourmaline (Table 4.2).

From the information outlined above it is clear that the highest concentrations of small dense minerals occur in the poorly sorted fine sands whereas the relatively larger lighter minerals are enriched in the silts and clays. For instance, there is a strong negative correlation (-0.71) between chlorite and mean grain size in contrast to the strong positive correlation (0.87) between zircon and mean grain size. The relationship between sample texture and heavy mineral composition may have significant implications upon the general validity of these results and their ability to trace sedimentary transport paths.

The origin of sediments within the Taf Estuary and the barrier complex

The sediments within the barrier complex and the Taf Estuary may originate from a number of possible sources, comprised mainly of drifts derived from either Welsh or Irish Sea Ice (Griffiths, 1939; Cambell and Bowen, 1989). The proportion of foreign minerals within the Irish Sea Drift varies in response to the contribution from 'local' sources, and the Welsh drifts maybe subdivided on the basis of local erratics. Other sources include glacio-fluvial material of both Irish Sea and Central Welsh origin, together with other materials of mixed provenance. All these deposits contain their own characteristic suite of minerals which complicates any attempts to retrace sediment transport paths.

In this study the estuarine and back-barrier sediments are compared to five potential source materials and six surface grab samples from Carmarthen Bay. The five potential sources include Late Devensian loess from Eastern Slade on the Gower Peninsula, till from Broughton Bay on the Gower Peninsula (deposit derived from Central Welsh Ice which has reincorporated Irish Sea till in Carmarthen Bay), Breconshire Drift (Welsh Origin) from Langland Bay on the Gower Peninsula, glacigenic material within the Taf Estuary and soil developing upon the Ordovician Llandeilo Mydrim shales northwest of St Clears (Table 4.3).

Mineral	CB4	CB31	CB55	CB78	CB101	CB121	Taf Drift	St Clears soil	Loess	Broughton Bay till	Breconshire Drift
Garnet	24.0	42.5	40.2	41.5	33.8	47.6	11.3		4.9	6.8	1.4
Rutile	3.9	6.0	12.4	7.5	4.4	3.8	3.2		11.4	4.5	42.2
Zircon	18.1	13.7	19.2	8.4	15.9	12.0	15.1	1.2	7.3	9.7	5.2
Apatite	4.6	1.7	1.0	4.5	2.1	1.0	1.3		2.4	3.9	3.8
Siderite					8.3	7.2					
Tourmaline	55.3	3.5	7.6	5.5	9.3	3.4	8.0	0.3	8.9	2.6	12.8
Andalusite	6.9	2.8	1.0	1.0	1.0	0.6				2.9	
Brookite									3.3		0.95
Staurolite	0.7	7.0	3.1	6.5	3.1	3.1	3.2	0.3		2.3	
Kyanite	1.6	1.4	3.4	2.0	1.4						
Amphibole	10.9	2.8	2.4	4.5	5.7	4.1					
Hornblende	3.6	3.5	1.4	3.5	1.7	1.0	4.5	0.3	3.2	0.6	1.4
Barkevicite				0.5			1.3	0.6	4.1	0.6	
Blue Green Amphiboles											
Glaucophane		0.7					0.6			0.3	
Chloritoid										0.3	
Chlorite	10.2	3.5	0.7	1.0	3.4	1.0	34.7	95.4	41.5	59.7	32.3
Epidote	1.3				1.3			0.6		0.3	
Clinozoizite							1.2		4.1	0.7	
Zoisite	2.6	0.7	0.7	2.0	2.7	3.4	1.2	0.3	3.2	2.6	
Pyroxene			3.1	0.5		0.3	3.5				
Augite	3.6	10.2	2.4	4.5	2.6	2.7	6.8		3.2	1.3	
Diopside					1.4	1.4			0.8		
Opaque %	58.9	62.3	62.8	53.8	61.2	63.8	68.9	31.8	91.0	82.9	95.5
Total	740	755	782	433	748	806	1000	481	1249	1803	4703
Total Non-Op	304	285	291	200	290	292	311	328	123	308	211

Table 4.3 Composition of heavy mineral assemblages from potential source materials.

The heavy minerals within the till from Broughton Bay, the Local Welsh till, the drift within the Taf Estuary and the loess from Eastern Slade are dominated by chlorite and contain greater or lesser amounts of zircon, garnet, rutile and tourmaline (Table 4.3). In seeking the source of minerals within the Irish Sea till Griffiths (1939) computed a heavy mineral assemblage typical of that deposit. The critical assemblage of foreign minerals, contained within the Irish Sea till, consists of staurolite, kyanite, chloritoid, epidote, andalusite and blue/green amphiboles (Griffiths, 1939; Case, 1983). If these minerals are identified in a particular deposit were derived from materials introduced into the area by the invasion of Irish Sea Ice.

The extremely high proportion of chlorite (59.7%) in till from Broughton Bay represents the incorporation of Lower Palaeozoic Shales by the advancing ice mass (Griffiths, 1939). The high frequency of 'local' minerals within this till results in a reduction in the total number of foreign minerals derived from Irish Sea till reincorporated in Carmarthen Bay, which only account for 7% of the total non-opaque heavy mineral assemblage in this sample (Table 4.3).

Within the Taf Estuary a morainic ridge of poorly sorted red diamicton extends from the Devonian Old Red Sandstone cliff line, on the east side of the estuary, beneath the saltmarsh and across the sand and mudflats. This feature, known as Black Scar, is thought to represent either a halt stage or a slight readvance during the retreat of the Towy glacier in the Late Devensian (Griffiths, 1939; Bowen, 1970). A sample of this drift, taken from a field above the saltmarsh, has relatively high percentages of zircon, garnet and tourmaline, with chlorite amounting to only 34.7% of the non-opaque heavy mineral assemblage (Table 4.3). The relatively high percentages of garnet, zircon and tourmaline together with the deposits diagnostic red colour reflects the close proximity of Devonian Old Red Sandstone. Foreign minerals within this deposit indicate that, if this feature was formed by a slight readvance in the retreating Towy glacier, the ice must have reincorporated Irish Sea till (Griffiths, 1939).

The occurrence of kyanite and blue/green amphiboles within the windblown sediments from Eastern Slade indicates that these materials may be partly derived from Irish Sea till.

The heavy mineral suite within the soil sample, taken from the floodplain adjacent to the River Taf, is composed almost exclusively of chlorite (95.4%) with occasional grains of zircon, tourmaline, staurolite, blue/green amphiboles, hornblende, epidote and zoisite (Table 4.3). The

trace amounts of foreign minerals within these soils may be derived from the considerable quantities of drift to the north and west of St Clears. These drifts are thought to represent the remains of an outwash fan generated by the Towy glacier during the Late Devensian maximum (Griffiths, 1939). As the Towy glacier is believed to have reincorporated Irish Sea till, these deposits contain both Irish Sea and Central Welsh material.

Sediments offshore in Carmarthen Bay are composed of medium to fine sand which is well to moderately well sorted and has either a strong negatively skewed or symmetrical distribution (Table 4.1). The heavy mineral fractions in all six Carmarthen Bay samples are dominated by an assemblage composed of garnet, zircon, augite, apatite, hornblende, and amphibole (Table 4.3). In contrast to the estuarine and back barrier sediments these sands contain very low frequencies of chlorite, which on average does not amount to more than 3.5% of the non-opaque assemblage. The relative proportion of foreign minerals within the Carmarthen Bay sands varies from 7.9% (CB55) to 11.2% (CB31) and includes andalusite, staurolite, kyanite and epidote grains.

All fourteen samples taken from the back-barrier and saltmarsh sediments contain foreign minerals derived from Irish Sea Drift. Within the Delacorse Marsh sediments the relative proportion of foreign minerals is highest in the sands at the base of the sequence (4.7% to 10.0%) and lowest in the clays at the top of the sequence (1.3% to 3.7%). This foreign component is composed of andalusite, epidote, chloritoid and blue/green amphiboles; none of the samples contain the whole suite of foreign minerals. A similar decrease, in the observed frequency of foreign minerals, occurs in the back-barrier deposits. As the sediments fine upwards from sand (P1) into silt (P2) there is a corresponding decrease in the frequency of foreign minerals from 6.8% to 2.5%. The presence of foreign minerals within all the estuarine and back-barrier samples analysed is undisputable evidence that these sediments are partly derived from Irish Sea till.

Principle Component Analysis (PCA), applied to the untransformed non-opaque heavy mineral data, was utilised in order to compare the complex multivariate data sets identified in this study. The correlation coefficients derived from the first and second principle components account for 66.1% and 22.6% of the total variance within all twenty five samples. By plotting PC1 and PC2 on the y- and x-axes it is clear that the heavy mineral compositions of the Carmarthen Bay sands are very different to the saltmarsh and back-barrier deposit (Figure 4.21).

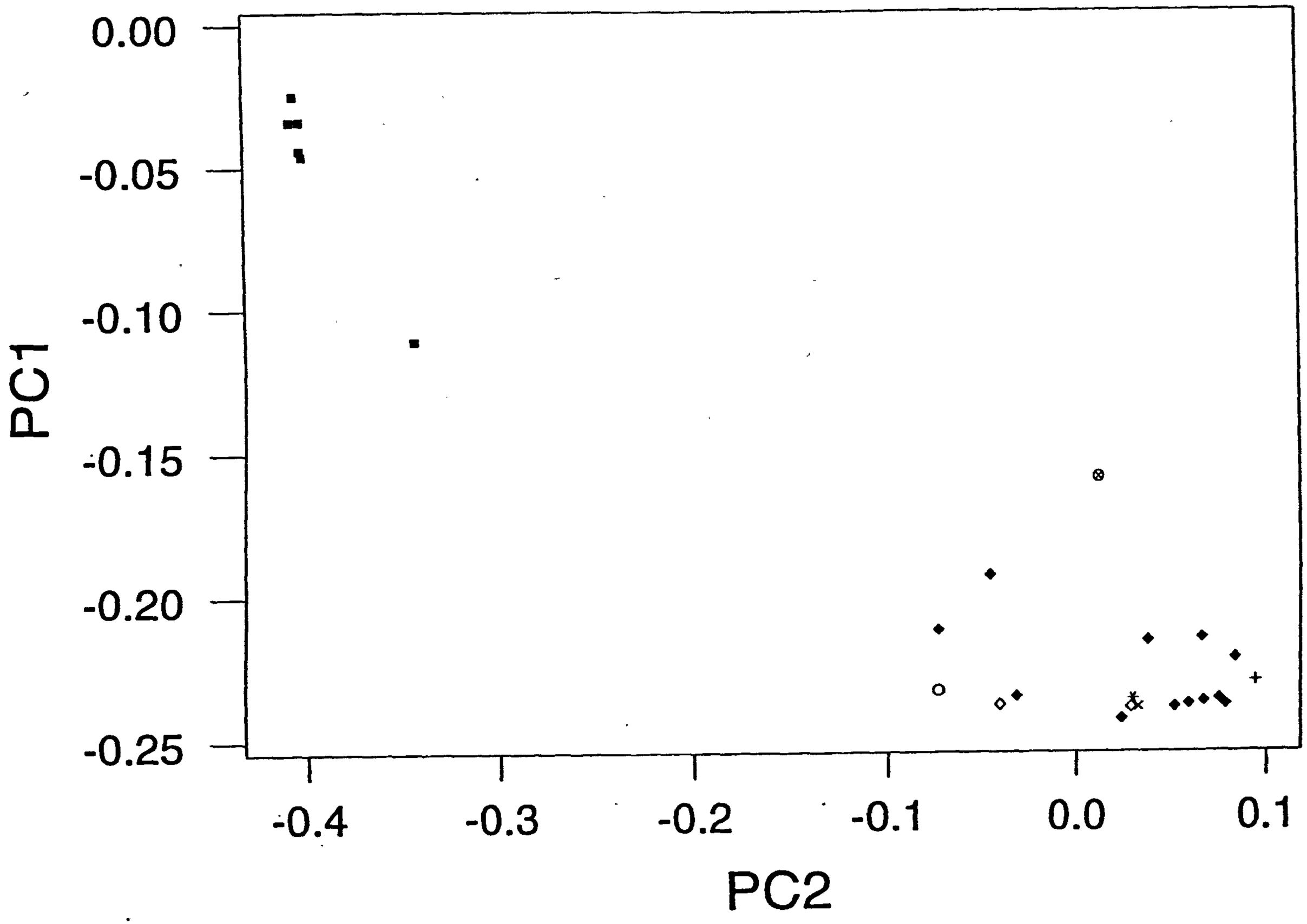

Figure 4.21 PCA applied to the untransformed non-opaque heavy mineral assemblages; estuarine samples (◆), back-barrier deposits (◊), Carmarthen Bay sands (■), loess (X), Irish Sea Drift (*), Breconshire Drift (⊗), moraine within the Taf Estuary (⊙), and the soil sample (+).

Barrie (1978) examined the distribution of heavy minerals within the surficial sediments in the Bristol Channel. He indicates that there is a progressive increase in the concentration of garnet from the deeper outer channel to mid-depth (approximately 30 metres below chart datum). As the channel shallows the relative proportion of garnet decreases and reaches a minimum in areas of shoaling. Barrie (1978) also discovered that, due to its small size and high density, zircon is concentrated on the beaches exposed to the intense southwesterly storms, such as Rossili and Kenfig. Although the sands at Ginst Point have not been analysed it is likely that the same processes concentrate zircon on the beaches adjacent to the Taf Estuary. This indicates that the variance accounted in PC1 (Figure 4.21) represents selective sorting within Carmarthen Bay, whereby differential entrainment, transport, and settling effectively concentrate zircon on the beaches and garnet offshore. Similar concentrations of garnet are not found in any of the potential sources analysed in this study.

The second principle component accounts for the major source of variance within the estuarine and back-barrier deposits (Figure 4.21). Although the back-barrier silt (P1) and the clay at the top of core 002 have heavy mineral compositions very similar to those within the Irish Sea Drift and loess, their foreign component (2.5% and 1.3% respectively) is much lower than in the sands at the base of the sequence. This indicates that the similarity results from the relative proportions of the major constituents within the heavy fraction and does not reflect the dissimilarity in the relative proportion and composition of the foreign component. The remainder of the silts and clays within Delacorse Marsh have heavy mineral assemblages comparable to soil sample, and the sands are similar in composition to the drift within the Taf Estuary. None of the marsh or barrier complex sediments analysed have compositions similar to the Breconshire Drift from Langland Bay.

Although at present there is a net westerly transport of material out of the Bristol Channel, recent studies suggest that in Carmarthen Bay, as in the Severn Estuary, bedload parting results in mutually evasive sediment transport (Stride and Belderson, 1990, 1991). Material is transported onshore by the flood tide and contributes to the infilling of the Taf Estuary. This hypothesis was supported by Jago (1974, 1980) who indicates that the Taf Estuary is currently being infilled by sand transported on-shore. As sea-level is believed to have attained its present level approximately 5,000 years BP (Heyworth and Kidson, 1982; Allen and Rae, 1988) it is likely that

the modern hydrodynamic regime was established soon after this time. This implies that any fine grained material contained within the offshore sediments, not removed by the advancing high energy shoreline, would have been removed rapidly. As the Bristol Channel and Carmarthen Bay sediments contain very little chlorite it is extremely unlikely that the chlorite within the estuarine sediments is derived from offshore. Barrie (1978) argues that sediment is presently entering the Bristol Channel via the rivers Taf, Towy and Severn. The Lower Palaeozoic shales within the catchment areas of the rivers Taf and Towy maybe a source of the large quantities of chlorite contained within Delacorse Marsh and back-barrier deposits.

The relatively high proportion of chlorite in the wind blown sediments on the Gower Peninsula suggests the tills derived from Irish Sea and Welsh ice, exposed in Carmarthen Bay and the Bristol channel, contained a relatively large amount of this mineral. As the transgressing high energy surf-zone, enhance storm waves and tidal scour, reworked the Pleistocene deposits on the continental shelf the fine grained material contained within these deposits would have been rapidly removed. The sands remaining offshore were subsequently reworked and selectively sorted; the small dense heavies became concentrated in the beach and estuarine sands whereas the large light minerals became concentrated in the estuarine and back-barrier silts and clays. Therefore when this portion of south Wales was first inundated a large proportion of the fine grained material and chlorite was supplied from the reworking of offshore sediments. During the later part of the Holocene this supply must have decreased as at present the contribution of fine-grained sediments from offshore is insignificant (Allen, 1991).

The analysis therefore reveals that at present heavy minerals are selectively sorted offshore and transported onshore by the flood tide (Jago, 1974, 1980). Once in the estuary the sands are mixed with material rich in chlorite and the subsequent distribution of these minerals in the estuarine sediments depends upon selective sorting by differential entrainment and settling. The fine-grained sediment and chlorite presently accumulating within the estuary is either derived from freshwater input via the Taf and Towy (Barrie, 1978), or is derived from the reworking of fine grained coastal sequences exposed within Carmarthen Bay. The relative decrease in the proportion of chlorite in the sediments at the top of cores 003 and 002 may represent either a temporal decrease in the contribution of chlorite from offshore sources or the complex patterns of sedimentation across the salt marsh.

Although it is clear that the sands within the barrier complex and the Taf Estuary are derived from Central Welsh and Irish Sea Drift, the exact origin of the fine-grained component supplied during the late-Holocene is uncertain. The study is limited by the small number of samples analysed and any conclusions drawn from this discussion should be regarded as preliminary. In this instance heavy mineral analysis reveals how sediment provenance can be evaluated by using a critical assemblage of minerals and how selective sorting mechanisms have operated throughout the Holocene in the back-barrier area and the Taf Estuary. These processes have a significant influence over the ultimate composition of heavy minerals contained within the sediments analysed and cannot be ignored when assessing sediment transport paths.

4.2.2 X-Ray Diffraction Analysis

Clay mineralogy and indications of sediment source

The XRDA results reveal that there is little or no variation in the clay mineral compositions within the estuarine or back-barrier sediments (Figure 4.22). The samples are dominated by illite and contain lesser amounts kaolinite, smectite, vermiculite, chlorite and irregularly interstratified illite/vermiculite. Analysis of the clays within the Carmarthen Bay sample (CB101), the surface samples from Ginst Marsh and the river bank at St Clears show that these samples are extremely similar in composition to the samples taken from core 006, 103 and the back-barrier sediments (Figure 4.23). The data therefore indicates that there is relatively little spatial or temporal variation in the clay mineral compositions within the samples analysed.

Allen (1991) found that the clay minerals contained within the Severn Estuary are very similar in composition to the clays within the Taf Estuary and the adjoining back-barrier area. The assemblage is dominated by illite, expandable minerals, kaolinite and chlorite, which appear to be relatively unchanged throughout the tidal sediments. Allen (1991) argues that as the contribution of fine grained sediments from offshore is insignificant, the similarity between the fine grained saltmarsh deposits and the river input indicates the fine grained material within the Severn is derived from the river catchment. He also suggests that the intensity of the wind-wave climate and the strong tidal currents make the clay mineralogy within the Severn Estuary far less variable than within the river catchment.

(A)

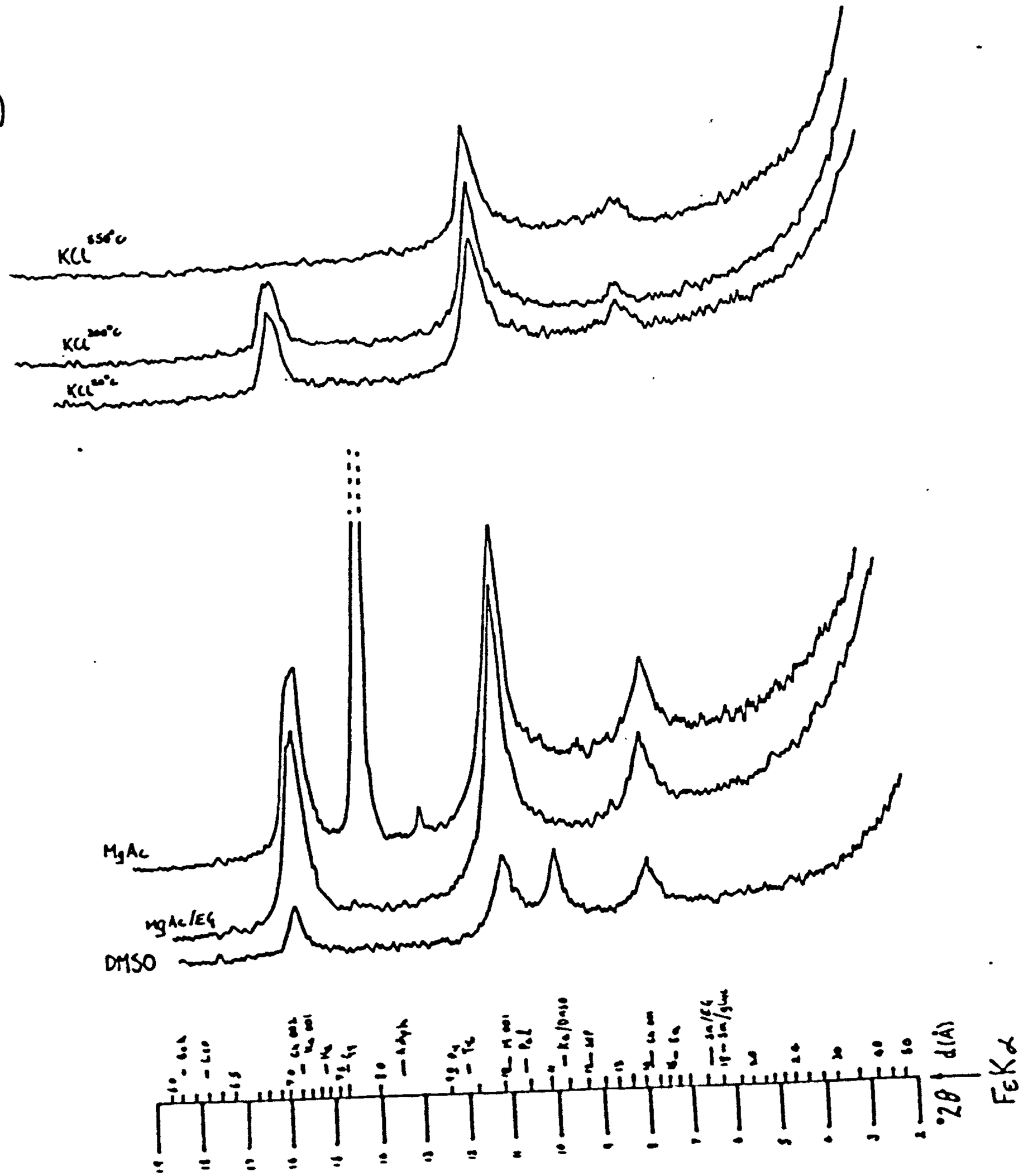

(B)

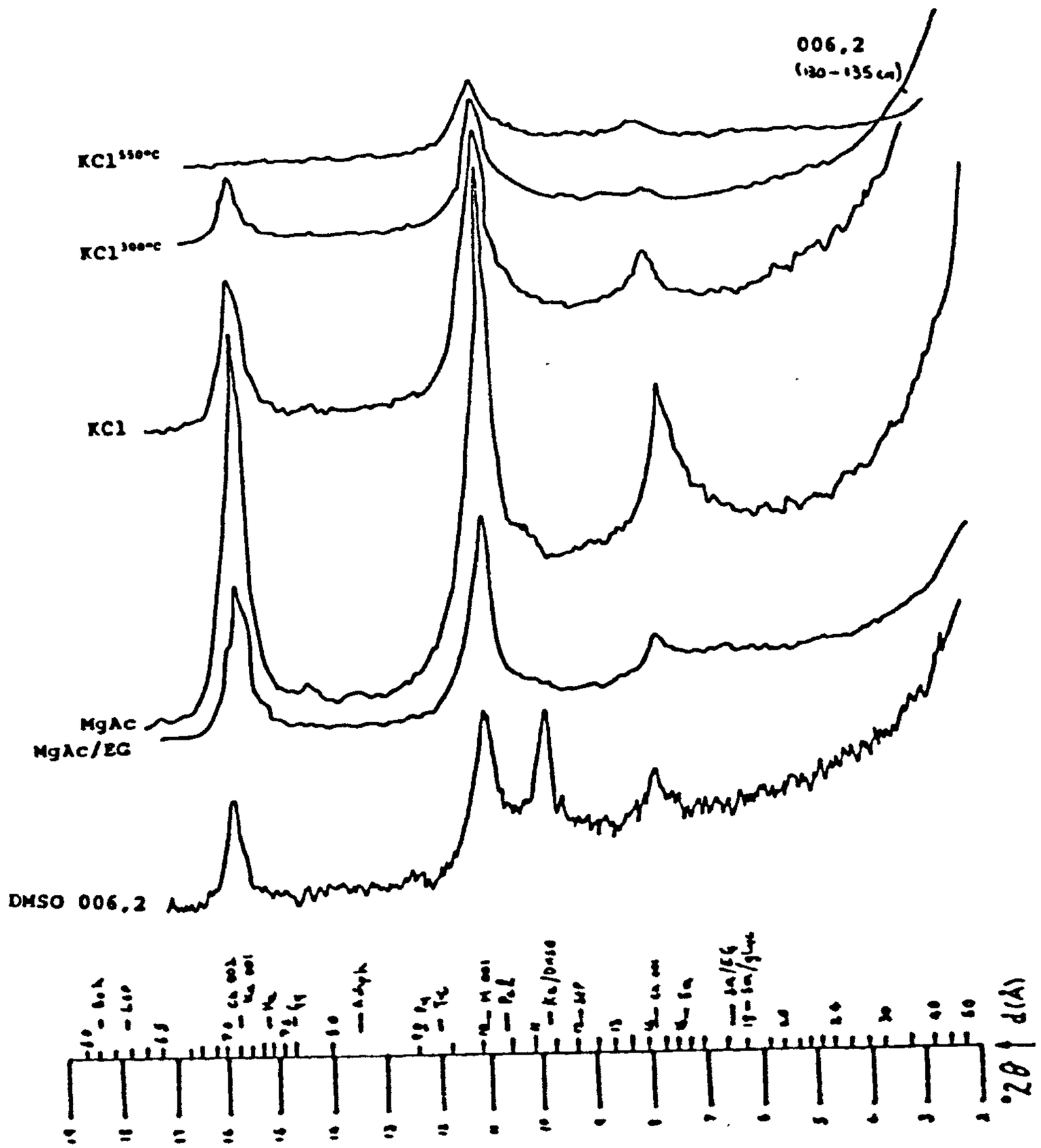

Figure 4.22 XRDA diffraction patterns for (a) the Delacorse Marsh sediments and (b) the Black Scar Marsh sediments.

(A)

KCl 550°C

KCl 350°C

KCl 80°C

Mg Ac

Mg Ac/EG

DMSO

°2θ d(Å) FeKα

(B)

KCl 550°C

KCl 350°C

KCl 80°C

Mg Ac

Mg Ac/EG

DMSO

°2θ d(Å) FeKα

Allen (1991) indicates that illite may be derived from the Lower Palaeozoic rocks in the Welsh Basin and the Triassic beds in the west Midlands and the margins of the Bristol Channel. Kaolinite may be derived from the Upper Palaeozoic sandstones within the south Wales coalfield, the Jurassic (Mesozoic) rocks in the Cotswolds and the Jurassic rocks in the Severn lowland. Chlorite on the other hand is thought to have been derived from the Old Red Sandstone (Devonian) in south-east Wales and the Welsh borders. This mineral may also be supplied by the older Carboniferous Limestone in south Wales or by the Lower Palaeozoic shales and slates within the Welsh Basin (Figure 4.24). Allen (1991) concludes that the macro-tidal flood dominated inner Bristol Channel and Severn Estuary constitute a system in which the provenances of fine and coarse sediment differ sharply. The fines are supplied by fresh-water input whereas the sands are supplied from well sorted reworked glacigenic material offshore.

It is therefore likely that the similarity in the composition of the clay minerals contained within the estuarine and back-barrier sands also results from intense mixing by strong tidal currents and wave activity. All the clay minerals contained within the samples analysed may be supplied from source rocks within the catchments of the rivers Taf, Towy and Gwendraeth. As illite is the most dominant clay mineral in marine sediments (Krouskopf, 1982; Wilson, 1987) it is not surprising that it is the major constituent within the sediments analysed.

The fines presently accumulating within the Taf Estuary may therefore be derived from fresh-water input. As no early Holocene sediments have been analysed conclusions cannot be made with regard to the long term provenance of fines within this system. It is possible that with changing landuse patterns and forest clearence, in the surrounding landscape, that the rivers draning into Carmarthen Bay were a major source of fine grained material during the Holocene. Furthermore, as the major proportion of material within the Irish Sea and Central Welsh Drifts is derived from local sources it would be extremely difficult to elucidate changing fine grained sediment transport paths on the basis of clay mineralogy.

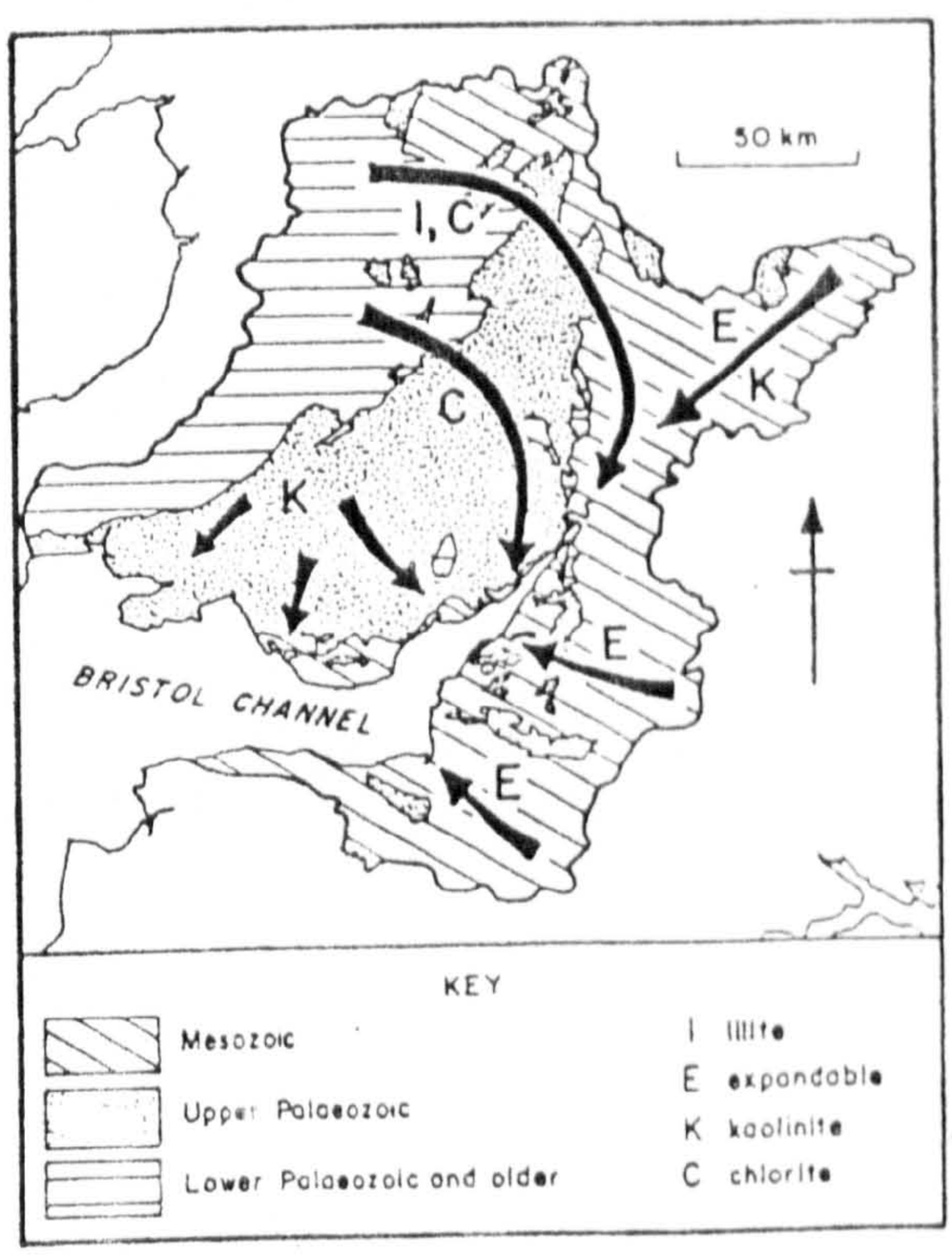

Figure 4.24 The major sources of clay minerals within the Severn Estuary and the lower Bristol Channel (Allen, 1991).

Although XRDA is less diagnostic than provenance studies based upon heavy mineral data, the clay mineral assemblages reflect the intensity of the hydrodynamics within Carmarthen Bay and the Taf Estuary and indicate that the sediment currently accumulating within the Taf Estuary may be derived from fresh water input.

4.3 Environmental Magnetism

4.3.1 Description and interpretation of geomagnetic measurements

West Marsh

The whole core initial susceptibility measurements (*k*) for sites 7, 12, 9, 4 and 11 are presented in figure 4.25; the measurements are quoted in SI units and relate to susceptibility per unit volume (Thompson and Oldfield, 1986).

At site 7 the lower nine metres of the sequence exhibit extremely variable levels of susceptibility, which range from 0 to 468 SI (Figure 4.25a). The highest peaks in *k* are measured in stratified silty clay beds, whereas the lowest *k* values correspond to organic detrital units. For instance, the black organic detritus between 3 and 4 metres depth contains little or no minerogenic material and consequently has no measurable *k* (Figure 4.25a). Above 3 metres depth the *k* values increase slightly, as the sediments fine upwards from shelly sand into silty clay, and remain relatively constant at 15 SI until approximately 0.20 m depth where *k* increases to 48 SI in the oxidised top soil (Figure 4.25a).

The susceptibility measurements at site 12 display a similar patterns to those obtained from site 7. In the lower nine metres of the sequence *k* is extremely variable and values range from 0 to 200 SI. The *k* peaks are measured in the silty clay and sandy silt beds, whereas the minimum values corresponds to organic detrital units (Figure 4.25b). Between 3 and 1 metres depth *k* increases initially to 31 SI, as the sediments grade from organic detritus into silty clay, and then diminishes as the relative proportion of organic detritus once again increases. Above this *k* gradually decreases to 9 SI as the deposits coarsen upwards into mottled brown sandy silt. There is no peak in susceptibility in the oxidised top soil at site 12 (Figure 4.25b).

The susceptibility of the sands, silts and clays at site 9 is far less variable than at those sites previously described (Figure 4.25c). Although the *k* does vary, background levels decrease from 15 SI at 7 metres depth to 6 SI at 0.4 metres depth, and a high *k* peak of 72 SI is measured in the

KEY

Silty Clay

Sandy Silt

Silty Clay containing organic detritus

Sandy Silt

Silty Sand

Organic Detritus

Sand containing shell frgaments

Sand

Red Boulder Clay containing large orientated clasts

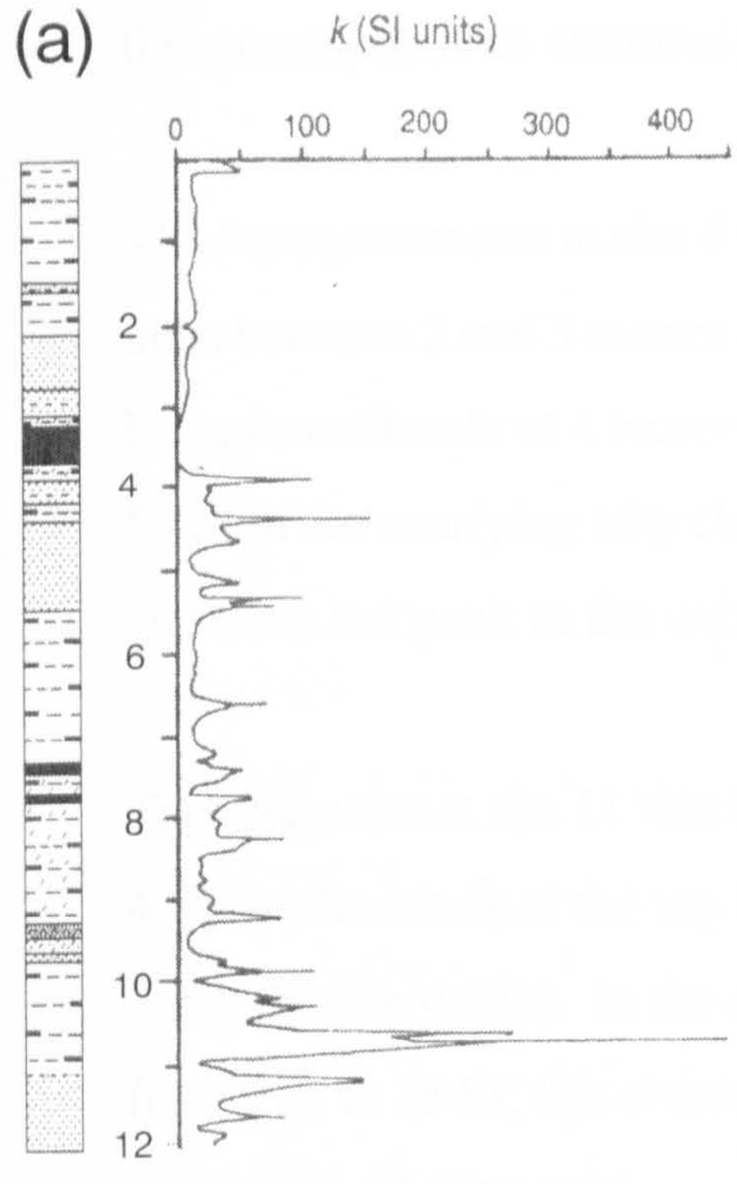

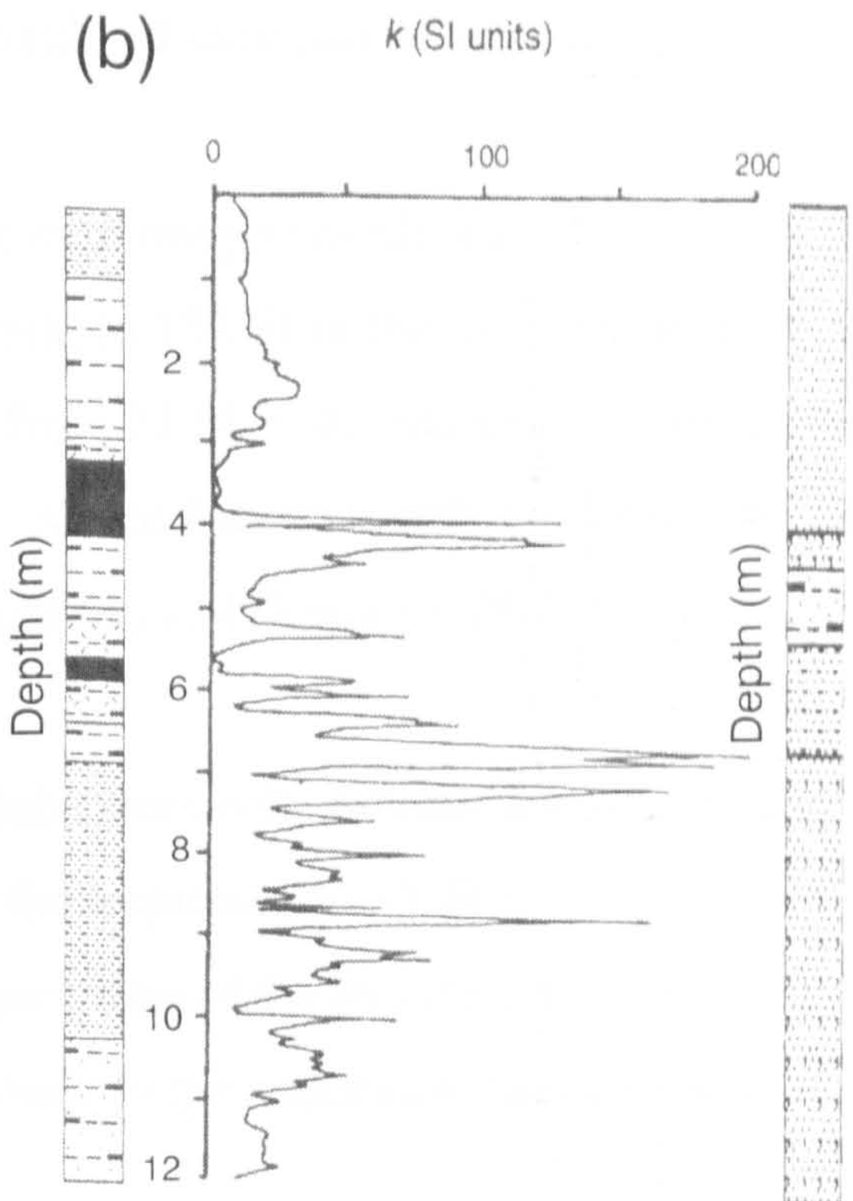

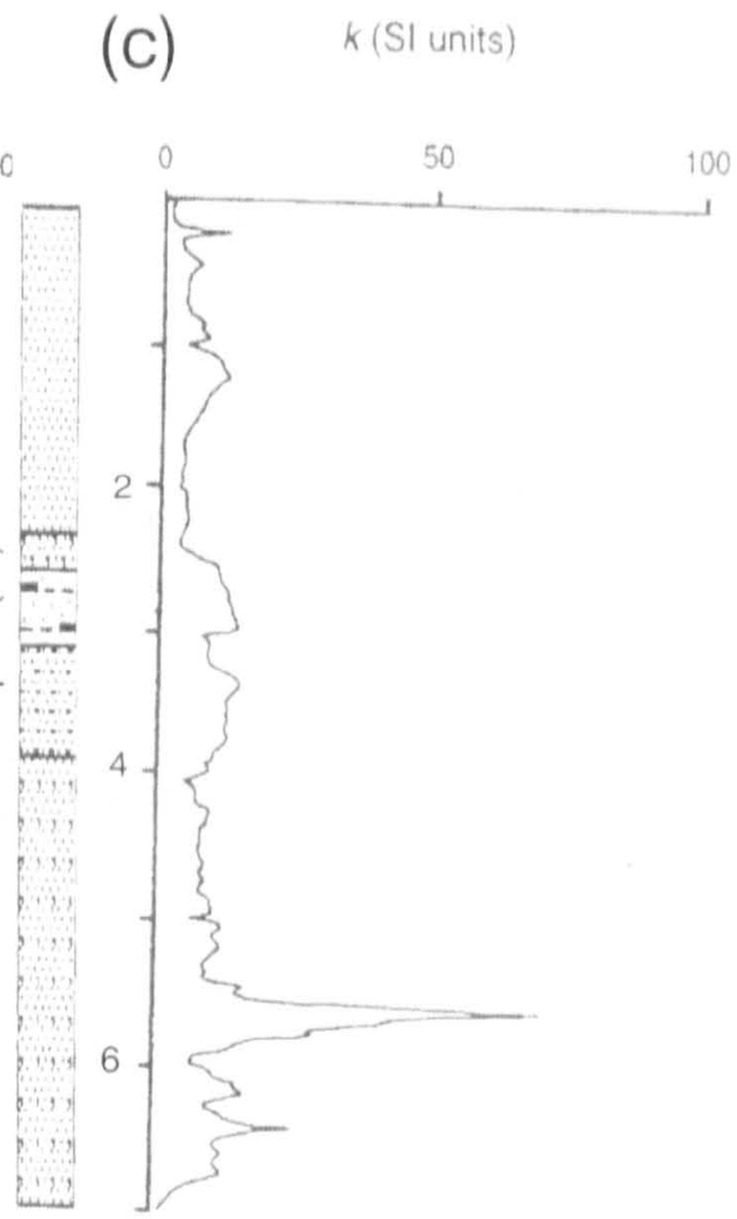

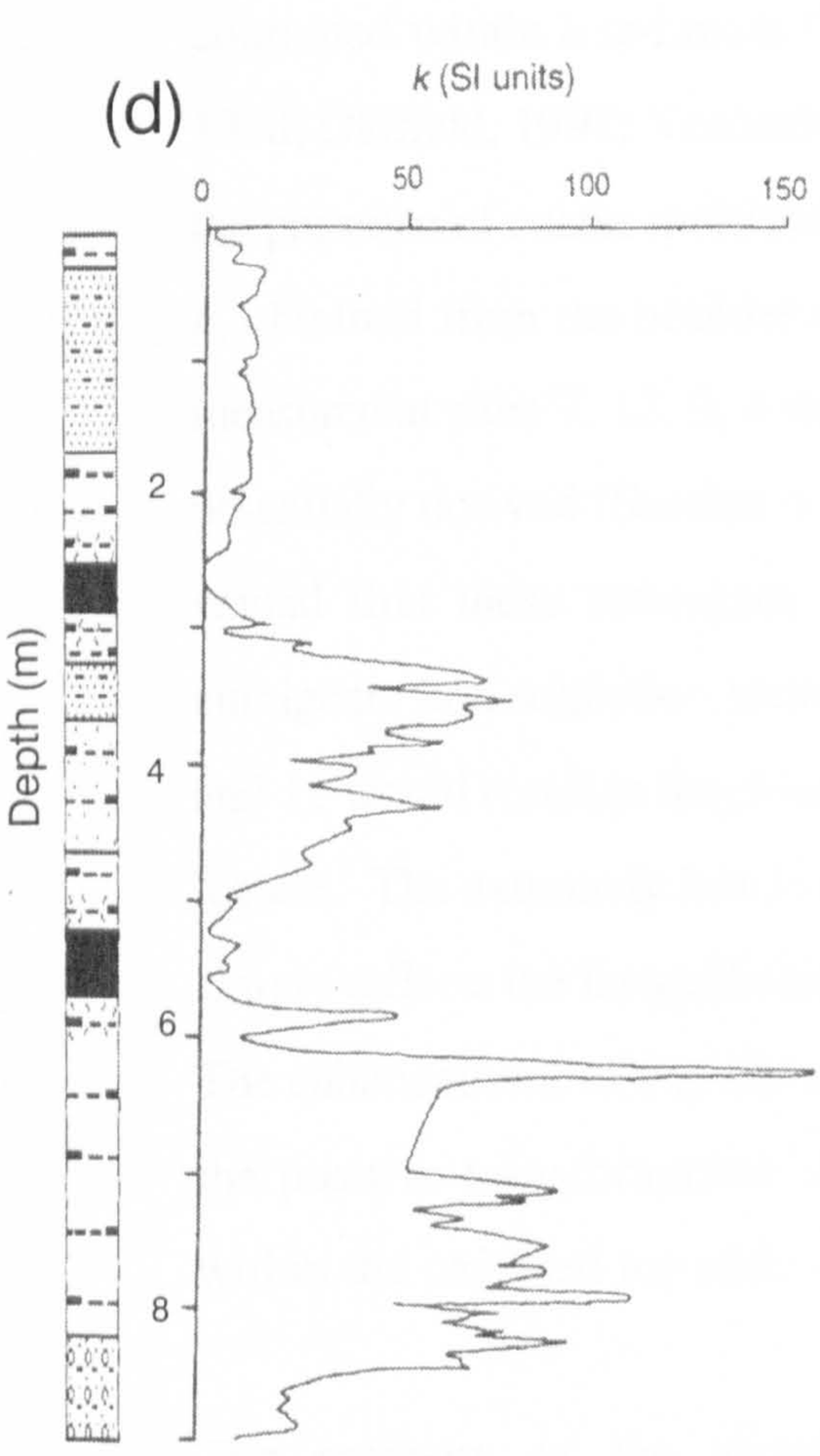

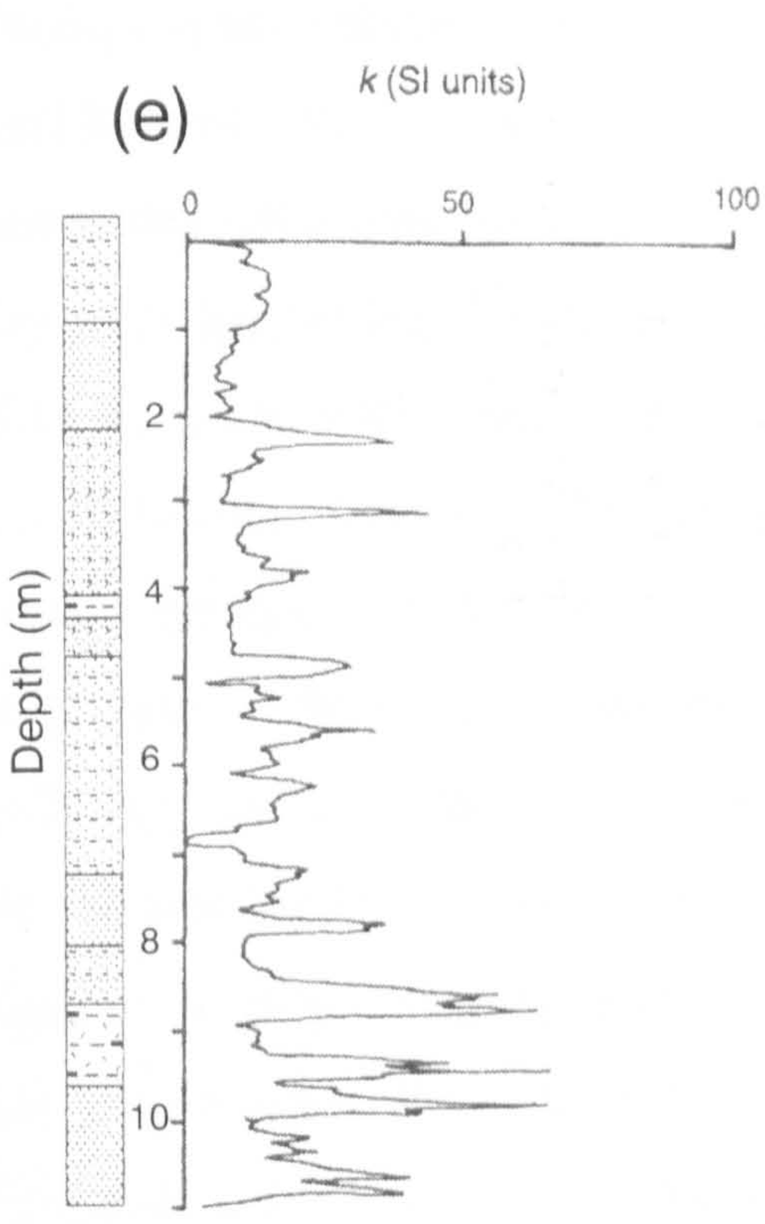

Figure 4.25 Whole core susceptibility (k) measurements for (a) site 7; (b) site 12; (c) site 9; (d) site 4; (e) site 11.

shelly sand at 5.60 metres depth. Susceptibility peaks in the upper 0.3 metres of the sequence; this corresponds to extremely oxidised sand just beneath the ground surface.

The *k* measurements at site 4 are extremely variable and range from 0 SI, in the organic detrital units between 2 and 3 metres depth, to 153 SI in the intervening silty clays (Figure 4.25d). The background levels of *k* increase from 22 SI in the red gravel layer at the base of the sequence to 53 SI in the overlying silty clay. Above 2 metres depth the *k* remains relatively constant at 22 SI and does not peak in the oxidised top soil (Figure 4.25d).

The sediments at site 11 also exhibit extremely variable levels of susceptibility which range from 4 SI, in the sands at the top of the sequence, to 65 SI in the silty clay between 9 and 10 metres depth (Figure 4.25e). In the upper metre of the sequence there is a sharp increase in susceptibility from 9 SI to 15 SI; this corresponds to the sediments fining upwards from well sorted fine sand into oxidised silty sand.

Susceptibility is directly proportional to the total quantity and size of the magnetic grains contained within a sediment (Thompson and Oldfield, 1986; Maher, 1988; Maher and Taylor, 1988; Oldfield, 1991; Verosub and Roberts, 1995). This magnetic property is very sensitive to the presence of coarse multidomain grains and the finest superparamagnetic grains. The level of *k*, obtained from the boulder clay at the base of site 4, indicates that the peaks in susceptibility measured at sites 7, 12, 9, 4 and 11 are much higher than in the material from which they were potentially derived (Section 4.2.1). Chemical analysis of two samples taken from sites 4 and 7 reveal that these sediments contain greigite (Jenkins pers com., 1996). The formation of authigenic iron sulphides, such as greigite, in the anoxic sands, silts and clays at sites 7, 12, 9, 4 and 11 would result in the extremely high and variable levels of susceptibility measured at these locales. The extremely low levels of *k* measured in the organic detrital units at sites 7, 12 and 11 simply reflects the insignificant quantity of minerogenic material contained within these deposits. The enhancement of *k* in the near surface sediments at site 7, 9, and 11 may be associated with the positive transformation of paramagnetic iron to ferrimagnetic or antiferrimagnetic forms within the oxidised top soil.

The majority of the variation in susceptibility within West Marsh is caused by the postdepositional processes which, under anoxic sulphide rich conditions, produce highly

magnetic authigenic iron sulphide minerals. Consequently, susceptibility measurements cannot be used to correlate specific depositional events within this area of the sedimentary basin.

East Marsh

A series mass specific magnetic measurements, percentages and quotients, obtained from the sediments recovered at sites 17, 20, 21, 22, 23 and 24, are plotted in figures 4.26 to 4.31.

The detailed measurements obtained from site 17 display differences in the composition of magnetic mineral assemblages within and between sedimentary units (Figure 4.26). The low field susceptibility measurements (*X*LF) remain low and relatively constant throughout the sequence, as does frequency dependent susceptibility (FD%). This suggests the sediments contain little coarse multidomain or extremely fine superparamagnetic material. Furthermore, there is relatively little material at or near to the small single domain / superparamagnetic boundary (SSD/SP ≈0.02μm). The shelly sand between 5.06 and 6.00 metres depth contains variable amounts of fine grained ferrimagnetic minerals with lesser amounts of imperfect antiferrimagnets; the magnetic component becomes coarser towards the top of this unit. SIRM values in the stratified clays, between 4.70 and 5.06 metres depth, indicates that the relative proportion of remanence carriers is greatest in the fine grained lenses; the magnetic assemblage is composed of generally coarse pseudo-single domain (PSD) and multidomain (MD) ferrimagnets with lesser amounts of imperfect antiferrimagnets and fine grained stable single domain grains (SSD). The silty sand unit which extends from 4.50 to 3.17 metres depth shows relatively little variation in the composition of the magnetic component (Figure 4.26). Between 3.15 and 2.00 metres depth, the relative proportion of remanence carrying minerals contained within the highly stratified silt, highly stratified silty clay, silty sand and clayey silt units increases. This is caused by greater quantities of coarse ferrimagnetic minerals, such as magnetite or maghaemite (Figure 4.26). Above this the relative proportion of remanence carriers decreases, as the sediments fine into grey silty clay, and the magnetic component is largely composed of fine grained antiferrimagnetic material, such as haematite or geotite. As the sediments grade from silty clay into sandy silt the magnetic component, composed mainly of imperfect antiferrimagnets, becomes coarser and the total amount of remanence carrying minerals reaches a minimum in the sandy silt at 1.02 metres depth. The SIRM values indicate that the sands at 0.6 metres depth contain a greater proportion of remanence carriers (Figure 4.26), which are largely composed of fine grained ferrimagnets and

Figure 4.26 Magnetic parameters, quotients and ratios for site 17.

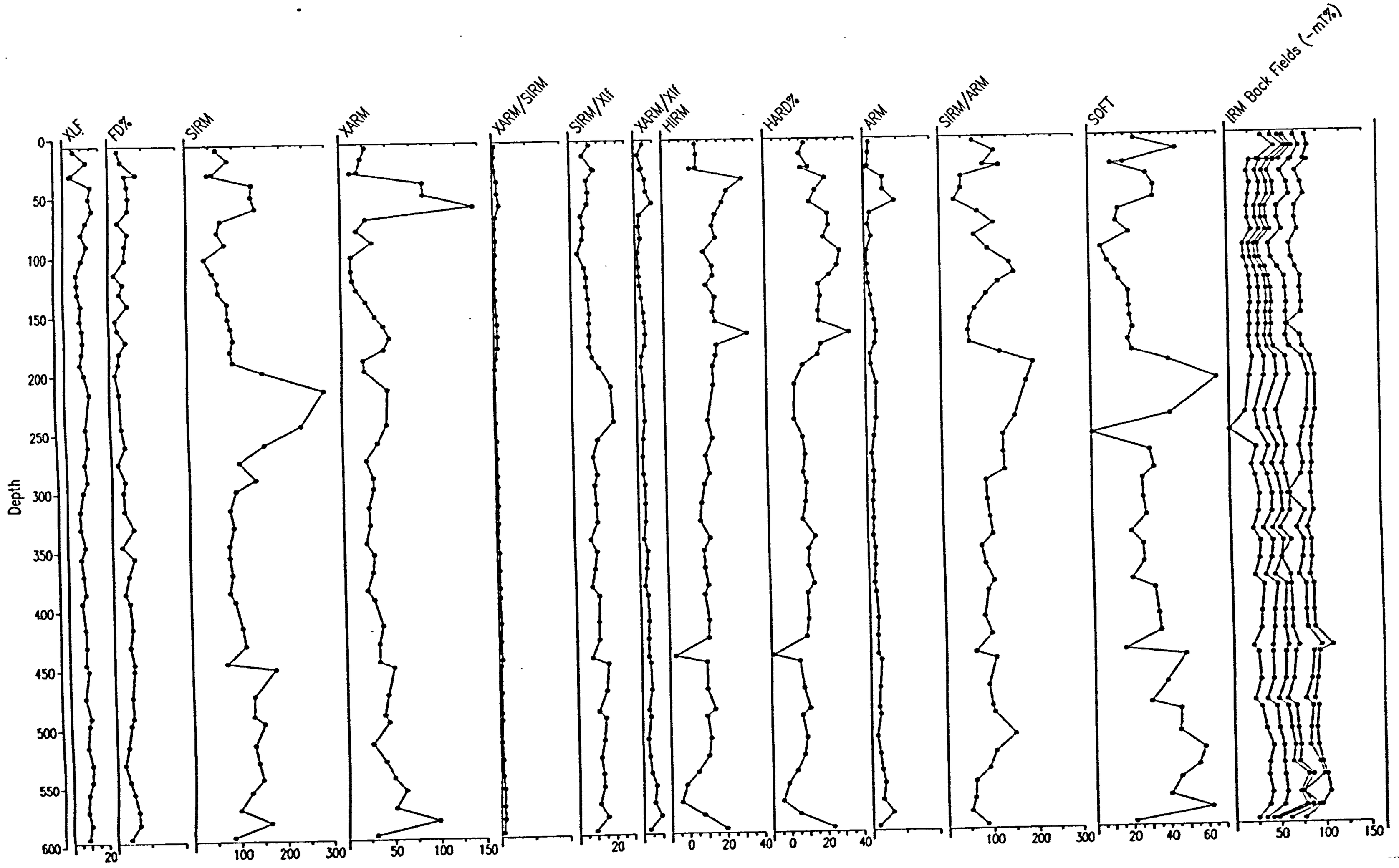

Figure 4.27 Magnetic parameters, quotients and ratios for site 24.

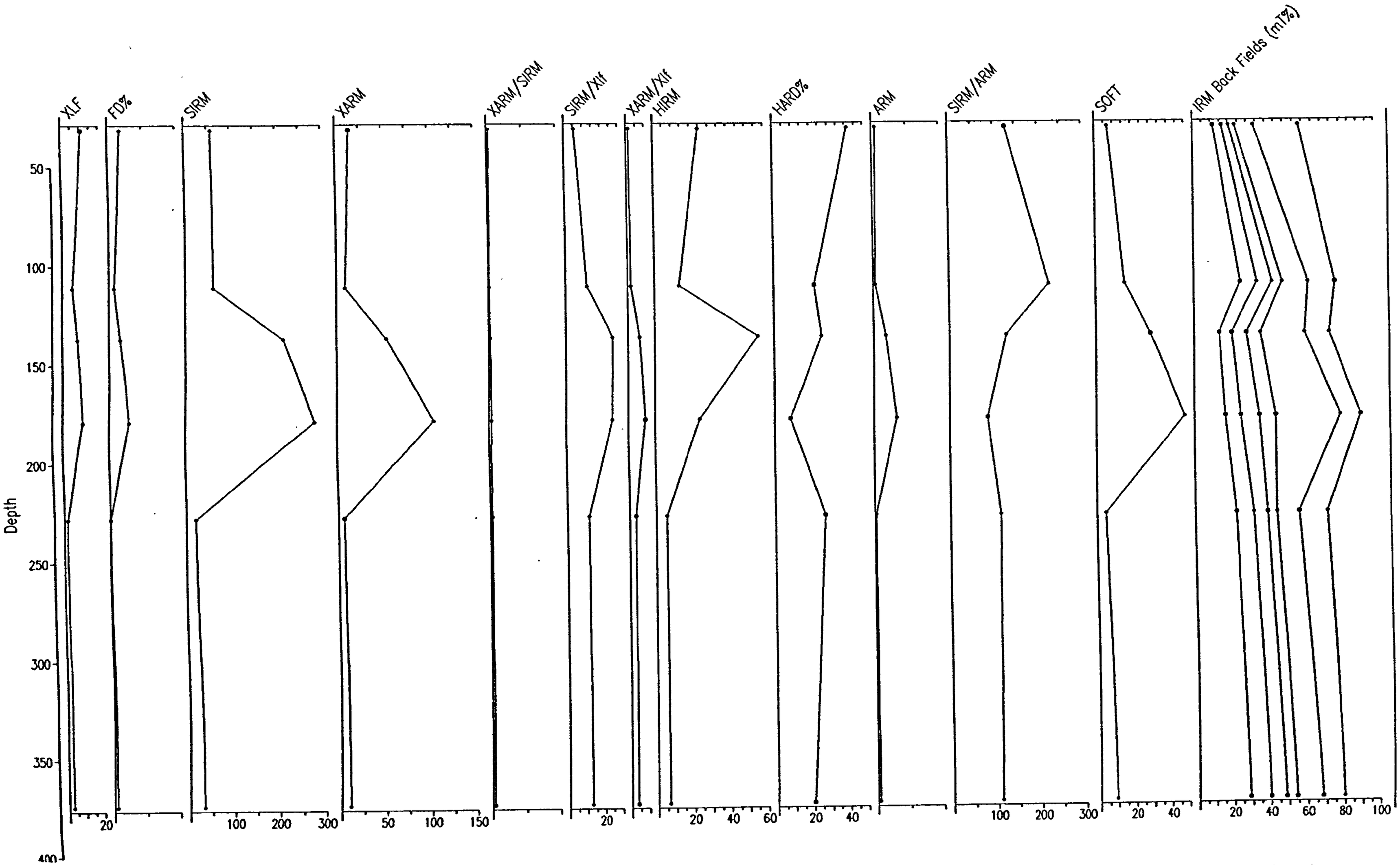

Figure 4.28 Magnetic parameters, quotients and ratios for site 20.

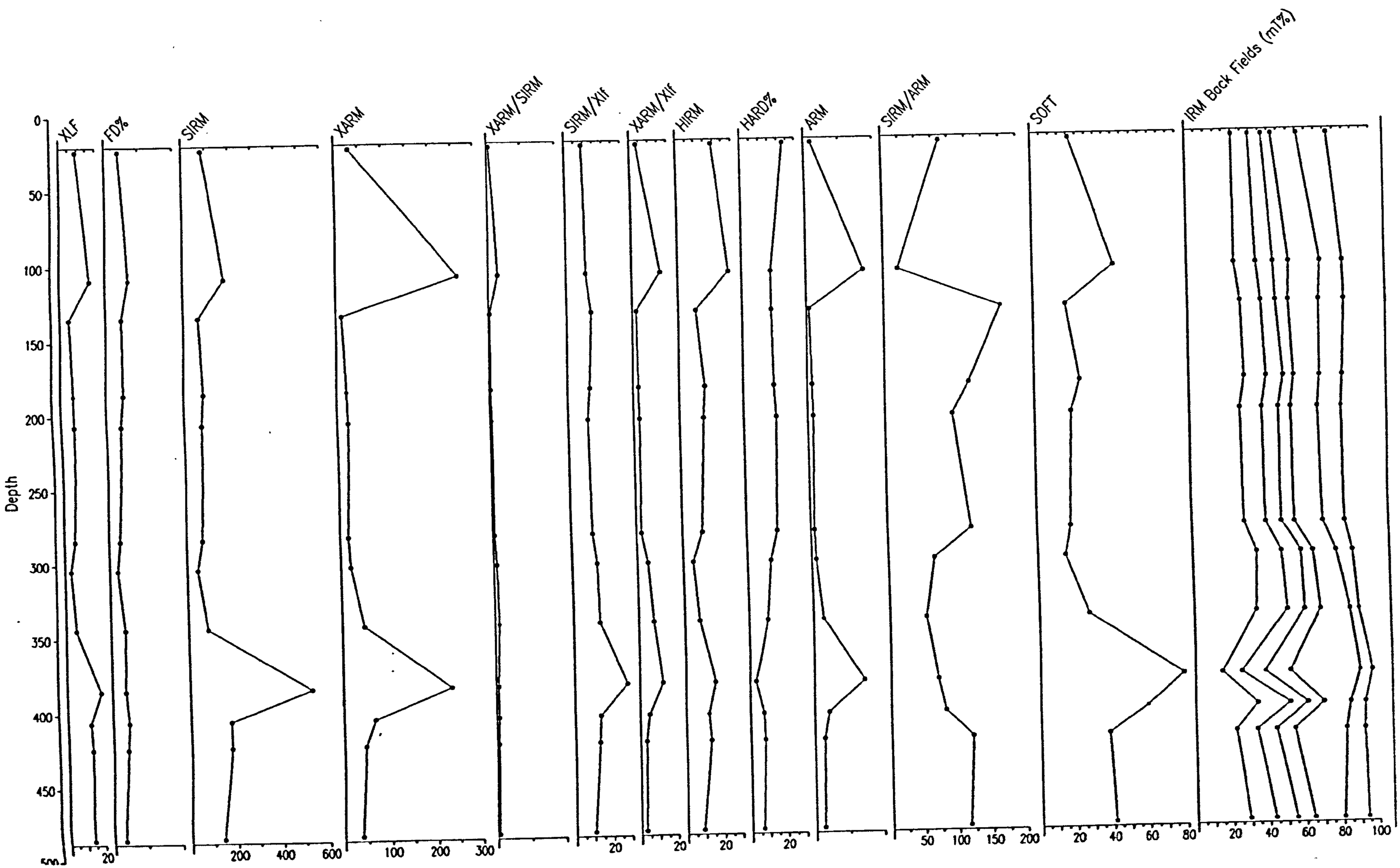

Figure 4.29 Magnetic parameters, quotients and ratios for site 23.

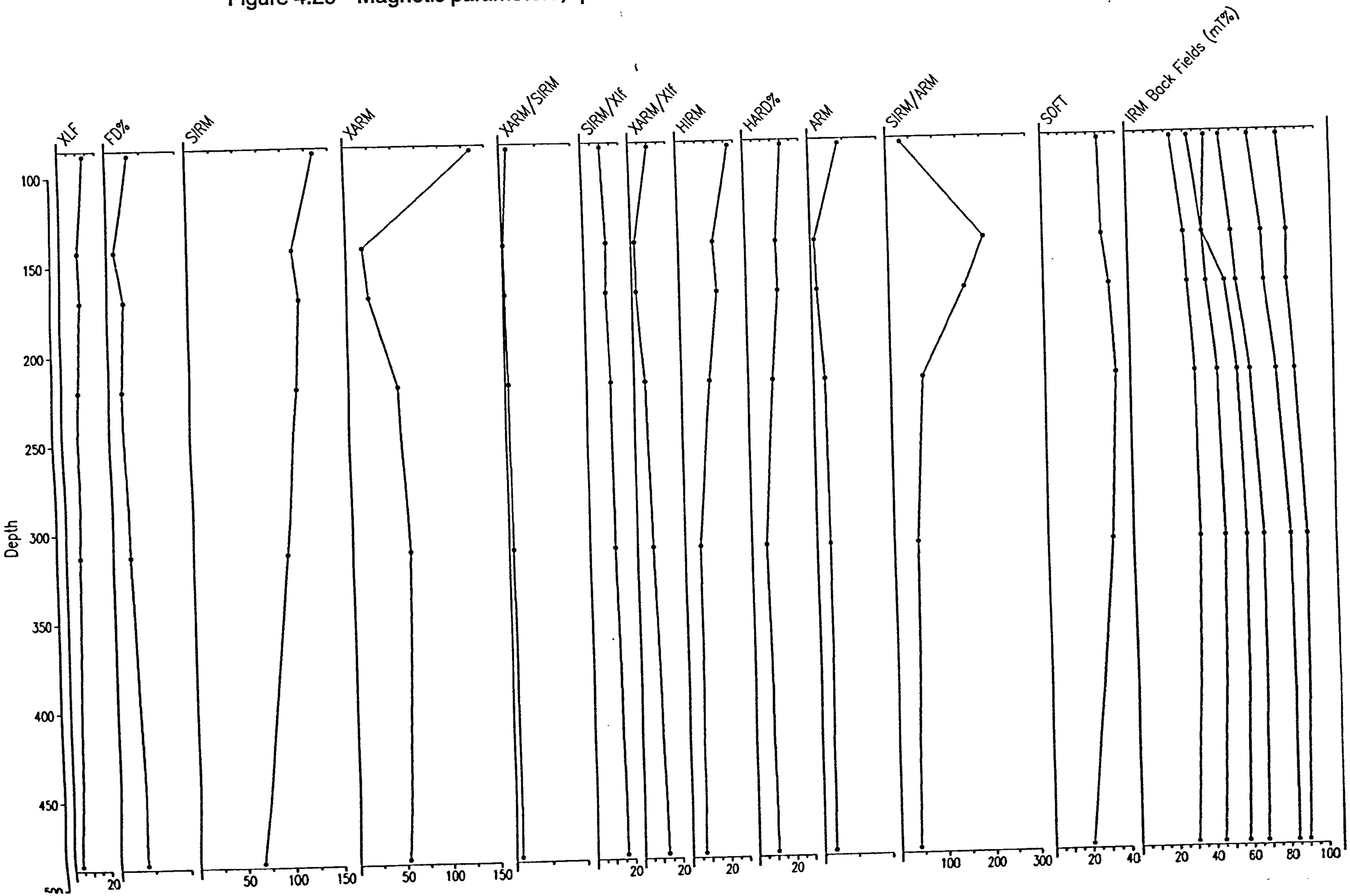

Figure 4.30 Magnetic parameters, quotients and ratios for site 21.

Figure 4.31 Magnetic parameters, quotients and ratios for site 22.

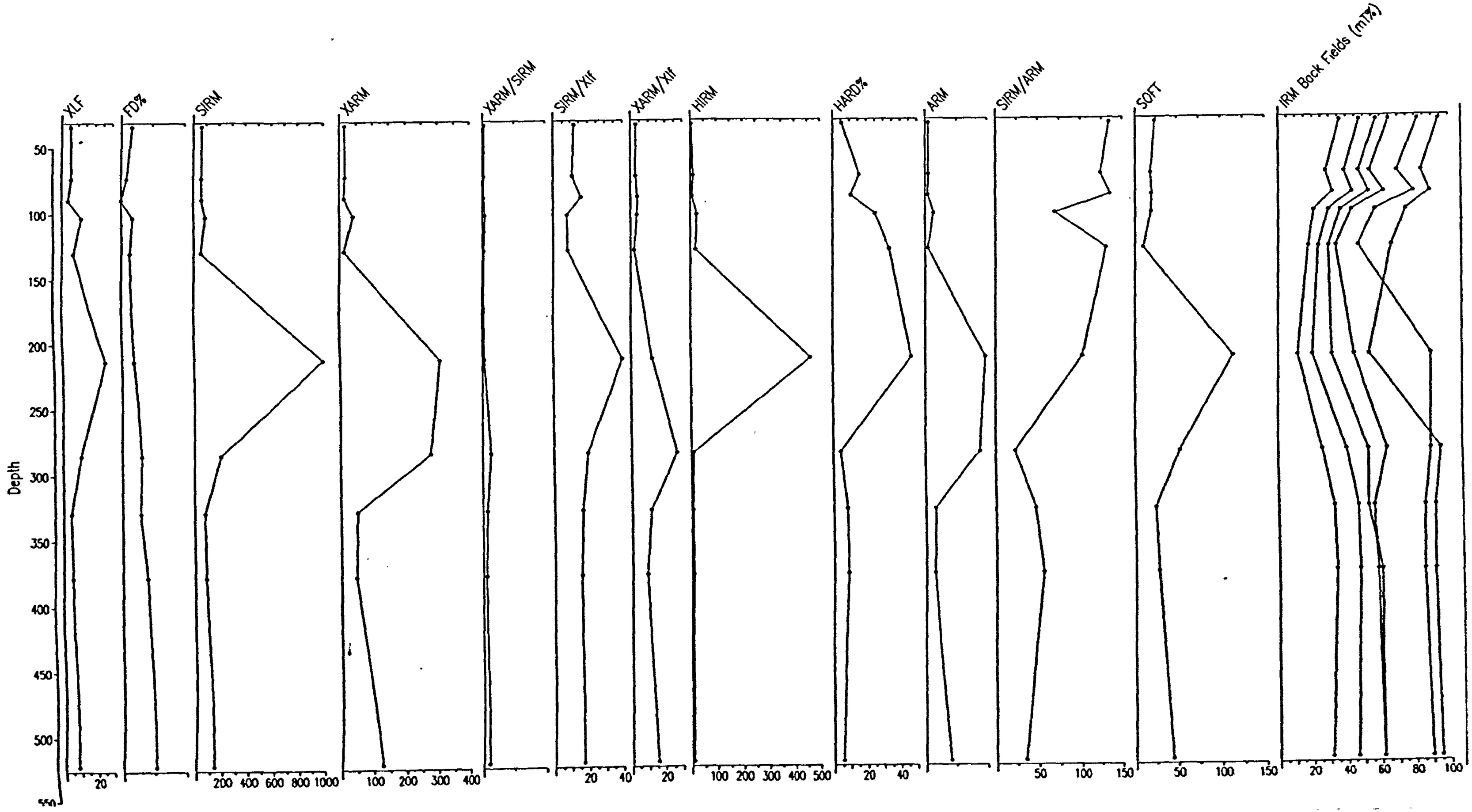

imperfect antiferrimagnets. The sands at 0.3 metres depth exhibit lower levels of susceptibility and contain an extremely small proportion remanence carrying minerals. These sediments also contain a greater amount of material at the SSD/SP boundary.

The shelly sands at the base of site 24 exhibit relatively low levels of *X*lf and SIRM and the magnetic minerals are dominated by coarse antiferrimagnetic and ferrimagnetic material (Figure 4.27). As the sediments grade into fine well sorted sand the *X*lf and SIRM increases sharply. The magnetic assemblages within this deposit do vary and are composed of either fine SSD, at or near to the SSD/SP boundary, and PSD ferrimagnets or coarse imperfect antiferrimagnets (Figure 4.27); *X*lf, FD% and SIRM values decrease towards the top of this unit. The overlying silty clay contains a high proportion of coarse imperfect antiferrimagnetic material.

At site 20 the *X*lf is greatest in the silty clay beds, at 3.85 and 1.09 metres depth, and remains relatively constant through the intervening silts and sands (Figure 4.28). These two clay beds contain a relatively high proportion or remanence carrying minerals, which are composed of predominately fine small single domain and pseudo single domain ferrimagnets, such as magnetite or maghaemite. The magnetic minerals, within the silts and sands at this locale are generally larger than in clay beds, and are dominated by imperfect antiferrimagnets.

As the sediments fine upwards from shelly sand into sandy silt and then into silty clay at site 23, there is a corresponding increase in the levels of *X*lf and the total number of remanence carrying minerals (Figure 4.29). The silts and sands between 1.7 and 4.9 metres depth contain magnetic assemblages composed of predominately fine imperfect antiferrimagnets and ferrimagnets. However, the silt at 1.42 metres depth is dominated by coarse ferri- and imperfect antiferrimagnetic minerals. As the sediments fine upwards into silty clay the magnetic component becomes finer, the relative proportion of viscous grains at the SSD/SP boundary increases as does the relative proportion of imperfect antiferrimagnetic material.

The *X*lf and FD% measurements at site 21 exhibit little or no variation and suggest that only small proportion of the magnetic minerals at this locale lie at the small single domain / superparamagnetic boundary (Figure 4.30). The relative proportion of remanence carriers peaks in the shelly sand at 3.19 metres depth and gradually diminishes as the sediments fine upwards into sandy silt and silty clay. The sands at 3.19 metres depth are dominated by fine grained SSD

and PSD ferrimagnets, whereas the silts and clays above this level contain a relatively coarser magnetic component. The proportion of imperfect antiferrimagnetic minerals increases as the sediments fine upwards, reaching a maximum at 0.28 metres depth.

The shelly sand at the base of site 22 exhibits low levels of *X*lf and the magnetic component is composed of relatively fine grained ferrimagnetic minerals and imperfect antiferrimagnets (Figure 4.31). As the sediments fine upwards into sandy silt there is a corresponding increase in the concentration of fine SSD and PSD ferrimagnets (Figure 4.28). The silty clay at 2.13 metres depth exhibits relatively high levels of *X*lf and SIRM, which indicates an increase in the quantity of both magnetic grains and remanence carrying minerals. The clays at this depth contain a large quantities of fine SSD, PSD and MD grains of both imperfect antiferrimagnetic and ferrimagnetic material. As the sediments coarsen upwards into well sorted sand there is a corresponding decrease in *X*lf and SIRM (Figure 4.31). The magnetic component within this unit is composed largely of coarse imperfect antiferrimagnets and ferrimagnets.

The magnetic mineral compositions of back-barrier deposits in East Marsh vary within and between the sedimentary units. As no grain size analysis was undertaken, in conjunction with the magnetic measurements, no attempt can be made to quantify the effects of grain size upon the magnetic parameters measured. It is clear that the composition of magnetic minerals contained within the back-barrier complex sediments are extremely variable making any attempt to correlate individual depositional units very difficult. The origin of SSD grains at or near to the SSD/SP boundary is uncertain as these minerals may form through postdepositional processes; however the large MD grains are likely to be detrital in origin (Oldfield, 1994).

4.3.2 Summary

The environmental magnetic measurements obtained from West Marsh and East Marsh prove extremely complex. The whole core susceptibility measurements from sites 7, 12, 9, 4 and 11 are overwhelmed by the susceptibility of authigenic greigite which obscures any subtle changes in susceptibility within the lower nine metres of the sequence. Consequently, any attempt to correlate specific depositional units within this area is significantly impaired.

Similarly, the complex nature of the more detailed measurements, obtained from sites 17, 24, 20, 23, 21 and 22, confounds any attempt to correlate deposits within East Marsh. The measurements do indicate the general composition of the magnetic material within these sediments, and displays how this fraction varies independently from the texture of sediment.

Before designing the experimental procedure, when using environmental magnetic techniques, the objectives of the study have to be clearly defined. It is inevitable that even when simply attempting to correlate sedimentary units, on the basis of their induced magnetic properties, a whole series of questions are raised regarding the validity of the measurements made. In this instance the magnetic measurements reflect the biological, chemical and physical complexity within this coastal barrier system.

Chapter 5

Geophysical surveys

5.1 Seismic surveys

5.1.1 Seismic refraction surveying

Description of refraction data

Seismic refraction data were acquired from 50 lines within the Pendine Burrows, West Marsh and East Marsh. However, due to poor data quality only 37 lines provide information suitable for refraction analysis (Figure 5.1). The data were processed using intercept times rather than the Generalised Reciprocal Method (Palmer, 1980), because there was insufficient overlap of the refraction arrivals on the normal and reverse spreads of each line. Consequently, refractor depths have only been determined for points immediately beneath the shot positions. Line positions, the number of layers, the velocity structure and corresponding refractor depths are summarised in table 5.1.

Four seismic facies have been identified, on the refraction data acquired within West Marsh, East Marsh and the Pendine Burrows, on the basis of compressional wave data. Each of these layers exhibits a range of seismic velocities and all four are present at only seven of the 37 sites analysed (Table 5.1).

For the upper most horizon (L1) the seismic velocity ranges from 241 to 590 m/s whereas the layer thickness varies between 0.8 to 3.92 metres (Table 5.1). As mentioned in section 3.1.5 velocities lower than the velocity through water (1500 m/s) generally indicate that air, gas or methane fills some of the pore spaces within the medium of propagation. *Low-velocity layers* (LVL) generally occur on land near the surface; they are characterised by low variable seismic velocities and the base of the LVL usually coincides roughly with the water table (Sheriff and Geldart, 1995). It is therefore possible that the low seismic velocities measured in L1 correspond to the aerated zone above the water saturated zone within the Pendine Burrows, West Marsh and East Marsh. The thickness of L1 is controlled by the water table height and the position of the

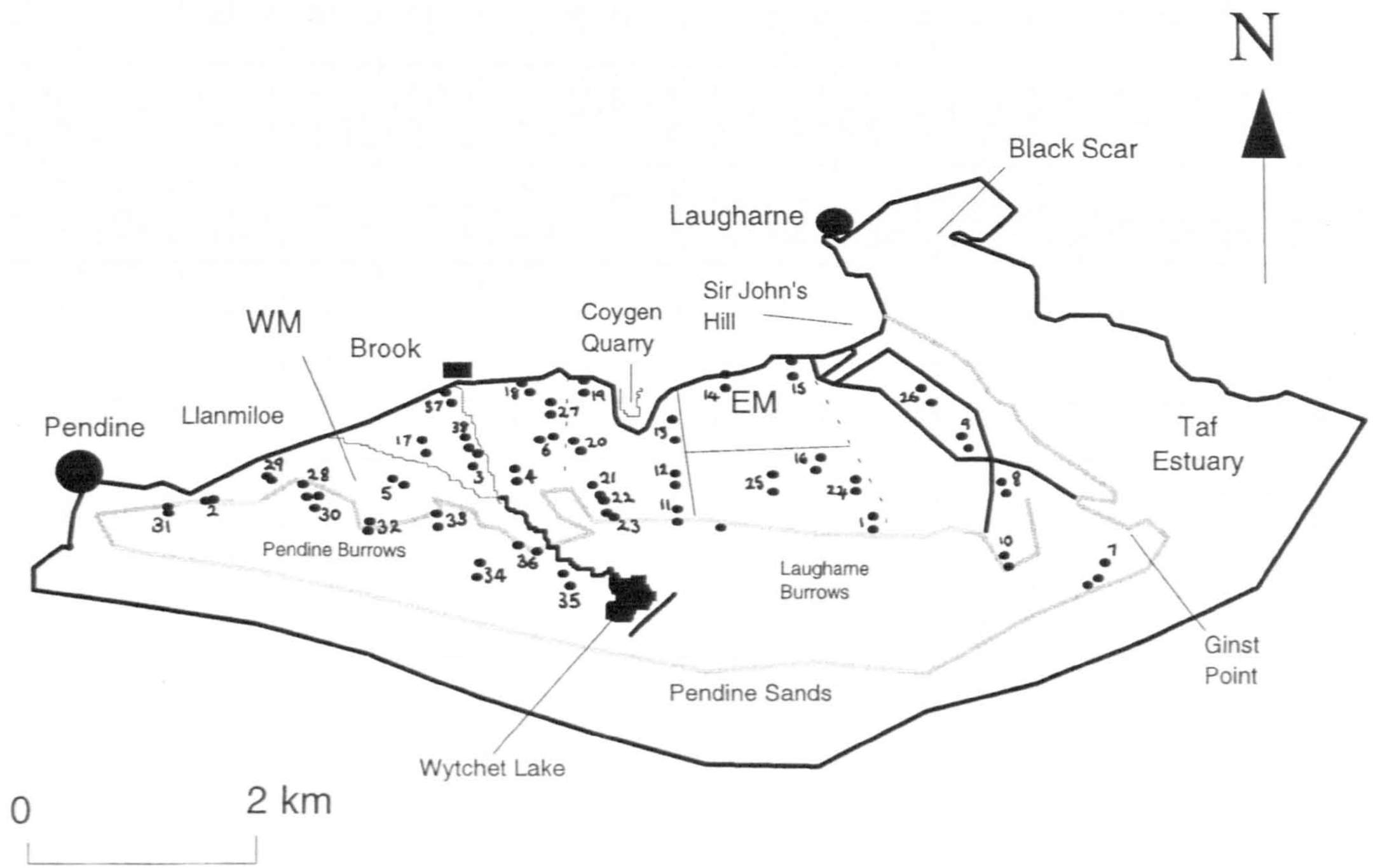

Figure 5.1 Distribution of refraction data within West Marsh (WM), East Marsh and Pendine Burrows; black points indicate shot point positions.

Line Number	Eastings	Northings	Number Layers	Velocities (metres/ sec)				Depth to refractors (metres)		
				Layer 1	Layer 2	Layer 3	Layer 4	H1	H2	H3
1	230500 230500	208110 207983	3	370	1348		4125	1.07 0.8		29.71 28.44
2	224612 224540	208270 208260	3	350		1897	5376		4.1 3.78	36.58 34.5
3	226990 226940	208700 208585	4	345	1481	2117	3486	1.67 1.99	18.03 22.1	39.64 41.13
4	227320 227335	208560 208440	4	241	1645	2222	3486	0.82 1.44	17.75 22.41	38.98 41.55
5	226220 226330	208470 208410	3	241	1447		3981	1.94 1.62		28.85 31.05
6	227535 227655	208830 208860	4	368	1527	2125	4640	1.48 1.58	12.8 23.15	37.2 51.44
7	232625 232570 232475	207670 207530 207460	2		1630		3945			24.58 23.35 25.97
8	231720 231675	208325 208430	4	460	1472	2417	6076	1.08 1.23	18.03 20.61	57.1 48.63
9	231370 231310	208750 208870	3	419	1477		3742	2.24 2.61		27.09 26.7
10	231740 231700	207640 207740	4	404	1574	2250	7484	2.4 2.46	18.8 36.3	64.2 62.3
11	228754 228754	208179 208053	3	590	1120		6965	1.6 3.92		29.37 25.29
12	228740 228740	208400 208510	3	441	1522		5951	1.56 1.89		20.52 19.62
13	228737 228711	208825 209018	3	441	1424		4069	1.95 1.67		26.1 22.43
14	229180 229180	209439 209319	3	419	1512		4428	1.56 1.99		18.09 20.43
15	229765 229770	209570 209430	3	404	1533		3886	1.68 1.5		18.41 21.2
16	229980 230020	208545 208663	3	397	1482		4423	1.9 1.5		28.3 26.3
17	226490 226525	208830 208710	3	384	1410		3021	2.6 2.25		29.2 22.77
18	227445 227380	209275 209365	4	427	1250	1923	3907	2 3.14	8.21 13.72	36.3 22.49
19	227925 227920	209385 209270	3	367		1992	4056		1.97 2.2	28.57 38.86
20	227895 227840	208725 208820	3	392	1544		2979	1.54 1.72		23.31 20.31
21	228000 228070	208400 208305	3	416	1610		3607	1.94 1.4		27.88 28.33
22	228110 228135	208260 208140	3	416	1509		3748	1.3 1.3		27.19 25.54
23	228190 229140	208100 208000	3	418	1515		3909	1.33 1.33		36.08 23.75
24	230345 230345	208460 208345	3	403	1669		3943	2.45 1.83		39.82 36.28
25	229598 229598	208506 208339	3	401	1488		3979	2.145 2.47		30.23 34.08
26	230940 231040	209320 209180	3	401	1458		4483	1.55 2.15		25.76 26.64
27	227630 227625	209065 209180	3	401		1783	3873		2.26 1.91	25.58 32.8
28	225440 225410	208295 208410	3	385	1495		3486	1.67 2.7		31.76 39.48
29	225130 225085	208450 208490	3	401	1157		3630	1.05 1.06		17.36 22.03
30	225510 225545	208190 208297	3	401	1452		3213	1.58 1.68		25.98 37.5
31	224200 224210	208205 208145	3	401	522**		5172	2.64 2.9		15.07 13.92
32	226000 226015	207970 208060	3	401	1708		3379	2.34 2.27		35.02 22.16
33	226620 226630	208140 208015	3	401	1553		6464	2.36 1.88		39.2 39.46
34	227000 226980	207675 207545	3	401		1896	4700		2.77 2	44.03 38.92
35	227745 227805	207570 207450	3	401	1644		10761	2.08 0.8		54.71 57.13
36	227345 227505	207840 207780	3	401	1573		2920	0.88 1.41		26.22 27.43
37	226700 226750	209280 209180	4	264	1247	2183	4371	1.41 0.99	12.19 9.39	30.82 30.19
38	226870 226910	208860 208755	3	295	1524		2839	2.08 2.47		29.98 27.89

** Partially saturated sand with a compressional wave velocity slightly > V1

Table 5.1 Seismic velocities and refractor depths obtained from refraction lines within the dunes and the back-barrier area

line relative to Ordnance Datum (OD) such that low water tables and increased height above OD increases L1 thickness. These assumptions are supported by data acquired from line 7, located on the foreshore at Ginst Point (Figure 5.1). Because the foreshore sediments were saturated no near-surface LVL was identified beneath line 7 (Table 5.1).

Layer 2 (L2) velocities range from 1120 to 1708 m/sec and thicknesses vary between 6.21 to 56.33 metres (Table 5.1). The seismic velocities measured in L2 are characteristic of partially or fully saturated unlithified sediments such as mud or sand (Telford *et al.*, 1990). The velocity range exhibited by L2 may be caused by variations in lithology (particle size), density, the effect of overburden pressure or the degree of saturation (Sheriff and Geldart, 1995). For instance, a deeply buried and fully saturated sand, subject to overburden pressure, is likely to exhibit higher seismic velocities than a partially saturated mud at or near to the ground surface. L2 may therefore represent partially or fully saturated unconsolidated sediment beneath the Pendine Burrows, West Marsh and East Marsh.

Layer 3 (L3) velocities range from 1783 to 2250 m/sec and thicknesses vary from 8.77 to 45.4 metres (Table 5.1). The seismic velocities measured in L3 are characteristic of glacial diamicton such as gravel and boulder clay (Telford *et al.*, 1990; Griffiths and King, 1982; Bennell *pers com.*, 1996). The large variation in velocity may be due to changes in the consolidation state and/or the composition of the deposit. L3 may possibly represent a layer of glacial diamicton beneath the Pendine Burrows, West Marsh and East Marsh.

Layer 4 (L4) is the lowest layer and has been identified beneath all 37 sites analysed. Velocities range between 2839 and 7484 m/s. These velocities are characteristic of lithified sandstone and limestone, both of which exhibit a wide range in velocity (Griffiths and King, 1982; Telford *et al.*, 1990). The Vp velocity of 10,761 m/s for L4 beneath line 35 is extremely high and must be regarded as anomalous and interpreted with some caution. Values of this order of magnitude are usually only encountered in the inner mantle.

As mentioned in section 3.1.5 the seismic velocity through sandstone is generally lower than the velocity through limestone; however, purely on the basis of velocity data it may be difficult to distinguish between low velocity limestone and high velocity sandstone (Telford *et al.*, 1990;

Sheriff and Geldart, 1995). It is therefore likely that *L4* represents the bedrock beneath the Pendine Burrows, West Marsh and East Marsh.

All four layers are identified beneath lines 3, 4, 6, 8, 10, 18 and 37 (Table 5.1). The seismic refraction data therefore suggests that at these sites the bedrock (*L4*) is overlain by a gravel (L3) and saturated sands and silts (L2). This latter unit becomes unsaturated towards the ground surface (L1). The data acquired along lines 3, 19, 27 and 34 indicates that beneath these sites the bedrock (*L4*) is overlain by a layer of gravel (L3) which is covered by a thin veneer of unsaturated sediment (L1). The surface of L3 is therefore located relatively near to the ground surface beneath lines 3, 19, 27 and 34.

At most of the remaining shot points it appears that the bedrock (*L4*) is overlain by sands and silts (L2) which become unsaturated near the ground surface (L1). Velocities characteristic of L3 were not identified on the seismic refraction data acquired from these sites. Although the refraction data indicate that the gravel/boulder clay facies (L3) is apparently absent from these sites, if L3 is relatively thin and exhibits little velocity contrast to either the over consolidated sands and silts above or the underlying bedrock then it is possible that the horizon may be hidden.

Comparison of refraction data to borehole information

The seismic facies identified in the refraction analysis compare well to the sequence of sediments described in boreholes recovered from West Marsh, East Marsh and the Pendine Burrows (Section 4.1). For instance, the lithology within West Marsh is dominated by sands and silts intercalated with organic detrital units, which in places overlie a layer of dense red Pleistocene gravel/boulder clay (Section 4.1.2). Seismic data at the same location (line 37) suggest that the gravel/boulder clay layer lies at a depth of between 12.2 and 9.4 metres beneath the ground surface (Table 5.1). Unfortunately, as the borehole at site 3 only penetrated to 5.5 metres depth the Pleistocene surface was not located beneath line 37 by coring. However, a borehole located in an adjacent field at site 4 shows that gravel/boulder clay is encountered at 8.23 metres beneath the ground surface (Section 4.1.2). Relief in the gravel surface may account for any difference in the depth to this layer between ground truth and refraction data.

This has two important implications upon the validity of the refraction data analysed in this study. First, the seismic facies, identified on the basis of compressional wave velocities, correspond to the main lithofacies described in boreholes recovered from the Pendine Burrows, West Marsh and East Marsh. The seismic refraction analysis is able to distinguish between saturated/unsaturated sands and clays, the gravel facies and the underlying bedrock and can therefore be used to map the distribution of these deposits beneath the ground surface. Second, in the areas investigated, saturated organic layers within the near surface sediments, do not appear to have a significant effect upon the recorded travel-times. If the velocity through the organic units was much lower than in the intervening sands and clays the depth to the gravel/boulder clay and bedrock surfaces would be overestimated.

A number of the refraction lines conducted within West Marsh yielded extremely poor data which was unsuitable for analysis; this occurred mainly in areas where the fine grained surface sediment was very dry and disturbed. The poor data quality at these sites is possibly due to the absorption and internal reflection of seismic energy within the near-surface LVL and may be affected by poor coupling between the geophones and the ground surface (Sheriff and Geldart, 1995). This problem may be overcome if the source was placed below the water table (Telford et al., 1990; Sheriff and Geldart, 1995). However, the relative thickness of Layer 1 gained at these locations corresponds to the extent of unsaturated and oxidized sediment described in the boreholes recovered from West and East Marshes.

Surface models derived from refraction data

The shot point heights, relative to Ordnance Datum, were determined from accurate levels obtained for the boreholes described in section 4.1. The depths to L4 and L3 were then converted into heights relative to OD and the data were contoured using UNIMAP© to produce structural models of the bedrock basement and the pre-Holocene surface(Figures 5.2 & 5.3); the latter was taken as the depth to the L3 surface where present or L4 in other areas. The contours were interpolated using a 'distance-weighted method'. The values are extrapolated to a region defined by the fossil cliffline (5m above OD) and the Mean High Water (MHW) level seaward of the dunes.

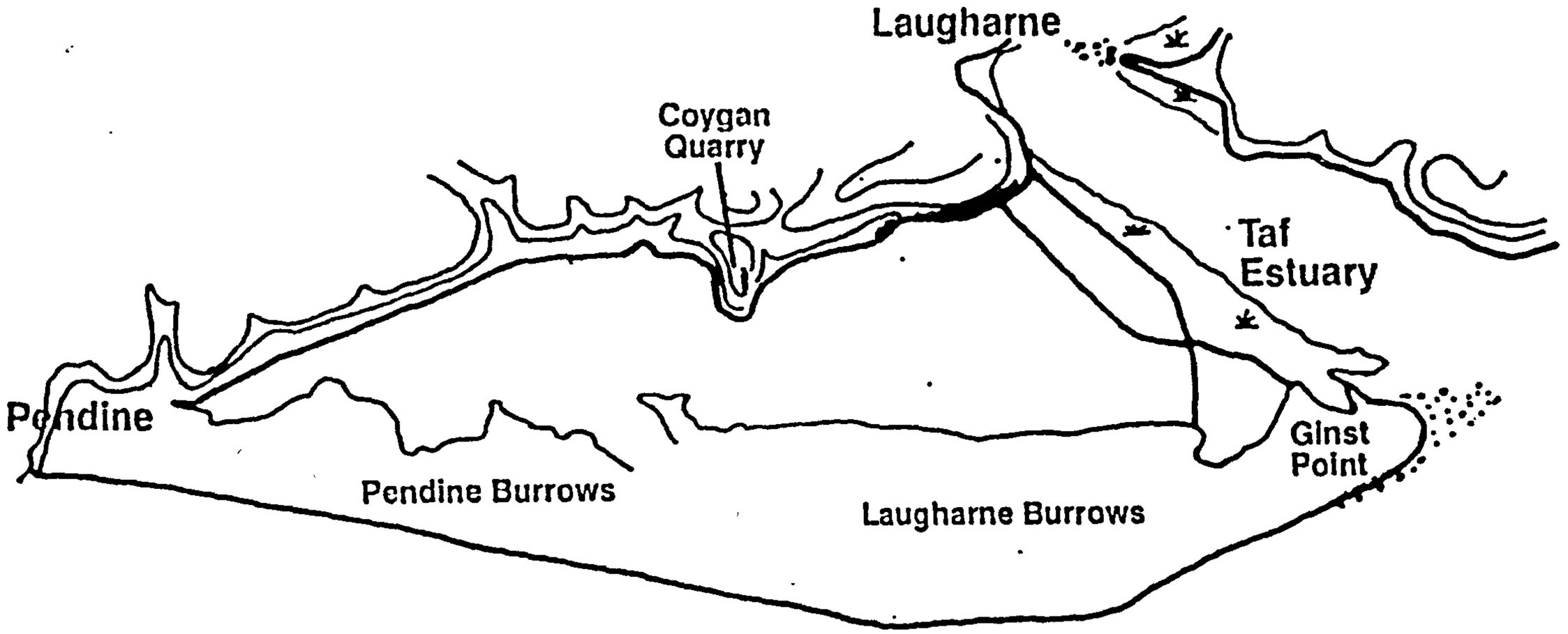
Laugharne
Coygan
Quarry
Taf
Estuary
Pendine
Pendine Burrows
Laugharne Burrows
Ginst
Point

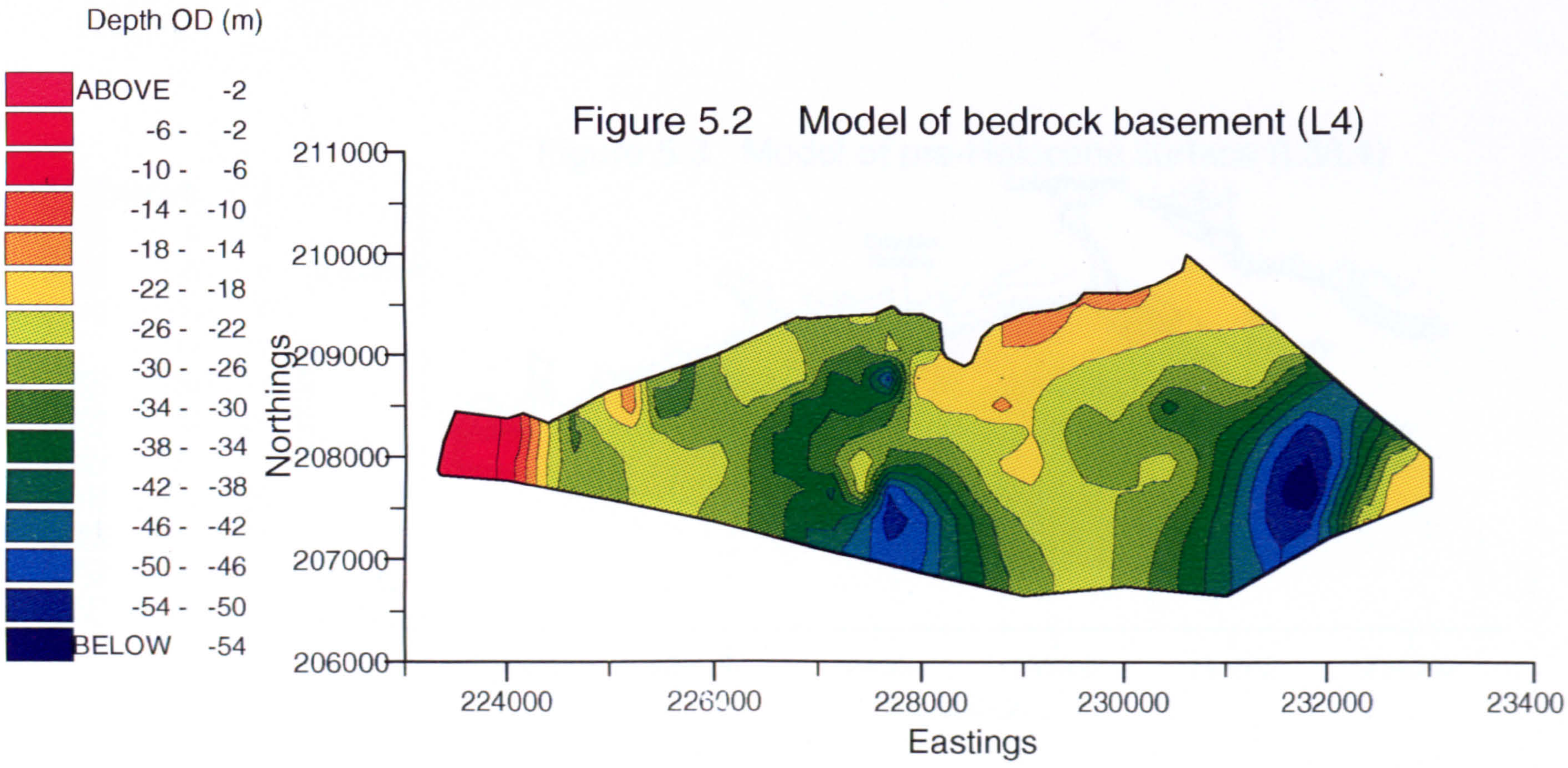

Figure 5.2 Model of bedrock basement (L4)

Figure 5.2 Model of bedrock basement (L4)

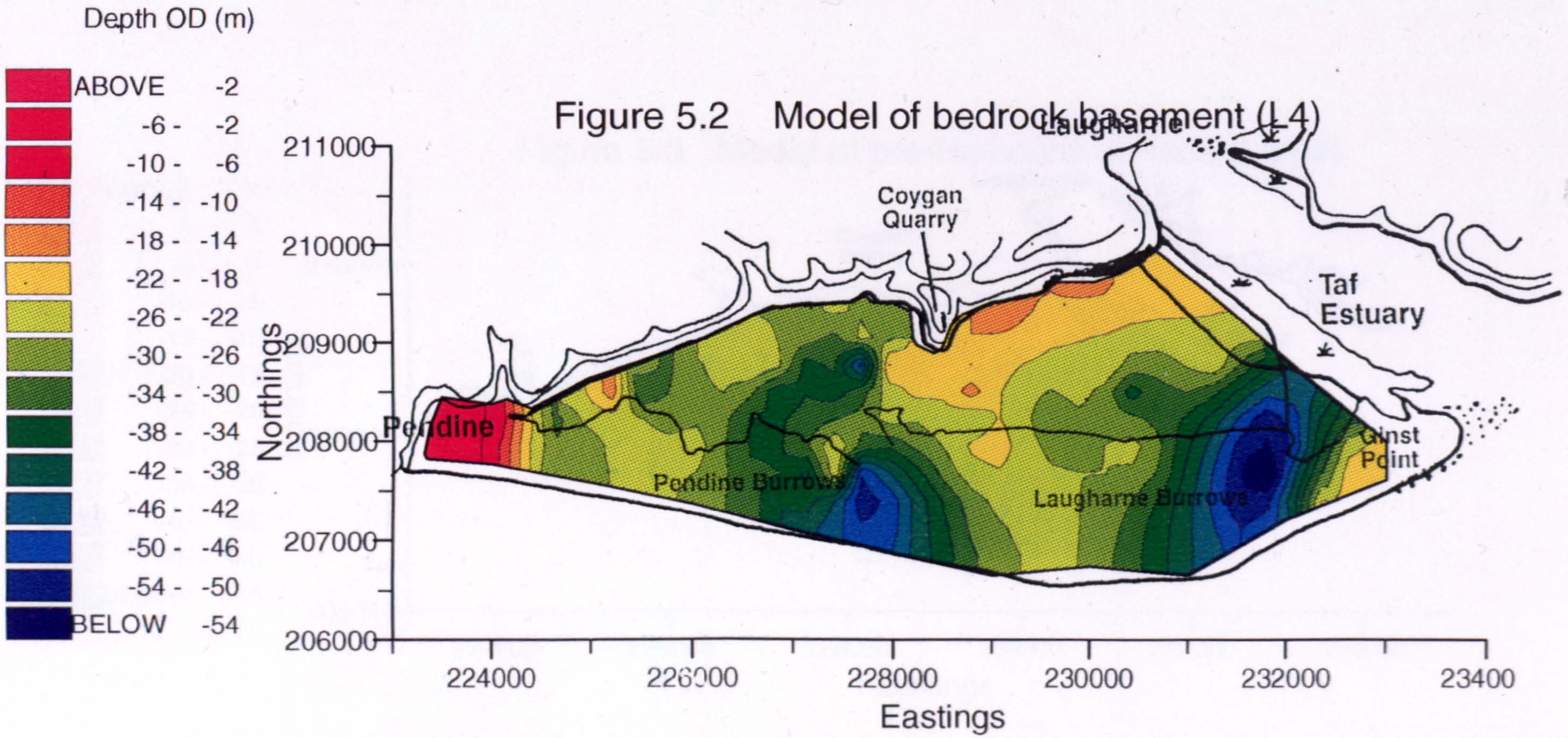

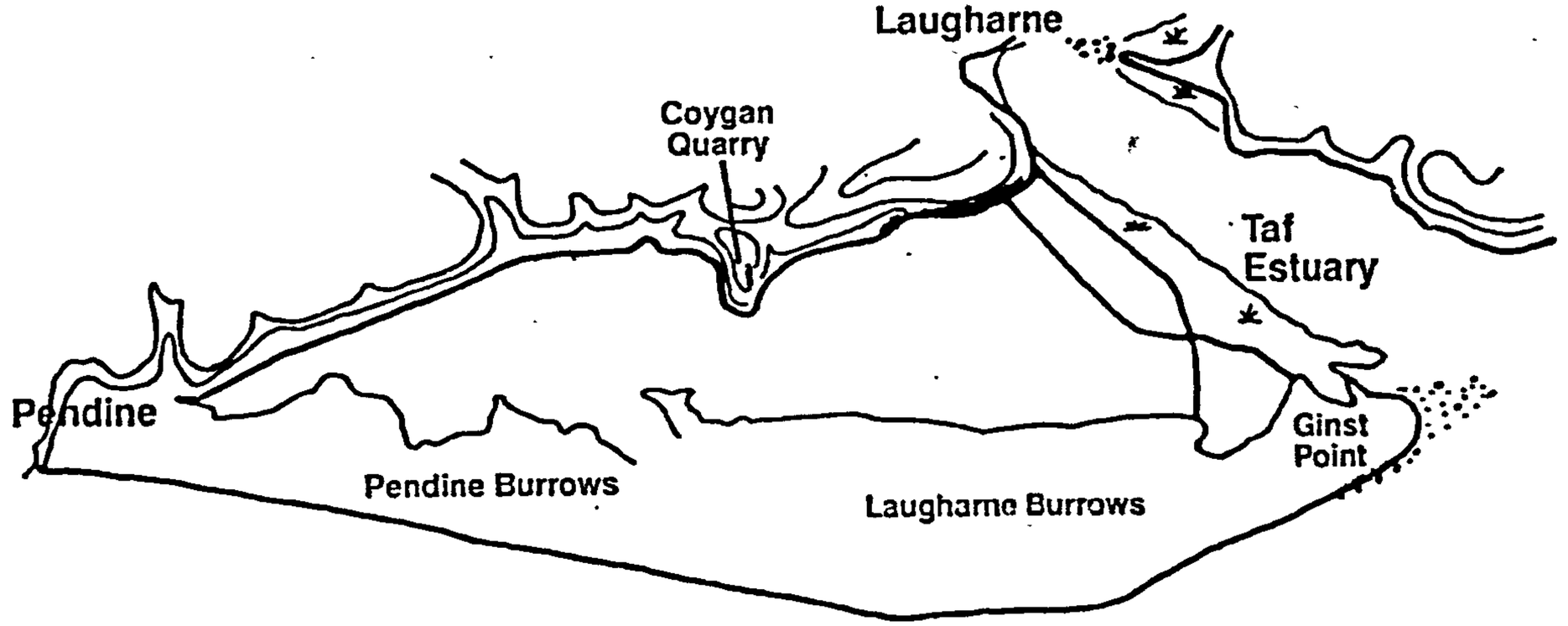
Laugharne
Coygan
Quarry
Taf
Estuary
Pendine
Ginst
Point
Pendine Burrows
Laugharne Burrows

Figure 5.3 Model of pre-Holocene surface (L3/L4)

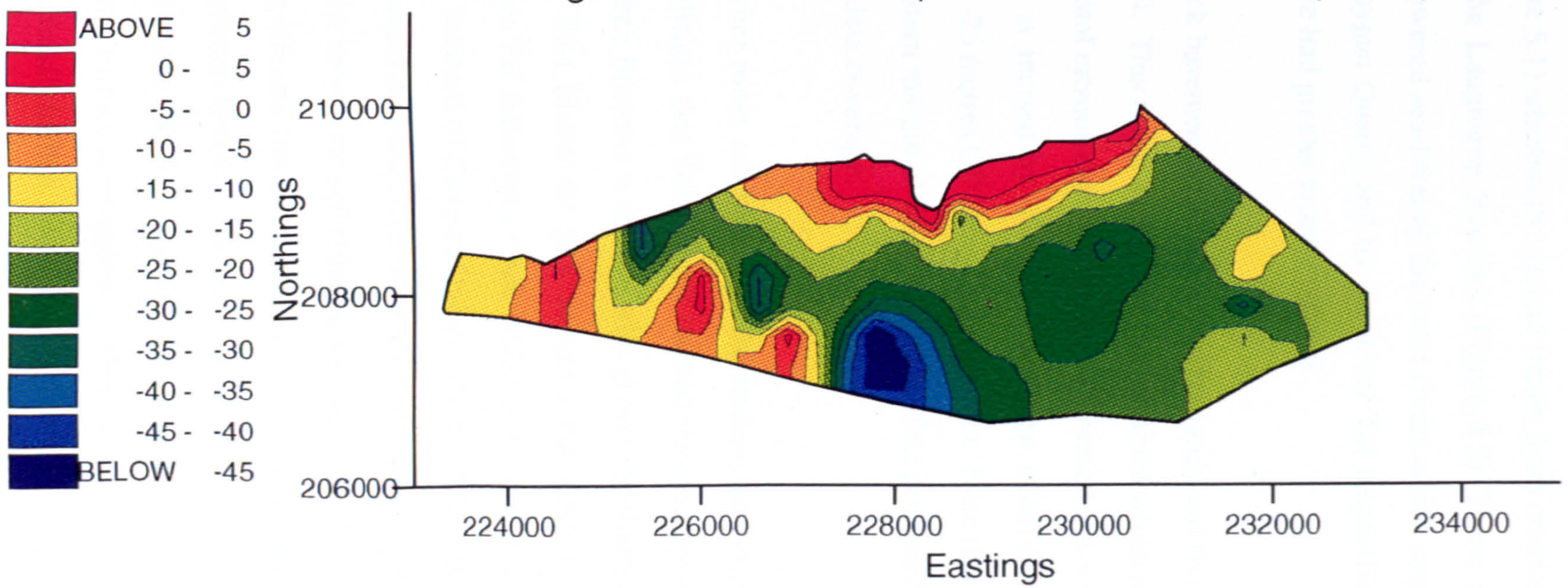

Figure 5.3 Model of pre-Holocene surface (L3/L4)

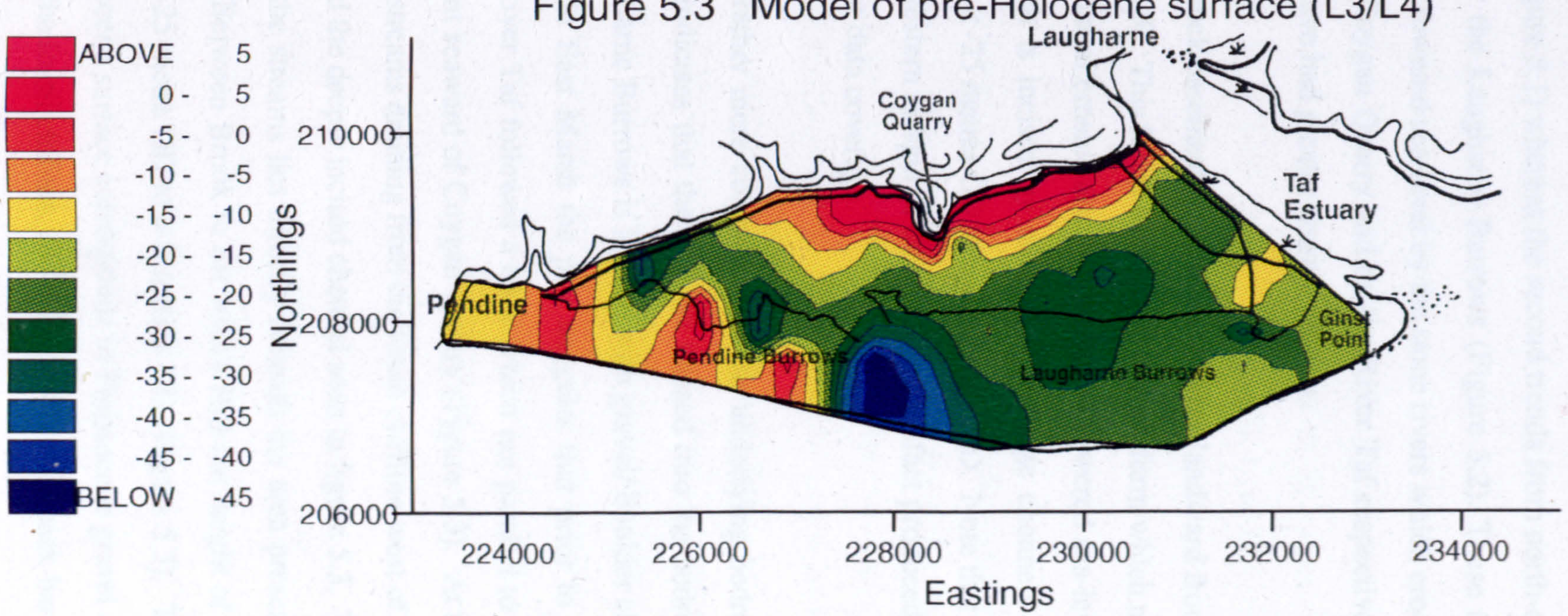

The refraction data indicates that two deeply incised depressions or channels have been eroded into the bedrock basement (Figure 5.2). The first extends from Brook in a sinuous fashion seawards beneath the Pendine Burrows (Figure 5.1) whereas the second trends from north-east to south-west from the Taf Estuary under the Laugharne Burrows (Figure 5.2). These two channels may have been formed at a time of lowered sea-level by the same rivers which eroded similar channels into the cliffline west of Coygan Quarry and by the River Taf respectively. During lower base-levels these rivers will have had greater erosive powers.

East of Coygan Quarry the height of the bedrock basement gradually increases landward from < -25 metres OD to > -18 metres OD (Figure 5.5). This forms a relatively flat platform which may represent a wave-cut platform formed by coastal erosion during a period of lowered sea-level. Although the bedrock beneath West Marsh is incised by numerous drainage channels the intervening areas also shelve gradually from < -25 metres OD to > -18 metres OD. Note that the dramatic increase in bedrock height in the western margin of the plot is an artifact produced by UNIMAP© extrapolating when there is poor data coverage.

The shape of the pre-Holocene surface is rather more complex than the underlying bedrock surface (Figure 5.3). The refraction data indicates that the channel incised into the bedrock basement beneath East Marsh and the Laugharne Burrows is infilled with gravel/ boulder clay. Although, the data coverage is poor within East Marsh the plot suggests that prior to the formation of the Laugharne Burrows the River Taf followed a route which ran parallel to the fossil cliffline from Sir John's Hill to a point seaward of Coygan Quarry (Figure 5.3). At this point the River Taf possibly combined with streams draining from the fossil cliffline west of the quarry and subsequently may have excavated the deeply incised channel seen in figure 5.3. The possible confluence of the River Taf and the streams lies directly beneath the area presently occupied by Wytchet Lake (Figure 5.1). Between Brook to Sir John's Hill the height of the gravel surface increases landward from < -25 metre OD to > 0 metres OD (Figure 5.3). This sharp increase in the height of the pre-Holocene surface corresponds to Pleistocene gravel and boulder clay identified along this portion of the fossil cliffline, above the level of the back-barrier sediments.

The seismic refraction data indicates that the Pendine Burrows lie on top of a gravel ridge (L3) which extends from < -10 to > 0 metres OD (Figures 5.1 & 5.3). However, the area beneath West

Marsh has been excavated (Figure 5.3), possibly by streams draining from the fossil cliffline, to form a relatively deep channel which extends from Llanmiloe beneath Wytchet Lake (Figure 5.1). The variation in the height of the gravel/boulder clay ridge (L3), beneath the Pendine Burrows, may represent either fluvial erosion, possibly by meandering channels, or erosion by coastal processes; this feature has been truncated by the interpreted former course of the River Taf (Figure 5.3). Lithological evidence from cores recovered in West Marsh suggests that these materials are glacial in origin and may therefore represent either terminal or lateral moraine deposited by a readvance of Central Welsh Ice (Towy Glacier) during the Late Devensian (Scourse pers comm. 1996).

Implications for barrier formation and development

The model of the pre-Holocene surface, derived from seismic refraction data acquired within the Pendine Burrows, West Marsh and East Marsh (Figure 5.3), has important implications for the formation and subsequent development of the barrier-complex. During the Holocene transgression rising relative sea-levels would have inundated West Marsh and the advancing high energy surf zone was probably prevented from reworking the fossil cliffline west of Coygan by the gravel ridge beneath the Pendine Burrows; this explains the slope of the fossil cliffline west of Coygan. If this feature represents Pleistocene material deposited during the Late Devensian then the model suggests that the barrier may have initially formed through the submergence of the antecedent topography. High sediment supply during the Holocene is likely to have led to the subsequent formation of the barrier and the infilling of the deeply incised channel beneath Wytchet Lake (Figure 5.3).

Even during any periods of reduced sediment supply but continued sea-level rise, the gravel ridge beneath the Pendine Burrows would have pinned the barrier in place and prevented it from being overstepped and ultimately reworked. Since no similar feature occurs beneath the Laugharne Burrows it is probable that once sea-levels stabilised the barrier extended laterally as a 'barrier-spit' by longshore transport.

5.1.2 Seismic reflection surveying

Description of land based shallow reflection data

High resolution seismic profiles were conducted within West and East Marshes and upon the foreshore of Pendine Sands. Data obtained from preliminary investigations within the back-barrier area, using both a sledge hammer/steel plate and a 12-gauge Buffalo Gun to generate shots (Brabham and McDonald, 1992), were extremely poor in quality and unsuitable for analysis. In the majority of the records the sub-surface reflectors were obscured by low frequency (<50Hz) surface waves. It is possible that a large proportion of the seismic energy, generated by both types of source, is either absorbed or internally reflected within a near-surface LVL (Telford et al., 1990; Sheriff and Geldart, 1995). However, reflection data acquired during the winter months, when the fields within West Marsh and East Marsh become water logged, showed only a marginal improvement in data quality. The near-surface sediments, composed predominately of highly stratified silts and clays intercalated with biogenic sediment (section 4.1) may therefore be unsuitable for the acquisition of high resolution seismic reflection data.

The data acquired from three transects on Pendine Sands (Figure 5.4) were processed and the stacked sections are displayed in figures 5.5, 5.6 and 5.7. The final sections reveal two main sub-surface reflectors which are thought to represent the boundary between the L2 and L3 horizons of the refraction analysis and the interface between L3 and L4 horizons; the reflectors were identified using velocity data derived from normal-moveout correction and refraction analysis (Sheriff and Geldart, 1995). For simplicity, the geological interpretations displayed beneath each of the sections are based on an average velocity of 1650 m/sec.

The surface sediment along the first 55 metres of transect 1 (SN 2711 0714 to SN 2707 0698) was unsaturated when the survey was conducted. Consequently any sub-surface reflectors are concealed by low frequency noise (Figure 5.5). As the near surface sediments become saturated the data quality increases significantly. From 55 to 154 metres the gravel and bedrock surfaces exhibit little or no relief and appear to be horizontal and parallel to one another (Figure 5.5). The depth to the L3 varies between 19.6 to 21.2 metres whereas the bedrock lies between 25.7 and 26.6 metres depth. An internal reflector within the gravel facies is indicated by the dashed line (Figure 5.5). Considering the gradient of the foreshore the reflection data implies that the gravel

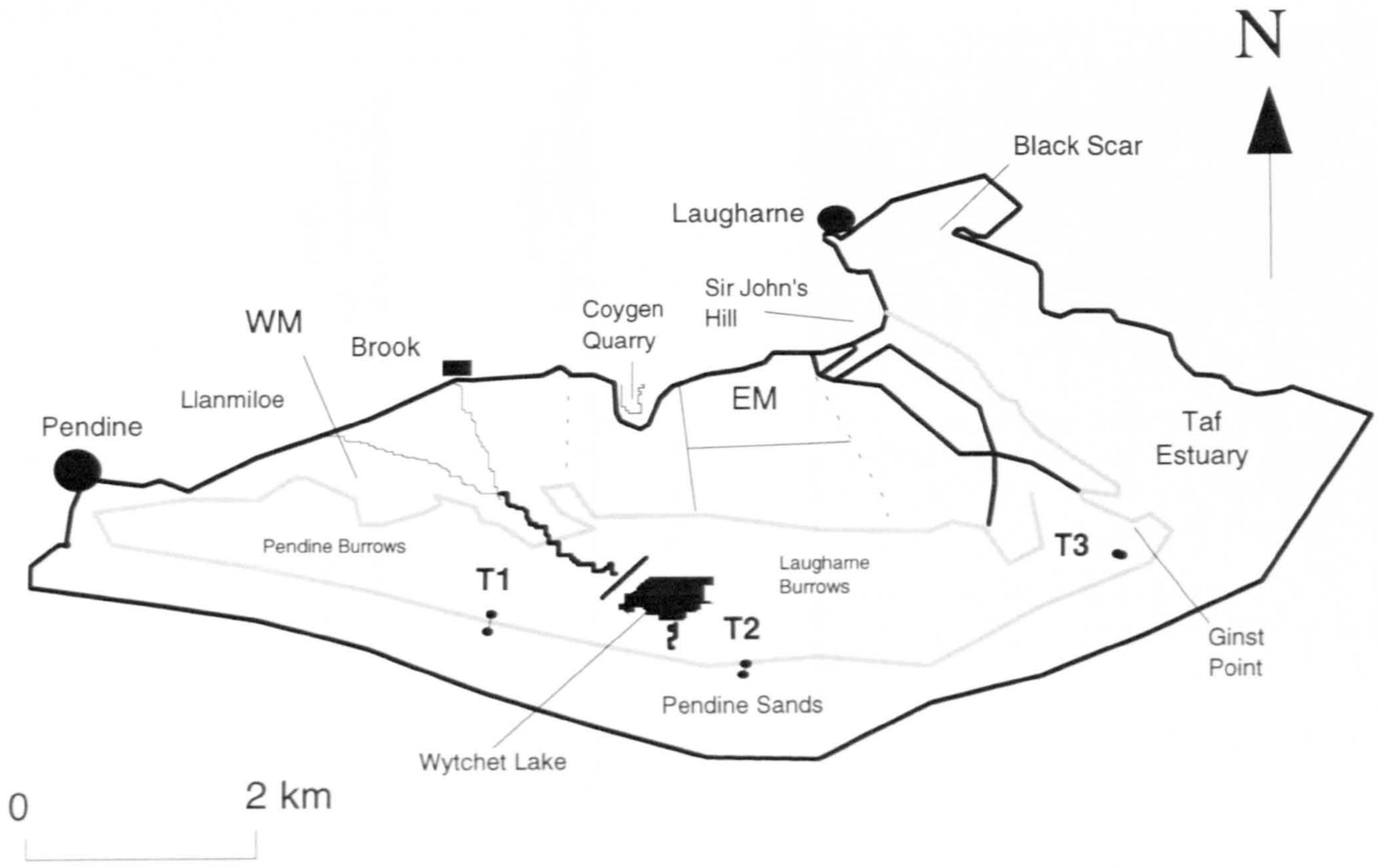

Figure 5.4 Position of reflection profiles on Pendine sands

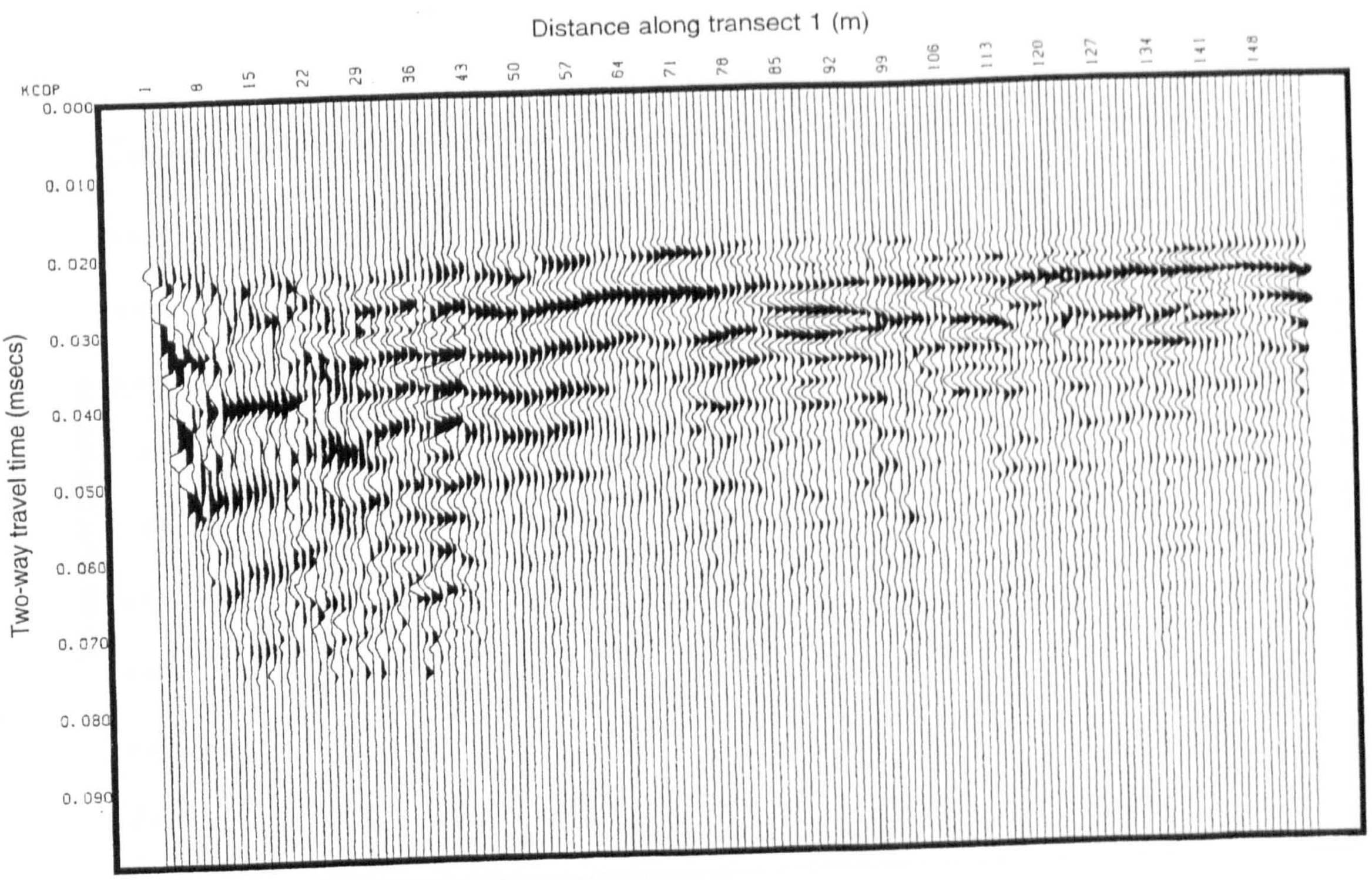

Figure 5.5 Final processed section for Transect 1; the geological interpretation is based on an average velocity of 1650 m/sec.

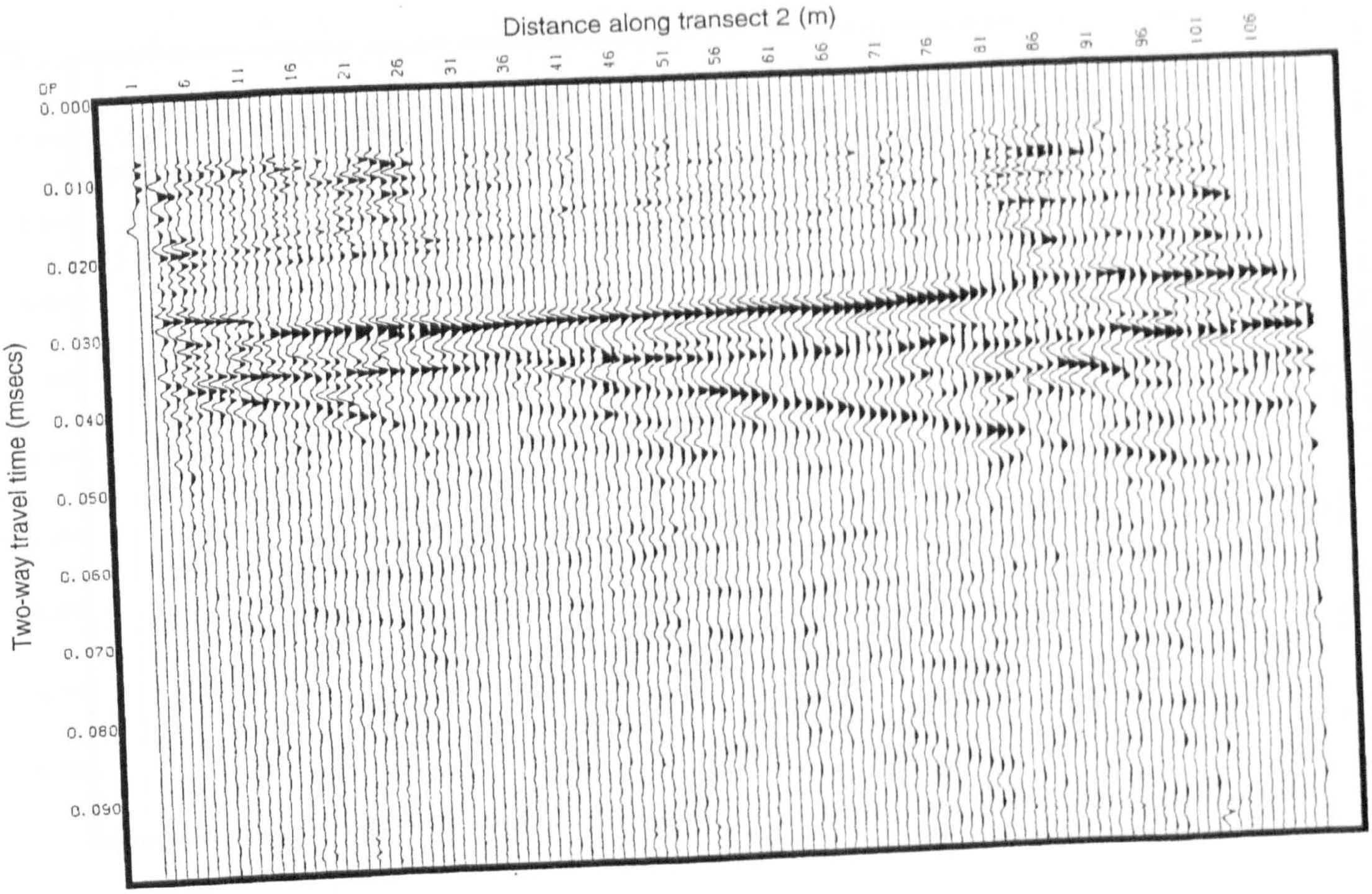

Figure 5.6 Final processed section for Transect 2; the geological interpretation is based on an average velocity of 1650 m/sec.

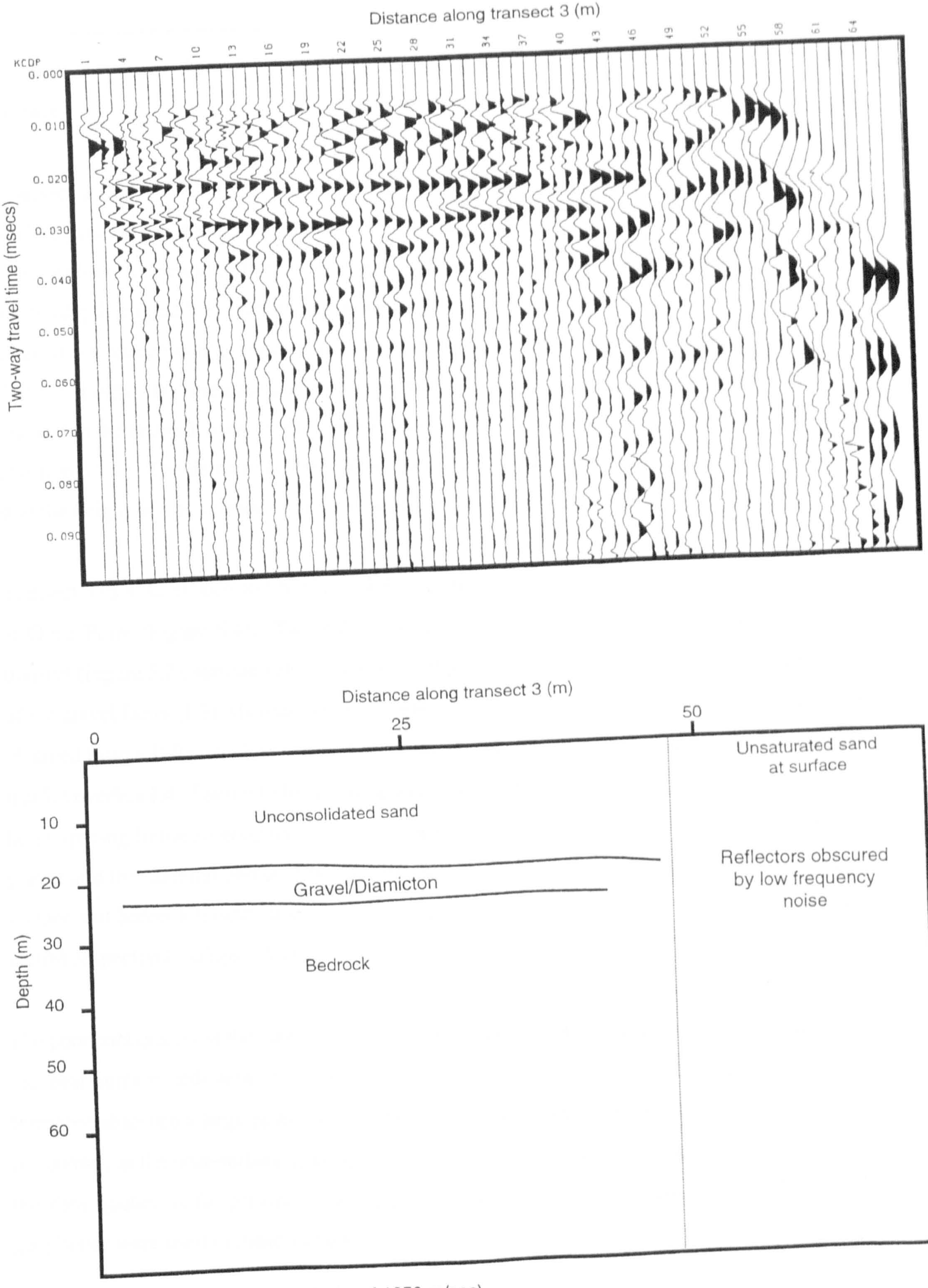

Figure 5.7 Final processed section for Transect 3; the geological interpretation is based on an average velocity of 1650 m/sec.

and bedrock surfaces beneath transect 1 dip gently offshore, approximately parallel to the beach surface.

Transect 2 (SN 2936 0666 to SN 2933 0656) yielded high data quality (Figure 5.6). The L3 surface exhibits slight relief and lies between 21.1 and 23.3 metres depth. In contrast the bedrock (L4) appears horizontal at the start of transect 2 but then dips from approximately 28 to > 42 metres depth (Figure 5.6). Internal reflectors within the L2 and L3 layers are indicated by dashed lines; these reflectors may represent changes in sediment composition and density (Sheriff and Geldart, 1995). The increase in the depth to the L4 surface along transect 2 corresponds to the channel in the bedrock basement beneath Wytchet Lake, identified using seismic refraction data (Section 5.1.1). The depth of L3 beneath transect 2 is comparable to transect 1 and but suggests that the height of this surface increases slightly beneath the lower shoreface (Figure 5.6).

Transect 3 (SN 3270 0669 to SN 3274 0668) is a relatively short profile located on the foreshore at Ginst Point (Figure 5.4). Two reflectors can clearly be seen in the first 45 metres of the transect (Figure 5.7); seismic velocities indicate that the upper reflector corresponds to the surface of the gravel facies (L3) whereas the lower represents the bedrock surface (L4). Refraction data obtained from a 120 metre line adjacent to transect 3 indicates that L3 is absent from this area and that L2 overlies L4. Failure to locate the gravel, using refraction analysis, can either be due the large spacing between geophones or due to a small acoustic impedance contrast between the gravel and the material above or below this unit - yielding a weak refraction event. The gravel surface and bedrock basement show little relief and lie between 15.8 to 16.4 and 23.9 and 24.6 metres respectively (Figure 5.7).

The poor data quality at the start of transect 1 and at the end of transect 3 was largely caused by the near-surface sediments becoming unsaturated. Low velocity unsaturated sands on the foreshore absorbed a large proportion of the seismic energy and generated low frequency noise. In contrast, as the near-surface sediments along transect 2 remained saturated during the survey the data quality is far greater. Data quality would have been improved if high-frequency geophones were used in these surveys.

Discussion of high-resolution seismic reflection data

Using velocity data obtained from refraction analysis and the *normal-moveout* velocity (stacking velocity), it is possible to relate the two main reflectors identified on the high-resolution seismic profiles to the boundary between sand and gravel (L2/L3 boundary in section 5.1.1), and the interface between gravel and bedrock (L3/L4 boundary in section 5.1.1). The reflection data suggests that the pre-Holocene surface beneath the foreshore dips gently offshore, roughly parallel to the contemporary beach surface, at a depth of approximately 20-22 metres. In contrast to the dunes and back barrier area the pre-Holocene surface beneath the Pendine Sands exhibits little or no relief, which may represent intense reworking by a high energy surf-zone during the Holocene transgression.

The reflection data indicates that the gravel ridge located beneath the Pendine Burrows (section 5.1.1), does not extend beneath the contemporary foreshore. Furthermore, no back-barrier facies (mud, silt or peat) have been identified on the seismic profiles. The reflection data possibly supports the hypothesis that the barrier formed through the inundation of a gravel ridge, upon which Holocene sediment accumulated. If the Pendine Burrows were formed through the retreat of an offshore barrier, in response to rapid sea-level rise during the early Holocene, any evidence of barrier roll-over has been removed from the shoreface sediments.

Although the acquisition system used was not suited to this type of work (e.g the low resonant frequency geophones had too great a frequency bandwidth and the cables had different polarities) good quality high-resolution seismic reflection data were obtained from Pendine Sands. On the foreshore, data quality was drastically improved when the near-surface sediments were fully saturated. However, due to the composition of the near-surface sediment within the back-barrier area the quality of data acquired within West Marsh and East Marsh was very poor.

5.1.3 Marine reflection profiling

Description of shallow marine reflection data

The quality of the data acquired using the SEISTEC system were lower than expected; this was due to a tear in a rubber membrane within the boomer source which was identified after the survey was completed (Bennell *pers com.*, 1996). Two main reflectors were identified on the majority of the records acquired within the Taf Estuary. Using velocity data obtained from refraction analysis along with the exposure of local Pleistocene gravel and boulder clay deposits theses reflectors are interpreted as the pre-Holocene surface (L3) and the bedrock basement (L4).

Two typical sections of marine data, acquired within the estuary (Figure 5.8), are presented in figures 5.9 and 5.10 along with the corresponding geological interpretations. The sections show both reflectors and indicate that a channel incised into the bedrock basement is infilled with Pleistocene material (Figures 5.9 & 5.10).

The depths to the gravel and bedrock surfaces were converted into depths relative to Ordnance Datum using tide gauge data, and were then contoured in UNIMAP© using a distance weighted method. Models of the bedrock basement (L4) and the pre-Holocene surface (L3) beneath the survey area (Figure 5.8) are presented in figures 5.11 and 5.12.

The depth of the bedrock basement increases from < -14 metres OD in the southwestern portion of the survey area to > -2 metres adjacent to the fossil cliffline on the eastern side of the estuary (Figure 5.11). The marine reflection survey locates a relatively shallow channel in the bedrock basement which extends from north-east to south-west and is thought to extend beneath the contemporary saltmarsh and the back-barrier deposits (Figure 5.11).

The height of the pre-Holocene surface ranges from <-14 to > 2 metres OD (Figure 5.13). The model indicates that a channel, eroded into the pre-Holocene surface by the course of the River Taf (Figure 5.12), extends from Black Scar around the base of Sir John's Hill and beneath East Marsh (Figure 5.8). The gravel ridge exposed at Black Scar could not be accurately delimited because the water depth over this feature was too shallow for the survey vessel. Because of this

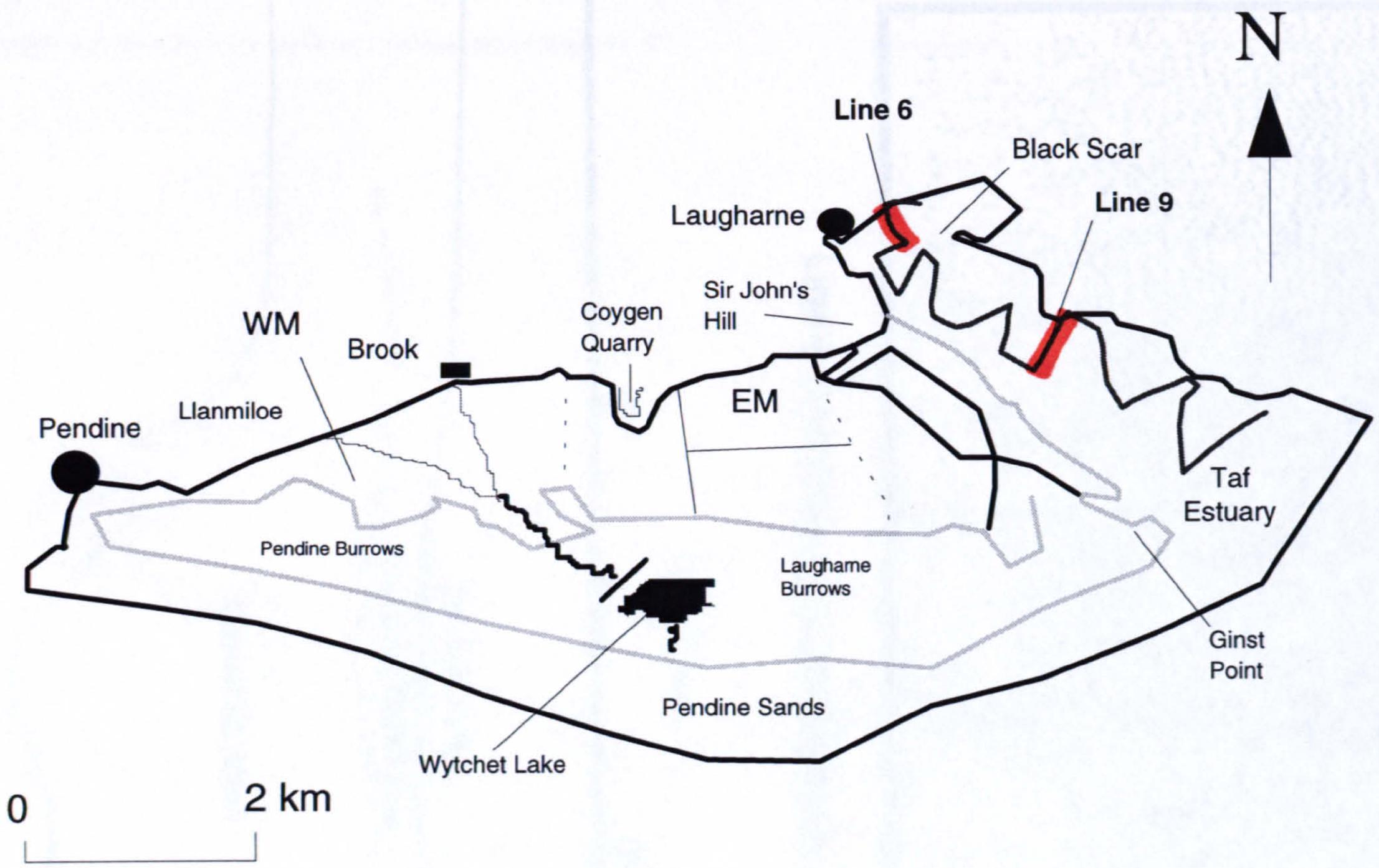

Figure 5.8 Marine reflection survey track within the Taf Estuary

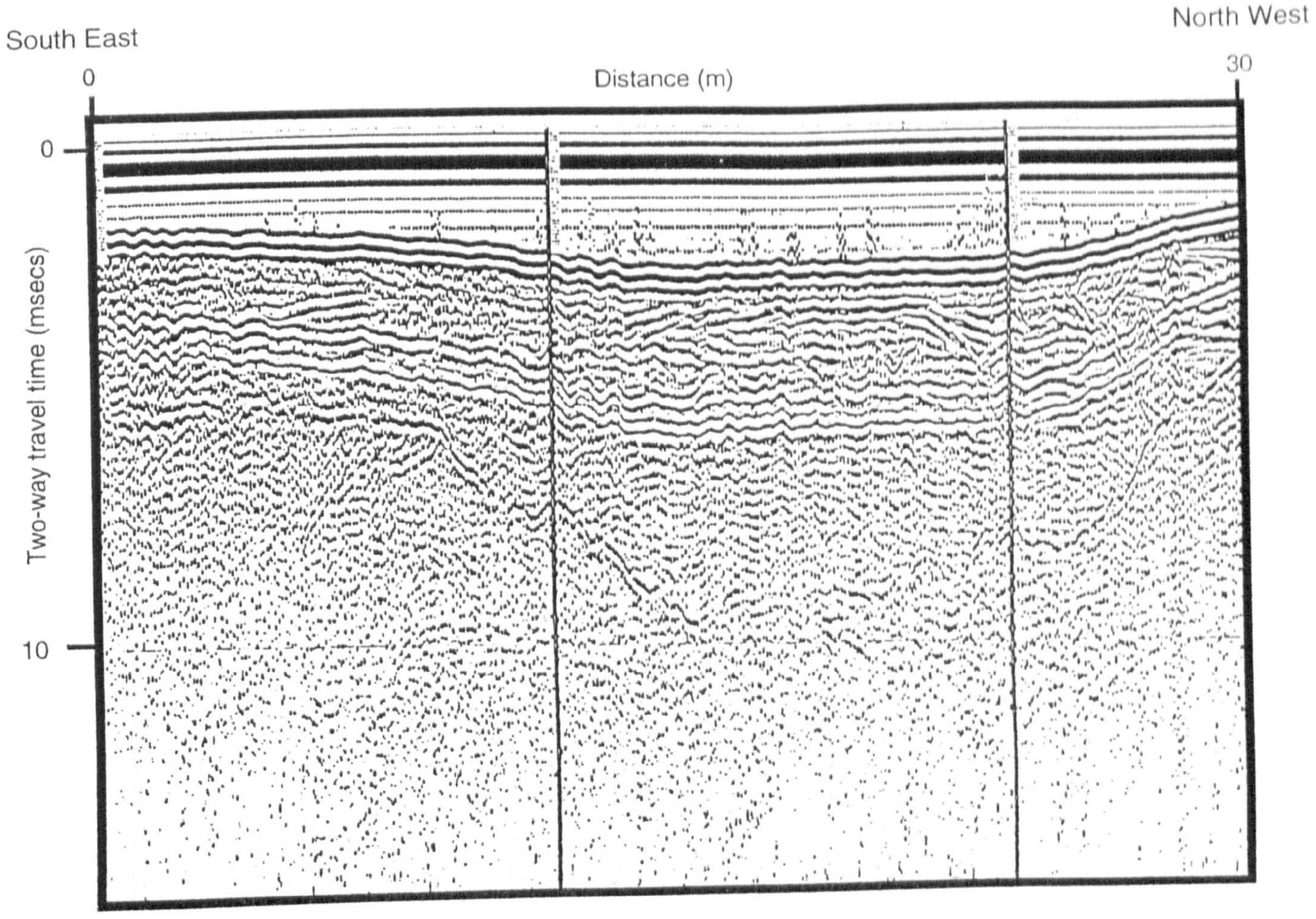

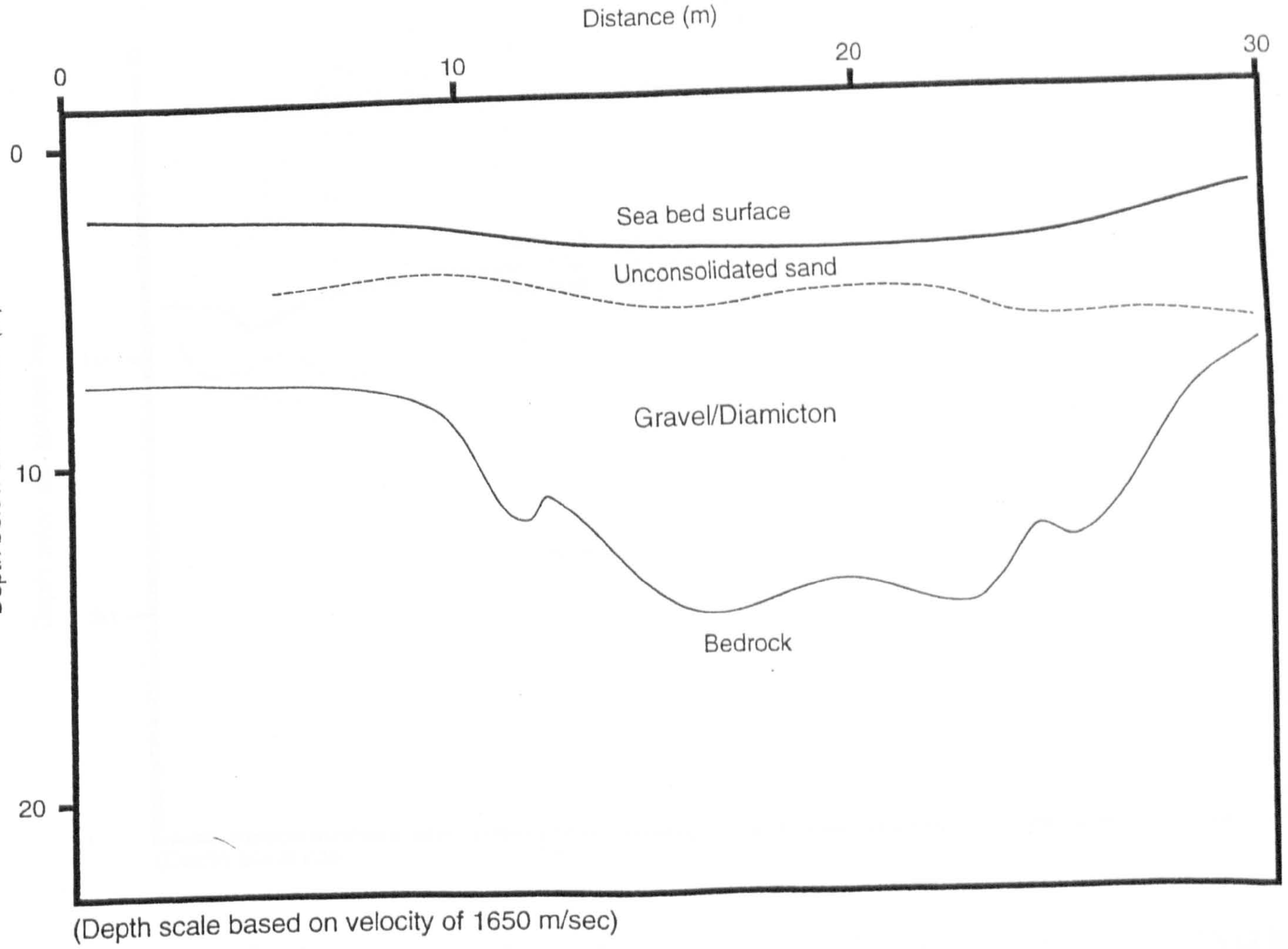

Figure 5.9 A section of marine reflection data recorded using the SEISTEC along line 6; the geological interpretation is based on an average velocity of 1650 m/sec.

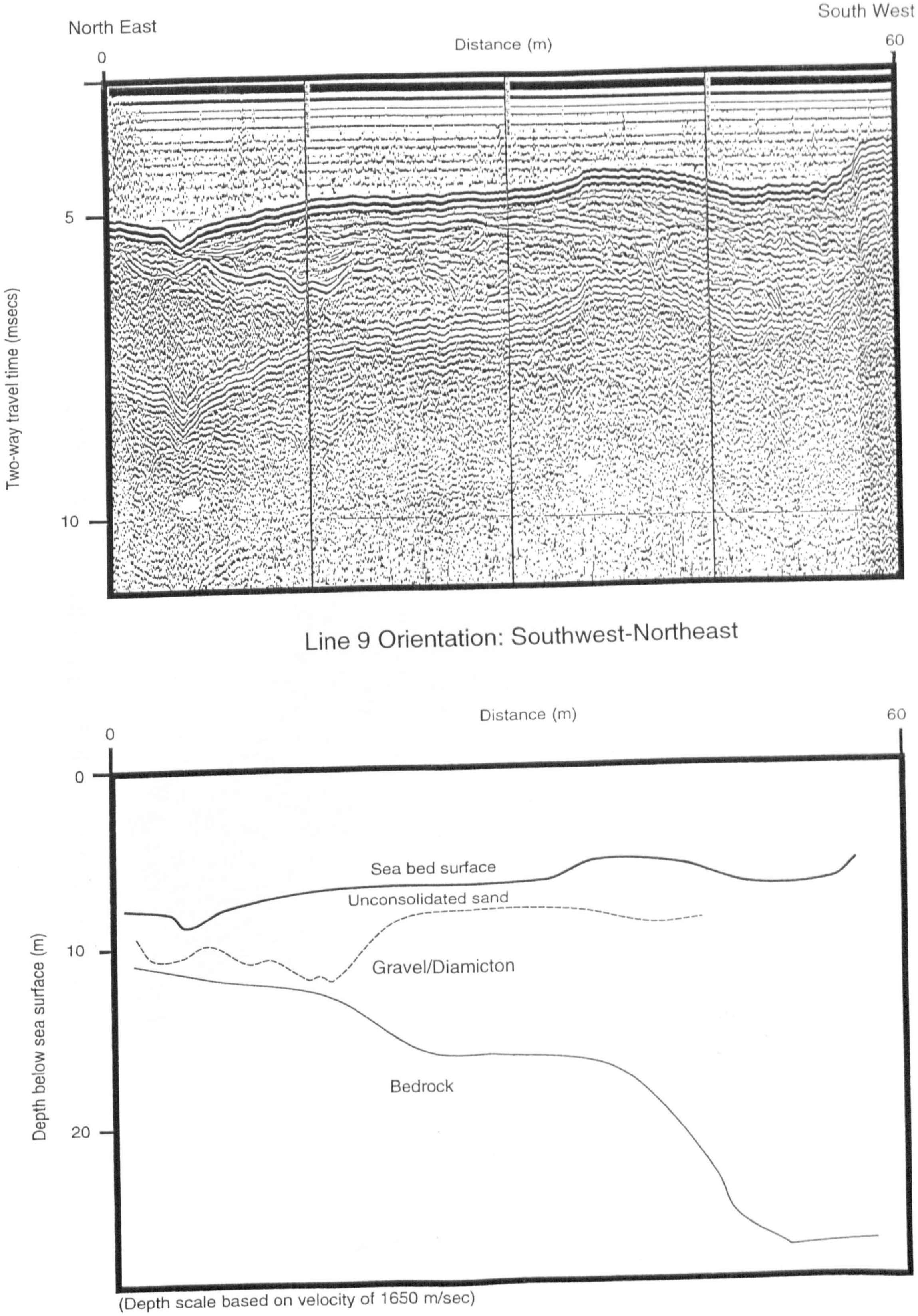

Figure 5.10 A section of marine reflection data recorded using the SEISTEC along line 9; the geological interpretation is based on an average velocity of 1650 m/sec.

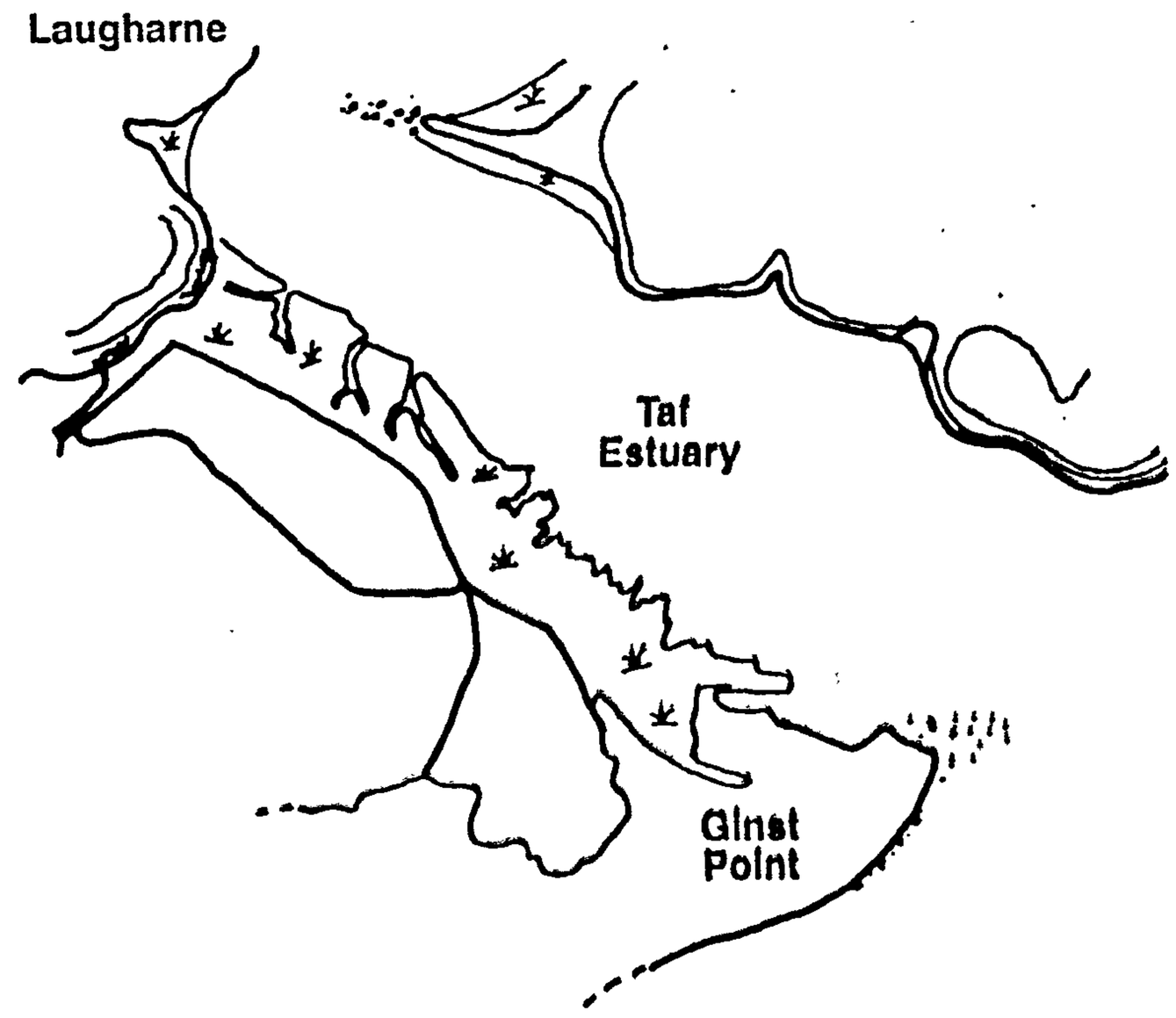
Laugharne
Taf
Estuary
Giant
Point

Figure 5.11 Model of bedrock basement

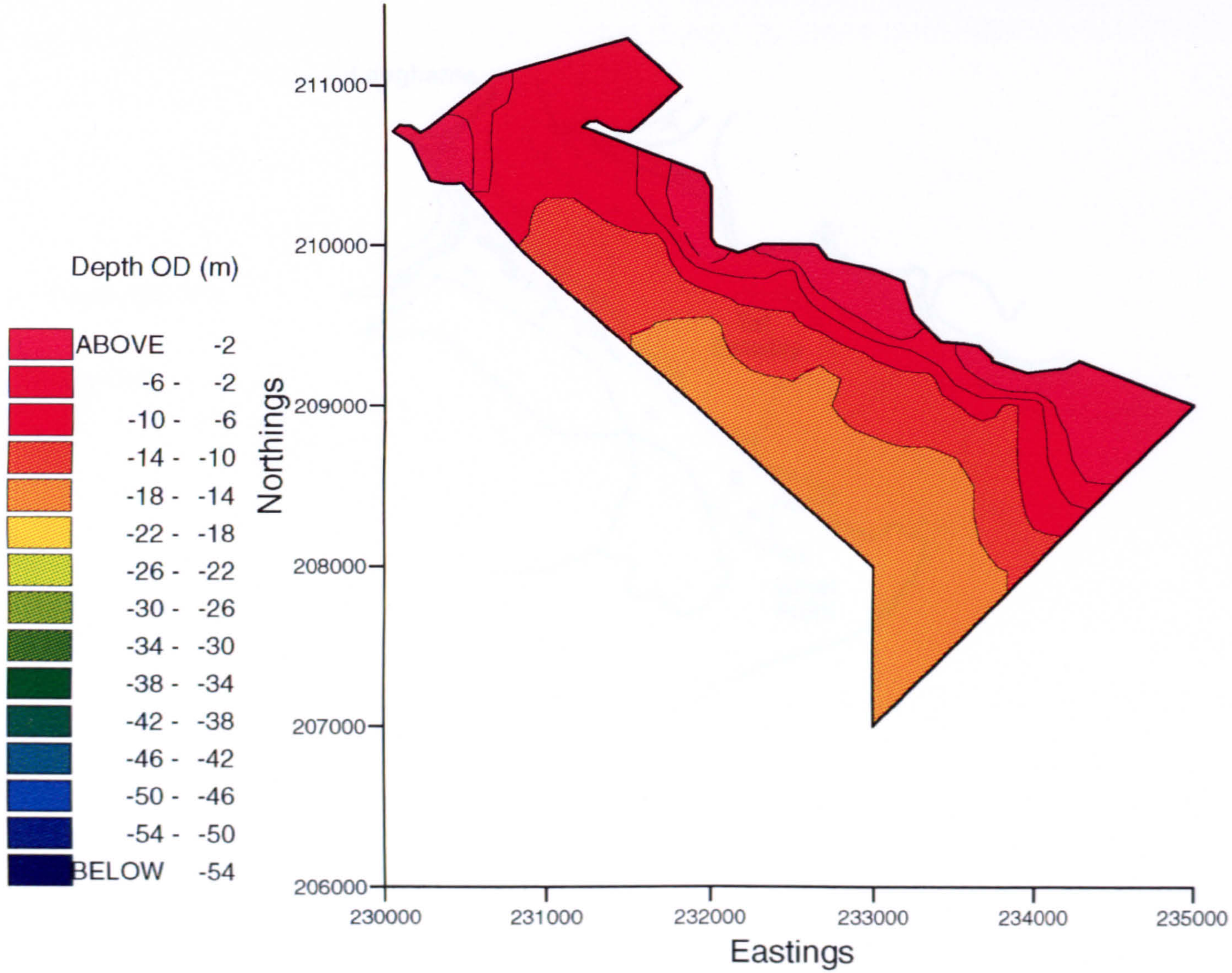

Figure 5.11 Model of bedrock basement

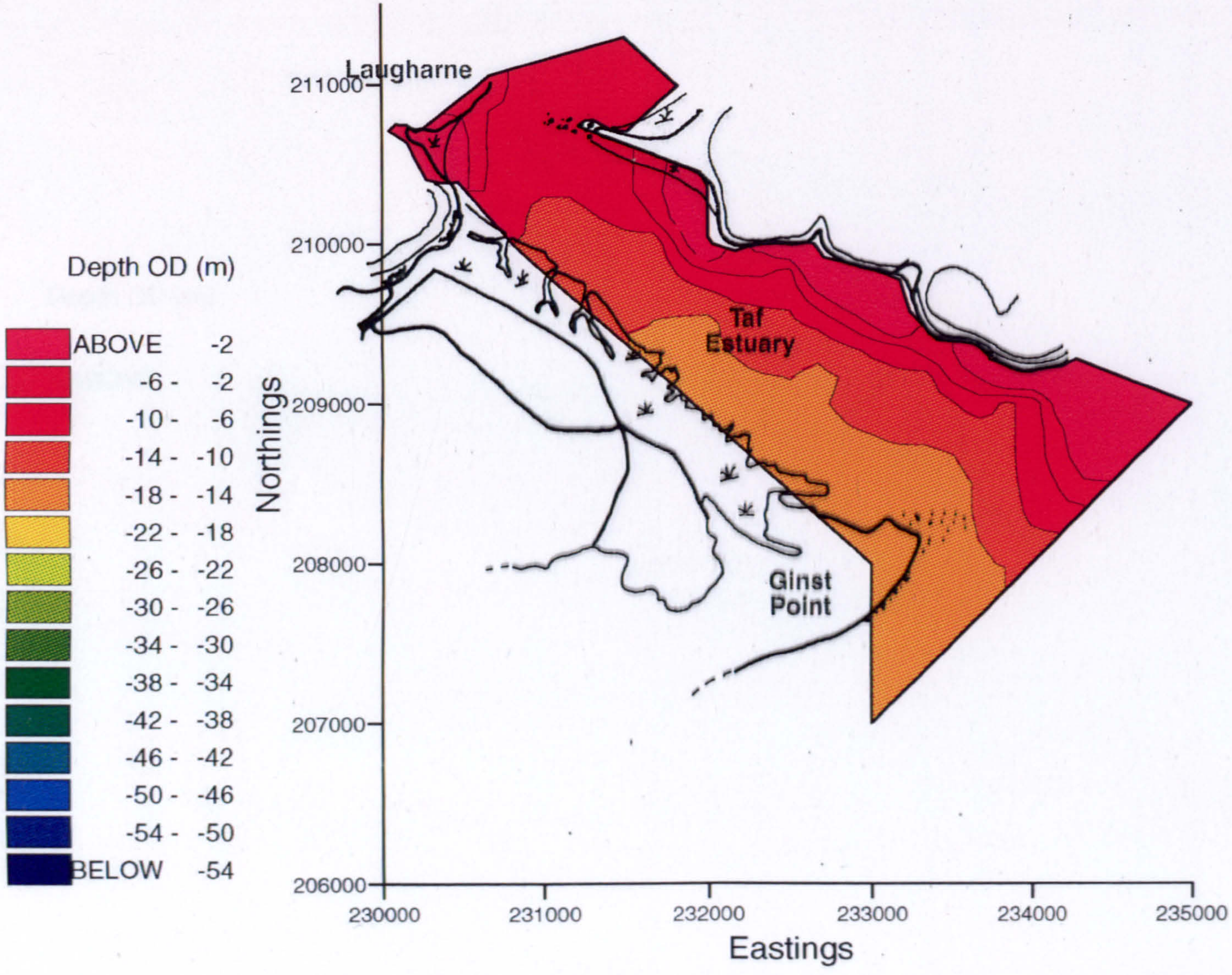

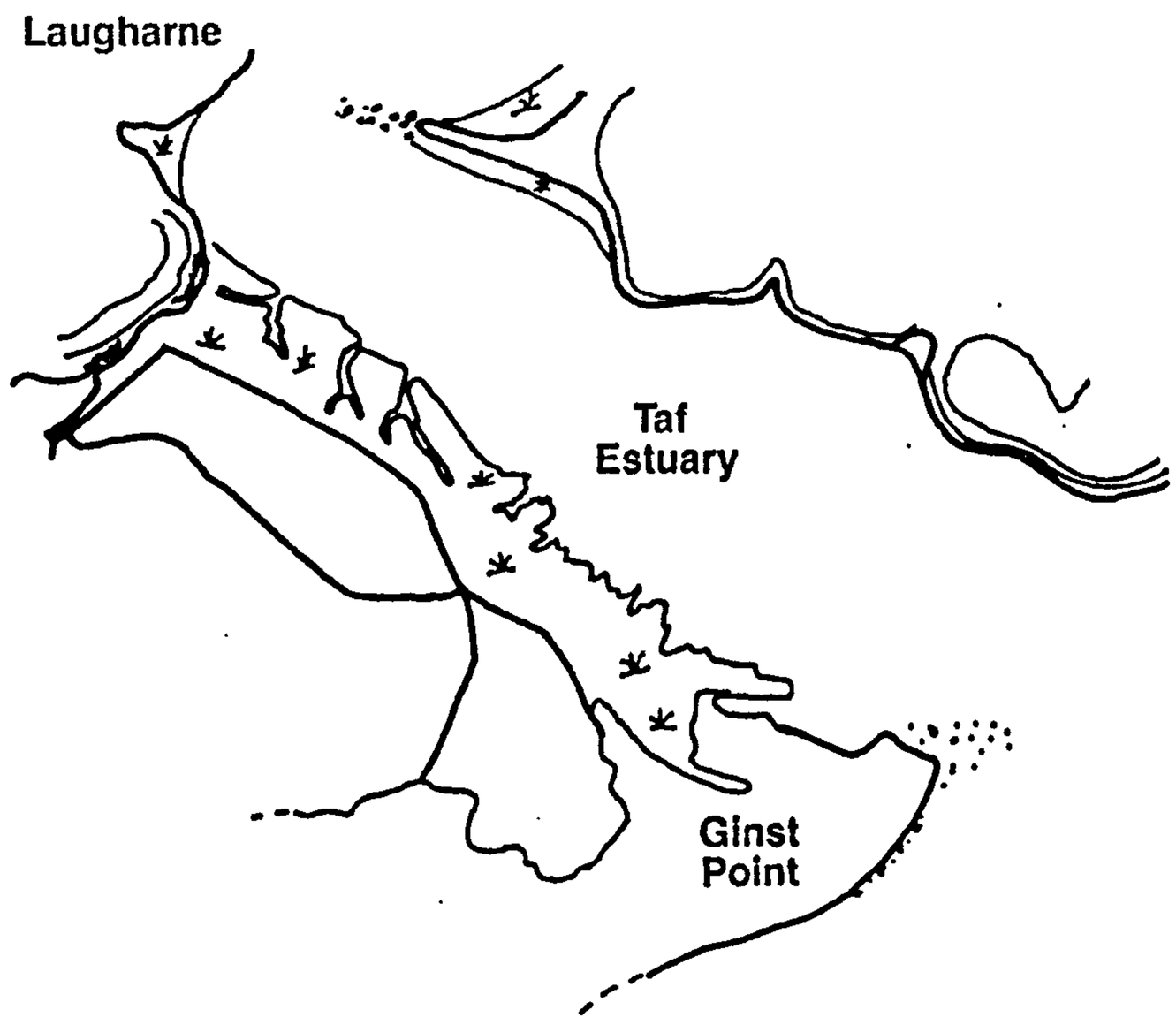
Laugharne
Taf
Estuary
Ginst
Point

Figure 5.12 Model of pre-Holocene surface

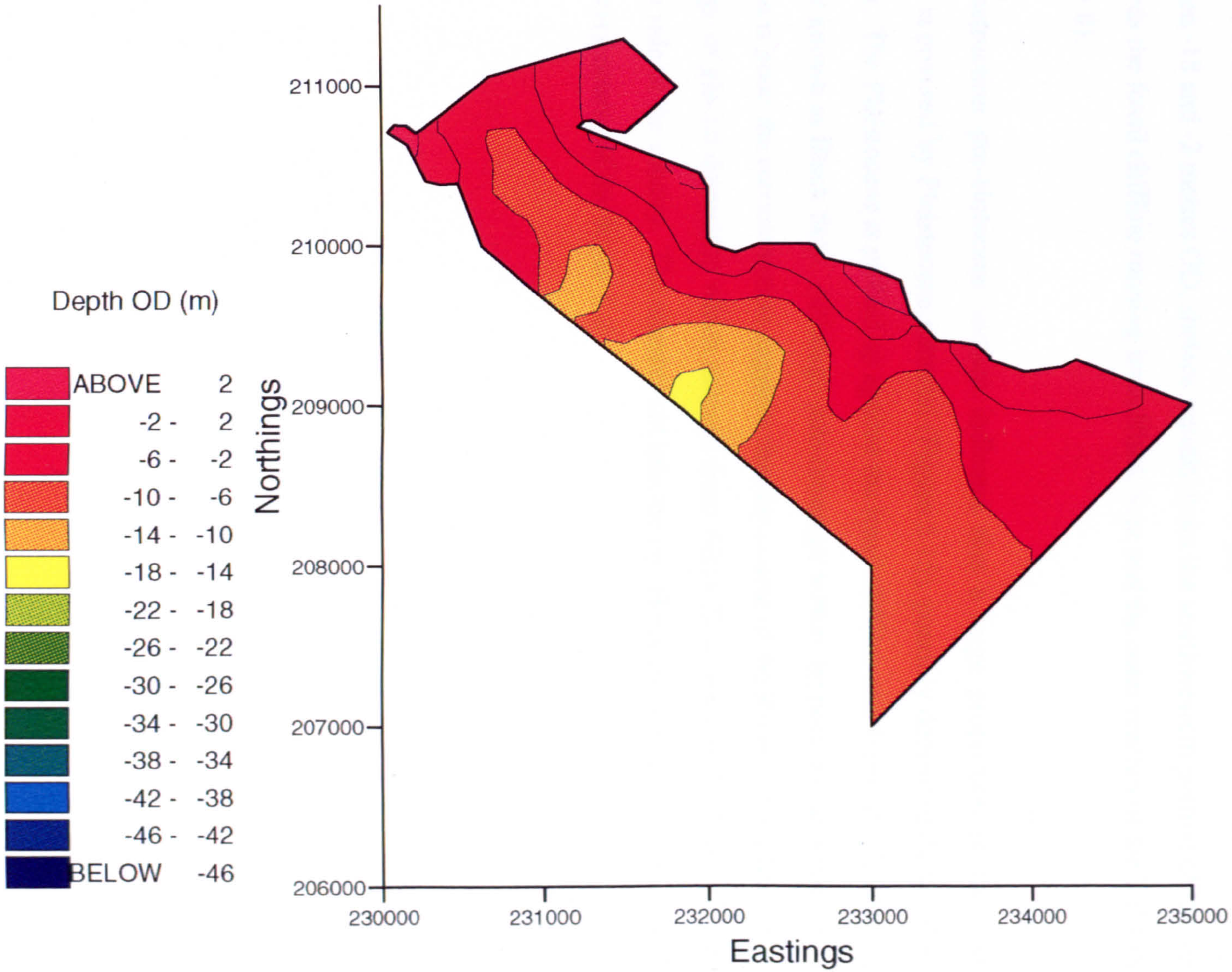

Figure 5.12 Model of pre-Holocene surface

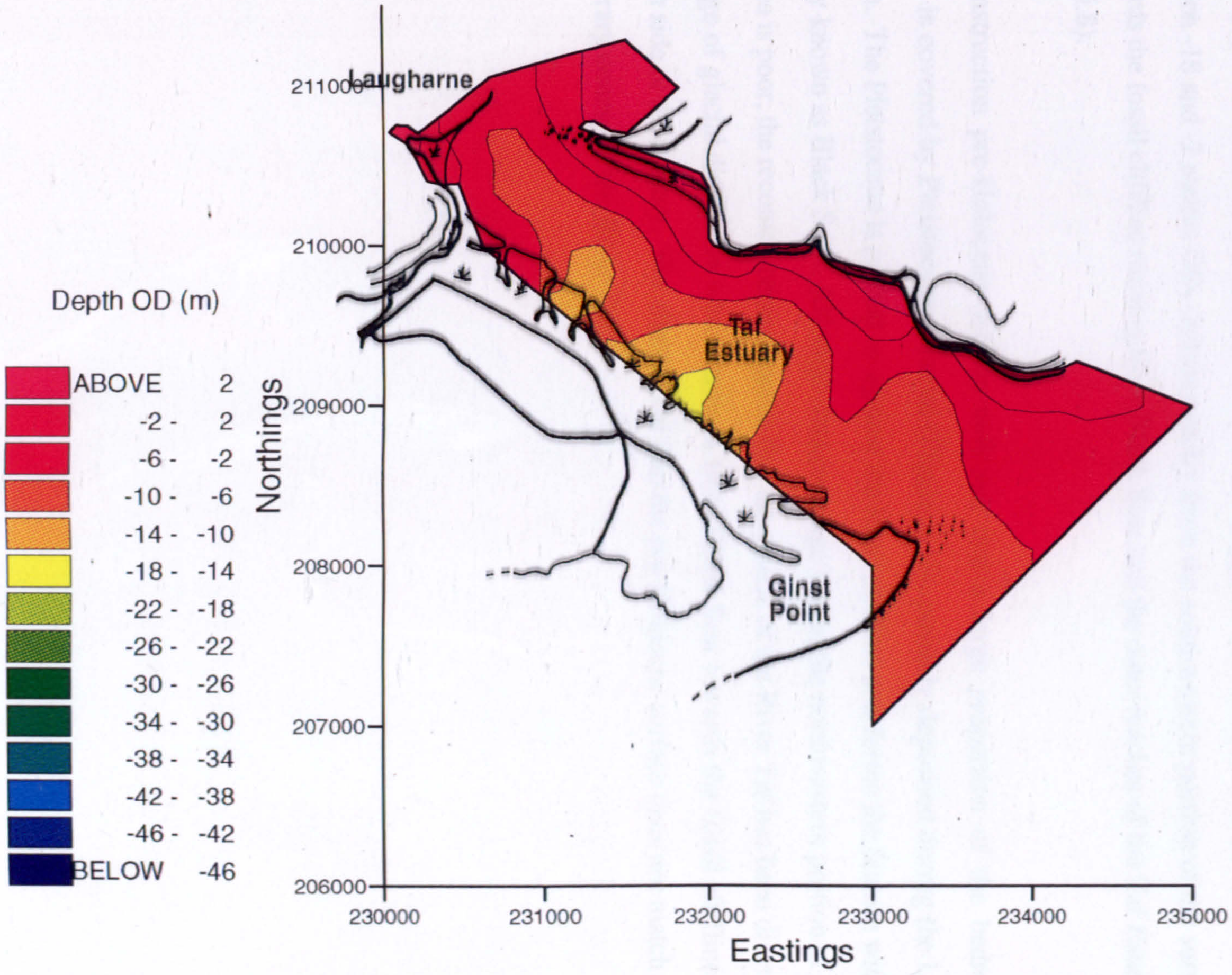

it is believed that the model does not truly represent the pre-Holocene surface in the extreme northeastern portion of the survey area (Figure 5.12).

Discussion of shallow marine reflection data

The two reflectors identified on the marine records have been interpreted as the pre-Holocene surface (L3) and the bedrock basement (L4). The data suggests that the bedrock basement, which lies between -18 and -2 metres OD, shelves rapidly from the southwestern portion of the survey area towards the fossil cliffline running from Black Scar and the outer reaches of the Taf Estuary (Figures 5.8).

The reconstruction pre-Holocene surface indicates that a large proportion of the bedrock basement is covered by Pleistocene material (Figure 5.15), possibly deposited during the Late Devensian. The Pleistocene is pushed up against the fossil cliffline and forms the feature within the estuary known as Black Scar. Although data coverage within the northwestern portion of the survey area is poor, the reconstruction suggests that the course of the River Taf has been diverted by the ridge of glacial diamicton which extends from Black Scar towards the fossil cliffline on the eastern side of the estuary. The channel cut into the pre-Holocene surface does not match the contemporary course of the River Taf.

5.2 Electrical resistivity surveying

Description of resistivity data

Twenty four Schlumberger depth probes were conducted within East Marsh and the data were processed using RESIX-PLUS. The results were inconclusive in that the technique failed to locate the bedrock surface beneath the majority of sites investigated. In the areas adjacent to the fossil cliffline the resistivity model data compares well to the depths obtained from refraction analysis. However, at sites located seaward of the cliffline the bedrock was not detected even with a current base separation of 300 metres.

The failure of resistivity techniques to locate the bedrock beneath East Marsh could be related to the composition of the pore fluid. If the pore fluid salinity or the degree of saturation (*i.e.* the electrical permeability) increases with depth, the current may leak laterally along the boundary possibly preventing the current field from penetrating down to the bedrock. It is possible that differences in the electrical permeability of the back-barrier sediments may have led to the general failure of this technique.

Due to the failure of resistivity depth probes within East Marsh similar measurements were not conducted in the West Marsh area. With hindsight resistivity methods may have been more successful in locating the bedrock surface behind and on the Pleistocene ridge identified by refraction surveys.

5.3 Summary

On the basis of seismic velocity data the main refractors and reflectors identified in the refraction analysis, the high-resolution seismic profiles and the shallow marine reflection survey were interpreted as representing the interface between sand and gravel and the boundary between gravel and bedrock. These three data sets were combined and contoured in UNIMAP© to produce reconstructions of the bedrock basement and the pre-Holocene surface (Figures 5.13 & 5.14). The heavy black line drawn over the diagrams represents the MHW level from Sir John's Hill to Ginst Point, the MHW level seaward of the dunes, and the five metre contour behind the Pendine and Laugharne Burrows.

The bedrock basement is intersected by two deeply incised channels, which may represent erosion by the River Taf and streams draining from the fossil cliffline west of Coygan Quarry (Figure 5.13). However, although one can speculate on the possible origin of the majority of the features, displayed on the bedrock basement model, it is likely that this surface has been subject to successive stages of erosion during the Pleistocene. For this reason the interpretation of the bedrock basement surface model will be extended no further.

The pre-Holocene surface suggests that, prior to the formation of the Laugharne Burrows, the River Taf followed a course roughly parallel to the fossil cliffline from Sir John's Hill to a point beneath Wytchet Lake (Figure 5.14). By combining the reflection data, acquired on the Pendine Sands, with the refraction data the model clearly indicates that gravel ridge beneath the Pendine Burrows does not extend beneath the foreshore. It is obvious that this feature played an integral role in the formation and subsequent development of the barrier complex (Figure 5.14).

The thickness of Pleistocene (Figure 5.15) and the shape of the basin beneath West Marsh (Figure 5.14) suggest that the gravel, beneath the western portion of the barrier complex, may represent terminal deposits formed by a readvance of the inland Welsh Ice, during the Late Devensian; the lithological evidence, acoustic properties and extent of the gravel show that these deposits do not represent a storm gravel ridge. Water draining from the fossil cliffline west of Coygan Quarry has modified these deposits, excavating the area behind the ridge (Figure 5.14). The extremely thick deposits beneath Laugharne Burrows represent the amount of Pleistocene infill occupying the deeply incised bedrock channel (Figure 5.15)

Figure 5.13 Bedrock basement beneath study area

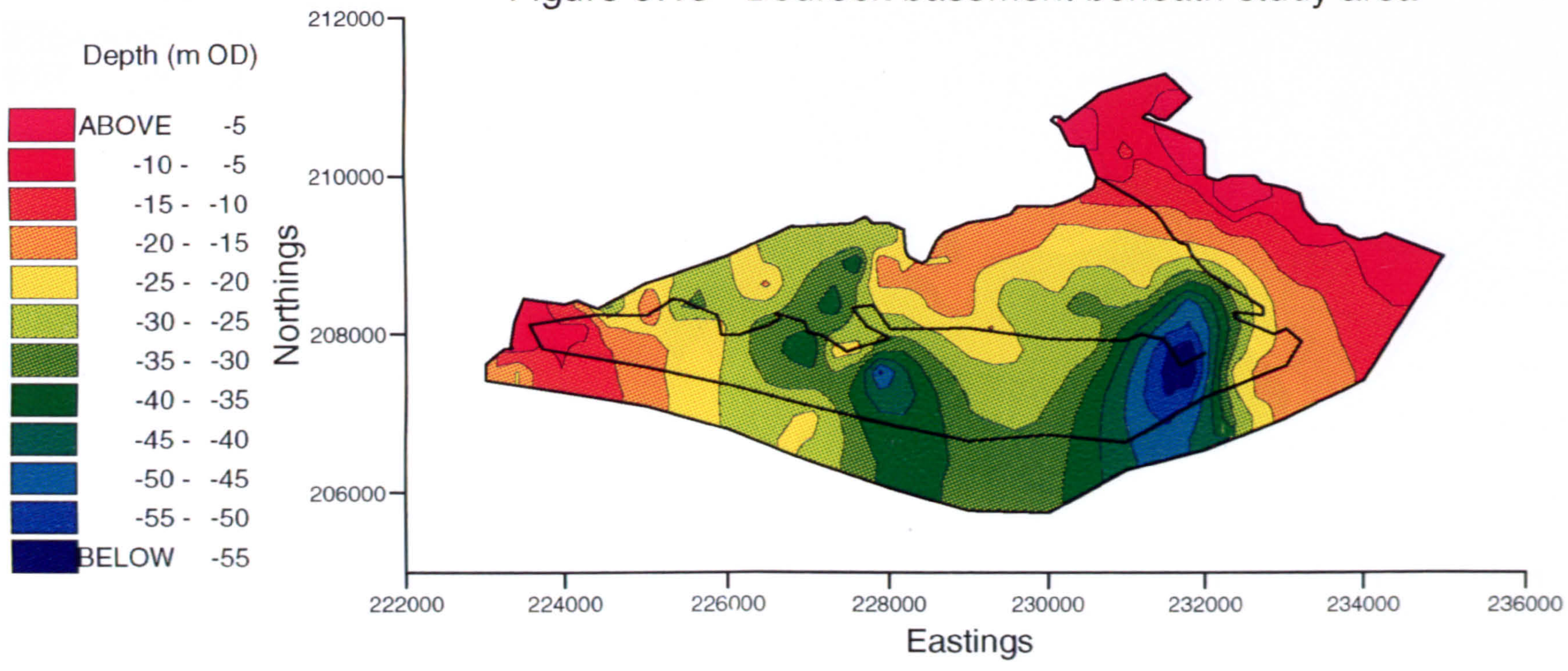

Figure 5.14 Pre-Holocene beneath the study area

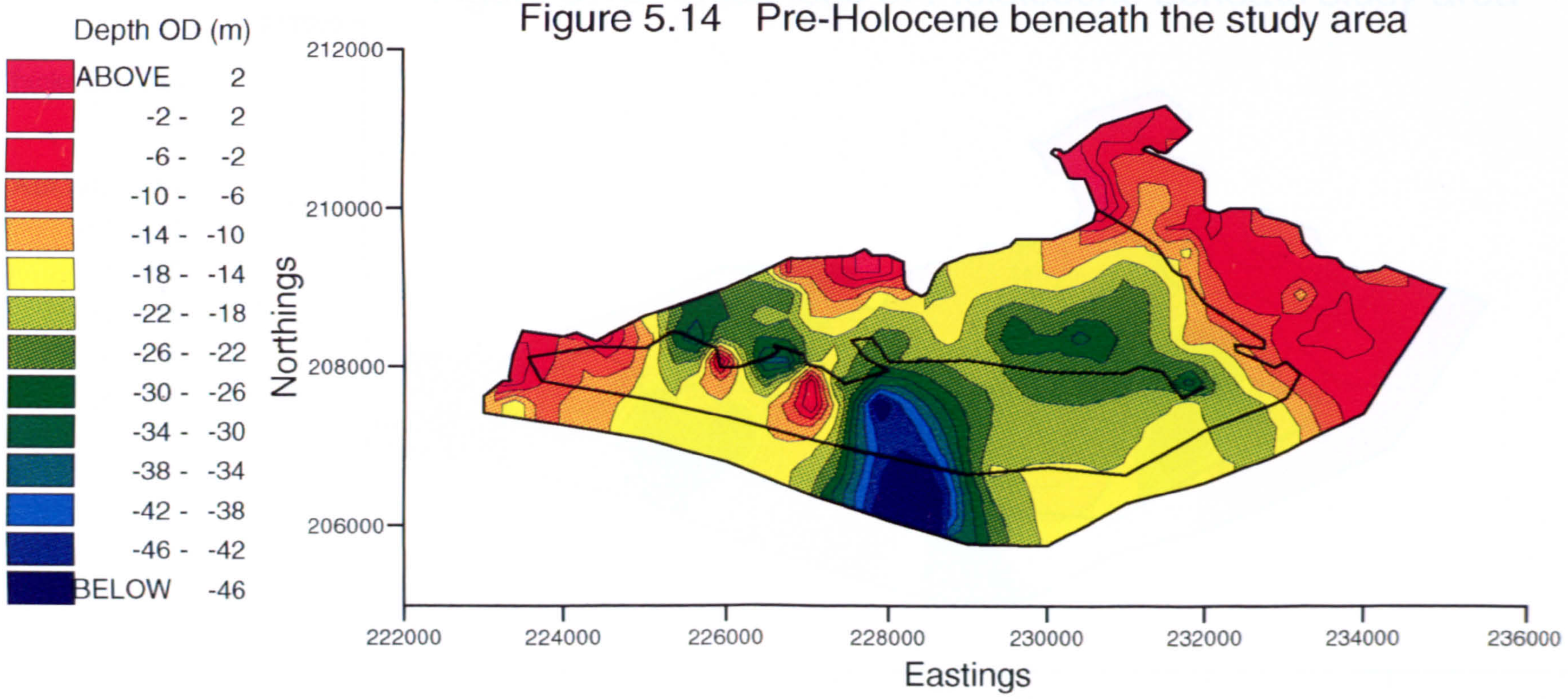

Figure 5.15 Thickness of Pleistocene beneath study area

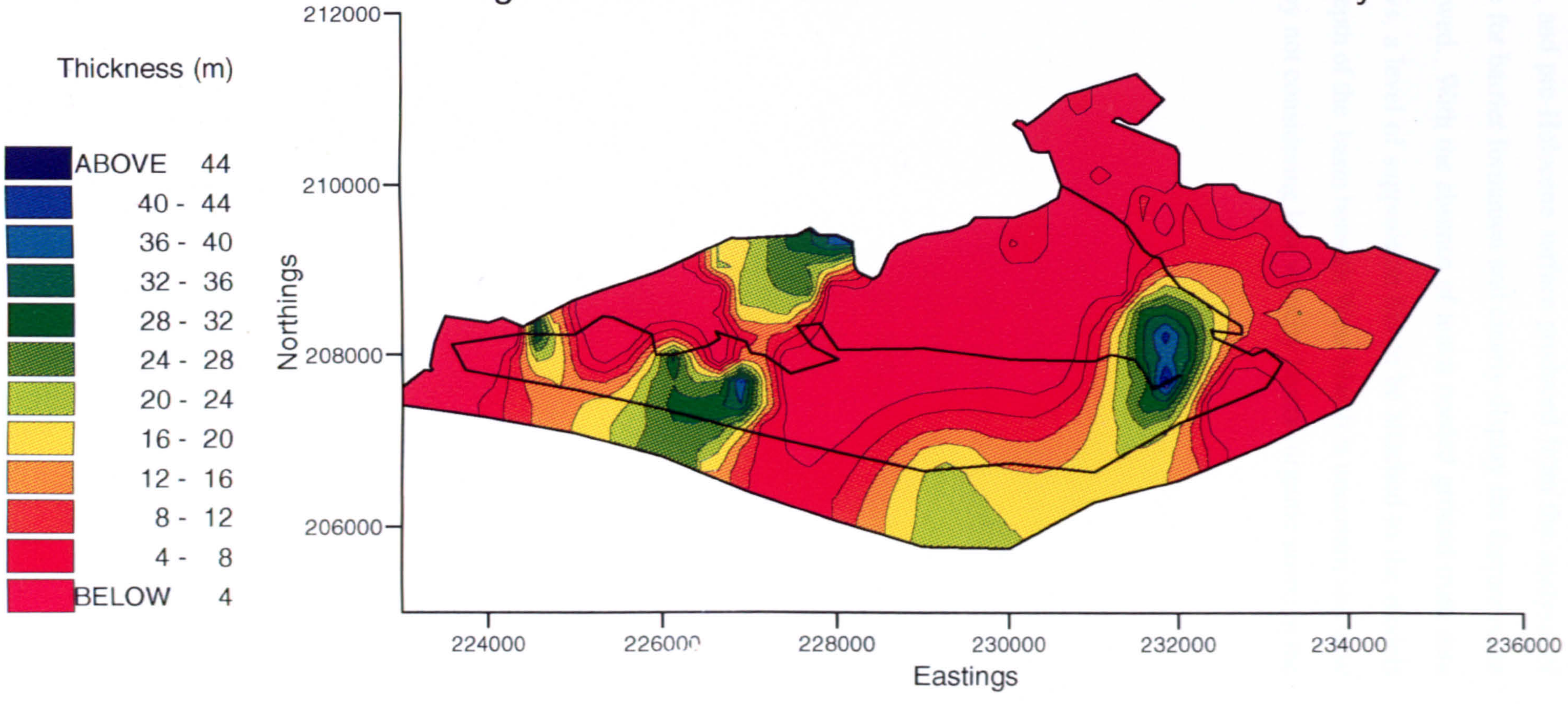

The reconstructions of the bedrock and pre-Holocene surface produced from the analysis of seismic data provide good evidence for barrier formation and clearly display the former route along which the River Taf once flowed. With the absence of much needed ground truth data within West Marsh and the Burrows, a level of supposition has to be attached to the models produced in this study. The actual depth of the basin beneath West Marsh is uncertain and may have been overestimated in places by not considering low velocity layers (organic units) in the analysis of data from this area.

Chapter 6

Palaeoenvironments and Radiocarbon Dating

6.1 Foraminifera

6.1.1 Description of foraminiferal data

Foraminiferal analysis was conducted on sub-samples taken from the sediments recovered at sites 12, 4, 11, 17, 20 and 22 (Figure 6.1). The sampling strategy was designed to examine changes in the foraminiferal compositions both within and between distinct sedimentary facies. The data is presented as percentages of the total number of foraminifera counted at each level and depths are discussed in metres beneath the ground surface; the ecological requirements of the most abundant species are summarised in table 6.1.

Site 12

Foraminifera were identified between 11.30 and 6.34 metres and at 5.10 and 4.80 metres. Samples taken from between 6.34 and 5.10 metres, and above 4.40 metres, contained no foraminiferal tests. On the basis of assemblage composition the foraminifera have been subdivided into three zones:

Zone 12-1: The foraminifera in zone 12-1, which extends from 11.30 to 10.57 metres, are composed of hyaline and porcelaneous tests, dominated by *Haynesina germanica*, *Elphidium williamsoni* and *Quinqueloculina seminulum*. These fine grained clayey silts at the base of the sequence also contain smaller numbers of *Cibicides lobatalus*, *Bolivina robusta*, *Elphidium excavartum*, *Miliolinella subrotunda*, *Rosalina anomala* and *Ammonia batavus*.

Zone 12-2: Extends from 10.57 to 6.57 metres and is defined by decrease in the relative proportion of porcelaneous tests. The sediments in this zone grade from clayey silt into highly stratified sandy silt at 10.15 metres; the latter is overlain by organic-rich silty clay (Figure 6.2).

Order FORAMINIFERIDA		Authority	Mode of life	Substrate	Salinity	Depth
Suborder TEXULARIINA						
	Trochamina inflata	Montagu	epifaunal or infaunal, free	muddy sediment	brackish-hypersaline	interidal marhes
	Jadammina macracens	Brady	epifaunal, free	mud-silt	brackish-hypersaline	interidal marshes
Suborder MILIOLINA						
	Quinqueloculina cliarensis	Heron-Allen & Earland	epifaunal, free or clining	plants or sediment	marine-hypersaline	hypersaline lagoons- marine shelf
	Quinqueloculina seminulum	Linnaeus				
	Quinqueloculina stalkeri	Loeblich & Tappan				
	Quinqueloculina bicornis	Walker & Joacob				
	Miliolinella subrotunda	Montagu	epifaunal, clinging	plants or hard substrates	marine-hypersaline	marine-hypersaline lagoons & marshes
Suborder ROTALIINA						
	Lagena clavata	d' Orbigny	infaunal, free	sand	marine	intertidal-shelf
	Lagena semistriata	Wiliamson				
	Lagena sulcata	Walker & Jacob				
	Fissurina elliptica	Cushman				
	Oolina hexagona	Williamson				
	Oolina squamosa	Montagu				
	Oolina williamsoni	Alcock				
	Bulimina elongata	d'Orbigny	infaunal, free	mud to fine sand	marine	inner shelf-bathyl
	Bulimina gibba	Foransini				
	Bulimina marginata	d'Orbigny				
	Stainforthia fusiformis	Williamson				
	Bolivina pseudoplicata	Heron-Allen & Earland	infaunal-epifaunal, free	muddy sediment	marine	inner shelf-bathyl
	Bolivina robusta	Brady				
	Rosalina anomala	Terquem	epifaunal, clinging or attached	hard substrates	marine	lagoons-inner shelf
	Asterigirata mamillia	Williamson	epifaunal, free	sediment	marine	inner shelf (0-100m)
	Cibicides lobatalus	Walker & Jacob	epifaunal, attached	hard substrates	marine	lagoons, shelf-bathyl
	Planorbulina distoma	Terquem	epifaunal, attached	hard substrates	marine	inner shelf
	Hayensina germanica	Ehrenburg	infaunal, free	mud-silt	brackish-marine	interidal
	Nonion labradoricum	Dawson	infaunal, free	mud-silt	marine	shelf
	Nonionella miocenica	Cushman	infaunal, free	mud	marine	shelf
	Ammonia becarii var. batavus	Hofker	infaunal, free	muddy sand	brackish, marine, hypersaline	brackish-hypersaline lagoons, inner shelf
	Ammonia batavus	Hofker				
	Elphidium crispum	Linne'	keeled: epifaunal, free	sand, vegitation	marine-hypersaline	inner shelf
	Elphidium ertandi	Cushman	non-keeled: infaunal,free	mud-sand	brackish-hypersaline	brackish-hypersaline marshes & lagoons, inner shelf
	Elphidium excavatum	Terquem				
	Elphidium incertum	Williamson				
	Elphidium gerthi	Van Voorthuysen				
	Ephidium macellum	Fichtel & Moll				
	Elphidium margaritaceum	Cushman				
	Elphidium williamsoni	Haynes				
	Globoqudrina hexagona	Natland				

Table 6.1 Authorities and ecological requirements for the foraminifera identified in the back barrier complex sediments

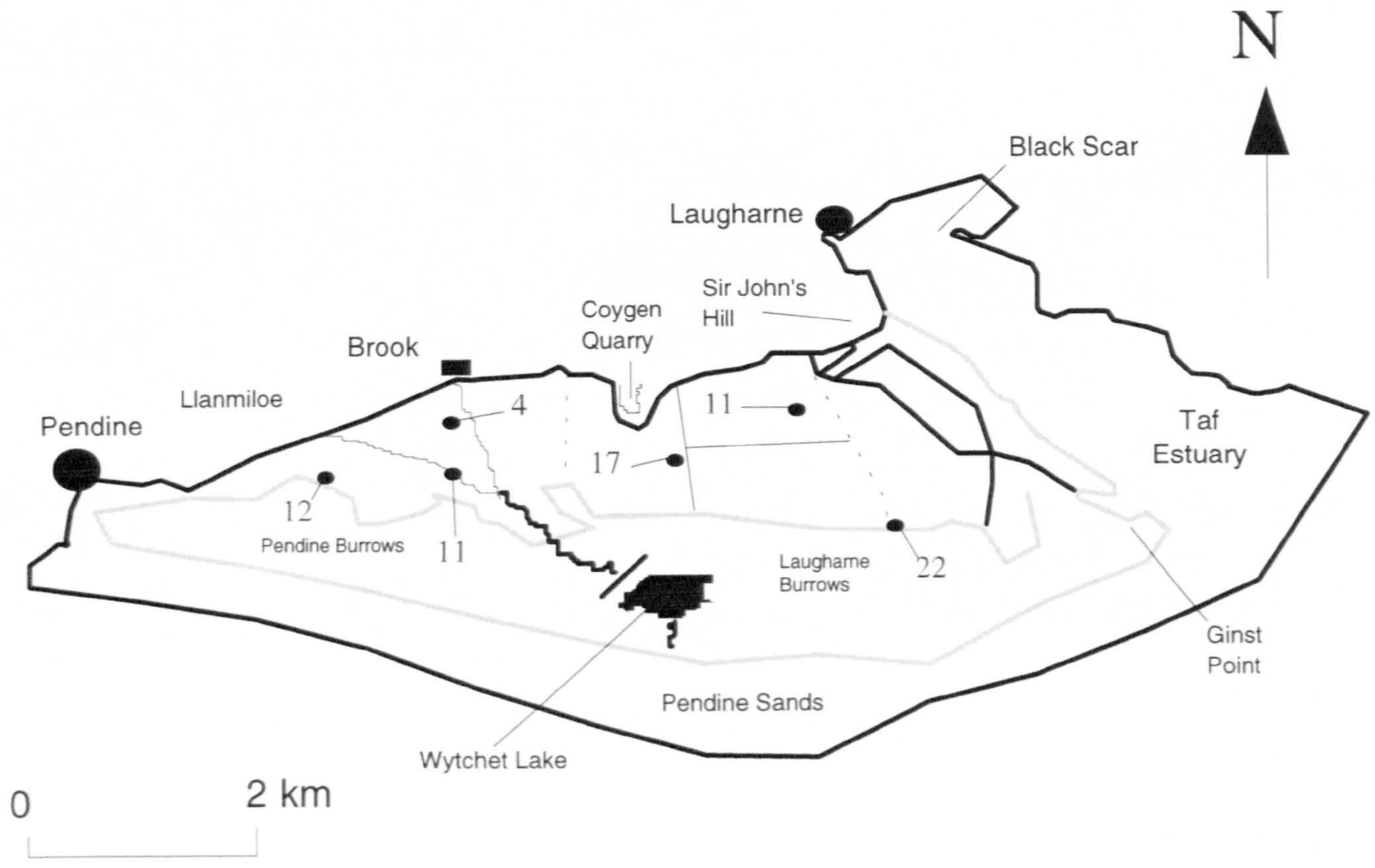

Figure 6.1 Location of sites 12, 4, 11, 17, 20 and 22

Figure 6.2 Foraminiferal diagram for site 12.

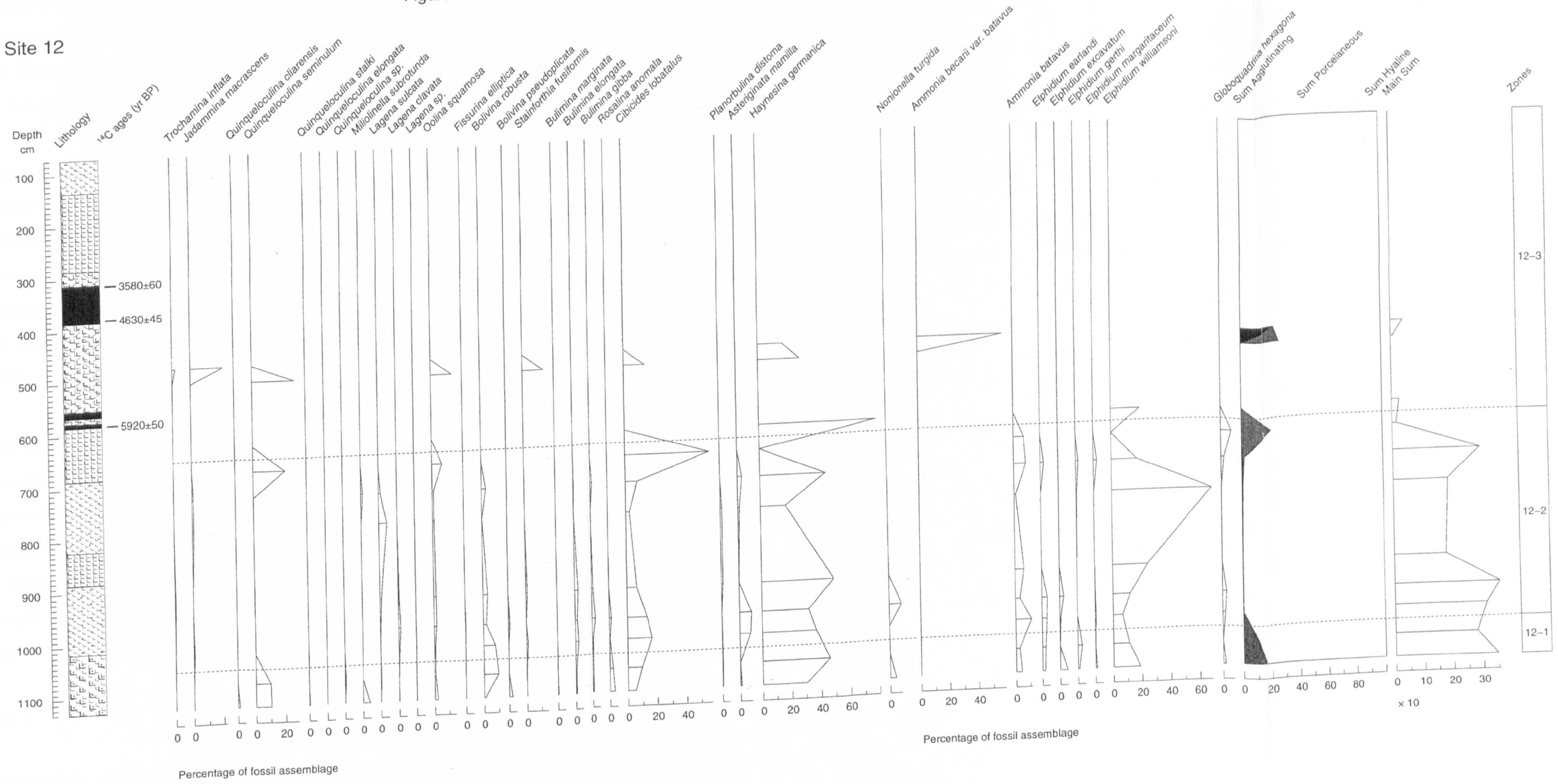

The Foraminifera at the base of zone 12-2 are dominated by *Haynesina germanica, Cibicides lobatalus, Elphidium williamsoni, Asteriginata mamilla, Nonionella turgida* and *Ammonia batavus* (Figure 6.2). Between 9.43 and 7.88 metres the relative proportion of *Elphidium williamsoni* increases sharply from 24% to 69%; this corresponds to a similar decrease in the frequency of *Haynesina germanica.* From 7.88 to 7.30 metres the relative proportion of *Elphidium williamsoni, Lagena sulcata* and *Planorbulina distoma* decreases. This corresponds to an increase in *Haynesina germanica, Ammonia batavus, Cibicides lobatalus, Bolivina robusta* and *Asteriginata mamilla* (Figure 6.2).

As the sediment fines upwards into organic-rich silty clay at 6.85 metres there is a corresponding increase in *Cibicides lobatalus, Quinqueloculina seminulum, Oolina squamosa* and *Globoquadrina hexagona;* this coincides with a thin bed of silty sand at the base of the silty clay facies. This sandy bed also contains relatively few *Haynesina germanica* or *Elphidium williamsoni* tests (Figure 6.2). The foraminiferal assemblage preserved within the silty clay at 6.34 metres is composed entirely of *Haynesina germanica* (80%) and *Elphidium williamsoni* (20%).

Zone 12-3: Although the organic-rich silty clay between 4.55 and 3.32 metres contains very few foraminifera, sub-samples from 5.10 and 4.80 metres depth contained seven and 41 tests respectively. The foraminifera at 5.10 metres are dominated by *Quinqueloculina seminulum, Haynesina germanica, Oolina squamosa* and *Cibicides lobatalus.* Between 5.10 and 4.80 metres the relative proportion of *Ammonia becarii var. batavus* and *Jadammina macrescens* increases sharply to 59% and 22% respectively. This level also contains *Haynesina germanica* and *Trochammina inflata* (Figure 6.2).

Site 4

Foraminifera were identified between 8.19 and 2.15 metres and on the basis of assemblage composition the foraminifera at site 4 have been sub-divided into three zones.

Zone 4-1: Extends from 8.19 to 4.69 metres and is dominated by agglutinating and hyaline tests. The lithology consists of an organic-rich silty clay facies intercalated with a organic detritus.

KEY

Silty Clay

Sandy Silty Clay

Silty Clay containing organic detritus

Sandy Silt

Silty Sand

Organic Detritus

Sand

Figure 6.3 Foraminiferal diagram for site 4.

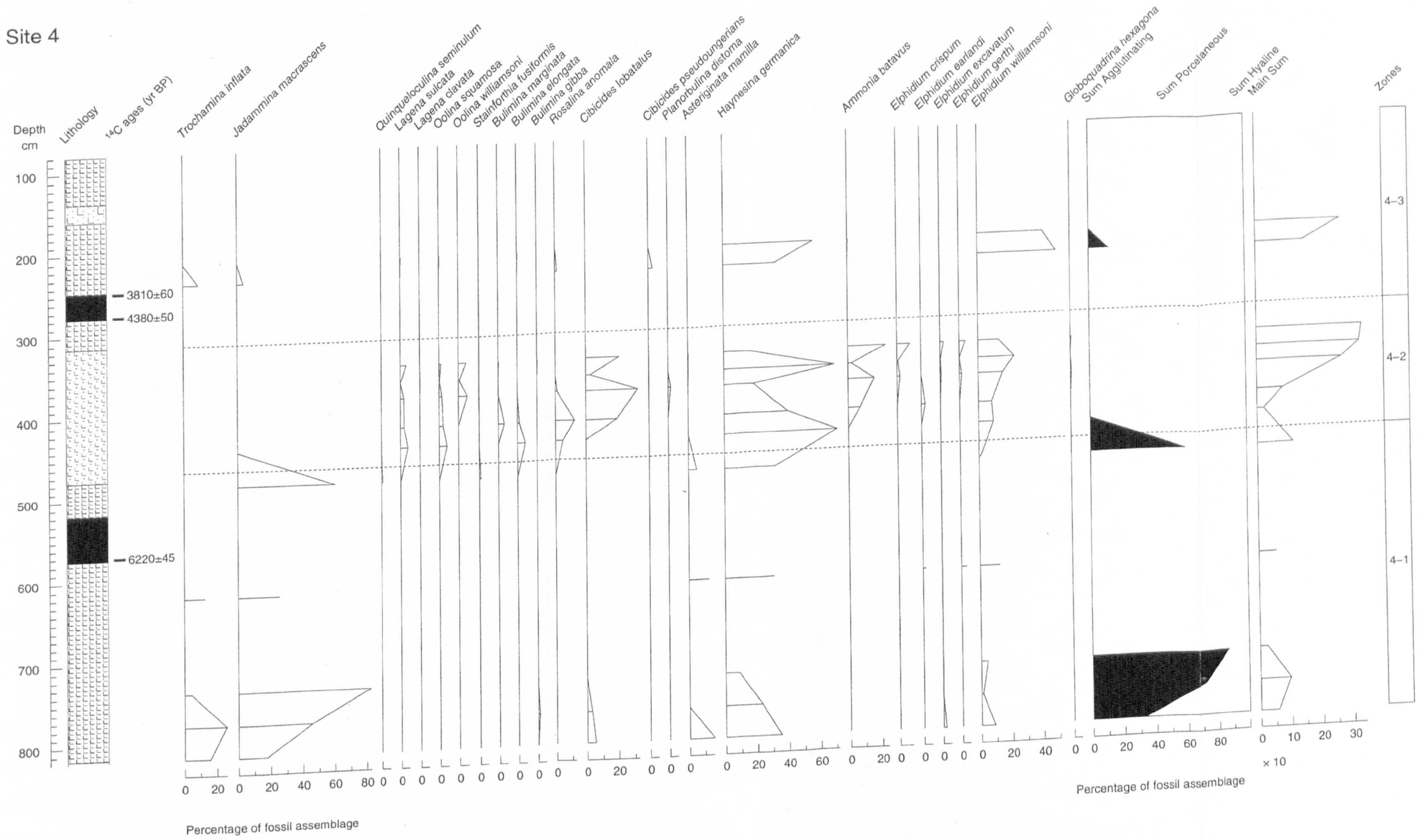

Highly stratified silty clay at the base of zone 4-1 contains a foraminiferal assemblage dominated by *Haynesina germanica, Jadammina macrescens, Trochammina inflata* and *Asteriginata mamilla.* These clays also contain fewer numbers of *Elphidium williamsoni* and *Cibicides lobatalus.* Between 8.19 and 7.40 metres the relative proportion of *Jadammina macrescens* increases sharply to 83%; this corresponds to an initial increase in the frequency of *Trochammina inflata* and to a decrease in *Haynesina germanica, Elphidium williamsoni, Cibicides lobatalus* and *Asteriginata mamilla* (Figure 6.3). No foraminifera are preserved in the highly stratified silty clay between 7.40 and 6.24 metres depth.

The clay at 6.24 metres depth contains fewer *Jadammina macrescens* and a greater proportion of *Haynesina germanica, Trochammina inflata, Asteriginata mamilla* and *Elphidium williamsoni* tests. The silty clay, organic detritus and organic-rich silty clay between 6.24 and 4.88 metres depth contains no foraminiferal tests (Figure 6.3).

At 4.88 metres the foraminifera are dominated by *Jadammina macrescens* and *Haynesina germanica* which account for 60% and 32% of the assemblage respectively. These sediments also contain small numbers of *Asteriginata mamilla, Elphidium williamsoni* and *Quinqueloculina seminulum* (Figure 6.3). As the sediments grade from silty clay into silty sand at 4.78 metres the relative proportion of *Jadammina macrescens* decreases sharply. This marks the upper boundary of zone 4-1.

Zone 4-2: Extends from 4.69 to 3.15 metres and is dominated by hyaline tests. The sediments are composed predominantly of stratified silty sand.

At 4.46 metres 4-2 *Haynesina germanica* increases sharply from 32% to 72%. These sands also contain *Elphidium williamsoni, Lagena sulcata, Oolina squamosa, Bulimina elongata* and *Rosalina anomala* (Figure 6.3). Between 4.46 and 3.87 metres *Haynesina germanica* decreases sharply to 19%; this corresponds to an increase in the frequency of *Cibicides lobatalus, Ammonia batavus* and *Elphidium williamsoni.* The silty sand between 4.46 and 3.87 metres also contains fewer *Rosalina anomala, Lagena sulcata, Oolina squamosa, Oolina williamsoni, Bulimina marginata, Bulimina elongata, Planorbulina distoma, Elphidium crispum, Elphidium earlandi, Elphidium excavartum, Elphidium gerthi* and *Globoquadrina hexagona* test (Figure 6.3).

KEY

- Silty Clay
- Sandy Silty Clay
- Silty Clay containing organic detritus
- Sandy Silt
- Silty Sand
- Organic Detritus
- Sand

The sharp increase in *Haynesina germanica* between 3.87 and 3.68 metres corresponds to a decrease in *Cibicides lobatalus*, *Ammonia batavus*, *Lagena sulcata*, *Oolina squamosa* and *Oolina williamsoni* (Figure 6.3). Above this *Haynesina germanica* and *Elphidium williamsoni* decrease sharply; this coincides with an increase in the frequency of *Ammonia batavus*, *Cibicides lobatalus* and *Elphidium crispum*. No foraminiferal tests are contained in the silty sand, silty clay and organic detritus between 3.47 and 2.40 metres depth (Figure 6.3).

Zone 4-3: Extends above 3.15 metres. The sediments are composed organic-rich silty clay facies intercalated with organic detritus. The organic rich silty clay at 2.40 metres contains a fossil assemblage dominated by *Elphidium williamsoni*, *Haynesina germanica*, *Trochammina inflata* and *Jadammina macrescens*. Between 2.40 and 2.15 metres the relative proportion of *Haynesina germanica* increases to 56.7%; this corresponds to a reduction in the numbers of *Elphidium williamsoni*, *Trochammina inflata* and *Jadammina macrescens* (Figure 6.3).

Although the foraminifera are relatively well preserved between 2.40 and 2.15 metres no tests are contained in the silty clays or sandy silts above these levels (Figure 6.3).

Site 11

Foraminifera were identified in the sediments between 10.88 an 0.31 metres at site 11 and on the basis of fossil assemblage composition have been subdivided into four zones.

Zone 11-1: Extends from 10.88 to 8.19 metres and the foraminifera are dominated by agglutinating and hyaline species. The sediments in zone 11-1 fine upwards from silty sand into organic-rich silty clay and then grade into highly stratified silty sand (Figure 6.4).

As the sediments fine upwards into silty clay at the base of zone 11-1 the relative proportion of *Haynesina germanica* increases sharply from 28% at 10.88 metres to 87% at 10.70 metres. This corresponds to a decrease in the relative proportion of *Elphidium williamsoni* and *Cibicides lobatalus*. These sediments also contains trace amounts of *Asteriginata mamilla, Rosalina anomala, Nonionella turgida*, and *Ammonia becarii* var. *batavus* (Figure 6.4).

KEY

- Silty Clay
- Sandy Silty Clay
- Silty Clay containing organic detritus
- Sandy Silt
- Silty Sand
- Organic Detritus
- Sand

Figure 6.4 Foraminiferal diagram for site 11.

Site 11

Depth cm

Lithology

Trochamina inflata
Jadammina macrascens
Spiroloculina sp.
Quinqueloculina cliarensis
Quinqueloculina seminulum
Quinqueloculina bicornis
Quinqueloculina elongata
Quinqueloculina sp.
Miliolinella subrotunda
Lagena sulcata
Lagena clavata
Lagena semistriata
Lagena sp.
Oolina squamosa
Oolina williamsoni
Oolina hexagona
Fissurina elliptica
Bolivina pseudoplicata
Buliimina marginata
Buliimina elongata
Buliimina gibba
Uvigerina peregrina
Rosalina anomala
Cibicides lobatalus
Cibicides pseudoungerians
Planorbulina distorna
Asterigininata mamilla
Haynesina germanica
Nonion labradoricum
Nonionella turgida
Astronoion
Ammonia becarii var. batavus
Ammonia batavus
Elphidium crispum
Elphidium earlandi
Elphidium excavatum
Elphidium gerthi
Elphidium incertum
Elphidium macellum
Elphidium margaritaceum
Elphidium williamsoni
Globoquadrina hexagona
Neogloboquadrina pachyderma
Gavelinopsis praegeri
Lamarckina haliotidea
Sum Agglutinated
Sum Porcelaneous
Sum Hyaline
Main Sum

Zones: 11–5, 11–4, 11–3, 11–2, 11–1

Percentage of fossil assemblage

× 10

Towards the top of the clay unit *Jadammina macrescens* increases sharply from 2% to 64%; this corresponds to a reduction in the relative proportion of *Haynesina germanica.* The deposits at 9.72 metres also contain a small amount of *Trochammina inflata* and *Cibicides lobatalus* (Figure 6.4).

Associated with the coarsening upwards of the sequence towards the top of zone 11-1 is an increase relative proportion of *Elphidium williamsoni* which amounts to 34% of the assemblage at 8.68 metres. This corresponds to a decrease in the frequency of *Jadammina macrescens* and *Trochammina inflata* and to a slight increase in the number of porcelaneous and *Haynesina germanica* tests (Figure 6.4).

Zone 11-2: Extends from 8.19 to 5.60 metres. The sediments grade from highly stratified silty sand into sandy silt at 6.62 metres. The foraminifera exhibit little variation and are dominated by *Cibicides lobatalus, Quinqueloculina seminulum* and *Haynesina germanica.* These sediments also contain small numbers of *Ammonia batavus, Ammonia becarii* var. *batavus, Miliolinella subrotunda, Planorbulina distoma, Elphidium crispum* and *Elphidium williamsoni* (Figure 6.4).

Zone 11-3: Extends from 5.60 to 4.66 metres and corresponds to a sharp increase in the relative proportion of *Haynesina germanica*, from 10% at 5.72 metres to 78% at 5.48 metres. These silts and clays also contain a greater number of *Elphidium williamsoni* and fewer *Cibicides lobatalus* and *Quinqueloculina seminulum* tests (Figure 6.4).

Zone 11-4: The sediments in zone 11-4, which extends from 4.66 to 1.49 metres, are composed mainly of highly stratified sand which contains reworked shell fragments. The boundary between zones 11-3 and 11-4 corresponds to a sharp decrease in the relative proportion of *Haynesina germanica* which is associated with an abrupt contact between clayey silt and the overlying sand.

The foraminiferal assemblages within this zone are composed predominately of hyaline and porcelaneous tests which are dominated by *Cibicides lobatalus, Quinqueloculina seminulum, Ammonia batavus* and *Asteriginata mamilla.* The increase in *Ammonia batavus, Quinqueloculina seminulum* and *Elphidium williamsoni* at 2.60 metres corresponds to a thin bed of silty clay within the shelly sand facies.

Zone 11-5: Extends from 1.49 to 0.31 metres and is defined by a sharp decrease in the relative proportion of porcelaneous tests *i.e. Quinqueloculina seminulum.* The lower boundary of zone 11-5 also corresponds to a slight increase in *Haynesina germanica* and is associated with a gradual fining upwards of the sequence from sand into sandy silt.

The foraminifera in zone 11-5 are dominated by *Cibicides lobatalus, Ammonia batavus* and *Elphidium williamsoni.* The sharp increase in *Elphidium williamsoni* at 0.91 metres corresponds to a thin silty clay bed within the sandy silt facies. Although the tests are more poorly preserved in the near-surface oxidised sediment, analysis of these deposits indicates a sharp increase in the relative proportion of *Ammonia batavus* at the top of zone 11-5.

Site 17

Foraminifera were identified between 5.89 and 1.84 metres and have been sub-divided into two zones. No forams were identified in the sediments above 1.84 metres (Figure 6.5).

Zone 17-1: Extends from 5.89 to 2.53 metres and is dominated by hyaline and porcelaneous tests. The sediments at the base of zone 17-1 fine upwards from shelly sand into stratified silty clay which then grades sharply into fine sand. The sediments then fine upwards into sandy silt and then into silty clay.

The foraminifera in the shelly sand at the base of zone 17-1 are dominated by *Cibicides lobatalus* and contain fewer numbers of *Elphidium williamsoni, Planorbulina distoma, Haynesina germanica, Miliolinella subrotunda* and *Quinqueloculina seminulum* (Figure 6.5). These sands also contain trace amounts of *Asteriginata mamilla, Ammonia becarii* var. *batavus, Oolina williamsoni, Elphidium margaritaceum* and *Elphidium macellum.* Between 4.97 and 4.84 metres *Miliolinella subrotunda* and *Lagena sulcata* increase; this corresponds to a decrease in *Cibicides lobatalus, Asteriginata mamilla* and *Quinqueloculina seminulum* (Figure 6.5). The change in the foraminiferal composition coincides with a clay bed within the highly stratified silty clay facies.

The composition of foraminifera assemblages varies only slightly as the sediments grade from sandy silt into silty clay at the top of zone 17-1. The assemblage is dominated by *Cibicides*

KEY

Silty Clay

Sandy Silty Clay

Silty Clay containing organic detritus

Sandy Silt

Silty Sand

Organic Detritus

Sand

Figure 6.5 Foraminiferal diagram for site 17

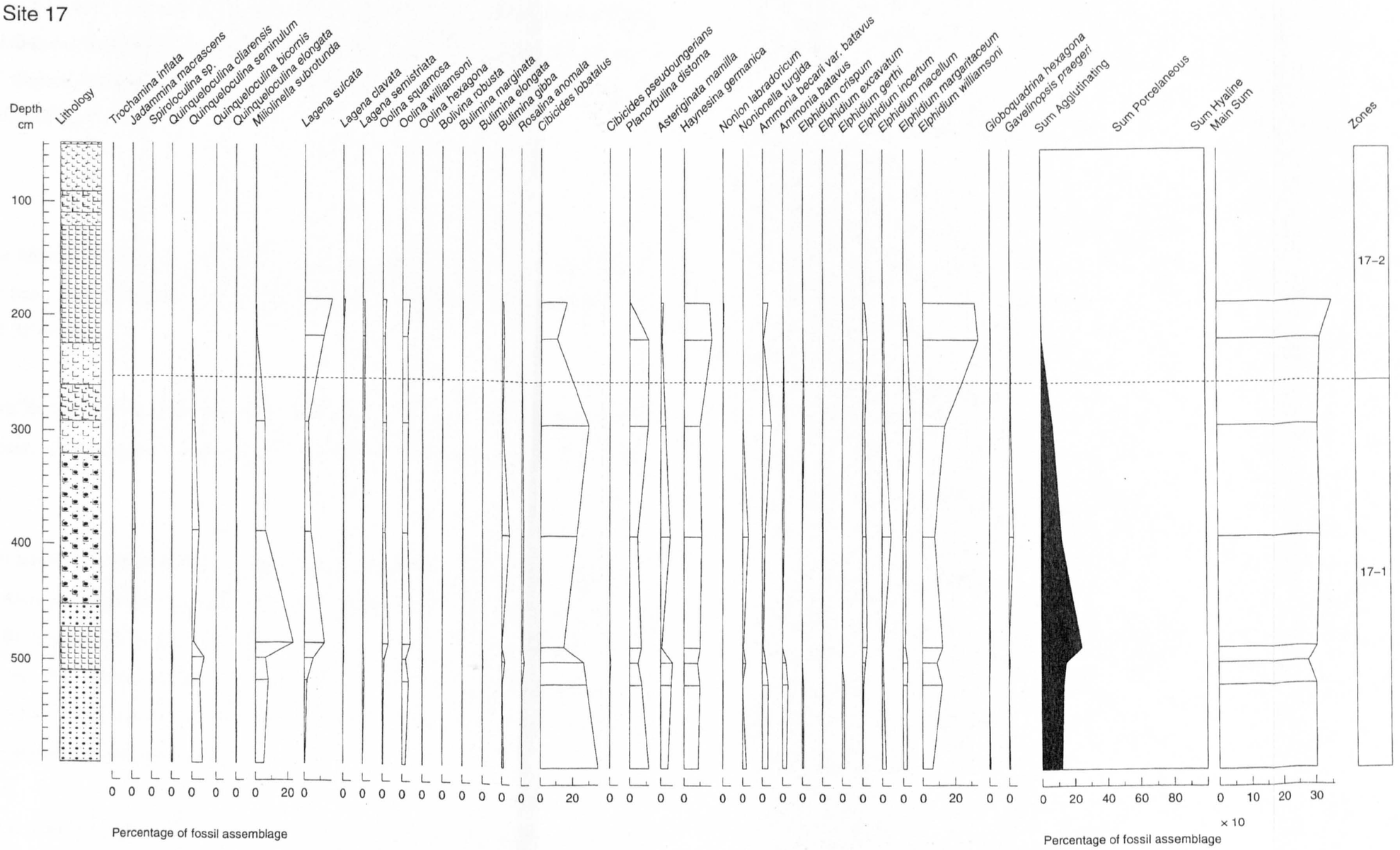

lobatalus, Elphidium williamsoni, Planorbulina distoma, Haynesina germanica, Milionella subrotunda and *Quinqueloculina seminulum* (Figure 6.5).

Zone 17-2: Extends upwards from 2.53 metres and is defined by a sharp decrease in *Cibicides lobatalus*. The sediments are composed stratified silty clay (Figure 6.5).

The foraminifera at 2.16 and 1.84 metres are dominated by *Elphidium williamsoni* and also contain *Cibicides lobatalus, Lagena sulcata* and *Haynesina germanica.* These levels also contain trace amounts of *Oolina williamsoni, Elphidium incertum, Elphidium margaritaceum* and *Asteriginata mamilla* (Figure 6.5).

Site 20

Foraminifera were identified between 5.19 and 1.35 metres and on the basis of assemblage composition have been sub-divided into three zones. No foraminifera were identified in the sediments above 1.35 metres.

Zone 20-1: Extends form 5.19 to 4.18 metres. The sediments fine upwards from highly stratified sandy silt at the base of the sequence into a series of stratified silty clay and clayey silt beds (Figure 6.6).

The foraminifera in zone 20-1 are dominated by *Haynesina germanica* and *Cibicides lobatalus,* and contain fewer *Ammonia batavus, Elphidium gerthi, Elphidium williamsoni* and *Asteriginata mamilla* (Figure 6.6). The relative proportion of *Haynesina germanica* increases sharply between 5.19 and 4.85 metres; this corresponds to a decrease in *Cibicides lobatalus, Quinqueloculina seminulum, Ammonia batavus* and *Miliolinella subrotunda* and coincides with the boundary between silty sand and sandy silt (Figure 6.6).

Zone 20-2: Extends from 4.18 to 2.94 metres and is marked by a sharp decrease in *Haynesina germanica.* The sediments are composed of predominantly of shelly sand which is intercalated with a thin layer of dark grey silty clay.

KEY

Silty Clay

Sandy Silty Clay

Silty Clay containing organic detritus

Sandy Silt

Silty Sand

Organic Detritus

Sand

Figure 6.6 Foraminiferal diagram for site 20

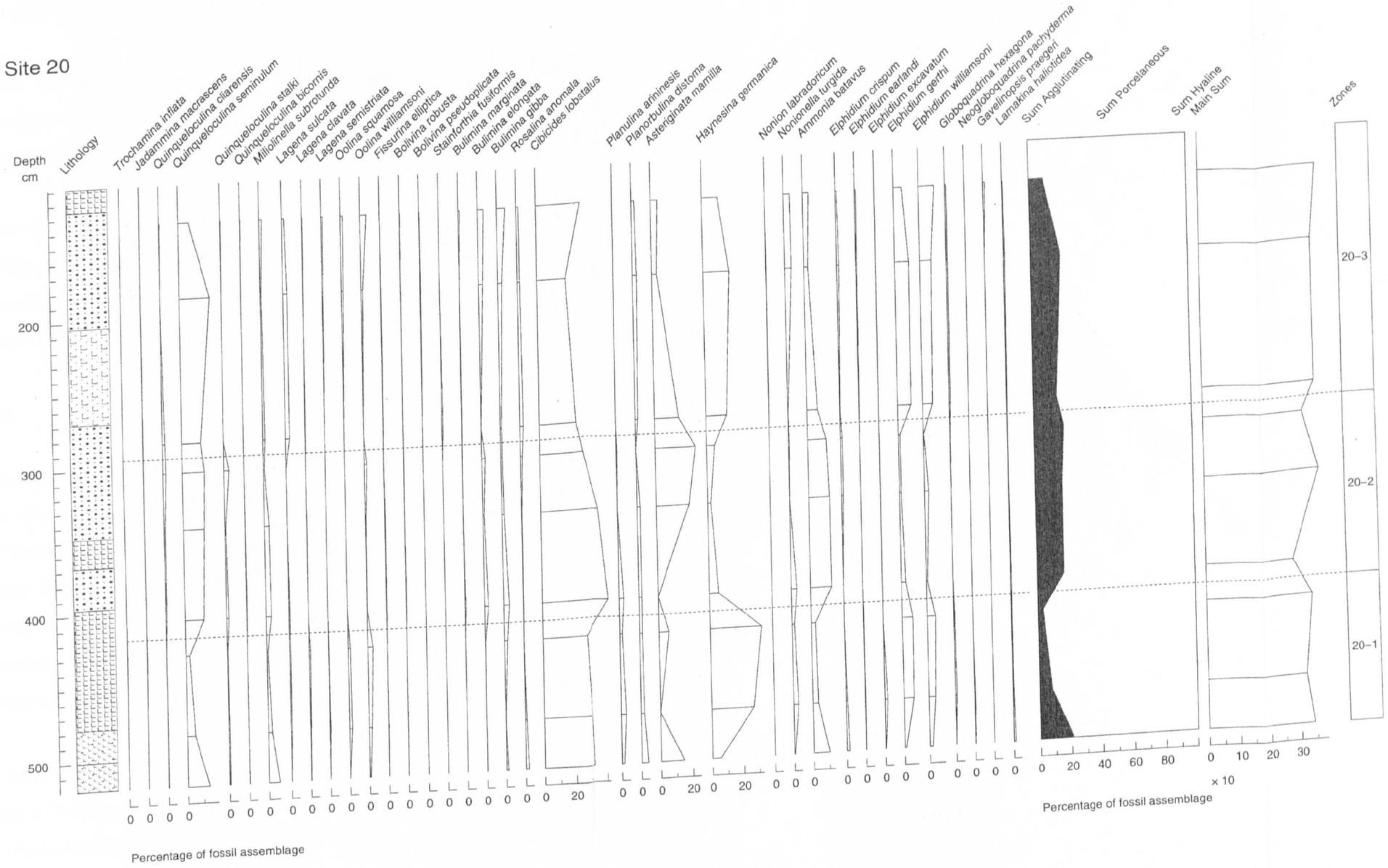

The foraminifera are dominated by *Cibicides lobatalus* and contain fewer *Quinqueloculina seminulum, Asteriginata mamilla* and *Ammonia batavus* (Figure 6.6). The relative increase in the proportion of *Asteriginata mamilla* between 4.06 and 3.44 metres corresponds to a decrease in *Cibicides lobatalus.* The relative proportion *Quinqueloculina seminulum* and *Ammonia batavus* remain relatively constant throughout zone 20-2.

Zone 20-3: Extends from 2.94 to 1.35 metres and is defined by a decrease in *Cibicides lobatalus, Asteriginata mamilla* and *Ammonia batavus.* The sediments in zone 20-3 grade from shelly sand into silty sand and then into silty clay; the latter is overlain by shelly sand (Figure 6.6).

The base of zone 20-3 exhibits an increase in the relative proportion of *Haynesina germanica, Elphidium gerthi* and *Elphidium williamsoni.* All the levels in zone 20-3 contain foraminifera dominated by *Cibicides lobatalus, Haynesina germanica, Quinqueloculina seminulum, Elphidium gerthi* and *Elphidium williamsoni* (Figure 6.6).

Site 22

Foraminifera were identified between 5.22 and 0.73 metres. No foraminifera were contained in the silty clay between 2.83 and 1.03 metres (Figure 6.7). The sediments fine upwards from shelly sand at the base of the sequence into silty clay which is overlain by a layer of shelly sand. The boundary between the two latter facies is marked by an abrupt erosional contact. The foraminifera identified at site 22 are dominated by *Cibicides lobatalus, Ammonia batavus* and *Quinqueloculina seminulum.* These sediments also contain small amounts of *Miliolinella subrotunda, Asteriginata mamilla, Elphidium crispum* and *Elphidium williamsoni.*

The relative proportion of *Ammonia batavus* and *Quinqueloculina seminulum* increase between 5.22 and 3.79 metres; this corresponds a decrease in *Cibicides lobatalus, Miliolinella subrotunda* and *Elphidium williamsoni.* The silty clay at 1.03 metres contains and assemblage dominated by *Ammonia batavus* and *Cibicides lobatalus* and contains *Jadammina macrescens.* As the sediments grade abruptly into shelly sand there is a corresponding sharp decrease in *Jadammina macrescens* and *Ammonia batavus*; this coincides with an increase in *Cibicides lobatalus* and

KEY

Silty Clay

Sandy Silty Clay

Silty Clay containing organic detritus

Sandy Silt

Silty Sand

Organic Detritus

Sand

Figure 6.7 Foraminiferal diagram for site 22

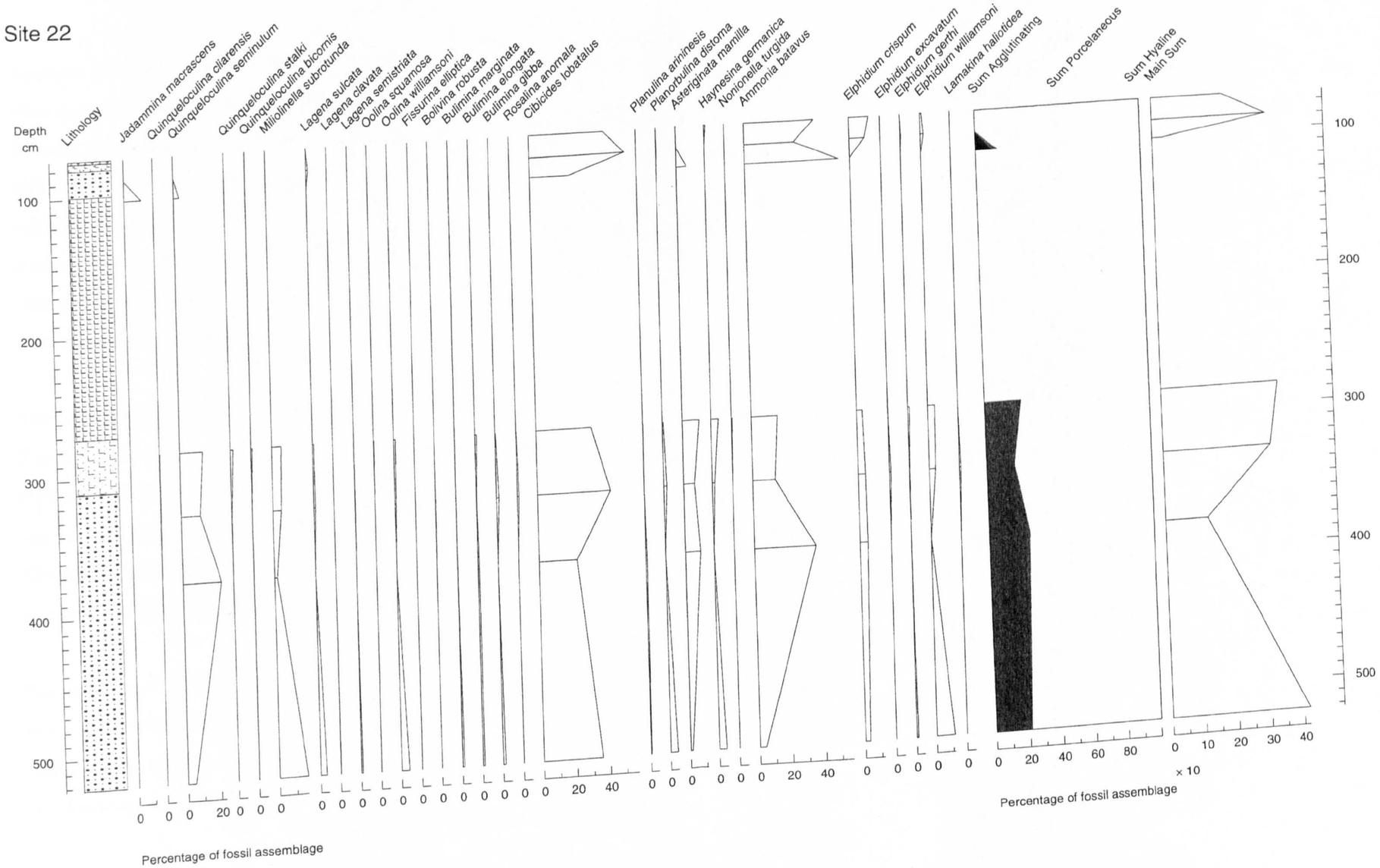

Elphidium crispum (Figure 6.7). The sandy silt at 0.73 metres contains a greater proportion of *Ammonia batavus* than the underlying shelly sand.

6.1.2 Modern foraminiferal associations in the Taf Estuary

Analysis of modern foraminifera, contained in sub-samples taken from the Taf Estuary, shows clear zonation across Delacorse Marsh (Figure 6.8). Sediments recovered from the marsh creeks, the mud flats adjacent to the main channel and sand flats in the main channel also exhibit distinct differences in foraminiferal composition. Delacorse marsh can be sub-divided into high marsh, mid marsh and low marsh, each possessing a characteristic foraminiferal association. The analysis was conducted during 9/94 and 9/95 by the final year Geological Oceanography and Ocean Science class at the School of Ocean Sciences; the modern data used in this study are summarised in appendix 6.1.

The high marsh sediments are dominated by *Jadammina macrescens* and commonly contain *Trochammina inflata*. The relative proportion of *Jadammina macrescens* varies from 50% to 80% whereas *Trochammina inflata* ranges from 14% to 36% of the total assemblage. Additional species occurring in the high marsh include *Quinqueloculina seminulum, Haynesina germanica, Elphidium williamsoni, Miliammina fusca* and *Ammonia batavus*; these species generally occur as a small or trace proportion of the total assemblage.

The mid marsh association is dominated by both *Trochammina inflata* and *Jadammina macrescens* which amount to 57% to 68% and 34% to 56% of the total assemblage respectively. Additional species include *Quinqueloculina seminulum, Elphidium williamsoni, Haplophragmoides wilberti* and *Miliammina fusca.*

The low marsh is dominated by *Trochammina inflata, Jadammina macrescens* and *Elphidium williamsoni*; the relative proportion of these three species varies between 16% to 45%, 19% to 27% and 17% to 50% of the total assemblage respectively. The low marsh sediments also contain *Haynesina germanica, Lagena sulcata, Cibicides lobatalus, Haplophragmoides wilberti* and *Ammonia batavus.*

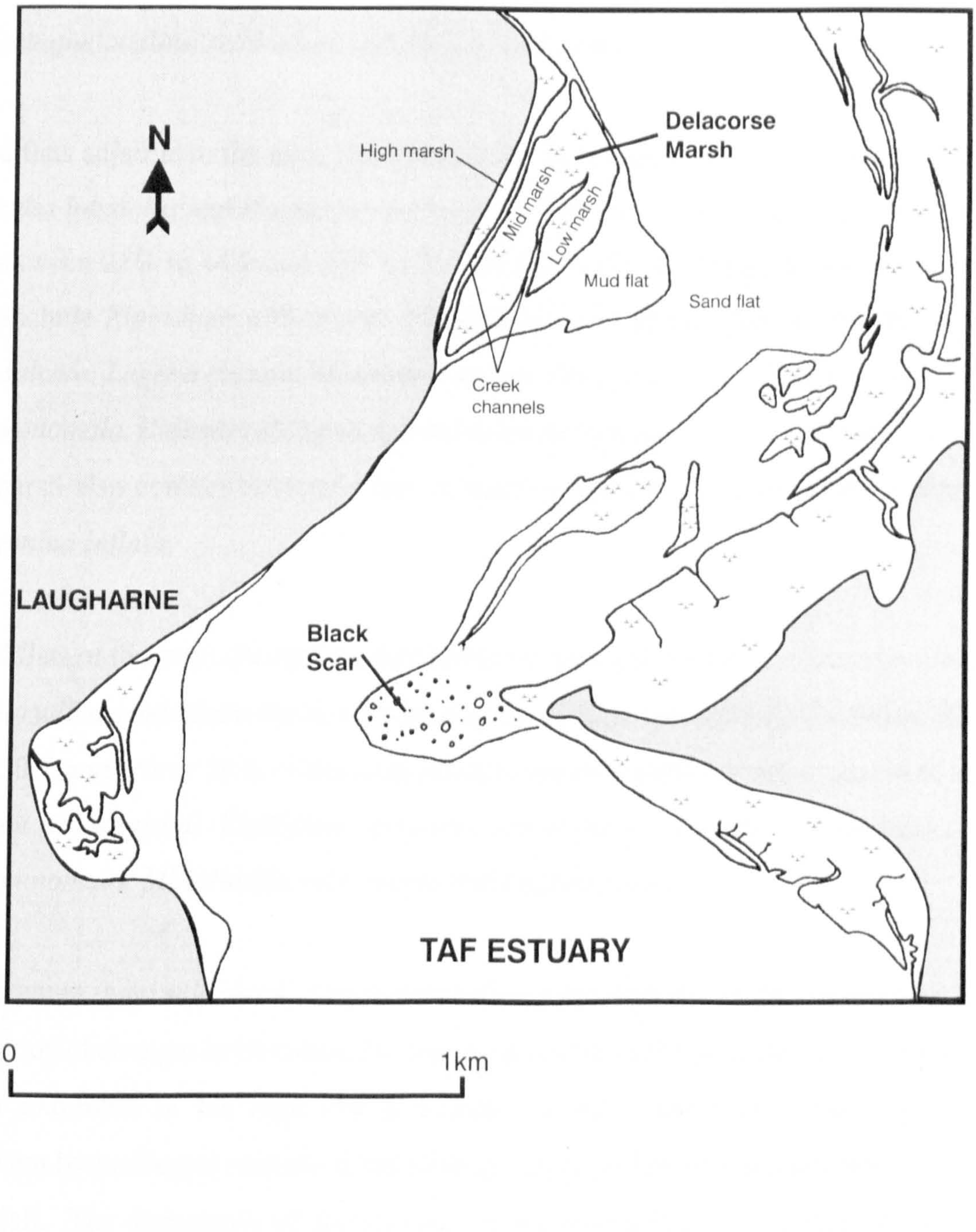

Figure 6.8 Location of Delecorse Marsh

The total populations within the creeks are dominated by *Haynesina germanica* and contain a relative high proportion of *Elphidium williamsoni, Jadammina macrescens* and *Trochammina inflata.* Additional species include *Cibicides lobatalus, Planorbulina distoma, Rosalina anomala, Bulimina elongata, Ammonia batavus, Elphidium excarvartum, Elphidium crispum, Miliammina fusca, Quinqueloculina seminulum* and *Miliolinella subrotunda.*

The mud flats adjacent to the main channel contain an extremely diverse assemblage dominated by *Cibicides lobatalus* and *Haynesina germanica.* The relative proportion of these two species varies between 21% to 44% and 10% to 33% of the total assemblage respectively. Additional species include *Elphidium williamsoni, Miliolinella subrotunda, Quinqueloculina seminulum, Lagena sulcata, Lagena clavata, Ammonia batavus, Oolina williamsoni, Planorbulina distoma, Rosalina anomala, Bulimina elongata* and *Bulimina marginata.* The mud flat sediments adjacent to the marsh also contain extremely low or trace frequencies of *Jadammina macrescens* and *Trochammina inflata.*

The sand flats of the main channel are dominated by *Ammonia batavus, Cibicides lobatalus* and *Quinqueloculina seminulum*; the relative proportion of these species varies between 13% to 43%, 10% to 38% and 9% to 39% of the total assemblage respectively. Additional species include *Elphidium williamsoni, Elphidium crispum, Asteriginata mamilla, Planorbulina distoma, Rosalina anomala, Miliolinella subrotunda* and *Lagena sulcata.*

The differences in foraminiferal composition between the high marsh, mid-marsh and low marsh are a function of changes in elevation and salinity across the surface of Delacorse marsh. The low diversity exhibited in the high marsh reflects the high levels of stress imposed on this environment by prolonged periods of exposure or increased freshwater input from surface runoff and rainfall. The dominance of *Jadammina macrescens* reflects the ability of this species to compete successfully in the highly stressed brackish marsh environment. As the low and mid-marshes are more frequently inundated by the tide, foraminiferal diversities increase from the high to low marshes. The marsh foraminifera contain relatively few allochthonous tests transported from adjacent environments by tidal waters. Consequently, the dead assemblages accumulating on the marsh surfaces differ only slightly from the live population (Murray, 1991).

The interrelationships between the factors controlling the formation of the total population accumulating within the marsh creeks and upon the mud and sand flats in the main channel is extremely complex as these environments contain allochthonous and autochthonous components and are significantly influenced by post-mortem transport processes. The proportion of exotic tests is relatively lower in the creek sediment than on the mud and sand flats; the allochthonous component is comprised of *Cibicides lobatalus, Planorbulina distoma, Asteriginata mamilla, Rosalina anomala, Bulimina elongata, Bulimina marginata* and *Globoquadrina hexagona.* These species are derived from the Celtic Sea and the Bristol Channel and transported by storm waves and high energy tidal currents to marginal marine environments where they are deposited. For instance, *Cibicides lobatalus* is epifaunal and attaches itself to hard substrates such as rock surfaces or shells; the test can be described as plano-convex with a flat dorsal attachment side and moderately raised ventral side (Haynes, 1973). Upon death the test can be detached from the substrate and transported onshore as either suspended or bed load. Although *Cibicides lobatalus* maybe suited to living in the main channel the greatest concentrations of this species are found upon in the mud flat sediment. In contrast *Ammonia batavus*, which commonly occurs on marshes and in near-marine environments (Murray, 1991), is found in greatest numbers upon the sand flats in the main channel. *Ammonia batavus* tests are biconvex and roughly twice as wide as high (Haynes, 1973). This indicates that due to their test architecture once entrained into the flow *Cibicides lobatalus* is hydrodynamically lighter than *Ammonia batavus* and are consequently enriched in the fine grained mudflat sediments. Both allochthonous and autochthonous foraminifera accumulating within the main channel of the Taf Estuary are selectively sorted in the high energy tidal regime.

6.1.3 Comparison of modern and of fossil assemblages

Principle components analysis was used to compare the modern data with the fossil assemblages. Samples representative of the high marsh, mid marsh, low marsh, creeks, mud flats and sand flats (Appendix 6.1) were included in the analysis in an attempt to identify biofacies in the down core studies.

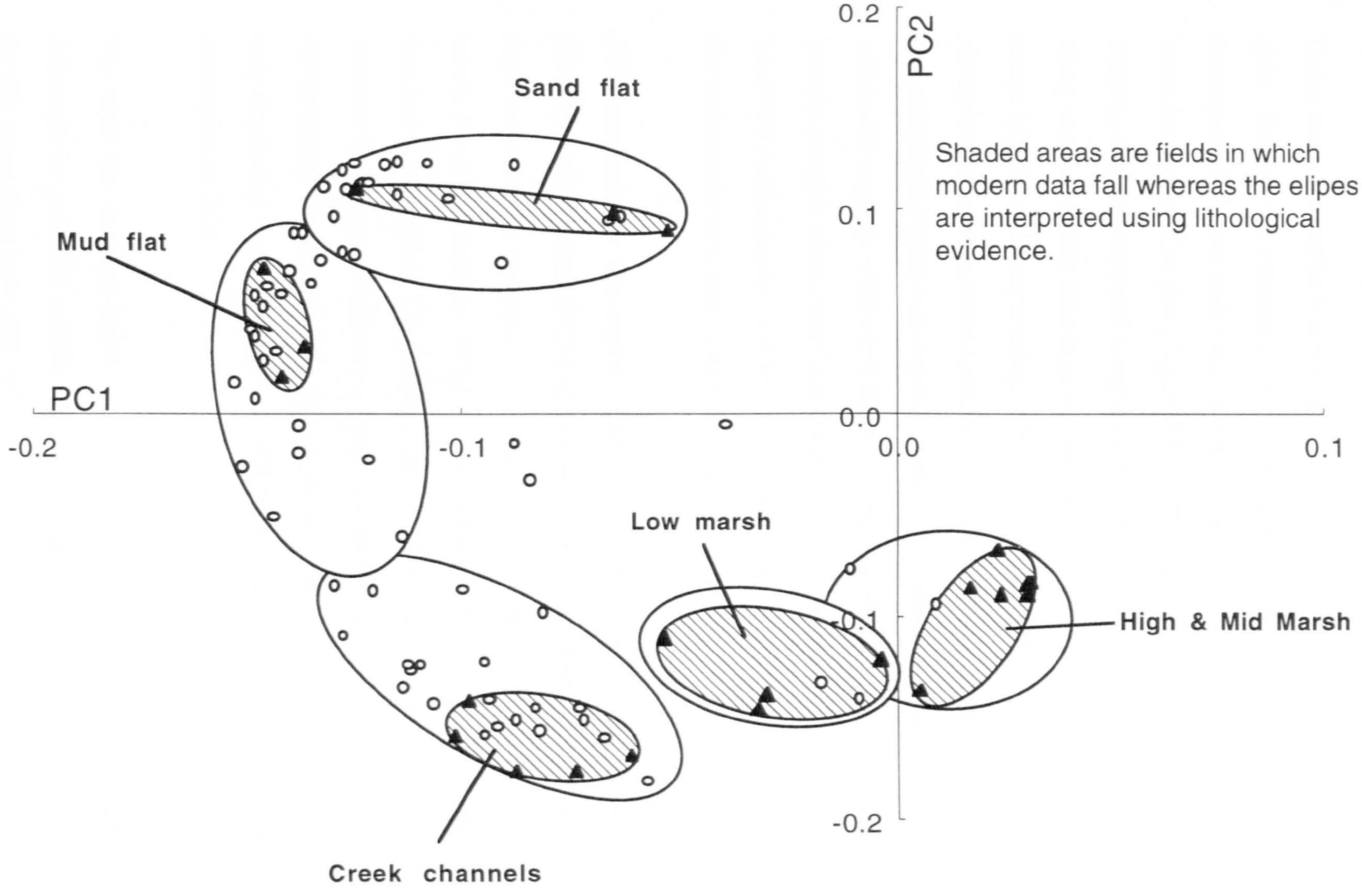

Figure 6.9 PCA applied to both modern (solid triangles) and fossil (circles) data.

Figure 6.9 displays the first and second principle component, for the modern and fossil data, which account for 44% and 23% of the total variance within the data set respectively. The modern samples and fossil data are displayed as solid triangles and circles respectively; the axes values represent the correlation coefficients between the samples and the principle components.

Using modern samples it is possible to define the areas occupied by the six biofacies on the PCA plot. Due to the considerable variability in the data set, multivariate analysis is unable to distinguish between high and mid-marsh samples; these two associations are displayed as one biofacies on the PCA plot (Figure 6.9). Although the low and high/mid-marsh biofacies overlap slightly, modern and fossil samples within these two environments can be clearly distinguished using supplementary lithological evidence. The PCA analysis suggests that the creek and low marsh biofacies do not overlap. The boundary between the creek and mud flat samples is less clearly defined; the relative similarity between the foraminiferal composition of creek and mud flat sediment samples will depend upon the proximity of a particular creek to the main channel within the estuary. Although the mud and sand flat biofacies overlap slightly the position of modern samples within this final biofacies can be used to distinguish fossil samples derived from these two environments. Differences between fossil assemblages and modern populations reflect the taphonomic processes active during fossilization.

PC1 accounts for the major differences between high/mid marsh, low marsh and creek environments whereas PC2 explains the principal differences between these biofacies and the mud and sand flat samples. PC1 may represent stresses such as salinity, temperature and pH across the marsh surface, which are controlled primarily by the duration of exposure between successive high tides. For instance, high/mid-marsh samples are positively correlated to PC1 whereas the low marsh and creek samples exhibit a negative correlation to stress; these latter two environments are inundated by each successive high tide whereas the high and mid-marshes are only flooded by higher spring tides. The mud and sand flat samples display the strongest negative correlation to PC1.

The mud flat samples exhibit both negative and positive correlations to PC2 (Figure 6.9). Although the sand flat samples possess the greatest positive correlation to PC2 the coefficients for this component vary only slightly within this environment. It likely that PC2 represents the

intensity of hydrodynamic processes within the system; the intensity increases from the relatively low energy low marsh and creek to the mud and sand flats within the main channel. As would be expected the hydrodynamic intensity varies only slightly across the sand flats in the main channel; however, the major cause of variance within this environment is described by PC1 (Figure 6.9). During low water certain areas of the sand flats within the main channel of the Taf Estuary are exposed whereas others are covered by fresh water draining from the catchment area. This produces a gradient of stresses across the sand flats from saline pools and exposed sand banks to sediment immersed in fresh water.

The three samples which fall outside of the envelopes, used to define the five biofacies described above, have foraminiferal compositions intermediate of mud/sand flat and marsh environments. These samples may represent hyper-saline marsh environments subject to high energy tidal or storm processes. For instance, storm waves set up by storm surges may breach the barrier and flood the back barrier area. Foraminifera contained within the storm water may settle out of suspension and contribute to the total population accumulating upon the back barrier marsh surfaces at that time.

It should be noted that the interpretation is qualitative, based upon the relationships between modern samples obtained from known environments; no attempt has been made to quantify the principle components described in this study. However, modern foraminifera supported by lithological evidence can be used to interpret the foraminiferal associations identified at sites 4, 12, 11, 17, 20 and 22.

6.1.4 Interpretation of fossil data

Site 12

The PCA data suggests that zone 12-1 represents a relatively high energy marsh creek environment which is overlain by a low energy mud flat. The boundary between zones 12-1 and 12-2 may represent a slight positive tendency in sea-level. Through zone 12-2 the environment gradually changes from mudflat back into a creek. However, at the top of zone 12-2 the

sediments grade into a thin bed of silty sand which is defined by the PCA data as a high energy sandflat environment. Although, the modern foraminiferal data used to define the sandflat facies was obtained from the estuary and not open marine sands in Carmarthen Bay, the relative proportion of exotic tests, the composition of the sands and the proximity of site 12 to the barrier dunes suggest that these sediments probably represent washover deposits. Zone 12-3 shows the accumulation of creek and marsh sediments above the sandflat deposits. The boundary between zones 12-2 and 12-3 represents an acretionary sequence and the development of back-barrier salt marshes.

Poor preservation between 6.34 and 5.10 metres may represent the dissolution and destruction of foraminiferal tests within mid and high marsh sediments or indicate that these sediments were deposited by terrestrial processes. The sediments at 5.10 and 4.80 metres represent mud flat and low/mid marsh environments. The relatively high proportion of *Quinqueloculina seminulum* and *Ammonia becarii* var. *batavus* suggests that these samples may represent hypersaline mud flat and marsh associations.

Site 4

The samples at the base of zone 4-1 indicate that the environment gradually develops from creek facies at 8.19 metres through low marsh into high/mid marsh at 7.4 metres. Poor test preservation between 7.40 and 6.24 metres may result from the dissolution foraminifera in the oxidised near surface sediments within the marsh sediments. Above this the sample at 6.24 metres indicates that the high/mid-marsh biofacies is overlain by creek deposits which inturn are replaced by a low marsh sediment at 4.88 metres. As the sediments grade from silty clay at the top of zone 4-1 to silty sand at the base of zone 4-2 the foraminiferal data indicates that environment changes from low marsh into creek biofacies. The boundary between zones 4-1 and 4-2 may represent a slight positive tendency in sea-level.

The foraminifera indicate that through zone 4-2 the environment progressively changes from a creek into low and high energy mud flat. The boundary between zones 4-2 and 4-3 corresponds to a transition from high energy mud flat to marsh creek biofacies. Poor preservation of foraminiferal tests at site 4 is either due to dissolution in marsh sediments or to the introduction

of terrestrial sediment. The boundary between zones 4-2 and 4-3 represents an acretionary sequence and the progradation of back-barrier saltmarshes.

Site 11

At the base of zone 11-1 the sediments fine upwards into silty clay. This corresponds in a gradual change from creek to high/mid marsh biofacies between 11.30 and 9.72 metres. The marsh deposits are overlain by marsh creek deposits which extend to the top of zone 11-1.

The boundary between zones 11-1 and 11-2 is rather abrupt and marked by a transition from creek to lower mud flat deposits. At the top of zone 11-2 the mud flat facies is replaced by sand flat deposits. The boundary between zones 11-2 and 11-3 are represent by rapid change from sand flat into creek biofacies. The highly stratified sand between 4.66 and 1.49 metres represents intercalated mud flat and sand flat deposits. The boundary between zones 11-4 and 11-5 is defined by a rapid change from sand flat to mud flat deposits. However, towards the top of zone 11-5 the deposits grade from mud flat into brackish sand flat deposits.

Due to the proximity of site 11 to the former tidal inlet, now occupied by Wytchet Lake, it is probable that the sand and mud flat deposits identified at this local accumulated in the main channel behind the Pendine Burrows. If the tidal inlet remained fixed in approximately in the same position during the Holocene transgression, then the biofacies changes identified at site 11 may represent the changing position of the main channel behind barrier. However, if sediment by-pass did not occur then the Pendine Burrows may have extend in a longshore direction and the biofacies at site 11 may represent changes in the stability and longshore development of the Pendine Burrows.

Site 17

The shelly sand at the base of site 17 represents a high energy lower mud flat or sand flat environment; this classification is based on foraminiferal evidence and does not relate to the textural composition of these particular sands. Between 4.97 and 4.84 metres the sediments grade

into silty clay; this corresponds to a change from mud flat to creek facies. The sandy silt and silty clay between 4.84 and 2.53 metres represent mud flat deposits. The boundary between zones 17-1 and 17-2 is marked by a change from mud flat into creek biofacies. Poor preservation above 1.84 metres may be caused by the dissolution of foraminiferal tests in oxidised near-surface sediment. The gradual transition from mud flat into creek facies probably represents the simple progradation of the mud flats within the back-barrier area. Conversely, the change from creek into mud flat facies between 4.84 and 3.87 metres may represent barrier instability or changing patterns of sedimentation within an accretionary back-barrier environment.

As sea-level changes invariably influence barrier stability the relationship between barrier development, sea-level and sediment supply further complicates the interpretation of these back-barrier facies changes.

Site 20

The sediments at the base of zone 20-1 grade from sandy silt into silty clay; this corresponds to a change in the foraminiferal composition from mud/sand flat into mud flat associations. The mud flat deposits extend to the top of zone 20-1 where they grade into sand flat deposits. The sand flat deposits of zone 20-2 extend to 2.94 metres where they are replaced by a second mud flat facies. Poor preservation above 1.35 metres may represent dissolution in oxidised near-surface sediment.

The two successive phases of mud flat development at site 20 may either represent slight regressive phases in sea-level rise or two successive phases of barrier-spit longshore extension in response to increased sediment supply and or changing oceanographic conditions.

Site 22

The PCA analysis indicates that the shelly sand and silty sand between 5.22 and 2.13 metres represents sand flat deposits. The silty sand bed within the silty clay unit at 1.03 metres contains

a foraminiferal assemblage indicative of hyper-saline sand flat deposits; the relatively low frequencies of *Jadammina macrescens* in this level indicates the proximity of this site to an adjacent saltmarsh. The absence of foraminifera in the stratified silty clay between 2.83 and 1.03 metres may represent either post-depositional dissolution during fossilization/diagenesis or the introduction of terrestrial sediment. The composition and structure of these sediments suggests that these deposits may represent salt marsh deposits; however, no other direct evidence exists to draw a conclusion.

The sequence at site 22 is overlain by a layer of shelly sand which represents sand flat facies. However, as these sediments lie above 3.68 metres OD it is probable that they represent wash-over deposits rather than deposits which have accumulated within the main channel.

6.1.5 Summary

By comparing modern foraminiferal populations to fossil data, using PCA analysis, it is possible to identify the sedimentary environment in which a particular deposit formed. Problems associated with the modification of the total populations, by post-mortem transport, are avoided as the modern data sets include this taphonomic variable. However, it is clear that the marsh assemblages are modified by post-depositional dissolution. Some of the stratified silty clays analysed contained no foraminiferal tests whilst their structure is extremely similar to saltmarsh deposits. In particular the organic- rich silty clay, in contact with the organic detrital units, at sites 12 and 4 contained very few foraminifera. The available foraminiferal information suggests that these organic units have accumulated above the Mean High Water Spring Tide levels and therefore probably represent terrestrial sediment.

The fossil data obtained from site 12 suggests that at the base of the sequence the sediments grade from saltmarsh and creek deposits into mud flat facies. These sediments are then replaced by creek and saltmarsh deposits which grade into the lower organic unit at site 12. The organic bed is replaced by saltmarsh sediment which extends to the base of the upper organic unit. These organics are also replaced by fine grained silty clay which extends to the ground surface. Although poor foraminiferal preservation prevents the identification of fine grained facies it is

likely that they represent the accumulation of saltmarsh sediments. A similar pattern of development is exhibited by the foraminiferal associations identified at site 4. The silty clay in contact with the Pleistocene boulder clay and gravel at the base of the sequence have been identified as creek deposits. These grade into saltmarsh sediment which is overlain by an organic detrital bed. The organics are replaced by a second phase of salt marsh development overlain by creek and mud flat sediment. The mud flat facies grades into creek and marsh deposits which extend to the base of the upper organic unit at site 4. As at site 12 the organics are once again replaced by fine grained silty clay. Differences in sedimentary facies, identified between the organic beds at sites 12 and 4, indicate the proximity of those two sites to the main channel. The accumulation organic sediment at sites 12 and 4 may represent negative phases in sea-level rise during the late Holocene.

The sedimentary facies identified at site 11 are dominated by mud flat and sand flat sediment. The foraminiferal assemblages suggests that site 11 has been influenced by the position of the main channel and or tidal inlet. This suggests that the tidal inlet, between the Pendine and Laugharne Burrows, may have continued to regulate back-barrier sedimentation up until the construction of the sea-wall defences, during the 18th and 19th centuries.

The shelly sand at the base of sites 17, 20 and 22 represent high energy sand flat deposits which contain a high proportion of open shelf tests derived from offshore. At sites 17 and 20 these sediments grade into mud flat sediment which is replaced by a second phase of sand flat development. These deposits are overlain by mud flat and creek sediments; however, although the lithological evidence suggest the subsequent development of saltmarshes, poor preservation within the oxidised near surface sediment prevents the identification of this facies using foraminifera.

The facies identified at site 22 show that the sand flat deposits at the base of the sequence extend to 2.13 metres where they grade into mud flat deposits. These fine grained sediments are overlain by a sand flat facies which extends to the ground surface. The height of these sediments above Ordnance Datum suggests that they may represent wash-over deposits. However, other possible criteria used to identify wash-over deposits are absent in these sediments.

The two phases of mud flat development at site 17 and 20 may represent two successive stages of longshore barrier development barrier. This may be linked to either increased sediment supply or to a stillstand or slight regressive phase in sea-level rise. The absence of the lower mud flat unit at site 22 may imply that the sediment has either been removed or that the barrier extended east of this locale only on one occasion during the late Holocene.

6.2 Pollen analysis

6.2.1 Description on pollen analytical data.

Pollen analysis was used to reconstruct vegetational development and palaeoenvironments at three sites within West Marsh (Figure 6.10). The sampling strategy is designed to investigate changes in the composition of pollen within and between the organic beds recovered from sites 7, 12 and 4.

Site 7

The inorganic sediments recovered from site 7 contained extremely low frequencies of pollen (<3000 grains cm^{-3}); as a result the majority of the levels analysed are restricted to the organic layers. On the basis of pollen assemblage composition the sequence has been sub-divided into five local pollen assemblage zones (LPAZ).

LPAZ 7-1: Extends from 9.89 to 5.54 metres. The spectrum at 9.89 metres is dominated by *Pinus* which is predominately composed of detached bladders. *Quercus*, Cyperaceae and Poaceae pollen maintain relatively high frequencies while *Alnus*, *Corylus* and Chenopodiaceae all occur in relatively small numbers (Figure 6.11). This level also contains a relatively high proportion of indeterminable pollen which are either broken or crumpled. The organic-rich sand at 9.37 metres contains an extremely small amount of pollen (Figure 6.12).

The pollen concentration increases dramatically to >150,000 grains cm^{-3} in the sandy organic layer between 9.35 and 9.27 metres. This level contains pollen dominated by Cyperaceae and *Quercus* with a smaller proportion of Poaceae, *Corylus* and *Pinus*. Although these organics contain *Alnus* pollen the values remain extremely low (Figure 6.11). No pollen were identified in the stratified silty clay between 9.27 and 7.72 metres.

The organic detritus between 7.75 and 7.63 metres contains pollen dominated by *Quercus* with a smaller proportion of Poaceae, Chenopodiaceae, *Corylus*, Cyperaceae and *Pinus* taxa. The reduction in Cyperaceae pollen towards the top of this thin organic layer coincides with a slight

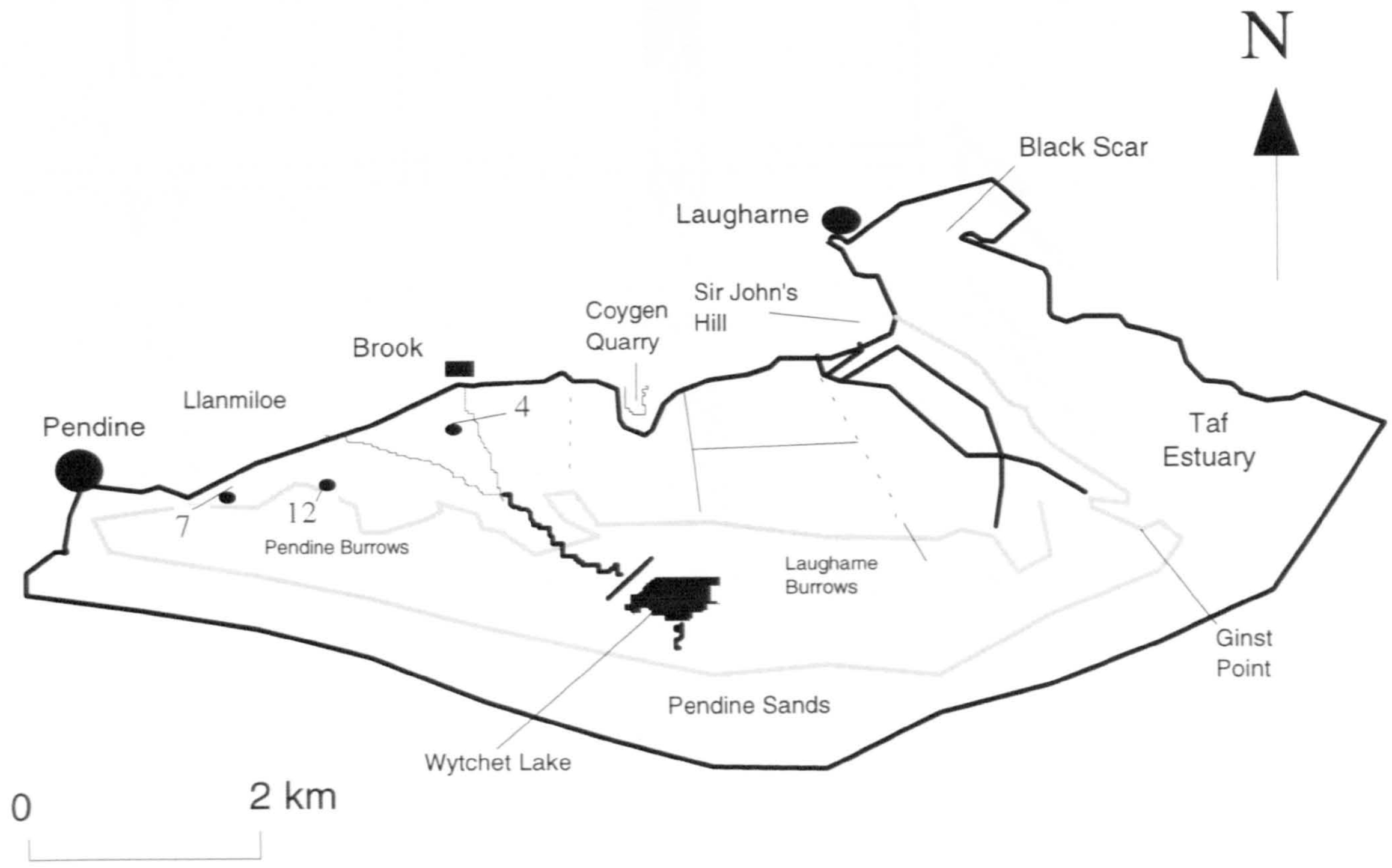

Figure 6.10 Location of sites 7, 12 and 4.

Figure 6.11 Pollen diagram for site 7.

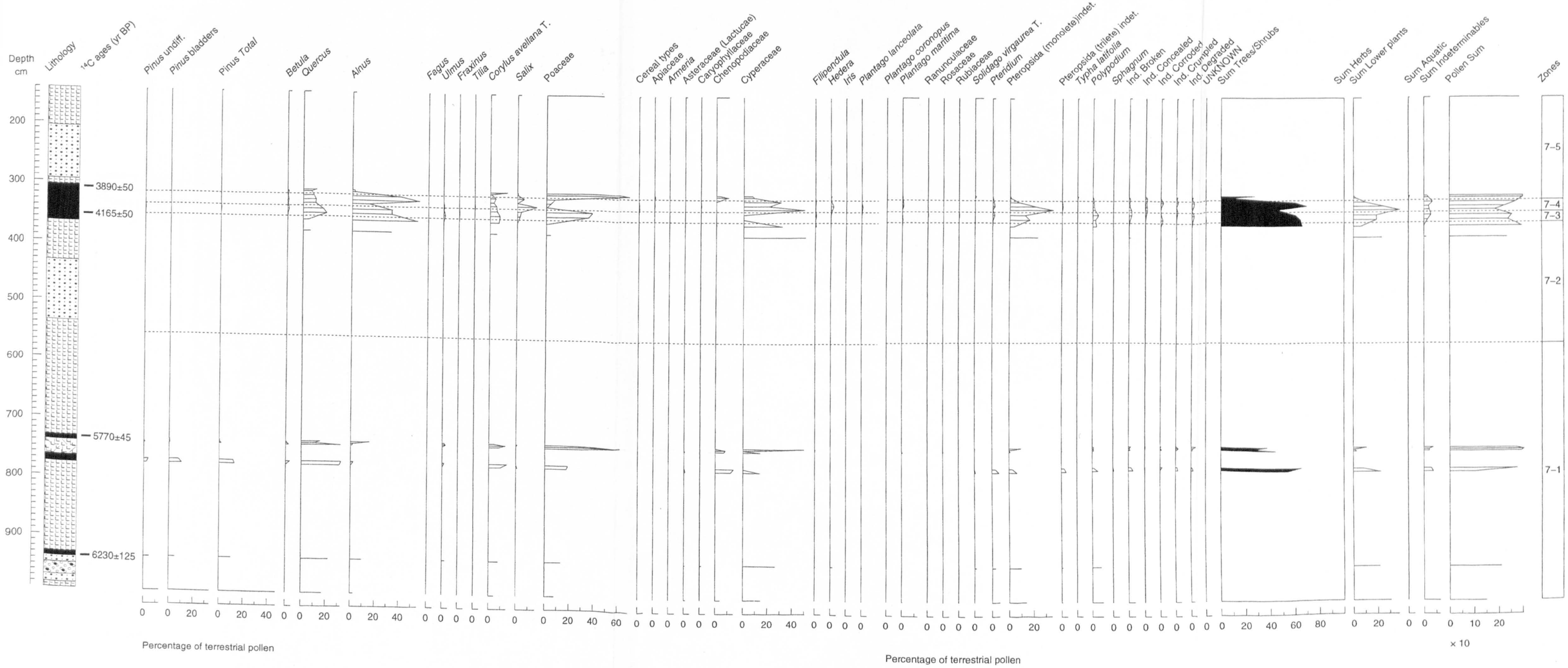

Figure 6.12 Pollen concentration diagram for site 7.

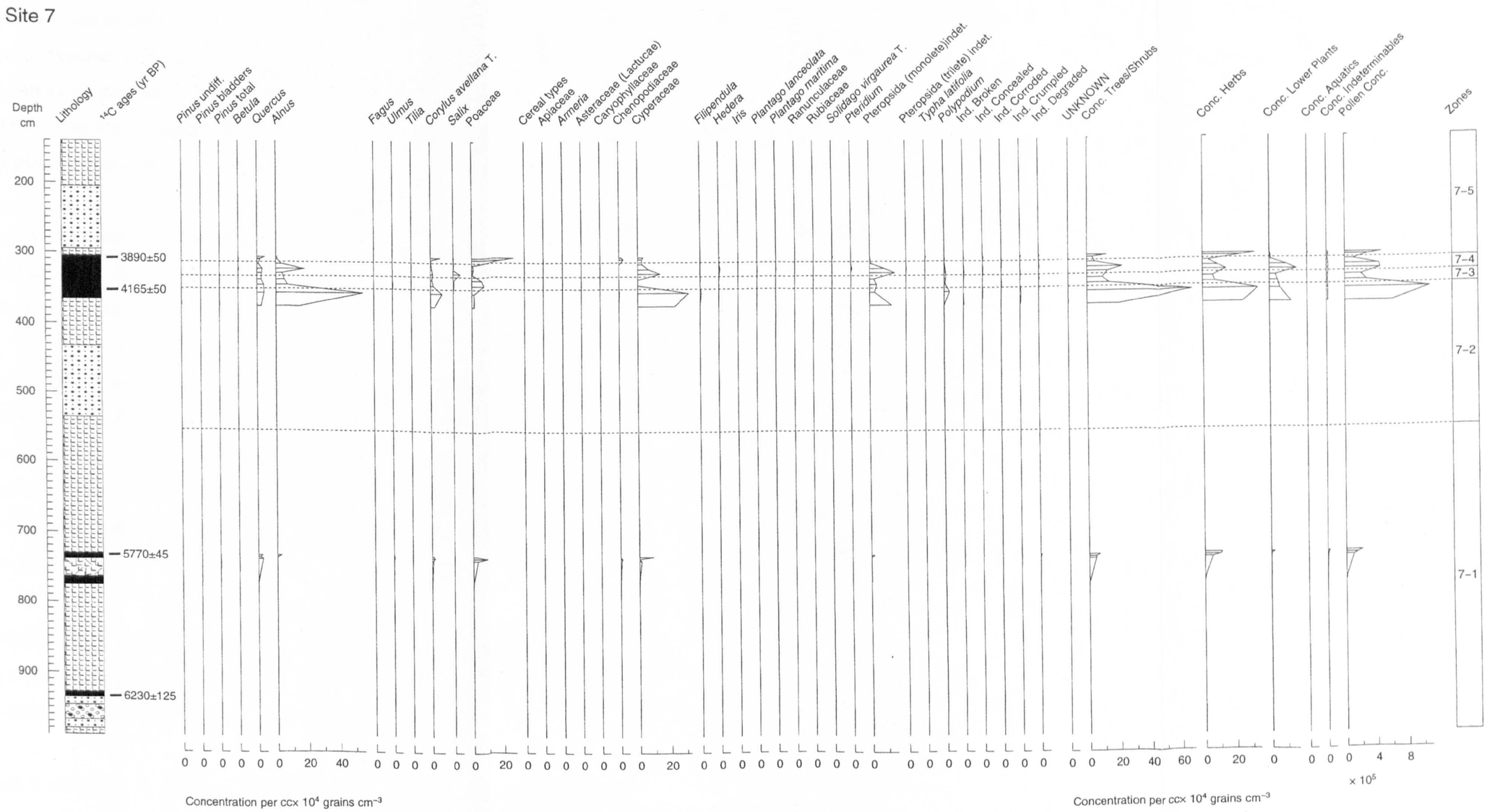

increase in the amount of *Betula*, *Alnus*, Poaceae and *Corylus* pollen. The organic-rich silty clay between 7.63 and 7.38 metres contained no pollen.

The pollen concentration within the organic detritus between 7.38 and 7.30 metres varies between 101,770 and 213,469 grains cm^{-3} (Figure 6.12). The assemblage identified at 7.38 metres is dominated Poaceae, *Quercus* and Cyperaceae with lower frequencies of *Corylus* and Chenopodiaceae. Between 7.38 and 7.35 metres the frequency of Poaceae increases dramatically; this corresponds to a decrease in *Quercus* and Cyperaceae pollen (Figure 6.11). Above this the relative proportion of Poaceae pollen decreases sharply whereas Cyperaceae recovers. The organics at 7.32 metres also contain a greater amount of *Alnus* and *Quercus* pollen and fewer Chenopodiaceae grains than the underlying level. The frequency of indeterminable grains and spores from lower plants increases between 7.35 and 7.32 metres (Figure 6.11).

Because no pollen were identified in the sands and silts between 7.32 and 3.76 metres the boundary separating LPAZ 7-1 & 7-2 is placed between these two levels; this boundary does not represent a specific level at which a vegetational change occurs.

LPAZ 7-2: Extends to 3.51 metres and is marked by a sharp rise in *Alnus* pollen. The organic-rich silty clay at 3.76 metres contains pollen dominated by Cyperaceae and *Alnus* with a smaller amount of *Quercus*, *Corylus* and Poaceae (Figure 6.11). As the sediments grade into organic detritus at 3.66 metres the *Alnus* curve increases from 33% to 54%; this corresponds to a decrease in Cyperaceae pollen from 51% to 32%. Other common taxa within this level also include *Quercus*, *Corylus* and Poaceae.

LPAZ 7-3: Extends from 3.51 to 3.26 metres and is defined by a sharp decrease in Cyperaceae and *Alnus* pollen, corresponding to an increase Poaceae and a slight rise in *Salix*. *Quercus* and *Corylus* pollen maintain relatively high levels throughout this zone.

LPAZ 7-4: Extends from 3.33 to 3.13 metres. The opening of LPAZ 7-4 is marked by a sharp decline in Poaceae, associated with an increase in the relative proportion of Cyperaceae and *Salix* pollen. *Alnus, Quercus* and *Corylus* pollen frequencies remain relatively low (Figure 6.11).

KEY

Silty Clay

Sandy Silty Clay

Silty Clay containing organic detritus

Sandy Silt

Silty Sand

Organic Detritus

Sand

Between 3.29 and 3.23 metres the *Salix* and Cyperaceae pollen diminish whereas *Alnus* increases sharply to 56%. The pollen composition varies only slightly between 3.23 and 3.16 metres.

LPAZ 7-5: Extends above 3.13 metres and is marked by a sharp rise in the Poaceae curve. This corresponds to a fall in *Alnus* and Cyperaceae while Chenopodiaceae and *Corylus* pollen increase. *Quercus* and *Corylus* curves only exhibit a slight variation throughout the upper organic unit at site 7 and the pollen concentrations within this layer range between 110,000 and 400,000 grains cm^{-3}.

No pollen were identified in the silts, clays and sands between 3.05 and 1.40 metres. The pollen concentration in the organic-rich silty clay at 1.40 metres is relatively high at 41,477 grains cm^{-3} (Figure 6.12). The pollen composition at this level is extremely similar to the organics at 3.06 metres. The spectrum is dominated by Poaceae and contains a relatively high proportion of Chenopodiaceae and *Plantago maritima* (Figure 6.11). *Quercus*, *Alnus* and *Corylus* pollen maintain low values.

Site 12

Although relatively few pollen grains were identified in the majority of the inorganic sediments a number of levels contained pollen in sufficient concentration to be included in the pollen diagram. On the basis of pollen assemblage composition the sequence at site 12 has been sub-divided into four local pollen assemblage zones (Figure 6.13).

LPAZ 12-1: Extends from 8.76 to 5.39 metres. The silty clay between 8.76 and 8.37 metres contains pollen dominated by *Quercus* and Poaceae with lower frequencies of *Corylus*, *Pinus*, Chenopodiaceae, *Ulmus*, Cyperaceae and *Alnus* (Figure 6.13). The pollen concentration between 8.76 and 8.37 metres is relatively high, varying between 65,000 and 55,00 grains cm^{-3} (Figure 6.14). No pollen were identified in the sandy silt and silty clay between 8.37 and 5.80 metres.

The organics at 5.80 metres contains a greater proportion of Poaceae and Cyperaceae and fewer *Quercus, Pinus, Ulmus* and *Corylus* pollen than the silty clay at 8.37 metres (Figure 6.13). *Betula* and *Alnus* pollen continue to occur in relatively low numbers and the total pollen concentration

KEY

Silty Clay

Sandy Silty Clay

Silty Clay containing organic detritus

Sandy Silt

Silty Sand

Organic Detritus

Sand

Figure 6.13 Pollen diagram for site 12.

Site 12

Depth cm

Lithology

^{14}C ages (yr BP)

3580±60

4630±45

5920±50

Pinus Undiff.
Pinus Bladders
Pinus Total
Betula
Quercus
Alnus
Fagus
Ulmus
Fraxinus
Tilia
Corylus avellana T.
Juniperus
Salix
Poaceae
Apiaceae
Armeria
Asteraceae (Lactucae)
Caryophyllaceae
Chenopodiaceae
Cyperaceae
Ericaceae sp.
Filipendula
Iris
Liliaceae
Plantago lanceolata
Plantago coronopus
Plantago maritima
Rosaceae
Rubiaceae
Solidago virgaurea T.
Pteridium
*Pteropsida (monolete)*indet.
Pteropsida (trilete) indet.
Sparganium type
Typha latifolia
Polypodium
Sphagnum
Ind. Broken
Ind. Concealed
Ind. Corroded
Ind. Crumpled
Ind. Degraded
UNKNOWN
Sum Trees/Shrubs
Sum Herbs
Sum Lower plants
Sum Aquatic
Sum Indeterminables
Pollen Sum
Zones

12–4
12–3
12–2
12–1

Percentage of terrestrial pollen

× 10

Figure 6.14 Pollen concentration diagram for site 12.

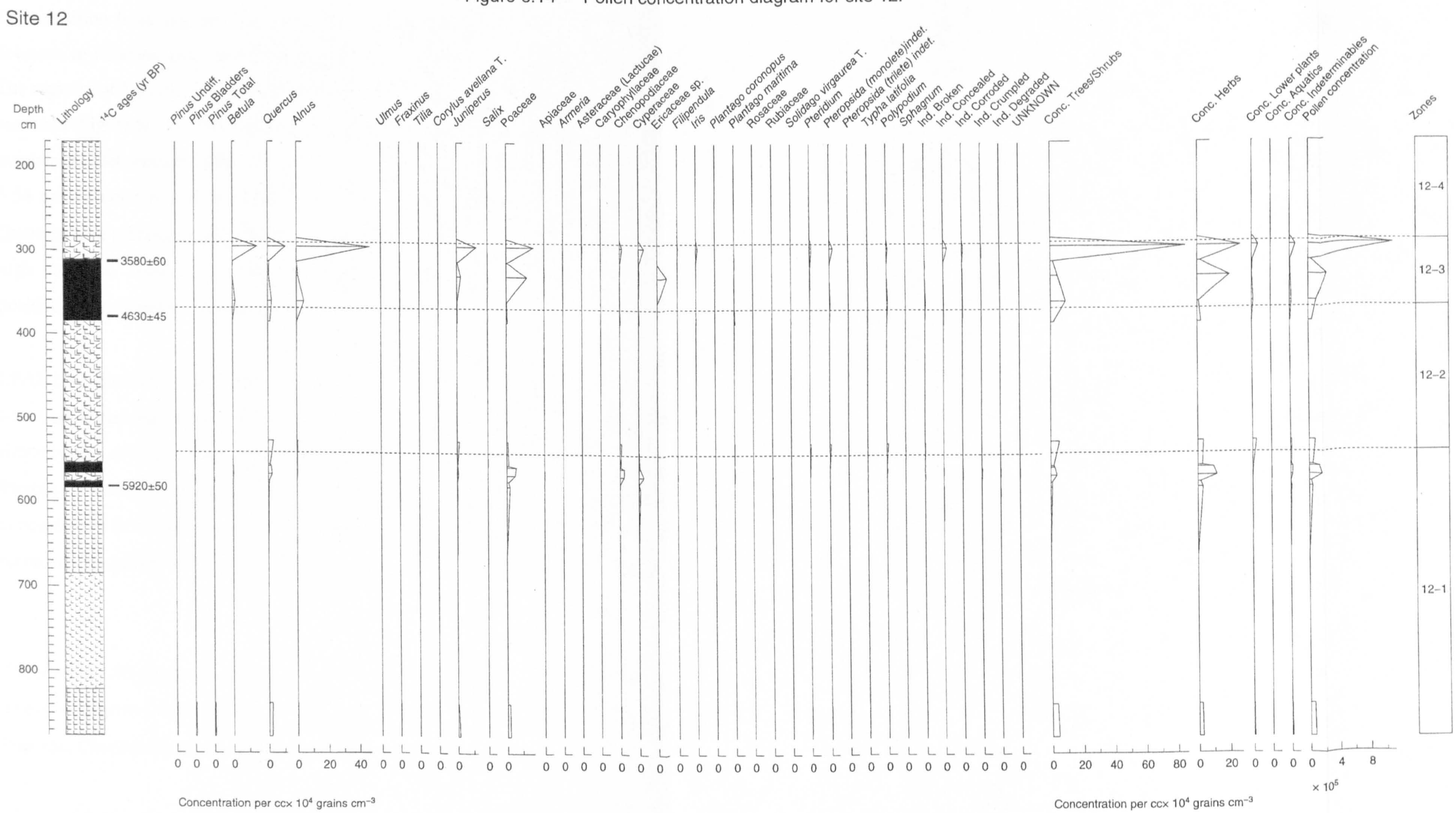

remains relatively high at 42,300 grains cm^{-3} (Figure 6.14). As the sediments grade into organic rich silty clay at 5.76 metres the relative proportion of *Quercus, Pinus* and Chenopodiaceae pollen increases whereas Cyperaceae and Poaceae diminish. The *Corylus* and *Betula* curves do not vary as the sediments grade from organic into inorganic sediment.

The transition from organic-rich silty clay to organic detritus at 5.66 metres is marked by a decrease in Poaceae and a corresponding increase in Cyperaceae and Chenopodiaceae pollen. The organics at 5.66 metres also contain *Quercus, Corylus* pollen and a small amount of *Plantago maritima* (Figure 6.13). The pollen concentration is extremely high and only a relatively small number of indeterminable grains were recorded within this level. The organics between 5.66 and 5.54 metres contain pollen dominated by Poaceae with variable amounts of Cyperaceae and *Quercus*. The percentage data indicates that Chenopodiaceae pollen, which is occurs in relatively high numbers between 5.66 and 5.54 metres, is negatively correlated to Cyperaceae and positively correlated to Poaceae (Figure 6.13).

LPAZ 12-2: Extends from 5.39 to 3.68 metres and is marked by a fall in Poaceae and Cyperaceae, which coincides with a rise in *Quercus* pollen. The pollen assemblage identified in the organic-rich silty clay at 5.25 metres contains a greater quantity of *Corylus*, Chenopodiaceae, *Alnus*, *Tilia*, Pteropsida and *Polypodium* than the underlying levels (Figure 6.13). Furthermore, the pollen concentration is >76,000 grains cm^{-3} (Figure 6.14) and relatively few indeterminable grains were recorded. No pollen were identified in the organic-rich silty clay between 5.25 and 3.85 metres.

The level at 3.85 metres was sub-sampled from the boundary between clay and organic detritus. These sediments contain pollen dominated by *Quercus* and a relatively high proportion of Poaceae, Chenopodiaceae, *Plantago maritima*, Cyperaceae and *Corylus* (Figure 6.13).

LPAZ 12-3: Extends from 3.68 to 2.90 metres and is defined by a sharp rise in *Alnus* and *Betula* pollen. This corresponds to a fall in *Quercus*, Poaceae, *Corylus*, Poaceae, Chenopodiaceae, Cyperaceae and *Plantago maritima* (Figure 6.13). The pollen concentration at 3.60 metres is extremely high and this level contains relatively few indeterminable grains. Between 3.45 to 3.22 metres *Corylus*, Poaceae and *Calluna* pollen increase whereas *Alnus*, *Quercus* and *Betula* all

decline in number (Figure 6.13). Above this the relative proportion of *Quercus*, *Corylus* and Cyperaceae increase whereas Poaceae and *Calluna* pollen diminish. The organic detritus at 3.13 metres show an increase in Chenopodiaceae and *Plantago maritima* pollen (Figure 6.13). Between 3.13 and 2.95 metres *Alnus* and *Betula* both increase in quantity whereas *Quercus*, *Corylus*, Poaceae and Cyperaceae pollen diminish.

LPAZ 12-4: Extends above 2.90 metres and is marked by an expansion in *Quercus* and Cyperaceae pollen; this coincides with a fall in *Betula*, *Alnus*, *Corylus* and Poaceae. These changes in assemblage composition within LPAZ 12-4 correspond to both a decrease in the total pollen concentration (from >1,100,000 to < 6,000 grains cm^{-3}) and to a sharp increase in the relative proportion of Pteridium, *Polypodium* and indeterminable pollen (Figures 6.13 & 6.14). No pollen were identified in the silty clay between 2.85 and 1.70 metres.

The pollen contained within the silty clay at 1.70 metres are dominated by Poaceae, *Corylus*, *Alnus*, *Quercus* and *Calluna*. These sediments also contain relatively few indeterminable grains and a high total pollen concentration (Figure 6.14).

Site 4

The sampling strategy at site 4 was designed to examine vegetational changes within the upper organic layer and any subsequent variation in pollen composition, associated with the transition from organic detritus into organic rich silty clay. On the basis of pollen composition the upper 2.89 metres of the sequence can be sub-divided into three local pollen assemblage zones (Figure 6.15).

LPAZ 4-1: Extends up to 2.70 metres. The pollen spectra identified within the organic-rich silty clay at the base of the sequence are dominated by Cyperaceae and *Polypodium* and contain a small amount of *Pinus*, which is predominately represented by broken bladders. These inorganic sediments contain a relatively large amount of indeterminable grains and have a low pollen concentration (Figure 6.16). As the sediments grade into organic detritus, between 2.89 and 2.80 metres, the pollen concentration increases sharply from <10,000 to >170,000 grains cm^{-3}. This corresponds to a sharp decline in Cyperaceae and a rise in Poaceae pollen. *Quercus*, *Corylus* and

KEY

Silty Clay

Sandy Silty Clay

Silty Clay containing organic detritus

Sandy Silt

Silty Sand

Organic Detritus

Sand

Figure 6.15 Pollen diagram for site 4.

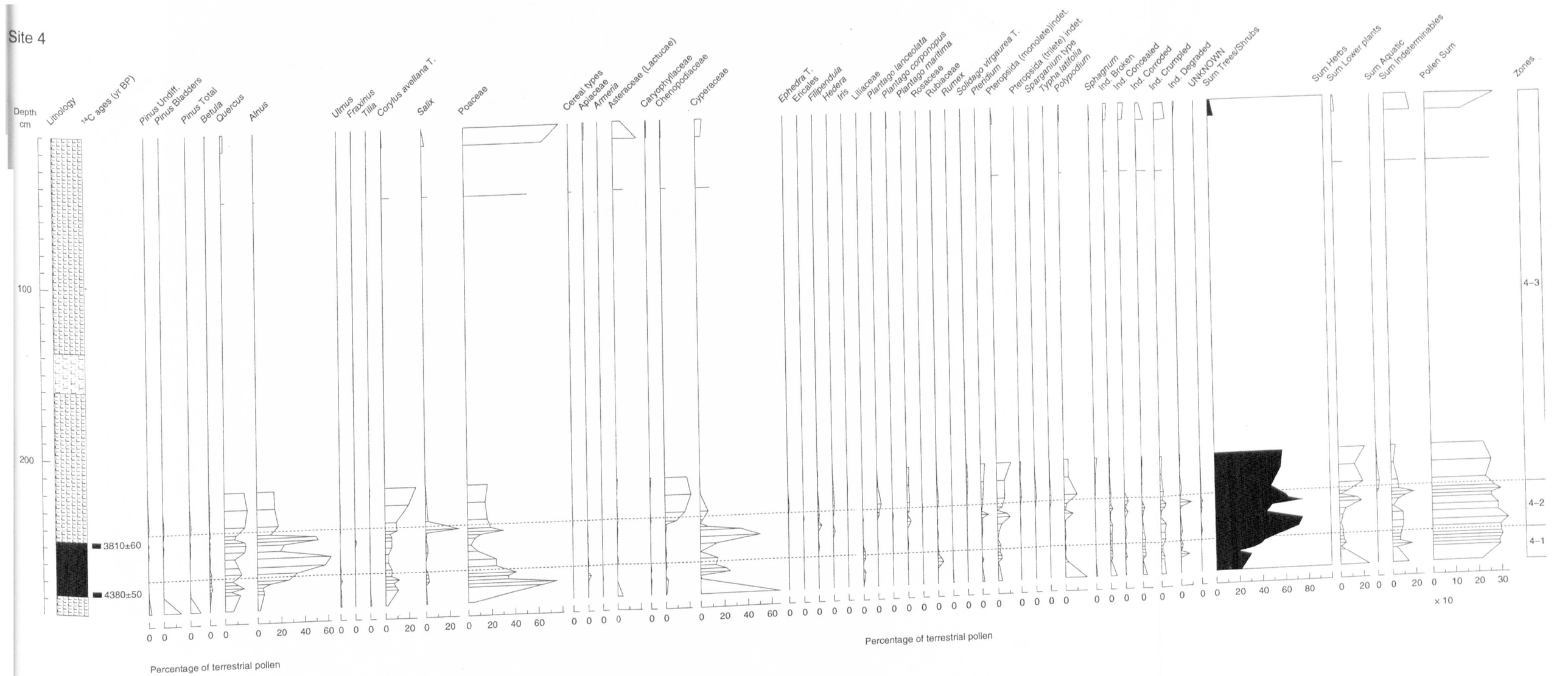

Figure 6.16 Pollen concentration diagram for site 4.

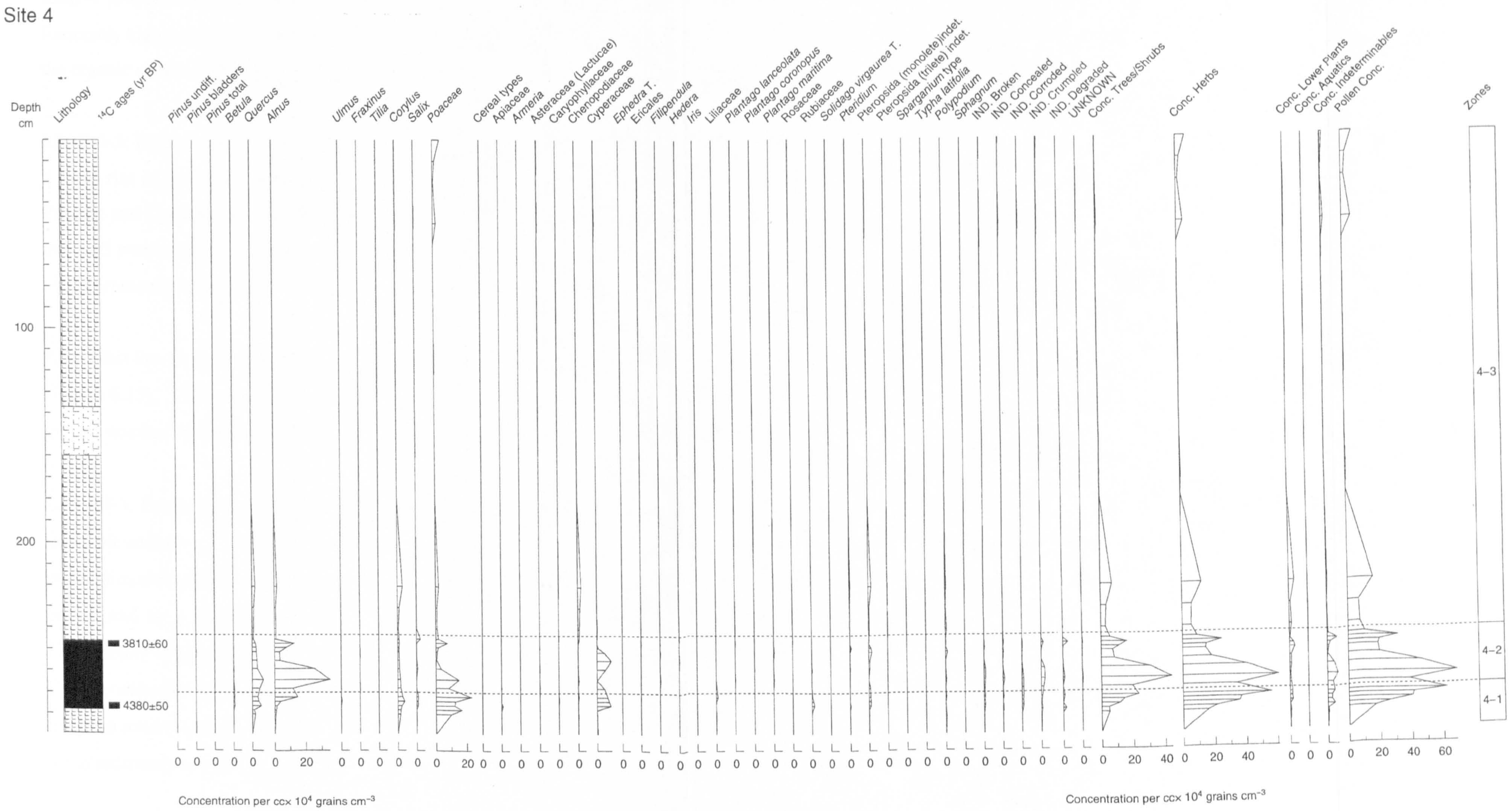

Alnus pollen maintain relatively constant frequencies through this zone whereas *Betula*, *Ulmus*, Chenopodiaceae, Pteropsida and *Polypodium* occur in small numbers (Figure 6.15). Between 2.78 and 2.76 metres the relative proportion of Poaceae decreases sharply; this corresponds to a sharp rise in the Cyperaceae curve. The percentage data indicates that through LPAZ 4-1 the relative proportions of Poaceae and Cyperaceae pollen exhibit a strong negative correlation. Extremely high pollen concentrations are recorded in the majority of the levels sub-sampled from the organic sediment (Figure 6.16).

LPAZ 4-2: Extends from 2.70 to 2.43 metres. The lower boundary of LPAZ 4-1 is marked by a sharp rise in the relative proportion of *Alnus* pollen which this corresponds to a decrease in Poaceae and Cyperaceae. The *Quercus* and *Corylus* curves exhibit little variation. Between 2.59 and 2.55 metres the *Alnus* pollen frequency falls whereas Cyperaceae exhibits rapid expansion and *Quercus* rises slightly.

Above this the *Alnus* and Poaceae curves recover while Cyperaceae and *Quercus* pollen diminish (Figure 6.15). These organics also contain a relatively high proportion of *Salix* pollen and a greater number of Chenopodiaceae and *Plantago maritima* than the underlying level.

LPAZ 4-3: Extends above 2.43 metres and corresponds to the boundary between organic and inorganic sediment. As the organic detritus grades into organic rich silty clay *Alnus* and *Salix* pollen diminish rapidly (Figure 6.15). This corresponds to a significant rise in Chenopodiaceae pollen and to a slight rise in *Quercus*, Cyperaceae, *Plantago maritima*, Pteropsida and *Polypodium* (Figure 6.15). Between 2.40 and 2.30 metres Cyperaceae declines whereas Chenopodiaceae and *Corylus* curves continue to increase. *Quercus*, *Alnus* and Poaceae pollen maintain relatively high values between 2.40 and 2.20 metres. The pollen concentrations within these sediments is much lower than in the underlying organic detritus.

Although ten levels were sub-sampled from the clay, silt and sand between 2.40 and 0.10 metres only three contained pollen in sufficient quantity for analysis (Figure 6.16). Pollen contained within the silty clay at 0.50, 0.20 and 0.10 metres are dominated by Poaceae with fewer numbers of *Quercus*, *Alnus*, *Corylus*, *Salix*, Asteraceae, Chenopodiaceae, Cyperaceae, Pteropsida and *Polypodium* than the underlying sediment (Figure 6.15). The pollen concentration varies between

73,000 to 29,000 grains cm^{-3} and the levels contain a high number of crumpled, corroded or broken grains (Figure 6.16).

6.2.2 Pollen sources in West Marsh and regional vegetation succession during the Holocene

Prior to the interpretation of pollen analytical data one must first consider the various sources of pollen within the study area. Knowing the potential origin of pollen contained within the organic and inorganic sediments described in West Marsh, it may possible to assess whether the spectra represent local, extra-local or regional vegetational development.

West Marsh is a low-lying area which covers approximately 5 km^2 and is fed by springs, streams and small rivers draining from the fossil cliffline between Pendine and Coygan Quarry (Figure 6.10). The various potential pollen sources in West Marsh (Figure 6.17) include pollen derived from local vegetation (Cl), pollen from freshwater inwashing (Cw), pollen supplied via air movements within the trunk-space (Ct), pollen supplied by the canopy (Cc) and pollen from rainfall (Cr). Jacobson and Bradshaw (1981) suggested that the local component is composed of Cl, Cw and Ct; the extra-local component is derived from Ct, Cw and Cc; whereas the regional component is largely supplied via Cc and Cr (section 3.2.4).

The relative contribution from each of these sources may vary in response to vegetational development within the back-barrier area, increased freshwater discharge, or tidal inundation. During periods of saltmarsh development and inorganic sediment accumulation, the Cl may originate from local saltmarsh vegetation. The predominance of tree-less vegetation, on the low lying back-barrier marsh surface, indicates that the Cw, Ct and Cc components are derived from extra-local forest communities growing upon the fossil cliffline (Figure 6.17a). Regional pollen may be supplied by Cc, Cr and are possibly contained within the coastal and estuarine waters.

Although the organic sediments contain a minerogenic component they are largely composed of plant debris, which have accumulated at a rate exceeding the combined effects of plant respiration, herbivore consumption and microbiological decomposition. Due to the inherent

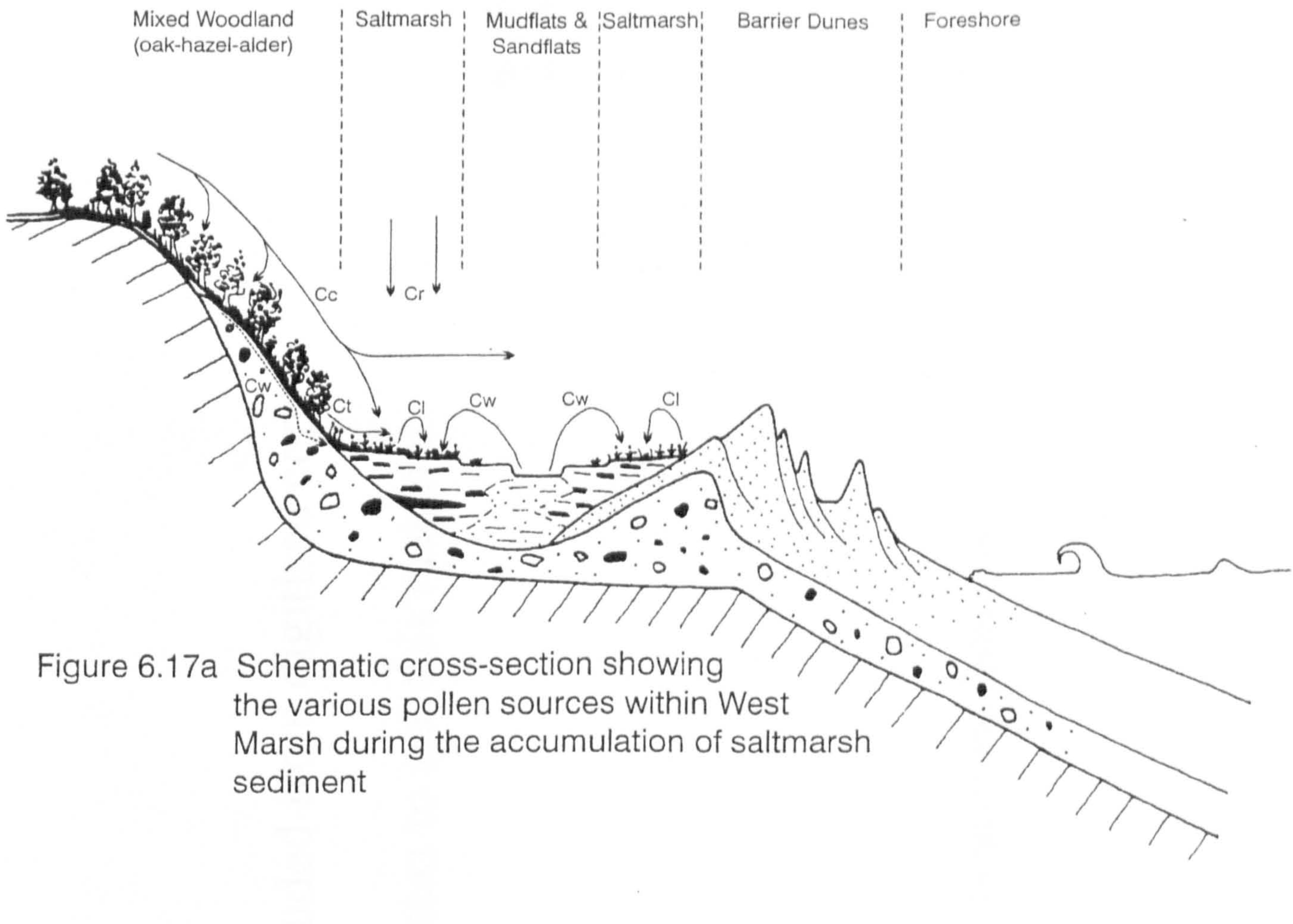

Figure 6.17a Schematic cross-section showing the various pollen sources within West Marsh during the accumulation of saltmarsh sediment

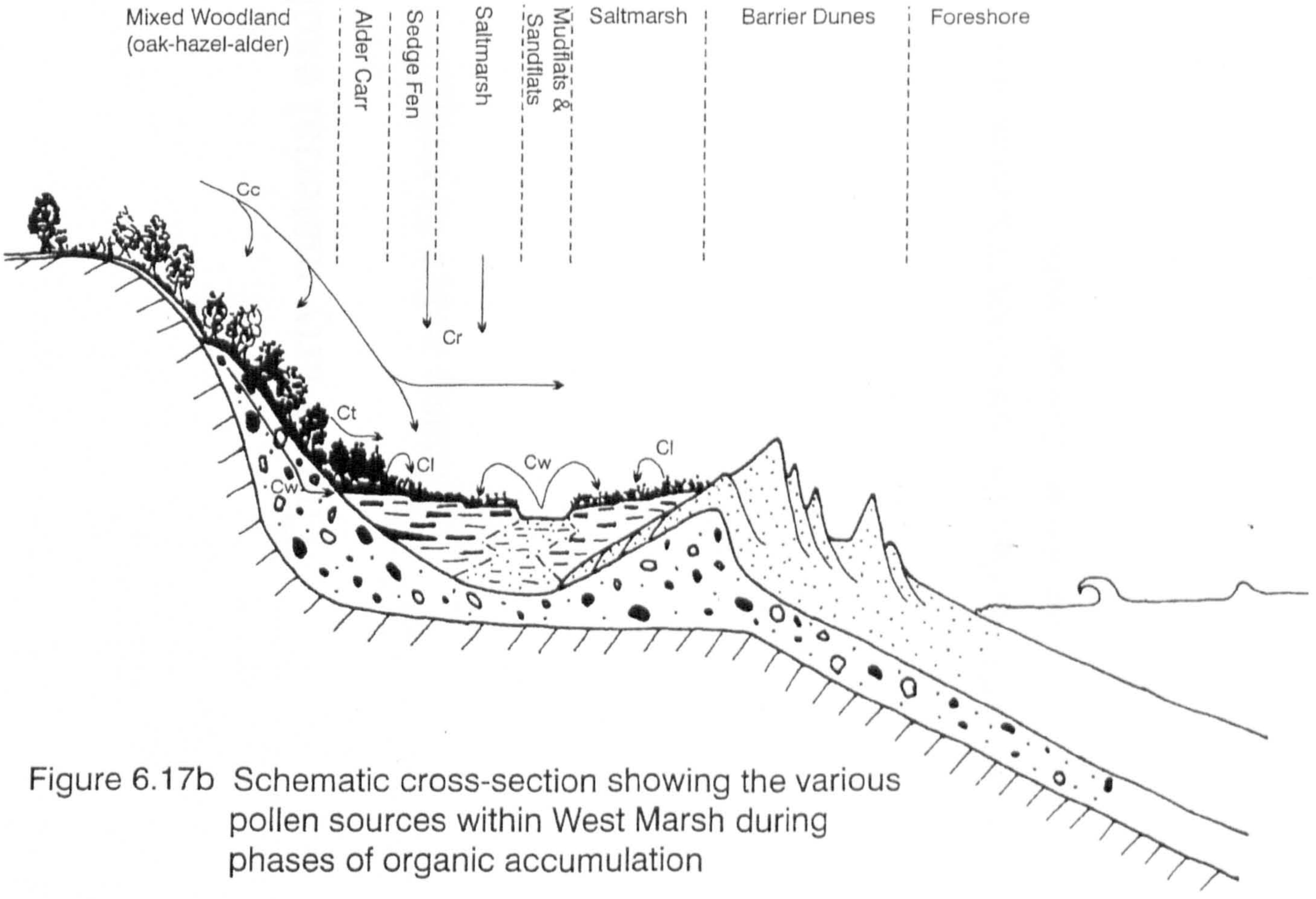

Figure 6.17b Schematic cross-section showing the various pollen sources within West Marsh during phases of organic accumulation

PAGE/PAGES
EXCLUDED
UNDER
INSTRUCTION
FROM
UNIVERSITY

topography of the marsh surface, the hydrology within West Marsh may have been extremely complex during periods of organic accumulation. The density of alder carr, sedge fen, and open grass vegetation within these rhetotrophic mires indicates that these organic detrital units may contain a large proportion of local pollen, derived from Cl, Ct and Cw (Figure 6.17b). The extra-local pollen component, supplied by Cw, Ct, and Cc from mixed woodland growing upon the fossil cliffline, would continue to be of significance and a smaller proportion of regional pollen may be derived from Cc and Cr (Figure 6.17b).

The organic and inorganic sediments in West Marsh are therefore likely to contain local, extra-local and regional pollen; however, the relative contribution from each of these components may vary in response to barrier complex development. Consequently, the succession of sub-environments within West Marsh might have received differing amounts of local and extra-local pollen depending upon the density of local vegetation and the degree of inwashing into the sedimentary basin. Because the back-barrier sediments may contain a regional component it is necessary to discuss and compare the study area to a well-dated continuous record of Holocene vegetational succession.

Tregaron south east bog (Dyfed) is the nearest continuous well-dated record of Post-glacial vegetational development in Wales. The stratigraphy was first analysed by Godwin and Mitchell (1938), who provide a description of the site and stratigraphy at Cors Goch Glan Teifi; this sequence shall provide the basis for comparison with the incomplete sequences described in West Marsh.

Godwin and Mitchell (1938) sub-divided the sequence at Cors Goch Glan Teifi into six pollen assemblage zones (Figure 6.18), which were subsequently radiocarbon dated by Hibbert and Switsur (1976):

1) *Betula-Pinus-Salix-Juniperus* Zone: Extends from 4.17 to 4.05 metres. *Betula* pollen dominates the tree taxa within this zone (Figure 6.18). *Juniperus* and *Salix* occur in relatively high frequencies whereas *Pinus* pollen is present in low but constant numbers. Other taxa include *Empetrum* and *Sorbus*. The opening of this zone is dated at 10,200 ± 220 BP.

2) *Betula-Pinus-Corylus* Zone: Extends from 4.05 to 3.94 metres. This zone shows the continued dominance of *Betula* pollen while *Pinus* exhibits a small increase (Figure 6.18). The rapid expansion of *Corylus* pollen marks the beginning of this zone whereas *Juniperus* and *Salix* both remain relatively low. This zone begins at 9750 ± 220 BP.

3) *Corylus-Pinus* Zone: Extends from 3.94 to 3.50 metres. Initially *Corylus* pollen rises rapidly and then remain relatively constant whereas *Betula* and *Juniperus* decline while *Pinus* and *Salix* maintain low values. *Ulmus* and *Quercus* pollen increase through this zone. The *Ulmus* pollen rise has been dated at 9550 ± 200 BP. , the zone opens at 9300 ± 190 BP. and the level at which *Pinus* exceeds *Betula* is dated at 8285 ± 150 BP.

4) *Pinus-Corylus-Quercus* Zone: Extends from 3.50 to 2.37 metres. *Pinus*, *Ulmus* and *Quercus* pollen all rise whereas *Betula* and *Salix* fall while *Corylus* representation remains high. This zone commences at 8150 ± 150 BP. and *Alnus* first appears at 7130 ± 180 BP.

5) *Quercus-Ulmus-Alnus* Zone: Extends from 2.37 to 1.68 metres. The opening of this zone is defined by a marked rise in *Alnus* pollen while *Pinus* frequencies fall (Figure 6.18). *Quercus* pollen values rise to a maximum in this zone whereas *Tilia* and *Fraxinus* pollen first appear. The start of this zone is dated at 6990 ± 180 BP., the *Alnus* pollen rise is completed by 6530 ± 110 BP., and *Tilia* pollen attains continuous representation by 5980 ± 100 BP.

6) *Quercus-Alnus* Zone: Extends from 1.68 to 0.30 metres. The start of this zone is marked by a fall in *Ulmus*, *Tilia* and *Fraxinus* pollen. *Quercus* and *Alnus* pollen dominate this upper zone. The opening of zone six is dated at 4990 ± 70 BP. and the decline in *Ulmus* is dated 4890 ± 70 BP.

Hibbert and Switsur (1976) also provide dates for two phases *Plantago* pollen expansion along with the timing of a slight recovery in *Ulmus* and *Fraxinus*. The affect of anthropogenic activity at Tregaron south east bog has been dated at 2920 ± 50 BP.

The well dated sequence at Tregaron provides a basis for the comparison of sites 7, 12 and 4 to regional vegetation development during the Holocene. The rise in *Ulmus* and *Alnus* along with

the subsequent *Ulmus* decline represent regional vegetational indicators which can be used to determine the timing of events within the sequence.

6.2.3 Vegetational development within West Marsh

When pollen data are presented in percentage form problems arise from the individual taxa curves being inter-dependent. For instance, an increase in the influx of one particular taxa will lead to the suppression of percentages derived for the other taxa when they maintain at the same concentration. Therefore changes in the relative proportion of taxa obtained from percentage diagrams may not actually represent the ecological development at a particular site but may be an artifact of the percentage calculations. These problems can be overcome by analysing the concentration of particular taxa within the sequence. To assist in the interpretation of fossil pollen-analytical data the ecological and environmental requirements of certain tree, shrub, herb and lower plants taxa are summarised in appendix 6.2.

Site 7

LPAZ 7-1: Cyperaceae, Poaceae and Chenopodiaceae, identified within the silty clay at 9.86 metres, indicate the local abundance of sedge fen and saltmarsh vegetation at or above MHWST level (Godwin, 1975). *Quercus, Alnus* and *Corylus* pollen may be derived from forest communities located either locally or in the surrounding landscape. However, the high percentage of *Pinus* bladders, the low pollen concentration and the relatively high proportion of indeterminable grains indicates that this level contains a significant reworked component supplied probably via aquatic transport; pine bladders may either be derived from older sediments within the catchment or represent long-distance transport.

The spectrum identified at 9.31 metres suggests that the organic layer between 9.35 and 9.27 metres may represent the development and subsequent accumulation of treeless mire vegetation, dominated by sedges and grasses; these pollen are likely to represent local vegetation whereas *Quercus, Corylus, Pinus, Alnus* and *Ulmus* pollen indicate the presence of oak-hazel-alder woodland adjacent to the site of preservation. Alder may flourish in wetter areas, such as on

stream banks, forming part of the oak canopy whereas hazel may grow in open areas within the oak woodland. The absence of pollen within the silty clay between 9.27 and 7.72 metres maybe an indication of either poor pollen preservation or high sediment supply in a near-shore environment.

The high proportion of *Quercus* and *Corylus* pollen, identified within the organic detritus between 7.75 and 7.63 metres, indicates the continued development of mixed oak-hazel woodland in the surrounding landscape with occasional birch, alder and elm; oak-hazel stands may extend locally into relatively dry areas within the back-barrier environment. The high proportion of *Pinus* bladders and extremely low pollen concentrations throughout this organic unit suggest that these sediments contain reworked pollen. Chenopodiaceae pollen values indicate the local abundance of saltmarsh species such as *Salicornia* sp., *Atriplex* sp., *Suaeda maritima* and *Halimione portulacoides*, which are widespread on the coasts of Britain today. The frequency of Poaceae and Cyperaceae pollen implies the predominance of local treeless vegetation with occasional stands of sedges in areas subject to water-logging. Similar vegetational patterns can be observed within the Taf Estuary at present; sedges grow between Highest High Water Springs (HHWS) and Mean High Water Springs (MHWS) and are influenced by local salinity and waterlogging. The absence of pollen, within the organic-rich silty clay between 7.63 and 7.38 metres may be a result of destructive processes during oxidation or increased sediment supply in a near-shore environment.

Quercus and *Corylus* pollen, identified within the organics between 7.38 and 7.30 metres, suggest the continued development of mixed forest communities adjacent to site 7. However, the extremely high proportion of Poaceae throughout this unit may indicate the predominance of local grass dominant saltmarsh vegetation. The concentration data suggests that the decrease in *Quercus*, Poaceae and salt-tolerant pollen at 7.32 metres reflects the local expansion of alder carr and sedge fen communities (Godwin, 1975); the change from grass-dominant saltmarsh to freshwater carr and fen habitats may represents a decrease in marine influence. The scarcity of pollen in the inorganic sediments between 7.32 and 3.76 metres may result from destruction of sporopollenin during oxidation, increased sediment supply in a near-shore environment or a combination of these processes.

LPAZ 7-2: The rise in *Alnus* indicates the local development of alder carr in areas subject to waterlogging. The inorganic and organic sediment between 3.76 and 3.51 metres is therefore likely to have accumulated within a freshwater environment dominated by alder and sedges; however, as *Alnus* can often be locally over-represented in carr communities care should be taken when interpreting these environments. Although the majority of oak and hazel pollen is likely to be derived from extra-local mixed forest in the surrounding landscape, *Quercus* may grow locally in dry areas behind the barrier. As the sediments grade from inorganic into organic sediment at 3.66 metres the concentration of both *Alnus* and Cyperaceae pollen increase (Figure 6.12); the dramatic rise in alder pollen which corresponds to the transition into organic sediment and results in the suppression of sedge on the percentage diagram (Figure 6.11). This indicates the continued development and accumulation of alder carr and sedge fen vegetation.

LPAZ 7-3: The sharp rise in Poaceae pollen indicates the development of treeless vegetation and possibly a fall in the local water table. The slight increase in *Quercus* and *Corylus* pollen frequencies may represent the local development of oak-hazel stands within the back-barrier environment (Figure 6.12).

LPAZ 7-4: The sharp rise in Cyperaceae pollen indicates a local increase in waterlogging, suggesting a transition from grass-dominant saltmarsh vegetation to freshwater fen communities. The increase in willow pollen may represent the initial development of local stands of *Salix*. The expansion of *Alnus* pollen between 3.29 and 3.23 metres causes a reduction in the concentration of Cyperaceae and *Salix* pollen, indicating the local replacement of sedge and willow by alder carr. The initial rise in Cyperaceae pollen at the onset of LPAZ 7-4 may possibly represent local changes in the distribution of sedge in response to hydrological and ecological changes within the back-barrier environment.

LPAZ 7-5: The rise in Poaceae pollen possibly implies a transition from freshwater alder carr to grass-dominant saltmarsh vegetation. This corresponds to an increase in Chenopodiaceae and extra-local pollen, which indicates greater marine and tidal influence and the possible development of saltmarsh vegetation.

The succession of plant communities within the back-barrier environment at site 7 occur in response to complex interrelationships between local hydrology and salinity. For instance, fluctuations in the frequency of alder, sedge and grass pollen reflect changes in the extent and distribution of wetter and drier areas behind the barrier.

Site 12

LPAZ 12-1: Pollen identified in the silty clay between 8.76 and 8.37 metres indicates the possible presence of extra-local pollen derived from mixed oak-hazel woodland adjacent to the site of preservation. The forest vegetation contains a high proportion of oak and hazel pollen with less elm, birch, alder, beech and pine. As previously indicated the relatively low concentrations of *Pinus* pollen must be interpreted with some caution as it may represent long-distance transport or reworking within the catchment. The local vegetation is dominated by Poaceae pollen and indicates the local presence of salt-tolerant species and Cyperaceae; this is indicative of grass-dominant saltmarsh vegetation growing at or above MHWST level.

The pollen data indicates that the organics at 5.80 metres may represent pollen derived from the development and accumulation of local treeless vegetation, dominated by Poaceae and Cyperaceae. *Quercus, Corylus, Betula* and *Alnus* pollen indicate the continued development of mixed woodland adjacent to site 12 or the local development of oak-hazel and alder-birch stands within the back-barrier environment. As the sediments grade into organic-rich silty clay at 5.76 metres the extra-local and Chenopodiaceae pollen increase whereas Poaceae and Cyperaceae diminish. The remainder of the organic and inorganic sediments in LPAZ 12-1 contain pollen indicative of local treeless vegetation dominated by Poaceae with Chenopodiaceae and Cyperaceae in local abundance. The concentration data indicates that the apparent inverse relationship between Chenopodeaceae and Cyperaceae pollen is an artifact of the percentage calculations and that the contribution from extra-local plant communities varies only slightly through this zone.

LPAZ 12-2: The onset of LPAZ 12-2 is marked by an increase in the relative proportion of extra-local pollen and a decrease in the abundance of local pollen. As the concentration of *Quercus, Corylus, Alnus* and *Tilia* pollen does not increase through this zone the rise observed

on the percentage diagram (Figure 6.13) may be result from the interplay between local and extra-local pollen sources. These sediments do contain Chenopodiaceae and *Plantago maritima* pollen in sufficient quantity to suggest that these salt-tolerant plants occur in local abundance.

LPAZ 12-3: The rise in *Alnus* pollen at the onset of zone 12-3 possibly may represent the local expansion of alder carr vegetation within the back-barrier environment. The increase of alder, associated with a decrease in the concentration of Cyperaceae and Poaceae pollen, may suggest a transition from grass-dominant saltmarsh vegetation to fresh water carr at site 12. The rise in *Betula* pollen at 3.60 metres could also support this hypothesis (Godwin, 1975). The rise in Poaceae and Calluna pollen between 3.45 and 3.22 metres indicates the development of local grass-dominated vegetation and the possible clearance of mixed-woodland adjacent to the site of preservation; although this may be supported by the observed decrease in oak, hazel and alder pollen, local stands of *Quercus*, *Corylus* and *Alnus* are likely to have been replaced by grass-dominated vegetation (Figure 6.14). The increase in Cyperaceae, *Salix* and Chenopodiaceae pollen between 3.22 and 3.13 metres may represent the development of local saltmarsh vegetation accumulating at or above MHWST. The expansion of *Alnus* and *Betula* pollen between 3.13 and 2.95 metres indicates the local development of freshwater carr, which replaces the sedge, willow and saltmarsh vegetation. *Quercus* and *Corylus* pollen indicate that oak and hazel continue to be significant contributors to mixed forest communities within the surrounding landscape and that local stands of oak and hazel may have developed in dry areas behind the barrier.

LPAZ 12-4: The rise in the *Quercus*, Cyperaceae and *Pteridium* curves above 2.90 metres may represent a decrease in the abundance of local vegetation with a continued contribution from extra-local plant communities. Cyperaceae pollen maybe derived from local sedge stands, growing between HHWST and MHWST, whereas oak and bracken pollen may originate from the adjacent woodland. The lack of pollen between 2.85 and 1.70 metres may either be due to post-depositional oxidation, which is supported by the presence of mottling, or high sedimentation rates within a near-shore environment.

The pollen identified at 1.70 metres indicates the predominance of local treeless vegetation with continued development of extra-local mixed oak, alder, birch and hazel woodland, adjacent to the site of preservation.

Site 4

LPAZ 4-1: Pollen, identified within the organic rich silty clay at 2.89 metres, suggests that the local vegetation at that level was composed predominately of sedge with an extremely low contribution from extra-local forest communities; extra-local pollen is composed of *Pinus* bladders, *Quercus* and *Polypodium*. The relatively high proportion of indeterminable grains, pine bladders and Polypodium spores suggests that these sediments contain reworked pollen and have been subject to destructive processes during oxidation. The low pollen concentrations may also indicate low pollen input into a near-shore environment subject to high sediment supply.

The sharp rise in Poaceae, associated with the transition from inorganic to organic sediment, implies a change from sedge to local grass-dominant vegetation. Although the organics at 2.80 metres contain a high pollen concentration the proportion of *Quercus*, *Alnus* and *Corylus* pollen remain relatively low. The rise in the Cyperaceae curve between 2.78 to 2.76 metres maybe an indication of increased waterlogging at this locale. Differences in the relative proportion of sedge and grass in LPAZ 4-1 are likely to be localised and represent changes in water table height.

LPAZ 4-2: The rise in *Alnus* pollen is may represent the local expansion of alder carr at site 4. The concentration of Poaceae pollen remains relatively high and the minimum value of Cyperaceae coincides with a peak in the concentration of alder and grass pollen. This may indicate a gradual change from alder and sedge carr to slightly drier alder and grass communities. Above this the decline in *Alnus* and Poaceae, associated with the recovery of Cyperaceae pollen, indicate a switch to wetter conditions in which sedge becomes a significant component of the local vegetation.

The recovery of *Alnus* and Poaceae pollen towards the top of LPAZ 4-2 indicates a transition to slightly drier conditions. The pollen imply that local vegetation is composed of alder and grass with occasional stands of willow and local presence of salt-tolerant plants such as Chenopodiaceae and *Plantago maritima*. The extra-local component, composed of *Quercus, Corylus, Ulmus, Fraxinus* and *Pinus* pollen, remains relatively low and constant throughout this zone.

LPAZ 4-3: As the sediments grade from organic into inorganic *Alnus*, Poaceae and the total pollen concentration decrease sharply (Figure 6.16). The rise in Chenopodiaceae, *Plantago maritima* and Cyperaceae pollen suggest a transition from local freshwater carr to saltmarsh vegetation. The lower pollen concentration maybe an indication of increased sediment supply in a near-shore environment and the subsequent decline in sedge is likely to represent greater marine influence. The concentration of the extra-local pollen remains relatively low and exhibits little variation.

The extremely low pollen concentrations between 2.40 and 0.50 metres may represent reworking, destruction during oxidation, increased sediment supply or a combination of these processes. Pollen between 0.50 and 0.10 metres indicates that the local vegetation is dominated by Poaceae with the local presence of Cyperaceae, Chenopodiaceae and Asteraceae (Lactuceae). The latter includes *Aster tripolium* which at present is a common component of the saltmarsh vegetation within the modern Taf Estuary. Extra-local pollen values remain low in these sediments, indicating a reduced contribution from mixed woodland adjacent to site 4.

6.2.4 Summary

From consideration of the vegetational succession within West Marsh it is clear that pollen identified within the deposits recovered from sites 7, 12 and 4 generally represent local and extra-local plant communities. None of the main regional changes in vegetation, described at Tregaron south east bog, can be identified within the incomplete sequences from West Marsh. However, the majority of the organic sediments contain pollen of *Alnus* and *Quercus* indicating that these sediments accumulated after the *Alnus* rise of approximately 6990 years BP (Hibbert and Switsur, 1976). Although the silty clay at the base of site 12 contain *Ulmus* the exact point at which this tree declines is not clear; however, the pollen data does suggest that the silty clay at the base of site 12 was deposited prior to the *Ulmus* decline at approximately 4890 years BP (Hibbert and Switsur, 1976). The under-representation elm within West Marsh may be due to low pollen production, poor dispersal, and the fact that *Ulmus* is not a constituent of the local back-barrier vegetation.

During the accumulation of organic and inorganic sediments within West Marsh mixed oak-hazel-alder woodland dominated the fossil cliffline between Pendine and Coygan, the river catchments, and the landscape above Pendine, Llanmiloe and Brook (Figure 6.10). Alder formed part of the oak canopy in wetter areas whereas hazel will have developed in openings within the forest. The inorganic sediments generally contain very little pollen, largely derived from local and extra-local vegetation. Arboreal pollen is likely to be supplied by via air transport and freshwater discharge; grains introduced into the coastal and estuarine waters by rivers draining into Carmarthen Bay would be deposited upon the marsh and mudflat surfaces during high water. Where preserved, pollen derived from local vegetation indicates that the organic rich silty clay accumulated within an environment covered by grass-dominant saltmarsh vegetation. The low pollen concentrations observed within these sediments may result from the destruction of sporopollenin during oxidation, low pollen input, high sediment supply in a near-shore environment or a combination of these processes.

The organic detritus identified at sites 7, 12 and 4 represent the deposition and accumulation of plant debris within a predominately freshwater back-barrier environment. Although the area has largely been isolated from significant marine influence, during periods of organic accumulation the main successions in vegetation occur in response to local changes in hydrology and salinity; for instance, pollen indicative of saltmarsh vegetation have been identified within the upper organic unit at site 4. Analysis of the pollen analytical data highlights the complexity of local vegetational development within the back-barrier environment, the distribution of sub-environments within the system and the interplay between local, extra-local and regional pollen. The increase in *Alnus* pollen, observed within the upper organic units at all three sites, represents the local development of alder carr within West Marsh and not the regional rise in alder. Fluctuations in the relative frequency of *Alnus* and Cyperaceae represent the complex hydrology within the back-barrier area during periods of organic accumulation. Variations in the quantity of *Quercus* and *Corylus* pollen may represent periods of oak and hazel growth within drier areas behind the barrier. The difficulties encountered when reconstructing former vegetational succession within West Marsh are unsurprising. Modern coastal fen-carr environments, such as Oxwich Marsh on the Gower Peninsula, contain a whole series of sub-environments dominated by distinctive floras.

The transition from organic-rich silty clay into organic detritus corresponds to a gradual change from saltmarsh vegetation to sedge fen and then alder carr. Similarly, as the sediments grade from organic detritus into organic rich silty clay the pollen indicate a change from freshwater carr into saltmarsh vegetation. This suggests that the transition from freshwater organics to intertidal saltmarsh sediment represent continuous sedimentation under increasing marine influence. Although the majority of the organics units in West Marsh represent the accumulation of freshwater vegetation above the HHWST level they contain pollen indicative of grass-dominant saltmarsh vegetation which suggests that they were periodically subject to marine influence. For instance, when extremely high spring tides coincided with large storms it is possible the sea inundated the fen communities at the back of the saltmarsh.

6.3 Radiocarbon Dating

6.3.1 Radiocarbon results

Site 7

The organic bed between -5.60 to -5.53 metres OD is composed of organic-rich sand, which contains 10% organic matter. This level has been dated at 6230 ± 125 BP. (Table 6.2). The remaining three samples were taken from fine-grained silty organic detritus and fine-grained organic detritus. The organic content varies between 38% and 85% and the samples contain small fragments of wood and sedge (Table 6.2).

The organics between -3.62 and -3.59 metres OD have been dated at 5770 ± 45 BP.. The base of the upper organic bed between 0.20 and 0.23 metres OD is dated at 4165 ± 50 BP., whereas the top of this unit is dated at 3890 ± 50 BP. (Table 6.2).

Site 12

The samples taken from site 12 are composed of silty organic detritus and fine-grained organic detritus. The organic content varies between 20% and 60% and these samples contain small fragments of wood and sedge (Table 6.2).

The organics between -2.23 and -2.20 metres OD have been dated at 5920 ± 50 BP.. The base of the upper organic bed at -0.21 metres OD has been dated at 4630 ± 45 BP., whereas the top of this unit is measured at 3580 ± 45 BP. (Table 6.2).

Site 4

Samples taken from site 4 are composed of fine-grained organic detritus and fine-grained silty organic detritus. The organic content varies between 49% and 82% and the samples contain small fragments of wood and sedge (Table 6.2).

Site	Location NGR	Lab Ref.	Depth m	Depth OD	Date BP.	Stratigraphic position	Sample composition	% OM.
7	2246, 2084	SRR	9.35-9.32	-5.60 to -5.53	6230 +/- 125	Contact between sandy organics and silty clay	Sandy organic detritus	10
		SRR	7.34-7.31	-3.59 to -3.62	5770 +/- 45	Top of a thin organic layer	Fine grained silty organic detritus	38
		SRR	3.55-3.52	0.20 to 0.23	4165 +/- 50	Base of upper organic unit	Fine grained organic detritus	85
		SRR	3.10-3.07	0.65 to 0.68	3890 +/- 50	Top of upper organic unit	Fine grained silty organic detritus	46
12	2256, 2087	SRR	5.83-5.80	-2.23 to -2.20	5920 +/- 50	Base of a thin organic unit	Silty organic detritus	20
		SRR	3.81-3.78	-0.21 to -0.18	4630 +/- 45	Base of upper organic unit	Fine grained organic detritus	60
		SRR	3.15-3.12	0.45 to 0.48	3580 +/- 45	Top of upper organic unit	Fine grained silty organic detritus	37
4	2267, 2089	SRR	5.73-5.70	-1.81 to -1.78	6220 +/- 45	Base of lower organic unit	Fine grained organic detritus	82
		SRR	2.78-2.75	1.14 to 1.17	4380 +/- 50	Base of upper organic unit	Fine grained organic detritus	77
		SRR	2.49-2.46	1.43 to 1.46	3810 +/- 50	Top of upper organic unit	Fine grained silty organic detritus	49

Table 6.2 Radiocarbon dates obtained from organic level in West Marsh.

The organics between -1.81 and -1.78 metres OD are dated at 6220 ± 45 BP. The base of the upper organic bed between 1.14 and 1.17 metres OD is dated at 4380 ± 50 BP., whereas the top of this unit is has a ^{14}C age of 3810 ± 50 BP. (Table 6.2).

6.3.2 Discussion of ^{14}C dates

All ten samples contain a variable amount of allochthonous material composed principally of fine grained inorganic sediment, probably introduced via freshwater streams draining from the fossil cliffline and tidal in-washing, during periods of elevated sea-level. The organics probably represent *insitu* accumulation of organic detritus which have not been affected by oxidation or bioturbation.

Four brooks, with relatively small catchments, drain from the Lower Old Red Sandstone Measures into West Marsh. The streams presently draining into West Marsh do not originate from areas of limestone or calcareous soils and the palaeohydrology during the Holocene is not likely to have been too dissimilar. If so the levels of dissolved carbonate and inert carbon within the freshwater streams, at the time of organic accumulation, is likely to have been low. Furthermore, the low levels of aquatic pollen identified within the organics at sites 7, 12 and 4 indicate that sub-aquatic photosynthesis is unlikely to have further diluted ^{14}C levels within these deposits. On the basis of this evidence it is extremely unlikely that hard-water error has influenced the ^{14}C ages determined for sites 7, 12 and 4.

Other than the 'constant and unavoidable source of contamination' (Mook and Van de Plassche, 1986) during the formation of these organic deposits, contamination from root penetration is thought to be minimal as these units contain no recognisable roots and rootlets.

The relatively large standard deviation determined for the organic sand at site 7 is probably due to the extremely small amount of organics contained within this deposit. Increasing the measuring time or sample size would reduce the σ value. The gradual contacts between organic and inorganic sediment at sites 7, 12 and 4 indicates that the peat bed surfaces have not been eroded. The pollen data suggests that the sediments analysed within West Marsh accumulated

after the regional rise in *Alnus*, approximately 6990 years BP. (Hibbert and Switsur, 1976). On the basis of this evidence it is clear that the ^{14}C dates are accurate and have not been significantly affected by contamination or hard-water error.

Chapter 7

Discussion

7.1 Introduction

The sand barrier which now extends from Gilman Point near Pendine to the confluence of the rivers Taf, Towy and Gwendraeth at Ginst Point forms the landward portion of extensive intertidal sandflats within Carmarthen Bay (Figure 7.1). The barrier is comprised of two discrete dune systems known as the Pendine Burrows and Laugharne Burrows which were separated by the Wytchet tidal inlet prior to marsh reclamation between 1660 AD and the late 19th century (James, 1991). The back-barrier area can be divided into West Marsh and East Marsh which lie behind the two dune systems respectively. The Pendine/Laugharne barrier complex has formed within a region with one of the largest tidal ranges in the world; this is unusual as sand barriers elsewhere of similar dimensions are confined to micro- and meso-tidal environments (Hayes, 1975).

Boreholes undertaken behind the barrier reveal very different sedimentary sequences within West Marsh and East Marsh. Geophysical data obtained from refraction surveys, from high-resolution multi-channel reflection lines in the intertidal zone and from a shallow marine reflection survey within the Taf Estuary provide a information on the pre-transgressive surface beneath the study area. Foraminifera, contained within the minerogenic deposits, are used for the identification and interpretation of sedimentary facies changes within the back-barrier area; pollen analytical data describe vegetational and ecological changes within West Marsh during phases of organic accumulation. The evidence described and discussed in the preceding chapters is used to construct a series of cross-sections which show back-barrier facies development. On the basis of the facies changes within West Marsh and East Marsh a qualitative model is proposed which aims to describe the formation and subsequent evolution of the barrier system during the Holocene.

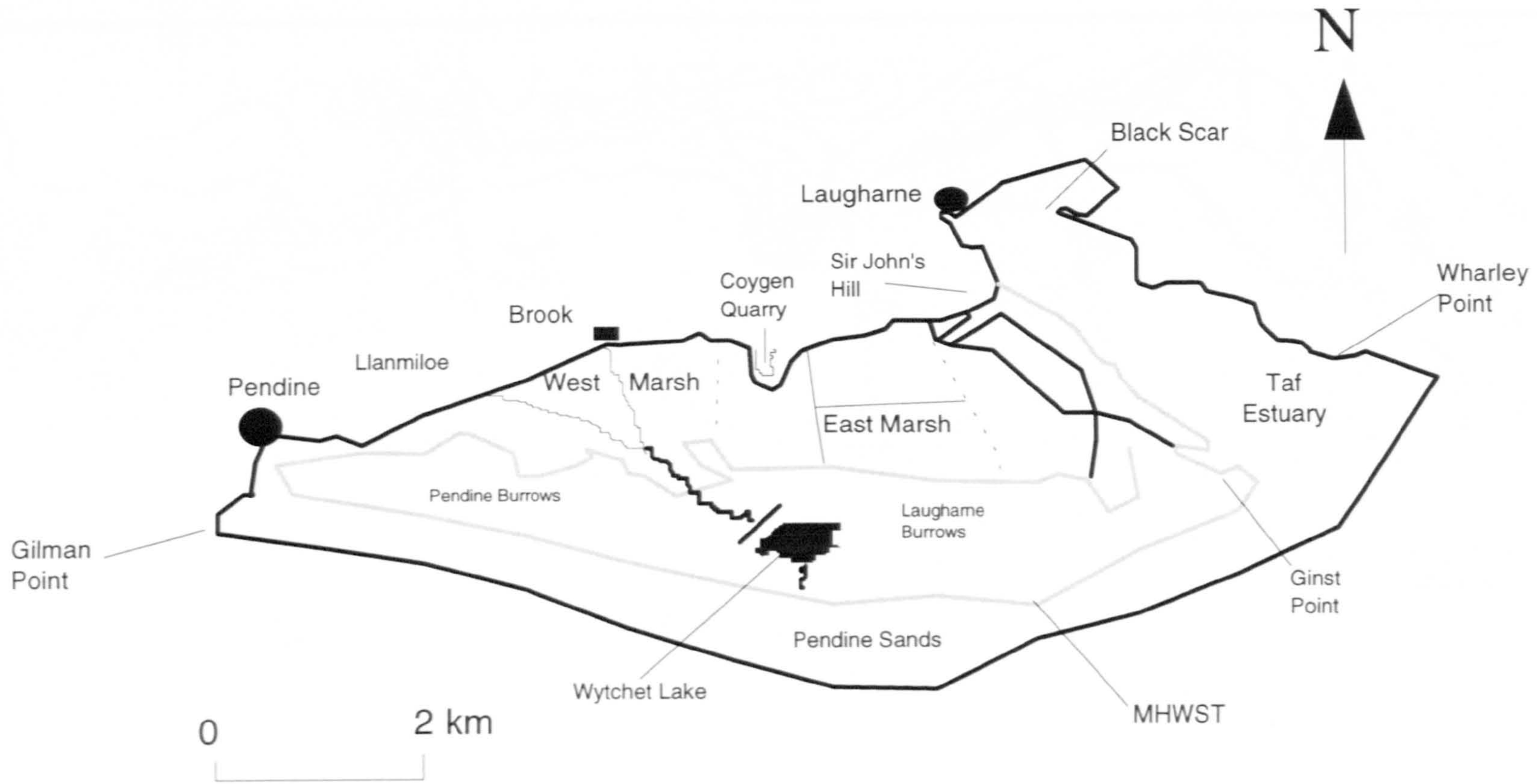

Figure 7.1 The Pendine/Laugharne barrier system

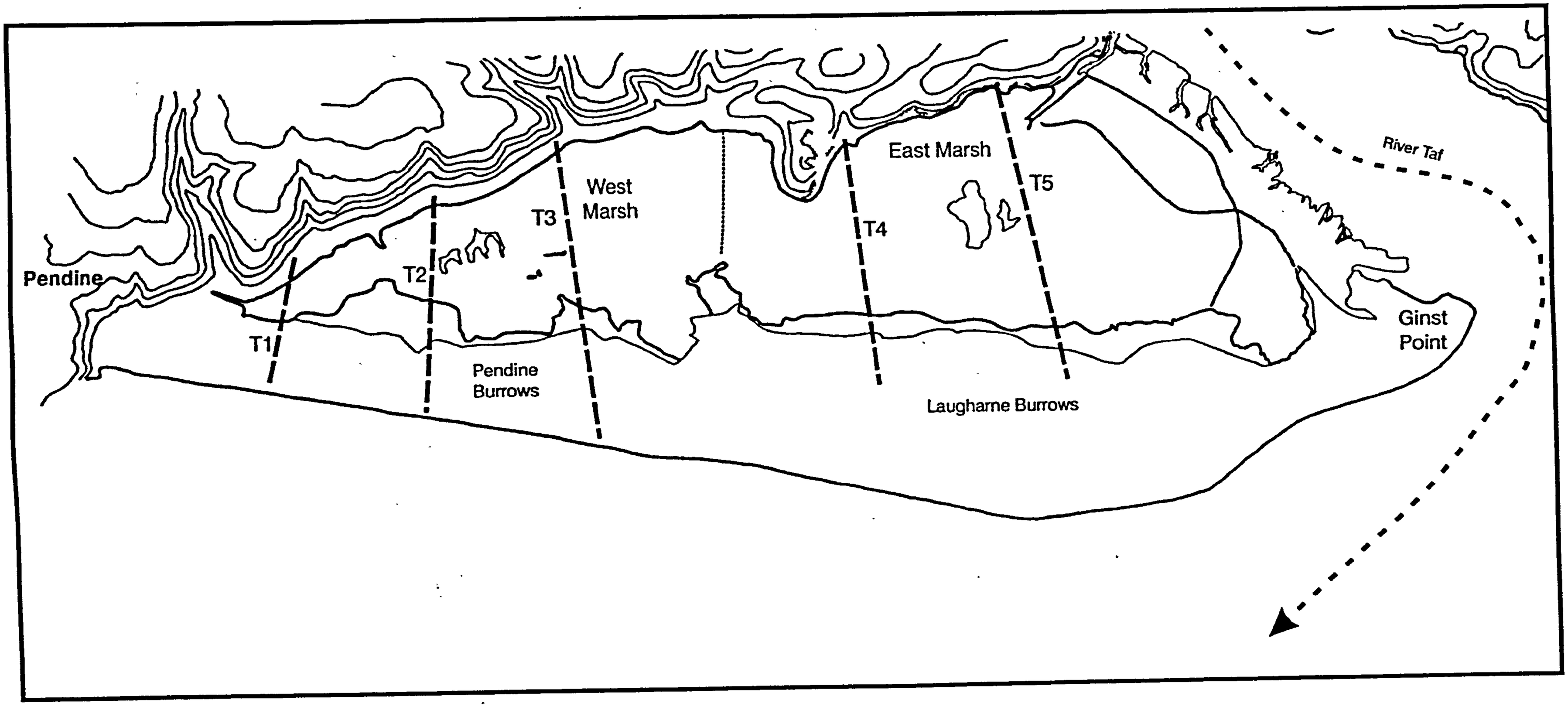

Figure 7.2 Position of stratigraphic sections in West Marsh and East Marsh.

Mechanisms which are believed to control barrier development are discussed in the context of the Pendine barrier. These include rates of relative sea-level rise and differential sediment supply, the tidal range, storm activity and the influence of the antecedent topography.

7.2 Sedimentary facies development

7.2.1 West Marsh

Biostratigraphic and lithostratigraphic evidence from boreholes recovered in West Marsh have been used to construct three cross-sections (Figure 7.2). The sediment sequences are dominated by stratified minerogenic saltmarsh facies intercalated with freshwater biogenic units, mudflat/sandflat sediment and occasional washover/blowout deposits.

Pendine Woodend section

The Pendine Woodend section (T1) extends from the fossil cliffline west of Llanmiloe across West Marsh and the Pendine Burrows (Figure 7.3). The stratified silty sand at the base of site 7 represents poorly-sorted sandflat sediment intercalated with finer deposits (section 6.1.6). This facies grades laterally into well-sorted medium fine sand between sites 7 and 8; the composition and distribution of these sands indicates that these deposits may represent washover or blowout events associated with periods of barrier breaching. The sandflat and washover facies are replaced by stratified silty clay, interpreted as consisting of mudflat and low marsh facies. Pollen data indicates that local saltmarsh vegetation and freshwater fen communities developed locally upon or adjacent to this area (Table 7.1). The saltmarsh facies at site 7 is intercalated with a unit of stratified sand and gravel. The base of the gravel layer is marked by an abrupt erosional contact and sands at the top of this unit contain a high proportion of organic material. This gravel layer does not occur at site 8 and has not been identified at any other locality within West Marsh; these deposits are believed to represent a former fluvial channel possibly generated by the stream draining from the fossil cliffline west of T1 (Figure 7.2). The organic-rich sands between -5.60 and -5.57 metres OD, which have been radiocarbon dated at 6230 ± 125 years BP, may have been

Key for lithological logs

Organic Detritus

Silty Clay

Stratified Sandy Silt / Silty Sand

Sand

Poorly sorted gravel

Key for lithological logs

Organic Detritus

Silty Clay

Stratified Sandy Silt / Silty Sand

Sand

Poorly sorted gravel

Site 7

	Height metres OD	Radiocarbon dates years BP	Lithology	Interpretation
Ground surface_	3.75 1.70		Sand grades into stratified silty clay which becomes mottled near the ground surface	Sandflat deposits grade into mudflat and marsh facies - development of grass-dominant saltmarsh vegetation
	1.70 0.80		Silty sand in sharp contact with stratified grey sand containing shell fragments	Abrupt change from creek channel facies into high energy sandflat deposits
	0.80 0.70		Organics grade into grey organic rich silty clay which is overlain by stratified sandy silt	Freshwater organics grade into saltmarsh and creek channel facies - local abundance of salt-tolerant species
	0.70 0.06	3890 +/- 50 (0.68 to 0.65 m OD) 4165 +/- 50 (0.23 to0 .20 m OD)	Silty clay grades into black organic detritus	Transition from sedge-dominant fen to alder-dominant carr - this is replaced by grass-dominant vegetation - freshwater fen - alder carr and grass-dominant saltmarsh vegetation
	0.06 -0.08		Silty sand grades into dark grey organic rich silty clay	Mudflat facies grades into creek channel and marsh deposits - local abundance of salt-tolerant species which are replaced by sedge fen
	-0.08 -1.56		Silty clay grades into highly stratified silty sand	Marsh deposits replaced by high energy mudflat and sand flat facies
	-1.56 -3.55		Black organic detritus grades into stratified grey silty clay	Marginal fresh/saline organic facies grades into high/mid- marsh deposits
	-3.55 -3.65	5770 +/- 45 (-3.56 to -3.59 m OD)	Organic rich silty clay grades into stratified organic detritus	Marsh facies is succeeded by marginal fresh/saline mire at or above MHWST level stratified by saltmarsh deposits
	-3.65 -5.50		Organic rich sand grades into organic rich silty clay	Freshwater fen replaced by marsh facies - local abundance of salt-tolerant vegetation
	-5.50 -6.10	6230 +/- 125 (-5.57 to -5.60 m OD)	Silty clay overlain by stratified grey sands, gravels and organic rich sand	Poorly sorted gravel over/under- lain by well sorted fluvial sand - accumulation and development of freshwater fen on top of the gravel bed
	-6.10 -7.25		Stratified grey silt grades into silty clay	Mudflat facies grades into creek channel and marsh deposits - local development of saltmarsh and freshwater fen vegetation
	-7.25 -8.25		Stratified grey silty sand grades into sandy silt	High energy sandflat deposits replaced by mudflat facies

Table 7.1 Facies development at site 7 during the Holocene

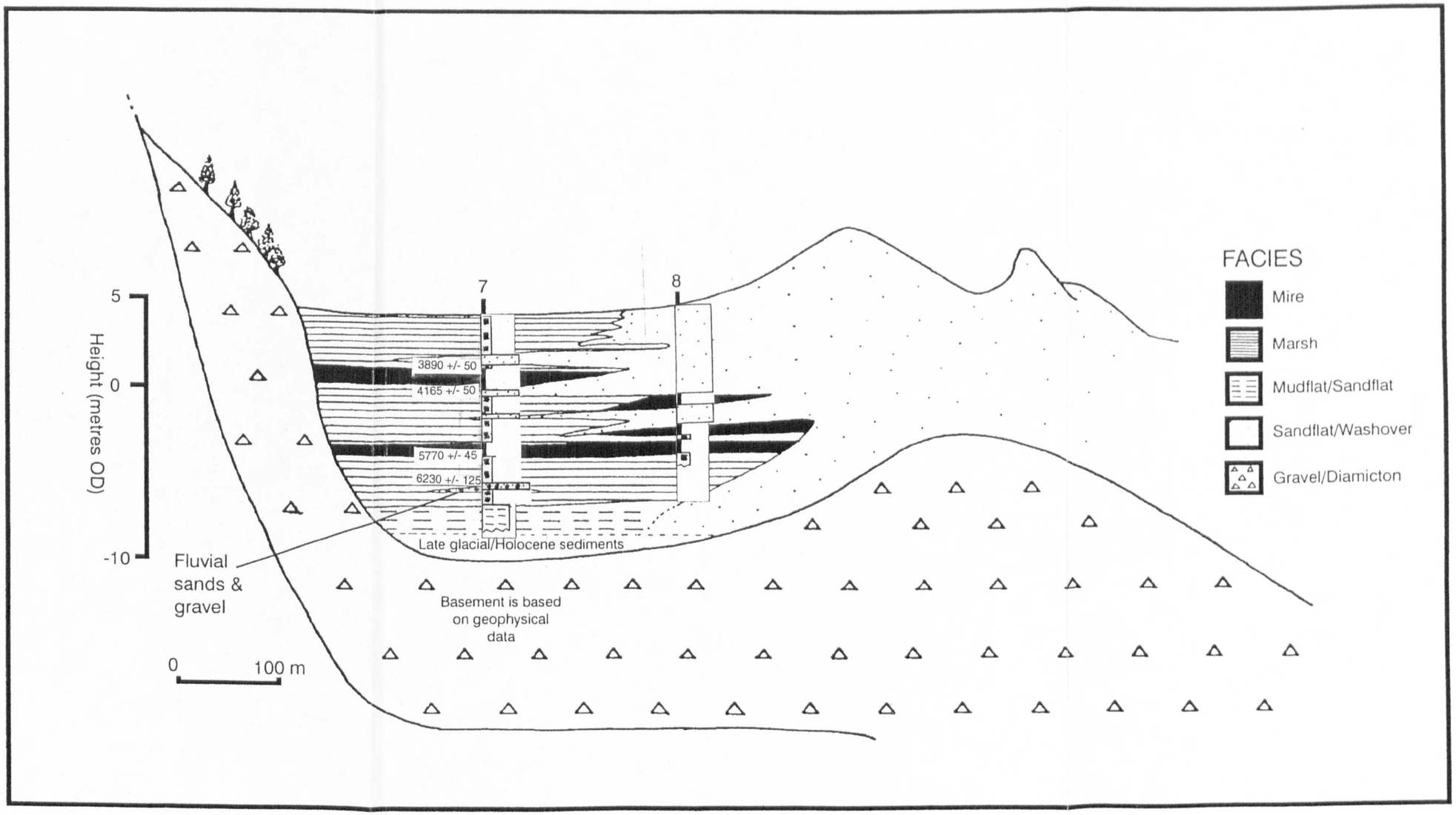

Figure 7.3 Stratigraphic section (T1) based on lithological data from sites 7 and 8.

deposited below MHWST level within a freshwater drainage channel. Pollen data indicates the local development of grass- and sedge-dominant fen communities (section 6.2.5).

The drainage channel is infilled with the saltmarsh deposits which continue up to -3.65 metres OD where the sediment grades from organic-rich silty clay into black organic detritus (Table 7.1). This organic layer occurs at sites 7 and 8 and is stratified by lenses of organic-rich silty clay (Figure 7.3). Pollen analysis indicates that these organics represent the local development of a freshwater mire with discrete lenses of saltmarsh sediment. The top of this organic unit has been radiocarbon dated as 5770 ± 45 years BP (Table 7.1). The stratified organics then grade into a stratified saltmarsh facies which is overlain by highly-stratified silts and sands.

At site 8 two organic units, between -3.55 and 0.06 metres OD, are interstratified and overlain by well-sorted medium fine sand (Figure 7.3). The latter continue up to the ground surface at site 8 and the boundaries between the organic and sand beds are marked by abrupt erosional contacts. As the sands extend across the back-barrier area it is possible that they may represent washover sediment deposited by storm waves breaching the barrier. Although pollen analysis was not conducted on the organics at site 8 the two upper organic levels probably represent the local development of freshwater vegetation above the MHWST level. The absence of these organic levels at site 7 is believed to reflect the complex hydrology within this area and variations in the height of the back-barrier surface rather than the removal of this deposit *i.e.* at this time the surface of site 7 may have been located below the MHWST level.

The stratified silt and sand facies between -1.56 and -0.08 metres OD at site 7, contains washover deposits which are replaced by a thin layer of organic-rich silty clay. Pollen analysis indicates that as these fine-grained marsh and mudflat deposits grade into organic detritus at 0.06 metres OD the local grass-dominant saltmarsh vegetation is replaced by sedge-fen and alder-carr communities (section 6.2). The base of these organics have been radiocarbon dated at 4165 ± 50 years BP whereas the top of this unit is dated at 3890 ± 50 years BP (Table 7.1). During this phase of organic accumulation alder-carr is replaced by grass- and sedge- dominant vegetation; this is then followed by a re-expansion of carr communities. These vegetational changes may reflect changes in the height of the local water table or the opening up of alder-carr. The contact between organic detritus and organic-rich silty clay and sandy silt at 0.70 metres OD corresponds

to a transition from alder-carr to grass-dominant saltmarsh vegetation. The fine-grained saltmarsh facies continues to 0.80 metres OD where they are replaced by well-sorted sand containing shell fragments. These sands extend across the back-barrier area and probably represent either washover or blowout deposits. The latter are overlain by fine-grained saltmarsh facies which becomes oxidised towards the ground surface.

Westmead section

The Westmead section (T2) extends from the fossil cliffline, east of Llanmiloe, across West Marsh and the Pendine Burrows (Figure 7.2). The silty sand facies at the base of the sequence represent high-energy sandflat deposits which grade laterally into well-sorted medium fine sand between sites 12 and 9 (Figure 7.4). These sandflats are replaced by mudflat deposits which grade into saltmarsh creek, low marsh and high/mid- marsh facies. Lithostratigraphic evidence from T2 indicates that the saltmarsh initially abutted against the fossil cliffline and subsequently extended across the mudflat and sandflat deposits towards the Pendine Burrows (Figure 7.4). The saltmarsh facies extends to approximately -2.21 metres OD at sites 5 and 12 where organic-rich silty clay is replaced by black organic detritus. The base of this unit is radiocarbon dated at 5920 ± 50 years BP (Table 7.2). Pollen analysis indicates that the lower organic unit at sites 5 and 12 represents the development of grass- and sedge-dominant vegetation at or above MHWST (section 6.2.5). The local abundance of salt-tolerant pollen may represent extra-local pollen from saltmarsh vegetation within the back-barrier area or indicate that these environments were periodically inundated by the tide. The lower organic unit is replaced by high/mid-marsh and low marsh facies which extend to approximately -0.28 metres OD where they are replaced by a second organic unit. At site 9 the silty clay between -1.95 and 0.28 metres OD are intercalated with well-sorted medium fine sand containing reworked shell fragments (Figure 7.4). These deposits may represent washover or blowout deposits introduced into the back-barrier area during periods of barrier instability. The lack of organics at sites 6 and 9 indicates that the hydrology at these locales may have been unsuitable for organic accumulation or that the organics have subsequently been removed.

The base of the upper organic unit at site 12 has been radiocarbon dated at 4630 ± 45 years BP whereas the top of this unit is dated at 3580 ± 60 years BP (Table 7.2). The transition from the

Key for lithological logs

Organic Detritus

Silty Clay

Stratified Sandy Silt / Silty Sand

Sand

Poorly sorted gravel

Site 12

Height metres OD	Radiocarbon date Years BP.	Lithology	Interpretation
Ground surface_ 3.6 2.05		Silty clay	Continued accumulation of saltmarsh facies
2.05 0.48		Organic detritus grades into silty clay	Fen communities replaced by grass-dominant saltmarsh vegetation; accumulation of high/mid-marsh facies
0.48 -0.08	3580 +/- 60	Black organic detritus	Local expansion of alder carr at site 12 replaces sedge fen vegetation at or above the HHWST level
-0.08 -0.28	4630 +/- 45	Organic rich silty clay grades into organic detritus	Saltmarsh vegetation replaced by grass and sedge, deposited in a predominately fresh water environment
-0.28 -1.95		Organics replaced by silty clay	Transition from freshwater fen into salt-marsh vegetation high/mid- marsh and low marsh facies are replaced by mudflat deposits
-1.95 -2.24	5920 +/- 50	Silty clay grades into organic detritus stratified by organic rich silty clay	Accumulation of grass- and sedge-dominant vegetation at or above MHWST level; saltmarsh vegetation occurs in local abundance
-2.24 -3.25		Silt grades into organic-rich silty clay intercalated with sandy silt beds	Creek channel deposits are replaced by low and high/mid- marsh facies marsh facies
-3.25 -4.65		Silty clay in sharp contact highly stratified sandy silt	Saltmarsh facies replaced by high energy mudflat and sandflat deposits
-4.65 -5.25		Sandy silt grades into organic-rich silty clay	Mudflat facies replaced by creek channel and marsh deposits; grass-dominant saltmarsh vegetation in local abundance
-5.25 -6.4		Silty clay replaced by sandy silt	Creek channel deposits replaced by high energy mudflat facies
-6.4 -7.05		Silt grades into silty clay stratified by numerous sand lenses	Transition from mudflat into marsh creek channel facies
-7.05 -8.4		Horizontally bedded silty sand grade into sandy silt	High energy sandflat deposits replaced mudflat facies

Table 7.2 Facies development at site 12 during the Holocene

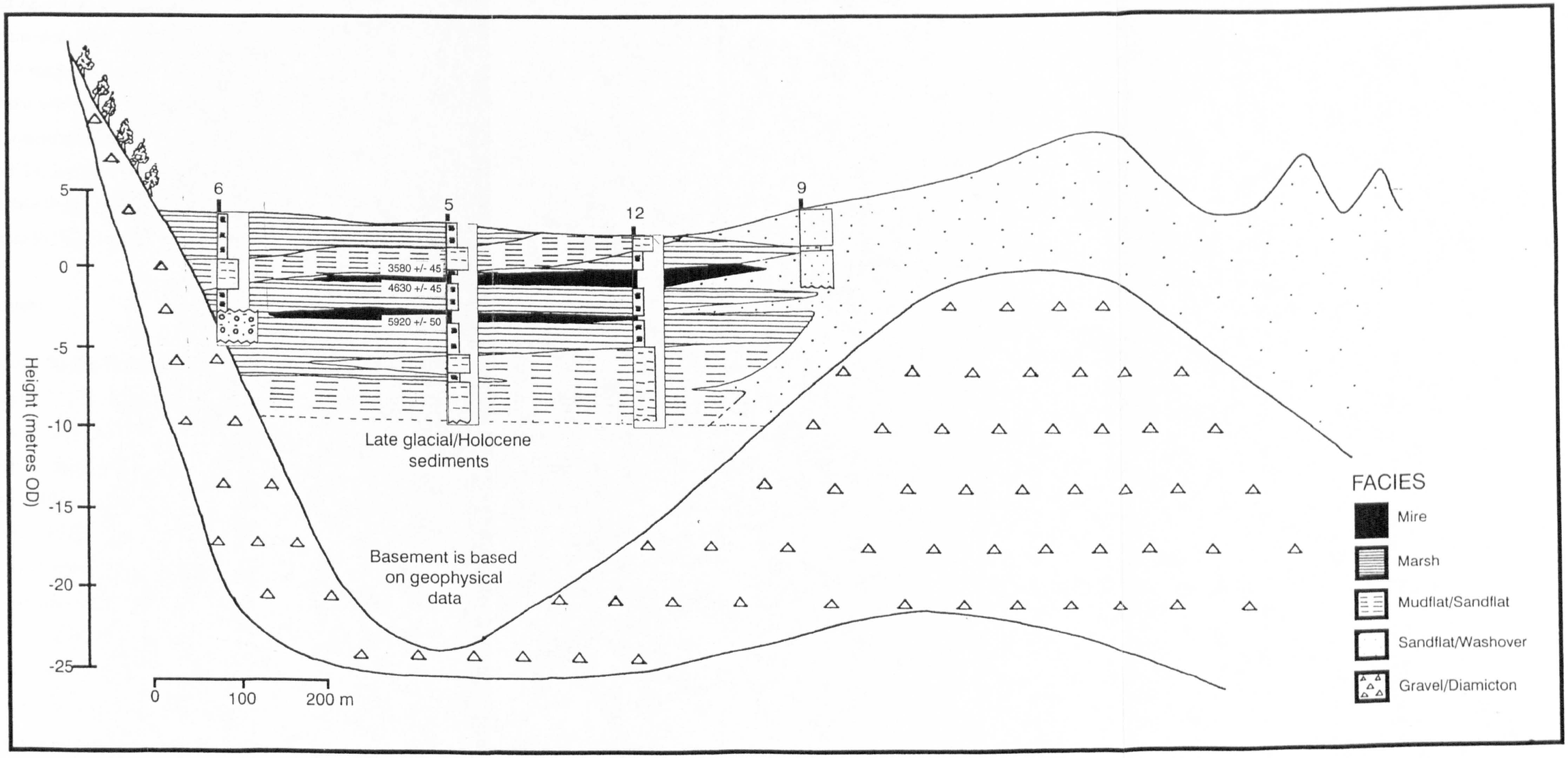

Figure 7.4 Stratigraphic section (T2) based on lithological data from sites 6, 5, 12 and 9.

marsh facies to organic detritus is marked by a switch from grass-dominant saltmarsh vegetation to sedge-dominant fen communities; the latter is replaced by alder-carr. The upper organic unit at sites 5 and 12 grades into a saltmarsh facies which corresponds to the local development of grass-dominant saltmarsh vegetation. Sandflat and mudflat deposits overlying the saltmarsh facies at site 6 suggests that as the back-barrier area was once again subject to greater marine influence a tidal inlet opened up adjacent to the fossil cliffline (Figure 7.4). The tidal inlet was forced to migrate towards the Pendine Burrows, over the underlying saltmarsh and organic facies at site 5 and 12, by the development of saltmarshes along the fossil cliffline (Figure 7.4). Lithological data from site 9 suggests that the inlet was ultimately infilled by washover deposits introduced into the back-barrier area by storm waves.

Brook Section

Brook Section (T3) extends from the fossil cliffline at Brook across West Marsh and the Pendine Burrows (Figure 7.2). Foraminifera contained within the highly-stratified silty clay at the base of site 4 show the development of creek channels and low marsh deposits which formed on top of Pleistocene till (section 6.1.6); this indicates that the high energy shoreface did not rework the pre-Holocene surface beneath site 4 (Table 7.3). These sediments are replaced by high/mid-marsh sediments which extend seawards towards the Pendine Burrows (Figure 7.5). At the base of site 11 well-sorted sand, possibly deposited within a tidal inlet or in response to washover/blowout events, is replaced by mudflat deposits which grade into high/mid-marsh facies (Table 7.4). These fine-grained sediments are believed to coincide with the saltmarsh facies at the base of site 4 and represent the same phase of back-barrier marsh development (Figure 7.5). At site 4 the saltmarsh facies continues up to -1.82 metres OD where fine-grained minerogenic sediment is replaced by black organic detritus (Table 7.3); the accumulation of freshwater biogenic sediment represents a regressive overlap defined by a decrease in marine influence. The base of this organic unit, which extends from -1.82 to -1.26 metres OD, has been radiocarbon dated at 6220 ± 45 years BP. Comparison of sites 4 and 11 indicates that while freshwater organics were accumulating in the area in front of Brook, saltmarshes probably continued to develop at site 11 where marine conditions persisted. The transition from freshwater organics to high/mid-marsh facies at site 4 corresponds to a change from saltmarsh facies to mudflat and then sandflat facies at site 11 (Table 7.4). The latter is composed predominantly of well-sorted sands

Key for lithological logs

Organic Detritus

Silty Clay

Stratified Sandy Silt / Silty Sand

Sand

Poorly sorted gravel

Site 4

Height (metres OD)	Radiocarbon date Years BP.	Lithology	Interpretation
Ground surface_ 3.92		Silty clay replaced by mottled dark brown clayey silt	Creek channel facies replaced by mudfla facies
2.35			
2.35		Organics overlain by silty clay	Transition into marsh and creek channel facies with the development of saltmarsh vegetation
1.46			
1.46	3810 +/- 60	Dark red organic detritus	Local expansion of alder carr upon a freshwater rhetotrophic mire above the HHWST level
1.22			
1.22	4380 +/- 50	Organic rich silty clay grades into black organic detritus	Local grass-dominated saltmarsh vegetation replaced by freshwater sedge fen
1.13			
1.13		Highly stratified sand grades into grey silty clay	Replacement of mudflat facies by low and high/mid- marsh facies; local freshwater fen dominated by sedge
0.77			
0.77		Silty clay overlain by sand stratified by thin layers of silty clay	Progressive change from creek channel facies into low/high energy mudflat
-0.86			
-0.86		Organics grade into highly stratified grey silty clay	Replacement of high/mid- marsh facies by low marsh and creek channel facies
-1.26			
-1.26		Black organic detritus composed of fine-grained detritus and horizontally compressed wood	The accumulation of plant debris between MHWST and HHWST in a predominately freshwater environment
-1.82	6220 +/- 45		
-1.82		Highly stratified grey silty clay	Replacement of creek channel facies by low marsh and high/mid- marsh deposits
-4.31			
-4.31		Poorly sorted dense red gravel/till	Deposited during the Late Devensian

Table 7.3 Facies development at site 4 during the Holocene

Site 11

	Height metres OD	Lithology	Interpretation
Ground surface_	3.99 2.63	Sand grades into highly stratified mottled brown sandy silt	Sandflat deposits are intercalated with a mudflat facies
	2.63 -0.73	Stratified grey sand	Mudflat deposits are replaced by a sandflat facies
	-0.73 -1.01	Sand replaced by stratified grey clayey silt containing lenses of well sorted sand	Creek channel deposits are stratified by thin lenses of sandflat sediment
	-1.01 -1.43	Sharp change from silty clay into shelly sand	Abrupt change from mudflat into sandflat facies
	-1.43 -2.66	Sand replaced by highly stratified grey silty sand which grades into stratified silty clay	Sandflat deposits grade into a mudflat facies which are succeeded by creek channel sediments
	-2.66 -4.56	Stratified grey sand containing shell fragments* intercalated with thin silty beds	Mudflat deposits grade abruptly into a sandflat facies
	-4.56 -5.66	Stratified grey silty sand in sharp contact with the under-lying unit	Creek channel facies are abruptly replaced by high energy mudflat deposits
	-5.66 -6.76	Stratified dark grey silty clay grades into organic rich silty clay	Mudflats are replaced by creek channel deposits which grade into high/mid-marsh facies; the latter are succeeded by creek marsh facies
	-6.76 -8.01	Well sorted grey sand overlain by silty clay	Sandflat facies grade into mudflat deposits

Table 7.4 Facies development at site 11 during the Holocene

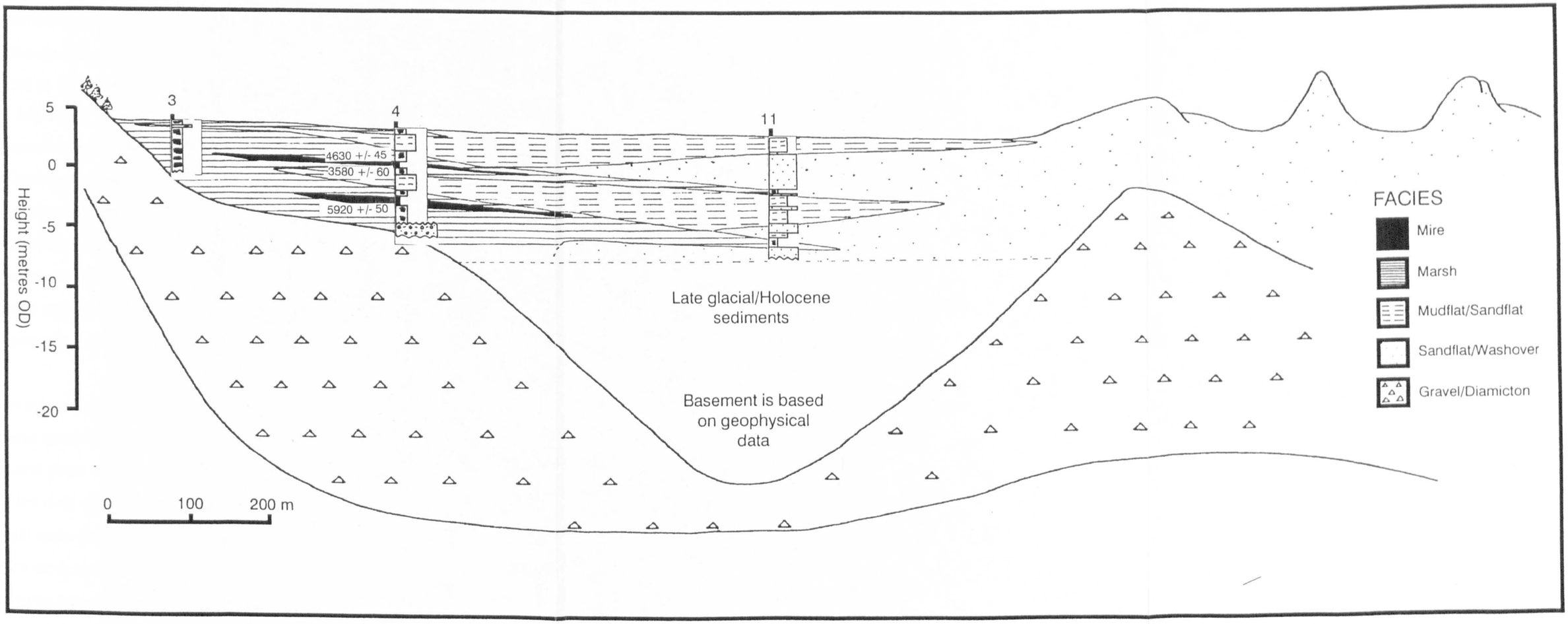

Figure 7.5 Stratigraphic section (T3) based on lithological data from sites 3, 4 and 11.

containing shell fragments, and is intercalated with thin beds of silty clay; these deposits may represent tidal inlet facies possibly deposited within an intertidal creek in the back-barrier environment.

Above this, the transgressive sequence from marsh to mudflat facies at site 4 suggest that the intertidal channel increased in width and the back-barrier area was subject to greater marine influence (Figure 7.5). However, the mudflat deposits at site 4 are replaced by a creek channel facies at 0.77 metres OD (Table 7.3). The latter grades into low-marsh facies which is overlain by high/mid- marsh sediment. Pollen analysis at site 4 indicates that sedge-dominant fen communities develop locally towards the top of this unit suggesting a decrease in marine influence and therefore a second regressive overlap. The contact between minerogenic and biogenic sediment at 1.13 metres OD corresponds to a transition from grass-dominant saltmarsh vegetation to a freshwater mire (Table 7.3). This is followed by the local expansion of alder-carr vegetation at site 4 and implies that freshwater conditions persisted at this locale. The base of this upper organic unit at site 4 has been dated at 4380 ± 50 years BP where as the top of these organics are dated at 3810 ± 60 years BP.

The upper biogenic unit at site 4 coincides with the formation and accumulation of mudflat and marsh creek deposits at site 11 (Table 7.4). These regressive sequences probably represent a second phase of barrier stability and decreasing marine influence within West Marsh. However, pollen data indicates that as the upper organic unit grades into minerogenic marsh at site 4 the vegetation switches from alder-carr to salt-tolerant vegetation; this corresponds to a transition from creek and mudflat facies to sandflat sediment at site 11. The latter may represent washover material deposited in response to storm waves breaching the barrier (Figure 7.5). Above this the marsh and sandflat facies are replaced by mudflat deposits which ultimately extend across the marsh surface at site 3 (Figure 7.5). Lithostratigraphic data from sites 3 and 4 suggest that during the late Holocene marshes began to prograde seawards from the fossil cliffline at Brook acrossthe intertidal sand and mudflats.

7.2.2 East Marsh

Biostratigraphic and lithostratigraphic data from boreholes recovered in East Marsh have been used to construct two transects within East Marsh. In contrast to West Marsh the sediments behind the Laugharne Burrows are dominated by sandflat and mudflat facies which are intercalated with relatively thin layers of minerogenic saltmarsh sediment. No biogenic saltmarsh or freshwater deposits were identified within East Marsh.

Causeway Section

Causeway section (T4) extends from the fossil cliffline adjacent to Coygan Quarry across East Marsh and the Laugharne Burrows (Figure 7.2). Foraminifera contained within the well sorted shelly sand at the base of site 17 identify these deposits as a high energy sandflat facies (Table 7.5). The height of the sandflat deposits at the base of the sequence increases towards the fossil cliffline (Figure 7.6). These sands may represent deposition within a sandy bay possibly prior to the formation of the Pendine Burrows. At sites 16 and 17 the sands are replaced by silty clay intercalated with sandflat sediment (Figure 7.6). These deposits contain whole *Cerastoderma edule* shells (Table 7.5) which are indicative of clean sand, muddy sand, mud or muddy gravel deposited within open bays or brackish estuaries. *Cerastoderma edule* are commonly found around the British Isles between the mid-tide level and low water (Tebble, 1976).

At sites 15 and 19 well sorted sand at the base of the sequence grades into a fine-grained saltmarsh facies. These deposits represent the formation and development of saltmarshes adjacent to the fossil cliffline at Coygan and behind the Laugharne Burrows, separated by an intertidal drainage channels. At sites 18 and 19 the saltmarsh facies is overlain by well-sorted medium fine sand which extends across the mudflat deposits at the base of sites 16 and 17 (Figure 7.6). This facies may represent beach and barrier sands deposited into the back-barrier area by storm waves during a period of barrier instability. Above this the sand grades back into stratified mudflat sediment (Figure 7.6).

The saltmarsh adjacent to the fossil cliffline at Coygan appears to have subsequently extended across the mudflat/sandflat facies identified beneath sites 16 and 17 (Table 7.5). However, the saltmarsh deposits at sites 15, 16 and 17 are overlain by intertidal channel deposits; this

Key for lithological logs

Organic Detritus

Silty Clay

Stratified Sandy Silt / Silty Sand

Sand

Poorly sorted gravel

Site 17

Height metres OD	Lithology	Interpretation
Ground Surface_ 4.3	Strong mottled brown sand	Abrupt change into sandflat facies
3.83		
3.83	Mottled brown sandy silty	Mudflat deposits replace creek channel facies
3.43		
3.43	Stratified silty clay intercalated with a thin bed of sandy silt	Mudflat deposits grade into creek channel
2.12	facies	
2.12	Highly stratified silty sand	Creek channel facies are replaced by mudflat
1.76	deposits	
1.76	Highly stratified poorly sorted silty	Mudflat sediments grade into a marsh
1.44	clay containing shell fragments	creek channel facies
1.44	Highly stratified silty sand with clay laminations and shell	Sandflat deposits grade into mudflat sediment
1.16	fragments	
1.16	Silty sand containing reworked	Washover deposits are replaced by a high
-0.15	shell energy fragments	sandflat facies
-0.15	Well sorted medium/fine sand in	Barrier dune facies deposited during
-0.32	sharp contact with underlying unit	washover event
-0.32	Highly stratified silty clay	Mudflat facies grades into creek channel
-0.76	intercalated with shelly sand** sediment	deposits which are intercalated with sandflat
-0.76	Grey shelly sand	High energy sandflat facies is replaced by
-1.7	mudflat deposits	

Table 7.5 Facies development at site 17 during the Holocene

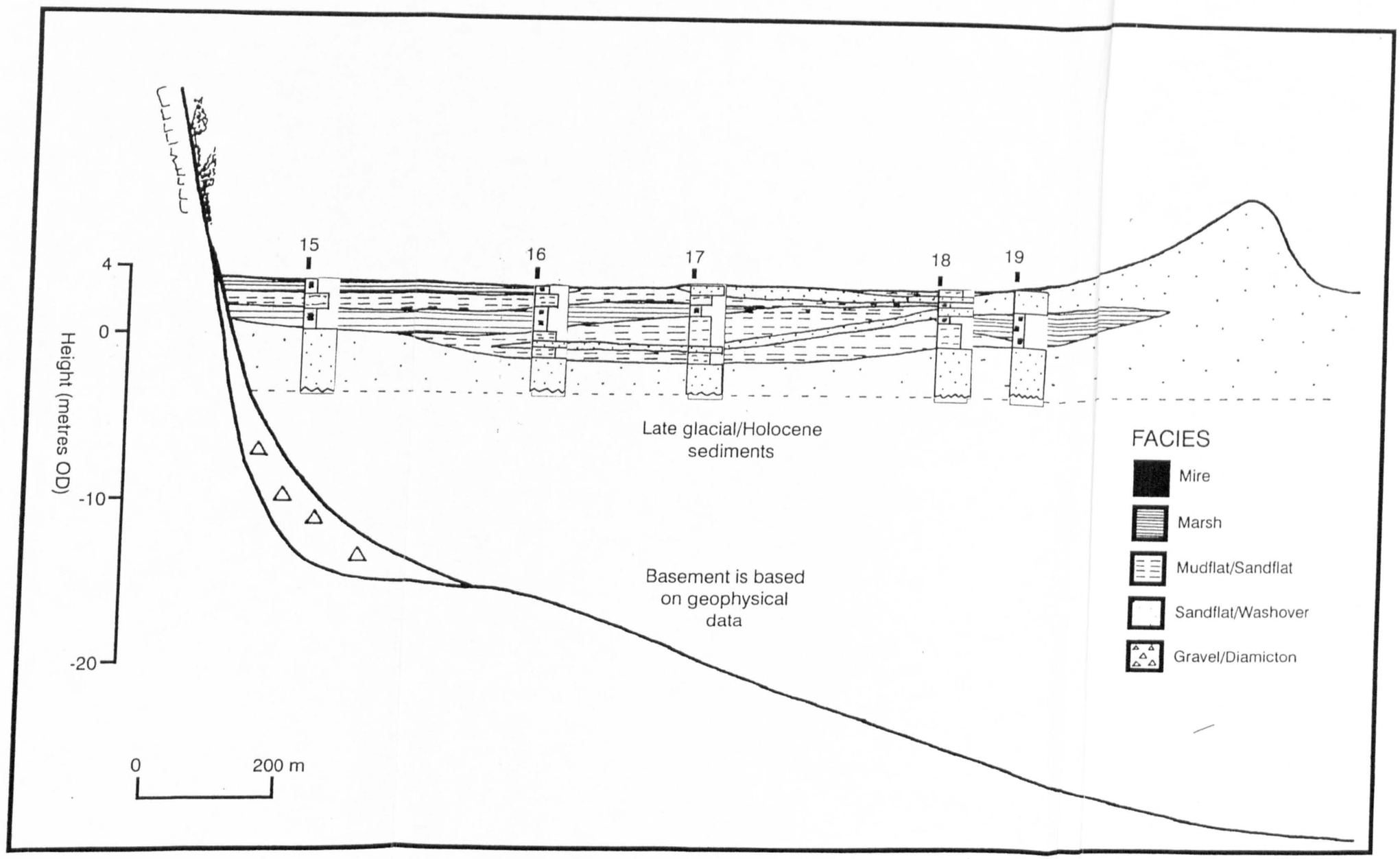

Figure 7.6 Stratigraphic section (T4) based on lithological data from sites 15, 16, 17, 18 and 19.

Site 20

	Height metres OD	Lithology	Interpretation
Ground surface_	4.59 3.71	Silty replaced by highly stratified mottled brown sandy silt	Abrupt change from creek channel facies into a mudflat facies
	3.71 3.35	Sand replaced by mottled grey silty clay stratified at base	Sandflat facies grades into mudflat deposits which are overlain by marsh/creek channel sediment
	3.35 2.54	Silty sand grades into shelly sand	Mudflat deposits are replaced by a sandflat facies
	2.54 1.88	Sand replaced by shelly silty sand	Sandflat facies grades into mudflat deposits containing reworked shell fragments
	1.88 1.09	Silty clay int sharp contact with dark grey shelly sand containing whole Cerastoderma edule shells	Abrupt change from mudflat into sandflat facies
	1.09 0.88	Sand grades into grey silty clay	Mudflat sediment replaces high energy sandflat facies
	0.88 0.68	Silty clay in sharp contact with dark grey shelly sand	Abrupt change from mudflat into sandflat facies
	0.68 -0.15	Silt replaced by highly stratified grey silty clay	Mudflat facies grade into creek channel deposits
	-0.15 -0.39	Sand grades into highly stratified grey sandy silt	Sandflat facies are replaced by transitional mud-/sand- flat deposits
	-0.39 -0.91	Dark grey shelly sand containing whole Cerastoderma edule shells	High energy sandflat facies

Table 7.6 Facies development at site 20 during the Holocene

Site 22

	Height metres OD	Lithology	Interpretation
Ground surface_	4.70 4.41	Brown mottled sand containing no shell fragments	Washover/blowout deposits derived from barrier dunes
	4.41 3.68	Silty clay in sharp contact with shelly sand which grades into brown mottled shelly sand	Abrupt change from mudflat into sandflat/Washover facies which become oxidized
	3.68 2.04	Dark grey silty clay stratified by shelly sand lenses above 3.13 metres OD	Mudflat deposits grade into creek channel and marsh facies which are stratified by sandflat/Washover sediment
	2.04 1.67	Sand replaced by silty sand containing shell fragments	Well sorted sandflat deposits grade into poorly sorted mud- / sand- flat facies
	1.67 -0.80	Dark grey shelly sand	High energy sandflat deposits

Table 7.7 Facies development at site 22 during the Holocene

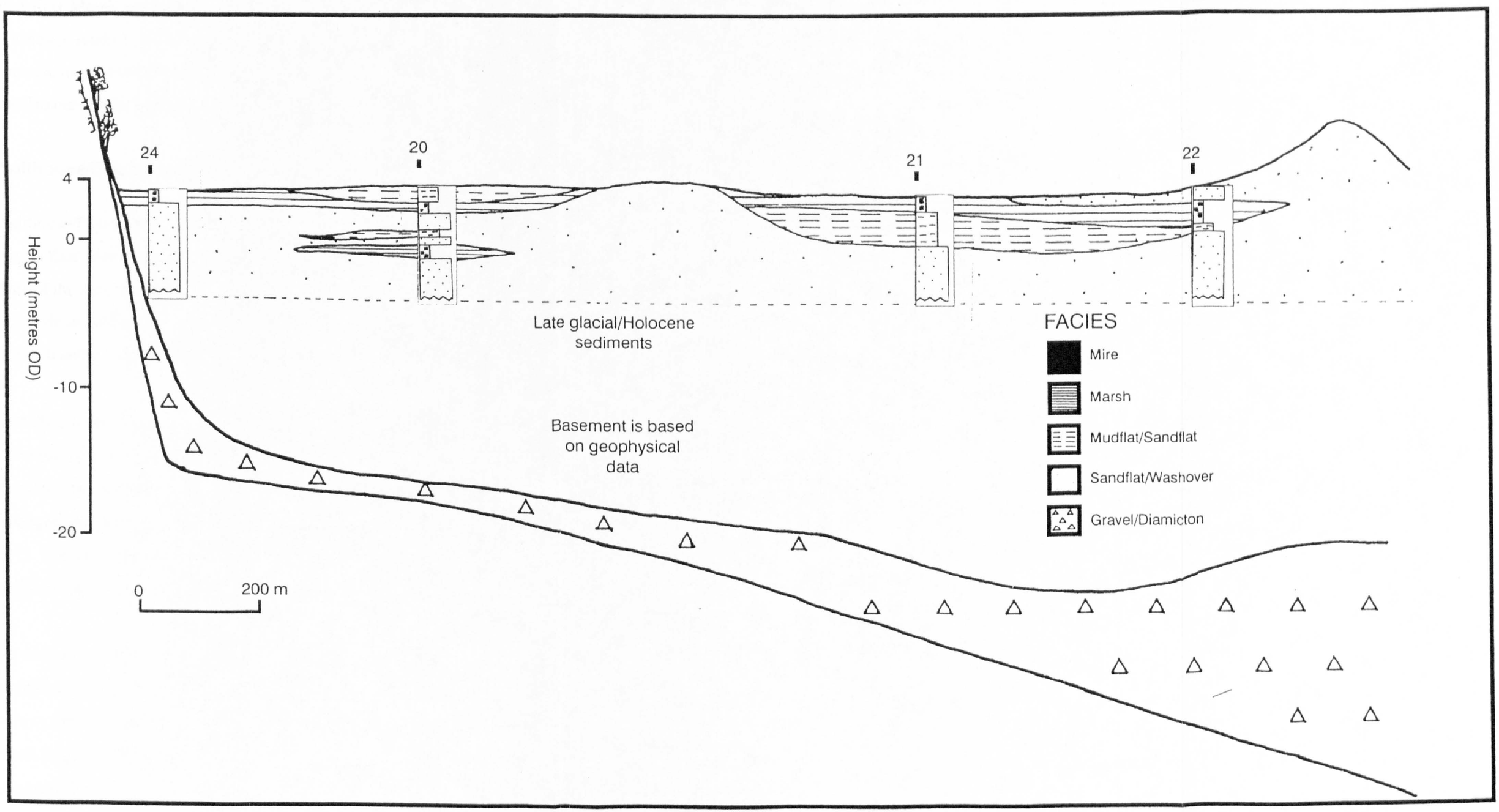

Figure 7.7 Stratigraphic section (T5) based on lithological data from sites 24, 20, 21 and 24.

transgressive sequence indicates a widening of the channel behind the Laugharne Burrows and that East Marsh was subjected to greater marine influence. An abrupt change to well-sorted washover sands at the top of sites 17, 18 and 19 indicates barrier instability and a continued increase in marine influence (Figure 7.6). Lithological data from site 15 suggests that during the late Holocene saltmarsh deposits once again extended from the fossil cliffline adjacent to Coygan.

Salthouse/Easthouse Section

Salthouse/Easthouse Section (T5) extends from the fossil cliffline adjacent to Salthouse Farm across East Marsh and the Pendine Burrows (Figure 7.2). As at Causeway the sediments at the base of the sequence are of composed well sorted shelly sand, which contain whole *Cerastoderma edule* shells, indicative of an open bay or brackish estuary (Figure 7.7). Foraminiferal data from sites 20 and 22 indicate that these deposits represent high-energy sandflat facies.

Site 20 is located landwards of the back-barrier island upon which Malthouse and Hurst House are built (Figure 7.2). The sands at the base of the sequence are overlain by interstratified mudflat, sandflat and saltmarsh creek sediment (Table 7.6). Above this the mudflat facies changes abruptly into sandflat facies which contains whole *Cerastoderma edule* shells (Figure 7.7). The latter extend to approximately 3.35 metres OD where high energy sandflat deposits are replaced by mudflat and saltmarsh creek deposits (Table 7.6).

In contrast, the shelly sand at the base of site 22 continues up to -0.80 metres OD where the sediments grade into mudflat and marsh deposits (Table 7.7). Above this the stratified marsh, which extends landward towards site 20, changes abruptly into sand which contains numerous shell fragments (Figure 7.7). The latter are believed to represent washover dune and beach deposits (Table 7.7)

Key for lithological logs

Organic Detritus

Silty Clay

Stratified Sandy Silt / Silty Sand

Sand

Poorly sorted gravel

7.3 Coastal evolution

The evolution of the Pendine barrier during the mid and late Holocene is well documented by lithostratigraphic and biostratigraphic evidence which is calibrated by radiocarbon dates obtained from organic levels in West Marsh. Although, no direct evidence is available for coastal changes in the Bristol Channel and Carmarthen Bay during the Late Devensian and early Holocene, geophysical data, borehole information and published sources can be used to 'infer' environmental changes during this period.

7.3.1 Deglaciation and the onset of the Holocene transgression (18,000-10,000 BP)

During the Late Devensian deglaciation glacigenic sediments in the Bristol Channel and Celtic Sea, underwent a short period of intense erosion. Meltwater channels generated by the retreating glaciers rapidly excavated certain areas of drift. Channel development, confined to a relatively short period between the retreat of Devensian ice sheets and the succeeding Holocene transgression, was greatest in shallow areas. Garrard and Dobson (1974) suggest that these channels were forced to run obliquely to the general gradient of the shelf by barriers which blocked their obvious seaward routes. Late Devensian loess deposits along the coast of South Wales indicate that sediments of glacial-fluvial origin were entrained by intense south-westerly or westerly winds which influenced the continental shelf during lowered sea-level (Case, 1983). Similar deposits may have generated extensive aeolian deposits which subsequently formed the barriers within the Bristol Channel and Carmarthen Bay during lowered sea-level (Garrard and Dobson, 1974). The landward transport of silt- and sand-sized particles would have been further enhanced by reworking within the surf zone; reworked sands exposed on the shoreface will have been entrained and transported onshore by intense storm winds. This 'hand-over' of sediment may have been reinforced during the period of lowered sea-levels by greater tidal amplitudes (Austin, 1991) exposing wider expanses of reworked sediment during low tide.

As the high-energy environment of the surf zone transgressed the exposed drifts, the surface of the glacial-fluvio deposits was reworked to produce a thin cover of gravel lag which rests upon

a distinct plane of marine erosion (Garrard and Dobson, 1974). Pre-Quaternary foraminifera, identified in early Holocene sediments within Swansea Bay and its approaches, highlight the vigorous reworking of the Celtic seabed during the Late Devensian (Culver and Banner, 1979). Flood tidal currents would have added their kinetic energy to the easterly and north-easterly wave induced currents which eroded the periglacially modified chalks, silts and sands offshore. Episodic regressive phases in relative sea-level rise would have further enhanced this erosion by re-exposing previously reworked sediment.

7.3.2 Formation and evolution of the Pendine and Laugharne Burrows

Back-barrier facies development is controlled primarily by the stability of the coastal barrier, the composition and volume of sediment supply into the back barrier area, tidal regime, storm activity and local changes in relative sea-level. Although, the shoreface reacts instantly to changes in the wave/wind climate and sediment supply, environmental changes within the back-barrier area often exhibit a delayed response to the processes acting upon the seaward side of the barrier. Depending upon the magnitude of the events, back-barrier tidal inlet sequences record both long- and short-term changes in coastal configuration and stability. Hypotheses describing the evolution of barrier systems can therefore be inferred from evidence derived from back-barrier facies development.

The Pendine Burrows, Laugharne Burrows and adjoining back-barrier deposits represent an extremely complex coastal system which has evolved in response to oceanographic processes, changing sedimentary dispersal patterns and relative sea-level changes during the Holocene. The hypothesis describing the evolution of this system is based on geophysical data and the interrelationships between back-barrier facies recovered in cores. Radiocarbon dating of organic units recovered in West Marsh provides the basic chronological framework used to constrain this hypothesis. The absence of similar organic deposits within East Marsh means that changes within this portion of the system are not accurately calibrated; however, the stratigraphic position of these sequences suggest the deposits in East Marsh represent a later stage of barrier development than sediments described in West Marsh.

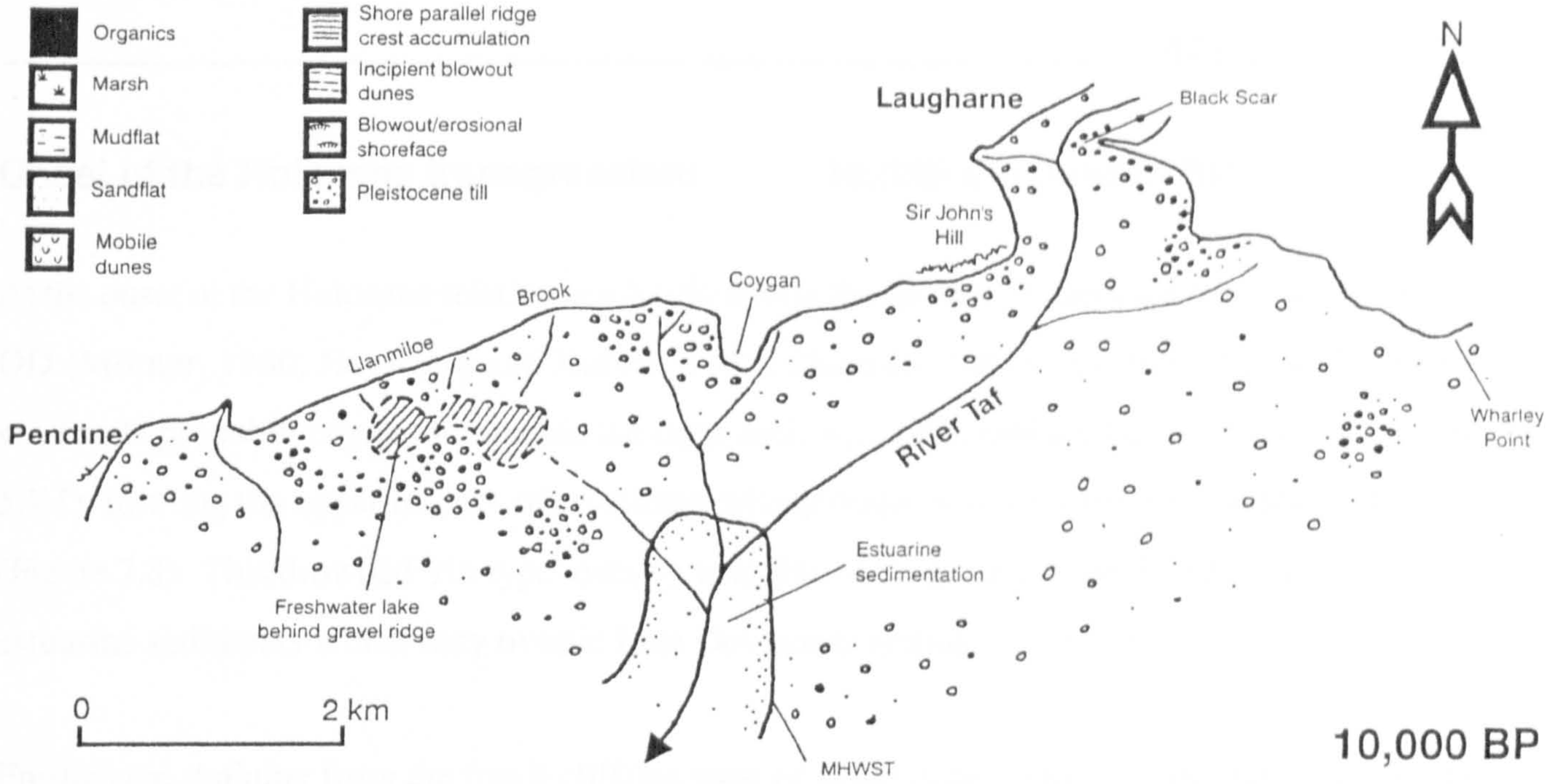

Figure 7.8 Coastal configuration at the onset of the Holocene transgression

Figure 7.9 Coastal configuration at 9,000 years BP

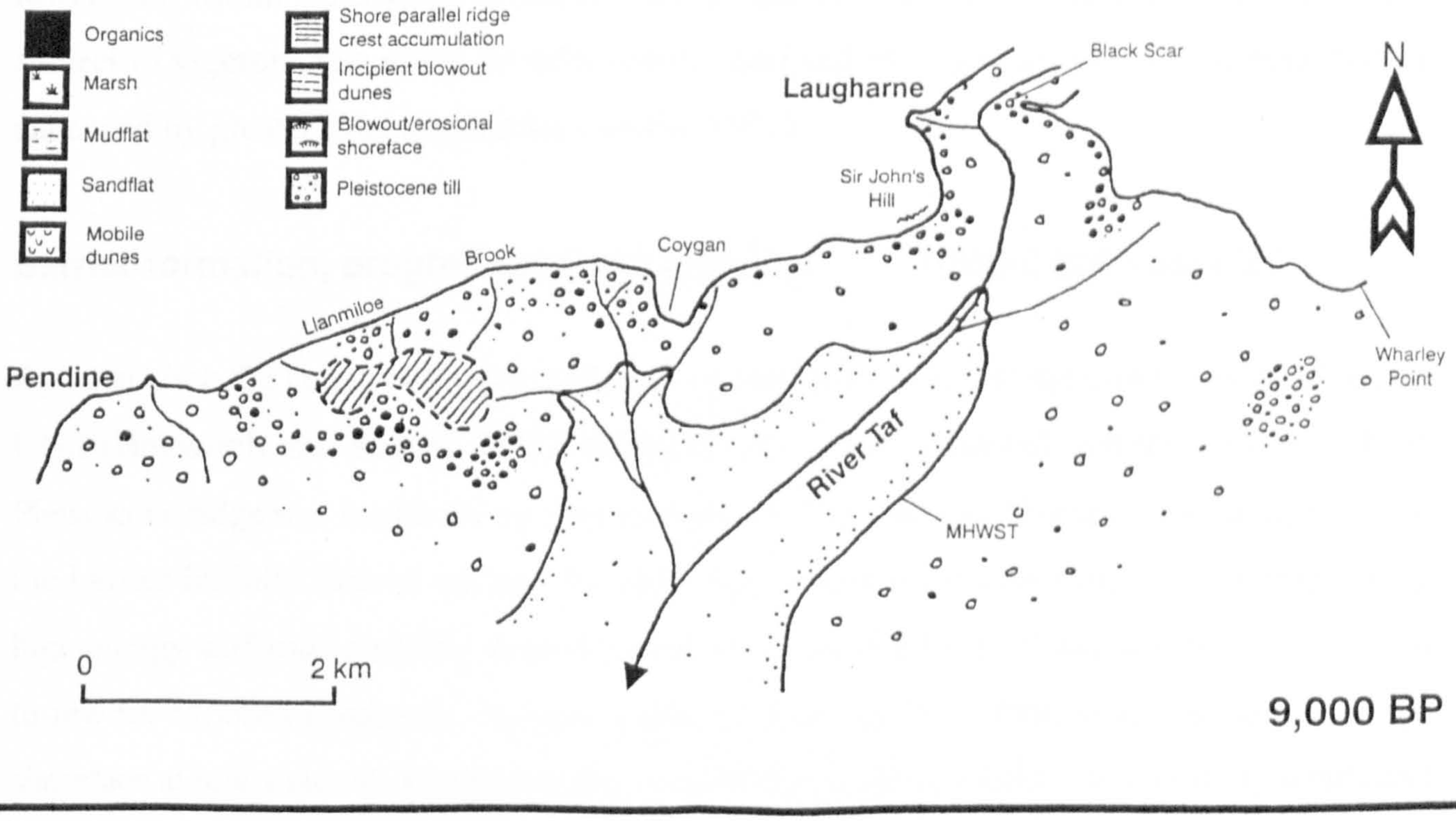

Onset of the Holocene transgression: 10,000-8,000 years BP

At the onset of the Holocene relative sea-levels within the Bristol Channel were below -35 metres OD (Mörner, 1980; Heyworth and Kidson, 1982; Shennan, 1983). By 10,000 years BP rising sea-levels probably began to inundate the deep melt water channel seaward of Coygan (section 5.1.1), forming the upper reaches of an estuary whose origin was located some distance offshore (Figure 7.8). This drowned 'ria-type' estuary would have been initially infilled by early Holocene estuarine sediments which may overlie Late Devensian channel sequences.

Freshwater, draining from the fossil cliffline west of Coygan may have accumulated behind the ridge of Pleistocene till which extends from Pendine to a point seaward of Brook (Figure 7.8). As streams and small rivers continued to drain into this enclosed impermeable basin, water probably spilt over the Pleistocene ridge and in doing so excavated drainage channels in the surface of this feature (Figure 7.8). Although no evidence is available at present, Late Devensian and early Holocene lacustrine sediment may be preserved beneath the back-barrier deposits recovered from this part of West Marsh.

Between 10,000 and 8,000 years BP the rapidly rising sea-levels will have continued to inundate the Taf valley (Figure 7.9). Because the gradient of the Pleistocene surface east of Coygan is far lower than within the deeply incised meltwater channel (section 5.3), this area may have been subject to vigorous reworking by tidal scour; flood and ebb currents would have been further enhanced by greater tidal amplitudes (Austin, 1991).

Barrier formation, progradation and stability: 7,500-5,500 years BP

By comparing the height of the pre-Holocene surface (section 5.3) to the position of relative sea-level (Heyworth and Kidson, 1982; Shennan, 1983) it is estimated that the area behind the Pleistocene ridge was inundated by approximately 7,500 years BP (Figure 7.10); it appears that the barrier initially formed through the drowning of this antecedent ridge. The transgressing high-energy surf zone probably abutted against the seaward portion of this feature and continued to rework exposed glacigenic deposits within Carmarthen Bay. Fine sands exposed upon the shoreface at low water were probably entrained by strong westerly and south westerly winds and deposited on the irregular surface of both the barrier and Pleistocene deposits landward of the

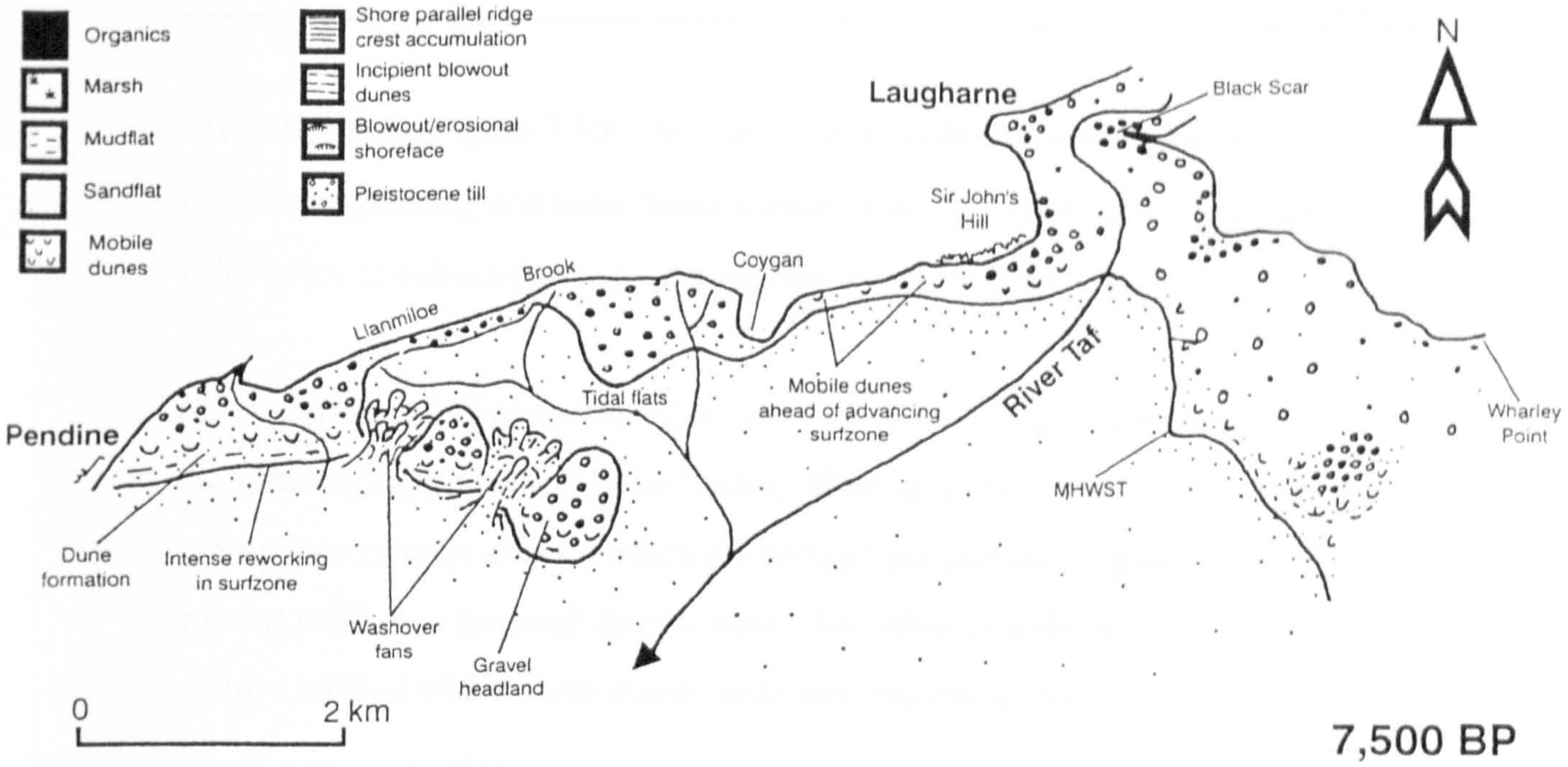

Figure 7.10 Barrier formation through mainland detachment of antecedent topography

Figure 7.11 Barrier progradation in response high sediment supply

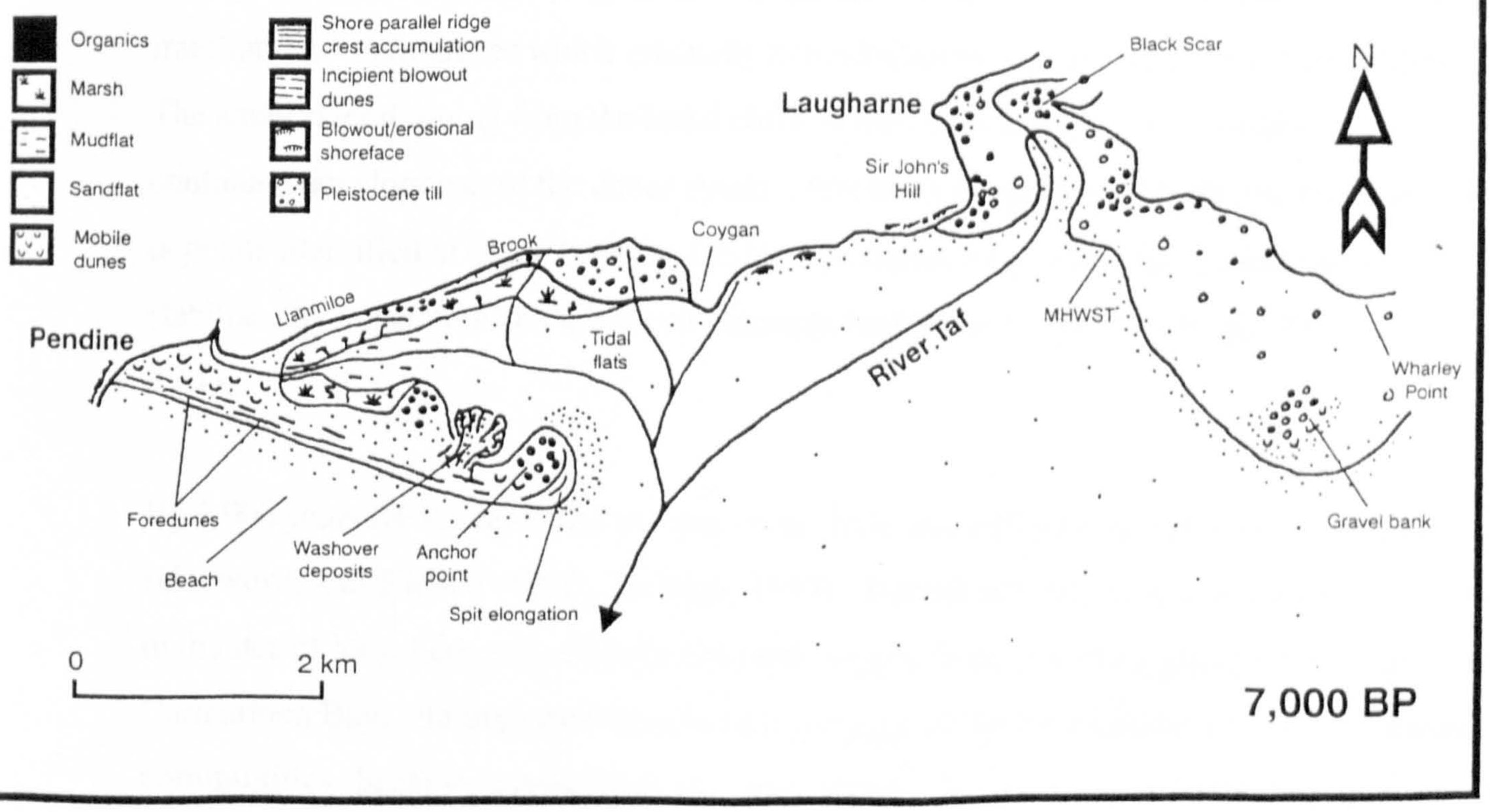

MHWST level (Figure 7.10). Self-sustaining mobile dunes probably migrated landward ahead of the transgressing surfzone; these aeolian deposits may have accumulated upon the Pleistocene ridge prior to submergence by the rapidly rising relative sea-level.

Fine-grained sediment contained within the turbid coastal waters began to infill the basin behind the submerging gravel and dune barrier. With continued relative sea-level rise storm set-up and run-up, waves were able to breach the barrier and introduce coarse washover deposits and/or tidal current infill into the back-barrier area. The deep channel adjacent to the barrier was probably rapidly infilled with coarse clastic sediment reworked from longshore and offshore sources.

Between 8,000 and 7,000 years BP extremely high rates of sediment supply stabilised the barrier and allowed this feature to prograde, even under conditions of continued rapid relative sea-level rise (Figure 7.11). Although the barrier may have been periodically over-topped, when intense westerly and south westerly storms coincided with high spring tides, the Pleistocene ridge upon which this feature is anchored prevented its breakdown or landward migration *i.e.* when the wave climate changed and sediment was stripped from the seaward portion of the dunes by storm waves the landward translation of the shoreface was probably prevented by the re-exposure of the gravel ridge.

The upward and longshore progradation of the barrier facilitated the development of back-barrier mudflats and saltmarshes which gradually extended across the inter-tidal sandflats (Figure 7.11). The small river draining from the fossil cliffline west of Llanmiloe was probably diverted by the continued development of the dunes system; this stream may have introduced the coarse fluvial deposits identified at site 7 (section 7.2.1). The dunes were supplied by wind blown sediment, stabilised by vegetation and advanced seawards forming a series of shore parallel ridges (Figure 7.11).

By 6,000 years BP the rapid rise in relative sea-level was replaced by a phase of more gradual rise (Heyworth and Kidson, 1982; Shennan, 1983). Barrier stability was maintained by continued high rates of longshore and offshore sediment supply from reworked glacigenic material within Carmarthen Bay. Saltmarshes occupied the majority of the back-barrier area and freshwater fen communities became established in areas above the level of MHWST subject to local

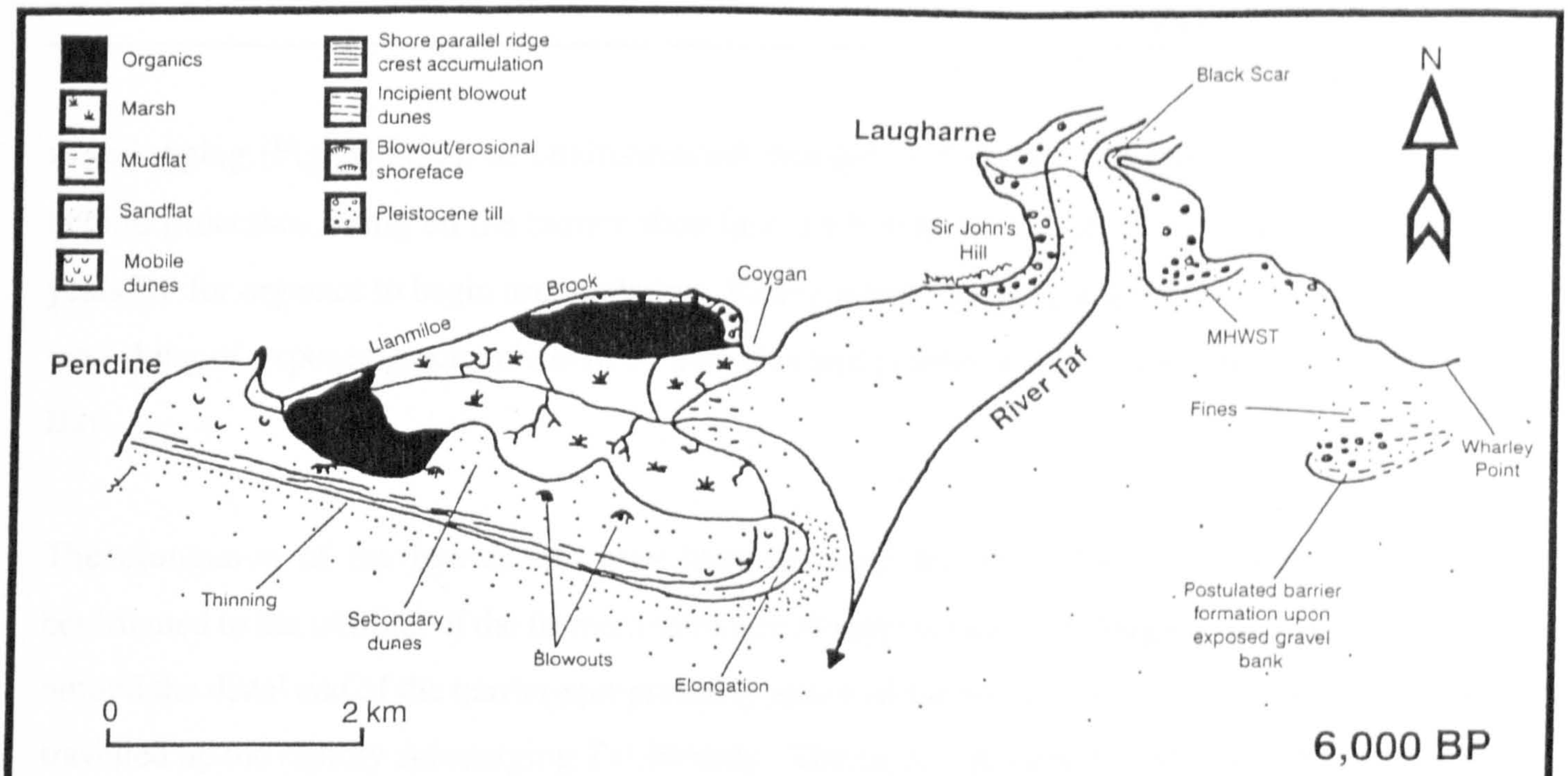

Figure 7.12 Barrier stability, marsh development and organic accumulation

Figure 7.13 Barrier breaching and breakdown

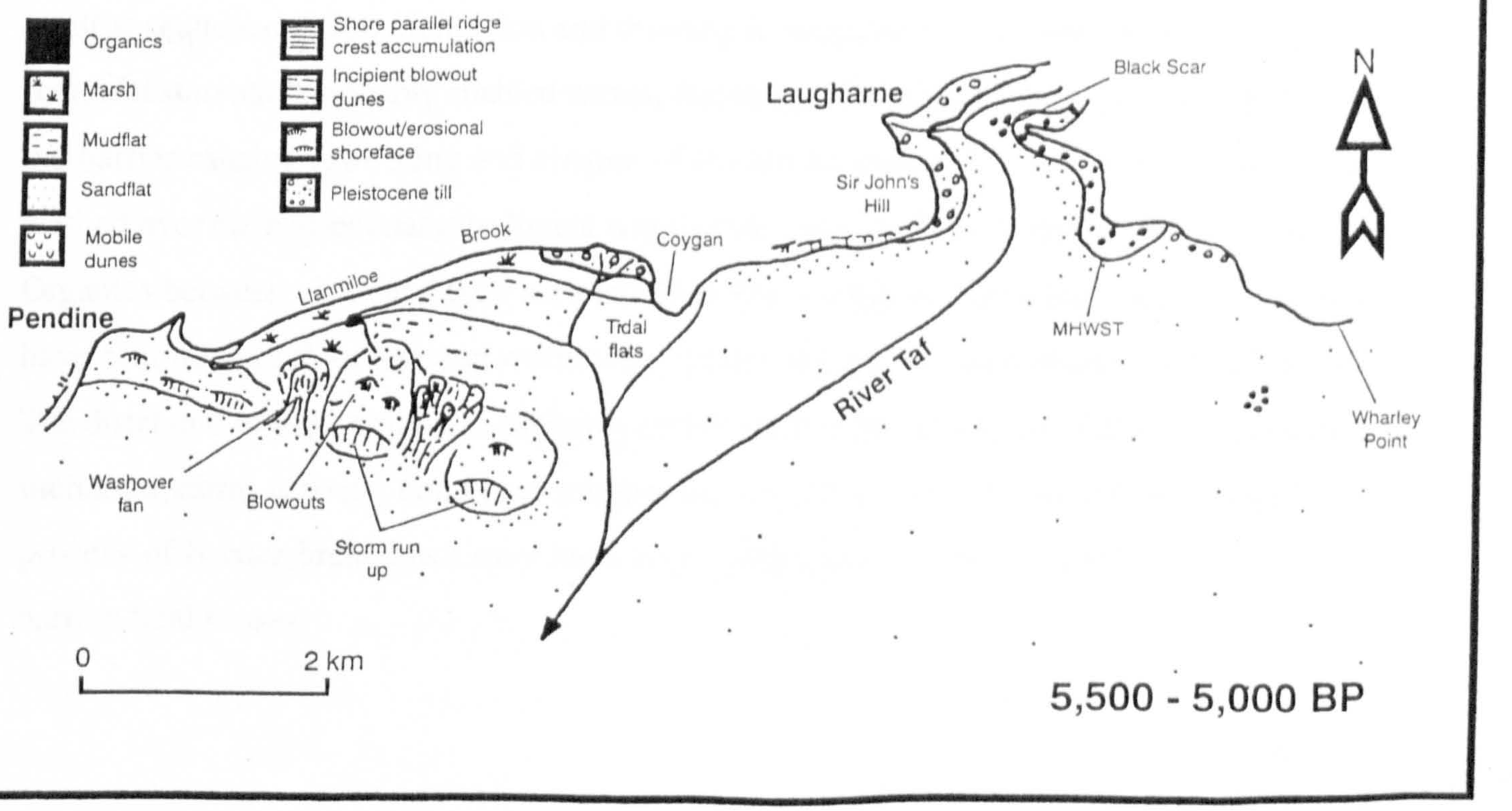

waterlogging (Figure 7.12); as environmental changes within the back-barrier area often lag behind processes acting on the barrier shoreface the barrier had to be well developed by 6200 years BP for organics to begin accumulating. Fine-grained sediment was also supplied from the reworking of exposed glacigenic drift of Irish Sea and central Welsh origin within Carmarthen Bay.

The elongation of the barrier spit may have diverted the River Taf towards the east and contributed to the infilling of the former meltwater channel seaward of Coygan. Waves refracting around the distal end of the barrier-spit probably attacked the fossil cliffline east of Coygan and travelled up the rapidly submerging Taf Estuary. The highly-stratified sands and silts, exposed along the fossil cliffline west of Wharley Point and beneath the intertidal sandflats seawards of Ginst Point (Figure 7.1), may have accumulated behind a low barrier which formed above a drowned gravel bank (Figure 7.12); however, other than the occurrence of these fine-grained deposits no evidence has been found to support this hypothesis. It is possible that these deposits accumulated behind a landward migrating barrier but this is mere speculation.

Barrier instability, breakdown and reworking : 5,500-5,000 years BP

Between 5,500 and 5,000 years BP the barrier system became unstable. Regressive saltmarsh and freshwater organic deposits within West Marsh were replaced by transgressive mudflat and sandflat sequences. Spit elongation and thinning in response to increased storm activity and or sediment starvation probably enabled waves, during periods of storm run up and set-up, to breach the barrier causing reworking and erosion of the barrier dunes (Carter, 1988); as storm waves washed over the barrier coarse sediment was introduced into the back-barrier area (Figure 7.13). Organics between -3.55 and 0.06 metres OD at site 8 suggests that freshwater vegetation may have continued to flourish upon washover deposits in areas elevated above the MHWST level. The distal end of the barrier was probably then broken down and reworked under conditions of increased storm activity, continued relative sea-level rise and reduced sediment supply. The process of barrier breakdown may have been accelerated by wind erosion and scour though narrow tidal passes.

The total breakdown and reworking of the barrier was prevented by the Pleistocene ridge. Rather than migrating landwards, the western portion of this feature was fixed in position by the antecedent topography which preserved the large majority of the back-barrier deposits within West Marsh (Figure 7.13). Tidal scour and wave action probably reworked the majority of the fine grained back-barrier sediments deposited east of Coygan. This may have been compounded by high tidal amplitudes which exposed great expanses of these sediments to wave action and tidal scour during the tidal cycle.

Barrier progradation and stability: 5,000-3,500 years BP

Lithostratigraphic and biostratigraphic evidence indicates that between 5,000 and 4,500 years BP the barrier-spit became stable began to extend eastward probably in response to either reduced storm activity, increased sediment supply or to a change in the rate of relative sea-level rise (Figure 7.14). During constructive periods the aeolian sediment, entrained by southwesterly winds from the beach surface, supplied low accreting dunes which were rapidly colonised by pioneer vegetation and wave continued to build up the beach profile. However, during destructive phases storm waves stripped sediment from the beach causing significant erosion along the seaward side of the barrier. Constructive and destructive processes acting on the shoreface probably generated a series of low shore-parallel ridges which were periodically breached by storm waves.

As the barrier extended in a longshore direction it is likely that the tidal inlet seawards of Coygan was forced to migrate ahead of the advancing spit re-curve deposits. Saltmarshes began to develop within West Marsh and the distal end of the spit extended east of Coygan, diverting the course of the River Taf (Figure 7.15). By 4,500 years BP a freshwater mire began to develop behind the barrier, in areas above MHWST subject to local freshwater waterlogging. Sedge-dominant fen communities were replaced by alder carr which probably extended from the dunes and the fossil cliffline towards the centre of West Marsh. The accumulation and preservation of organics were largely controlled by the local hydrology and variations in the elevation of the organic beds reflects the uneven morphology of the back-barrier area. With the continued extension of the barrier saltmarshes probably began to develop in the area east of Coygan (Figure 7.15). The stability exhibited by the barrier between 4,500 and 3,500 years BP indicates that

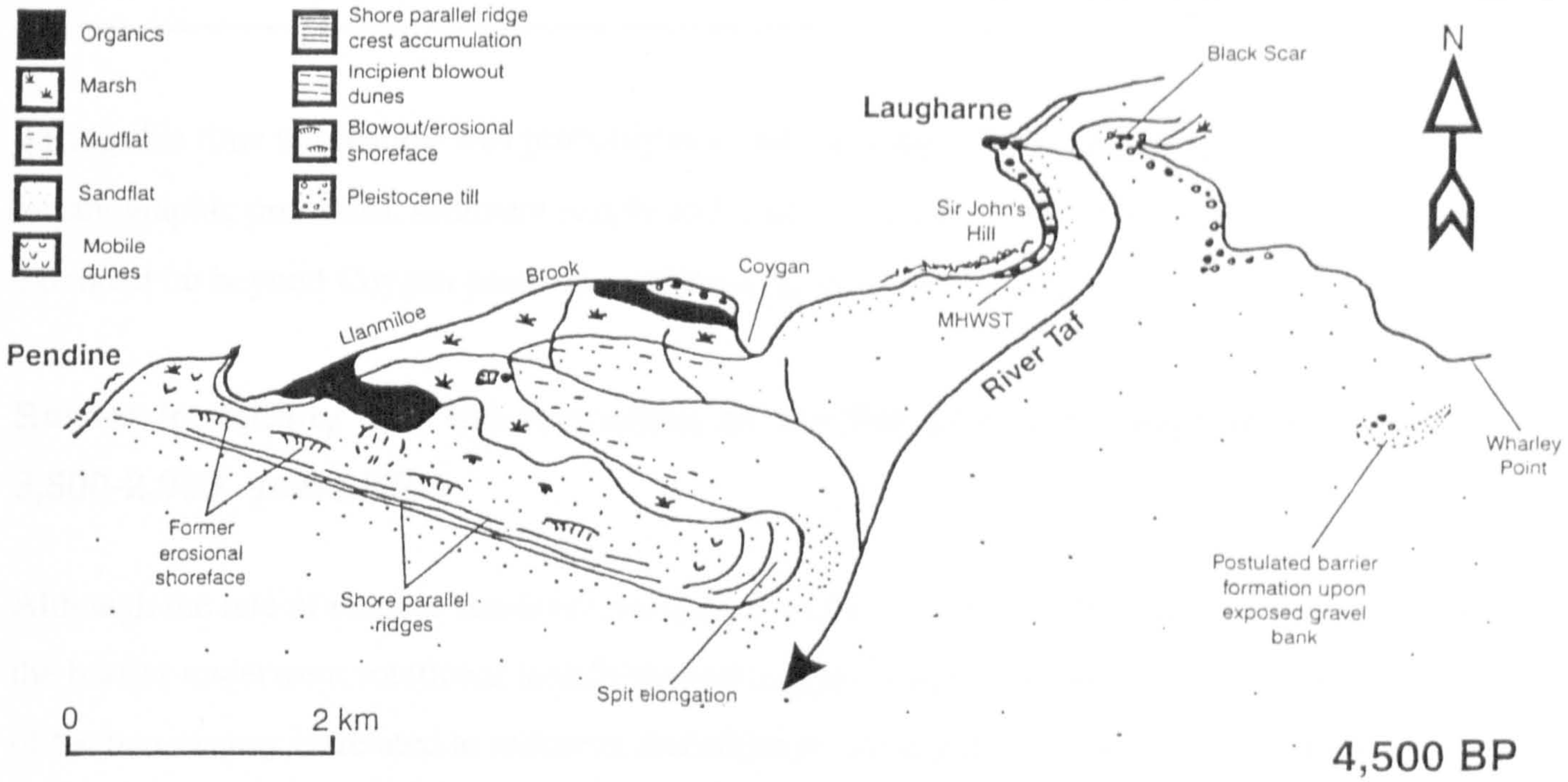

Figure 7.14 Barrier progradation, marsh development and organic accumulation

Figure 7.15 Barrier thinning and spit elongation

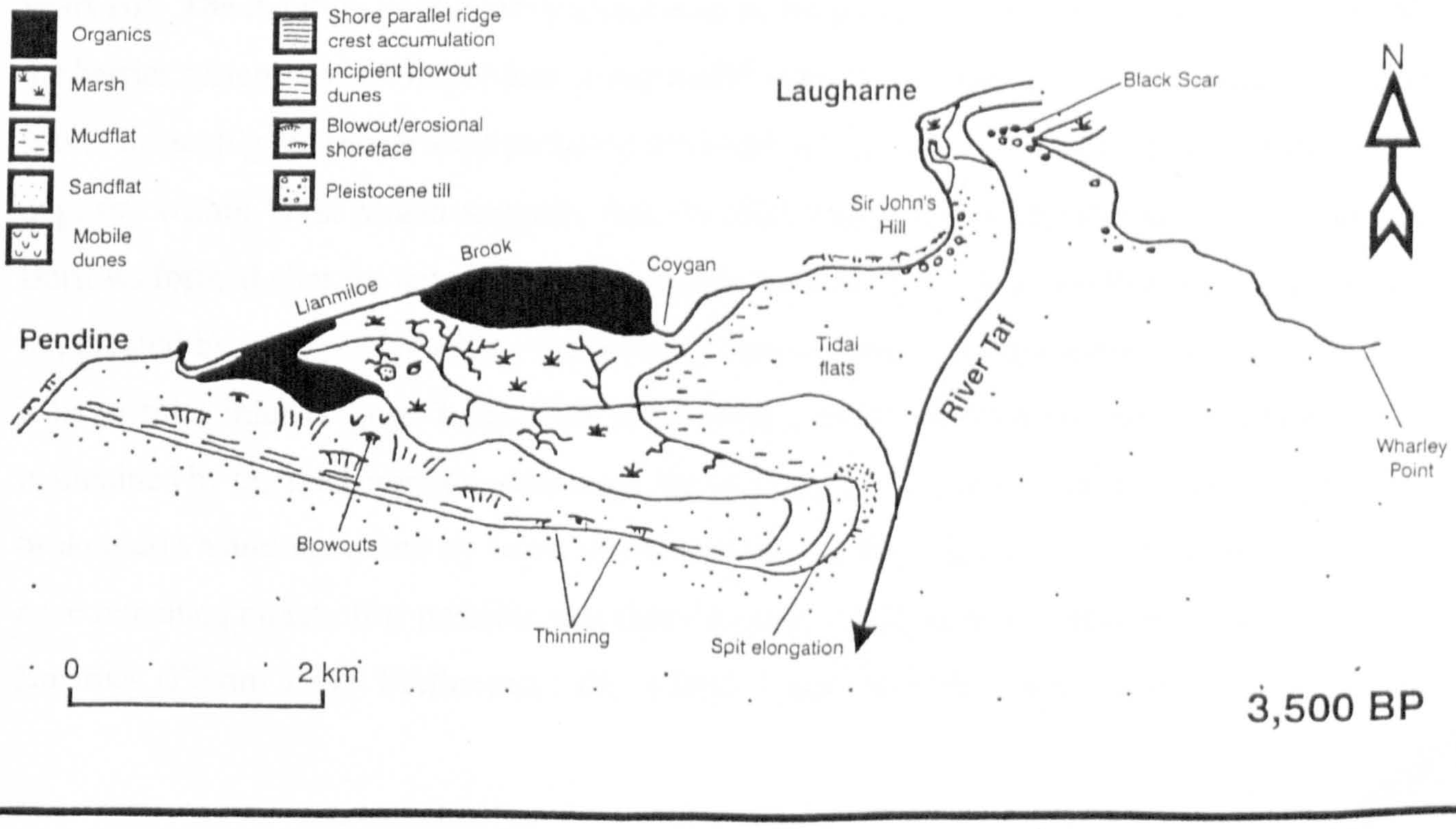

during this time the feature was probably in a state of long-term dynamic equilibrium with the oceanographic processes, sediment supply and relative sea-level rise. It is likely that the barrier extended far beyond Coygan possibly reaching a point seawards of Sir John's Hill (Figure 7.15).

Barrier instability and the formation of the Pendine and Laugharne Burrows: 3,500-2,000 years BP

Although the rate of relative sea-level rise began to diminish by approximately 3,000 years BP, the barrier underwent rotational instability and in-place narrowing (Figure 7.16). The thinning of the barrier may be related to sediment starvation or increased storm activity. In order to satisfy sediment transport requirements material eroded from the seaward side of the barrier was probably deposited at the distal end of the spit by waves refracting around this feature. The landward migration of the eastern portion of the barrier may have caused this feature to rotate counter-clockwise about a thinning mid-point which was fixed in place by the antecedent topography. The barrier shoreface was eroded and eventually breached by storm waves which created washover fans in the back-barrier area. Within West Marsh accretionary saltmarsh and freshwater organic sequences are replaced by transgressive mudflat and sandflat deposits. The barrier system then became unstable and began to breakdown.

However, this phase of breakdown was very different to the instability between 5,500 and 5,000 years BP. The duration or organic accumulation in West Marsh suggests that by 3,500 years BP the barrier system was far larger than at any earlier stage in its evolution. Inlets created by storm waves breaching the barrier were probably modified by tidal scour. The nature of the back-barrier deposits within West Marsh suggests that the tidal inlet dividing the Pendine and Laugharne Burrows formed after the second phase of organic accumulation. It is possible that a narrow tidal jet, created by a storms breaching the thinning centre portion of the barrier, opened up to form a large tidal inlet (Figure 7.16). This inlet became fixed in position and was subsequently maintained by the tidal currents. Although, the majority of the barrier system east of Coygan was broken down and reworked by wave action and tidal scour, a portion of the barrier dunes may have remained intact. It is possible that these deposits initiated the formation of the Laugharne Burrows (Figure 7.17). Furthermore the 'island' upon which Malthouse and Hurst House are

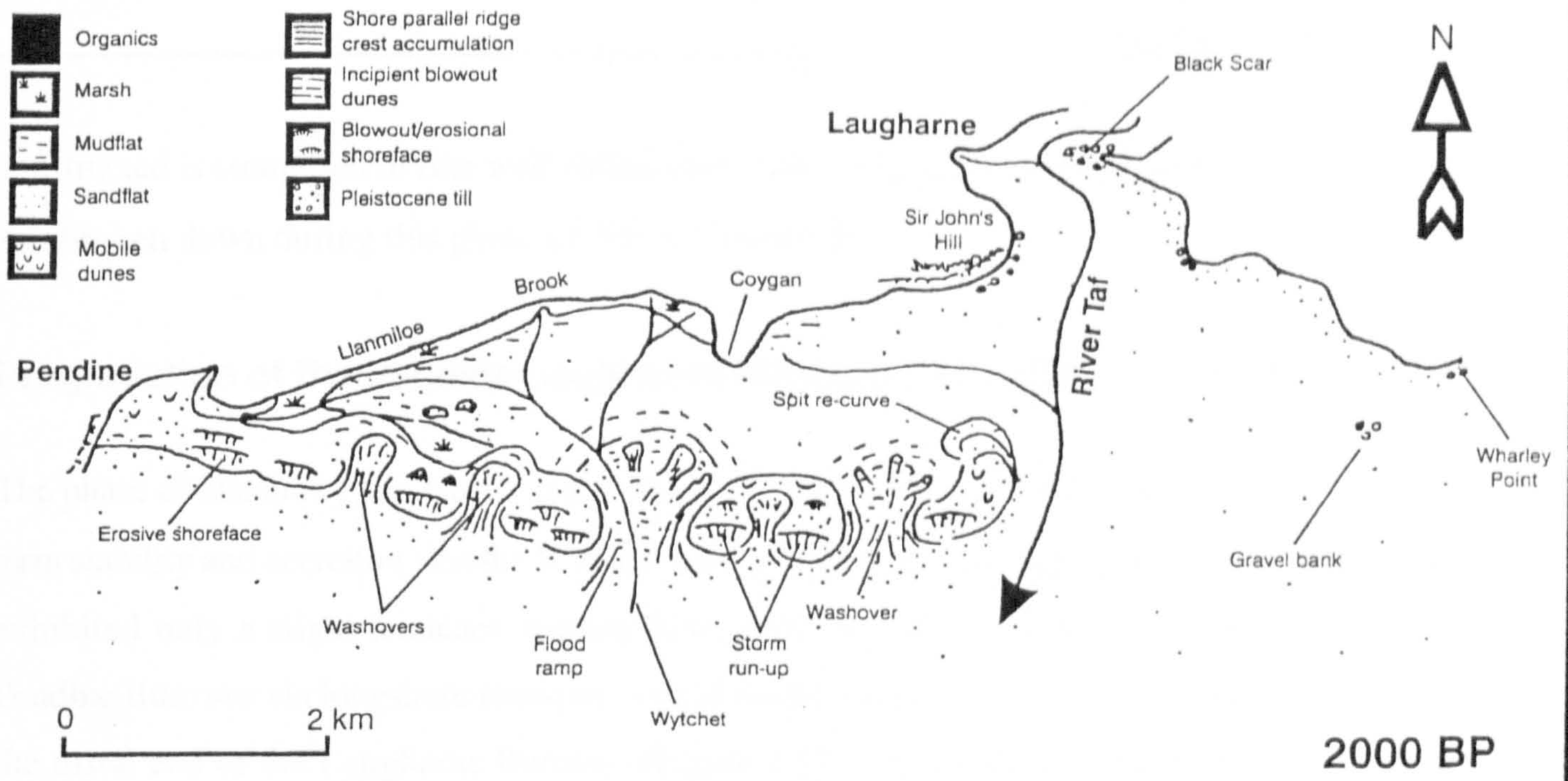

Figure 7.16 Barrier breaching and breakdown

Figure 7.17 Formation of the Pendine and Laugharne Burrows

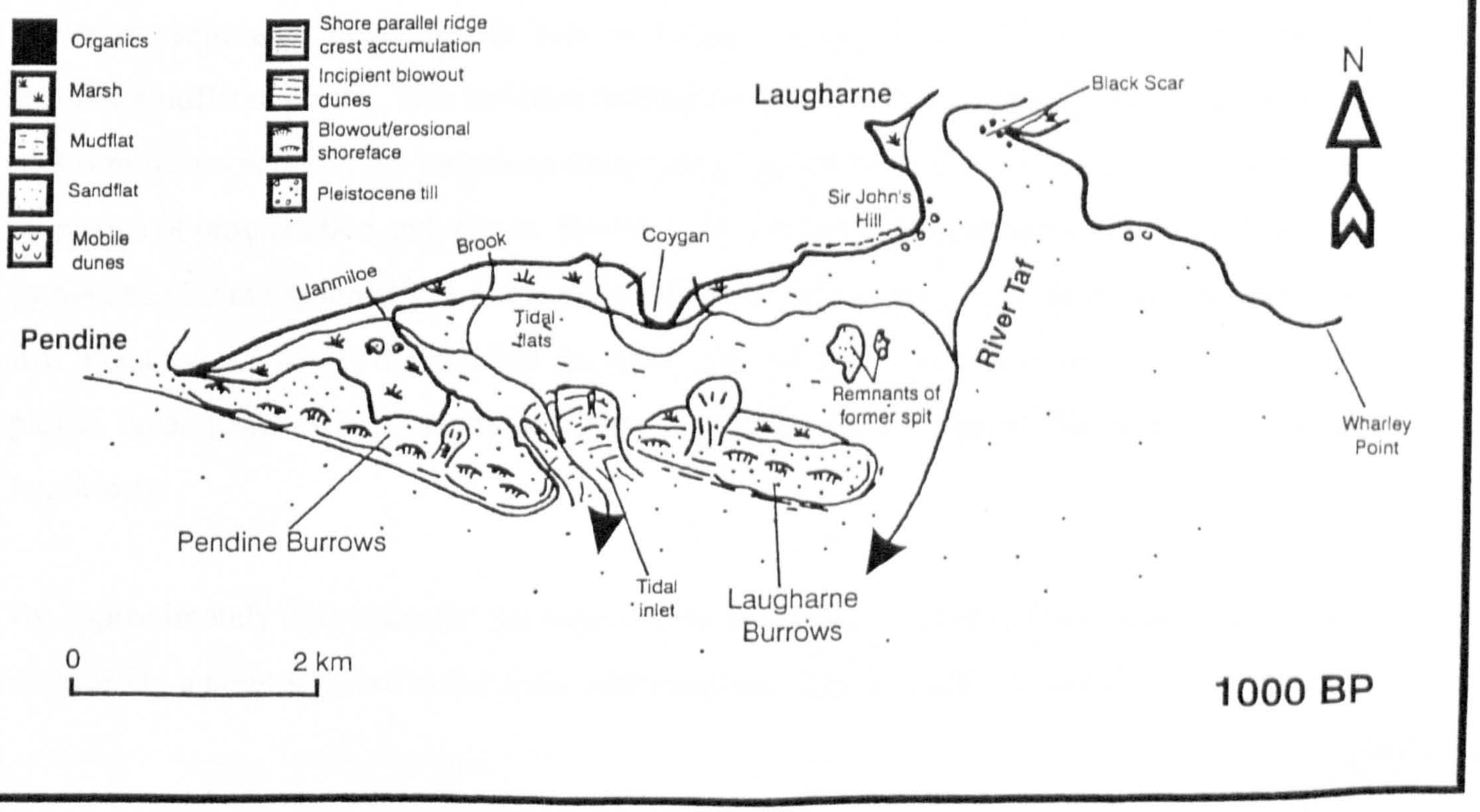

constructed is composed of fine well-sorted sand which may represent the remnants of a former spit broken down during this phase of barrier instability.

Progradation of the Pendine Laugharne Burrows: 2,000-500 years BP

The phase of instability and barrier-spit breakdown after 3,500 years BP was succeeded by long-term stability and accretion. As the Wytchet Inlet probably remained in dynamic equilibrium and exhibited only a slight tendency toward down drift migration, sediment travelling along the Pendine Burrows via longshore transport would have by-passed this inlet and been deposited at the distal end of the Laugharne Burrows (Figure 7.17). In response to reduced storm activity continued sediment supply and possibly decreasing rates of relative sea-level rise (Heyworth and Kidson, 1982) the Pendine and Laugharne Burrows advanced seawards (Figure 7.18). Wind and wave activity constructed a series of shore parallel beach/dune ridges along the upper foreshore. West Marsh was infilled with fine-grained sediment and saltmarshes developed along the fringes of the dunes and the fossil cliffline. However, the proximity of the Wytchet inlet probably influenced back-barrier facies development within West Marsh and may have prevented the development of freshwater communities within this area.

As the Laugharne Burrows extended eastward, the area behind this portion of the barrier was also infilled with fine-grained sediment and saltmarshes replaced coarser sandflat and mudflat facies. However, saltmarsh development east of Coygan is punctuated by coarse washover and sandflat/mudflat deposits. This indicates that the Laugharne Burrows were periodically breached by storm waves and that the longshore extension of this feature was not continuous but marked by phases of progradation and retreat. Because this portion of the barrier was not fixed in place by the antecedent topography and was drift aligned the configuration of the Laugharne Burrows was probably different to the Pendine Burrows. Intense storm activity may have resulted in the partial breakdown of the Laugharne Burrows which possibly caused this feature to migrate landwards.

By approximately 500 years BP the barrier, now consisting of two discrete dune systems, had extended to a point seaward of Sir John's Hill and was able to maintain a profile of equilibrium

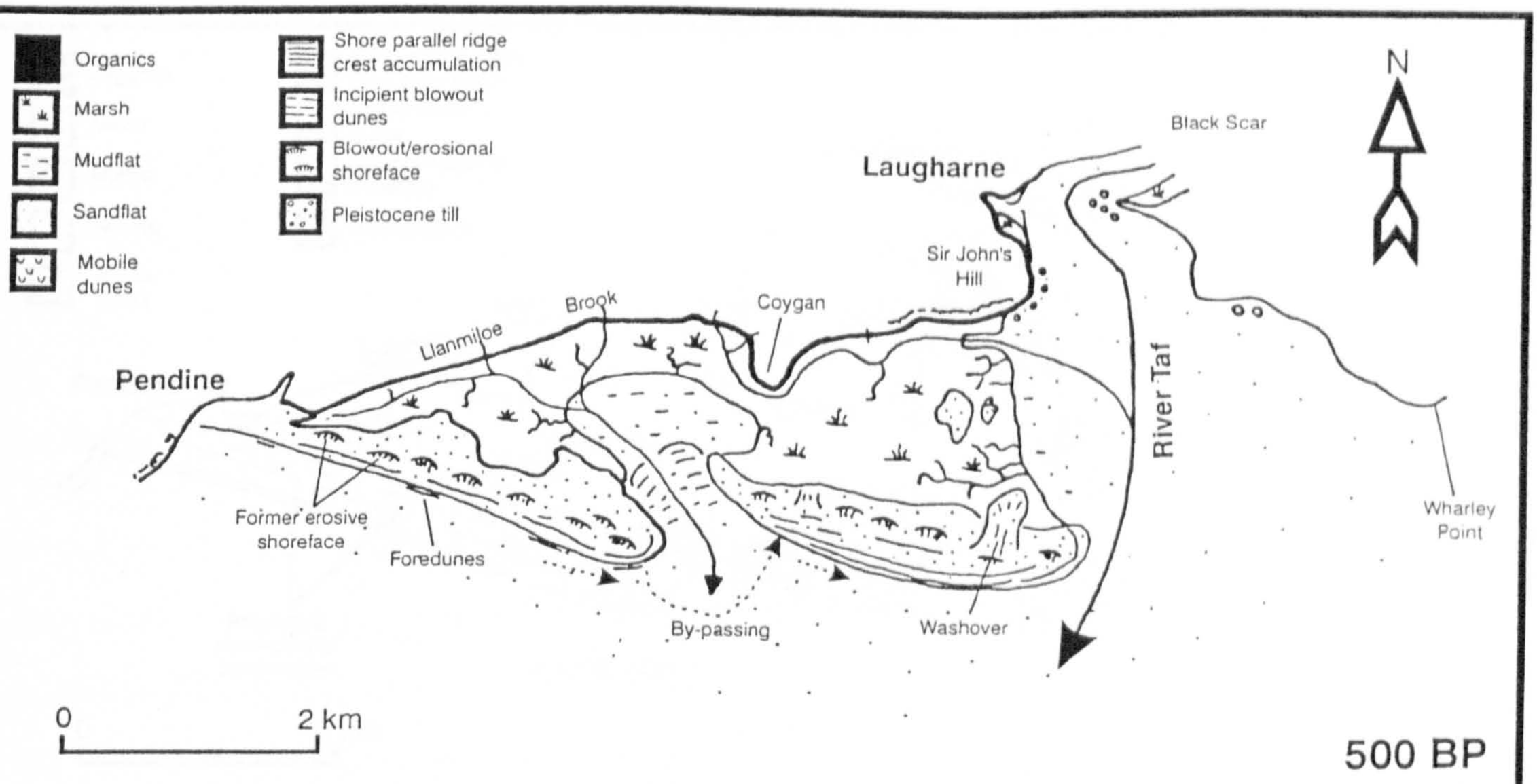

Figure 7.18 Dynamic equilibrium and sediment by-passing

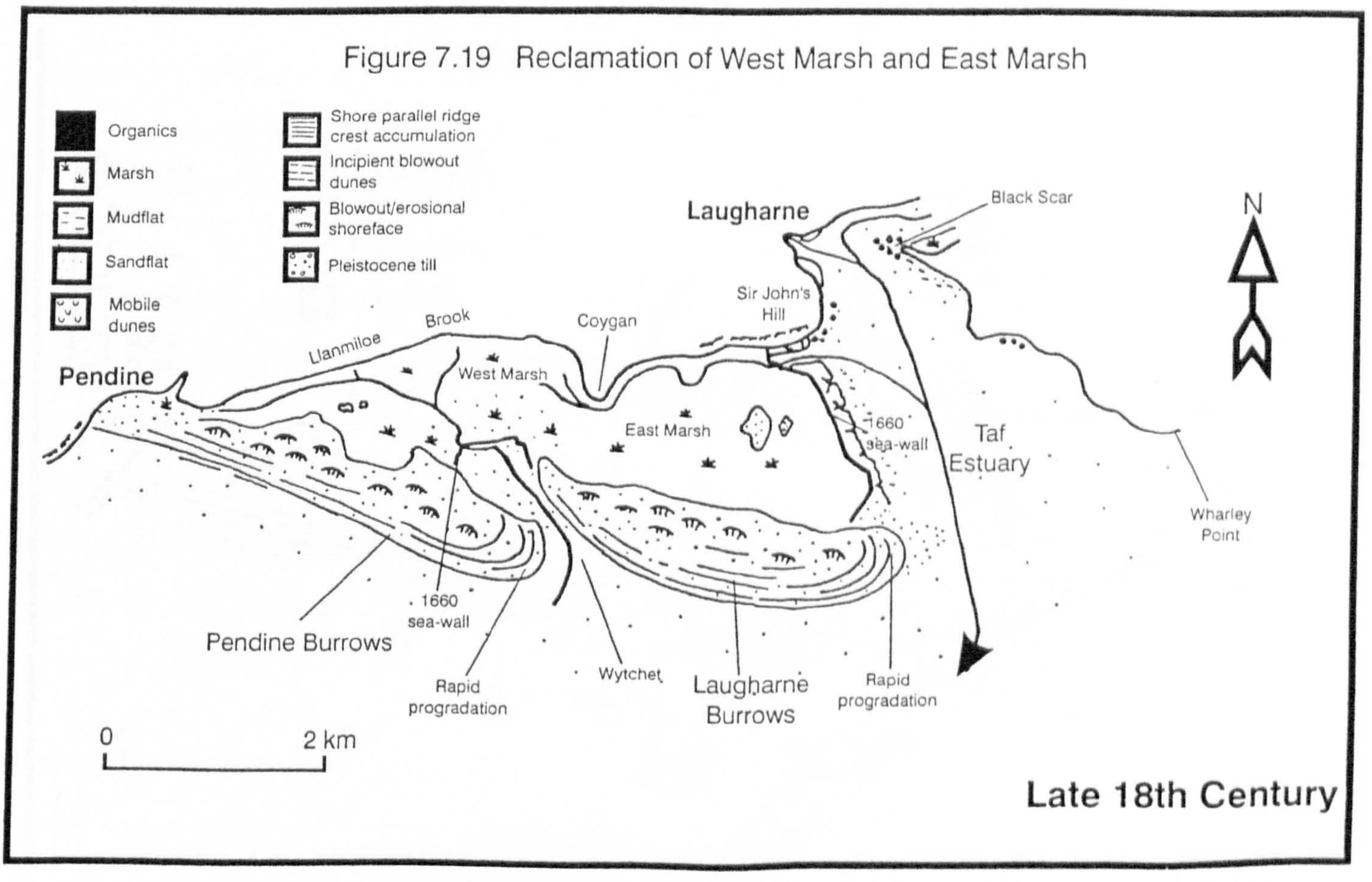

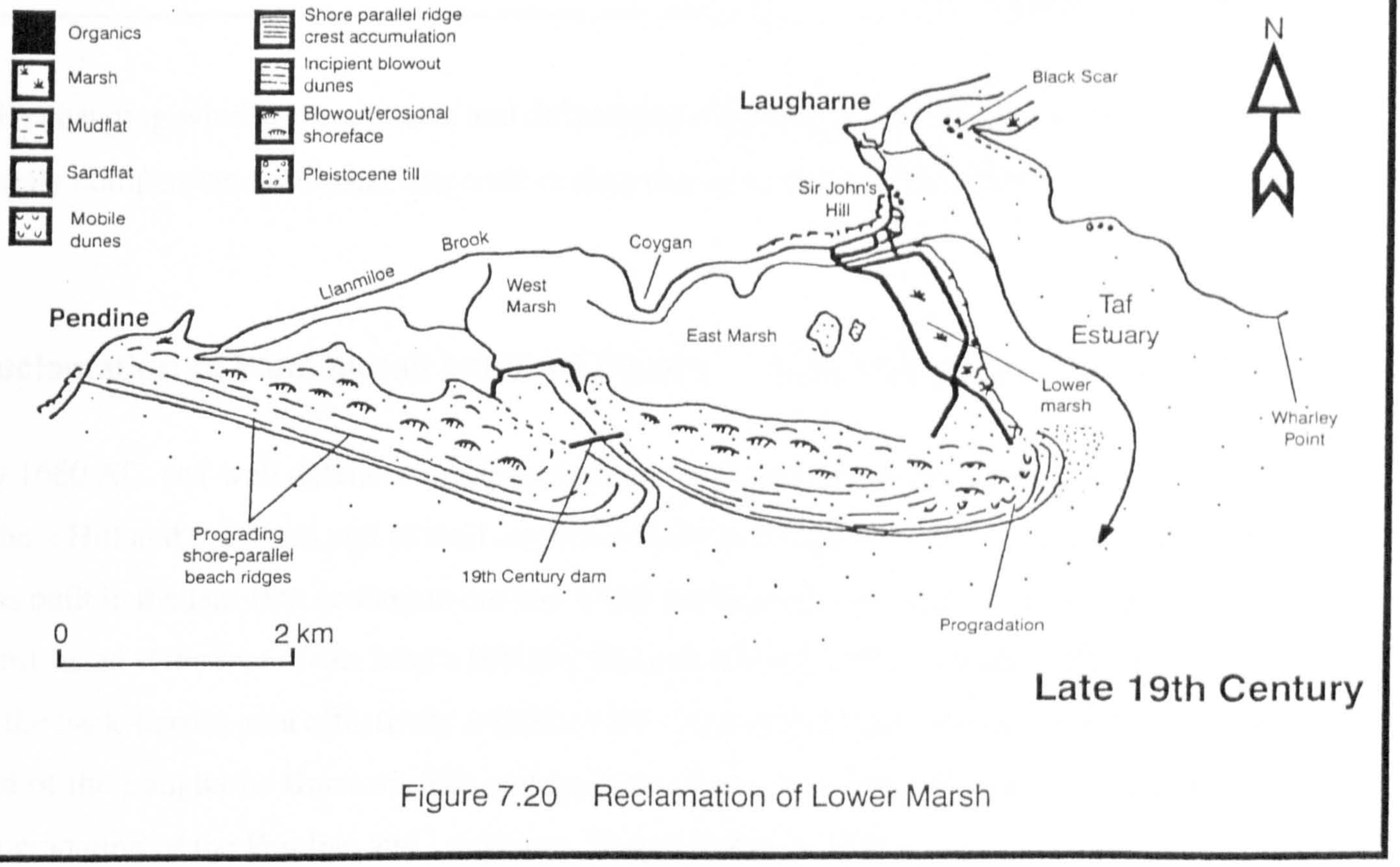

Figure 7.20 Reclamation of Lower Marsh

Figure 7.21 Contemporary barrier system

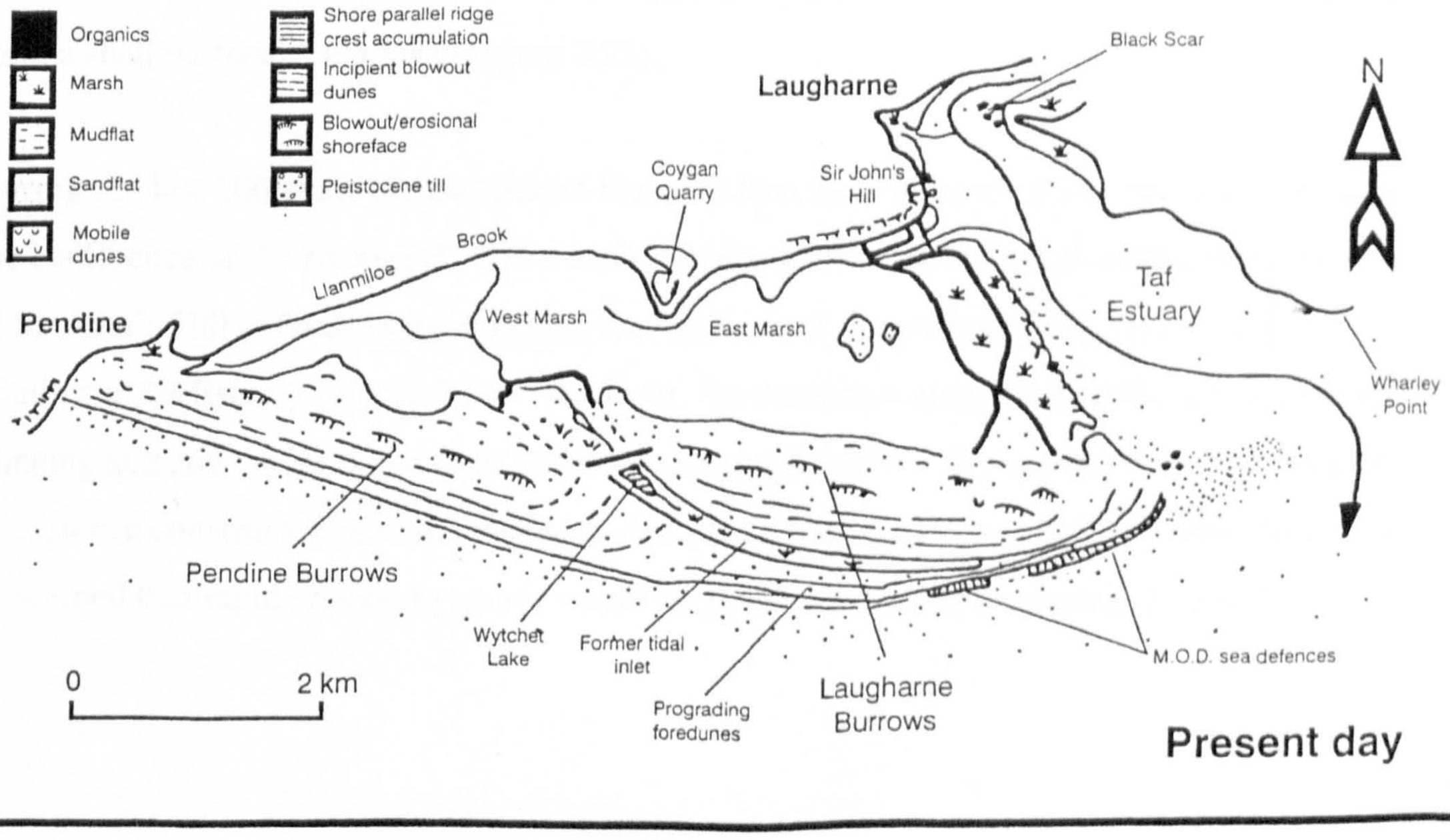

with changing wind/wave climates and differential sediment supply (Figure 7.18) *i.e.* sediment supply compensated sediment dispersal in response wind and wave erosion

.

Reclamation of West Marsh and East Marsh: Late 17th century to present day

By 1660 AD. sea-wall defences had been constructed across the Wytchet Inlet and between Sir John's Hill and the distal end of the Laugharne Burrows (Figure 7.19). A second embankment was built in the late 18th century to enclose lower marsh and by the 19th century dams had been constructed at the foot of Sir John's Hill and across the Wytchet Inlet (Figure 7.20). Reclamation of the back-barrier area effectively stabilised the barrier-spit by preventing erosion at the distal end of the Laugharne Burrows. The construction of sea-wall defences has promoted the rapid progradation of the Pendine and Laugharne Burrows (James, 1991).

The closure of the Wytchet Inlet resulted in sediment accumulation at the distal end of the Pendine Burrows because the position of this pass could not be maintained by tidal currents. Freshwater accumulating within West Marsh was diverted along a series of man-made ditches and drained out onto the Pendine Sands via Wytchet brook (Figure 7.20). However, with continued sediment supply, via southwesterly winds and longshore transport, the Pendine Burrows extended eastwards in front of the Laugharne Burrows impounding Wytchet brook to form a shallow freshwater lake (Figure 7.21).

During the last 100 years the Laugharne Burrows have continued to extend eastwards towards the confluence of the rivers Taf, Towy and Gwendraeth; saltmarshes now extend from the foot of Sir John's Hill to Ginst Point along the seaward side of the embankment, across the sandflats within the Taf Estuary (Figure 7.21). However, the continued elongation of the spit has caused thinning and erosion along the front of the Laugharne Burrows. During the 1970s the Ministry of Defence constructed sea-wall defences along the distal end of the barrier because they were concerned that rapid erosion by storm waves might lead to barrier breaching (Figure 7.21).

7.4 Mechanisms controlling Holocene barrier formation and evolution in south west Wales

The proposed hypothesis of barrier development describes the initiation, progradation and stability of the barrier system between 8,000 and 5,500 years BP. This is followed by a phase of erosion, barrier instability, breakdown and reworking between 5,500 and 5,000 years BP; during this period the shoreface was unable to maintain its position in response to increased storm activity and or reduced sediment supply. During barrier breakdown, the western portion of this feature was fixed in place by the antecedent topography which prevented the total breakdown and reworking of the system. Consequently, the back-barrier sediments deposited within West Marsh are preserved whereas tidal inlet sequences east of Coygan were probably reworked by wave action and tidal scour. Between 5,000 and 3,500 years BP the barrier underwent a second phase of initiation, progradation and long-term stability during which time the net input of sediment must have exceeded net dispersal by storm waves. This was followed by a second phase of barrier instability, breakdown and reworking which led to the formation of two discrete dune systems by storm-waves breaching the thinning spit. The succeeding phase of barrier progradation resulted in the longshore development of the Laugharne Burrows and the seaward advance of the two dune systems. The tidal inlet separating the dunes lies above the former meltwater channel which is probably filled with early Holocene estuarine sediment overlain by shoreface sands and spit re-curve deposits.

Seismic surveys show that the Pendine Burrows rest upon a ridge of Pleistocene till which extends from the cliffline at Pendine to a point seawards of Coygan. The area behind this feature has been excavated by freshwater streams and rivers draining from the fossil cliffline. At sites 3, 4 and 6 the Pleistocene material is unconformably overlain by fine grained mudflat and saltmarsh deposits. The absence of coarse beach sands or gravel lag deposits in contact with the pre-transgressive surface indicates that the high energy shoreface did not overstep this feature and rework the base of the fossil cliffline west of Coygan. It is proposed that the barrier formed initially in response to the in-place drowning of the antecedent topography. Rapid relative sea-level rise during the early Holocene inundated the area behind the ridge, introducing fine reworked sediment from exposed glacial drift within Carmarthen Bay. High-resolution reflection data acquired on the Pendine Sands show that the Pleistocene surface seaward of the ridge is

extremely flat and roughly parallel to the contemporary beach surface (section 5.1.2); this surface represents a distinct plane of marine erosion. The uneven morphology of the Plestocene ridge probably represents reworking wave action and erosion by freshwater drainage networks.

Small mobile dunes, sustained by sands entrained from the shoreface at low tide by strong westerly and southwesterly winds, probably became attached the ridge forming a low dune belt. Sand binding perennial dune grasses, such *Ammophilia arenaria* or *Carex arenaria*, may have rapidly colonised these dunes and in doing so would have stabilised the sands and promoted further sediment accumulation. The age of the lower biogenic sediments within West Marsh indicates that this feature predates similar barrier systems which are believed to have formed along the coast of south west Wales and Cornwall by approximately 6,000 years BP (Lewis, 1992; Healy, 1995). By 8,000 years BP it is likely that the transgressing shoreface began to rework extensive glacial deposits within Carmarthen Bay. Sediment would have been supplied to the barrier via longshore transport, from eroding glacial material west of Gilman Point, and from the reworking of relict sediments offshore. Once the sediment reached the barrier system it would have been partitioned across an energy gradient resulting in coarse sands being concentrated on the shoreface and fines transported into the back-barrier area. Relative sea-level rise would have ensured a continuous supply of sediment by exposing fresh areas of drift to erosion in the coastal zone.

The regressive overlap at the base of the sequence within West Marsh suggests that once the shoreface had established an equilibrium profile, in response oceanographic processes, differential sediment supply and relative sea-level rise, the barrier was able to prograde eastwards as a **spit**; provided that the wave climate, sediment supply and the rate of relative sea-level rise did not vary significantly the barrier would have been able to exhibit 'long-term' stability. Furthermore, the high relief of the fossil cliffline behind the barrier would have promoted spit development rather than the landward retreat of the barrier (Swift, 1975). The transition from mudflat to intertidal marsh at the base of the sequence within West Marsh is therefore a manifestation of long-term barrier stability.

Foraminiferal and pollen analyses indicate that the transition from minerogenic to organic sediment at sites 7, 12 and 4 corresponds to a decrease in marine influence *i.e.* from a saltmarsh

to a freshwater fen/swamp. Although, this negative tendency in sea-level may be interpreted as a regressive phase in relative sea-level rise, Jennings *et al.* (1995) argue that barrier systems are extremely complex and regressive/transgressive facies changes may simply represent phases of barrier stability and instability. For instance, if the surface of the marsh became elevated above the MHWST level, in response to rapid sedimentation during extremely high spring tides or a storm event, then freshwater vegetation may be able to develop at these sites above marine influence (Jennings *et al.*, 1995). Provided the surface of the mire remained above the MHWST level then freshwater organics would continue to accumulate if hydrological conditions were suitable. It is likely that the organics beds between -3.55 and 0.06 metres OD at site 8 represent freshwater communities accumulating upon washover deposits which were elevated above the MHWST level. However, conventional radiocarbon dates from organic deposits at sites 7, 12 and 4 indicate that organics of similar ages were accumulating at very different elevations within the back-barrier area; at 6,220 ± 45 years BP freshwater organics were accumulating at an elevation of -1.82 metres OD at site 4, by 5920 ± 50 years BP organics began to accumulate at an elevation of -2.21 metres OD at site 12, whereas organic accumulation continued at site 7 until 5770 ± 45 years BP at a height of -3.56 metres OD. The radiocarbon dates from the upper organic levels indicate that this second phase of biogenic accumulation was greatest at site 12, which was at that time lower than sites 4 and 7. Although, sediment compaction invoked during consolidation and by the coring procedure may account for some of the difference in elevation, similarities in the thickness of the organic units and overlying/underlying clays suggest that the differences in elevation are not an artifact of recovery or post-depositional processes.

For freshwater organics to accumulate at very different elevations within West Marsh between 6,200-5,700 years BP and between 4,500-3,500 years BP, while marine conditions persisted locally within the back-barrier area, the height of local relative sea-level probably fell. The organic levels at sites 7, 12 and 4 are believed to represent two regressive phases in local relative sea-level rise at Pendine. Organic accumulation in West Marsh was controlled primarily by the height of the local water table and reflects the complex hydrological patterns and uneven morphology within the back-barrier area. Fine grained organic-rich minerogenic sediment intercalated with the lower organic unit at sites 7, 12 and 4 indicates that during the first regressive phase (6220 to 5770 years BP) the position of local relative sea-level was fluctuating within West Marsh. Minerogenic lenses contained within the organic unit, are thickest at sites

7 and site 12 which lie below site 4 where biogenic accumulation is punctuated by thin lenses of saltmarsh sediment. In contrast, the upper organic units at sites 7 and 12 contain no minerogenic sediment whereas the organics at site 4 contain thin lenses of organic rich silty clay. The latter may represent the erosion and redeposition of sediment at site 4 by freshwater streams draining over the former marsh surface. The elevation and duration of organic accumulation between 4,630 and 3,580 years BP at sites 7, 12 and 4 suggests that the height of MHWST probably varied only slightly within West Marsh during this second regressive phase in relative sea-level rise.

Allen (1990) describes a series of peat levels within the Severn Estuary which occur several metres below the present marsh surface and can be found two metres above OD; the thickness of these deposits extends to over 1 metre. Conventional radiocarbon dates provided by Godwin and Willis (1964), Hawkins (1971), Heyworth and Kidson (1982) and Allen and Rae (1987) indicate that the oldest radiocarbon date is 6100 years BP whereas the youngest is 2180 years BP. Allen (1990) indicates that on the basis of mammalian remains, botanical character and root bases these deposits represent high marshes which were relatively infrequently flooded by the tide. The organic levels within the inner Severn Estuary are believed to represent a period of approximately 3000 conventional radiocarbon years when relative sea-levels fluctuated several times on a time scale of 500 to 1000 years (Allen, 1990).

It is likely that the organic sediments identified in West Marsh were deposited in response to the same episodic fluctuations in relative sea-level as described by Allen (1990). These fluctuations are however superimposed upon a gradual upward trend in local relative sea-level. The timing of these regressive phases corresponds to the change from rapid relative sea-level rise to a more gradual rise at approximately 6,000 years BP and the transition to slow relative sea-level rise at approximately 3,000 years BP (Heyworth and Kidson, 1982; Shennan, 1983). As discussed in section 2.2, reconstructions of former sea-level in south west Britain are complicated by the region being located on one of the widest continental shelves in the world, in an amphidromically complex situation, in a westerly storm belt, and by the large tidal range and crenellate coastline. As the coastal configuration and bathymetry changed within the Bristol Channel and Carmarthen Bay, in response to relative sea-level rise during the Holocene, the tidal range is believed to have decreased and the rate of change exhibited strong spatial gradients (Austin, 1991; Scourse and Austin, 1995). The fluctuations in relative sea-level within the Severn Estuary and West Marsh

may be linked to shifts in the position of tidal amphidromes and rapid changes in tidal range; however, until numerical models are able to accurately predict changes in the tidal amplitudes within the Bristol Channel in response to the Holocene transgression, the cause of the fluctuations in relative sea-level will remain unclear. Nevertheless, the two regressive phases in local relative sea-level rise at Pendine correspond to the changes in relative sea-level within the Severn Estuary over the same period (Allen, 1990). This indicates that relative sea-level rise within the Bristol Channel during the Holocene has been extremely complex. The smooth continuous curve produced by Heyworth and Kidson (1982) does not accurately represent the episodic nature of relative sea-level rise within this area.

Facies changes within West Marsh after 5770 and 3580 years BP indicate that the two phases of long-term stability were replaced by barrier instability, breaching and breakdown. The switch from freshwater organics to minerogenic marsh therefore indicates a positive tendency in sea-level. It is likely that if a large storms coincided with an extremely high spring tides then waves would have breached the barrier and introduced coarse washover deposits into West Marsh. However, if sediment supply continued to exceed erosion and dispersal then the shoreface would be able to re-establish an equilibrium profile and maintain long-term stability. This suggests that either the rate sediment supply decreased or the wave climate changed; although slight regressive phases in relative sea-level rise promote barrier stability and progradation it is unlikely that relative sea-level changes during the late Holocene were responsible for the phases of barrier instability described in this study.

Lewis (1992) suggested that the submerged forests exposed on the foreshore at Marros, Whitesands Bay, Lydstep and Pen-y-Bont formed behind a series of bay-head barriers which enclosed and protected the back-barrier areas. These barriers are believed to have formed in response to a fall in relative sea-level. Conventional radiocarbon dates show that organic accumulation continued at these sites during and after the breakdown of the Pendine/Laugharne barrier. Unlike the spit-barrier at Pendine these features were relatively enclosed and able to maintain an equilibrium with differential sediment supply and dispersal; they migrated landwards in response to relative sea-level rise permitting the continued accumulation of organic back-barrier facies. The formation of a whole series of barriers along the coastline probably affected the sediment budget and sediment dispersal within Carmarthen Bay. Sediment which would have

previously been supplied to the barrier at Pendine, from eroding glacigenic sediment via longshore transport, probably became trapped in smaller beach-barrier systems along the coastline. Although, reduced supply and changing sedimentary dispersal systems contributed to the eventual erosion of the barrier, oceanographic processes ultimately construct and destroy these features.

Prior to the construction of sea-wall defences at Ginst Point, the natural processes at the distal end of Laugharne Burrows could still be observed. During calm constructive periods low windblown dunes were able to form rapidly in front of the spit (Jago pers com., 1996). These deposits were colonised by vegetation and slowly built up over the calm summer months. However, during the winter months when storms combined with high spring tides, waves were able to breach the advancing dunes causing catastrophic erosion (Jago pers com., 1996). As storm activity within Carmarthen Bay is focused along the main intertidal drainage channels the wave heights increase progressively from Pendine to Ginst Point. Consequently, while the distal end of the barrier was periodically breached and broken down the centre of the barrier may have been able to prograde. Because the system exhibits long-term stability Ginst Point was able to re-establish a profile of dynamic equilibrium during calm constructive periods.

It is likely that during phases of long-term barrier stability and progradation the low vegetated dunes at the distal end of the spit advanced during calm constructive conditions and retreated during destructive storm events. As the spit extended eastwards its advance would have diverted the course of the River Taf; the distal end of the spit was probably attacked by large storm waves propagating up the intertidal channel excavated by the course of the Taf. Low frequency, high magnitude storm events are therefore superimposed upon the long-term evolution of the back-barrier area. The coarse sediments within East Marsh do not necessarily indicate the total breakdown of the Laugharne Burrows, but may represent the deposition of beach/dune sands by waves which periodically breached the barrier when strong southwesterly storms coincided with extremely high spring tides.

Changes in the growth and decay of the Pendine Barrier are therefore most probably due to changing oceanographic conditions which may by driven by climate changes in the North Atlantic during the Holocene. For instance, Lamb (1977, 1991) indicated that during the first

phase of the Little Ice Age (*ca.* 1350-1550 AD) the Polar climate zone began to expand toward the south. This forced the main westerly wind stream and cyclone tracks to move southwards and the subsequent increase in storm frequency had a profound effect on coastal development. It is very likely that these processes operated throughout the Holocene and are ultimately responsible for changing oceanographic conditions during the formation and development of the barrier at Pendine Sands.

As the shoreface responds instantly to changing wind and wave climates, increased storm activity could cause the rapid erosion and breakdown this feature. An increase in the frequency of westerly and southwestern storms could cause the barrier erosion and breakdown described in this study. Wind transport is a key factor in barrier dune development and is probably responsible for the long-term maintenance and recent development of the Pendine barrier system.

The absence of any datable horizons within East Marsh limits the applicability of the hypothesis because changes within this area of the system are not accurately calibrated. However, it is believed that the sequences within East Marsh formed over a much shorter time scale than those described within West Marsh. Lithostratigraphic data suggests that the Wytchet tidal inlet was created after 3,580 years BP during a period of barrier instability and breakdown. Neolithic finds within the Laugharne Burrows (SN 296076) are believed to represent a small settlement within the dunes (Cantrill, 1909; James, 1991); for such a settlement to be built the dunes were probably able to protect the inhabitants from strong southwesterly storms. As the Neolithic is believed to have continued up until approximately 4,000 BP in Europe (Challinor, 1978), the Laugharne Burrows may have been occupied during the second phase of long-term barrier stability between approximately 5,000 and 3,500 years BP. This supports the hypothesis that the Laugharne Burrows *per se* were formed by the breaching of the spit during the second phase of barrier instability.

This study has attempted to use multidisciplinary geophysical, biostratigraphic, lithological and minerogenic evidence to test hypotheses regarding the formation and subsequent evolution of the coastal sand barrier complex at Pendine. The proposed hypothesis of barrier evolution and the mechanisms explaining these changes represent one interpretation of the evidence described within the preceding chapters and by no means should be considered as definitive. Although, the

preferred hypothesis is to some degree supported by supplementary evidence from other sites within Carmarthen Bay (Allen, 1990; Lewis, 1992), it relies upon changing oceanographic conditions, the inherent episodic nature of local sea-level rise and assumes that sedimentary dispersal patterns within Carmarthen Bay have varied during the Holocene. The study does indicate that the gravel ridge beneath the Pendine Burrows played an integral role in the formation and subsequent survival of this feature and that many mechanisms have operated during the development of this system. If the western portion of the barrier had not been fixed in place by the antecedent topography it is very likely that the barrier at Pendine would either not have formed or would have been overstepped and reworked during the Holocene transgression. The ridge preserved the sediments within West Marsh and provided a platform from which the barrier subsequently developed. The evidence described in this study support theories which suggest that large barriers formed by mainland beach detachment and spit development is favoured in coastal areas with steep rugged relief (Hoyt, 1967; Swift, 1975). Although, the evolution of the Pendine barrier-spit exhibits some similarity to qualitative regional response-type models (McBride *et al.*, 1995), local topographic, oceanographic and sedimentological factors ultimately controlled the development of this particular system.

The study highlights the complexity of coastal barrier systems and the problems encountered when attempting to interpret back-barrier facies development. Information from numerous techniques are required to develop plausible hypotheses which aim to describe coastal barrier evolution. The barrier complex at Pendine has experienced significant changes in wave/wind climate, differential sediment supply, tidal range and possibly relative sea-level rise during the Holocene. The significance of antecedent topography indicates that the formation and evolution of this particular barrier is unique and should not be considered as a hypothesis for regional barrier evolution.

Chapter 8

Conclusions

8.1 Conclusions

This study uses a multidisciplinary approach to examine complex sequences within a large sand barrier system at Pendine Sands, South Wales. Lithostratigraphic, biostratigraphic and geophysical evidence is used to generate hypotheses which describe I) the formation and evolution of this feature during the Holocene and ii) the mechanisms which caused the changes in coastal configuration. The findings were as follows:

- Geophysical evidence shows that the western portion of the barrier (Pendine Burrows) rests on a ridge of Pleistocene glacigenic sediment; the area behind this feature has been excavated by freshwater draining into West Marsh from the fossil cliffline between Pendine and Coygan. The barrier at Pendine Sands initially formed in response to the drowning of the antecedent topography by rapidly rising relative sea-levels during the early Holocene (*ca.* 10,000-7,000 years BP). The ridge beneath the western portion of the barrier then played an integral role in the subsequent development and preservation of this feature. The evidence presented in this study does not suggest that the Pendine Barrier migrated landwards over back-barrier deposits in response to rising sea-levels during the early Holocene.

- Foraminifera and pollen contained within the back-barrier sequences are used to identify the sedimentary facies and local ecological changes within West and East Marshes; this information is used to interpret depositional environments within the back-barrier area and elucidate phases of barrier complex stability and instability. The proposed hypothesis of barrier development describes the initiation, progradation and stabilisation of the barrier system between 8,000 and 5,500 years BP. This was followed by a phase of erosion, barrier instability, breakdown and reworking between 5,500 and 5,000 years BP. During barrier breakdown the western portion of the feature was fixed in place by the

antecedent topography which prevented the landward migration and total reworking of the barrier dunes. Consequently, the back-barrier sediments deposited within West Marsh were preserved whereas tidal inlet sequences east of Coygan were reworked by wave action and tidal scour. Between 5,000 and 3,500 years BP the barrier underwent a second phase of progradation and stabilisation during which time sediment input must have exceeded sediment dispersal by storms. This was followed by a second phase of barrier instability, breakdown and reworking which led to the formation of two discrete dune systems by the breaching of the thinning spit by storm waves. The succeeding phase of barrier progradation resulted in the longshore development of the Laugharne Burrows and the seaward advance of the two dune systems. The tidal inlet separating the dunes lies directly above a former meltwater channel which is probably filled with early Holocene estuarine sediment, overlain by shoreface sands and spit re-curve deposits.

- The mechanisms which control barrier development at Pendine are related to oceanographic processes, sediment supply and relative sea-level change. Pollen, foraminiferal and lithostratigraphic evidence show that the two main periods of biogenic accumulation in West Marsh represent two regressive phases in relative sea-level change. These regressive phases triggered the initial stabilisation of the barrier and promoted longshore spit development; this was probably enhanced by the steep rugged relief of the cliffline between Pendine and Sir John's Hill. Rather than being a continuous process, long-term spit development is marked by relatively short periods of advance and retreat. The succeeding instability and reworking of the barrier dunes was caused by a change in the wave/wind climate, possibly driven by climatic changes in the North Atlantic during the Holocene. The ridge beneath the Pendine Burrows played a critical role in the response of this particular barrier system to changing oceanographic conditions and differential sediment supply; the antecedent topography ultimately prevented the total breakdown and or landward migration of this system in response to increased storm activity. Barrier stability was re-established when storm activity decreased and sediment was released from the reworking of smaller bay-head barriers within Carmarthen Bay. As these features were probably not fixed in the same way, they responded to increased storm activity by migrating landwards over their adjoining back-barrier deposits. Continued relative sea-level rise also exposed fresh glacigenic deposits which were

reworked by the surf zone. This increased the sediment budget within Carmarthen Bay and supplied a greater proportion of material to the barrier at Pendine Sands.

- Relative sea-level changes within the Bristol Channel and Carmarthen Bay were extremely complex during the Holocene. This study shows that the smooth gradual sea-level curves drawn for this region do not accurately represent local episodic changes which have had a significant effect on the configuration of the coastline.

- Reclamation of West and East Marshes for agricultural purposes during the 17th and 19th centuries has stabilized the system and promoted rapid spit development and sediment accumulation along the seaward side of the barrier. The configuration of the Pendine and Laugharne Burrows would be very different today if the seawall defences had not been erected and many of the mechanisms described above would continue to operate. Most of the sediment currently accumulating upon the upper foreshore of the Pendine Sands is supplied by southwesterly winds which influence the lower shoreface. The large expanse of sand flats which are exposed in Carmarthen Bay at low tide, and the frequency of strong southwesterly winds, were critical factors in the formation and development of the barrier dunes at Pendine Sands.

It can be concluded from this study that a number of mechanisms operated during the formation and development of the Pendine barrier system. Although the geomorphological response of this particular feature exhibits some similarity to regional response hypotheses, local sedimentological and topographic controls ultimately dictate the response of this barrier system to changing oceanographic conditions and relative sea-levels during the Holocene. The significance of antecedent topography indicates that the formation and evolution of the barrier at Pendine Sands is unique and should not be considered as universally applicable to regional barrier evolution.

8.2 Further Research

- The geophysical data used to elucidate the morphology of the pre-Holocene surface requires supplementary ground truth data from boreholes which penetrate the Pleistocene glacigenic sediments beneath West Marsh and East Marsh. This is necessary in order to calculate the absolute depth to the bedrock and Pleistocene beneath the study area. In addition more extensive marine reflection surveys within Carmarthen Bay would provide information on the pre-transgressive surface within the region. This data could be incorporated in palaeo-tidal models used to interpret local and regional eustatic changes in relative sea-level.

- Detailed studies of the modern hydrodynamic regime within Carmarthen Bay are required in order to elucidate and model possible sedimentary dispersal patterns during the Holocene transgression. This information can be used to establish the actual mechanisms which led to phases of barrier stability and instability at Pendine Sands.

- Relative sea-level rise within the Bristol Channel during the Holocene was extremely complex. Further work is required to determine whether the regressive and transgressive phases in relative sea-level rise at Pendine Sands represent regional changes or are simply a local phenomenon.

REFERENCES

ALLEN, P. 1964. Sedimentological models. *Journal of Sediment Petrology* **34**, 289-293.

ALLEN, J.R.L 1990. The Severn Estuary in southwest Britain: its retreat under marine transgression, and fine sediment regime. *Sedimentary Geology* **66**, 13-28.

ALLEN, J.R.L. 1991. Fine sediments sources, Severn Estuary and the inner Bristol Cannel, Southwest Britain. *Sedimentary Geology* 75, 57-65.

ALLEN, J.R.L. and RAE, J.E. 1988. Vertical salt-marsh accretion since the Roman period in the Severn Estuary, Southwest Britain. *Marine Geology* **83**, 225-235.

AUSTIN, R.M. 1991. Modelling Holocene tides on the NW European continental shelf. *Terra Nova* **3**, 276-288.

AUSTIN, W.E.N. 1991. Late Quaternary foraminiferal stratigraphy of the Western UK continental shelf. Unpublished Ph.D Thesis, University of Wales.

BARRIE, J.V. 1978. Heavy mineral distribution in bottom sediments of the Bristol Channel. Unpublished MSc Thesis, University of Wales.

BARRIE, J.V. 1980. Heavy mineral distribution in bottom sediments of the Bristol channel, UK *Estuarine and Coastal Marine Science* **11**, 369-381.

BAZYLINSKI, D.A., HEYWOOD, B.R., MANN, S. and FRANKEL, 1993. Fe_3O_4 and Fe_3S_4 in a bacterium. *Nature* **366**, 281.

BELDERSON, R,H., PINGREE, R.D. and GRIFFITHS, D.K. 1986. Low sea-level tidal origin of Celtic Sea sand banks: evidence from numerical modelling of M_2 tidal streams. *Marine Geology* **73**, 99-108.

BELKNAP, D.F. and KRAFT, J.C. 1981. Preservation potential of transgressive coastal Lithosomes on the U.S. Atlantic Shelf. *Marine Geology* **42**, 429-442.

BELKNAP, D.F. and KRAFT, J.C. 1985. Influence of antecedent geology on stratigraphic preservation potential and evolution of Delaware's barrier systems. Marine Geology 63, 235-262.

BERGLUND, B.E. and RALSKA-JASIEWICZOWA, M. 1986. Pollen analysis and pollen diagrams. In B.E. Berglund (ed) Handbook of Holocene Palaeoecology and Palaeohydrology. John Wiley & Sons, New York.

BERRYMAN, K.R., YOKO, O. and HULL, A.G. 1992. Holocene evolution of an estuary on a tectonically rising coast: the Pakarae River locality, eastern North Island, New Zealand. *Sedimentary Geology* **80**, 151-165.

BJÖRCK, S., PERSSON, T. and KRISTERSSON, I. 1978. Comparison of two concentration methods for pollen in minerogenic sediments. *Geol. Fören, I Stckholm Förh.* **100**, 107-111.

BIRKS, H.J.B. and BIRKS, H.H. Quaternary palaeoecology. Edward Arnold.

BLOOM, A.L. 1977. Atlas of sea-level curves. Cornell University, New York, *International Geological Correlation Programme 61.*

BOLTOVSKOY, E and TOTAH, V.I. 1992. Preservation index and preservation potential of some foraminiferal species. *Journal of Foraminiferal Research* **22**, 267-273.

BOULTON, G.S. 1992. The spectrum of Quaternary Global change: understanding the past and anticipating the future. *Geoscientist* **2**, 10-12.

BOUYSEE, P., HORN, R., LAPIERRE, F. and LE LANN, F. 1976. Etude des grands bancs de sable du sudest de la mer Celtique. *Marine Geology* **20**, 251-275.

BOWEN, D.Q. 1970. South-east and central South Wales. In C.A. Lewis (ed), The glaciations of Wales and adjoining regions. Longman, London, 177-228.

BOYD, R. and PENLAND, S. 1984. Shoreface translation and the Holocene stratigraphic record: Examples from Nova Scotia, The Mississippi Delta and Eastern Australia. *Marine Geology* **60**, 391-412.

BRABHAM, P.J. and McDONALD. 1992. Imaging a buried river channel in an intertidal area of South Wales using high-resolution seismic techniques. *Quarterly Journal of Engineering Geology* **25**, 227-238.

BREDEWOUT, J.W. and GOULTY, N.R. 1986. Some shallow seismic reflections. *First Break* **4**(12), 15-23.

BRIGGS, L.I. 1965. Heavy mineral correlation and provenances. *Journal of Sediment Petrology* **35**, 939-955.

CAMBELL, S. and BOWEN, D.Q. 1989. Quaternary of Wales. *Geological Conservation Review* A4.1.

CANTRILL, T.C. 1909. Shell mounds on Laugharne Burrows. *Archaeologia Cambrenis 6 Series* **9**, 433-472.

CARTER, R.M., CARTER, L. and JOHNSON, D.P. 1986. Submergent shorelines in the SW Pacific: evidence for an episodic post-glacial transgression. *Sedimentology* **33**, 629-649.

CARTER, R.W.G. 1988. Coastal environments. Academic Press, London, New York.

CARTER, R.W.G., FORBES, D.L., JENNINGS, S.C., ORFORD, J.D., SHAW, J. and TAYLOR, R.B. 1989. Barrier and Lagoon coast evolution under differing relative regimes: Examples from Ireland and Nova Scotia. *Marine Geology* **88**, 221-242.

CARTER, R.W.G., ORFORD, J.D., FORBES, D.L. and TAYLOR, R.B. 1990. Morphosedimentary development of drumlin-flank barriers with rapidly rising sea-level, Story Head, Nova Scotia. *Sedimentary Geology* **69**, 117-138.

CASE, D.J. 1983. Quaternary air-fall deposits in South Wales: loess and coversands. Unpublished Ph.D Thesis, University of Wales.

CHALLINOR, J. 1978. A dictionary of geology. University of Wales Press, Cardiff.

CHAPPEL, J. 1978. Chronological methods and the ranges of Quaternary physical change. In D. Walker and J.C. Guppy (eds), *Biology and Quaternary Environments*. Australian Academy of Science, Canberra.

CLAPHAM, A.R., TUTIN, A.R. and MOORE, D.M. 1987. Flora of the British Isles. Cambridge University Press.

CLARK, J.A., FARRELL, W.E. and PELTIER, W.R. 1978. Global changes in Post-glacial sea-level: A numerical calculation. *Quaternary Research* **9**, 265-287.

CLARK, J.S., OVERPECK, J.T., WEBB, T. III, and PATTERSON, W.A. III. 1986. Pollen stratigraphic correlation and dating of barrier-beach peat sections. *Review of Palaeobotany Palynology* **47**, 145.

COLEMAN, J.M. and SMITH, W.G. 1964. Late and recent rise in sea-level. *Geological Society of America Bulletin* **75**, 833-840.

CULVER, S.J. and BANNER, F.T. 1979. The significance of derived pre-Quaternary foraminifera in Holocene sediments of the north-central Bristol Channel. *Marine Geology* **101**, 203-207.

CURRAY, J.R. and MOORE, D.G. 1964. Pleistocene deltaic progradation of continental terrace, Costa de Layarit, Mexico. In Van Andel and Shor (eds), *Marine geology of the Gulf of California, American Association of Petroleum Geologists*, 193-215.

CURTIS, M. 1880. The antiquities of Laugharne, Pendine and their neighbours, 2nd Edition.

DAVIS, A.M. and BENNELL, J.D. 1988. Resolving overburden characteristics via shear wave propagation. *Proceedings of the ASEG/SEG Conference Adelaide*, 41-44.

DAVIS, M.B. 1973. Redeposition of pollen grains in lakes. *Limnol. Oceanogr.* **18**, 44-52.

DAVIS, R.A.Jr and KUHN, B.J. 1985. Origin and development of Anelote Key, west-penninsular Florida. *Marine Geology* **63**, 153-172.

DEBEAUMONT, E. 1845. *Lecons de géologie pratique*, Paris, 223-252.

DEER, W.A., HOWIE, R.A. and ZUSSMAN, J. 1992. An introduction to the rock forming minerals. Longman Scientific & Technical, Hong Kong.

DEVOY, R.J.N. 1987. Introduction: First principles and the scope of sea-surface studies. In R.J.N. Devoy (ed.) *Sea Surface Studies: A Global View*, London, Croom Helm, 1-33.

DOORNEBAL, J.C. and HELBIG, K. 1983. High-resolution reflection seismics on a tidal flat in the Dutch Delta: acquisition, processing and interpretation. *First Break* **1**(5), 9-20.

ELLWOOD, B.B. 1980. Induced and remanent magnetic properties of marine sediments as indicators of depositional processes. *Marine Geology* **38**, 233-244.

ERDTMAN, G. 1960. The acetolysis method. *Sevensk. Bot. Tisdskr.* **54**, 561-564.

FÆGRI, K. and IVERSEN, J. 1975. Textbook of pollen analysis. Munksgaard.

FÆGRI, K. and IVERSEN, J. 1989. Textbook of pollen analysis. John Wiley & Sons, New York.

FAIRBANKS, R.G. 1989. A 17,000-year glacio-eustatic sea-level record: influence of glacial melting rates on the Younger Dryas event and deep-ocean circulation. *Nature* **342**, 637-642.

FAIRBRIDGE, R.W. 1961. Eustatic changes in sea-level. *Physics and Chemistry of the Earth* **5**, 99-185.

FARINA, M., ESQUIVAL, D.M.S. and LINS DE BARROS, H.G.P. 1990. Magnetic iron-sulphide crystals from a magnetotactic organism. *Nature* 343, 256-258.

FLEMMING, N.G. 1982. Multiple regression analysis of earth movements and eustatic change in the United Kingdom in the past 9000 years. *Proceedings of the Geologists' Association* **93**, 113-125.

FOLK, R.L. 1966. A review of grain-size parameters. *Sedimentology* **6**, 73-93.

FRIHY, O.E., LOTFY, M.F. and KOMAR, P.D. 1995. Spatial variations in heavy minerals and patterns of sediment sorting along the Nile Delta, Egypt. *Sedimentary Geology* **97**, 33-41.

GARRARD, R.A. and DOBSON, M.R. 1974. The nature and maximum extent of glacial sediments off the west coast of Wales. *Marine Geology* **16**, 31-44.

GEHRELS, W.R. 1994. Determining relative sea-level change from salt-marsh foraminifera and plant zones on the coast of Maine, USA. *Journal of Coastal Research* **10**, 990-1009.

GILBERT, G.K. 1885. The topographic feature of lake shores. *U.S. Geological Survey 5th Annual Report*, 69-123.

GODWIN, H. 1975. History of the British flora: A factual basis for phytogeography. Cambridge University Press.

GODWIN, H. and MITCHELL, G.F. 1938. Stratigraphy and development of two raised bogs near Tregaron, Cardigan Shire. *New Phytologist* **37**, 425-455.

GODWIN, H. and WILLIS, E.H. 1964. Cambridge University natural radiocarbon measurements III. *Radiocarbon* **6**, 116-137.

GOLDSTEIN, S.T. and HARBEN, E.B. 1993. Taphofacies implications of infaunal foraminiferal assemblages in a Georgia saltmarsh, Sapelo Island. *Micropaleontology* **39**, 53-62.

GREENSMITH, J.T. and TUCKER, E.V. 1986. Compaction and consolidation. In O. Van de Plassche (ed.) *Sea-level Research: A manual for the collection and evaluation of data*, Norwich, Geo Books, 591-604.

GRIBBLE, C.D. 1988. Rutley's elements of mineralogy. 27th Edition, Unwin Hyman, London.

GRIFFITHS, J.C. 1939. The mineralogy of the glacial deposits of the region between the rivers Neath and Towy, South Wales. *Proceedings of the Geologists Association* **50**, 443-462.

GRIFFITHS, J.C. 1967. Scientific methods in the analysis of sediments. McGraw-Hill.

GRIFFITHS, D.H. and KING, R.F. 1982. Applied geophysics for geologists and engineers. 2nd Edition, Pergamon Press.

HAND, B.M. 1964. Hydrodynamics of beach and dune sedimentation. Unpublished Ph.D Thesis, Pennsylvania State University.

HARRIS, P.T. and COLLINS, M.B. 1988. Estimation of annual bedload flux in a macrotidal estuary: Bristol Channel, U.K. *Marine Geology* **83**, 237-252.

HARRIS, B.M. and COLLINS, M.B. 1991. Sand transport in the Bristol Channel: Bedload parting zone or mutually evasive sand transport pathways? *Marine Geology* **101**, 209-216.

HAWKINS, A.B. 1971. Sea-level changes around South West England. In D.J. Blackman (ed), *Marine Archaeology*. Butterworth, London.

HAYES, M.O. 1975. Morphology of sand accumulation in estuaries: An introduction to the symposium. In L.E. Cronin (ed.), *Estuarine Research* **2**, 3-22.

HAYNES, J.R. 1973. Cardigan Bay recent foraminifera (cruises of the R.V. Antur, 1962-1964). *Bulletin of the British Museum* (Natural History) *Zoology Supplement* **4**, 8-245.

HEALY, M.G. 1995. The lithostratigraphy of a Holocene coastal sediment sequence in Marazon Marsh, West Cornwall, U.K. with reference to relative sea-level movements. *Marine Geology* **124**, 237-252.

HERON, S.D., MOSLOW, T.F., BERELSON, W.M., HERBERT, J.R., STEELE, G.A.III. and SUSMAN, K.R. 1984. Holocene sedimentation of a wave dominated barrier-island shoreline: Cape Lookout, North Carolina. In B. Greenwood and R.A. Davis, Jr (ed.), *Hydrodynamics and Sedimentation in Wave Dominated Coastal Environments. Marine Geology* **60**, 413-434.

HEYWORTH, A. and KIDSON, C. 1982. Sea-level changes in Southwest England and Wales. *Proceedings of the Geologists' Association* **93**, 91-111.

HIBBERT, F.A. and SWITSUR, V.R. 1976. Radiocarbon dating of Flandrian pollen zones in Wales and Northern England. *New Phytologist* **77**, 793-807.

HINTON, A.C. 1992. Palaeotidal changes within the area of the Wash during the Holocene. *Proceedings of the Geologists' Association* **103**, 259-272.

HOYT, J.H. 1967. Barrier Island formation. *Geological Society of America Bulletin* **78**, 1125-1136.

HOYT, J.H. 1970. Development and Migration of Barrier Islands, Northern Gulf of Mexico: Discussion. *Geological Society of America Bulletin* **81**, 3779-3782.

HUGHES, T.J. 1987. Deluge II and the continent of doom: rising sea-level and collapsing Antarctic ice. *Boreas* **16**, 89-100.

HUNTLEY, B. and BIRKS, H.J.B. 1983. An atlas of past and present pollen maps for Europe: 0-13,000 years ago. Cambridge University Press.

KIDSON, C. 1982. Sea-level changes in the Holocene. *Quaternary Science Reviews* **1**, 121-151.

KIDSON, C. 1986. Sea-level changes in the Holocene. In O. Van de Plassche (ed) *Sea-level Research: A manual for the collection and evaluation of data*, Norwich, Geo Books, 27-64.

KIDSON, C. and HEYWORTH, A. 1979. Sea "level". *Proceedings 1978 International Symposium on Coastal Evolution in the Quaternary*. Sao Paulo, Brazil.

KINDLER, P. 1992. Coastal response to the Holocene transgression in the Bahamas: episodic sedimentation versus continuous sea-level rise. *Sedimentary Geology* **80**, 319-329.

KLINE, P. 1994. An easy guide to factor analysis. Routledge, London.

KNAPP, R.W. and STEEPLES, D.W. 1986. High-resolution common-depth point seismic reflection profiling: Instrumentation. *Geophysics* **51**, 276-282.

KROUSKOPT, K.B. 1982. Introduction to geochemistry. McGraw-Hill, London.

JACOBSON, G.L. and BRADSHAW, R.H.W. 1981. The selection of sites for paleoenvironmental studies. *Quaternary Research* **16**, 80-96.

JAGO, C.F. 1974. The sedimentology of estuarine and coastal plain deposits between Pendine and Wharley Point, Carmarthen Bay. Unpublished Ph.D Thesis, Imperial College London.

JAGO, C.F. 1980. Contemporary accumulation of marine sand in a macrotidal estuary, southwest Wales. *Sedimentary Geology* **26**, 21-49.

JAGO, C.F. and HARDISTY, J. 1984. Sedimentology and morphodynamics of a macrotidal beach Pendine Sands, South Wales. *Marine Geology* **60**, 123-154.

JAMES, T. 1991. Where the sea meets the land: The changing Carmarthenshire coastline. In H.James (ed), Sir Gâr: Studies in Carmarthenshire History, : essays in memory of W.H. Morris and M.C.S. Evans. *Carmarthenshire Antiquarian Society, Monograph Series No4.*

JENKINS, D.A. 1964. Trace element studies on some Snowdonian rocks, their minerals and related soils. Unpublished Ph.D Thesis, University of Wales.

JENNINGS, A.E. and NELSON, A.R. 1992. Foraminiferal assemblages zones in Oregon tidal marshes - relation to marsh flora zones and sea-level. *Journal of Foraminiferal Research* **22**, 13-29.

JENNINGS, A.E., NELSON, A.R., SCOTT, D.B. and ARAVENA, J.C. 1995. Marsh foraminiferal assemblages in the Valdivia Estuary, South-Central Chile: Relation to vascular plants and sea-level. *Journal of Coastal Research* **11**, 107-123.

JENNINGS, S.C., CARTER, R.W.G. and ORFORD, J.D. 1993. Late Holocene saltmarsh development under a regime of rapid relative sea-level rise: Chezzetcook Inlet, Nova Scotia. *Canadian Journal of Earth Sciences* **30**, 1374-1384.

JENNINGS, S.C., CARTER, R.W.G. and ORFORD, J.D. 1995. Implications for sea-level research of saltmarsh and mudflat accretionary processes along paraglacial barrier coasts. *Marine Geology* **124**, 129-136.

JOHASSON, K.E. and PATTERSON, R.T. 1992. Preservation potential of saltmarsh foraminifera from the Fraser River, British Columbia. *Micropaleontology* **38**, 289-301.

JONGERIUS, P. and HELBIG, K. 1988. Onshore high-resolution seismic profiling applied to sedimentology. *Geophysics* **53**, 1276-1283.

LAMB, H.H. 1977. Climate- present, past and future: Volume 2, Climatic history and the furture. Methuen, London.

LAMB, H.H. 1991. Historic storms over the North Sea, British Isles and Northwest Europe. Cambridge University Press.

LEWIS, M.P. 1992. The pre-history of South-West Wales, 7500-3600 BP. An interdisciplinary palaeoenvironmental and archaeological investigation. Unpublished Ph.D Thesis, University of Wales.

LI, M.Z. and KOMAR, P.D. 1992a. Longshore grain sorting and beach placer formation adjacent to the Columbia River. *Journal of Sediment Petrology* **62**, 429-441.

LI, M.Z. and KOMAR, P.D. 1992b. Selective entrainment and transport of mixed size and density sands: Flume experiments stimulating the formation of black sand placers. *Journal of Sediment Petrology* **62**, 584-590.

LOEBLICH, A.R. and TAPPAN, H.T. 1988. Foraminiferal genera and their classification. Von Nostrand Reinhold Company, New York.

LOUBERE, P., GARY, A. and LAGOE, M. 1993. Generation of the benthic foraminiferal assemblage: Theory and preliminary data. *Marine Micropaleontology* **20**, 165-181.

LOWRIGHT, R., WILLIAMS, E.G. and DACHILLE, F. 1972. An analysis of the factors controlling deviations in hydraulic equivalence in some modern sands. *Journal of Sediment Petrology* **42**, 635-645.

MACLAREN, C. 1842. The glacial theory of Professor Agassiz. *American Journal of Science* **42**, 346-365.

MAHER, B.A. 1988. Magnetic properties of some synthetic sub-micron magnetites. *Geophysical Journal* **94**, 83-96.

MAHER, B.A. and TAYLOR, R.G. 1988. Formation of ultrafine-grained magnetite in soils. *Nature* **336**, 368-671.

MANN, S., SPARKS, N.H.C., FRANKEL, R.B., BAZYLINSKI, D.A. and JANNASCH, H.W. 1990. Biomineralisation of ferrimegnetic gregite (Fe_3S_4) and iron pyrite (FeS_2) is a magnetotactic bacterium. *Nature* **343**, 258-261.

McBRIDE, R.A., BRYNES, M.W. and HILAND, M.W. 1995. Geomorphic response type model for barrier coastlines: A regional perspective. *Marine Geology* **126**, 143-159.

McFLAREN, E. 1961. Radiocarbon dating of Late Quaternary deposits, South Louisiana. *Geological Society of America Bulletin* **72**, 129-158.

McQUILLIN, R., BACON, M. and BARCLAY, W. 1984. An introduction to seismic interpretation: Reflection seismics in petroleum exploration. 2nd Edition, Graham & Trotman.

MILLER, R.D., PULLAN, S.E., STEEPLES, D.W. and HUNTER, J.A. 1992. Field comparison of shallow seismic sources near Chino California. *Geophysics* **57**, 693-709.

MILLER, R.D., ANDERSON, N.L., FELDMAN, H.R. and FRANSEEN, E.K. 1995. Vertical resolution of a seismic survey in stratigraphic sequences less than 100m deep in southeastern Kansas. *Geophysics* **60**, 423-430.

MILNER, H.B. 1962. Sedimentary Petrography: Volume II Principles and Applications. Gorge, Allen & Unwin Ltd.

MILSOM, J. 1989. Field geophysics. *Geological Society of London Handbook*, Open University Press.

MITCHELL, J.D. and STEPHENS, N. 1979. Is there evidence for a Holocene sea-level higher than that of today on the coasts of Ireland ?. *Colloques International du CRNS* **219**, 115-125.

MOOK, W.G. and VAN DE PLASSHE, O. 1986. Radiocarbon dating. In O. Van de Plassche (ed) *Sea-level Research: A manual for the collection and evaluation of data*, Norwich, Geo Books.

MOORE, P.D. and WEBB, J.A. 1978. An illustrated guide to pollen analysis. Hodder & Stoughton, London.

MOORE, P.D., WEBB, J.A. and COLLINSON, M.E. 1991. Pollen analysis. Blackwell Scientific Publications, London.

MÖRNER, N-A. 1980. The northeastern European "sea-level laboratory" and regional eustasy. *Palaeogeography, Palaeoclimatology and Palaeoecology* **29**, 281-300.

MÖRNER, N-A. 1984. Planetary, solar, atmospheric and endogene processes as origin of climatic changes on the Earth. In N-A. Mörner and W. Karlen (eds.) *Changes in a Yearly to Millenial Basis*, Dordrecht, Reidel, 483-507.

MÖRNER, N-A. 1987. Models of global sea-level changes. In M.J. Tooley and I. Shennan (eds.) *Sea-level Changes*, Basil Oxford, Blackwell Ltd, 332-354.

MUDIE, P.J. and BRYNE, R. 1980. Pollen evidence for historical sedimentation rates in California coastal marshes. *Estuarine and Coastal Marine Science* **10**, 305-316.

MURRAY, J.W. 1979. British nearshore foraminiferids. *Synopses of the British Fauna* No. 16. Acedemic Press.

MURRAY, J.W. 1991. Ecology and palaeoecology of benthic foraminifera. Longman, London.

MURRAY, J.W. and HAWKINS, A.B. 1976. Sediment transport in the Severn Estuary for the past 8000-9000 years. *Journal of the Geological Society London* **132**, 385-398.

OLDALE, R.N. 1985. A drowned Holocene barrier spit of Cape Ann, Massachusetts. *Geology* **13**, 375-377.

OLDFIELD, F. 1991. Environmental magnetism - A personal perspective. *Quaternary Science Reviews* **10**, 73-85.

OLDFIELD, F. 1994. Toward the discrimination of fine grained ferrimagnets by magnetic measurements in lakes and near-shore marine sediments. *Journal of Geophysical Research* **99**, 9045-9050.

OLDFIELD, F. and YU, L. 1994. The influence of particle size variations on the magnetic properties of the sediments from the north-eastern Irish Sea. Sedimentology 41, 1093-1108.

OTVOS, E.G.Jr. 1970a. Development and Migration of Barrier Islands, Northern Gulf of Mexico. *Geological Society of America Bulletin* **81**, 241-246.

OTVOS, E.G.Jr. 1970b. Development and Migration of Barrier Islands, Northern Gulf of Mexico. *Geological Society of America Bulletin* **81**, 3783-3788.

PANTIN, H.M. and EVANS, C.D.R. 1984. The Quaternary history of the central and south western Celtic Sea. *Marine Geology* **57**, 259-293.

PALMER, D. 1980. The generalized reciprocal method of seismic refraction interpretation. *Society of Exploration Geophysicists, Tulsa.*

PATTERSON, R.T. 1990. Intertidal benthic foraminiferal biofacies on the Fraser River Delta, British Columbia: Modern distribution and palaeoecological importance. *Micropaleontology* **36**, 229-244.

PIERCE, J.W. 1969. Sediment budget along a Barrier Island chain. *Sedimentary Geology* **3**, 5-16.

PREECE, R.C., SCOURSE, J.D., HOUGHTON, S.D., KNUDSEN, K.L. and PENNEY, D.N. 1990. The Pleistocene sea-level and neotectonic history of the eastern Solent, southern England. *Philosophical Transactions of the Royal Society of London* **328**, 425-477.

PRICE, W.A. 1963. Origin of barrier chain and beach ridge. *Geological Society of America Special Paper* **73**, 355.

PYE, K. 1984. Models of transgressive coastal dune building episodes and their relationship to Quaternary sea-level changes: A discussion with reference to evidence from Eastern Australia. In M.W. Clark (ed.) *Coastal Research: UK Perspectives*, University Press Cambridge, Geo Books, 81-104.

RAMPINO, M.R. and SAUNDERS, J.E. 1981. Evolution of the barrier islands of Southern Long Island, New York. *Sedimentology* **28**, 37-47.

RIGGS, S.R., CLEARY, W.J. and SNYDER, W.S. 1995. Influence of inherited geologic framework on barrier shoreface morphology and dynamics. *Marine Geology* **126**, 213-234.

RITTENHOUSE, G. 1943. The transportation and deposition of heavy minerals. *Geological Society of American Bulletin* **54**, 1725-1780.

ROY, P.S., THOM, B.G. and WRIGHT, L.D. 1980. Holocene sequences on an embayed high-energy coast: An evolutionary model. *Sedimentary Geology* **26**, 1-19.

RUBEY, W.W. 1933. The size distribution of heavy minerals within water laid sandstones. *Journal of Sediment Petrology* **3**, 3-29.

SAVIGEAR, R,.A.G. 1953. Some observations on slope development in South Wales. *Trans. Inst. Brit. Geog.* **18**, 31-52.

SCOTT, D.B. and MEDIOLI, F.S. 1978. Vertical zonation of marsh foraminifera as accurate indicators of former sea-level. *Nature* **272**, 528-531.

SCOTT, D.B. and MEDIOLI, F.S. 1980. Quantitative studies of marsh foraminiferal distributions in Nova Scotia - Implications for sea-level studies. *Cushman Foundation for Foraminiferal Research Special Publication* No 17, 58.

SCOTT, D.K. and LECKIE, R.M. 1990. Foraminiferal zonation of Great Sippewissett saltmarsh (Falmouth, Massachusetts). *Journal of Foraminiferal Research* **20**, 248-266.

SCOURSE, J.D. 1992. Quaternary sea-level change and coastal management. *Geoscientist* **2**, 13-16.

SCOURSE, J.D. and AUSTIN, R.M. 1995. Palaeotidal modelling of continental shelves: marine implications of a land bridge in the Strait of Dover during the Holocene and Middle Pleistocene. In R.C. PREECE (ed), Island Britain: a Quaternary perspective. *Geological Society London Special Publication No* 96.

SHENNAN, I. 1983. Flandrian and Late Devensian sea-level changes in England and Wales. In D.E. Smith and A.G. Dawson (eds.) *Shorelines and Isostasy*, 225-283.

SHENNAN, I. 1987. Holocene sea-level changes in the North Sea. In M.J. Tooley and I. Shennan (eds.) *Sea-level Changes*, Oxford, Basil Blackwell Ltd, 109-151.

SHENNAN, I. 1989a. Late Quaternary sea-level changes: Measurement, correlation, and future applications - the international significance of IGCP Project 200. *Journal of Quaternary Science* **4**, 3-5.

SHENNAN, I. 1989b. Holocene crustal movements and sea-level changes in Great Britain. *Journal of Quaternary Science* **4**, 77-89.

SHENNAN, I., Tooley, M.J., Davis, M.J. and Haggart, B.A. 1983. Analysis and interpretation of Holocene sea-level data. *Nature* **302**, 404-410.

SHENNAN, I., ORFORD, J. and PLATER A. 1992. Introduction: IGCP Project 274 Quaternary coastal evolution: case studies, models and regional patterns. *Proceedings of the Geologists' Association* **103**, 163-165.

SHEPARD, F.P. 1964. Thirty-five thousand years of sea-level. In: *Essays in Honour of K.O. Emery*, Los Angeles, University of Southern California Press, 1-10.

SHERIFF, R.E. and GELDART, L.P. 1995. Exploration seismology. 2nd Edition. Cambridge University Press.

SIMPKIN, P.G. 1993. Seismic profiling in shallow water: A novel approach. *Proceedings of the Institute of Acoustics* **15**, 279-286.

SLINGERLAND, R.L. 1977. The effects of entrainment on the hydraulic equivalence relationships of light and heavy minerals in sands. *Journal of Sediment Petrology* **47**, 753-770.

SLINGERLAND, R.L. 1984. The role of hydrolic equivalence relationships of light and heavy minerals in sands. *Journal of Sediment Petrology* **47**, 753-770.

SLOSS, L.L. 1962. Stratigraphic models in exploration. *Journal of Sediment Petrology* **32**, 415-422.

SMITH, R.K. 1987. Fossilization potential in modern benthic foraminiferal assemblages. *Journal of Foraminiferal Research* **17**, 117-122.

STRAHAN, A. 1909. The geology of the South-Wales coal-field. HMSO, London.

STRIDE, A.H. and BELDERSON, R.H. 1990. A reassessment of sand transport paths in the Bristol Channel and their regional significance. *Marine Geology* **92**, 227-236.

STRIDE, A.H. and BELDERSON, R.H. 1991. Sand transport in the Bristol Channel east of Bull Point and Worms Head: Bedload parting model with some indications of mutually evasive sand transport paths. *Marine Geology* **101**, 203-207.

STUART, A. 1924. The petrology of the dune sands off South Wales. *Proceedings of the Geologists Association* **35**, 316-331.

SWIFT, D.J.P. 1975. Barrier-Island Genesis: Evidence from the Central Atlantic Shelf, Eastern USA. *Sedimentary Geology* **14**, 1-43.

SWIFT, D.J.P., KOFOED, J.W., SAULSBURY, P.J. and SEARS, P. 1972. Holocene evolution of the shelf surface, Central and Southern Atlantic Shelf of North America. In D.J.P. Swift, D.B. Duane and O.H. Pilkey (Eds.) *Shelf Sediment Transport: Process and Pattern*, Stroudsburg, Dowden, Hutchinson and Ross, 499-574.

TAUBER, H. 1965. Differential pollen dispersion and the interpretation of pollen diagrams. *Danm. Geol. Unders. IIR* **89**, 1-69

TEBBLE, N. 1976. British bivalve seashells: A handbook for identification. 2nd Edition, H.M.S.O., Edinburgh.

TELFORD, W.M., GELDART, L.P. and SHERIFF, R.E. 1990. Applied geophysics. 2nd Edition, Cambridge University Press.

TERWINDT, J.H.J. 1988. Palaeotidal reconstructions of inshore tidal depositional environments. In P.L. de Boer, A. Van Gelder and S.D. Nio (eds.), *Tide-influenced sedimentary environments and facies*, Dordrecht, Reidel, 233-263.

THOM, B.G. and CHAPPELL, J. 1975. Holocene sea-level relative to Australia. *Search* **6**, 90-93.

THOMPSON, R. 1986. Modelling magnetization data using SIMPLEX. *Physics of the Earth and the Planetary Interiors* **42**, 105-112.

THOMPSON, R. and OLDFIELD, F. 1986. *Environmental Magnetism*, London, Allen & Unwin Ltd, 166-177.

TOOLEY, M.J. 1987. Sea-level Studies. In M.J. Tooley and I. Shennan (eds.), *Sea-level Changes*, Oxford, Basil Blackwell Ltd, 1-24.

TOOLEY, M.J. 1989. Floodwaters mark sudden rise. *Nature* **342**, 20-21.

TOOLEY, M.J. 1992. Recent sea-level changes. In J.R.L. Allen and K. Pye (eds.) *Saltmarshes: Morphodynamics, Conservation and Engineering Significance*, 19-40.

TRABANT, P.K. 1984. Applied high-resolution geophysical methods: Offshore geoengineering hazards. International Human Resources Development Corp., Boston.

TRAVERSE, A. 1988. Paleontology. Unwin Hyman, Boston.

TROELS-SMITH, J. 1955. Karakteriering af løsejordarter. *Danmarks Geologiske Undersøgelse Ser* IV, 3.

TRÖGER, W.E. 1956. Optishe bestimmung der gesteinsbildenden minerale: Teil 1 Bestimmungstabilen, E. Schwezerbart' sche Verlagsbuchhandlung, Stuttgart.

VAN DE PLASSHE, O. 1986. Introduction. In O. Van de Plassche (ed.), *Sea-level Research: a manual for the collection and evaluation of data*, Norwich, Geo-Books, 1-27.

VEROSUB, K.L. and ROBERTS, A.P. 1995. Environmental magnetism: Past, present and future. *Journal of Geophysical Research* **100**, 2175-2192.

WALCOTT, R.I. 1980. Rheological models and observational data of glacio-isostatic rebound. In N-A. Mörner (ed.) *Earth Rheology, Isostasy, and Eustasy*, Chester, John Wiley and Sons, 3-10.

WATKINS, R. 1991. Post glacial vegetational dynamics in lowland North Wales. Unpublished Ph.D Thesis, University of Wales.

WELTON, J.E. 1984. SEM petrology atlas. *The American Association of Petroleum Geologists*, Oklahoma.

WILSON, M.J. 1987. X-Ray powder diffraction methods. In M.J. Wilson (ed*), A handbook of determinative methods in clay mineralogy*. Blackie, Glasgow.

APPENDICES

Appendix 3.1

Multiple layer refraction shooting

(adapted from UCNW Engineering Seismology supplementary notes)

The analysis of several layers, at varying angles of dip, involves the break-down of time-terms into *shot-terms* (intercept time/delay time) and *geophone* terms. The delay time in any bed is equal to:

$$\frac{h}{v}.\ (\cos\ i\ +\ \cos\ e)$$

where h is the thickness of the bed related to the shot point, V is the velocity in that bed, and i and e are incident and emergent angles for any ray travelling through that bed. The total shot-term for any intercept time measured on the time-distance graph is given by:

$$\Sigma\ [\frac{h}{v}\ (\cos\ i\ +\ \cos\ e)]$$

The geophone term for any position along the ground surface is given by:

$$\frac{x}{V_\alpha}$$

where $V\alpha$ is the apparent surface velocity derived from the inverse slope of the time-distance graph. If V_1 is the surface velocity then:

$$V_\alpha\ =\ \frac{V_1}{\sin\ \delta}$$

where δ is the emergent angle (between ray and normal) at the surface.

Shot-terms (intercept-times)

"Plane Layer Forward Model"

Medium 1:

$I_1' = (2h_1' \cos\theta)/V_1$ Down slope

$I_1'' = (2h_1'' \cos\theta)/V_1$ Up slope

Medium 2:

$I_2' = (2h_2' \cos\theta)/V_2 + h_1'/V_1(\cos\alpha_1 + \beta_1)$ Down slope

$I_2'' = (2h_2'' \cos\theta)/V_2 + h_1''/V_1(\cos\alpha_1 + \beta_1)$ Up slope

Medium 3:

$I_3' = (2h_3' \cos\theta)/V_3 + h_2'/V_2(\cos\alpha_2^+ + \beta_1^+) + h_1'/V_1(\cos\alpha_2 + \beta_2)$ Down slope

$I_3'' = (2h_3'' \cos\theta)/V_3 + h_2''/V_2(\cos\alpha_2^+ + \beta_1^+) + h_1''/V_1(\cos\alpha_2 + \beta_2)$ Up slope

$\sin\alpha_1 = V_1/V_2 \sin[\theta_2 - (\phi_2-\phi_1)]$

$\sin\beta_1 = V_1/V_2 \sin[\theta_2 + (\phi_2-\phi_1)]$

$\sin\alpha_2 = V_1/V_2 \sin[\alpha_2^+ - (\phi_2-\phi_1)]$

$\sin\beta_2 = V_1/V_2 \sin[\beta_2^+ + (\phi_2-\phi_1)]$

$\sin\alpha_3^+ = V_2/V_3 \sin[\theta_3 - (\phi_3-\phi_2)]$

$\sin\beta_3^+ = V_3/V_3 \sin[\theta_3 + (\phi_3-\phi_2)]$

where:

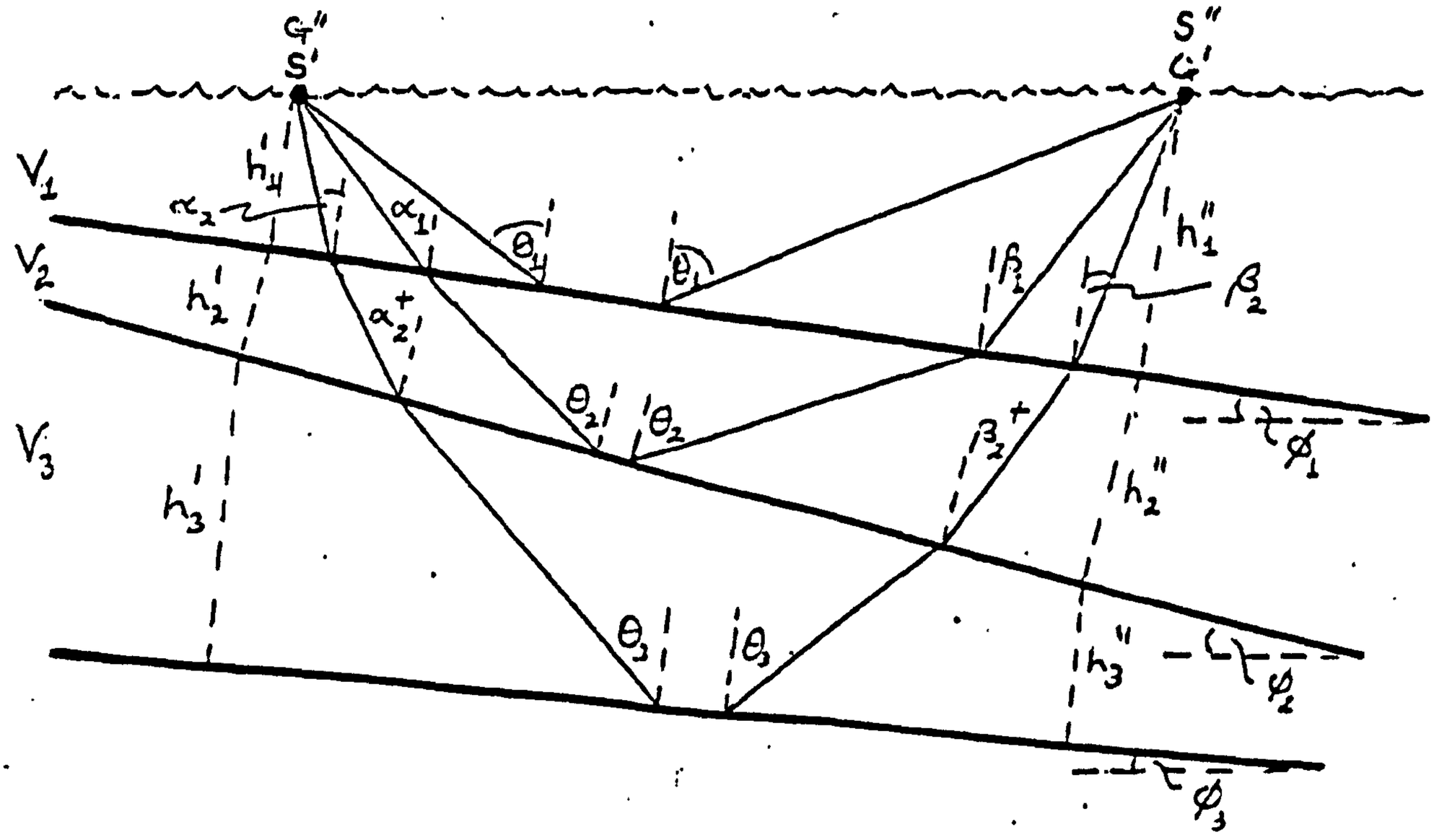

Appendix 6.1

Modern foraminiferal associations from the Taf Estuary

	Physiographic sub-environments within the Taf Estuary					
Species	High marsh	Mid Marsh	Marsh creek	Low Marsh	Mudflat	Sandflat
Trochammina inflata	12	57	7	16	3	0
Jadammina macrescens	80	34	22	19	1	0
Haplophragmoides wilberti	0	6	6	1	0	0
Miliammina fusca	0	1	0	0	2	0
Quinqueloculina seminulum	0	0	2	8	3	9
Miliolinella subrotunda	0	0	0	0	1	8
Lagena sulcata	2	0	1	0	1	1
Lagena clavata	0	0	0	0	1	0
Oolina squamosa	0	0	0	0	0	0
Oolina williamsoni	0	0	0	0	1	1
Bulimina marginata	0	0	0	0	0	0
Bulimina elongata	0	0	1	0	0	0
Bulimina gibba	0	0	0	0	0	0
Rosalina anomala	0	0	2	0	1	3
Cibicides lobatulus	0	0	5	0	21	38
Planorbulina distoma	0	0	2	0	13	5
Asteriginata mamilla	0	0	0	0	0	0
Hayensina germanica	6	0	38	5	33	1
Ammonia batavus	0	0	0	0	1	13
Elphidium williamsoni	0	2	13	51	14	20

Although variation does occur in each of the sub-environments this data represents the average composition of the foraminiferal associations identified within the Taf Estuary.

APPENDIX 6.2

Ecological and environmental requirements of certain tree, shrub, herb and lower plant taxa (derived from Godwin, 1975; Huntley and Birks, 1983; Clapham, Tutin & Moore, 1987)

Pinus spp. are generally tall forest-forming trees which occupy marginal habitats; when favourable conditions persist *Pinus* is capable of vigourous growth. Pines are prolific on dry, sandy soils such as dunes, on podsols, on peats, in montane and boreal environments, are secondary colonisers of abandoned cultivated areas and avoid water-logged areas (Huntley and Birks, 1983). The dominance of *Pinus* in the environments they inhabit may be a result of the poor soils pines tolerate, compounded by decomposition of an acidic litter. All species are prolific pollen producers and as a result high values of *Pinus* (>50%) are often recorded in modern treeless localities (Huntley and Birks, 1983).

Betula forms extensive natural woodlands in Europe in the sub-arctic, and generally occurs as secondary woods following forest clearance in lowland areas. Although birch grow on podsols they form mull humus and as they are high pollen producers their pollen is usually well dispersed. Consequently values >10% indicate local presence whereas values >25% indicate local birch-dominated woodland (Huntley and Birks, 1983).

The twenty-two European Oak species vary in stature from low shrubs to tall forest trees and they can range from being widespread to only locally significant (Huntley and Birks, 1983). Although *Quercus* exhibits considerable ecological variation, occurring in a whole variety of vegetation types and habitats, they are generally dominant or co-dominant in most European lowland forests and wet base-rich soils. These characteristics complicate the inference of local dominance; values ≥2% may represent local presence of oak whereas values >50% represent local dominance. When the *Quercus* frequency exceeds 10% oak is likely to be a significant contributor to the vegetation (Huntley and Birks, 1983).

Ulmus is a tall growing forest tree which frequently occurs in mixed canopies along with *Fraxinus, Quercus* and *Acer*, and are therefore characteristic of mesic mixed deciduous

woodland. Elms favour clay-rich soils and avoid waterlogged soils, shallow soils on freely-drained acidic or basic bedrock, and podsols. Pollen values ≥ 2% indicate local presence whereas 10% indicates that *Ulmus* amounts to a significant forest component (Huntley and Birks, 1983).

Alnus spp. are generally high pollen producers, their pollen maybe transported over long distances, and they are often abundant in wet or waterlogged environments (Huntley and Birks, 1983). Alder is generally abundant in fens and swamps forming carr communities associated with *Salix*, Cyperaceae, Poaceae and other hydrophilous herbs. *Alnus* commonly grows on peaty soils, where its litter forms part of the deposit, but can also flourish on silty or gravel substrates (Huntley and Birks, 1983). High pollen values can be recorded in areas of tree growth but it may be difficult to distinguish between local or widespread presence within the catchment.

The genus *Salix* includes 69 species of dwarf-shrubs, upright dwarf-shrubs, low shrubs, tall shrubs and trees native to Europe (Huntley and Birks, 1983). They are widely distributed and favour moist or waterlogged conditions on the edge of river banks or in fen carr. Willow is not a primary woodland species but may be locally dominant in carr or damp woodland. Local stands of *Salix* in carr communities may complicate the interpretation of pollen data and values > 2% indicate the local presence of *Salix*.

Corylus is a large shrub or small tree which generally occurs as an understorey species in mixed forests of *Quercus, Ulmus, Fraxinus* and *Tilia* with a mesic herb layer (Huntley and Birks, 1983). Hazel is found on a variety of soils but most commonly occurs on mull humus. Through determining the contribution of hazel to vegetation is complex, values greater than 25% indicate the presence of forests in which *Corylus* may be dominant.

Poaceae is the largest family of flowering plants and includes examples of almost every ecological type and life form (Clapham, Tutin & Moore, 1987). They occur in the majority of habitats from woodlands, dunes and shingles to steppes and aquatic environments. One common property of all the species is their basal rather than apical growth. Pollen values of up to 10% may occur in primarily wooded sites whereas values >25% imply the predominance of treeless vegetation (Huntley and Birks, 1983).

The Chenopodiaceae taxon includes over 100 genera and 1400 species of herbs and shrubs associated with either arid or saline environments (Clapham, Tutin & Moore, 1987). Although species are generally wind-pollinated the pollen is rarely transported over great distances and values > 1% indicate local presence whereas values >10% suggest the local abundance of Chenopodiaceae (Huntley and Birks, 1983). Examination of coastal and estuarine sites reveals that significantly high values of Chenopodiaceae can be recorded, reflecting the abundance with which the family grows in saltmarsh and other coastal environments Godwin (1975).

Although Cyperaceae grow in a whole variety of environments, and are ubiquitous in distribution, they favour cool, moist mires with treeless vegetation (Huntley and Birks, 1983). Sedges have capitalised upon the development of mires and waterlogged soils during the Holocene and their occurrence in the fossil record is an indication of the extent of treeless bog vegetation. Pollen frequencies > 10% occur consistently in areas where treeless vegetation persists whereas sporadic values of > 50% may be recorded in lacustrine sites where sedge swamps are surrounded by woodland (Huntley and Birks, 1983).

Plantains are annual or perennial herbs which flourish in unstable open treeless habitats and are common in coastal and inland sites. For instance, *Plantago lanceolata* is characteristic of grasslands whereas the halophytic salt tolerant species *Plantago maritima* has a strong preference to coastal sites and is likely to respond to eustatic changes in sea-level (Godwin, 1975). Although they produce large quantities of pollen they are poorly dispersed and occur in local abundance; consequently values >5% are rarely exceeded (Huntley and Birks, 1983).

Pteridium is primarily a woodland plant which avoids waterlogged soils and is still widespread throughout Europe within open forests, on acid soils and in locales where wind exposure may be too great for tree growth (Huntley and Birks, 1983). As bracken germinates after fire anthropogenic burning may have triggered the expansion of *Pteridium* into new areas during the late Holocene; the occurrence of spores indicates local abundance.

Polypodium spp. exhibit no significant soil preferences but occur as epiphytes on a wide variety of trees including *Quercus*, *Alnus*, *Fraxinus* and *Ulmus* (Huntley and Birks, 1983). Although they are prolific spore producers their low growth results in poor dispersal and spore values only exceed 3% in areas of abundant epiphytic growth. Relatively high *Polypodium* values, in the

absence of rupestral and epiphytic environments, may suggest that these resistant spores are an artifact of reworking and dissolution.